ISSN 0021-9673

VOL. 661 NOS. 1 + 2 FEBRUARY 11, 1994

COMPLETE IN ONE ISSUE

17th International Symposium on Column Liquid Chromatography Hamburg, May 9–14, 1993 Part II

JOURNAL OF CHROMATOGRAPHY A

INCLUDING ELECTROPHORESIS AND OTHER SEPARATION METHODS

SYMPOSIUM VOLUMES

ELSEVIER

JOURNAL OF CHROMATOGRAPHY A

INCLUDING ELECTROPHORESIS AND OTHER SEPARATION METHODS

Scope. The *Journal of Chromatography A* publishes papers on all aspects of **chromatography, electrophoresis** and related methods. Contributions consist mainly of research papers dealing with chromatographic theory, instrumental developments and their applications. In the *Symposium volumes*, which are under separate editorship, proceedings of symposia on chromatography, electrophoresis and related methods are published. *Journal of Chromatography B: Biomedical Applications* —This journal, which is under separate editorship, deals with the following aspects: developments in and applications of chromatographic and electrophoretic techniques related to clinical diagnosis or alterations during medical treatment; screening and profiling of body fluids or tissues related to the analysis of active substances and to metabolic disorders; drug level monitoring and pharmacokinetic studies; clinical toxicology; forensic medicine; veterinary medicine; occupational medicine; results from basic medical research with direct consequences in clinical practice.

Submission of Papers. The preferred medium of submission is on disk with accompanying manuscript (see *Electronic manuscripts* in the Instructions to Authors, which can be obtained from the publisher, Elsevier Science B.V., P.O. Box 330, 1000 AH Amsterdam, Netherlands). Manuscripts (in English; *four* copies are required) should be submitted to: Editorial Office of *Journal of Chromatography A*, P.O. Box 681, 1000 AR Amsterdam, Netherlands, Telefax (+31-20) 5862 304, or to: The Editor of *Journal of Chromatography B: Biomedical Applications*, P.O. Box 681, 1000 AR Amsterdam, Netherlands. Review articles are invited or proposed in writing to the Editors who welcome suggestions for subjects. An outline of the proposed review should first be forwarded to the Editors for preliminary discussion prior to preparation. Submission of an article is understood to imply that the article is original and unpublished and is not being considered for publication elsewhere. For copyright regulations, see below.

Publication information. *Journal of Chromatography A* (ISSN 0021-9673): for 1994 Vols. 652–682 are scheduled for publication. *Journal of Chromatography B: Biomedical Applications* (ISSN 0378-4347): for 1994 Vols. 652–662 are scheduled for publication. Subscription prices for *Journal of Chromatography A*, *Journal of Chromatography B: Biomedical Applications* or a combined subscription are available upon request from the publisher. Subscriptions are accepted on a prepaid basis only and are entered on a calendar year basis. Issues are sent by surface mail except to the following countries where air delivery via SAL is ensured: Argentina, Australia, Brazil, Canada, China, Hong Kong, India, Israel, Japan, Malaysia, Mexico, New Zealand, Pakistan, Singapore, South Africa, South Korea, Taiwan, Thailand, USA. For all other countries airmail rates are available upon request. Claims for missing issues must be made within six months of our publication (mailing) date. Please address all your requests regarding orders and subscription queries to: Elsevier Science B.V., Journal Department, P.O. Box 211, 1000 AE Amsterdam, Netherlands. Tel.: (+31-20) 5803 642; Fax: (+31-20) 5803 598. Customers in the USA and Canada wishing information on this and other Elsevier journals, please contact Journal Information Center, Elsevier Science Inc., 655 Avenue of the Americas, New York, NY 10010, USA, Tel. (+1-212) 633 3750, Telefax (+1-212) 633 3764.

Abstracts/Contents Lists published in Analytical Abstracts, Biochemical Abstracts, Biological Abstracts, Chemical Abstracts, Chemical Titles, Chromatography Abstracts, Current Awareness in Biological Sciences (CABS), Current Contents/Life Sciences, Current Contents/Physical, Chemical & Earth Sciences, Deep-Sea Research/Part B: Oceanographic Literature Review, Excerpta Medica, Index Medicus, Mass Spectrometry Bulletin, PASCAL-CNRS, Referativnyi Zhurnal, Research Alert and Science Citation Index.

US Mailing Notice. *Journal of Chromatography A* (ISSN 0021-9673) is published weekly (total 52 issues) by Elsevier Science B.V. (Sara Burgerhartstraat 25, P.O. Box 211, 1000 AE Amsterdam, Netherlands). Annual subscription price in the USA US$ 4994.00 (US$ price valid in North, Central and South America only) including air speed delivery. Second class postage paid at Jamaica, NY 11431. **USA POSTMASTERS**: Send address changes to *Journal of Chromatography A*, Publications Expediting, Inc., 200 Meacham Avenue, Elmont, NY 11003. Airfreight and mailing in the USA by Publications Expediting.

See inside back cover for Publication Schedule, Information for Authors and information on Advertisements.

0021-9673/94/$07.00

Printed in the Netherlands

For Contents see p. VII.

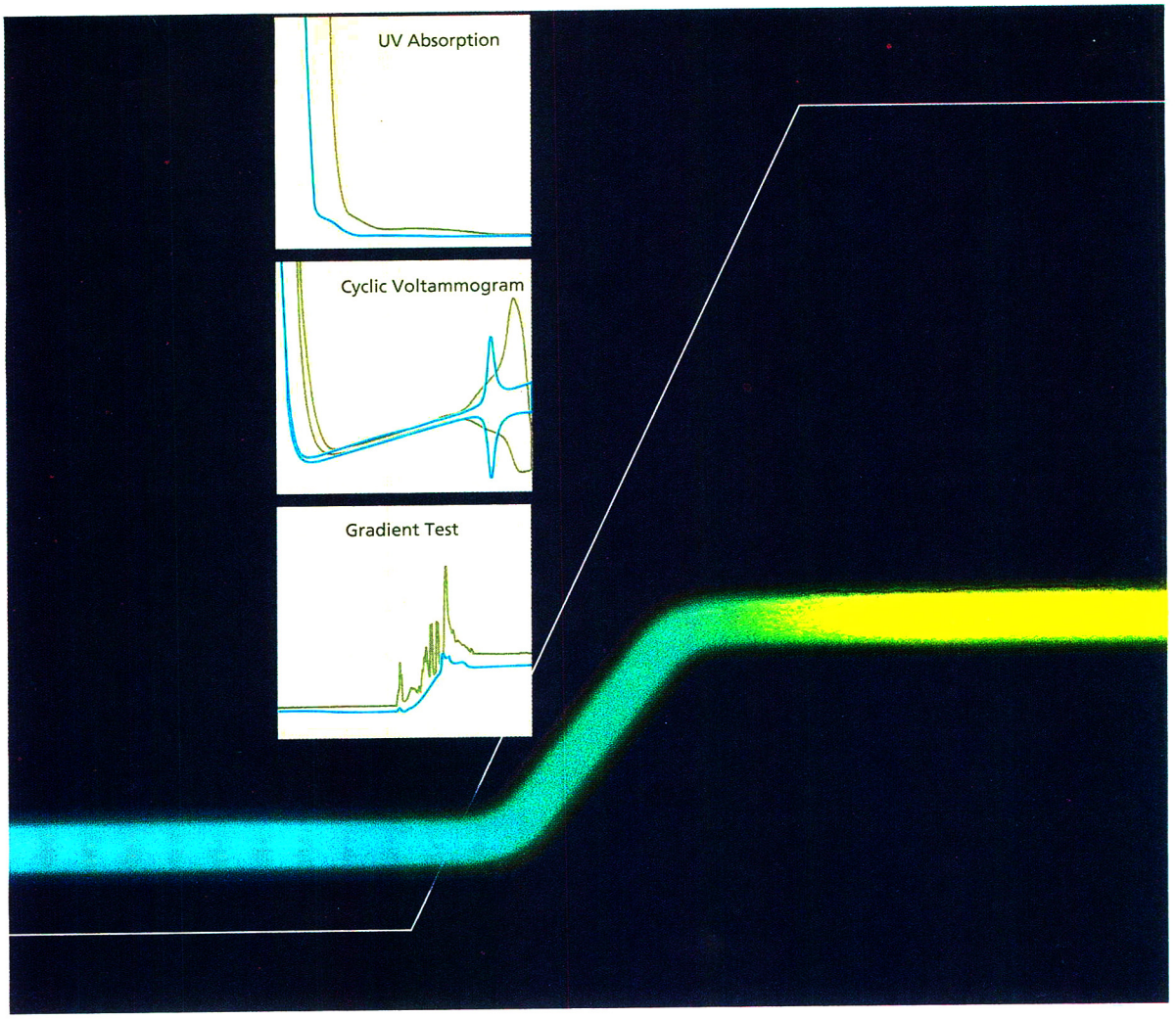

Reagents for Ion Pair Chromatography

Quality makes your decision easy

Are you looking for a high-purity and application-proven eluent additive ?

We offer ion pair reagents which meet unique and rigorous quality requirements:

- zero residue in the filter test
- extreme low UV absorption over a wide wavelength range
- absence of redox traces
- have passed a gradient test (except bromides).

Do you want a wide range of ion pair reagents to choose from ?

Besides all commonly used reagents our sales program includes distinct specialities such as

- tetraalkylammonium hydrogen sulfates
- phosphonium salts
- tetrabutylammonium dihydrogen phosphate.

Perhaps you prefer ion pair reagents in an easy-to-handle form
for example our ready-to-use concentrates in ampoules ?

Would you like to buy reagents for the pH adjustment of the eluent ?

Fluka is now introducing a unique series of application-tested phosphate concentrates in ampoules.

Have we aroused your curiosity ?

Please ask for
our new ion pair chromatography leaflet !

Fluka

Chemika-BioChemika

Switzerland: Fluka Chemie AG, Industriestrasse 25, CH-9470 Buchs/Switzerland, Telephone 081 755 25 11, Telex 855 282, Fax 081 756 54 49

Benelux: Fluka Chemie, B-2880 Bornem, Tel. (03) 899 13 01 France: Fluka S.a.r.l., F-38297 St.Quentin Fallavier, Tél. 74 82 28 00
Germany: Fluka Chemie, D-89231 Neu-Ulm, Tel. (0731) 973-3200 Great Britain: Fluka Chemicals Ltd, Gillingham, Tel. (0747) 82 30 97
Italy: Fluka Chimica, I-20151 Milano, Tel. (02) 33417-310 Japan: Fluka Fine Chemical, Chiyoda-Ku, Tokyo, Tel. 81-03-3255-4787
Spain: Fluka Química, E-28100 Alcobendas, Tel. (91) 661 99 77 USA: Fluka Chemical Corp., Ronkonkoma, N.Y., Tel. 516-467-0980

Organofluorine Compounds in Medicinal Chemistry and Biomedical Applications

Edited by **R. Filler**, **Y. Kobayashi** and **L.M. Yagupolskii**

Studies in Organic Chemistry Volume 48

An examination of the important role of fluorine in medicinal chemistry reveals that, in most cases, an organic compound needs be only lightly substituted with fluorine. Indeed, a single fluorine atom or a trifluoromethyl group, located in a key position of a bioactive molecule, can exert a profound pharmacological effect. Recently, developments in previously well-studied fields have been augmented by exciting reports in newer areas. The topics chosen by the authors are likely to be of broad interest and represent the work of established international leaders in their areas of research.

Keeping in mind the question *"what does fluorine provide that is so special?"*, the reader will find information on anticancer and antiviral agents and be brought up to date on volatile anesthetics and central nervous system agents, areas in which fluorine has played a pivotal role for almost forty years. Antibiotics receive special attention, with coverage of β-lactams and fluoroquinolone antibacterials. Newer applications of biologically-active fluorine compounds are reviewed, including cardiovascular drugs, fluoroamino acids and peptides, and the prostaglandins and leukotrienes of the arachidonic acid cascade. Biomedical applications, such as ^{18}F in positron emission tomography (PET) and fluorinated surfactants are exceptionally well covered. In the opening chapter, an overview of the field is given, including brief reports on areas not otherwise covered in the book, e.g. recent advances in antidiabetic and hypolipidemic agents.

Contents:

Fluoromedicinal chemistry - an overview of recent developments
(R. Filler).
Fluorine-containing antiviral and anticancer compounds
(L.W. Hertel, R.J. Ternansky).
Fluorine-containing cardiovascular drugs
(L.M. Yagupolskii, I.I. Maletina, B.M. Klebanov).
Recent developments in fluorine substituted volatile anesthetics
(D.F. Halpern).
Fluorinated β-lactams and biological activities of β-lactamase and elastase inhibitors
(O.A. Mascaretti, C.E. Boschetti, G.O. Danelon).
Fluoroquinolone carboxylic acids as antibacterial drugs
(D.T.W. Chu).
The role of fluorine in the chemistry of central nervous system agents
(A.J. Elliott).
New developments in the synthesis and medicinal applications of fluoroamino acids and peptides
(I. Ojima).
The fluoroarachidonic acid cascade
(A. Yasuda).
The synthesis and applications of F-18 compounds in positron emission tomography
(J.S. Fowler).
Fluorinated surfactants intended for biomedical uses
(J. Greiner, J.G. Riess, P. Vierling).
Subject index.

© 1993 394 pages Hardbound
Price: Dfl. 395.00 (US $ 225.75)
ISBN 0-444-89768-2

ORDER INFORMATION

For USA and Canada
ELSEVIER SCIENCE INC.
P.O. Box 945
Madison Square Station
New York, NY 10160-0757
Fax: (212) 633 3880

In all other countries
ELSEVIER SCIENCE B.V.
P.O. Box 330
1000 AH Amsterdam
The Netherlands
Fax: (+31-20) 5862 845

US$ prices are valid only for the USA & Canada and are subject to exchange rate fluctuations; in all other countries the Dutch guilder price (Dfl.) is definitive. Customers in the European Union should add the appropriate VAT rate applicable in their country to the price(s). Books are sent postfree if prepaid.

ELSEVIER SCIENCE B.V.

JOURNAL OF CHROMATOGRAPHY A

VOL. 661 (1994)

JOURNAL OF CHROMATOGRAPHY A

INCLUDING ELECTROPHORESIS AND OTHER SEPARATION METHODS

SYMPOSIUM VOLUMES

ELSEVIER
AMSTERDAM — LONDON — NEW YORK — TOKYO

Hamburg seen from the east
by Gabriel Engels (1648)

0021-9673/94/$07.00

Printed in the Netherlands

SYMPOSIUM VOLUME

17TH INTERNATIONAL SYMPOSIUM ON COLUMN LIQUID CHROMATOGRAPHY

PART II

Hamburg (Germany), May 9–14, 1993

Guest Editor

K.K. Unger

(Mainz, Germany)

The proceedings of the *17th International Symposium on Column Liquid Chromatography, Hamburg, May 9–14, 1993*, are published in two consecutive volumes of the *Journal of Chromatography A*: Vols. 660 and 661 (1994). The Foreword to the proceedings only appears in Vol. 660. A combined Author Index to both Vols. 660 and 661 only appears in Vol. 661.

VOL. 661, NOS. 1 + 2 JOURNAL OF CHROMATOGRAPHY A FEBRUARY 11, 1994

CONTENTS

17TH INTERNATIONAL SYMPOSIUM ON COLUMN LIQUID CHROMATOGRAPHY, HAMBURG, MAY 9–14, 1993, PART II

APPLICATIONS (*continued*)

Proteins and their constituents

Quantitative determination of a dipeptide in personal wash liquid by capillary electrophoresis
by D. Jones, A. Scarborough and C.M. Tier (Sharnbrook, UK) 1

High-performance liquid chromatographic separation of *cis–trans* isomers of proline-containing peptides. II. Fractionation in different cyclodextrin systems (Short Communication)
by S. Friebe, B. Hartrodt, K. Neubert and G.-J. Krauss (Halle/S., Germany) 7

Purification and analytical characterization of an anti-CD4 monoclonal antibody for human therapy
by A.H. Guse, A.D. Milton, H. Schulze-Koops, B. Müller, E. Roth, B. Simmer and H. Wächter (Erlangen, Germany), E. Weiss (Munich, Germany) and F. Emmrich (Erlangen, Germany) 13

Applications of amino acid derivatization with 6-aminoquinolyl-N-hydroxysuccinimidyl carbamate. Analysis of feed grains, intravenous solutions and glycoproteins
by S.A. Cohen (Milford, MA, USA) and K.M. De Antonis (Kingston, RI, USA) 25

Kinetic study of the adsorption of human serum albumin on immobilized antibody using the split-peak effect in immunochromatography
by J. Renard and C. Vidal-Madjar (Thiais, France) 35

Advances in the high-performance liquid chromatographic determination of phenylthiocarbamyl amino acids (Review)
by I. Molnár-Perl (Budapest, Hungary) 43

Ligand-exchange high-performance liquid chromatography of fluorine-containing phenylglycine and phenylalanine
by S.V. Galushko, I.P. Shishkina and V.A. Soloshonok (Kiev, Ukraine) 51

Liquid chromatographic–mass spectrometric studies on the enzymatic degradation of gonado-tropin-releasing hormone
by M. Brudel, U. Kertscher, H. Berger and B. Mehlis (Berlin, Germany) 55

High-performance liquid chromatography of amino acids, peptides and proteins. CXXXIII. Peak tracking of peptides in reversed-phase high-performance liquid chromatography
by A.J. Round, M.I. Aguilar and M.T.W. Hearn (Clayton, Australia) 61

Determination of peptide hydrophobicity parameters by reversed-phase high-performance liquid chromatography
by S. Rothemund, E. Krause, A. Ehrlich and M. Bienert (Berlin, Germany), E. Glusa (Erfurt, Germany) and P. Verhallen (Berlin, Germany) 77

Recombinant human insulin. III. High-performance liquid chromatography and high-performance capillary electrophoresis control in the analysis of step-by-step production of recombinant human insulin
by V.E. Klyushnichenko, D.M. Koulich, S.A. Yakimov, K.V. Maltsev, G.A. Grishina, I.V. Nazimov and A.N. Wulfson (Moscow, Russian Federation) 83

Synthesis and analysis of oxidation and carbonyl condensation compounds of tryptophan
by T. Simat, K. Meyer and H. Steinhart (Hamburg, Germany) 93

Determination of tryptophan and ten of its metabolites in a single analysis by high-performance liquid chromatography with multiple detection
by U. Caruso (Genova, Italy), B. Fowler (Basle, Switzerland) and G. Minniti and C. Romano (Genova, Italy) 101

Sensitive determination of N-terminal prolyl peptides by high-performance liquid chromatography with laser-induced fluorescence detection
by T. Toyo'oka, M. Ishibashi and T. Terao (Tokyo, Japan) 105

Miscellaneous biological applications

Column-switching liquid chromatographic method for the simultaneous determination of iothalamic acid and creatinine in biological fluids
by T. Seki, Y. Orita, S. Yamamoto and N. Ueda (Osaka, Japan) and Y. Yanagihara and K. Noguchi (Kanagawa, Japan) . . . 113

Thermospray liquid chromatography–mass spectrometry of flavonol glycosides from medicinal plants
by P. Pietta, R.M. Facino, M. Carini and P. Mauri (Milan, Italy) . . . 121

Evaluation of the analysis of cholesterol oxides by liquid chromatography
by B.H. Chen and Y.C. Chen (Taipei, Taiwan) . . . 127

Determination of catecholamines by automated pre-column derivatization and reversed-phase column liquid chromatography with fluorescence detection
by J. Kehr (Stockholm, Sweden) . . . 137

Correlative retention time peak identification method for glycated haemoglobin in high-performance liquid chromatography
by M. Ito, J. Miura, M. Ito, F. Umesato, K. Yasuda and Y. Takata (Katsuta, Japan) and B. Stanislawski (Darmstadt, Germany) . . . 143

On-line solid-phase extraction with automated cartridge exchange for liquid chromatographic determination of lipophilic antioxidants in plasma
by M. Hedenmo and B.-M. Eriksson (Mölndal, Sweden) . . . 153

Purification of human tumour necrosis factor by membrane chromatography
by J. Luksa, V. Menart, S. Milicic, B. Kus and V. Gaberc-Porekar (Ljubljana, Slovenia) and D. Josic (Vienna, Austria) . . . 161

Determination of glycoalkaloids in potato tubers by reversed-phase high-performance liquid chromatography
by R.J. Houben and K. Brunt (Groningen, Netherlands) . . . 169

Determination of aflatoxins in food by use of an automatic work station
by G. Niedwetzki and G. Lach (Hamburg, Germany) and K. Geschwill (Idstein/Ts., Germany) . . . 175

High-performance liquid chromatographic method for the simultaneous detection of malonaldehyde, acetaldehyde, formaldehyde, acetone and propionaldehyde to monitor the oxidative stress in heart
by G.A. Cordis (Farmington, CT, USA), D. Bagchi (Omaha, NE, USA) and N. Maulik and D.K. Das (Farmington, CT, USA) . . . 181

Pre-column derivatization of biogenic amines and amino acids with 9-fluorenylmethyl chloroformate and heptylamine
by J. Kirschbaum and B. Luckas (Stuttgart, Germany) and W.-D. Beinert (Darmstadt, Germany) . . . 193

Other applications

Determination of amines in wines by high-performance liquid chromatography with electrochemical coulometric detection after precolumn derivatization
by G. Achilli and G.P. Cellerino (Parabiago, Italy) and G. Melzi d'Eril (Pavia, Italy) . . . 201

Analytical study of polyoxyethylene surfactants of high degree of condensation by normal-phase liquid chromatography on *p*-nitrophenyl-bonded silica
by P.L. Desbène (Evreux, France) and B. Desmazieres (Mont Saint Aignan, France) . . . 207

Composition distribution separation of methyl methacrylate–methacrylic acid copolymers by normal-phase gradient elution high-performance liquid chromatography
by T.C. Schunk (Rochester, NY, USA) . . . 215

Quantitative polymer composition characterization with a liquid chromatography–Fourier transform infrared spectrometry–solvent-evaporation interface
by T.C. Schunk (Rochester, NY, USA) and S.T. Balke and P. Cheung (Toronto, Canada) . . . 227

Retention behaviour of tributylphenol ethylene oxide oligomers on an alumina high-performance liquid chromatographic column
by E. Forgács and T. Cserháti (Budapest, Hungary) . . . 239

ELECTROPHORESIS

Simultaneous determination of benzotriazole copper inhibitor and microbiocidal isothiazolinenones by high-performance liquid chromatography
by A. Iob, F. Al-Yousef, B.S. Tawabini, A.I. Mohammed and N.M. Abbas (Dhahran, Saudi Arabia) 245

Low-molecular-mass p*I* markers for isoelectric focusing
by K. Šlais and Z. Friedl (Brno, Czech Republic) 249

Factors affecting the performance of sodium dodecyl sulfate gel-filled capillary electrophoresis
by K. Tsuji (Kalamazoo, MI, USA) 257

Numerical algorithms for capillary electrophoresis
by S.V. Ermakov, M.S. Bello and P.G. Righetti (Milan, Italy) 265

Analysis of derivatized peptides by capillary electrophoresis
by K.M. De Antonis and P.R. Brown (Kingstown, RI, USA) and Y.-F. Cheng and S.A. Cohen (Milford, MA, USA) 279

Indirect fluorescence determination of lactate and pyruvate in single erythrocytes by capillary electrophoresis
by Q. Xue and E.S. Yeung (Ames, IA, USA) 287

Comparative study of non-porous anion-exchange chromatography, capillary gel electrophoresis and capillary electrophoresis in polymer solutions in the separation of DNA restriction fragments
by C. Sumita, Y. Baba, K. Hide, N. Ishimaru, K. Samata, A. Tanaka and M. Tsuhako (Kobe, Japan) 297

Electrophoresis of proteins in uncoated capillaries with amines and amino sugars as electrolyte additives
by D. Corradini, A. Rhomberg and C. Corradini (Rome, Italy) 305

Preparation and characterization of a stable polyacrylamide sieving matrix-filled capillary for high-performance capillary electrophoresis
by M. Nakatani (Hyogo, Japan) and A. Skibukawa and T. Nakagawa (Kyoto, Japan) 315

AUTHOR INDEX VOLS. 660 AND 661 323

Journal of Chromatography A, 661 (1994) 1–6
Elsevier Science B.V., Amsterdam

CHROMSYMP. 2917

Quantitative determination of a dipeptide in personal wash liquid by capillary electrophoresis

David Jones, Ann Scarborough and Christopher M. Tier

Analytical Section, Unilever Research, Colworth House, Sharnbrook, Bedfordshire, MK44 1LQ (UK)

ABSTRACT

The dipeptide alanylglutamine is quantified in a commercial personal cleaning fluid using micellar electrokinetic capillary chromatography. Quantitation is achieved using an internal standard approach with either normalised peak height or area measurements. Correlation coefficients for the calibration graphs were typically 0.999 with data generated over a two-month period and using different capillaries. The data was in good agreement with that of an HPLC approach which utilised pre-column derivatisation with dabsyl chloride.

INTRODUCTION

Since Virtanen [1] described the advantages of using small diameter tubes in 1974, capillary electrophoresis (CE) has enjoyed an exponential growth rate in terms of published papers. In 1991 a CE data base [2] estimated that there were in excess of over 700 publications in the open literature. However, an analysis of these papers [3] reveals that a sizeable proportion are either reviews or deal with instrumental modification, techniques or theory. Papers that detail analytical applications are therefore in the minority, and those that describe quantitative assays are relatively few [4–6]. Although remarkable qualitative separations have been demonstrated [7], in order to exploit CE to the full, it will have to be proven as a robust technique capable of providing quantitative data of a comparable quality to that of HPLC and GLC.

In this paper, CE has been investigated as a means of quantifying the level of a dipeptide (alanylglutamine) in a personal cleaning fluid undergoing stability trials. This particular problem was chosen not just as a suitable test-bed to examine quantitative aspects of the technique, but also because it represents a relatively complex sample matrix. Hence it provides a good test of the techniques quantitative ability in a "real sample" situation. For comparative purposes, data produced by CE are compared with that generated via an HPLC approach that utilises pre-column derivatisation.

EXPERIMENTAL

Equipment

Electrophoresis was carried out on a model 270A capillary electrophoresis system from Applied Biosystems using a 122 cm × 50 μm I.D. fused-silica capillary. Data collection, as for HPLC, was undertaken with Multichrom software from VG Instruments running on a μVAX computer.

HPLC was carried out using a Spectra Physics Model SP8800, a LiChrospher 100 reversed-phase column from Merck (12.5 cm × 0.5 cm I.D.) and a Model SA6500 UV–Vis detector from Severn Analytical. Sample injection was carried out using a Model 710 WISP autosampler from Millipore.

0021-9673/94/$07.00
SSDI 0021-9673(93)E0892-X

Materials

Tricine [N-tris(Hydroxymethyl)methylglycine], sodium dodecyl sulphate, triglycine and norvaline (2-aminopentanoic acid) were all purchased from Sigma and the dipeptide alanylglutamine from Nova Biochem. Acetonitrile was HPLC grade and the water was Milli Q (Millipore) with a resistivity >18 MΩ. Dabsyl chloride (4-dimethylaminoazobenzene-4′-sulphonylchloride) was double recrystallised from Pierce. All other reagents were of Analar grade.

Capillary electrophoresis

Conditions. The running buffer was 20 m*M* tricine pH 7.5 with varying levels of sodium dodecyl sulphate (SDS). An applied voltage of 25 kV equivalent to a field strength of 205 V cm^{-1} was used throughout. The column was maintained at a temperature of 55°C and detection was at 200 nm (rise time 0.5 s). Hydrodynamic injections of 3 s were carried out and a wash cycle consisting of 2 min of 0.1 *M* NaOH followed by 4 min running buffer was done after each injection.

Sampling. Approximately 0.6 g personal cleaning fluid was accurately weighed into a 25 cm^3 flask and 1 cm^3 of a 2.1 mg cm^{-3} solution of triglycine internal standard added. The flask was made up to volume with running buffer and thoroughly mixed. An aliquot of this solution was passed through a 0.45-μm filter prior to electrophoresis.

Calibration. Dipeptide levels in cleaning fluid were quantified using a series of dipeptide calibration standards dissolved in running buffer and containing triglycine internal standard. Initial work incorporated the cleaning fluid base into these standards but it was subsequently removed for a comparative experiment. Using independent stock solution of dipeptide and triglycine, both at a concentration of 2 mg cm^{-3}, calibration standards containing 80 μg cm^{-3} triglycine and from 24 to 240 μg cm^{-3} dipeptide were formulated. Cleaning fluid base was present at a level of 24 mg cm^{-3} (*i.e.* the same as for the samples) and the solutions were made up to volume with running buffer.

Quantitation. All quantitative work was undertaken with the use of internal standard normalisation using both peak height and area measurements. Calibration plots of dipeptide normalised peak height or area *versus* concentration were obtained over a two-month period.

HPLC

Sampling. Cleaning fluid (0.5 g) was accurately weighted into a volumetric flask (in duplicate), norvaline internal standard solution added, and the volume made up to 100 cm^3 with water. After mixing, an aliquot of this solution was filtered through a Whatman 541 and the filtrate used for derivatisation.

Calibration. As with the electrophoresis work, dipeptide levels in cleaning fluid were quantified using a series of dipeptide calibration standards containing cleaning fluid base and norvaline internal standard. The dipeptide concentration range was from 5 to 40 μg cm^{-3} with an internal standard concentration of 10 μg cm^{-3}.

Derivatisation. Both samples and standards were derivatised in an identical manner. Aliquots of 200 μl of sample or standard were dispensed into a low volume autosampler vial and then taken to dryness. The residue was dissolved in 20 μl of 50 m*M* sodium bicarbonate buffer pH 8.1 and then derivatised with 40 μl of dabsyl chloride solution in acetonitrile (4 mmoles cm^{-3}). The tubes were then stoppered, vortexed and incubated at 70°C for 12 min. After cooling, 440 μl of 50 m*M* sodium phosphate pH 7.0–ethanol (1/1, v/v) was added to each tube, and after vortexing, an aliquot of this solution taken for chromatography. The dipeptide derivative was separated on a reversed-phase column using a 40-min gradient from 20 m*M* sodium acetate–dimethylformamide (96:4) pH 6.4 to acetonitrile, with detection in the visible at 436 nm.

Quantitation. Dipeptide peak areas for both calibration standards and samples were determined and then normalised by dividing by the area of the internal standard. A calibration graph of normalised dipeptide peak area *versus* concentration was constructed and used to calculate dipeptide concentration in samples.

RESULTS AND DISCUSSION

Electrophoretic conditions

Cleaning fluids are complex formulations comprising a combination of surfactant types in

combination with other functional components such as conditioning agents, preservatives and pearlising agents. Using tricine buffer at pH 7.5, the dipeptide was found to migrate close to a number of other cleaning fluid constituents (Fig. 1a). By the addition of SDS above the critical micelle concentration, the separation mode can be changed from free solution electrophoresis to micellar electrokinetic capillary chromatography (MECC). In this mode, the negatively charged micelles migrate towards the anode, carrying with them any species that can partition into the micelle. Since at pH 7.5 however, the electro-osmotic flow is very rapid, the micelles will still eventually be swept to the cathode. Although both the dipeptide and cleaning fluid surfactants can partition into the micelle, the latter does so far more strongly.

The net effect is to retard the migration of the surfactant more than that of dipeptide (Fig. 1b). At 50 m*M* SDS most of the residual material migrating underneath the dipeptide can be removed and a clean separation achieved with the internal standard (Fig. 1c).

Migration time

Table I shows a typical set of data obtained from a calibration run, with dipeptide levels in

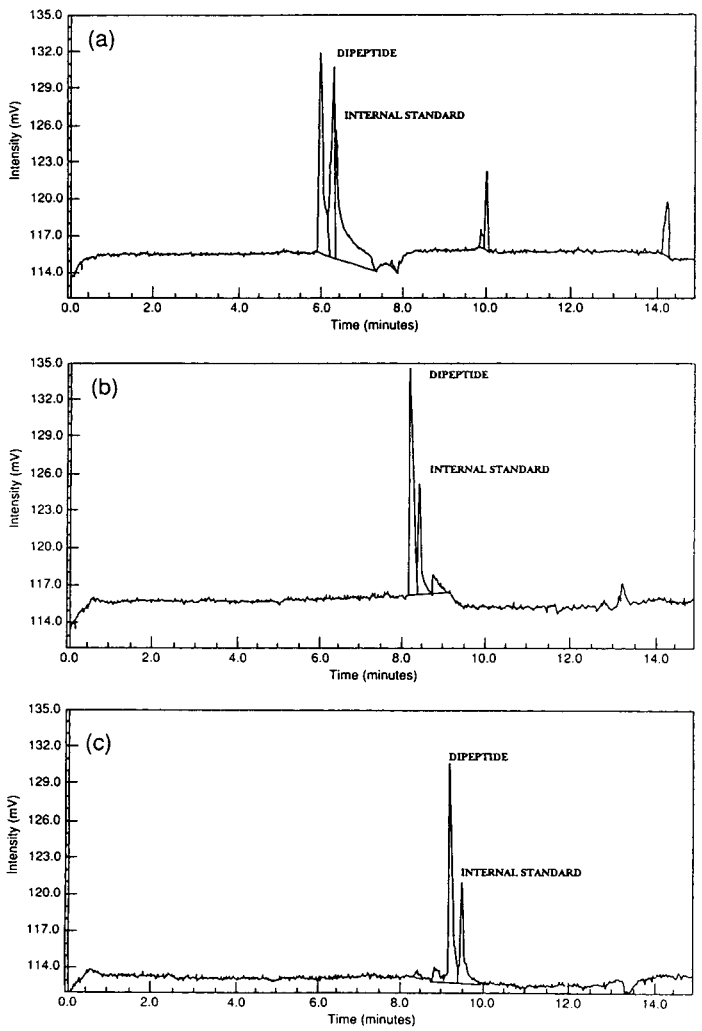

Fig. 1. Separation of dipeptide from cleaning fluid components. (a) Tricine buffer only; (b) tricine buffer with 20 m*M* SDS; (c) tricine buffer with 50 m*M* SDS.

TABLE I

MIGRATION TIME AND PEAK HEIGHT/AREA DATA FROM A CE CALIBRATION RUN

Internal standard (I.S.)			Dipeptide				Dipeptide/I.S.	
Migration time (min)	Peak height ($\mu V \cdot 10^{-2}$)	Peak area ($\mu Vs \cdot 10^{-2}$)	Migration time (min)	Peak height ($\mu V \cdot 10^{-2}$)	Peak area ($\mu Vs \cdot 10^{-2}$)	Level in cleaning fluid (%, w/w)	Normalised height	Normalised area
14.74	67.4	440.5	14.0	14.3	75.4	0.10	0.21	0.17
14.53	67.0	434.8	13.8	14.0	79.9	0.10	0.21	0.18
14.19	66.7	435.7	13.5	35.1	206.0	0.24	0.53	0.47
13.95	68.2	445.9	13.3	33.7	190.3	0.24	0.49	0.43
13.69	64.8	403.7	13.0	63.8	363.5	0.52	0.99	0.90
13.50	64.6	414.4	12.9	65.1	366.3	0.52	1.01	0.88
13.23	63.2	394.8	12.6	96.2	536.3	0.72	1.52	1.36
13.08	63.9	405.7	12.5	65.4	526.3	0.72	1.49	1.30
12.68	60.7	367.2	12.1	123.8	677.7	1.01	2.04	1.85

cleaning fluid ranging from 0.1 to 1.01%. It is important to note that with on-column detection in CE, any change in migration time will affect the speed at which the band passes the detector window. Hence a slower band will exhibit an apparently larger peak area [8]. Consequently it is important to ensure that the migration times within a run are reproducible (good repeatability) or to correct (normalise) the areas using *e.g.* the migration time of the band, or a suitable internal standard. From all the data generated during this study, this problem can be seen most clearly from the data in Table I. The migration times for both the triglycine and dipeptide progressively decrease; resulting in a steady increase to peak areas. All quantitative work was therefore conducted on peak height or area measurements that had been normalised with respect to that of the internal standard.

Calibration curves

Linearity of response, *i.e.* peak height/area of dipeptide *versus* concentration, was determined over three separate days during a two-month period for standards containing cleaning fluid base. The data in Table II shows the results for the correlation coefficients obtained following a least squares linear regression analysis. For both normalised height or area measurements good linearity is obtained indicating either approach is suitable for quantitation. The data from run 4 was obtained for a calibration standard in the absence of cleaning fluid base, *i.e.* in run buffer only, and demonstrates an improvement in linearity. The matrix in which the sample is injected can pose problems in CE [9]. If it is different between sample and standard then it can cause a change to the band migration time. In this particular assay, however, no such problems are encountered indicating that omission of the cleaning fluid base is not only a simpler approach but that the quality of the data is improved. The calibration graphs obtained from run 4 are shown in Figs. 2 and 3.

As a final point it should be noted that two different capillaries of identical dimensions were used to generate the above data, demonstrating

TABLE II

LINEAR REGRESSION ANALYSIS OF CE CALIBRATION DATA

Run No.	Correlation coefficient	
	Peak height	Peak area
1	0.9981	0.9981
2	0.9964	0.9949
3	0.9992	0.9984
4	0.9998	0.9998

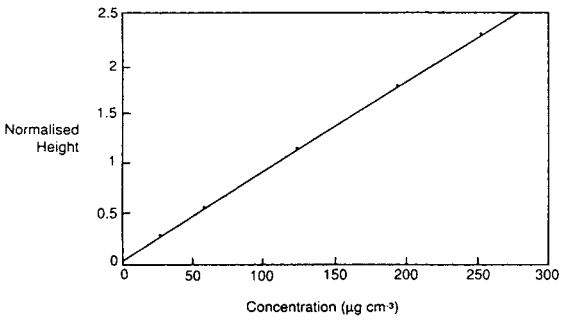

Fig. 2. Dipeptide concentration *versus* normalised peak height.

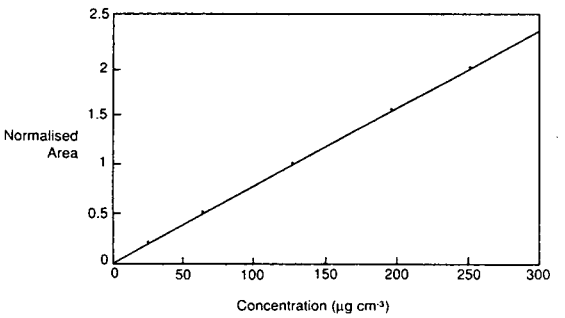

Fig. 3. Dipeptide concentration *versus* normalised peak area.

that variation in capillary characteristics does not pose problems of reproducibility.

Levels of dipeptide in cleaning fluid

The calibration graphs obtained in the preceding section were used to calculate alanylglutamine levels in cleaning fluid undergoing stability trials. The dipeptide was incorporated at a nominal 0.4% (w/w) and the sample divided in two. One of these was frozen down (−20°C) and the other placed in a fixed temperature cabinet (37°C). Samples were taken from these two storage trials and CE data generated using both normalised peak height and area measurements. The data obtained are presented in Table III and shows that essentially there is no difference between the two approaches.

The 17-week data was generated on two consecutive days, with the first −20°C and 37°C data set obtained with run 3 calibration (Table II) and the second set with run 4. The difference between these, was that run 3 was generated with cleaning fluid base in the calibration standard, whilst for run 4 it was omitted. Clearly both approaches give the same result and since an improved correlation coefficient is obtained for standards with no added base, this is the preferred procedure.

The data in Table III can be condensed by averaging the peak height and area result, as well as the two sets of 17-week data. Table IV gives the averaged CE data compared to that obtained via HPLC and shows good agreement between the two techniques. As far as the dipeptide is concerned, storage at 37°C leads to a rapid loss from 0.39% to 0.28% after four weeks and then to 0.24% after ten weeks. At this point the decomposition levels off.

CONCLUSIONS

From this study it is apparent that CE can be a viable technique for quantitative analysis, and more importantly is capable of quantifying ana-

TABLE III

CALCULATION OF DIPEPTIDE LEVELS IN CLEANING FLUID BY CE

Sample	Level of dipeptide in cleaning fluid (% w/w)			
	Normalised peak height (Mean)		Normalised peak area (Mean)	
Time 0	0.39, 0.36, 0.40	(0.38)	0.41, 0.40, 0.35	(0.39)
37°C/10 wks	0.25, 0.24, 0.25	(0.25)	0.22, 0.23, 0.24	(0.23)
−20°C/17 wks	0.34, 0.36	(0.35)	0.33, 0.35	(0.34)
37°C/17 wks	0.22, 0.23	(0.23)	0.21, 0.23	(0.22)
−20°C/17 wks	0.36, 0.34	(0.35)	0.36, 0.36	(0.36)
37°C/17 wks	0.25, 0.24	(0.25)	0.25, 0.25	(0.25)

TABLE IV

COMPARISON OF CE AND HPLC DATA

Sample	Level of dipeptide in cleaning fluid (% w/w)	
	CE	HPLC
Time 0	0.39	0.39
37°C/4 wks	ND[a]	0.28
37°C/10 wks	0.24	ND
−20°C/17 wks	0.35	0.33
37°C/17 wks	0.25	0.24

[a] ND = Not determined.

lytes in relatively complex matrices with the minimum of sample pre-treatment.

For this application data from the calibration graphs yielded correlation coefficients comparable to those which are typically achieved via the established techniques of HPLC and GLC. Peak height or area measurements were found to be equally suitable. One major requirement in CE however is the use of internal standards. Migration times are found to vary with CE, most likely due to changes in the zeta potential at the capillary wall. Consequently some form of normalisation must be adopted to allow for this variation, and this is probably best approached via the use of internal standards.

The data generated via the separate approaches of CE and HPLC was in good agreement, although admittedly on a limited data set. For this particular assay, however, the former technique is the preferred method since it is rapid and simple and obviates the need for pre-column derivatisation.

REFERENCES

1 R. Virtanen, *Acta Polytechn. Scand.*, 123 (1974) 1.
2 D. Perret, D. Goodall and G. Ross, *Capillary Electrophoresis, A Bibliography*. Chromatographic Society, Nottingham, 1991.
3 D. Perret and G. Ross, *Trends Anal. Chem.*, 11 (1992) 156.
4 S. Fujiwara and S. Honda, *Anal. Chem.*, 58 (1986) 1811.
5 M.T. Ackermans, J.L. Beckers, F.M. Everaerts, H. Hoogland and M.J. Tomassen, *J. Chromatogr.*, 596 (1992) 101.
6 H. Nishi, T. Fukuyama, M. Matsuo and S. Terabe, *J. Chromatogr.*, 515 (1990) 233.
7 A. Guttman, A.S. Cohen, D.N. Heiger and B.L. Karger, *Anal. Chem.*, 62 (1990) 137.
8 X. Huang, W.F. Coleman and R.N. Zare, *J. Chromatogr.*, 480 (1989) 95.
9 R. Weinberger, E. Sapp and S. Moring, *J. Chromatogr.*, 516 (1990) 271.

Journal of Chromatography A, 661 (1994) 7–12
Elsevier Science B.V., Amsterdam

CHROMSYMP. 2940

Short Communication

High-performance liquid chromatographic separation of *cis–trans* isomers of proline-containing peptides

II. Fractionation in different cyclodextrin systems

S. Friebe, B. Hartrodt, K. Neubert and G.-J. Krauss*

Martin-Luther-University Halle, Department of Biochemistry/Biotechnology, Weinbergweg 16a, 06099 Halle/S. (Germany)

ABSTRACT

β-Cyclodextrin-bonded silica is demonstrated to be a suitable stationary phase for high-performance liquid chromatography of conformational isomers of proline-containing peptides. In contrast to reversed-phase chromatography, the principle of inclusion complexation shows significant selectivities in conformer resolution based on a variety of interactions. New results of inclusion HPLC of biologically active oligopeptides related to β-casomorphin on stationary phases containing bonded cyclodextrins of different internal diameters indicate a steric discrimination process during the conformer separation. β-Cyclodextrin used as a mobile phase additive in reversed-phase systems is shown to offer the opportunity to investigate conformational changes using commercially available reversed-phase columns.

INTRODUCTION

Recently, we described the HPLC separation of *cis–trans* isomers of proline-containing oligopeptides on β-cyclodextrin (β-CD)-bonded silica [1].

Proline-containing peptides are unique in terms of their capacities to form peptide bond conformers. Xaa–Pro peptide bonds can adopt two different conformations (*cis* and *trans*), which can be simultaneously present in solution because of the energy barriers of rotation about the peptidyl–proline imidic bond [2,3]. Quantitative data describing this type of conformational interconversion can be obtained by different spectroscopic and kinetic methods [4–8].

Reversed-phase high-performance liquid chromatographic studies of di- and oligopeptides containing proline have been published by Melander *et al.* [9] and others [10,11]. Conformers were resolved by the solvophobic interaction of different hydrophobic surface areas of the *cis* and *trans* isomers with the hydrocarbons of reversed-phase silica gel. Low-temperature chromatography was introduced to diminish interconversion rates and to improve the resolution of isomer peaks, but the relaxation times of conformational changes have to be in the same time scale as the chromatographic runs. However, the comparatively small differences in hydrophobic surface areas result in inefficient chromatographic resolution of conformers.

* Corresponding author.

0021-9673/94/$07.00
SSDI 0021-9673(93)E0945-Q

In contrast to reversed-phase chromatography, the inclusion principle shows significant selectivities in conformer separation caused by a variety of selective interactions, such as host–guest and hydrophobic interactions, hydrogen bonding and dipole–dipole interactions. Peptides bearing aromatic amino acids N-terminally bonded to proline have been shown to be separated with relative chromatographic resolution (R_s) values suggesting a steric hindrance of isomer interconversion.

In this paper chromatographic data of new proline-containing peptides of the β-casomorphin type will be presented, which demonstrate that β-CD-bonded silica is applicable as a stationary phase in HPLC for conformer separation of small oligopeptides in a common manner. Using stationary phases with bonded cyclodextrins of different internal diameters we demonstrate that peak splitting is in fact a result of inclusion complexation. Moreover, β-CD added to the mobile phase also offers the opportunity to use selective interactions between peptide structure and toroid shape of cyclodextrins.

EXPERIMENTAL

Materials

Optically pure dipeptides were purchased from Bachem Biochemica (Heidelberg, Germany) and β-cyclodextrin from Merck (Darmstadt, Germany). The β-casomorphin peptides were synthesized by conventional solution methods [12]. Their purity was checked by analytical TLC, HPLC, field desorption mass spectrometry and amino acid analysis.

Chiral α-, β- and γ-cyclodextrin Si-100 (10 μm) columns were purchased from Serva Feinbiochemica (Heidelberg, Germany) and 250-4 LiChroSpher RP-8 (10 μm) from Merck. All solvents and chemicals were of high purity.

Apparatus

HPLC measurements were performed with a Merck-Hitachi LiChroGraph system using a L-6200 low-gradient pump, a L-3000 photodiode array detector and an HM-computing integrator. The columns and the eluents were immersed in a Lauda RM 6 constant-temperature bath.

HPLC conditions

Two chiral β- (α-, γ-) cyclodextrin Si-100 (10 μm) columns, 125 × 4.6 mm, were connected. Chromatographic experiments were performed isocratically using various 0.02 *M* ammonium dihydrogenphosphate–acetonitrile mixtures. The analyte absorptions were monitored at 210 nm. Before elution the columns were equilibrated with the mobile phase at 5°C for 60 min. Peak splitting as a result of isomerization kinetics was demonstrated by peak collection and rechromatography of the fractions.

RESULTS AND DISCUSSION

In order to evaluate inclusion HPLC on β-CD-bonded silica columns for the study of conformational changes in the peptide bond, a number of dipeptides and oligopeptides related to β-casomorphins were investigated on cyclodextrins with different internal diameters.

β-Casomorphins represent compound with opioid activities that may be released from the milk protein β-casein by proteolytic fragmentation. The insertion of D-amino acids into the sequences improves the proteolytic stability of such peptides and partially significantly enhances and prolongs opioid activity [12]. Moreover, des-Tyr^1-β-casomorphin analogues [13], show several interesting behavioural pharmacological effects.

In order to investigate the influence of the configuration of the internal amino acids Phe and Pro on the *cis–trans* isomerization about the X–Pro bond (X = Phe, D-Phe) the four diastereomers of such des-Tyr^1-β-casomorphins, Pro–Phe–Pro–Gly (labelled as LL), Pro–D-Phe–Pro–Gly (DL), Pro–D-Phe–D-Pro–Gly (DD) and Pro–Phe–D-Pro–Gly (LD), were analysed using the same chromatographic conditions described in ref. 1. As shown in Fig. 1, we achieved baseline separations with high chromatographic resolution between the two conformers for all four peptides. In the case of DL and LD the small peak (about 10%) was eluted before the large peak (about 90%), whereas surprisingly the elution order for LL and DD was reversed and, thus, the larger peak (about 70%) was eluted ahead of the smaller one (30%). On the under-

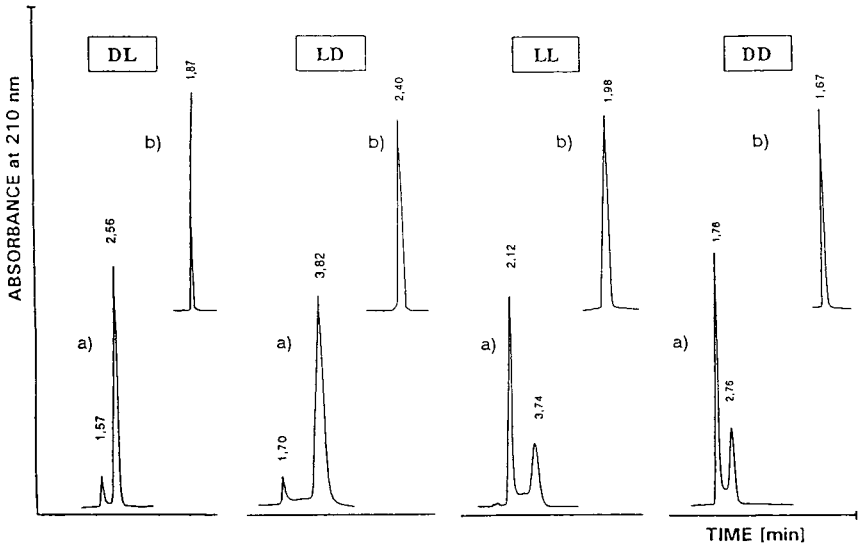

Fig. 1. Elution profiles of Pro–D-Phe–Pro–Gly (DL), Pro–Phe–D-Pro–Gly (LD), Pro–Phe–Pro–Gly (LL) and Pro–D-Phe–D-Pro–Gly (DD) on two connected 125 × 4.6 mm chiral β-cyclodextrin Si-100 (10 μm) columns: (a) at 2°C, (b) at room temperature. Mobile phase: 0.02 *M* ammonium dihydrogenphosphate (pH 6.2)–acetonitrile (70:30). Flow-rate: 3 ml/min.

standing that in each case the minor peak corresponds to the *cis* and the major one to the *trans* conformer, the calculated *cis–trans* ratio would be in agreement with data determined by NMR studies (*cis* content in aqueous solution: DL and LD about 10%, LL 35–40%, DD 25–30%) [13]. Molecular modelling studies are in progress in order to explore this phenomenon.

Furthermore, the high selectivity of β-CD silica as stationary phase for the study of conformational changes is demonstrated for β-casomorphin derivatives which contain two Xaa–Pro bonds in their sequence. In Fig. 2 the detected bonding isomers of these peptides are demonstrated. NMR spectroscopic studies of fractionated isomers are in progress to establish the elution order.

Starting from the hypothesis that the molecular dimension of bonded cyclodextrin can be adapted to the size and shape of the analyte, we tried to improve *cis–trans* isomer resolution by additional use of α- and γ-CD-bonded phases to allow isomer isolation of smaller and larger prolyl peptides.

We used an α-CD-bonded silica, formerly used for the separation of small peptide diastereomers composed of aliphatic amino acids [14], for the resolution of conformers of Xaa–Pro dipeptides (Xaa = Ala, Leu, Ile). The result was that only peak splitting without baseline separation was observed. Obviously, the cavity of the α-form is too small to include at least partially the investigated analytes.

γ-Cyclodextrin contains eight glucopyranose units, resulting in a larger internal diameter of 9.5 Å [15]. The corresponding silica was pos-

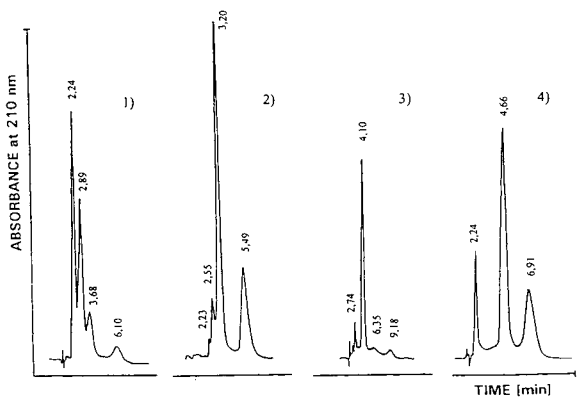

Fig. 2. Chromatographic patterns of oligopeptides bearing two Xaa–Pro bonds: Tyr–Pro–Phe–Pro–Gly (CM 5) (1), Phe–Pro–Phe–D-Pro–Gly (2), Tyr–D-Pro–Phe–Pro–NH_2 (3), Tyr–Pro–Phe–D-Pro–Gly (4). For chromatographic conditions see Fig. 1.

tulated to be suitable for enantiomer resolution of larger ring systems and cyclic peptides [16]. Using this stationary phase a number of oligopeptides of the β-casomorphin type were examined to be separated into *cis* and *trans* isomers. As shown in Fig. 3 our results demonstrate that γ-CD-bonded silica is, like β-CD, a suitable stationary phase for the study of conformational changes in proline-containing peptides, but in most cases the chromatographic resolution is poor compared with β-CD. The larger internal diameter enables analyte penetration into the hydrophobic cavity and, consequently, a solvophobic interaction, whereas additional interactions, such as hydrogen bonding and dipole–dipole interactions, seem to be less effective. Only pentapeptides, including β-casomorphin-5 (Tyr–Pro–Phe–Pro–Gly), are split into their *cis–trans* conformers with similar efficiency as on β-CD silica, in theory because the larger molecule fits better into γ-CD. However, for many oligopeptides, including cyclic peptides, the γ-CD-bonded stationary phase may represent an additional valuable tool to solve difficult separation problems.

Starting from the observed phenomenon that β-cyclodextrin-bonded silica gel shows the highest efficiency in separating peptide bond isomers, such as enantiomers, diastereomers and geometric and structural isomers, we showed that β-CD is a suitable mobile phase additive for reversed-phase systems. Several papers published recently describe the use of β-CD as a chiral selector in HPLC or capillary electrophoresis systems [17–20]. Small structural changes in analytes can be exploited by the interaction with the cyclodextrin toroid. Using reversed-phase systems published by Melander *et al.* [9] we investigated the effect of adding β-CD to the mobile phase on conformer resolution of the dipeptides Ala–Pro, Leu–Pro, Ile–Pro and Phe–Pro. The concentration of β-CD is limited by the poor solubility of the molecule. A 0.01 *M* β-CD solution proved to be the most suitable to take advantage of the β-CD–analyte interaction without interference on chromatographic devices. Fig. 4 demonstrates that *cis–trans* isomer resolution of dipeptides is noticeably improved if the mobile phase contains β-CD. The time scale of the interconversion rate decreases as a result of steric hindrance during inclusion complexation and, consequently, the flow-rate of mobile phase should not be as high

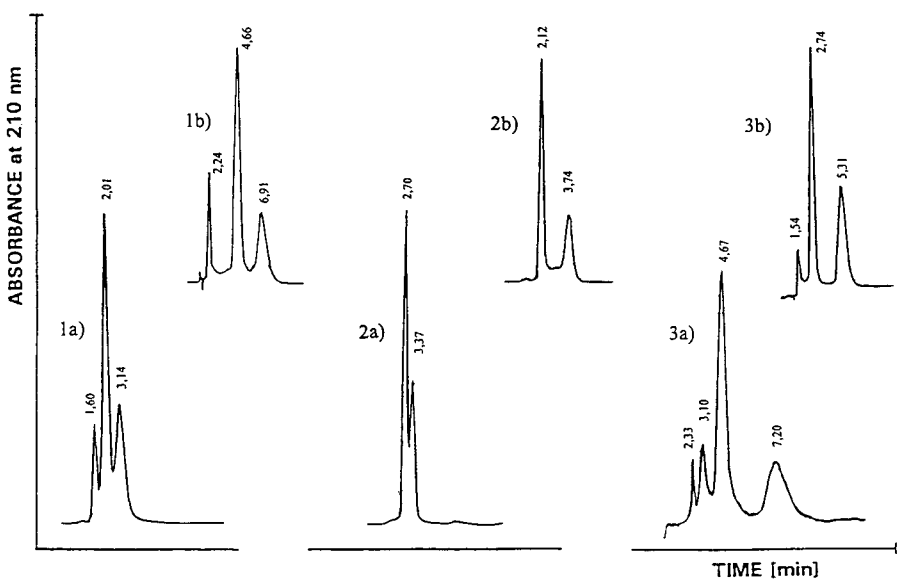

Fig. 3. Elution profiles of Tyr–Pro–Phe–Pro–Gly (1), Pro–Phe–Pro–Gly (2) and Phe–Pro–D-Phe–Pro–Gly (3). (a) On two connected 125 × 4.6 mm chiral γ-cyclodextrin Si-100 (10 μm) columns. Mobile phase: 0.02 *M* ammonium dihydrogenphosphate (pH 6.2)–acetonitrile (85:15). Flow-rate: 2 ml/min. (b) On two connected 125 × 4.6 mm chiral β-cyclodextrin Si-100 (10 μm) columns. For chromatographic conditions see Fig. 1. (1b) Flow-rate: 2 ml/min.

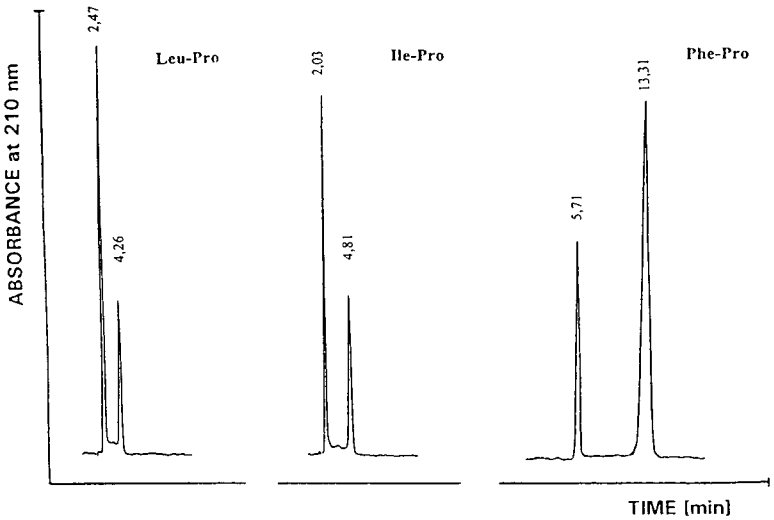

Fig. 4. Elution profiles of Leu–Pro, Ile–Pro and Phe–Pro on 250-4 LiChroChart, LiChroSpher 100 RP-8 (10 μm) at 5°C. Mobile phase: 0.02 *M* ammonium dihydrogenphosphate (pH 6.2)–methanol (95:5), 0.01 *M* β-cyclodextrin. Flow-rate: 2 ml/min.

as reported in reversed-phase systems. The typical plateaus between isomer peaks detected in reversed-phase systems disappear and the hydrophobic properties of peptides are shielded by the inclusion process. These features result in baseline separation and higher chromatographic resolution values, R_s. However, the process of inclusion of analytes in the cavity of β-CD can change seriously the conformer equilibrium in aqueous peptide solution. Thus, for example, in the case of Phe–D-Pro, we observed the complete disappearance of one isomer after several days, if the peptide was dissolved in the mobile phase containing β-CD. We separated only dipeptide conformers. Tetra- and pentapeptides were not investigated.

The application of β-CD as additive in mobile phase allows only the detection of conformational changes in prolyl peptides. The isolation of pure isomers is impossible because of the β-CD content in the fractions.

In conclusion, inclusion complexation with β-CD bonded to silica gel or dissolved in the mobile phase has been found to be a separation principle for the study of conformational changes in proline-containing peptides applicable in different HPLC systems. Separation of *cis–trans* peptide conformers on β-CD-bonded stationary phases has been established. The method is highly efficient, despite the fact that it requires a short time for the optimization of the chromatographic conditions, and allows conformer fractionation based on high chromatographic resolution. β-CD dissolved in the mobile phase of reversed-phase HPLC systems provides a versatile system for the investigation of *cis–trans* isomerism of the prolyl peptide bond using commonly available reversed-phase columns.

REFERENCES

1 S. Friebe, G.-J. Krauss and H. Nitsche, *J. Chromatogr.*, 598 (1992) 139–142.
2 C. Grathwohl and K. Wütherich, *Biopolymers*, 20 (1981) 2632–2633.
3 W.E. Stuart and T.H. Siddall, *Chem. Rev.*, 70 (1970) 517.
4 G. Fischer, H. Bang and C. Mech, *Biomed. Biochim. Acta*, 43 (1984) 1104–1111.
5 D. Hübner, G. Fischer, D. Ströhl, E. Kleinpeater, B. Hartrodt and W. Brandt, *Fresenius Z' Anal. Chem.*, 337 (1990) 131–132.
6 D. Hübner, T. Drakenberg, S. Forsen and G. Fischer, *FEBS Lett.*, 284 (1991) 79–81.
7 D. Hübner, B. Hartrodt, E. Kleinpeter, D. Ströhl, W. Brandt, H. Schinke, M. Wahab and G. Fischer, *Biochem. Biophys. Res. Commun.*, 177 (1991) 271–278.
8 J.T. Gerig, *Biopolymers*, 10 (1971) 2435–2443.
9 W.R. Melander, J. Jacobson and C. Horvath, *J. Chromatogr.*, 234 (1982) 269–276.
10 L. Rusconi, G. Perseo, L. Franzoi and P.C. Montecucchi, *J. Chromatogr.*, 349 (1985) 117–130.

11 J.C. Gesquiere, E. Diesis, M.T. Cung and A. Tartar, *J. Chromatogr.*, 478 (1989) 121–129.
12 K. Neubert, B. Hartrodt, I. Born, A. Barth, H.-L. Rüthrich, G. Grecksch, U. Schrader and C. Liebmann, in F. Nyberg and V. Brantl (Editors), *Proceedings of the 1st International Symposium on β-Casomorphins and Related Peptides*, Fyris-Tryck, Uppsala, 1990, pp. 15–20.
13 B. Hartrodt, H. Schinke, D. Hübner, G. Fischer and K. Neubert, in H. Teschemacher and V. Brantl (Editors), *Proceedings of the 2nd International Symposium β-Casomorphins and Related Peptides*, Verlag Chemie, Weinheim, 1993, in press.
14 I. Florance, A. Galdes, Z. Konteatis, Z. Kosarych, K. Langer and C. Martucci, *J. Chromatogr.*, 414 (1987) 313–322.
15 T.M. Ward and D.W. Armstrong, in M. Zief and L.Y. Cranein (Editors), *Chromatographic Chiral Separation (Chromatographic Science Series*, Vol. 40), Marcel Dekker, New York, 1988, pp. 131–163.
16 C.A. Chang, H. Ji and G. Lin, *J. Chromatogr.*, 522 (1990) 143–152.
17 K. Cabrera and G. Schwinn, *Int. Lab.*, 20 (1990) 28–32.
18 R.M. Mohseni and R.J. Hurtubise, *J. Chromatogr.*, 514 (1990) 19–27.
19 S. Terabe, Y. Miyashita, O. Shibata, E.R. Barnhart, L.R. Alexander, D.G. Patterson, B.L. Karger, K. Hosoya and N. Tanata, *J. Chromatogr.*, 516 (1990) 23–31.
20 S.A.C. Wren and R.C. Rowe, *J. Chromatogr.*, 603 (1992) 235–241.

Journal of Chromatography A, 661 (1994) 13–23
Elsevier Science B.V., Amsterdam

CHROMSYMP. 2929

Purification and analytical characterization of an anti-CD4 monoclonal antibody for human therapy

A.H. Guse*, A.D. Milton☆, H. Schulze-Koops, B. Müller, E. Roth and B. Simmer

Max-Planck-Gesellschaft, Klinische Arbeitsgruppe für Rheumatologie/Immunologie am Institut für Klinische Immunologie der Universität Erlangen-Nürnberg, Schwabachanlage 10, W-8520 Erlangen (Germany)

H. Wächter

Landesuntersuchungsamt für das Gesundheitswesen Nordbayern, Henkestrasse 9–11, W-8520 Erlangen (Germany)

E. Weiss

Institut für Anthropologie und Humangenetik, Richard-Wagnerstrasse 10/I, W-8000 Munich 2 (Germany)

F. Emmrich

Max-Planck-Gesellschaft, Klinische Arbeitsgruppe für Rheumatologie/Immunologie am Institut für Klinische Immunologie der Universität Erlangen-Nürnberg, Schwabachanlage 10, W-8520 Erlangen (Germany)

ABSTRACT

A purification process for the monclonal anti-CD4 antibody MAX.16H5 was developed on an analytical scale using $(NH_4)_2SO_4$ precipitation, anion-exchange chromatography on MonoQ or Q-Sepharose, hydrophobic interaction chromatography on phenyl-Sepharose and gel filtration chromatography on Superdex 200. The purification schedule was scaled up and gram amounts of MAX.16H5 were produced on corresponding BioPilot columns. Studies of the identity, purity and possible contamination by a broad range of methods showed that the product was highly purified and free from contaminants such as mouse DNA, viruses, pyrogens and irritants. Overall, the analytical data confirm that the monoclonal antibody MAX.16H5 prepared by this protocol is suitable for human therapy.

INTRODUCTION

Several methods for the purification of monoclonal antibodies (mAb) have been published (reviewed in ref. 1). The correct choice of the purification method mainly depends on the use for which the mAb is intended. Also, other parameters including source material, class and subclass of mAb may be important, as these may influence mAb behaviour in certain column chromatographic techniques. MAbs to be used for human therapy must be purified and the final product has to be analysed in accordance with the "guidelines on the production and quality control of monoclonal antibodies of murine origin intended for use in man" [2].

In this paper we describe the development of a purification schedule for the mouse anti-CD4 mAb MAX.16H5, which has been and is still used successfully in single-case treatments of

* Corresponding author. Present address: Universität Hamburg, Institut für Physiologische Chemie, Martinstrasse 52, D-20251 Hamburg, Germany.
☆ Present address: L.A.B. GmbH, Wegenerstrasse 13, W-7910 Neu-Ulm, Germany.

0021-9673/94/$07.00
SSDI 0021-9673(93)E0919-L

several autoimmune diseases (reviewed in ref. 3). CD4 (CD = cluster of differentiation) is a cell surface marker found on (i) the T lymphocyte helper subset, (ii) monocytes/macrophages and (iii) eosinophiles. MAX.16H5 recognizes a unique epitope in the first extracellular domain of the human CD4 molecule [4]. This epitope resides in the binding site of human immunodeficiency virus glycoprotein 120, as demonstrated by insertion mutants containing human CD4 sequences in a rat CD4 background [5].

The optimized purification protocol was scaled up to the preparative scale and gram amounts of mAb MAX.16H5 were produced. Analytical procedures for studying identity, purity and possible contamination showed that the final product fulfilled the criteria for use in man.

EXPERIMENTAL

Analytical-scale purification of mAb MAX.16H5

The purification protocol for mAb MAX.16H5 was set up using either milligram amounts of purified MAX.16H5 or ascites fluid containing milligram amounts of MAX.16H5 as samples. The computerized MT2 HPLC system (Kontron Instruments, Neufahrn, Germany) equipped with various fast protein (FPLC) columns (Pharmacia, Freiburg, Germany) as presented in the Results and Discussion section was used.

DNA-spiking experiments

Mixtures of mAb MAX.16H5 (0.5–1 mg) and 1 mg of calf thymus DNA (Boehringer, Mannheim, Germany) were chromatographed on an analytical scale on HiLoad Superdex 200 16/60 Prep grade columns (Pharmacia) using identical buffer systems as indicated for the preparative runs (see below). The elution protocols were adapted to the column sizes. The DNA content was measured in the MAX.16H5 fraction by fluorimetry using bisbenzimide H33258 [6].

Preparative-scale purification of mAb MAX.16H5

$(NH_4)_2SO_4$ precipitation. Ascites fluid containing mAb MAX.16H5 was precipitated with equal amounts of saturated $(NH_4)_2SO_4$ solution by dropwise addition at room temperature. To complete precipitation the solution was stirred for 2 h at room temperature and 1 h at 4°C. The precipitate was spun (4500 *g*, 30 min, 20°C) and the pellet was dissolved in the original volume of 50% saturated $(NH_4)_2SO_4$ solution. After a second centrifugation (11 300 *g*, 20 min, 20°C), the pellet was dissolved in half of the original volume of 50% saturated $(NH_4)_2SO_4$ solution. After a third centrifugation (11 300 *g*, 30 min, 20°C), the pellet was dissolved in 0.3 times the original volume in 20 m*M* Tris–HCl–40 m*M* NaCl (pH 7.5). This solution was again centrifuged (11 300 *g*, 15 min, 20°C) and the supernatant was used for subsequent steps.

Delipidation by n-hexane. To remove lipids, equal volumes of $(NH_4)_2SO_4$-precipitated material and *n*-hexane were vortex mixed. The phases were separated by centrifugation (338 *g*, 6 min, 4°C). The extraction was repeated twice. The final aqueous extract was centrifuged at 200 000 *g* (30 min, 4°C) to remove traces of remaining *n*-hexane.

Anion-exchange chromatography. A BioPilot system (Pharmacia) was used for all preparative column chromatographic steps. Detection was effected with a UV monitor set to 280 nm and with a conductivity monitor. Fractions of 10 ml were collected by a FRAC-100 fraction collector (Pharmacia) and were pooled manually. Pooled fractions corresponding to one peak were analysed for protein and IgG content (see below) and then further purified. After equilibration of the Q-Sepharose HP 35/100 column (Pharmacia) with low-salt buffer A [40 m*M* NaCl–20 m*M* Tris–HCl (pH 7.5)], the sample was loaded at 3.0 ml/min. The gradient for elution of column-bound material was as follows at a flow-rate of 3.6 ml/min [expressed as % of buffer B containing 1 *M* NaCl–20 m*M* Tris–HCl (pH 7.5)]: isocratic at 0% B for 36 ml; linear up to 15% B in 108 ml; isocratic at 15% B for 126 ml; linear up to 100% B in 72 ml; and isocratic at 100% B for 72 ml. Fractions were collected under sterile conditions in a laminar flow bench.

Hydrophobic interaction chromatography. Dry $(NH_4)_2SO_4$ was added to mAb MAX.16H5 solution eluted from Q-Sepharose to a final concentration of 0.5 *M*. The column (phenyl-

Sepharose HP 35/100; Pharmacia) was equilibrated with buffer A [0.5 *M* $(NH_4)_2SO_4$–70 m*M* KH_2PO_4–K_2HPO_4 adjusted to pH 7.2]. Loading of samples was done at flow-rates between 3 and 10 ml/min. The gradient for elution of column-bound material was as follows at a flow-rate of 10 ml/min [expressed as % of buffer B containing 70 m*M* KH_2PO_4–K_2HPO_4 (pH 7.2)]: isocratic at 0% B for 300 ml; linear up to 100% B in 700 ml; and isocratic at 100% B for 350 ml. Fractions were collected under sterile conditions in a laminar flow bench.

Ultrafiltration. The ultrafiltration apparatus (Amicon, Danvers, MA, USA) was made pyrogen-free by washing with 1 *M* NaOH for 2–3 h and was subsequently autoclaved. Concentration of mAb MAX.16H5 solution from hydrophobic interaction chromatography was done using MSO or XM50 membranes (Amicon). The solutions were concentrated in order to be used with the gel filtration columns listed below.

Gel filtration chromatography. Gel filtration was carried out on Superdex 200 Prep grade 35/600 or 60/600 (Pharmacia). The column was equilibrated with 75 m*M* NaCl–60 m*M* Na_2HPO_4–NaH_2PO_4 adjusted to pH 7.4. The samples (sample volume as rated in the manual from the column supplier) were chromatographed at flow-rates of 4 ml/min (35/600 column) or 11.7 ml/min (60/600 column). Fractions were collected under sterile conditions in a laminar flow bench.

Cleaning-in-place (CIP) procedures

The BioPilot system (Pharmacia) and BioPilot Q-Sepharose and phenyl-Sepharose columns were sterilized and made pyrogen-free by flushing with four column volumes of 1 *M* NaOH and subsequently by washing with 0.1 *M* NaOH at low flow-rates (0.5 or 1.0 ml/min) overnight. Superdex 200 columns were treated at a low flow-rate with one column volume of 1 *M* NaOH, resulting in a treatment period of *ca.* 3 h. After CIP, the columns were re-equilibrated by flushing with four column volumes of starting buffer. The pyrogen content of the columns was then checked by employing the Pyroquant 1 test (see below). Only if the column eluate was pyrogen-free were preparative runs started.

All buffers were prepared using pyrogen-free water (Ampuwa water, Fresenius, Bad Homburg, Germany) in pyrogen-free glassware and sterilized by filtration. All chemicals used were of German Pharmacopoeia (DAB) quality or analytical quality. Glassware for preparing buffers was made pyrogen-free by treatment with 1 *M* NaOH for 1 h followed by rinsing with Ampuwa water and drying overnight in an oven at >180°C. Buffers were tested with the Pyroquant 1 test to confirm their pyrogen-free state before use.

Protein determination

Protein was determined using the Bio-Rad protein determination kit according to manufacturer's instructions (BioRad, Munich, Germany) and immunoglobulin G (IgG) as a standard.

Analytical procedures on bulk final processed product (BFPP)

IgG-specific enzyme-linked immunosorbent assay (ELISA). Appropriate dilutions of standard and samples were incubated in goat anti-mouse IgG-coated Immuno Plate Maxi Sorp (Nunc, Roskilde, Denmark) 96-well plates for 1 h at 37°C. After washing, goat anti-mouse IgG– and IgM–alkaline phosphatase conjugates (Dianova, Hamburg, Germany) were added. After washing, the substrate *p*-nitrophenyl phosphate (Sigma, Deisenhofen, Germany) was added. The plates were measured in a Type 400 A ELISA-Reader (SLT-Labinstruments, Vienna, Austria) after 1 or 2 h at 450 nm.

Pro Ana Mabs assay. Concentration assays were performed with a Pro Ana Mabs system (Biolytika, Lund, Sweden) using a binding buffer of pH 5.0 and an elution buffer of pH 1.6 from Biolytika. The chromatographic system consisted of two M 510 pumps, an M 484 detector, an M 740 data module (all from Waters, Milford, MA, USA), a 1-ml sample loop and a Rheodyne injection valve. The chromatographic conditions were as follows: after injection, sample loading for 2 min and washing with binding buffer at a flow-rate of 2 ml/min, followed by desorption with elution buffer at a flow-rate of 3 ml/min for 2 min. Equilibration with binding buffer for at least 3 min at 2 ml/min was necessary before

injection of the next sample. The concentration of mAb was calculated from the peak area at 280 nm previously calibrated with a standard solution.

Sodium dodecyl sulphate–polyacrylamide gel electrophoresis (SDS-PAGE) and isoelectric focussing (IEF). SDS-PAGE was carried out using the Mini-Protean gel system and high-molecular-mass protein standards (for 7.5% gels under non-reducing conditions) or low-molecular-mass protein standards (for 12% gels under reducing conditions) from Bio-Rad. The buffer system introduced by Laemmli [7] was used. Alternatively, SDS-PAGE and IEF were carried out using the Pharmacia Phast system employing Phast gels following the manufacturer's instructions.

High-performance size-exclusion chromatography (HPSEC). For HPSEC, an HPLC system equipped with a WISP M 712 autosampler, an M 510 pump and an M 481 variable-wavelength detector (all from Waters) was used. The chromatography was carried out on a Protein Pak 300 sw column (Waters) using 0.05 *M* Tris–0.05 *M* Na_2SO_4 (pH 7.2) as the mobile phase. The sample size was 100 μl, the flow-rate was 0.5 ml/min and the detector was adjusted to 280 nm.

Cytofluorimetry. Flow cytometric analysis was performed by standard techniques. Briefly, $2 \cdot 10^5$ cells of a $CD4^+$ cell line (CB-15 [8]) were incubated first with human IgG (10 mg/ml) and washed twice. Appropriate dilutions of mAb MAX.16H5 were added, incubated on ice for 30 min and washed twice. Bound antibody was detected by fluorescein isothiocyanate-conjugated anti-mouse $F(ab)_2$ fragments (DAKO, Hamburg, Germany). Cells were analysed on an EPICS profile cell sorter (Coulter, Hialeah, FL, USA). MAX.16H5 preparations were compared with standards in dilution experiments using the percentage of stained cells and the mean fluorescence intensity as parameters.

Tests for pyrogenicity. The objective of the tests is the determination of the safety of the product with respect to the presence of pyrogenic material. The rabbit pyrogen test measures rises in body temperature of the rabbit induced by intravenous (i.v.) injection of the product to be examined. Rabbits were injected with mAb MAX.16H5 at 0.3 mg/kg body mass. The test was carried out according to the guidelines in the European Pharmacopoeia. Alternatively, the Pyroquant 1 test kit, an *in vitro* Limulus amoebocyte lysate assay, was used according to the manufacturer's instructions (Pyroquant Diagnostik, Walldorf, Germany). This test was usually employed to measure the pyrogen content of column eluates after CIP.

Sterility test. The solution to be tested for sterility was incubated at 37°C for at least 5–6 days and then checked by light microscopy for sterility.

Abnormal toxicity. In this test the safety of the product with respect to its parenteral or enteral toxicity was assessed. The test was carried out according to the European Pharmacopoeia.

Mouse DNA content. mAb solutions were concentrated by lyophilization and a maximum of 5 ml were digested in 10 m*M* Tris–HCl (pH 8.0)–10 m*M* EDTA–1% SDS with proteinase K (500 μg) overnight. Samples were extracted with phenol–chloroform–isoamyl alcohol and then with chloroform and the aqueous phase was precipitated with 10 pg of tRNA and 2.5 volumes of ethanol at −20°C. The precipitate was centrifuged at 15 000 *g* (4°C, 20 min) and washed once with 70% ethanol. The pellet was dissolved in 200 μl of 0.5 *M* NaOH and denatured at 95°C for 10 min. After cooling, the samples were transferred to a Hybond N^+ membrane (Amersham, Braunschweig, Germany) with the Manifold slot apparatus (Schleicher & Schüll, Dassel, Germany), and washed twice with 200 μl of SSC buffer [0.3 *M* NaCl–0.03 *M* sodium citrate (pH 7.0)]. DNA from Balb/c mice, that was sheared by short ultrasonic treatment in an ultrasound water-bath, was used as a standard. The concentration was determined by measuring the absorbance at 260 nm. Standard DNA and sample DNA were treated in an identical way as follows. DNA (1 ng and 500, 100, 50, 20, 10, 5, 2 and 0 pg) was applied in parallel on the filter. Bound DNA was detected with 20 ng of radiolabelled Balb/c mouse DNA prepared with 30-μCi [^{32}P]dATP by the polypriming method of Feinberg and Vogelstein [9]. Hybridization and washing were performed according to the protocol of

Church and Gilbert [10] with $5 \cdot 10^6$–$1 \cdot 10^6$ cpm/ml at 65°C overnight. Exposure for 3 h or overnight with an intensifying screen allowed the detection of 2–5 pg of DNA.

n-Hexane content. *n*-Hexane was determined using headspace GC. The GC apparatus (Perkin-Elmer F42) was equipped with a 2-m column packed with 5% Benton 34 and 5% DDP on Chromosorb W NAW (80–100 mesh). The samples (2-ml volume) containing 1 mg/ml of mAb MAX.16H5 were heated at 80°C for 2 h. Nitrogen was used as the carrier gas. The column oven was held at 100°C isothermally. Flame ionization detection (FID) was used. Calibration was done by running samples with and without addition of standard.

Pristane content. Pristane was extracted from an aqueous solution containing mAb MAX.16H5 (1 ml; mAb concentration 1 mg/ml) by addition of 0.5 g of NaCl and 1 ml of *n*-hexane and shaking for 30 min. The *n*-hexane extract was analysed for pristane on a DB1 fused-silica capillary (30 m × 0.32 mm I.D.). Nitrogen was used as the carrier gas. The temperature was programmed from 150 to 290°C at 5°C/min. FID was used. Calibration was done by running samples with and without addition of standard.

Viral content. Contamination with viruses was controlled by the mouse antibody production test. Briefly, 21-day-old anti-viral antibody-free Han:NMRI mice were injected with purified MAX.16H5 in solution. After 30 days, sera from injected mice were collected and tested for antibodies against the following viruses: hantaanvirus, lymphocytic choriomeningitis virus, reovirus type 3, sendaivirus, polyomavirus, ectromeliavirus, mouse rotavirus, K virus, mink virus of mice, mouse adenovirus, Theiler's encephalomyelitis virus, mouse hepatitis virus, pneumonia virus of mice, mouse cytomegalivirus, mouse thymic virus and mycoplasma pulmonis. Lactate dehydrogenase virus was tested in sera 4 days after infection.

RESULTS AND DISCUSSION

Preparation of mAbs for human therapy has to take into account the following requirements: (i) mAb must be separated from contaminating proteins present in ascites fluid or cell culture supernatant; (ii) other contaminating compounds such as mouse DNA, viruses, pyrogens and irritants have to be removed; and (iii) mAb must be sterile and pyrogen-free. As the final product is expected to contain a very high degree of active antibody, the biological activity of the mAb must be preserved during all purification steps.

Analytical-scale separations

One of the easiest ways to purify IgG mAbs is affinity chromatography on protein A or protein G matrices [1]. Although problems with mAb for human therapy sometimes occur when traces of protein A/G are co-eluted with mAb, these can be overcome by a second column chromatographic step, namely gel filtration to separate mAb and protein A/G. However, it is known that murine mAb of IgG subtype 1 bind to protein A/G with a lower affinity than other IgG subclasses [1]. Indeed, preliminary experiments revealed that mAb MAX.16H5 (IgG subclass 1) did not bind to protein A or protein G at all. Therefore, a schedule using other separation principles had to be developed.

Using anion-exchange chromatography on MonoQ 5/5 (Pharmacia), we observed binding of mAb MAX.16H5 with 40 m*M* NaCl–20 m*M* Tris–HCl (pH 7.5) and elution on increasing the NaCl concentration linearly to 150 m*M*. Raising the NaCl concentration subsequently to 1 *M* led to the elution of further material absorbing at 280 nm. Spiking experiments showed that DNA was also bound strongly to the column and eluted at 0.8–1.0 *M* NaCl (see also below). Several column runs using ascites fluid or purified MAX.16H5 were carried out to optimize the gradient. We ended up with the following gradient at a flow-rate of 0.5 ml/min: loading and washing at 40 m*M* NaCl, following by a linear gradient to 150 m*M* NaCl within 20 min, followed by isocratic elution for 10 min at 150 m*M* NaCl, followed by a linear gradient to 1 *M* NaCl in 10 min and then 10 min of isocratic elution at 1 *M* NaCl [eluents were buffered to pH 7.5 with 20 m*M* Tris–HCl (Fig. 1)]. This procedure resulted in a product that, on the protein level, was already more than 95% pure

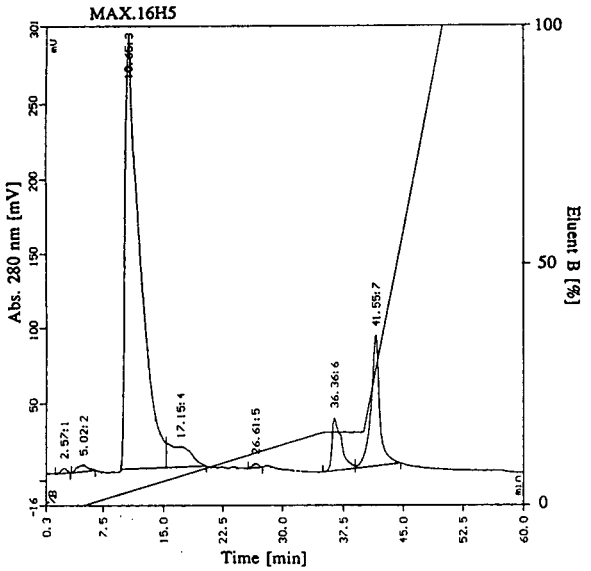

Fig. 1. Analytical-scale purification of $(NH_4)_2SO_4$-precipitated material from ascites fluid. A 1.75-mg amount of protein was analysed on MonoQ 5/5 using buffers A [40 m*M* NaCl–20 m*M* Tris–HCl (pH 7.5)] and B [1 *M* NaCl–20 m*M* Tris–HCl (pH 7.5)] and the following gradient at a flow-rate of 0.5 ml/min: 0 min, 0%; 5 min, 0%; 25 min, 15%; 30 min, 15%; 40 min, 100%; 50 min, 100% B. The pressure was *ca.* 30 bar. The elution position of mAb MAX.16H5 is indicated.

(Table I). However, a second run on MonoQ and especially on Q-Sepharose preparative columns, had to be carried out to obtain a higher removal rate of contaminating DNA (see below).

As the second step, hydrophobic interaction chromatography (HIC) was introduced (i) to purify the protein further, (ii) to remove DNA (see below) and (iii) to remove pyrogens. For analytical-scale chromatography two different matrices were used: alkyl-Sepharose and phenyl-Sepharose (both from Pharmacia). The mAb MAX.16H5 bound to both columns at high salt concentrations. For the alkyl-Sepharose matrix 1.5 *M* $(NH_4)_2SO_4$–70 m*M* K_2HPO_4–KH_2PO_4 (pH 7.2) was needed, whereas with the more hydrophobic phenyl-Sepharose only 0.5 *M* $(NH_4)_2SO_4$–70 m*M* K_2HPO_4–KH_2PO_4 (pH 7.2) was necessary. From both columns mAb MAX.16H5 could be eluted by decreasing the $(NH_4)_2SO_4$ concentration to zero. We finally chose phenyl-Sepharose as it turned out that no preparative alkyl-Sepharose columns were commercially available. As can be seen in Table I, no further protein purification on the analytical scale could be achieved. However, spiking experiments revealed a significant removal of DNA (see below).

Gel filtration was chosen as the final procedure using a Superdex 200 Prep grade column. Within a single step, (i) further protein purification, especially removal of potentially existing mAb dimers or polymers, (ii) an estimation of the molecular mass and (iii) an exchange of the buffer to phosphate-buffered physiological NaCl solution could be achieved. Material prepurified on MonoQ and phenyl-Sepharose on the analytical scale eluted as a single peak on Superdex 200 (Fig. 2, Table I).

DNA removal

Spiking experiments with calf thymus DNA were carried out on an analytical scale with optimized elution protocols for each chromato-

TABLE I

PURIFICATION OF mAb MAX.16H5 ON AN ANALYTICAL SCALE

Ammonium sulphate-precipitated material from ascites fluid containing 5 mg of protein was purified during subsequent runs on Mono Q 5/5 (two runs), phenyl-Sepharose and Superdex 200 Prep grade. For separation conditions, see Experimental.

Column type/method	Protein (mg)	mAb (mg)	Yield (%)
$(NH_4)_2SO_4$ precipitate	5.0	3.7	100
MonoQ 5/5 (1st run)	4.5	3.3	89
MonoQ 5/5 (2nd run)	3.0	3.0	81
Phenyl-Sepharose	2.7	2.7	73
Superdex 200 Prep grade	2.4	2.4	65

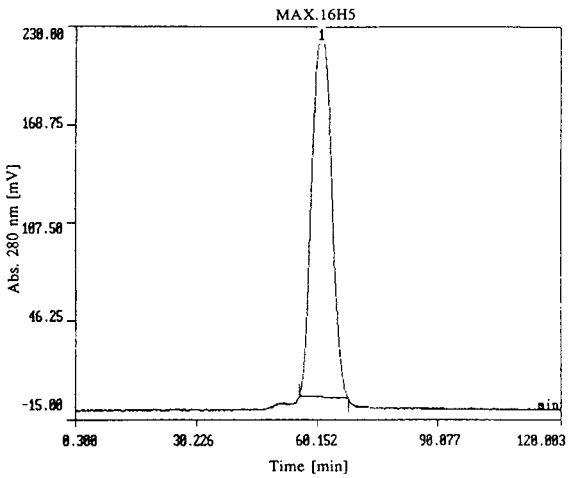

Fig. 2. Analytical-scale separation of mAb MAX.16H5 on Superdex 200 Prep grade. A 12.4-mg amount of mAb MAX.16H5 previously purified on MonoQ (two runs) and phenyl-Sepharose was chromatographed on HiLoad Superdex 200 Prep grade 16/60 using 75 m*M* NaCl–60 m*M* Na_2HPO_4–NaH_2PO_4 (pH 7.4) as elution buffer at a flow-rate 0.5 ml/min. The elution position of MAX.16H5 is indicated. In this particular preparation some high-molecular-mass contaminations were observed.

graphic step. As shown in Table II, the most significant removal was achieved by anion-exchange chromatography on Q-Sepharose. Phenyl-Sepharose was less effective, whereas gel filtration did not remove DNA significantly. As a factor of $>10^{12}$ has to be achieved for the whole purification procedure [2], a second run on Q-Sepharose was considered necessary.

Preparative-scale purification

Separation protocols optimized under analytical conditions were linearly scaled up using BioPilot columns with increased column diameter but identical or similar length. However, in some instances modifications were introduced to increase the separation efficiency.

Before chromatography, mAb MAX.16H5 was enriched from ascites fluid by $(NH_4)_2SO_4$ precipitation (Table III). Subsequently, a lipid extraction with *n*-hexane was carried out. This procedure appeared to be necessary as experiments on the analytical scale indicated that the lipid content in ascites fluid interfered with the column performance and reduced column lifetime. It is important to mention that the extraction with *n*-hexane did not reduce the biological activity of mAb MAX.16H5. Problems occurred, however, in removing traces of *n*-hexane and precipitated proteins of unknown nature from the aqueous solution. Therefore, an ultracentrifugation step had to be introduced. With this step the remaining traces of *n*-hexane could be removed satisfactorily. However, some precipitated protein remained in the solution, leading to significant sample loss during sterile filtration through 0.2-μm filters (Table III).

The material was chromatographed twice on Q-Sepharose HP 35/100 (Figs. 3 and 4). In the first step, a significant separation from material eluting closely after mAb MAX.16H5 and at higher salt concentrations was achieved (Fig. 3

TABLE II

REMOVAL OF ADDED DNA BY COLUMN CHROMATOGRAPHIC STEPS

Mixtures of mAb MAX.16H5 (0.5–1 mg) and 1 mg of calf thymus DNA were chromatographed on HiLoad Q-Sepharose HP 26/10, HiLoad phenyl-Sepharose HP 16/10 and HiLoad Superdex 200 16/60 Prep grade using identical buffer systems as indicated for the preparative runs under Experimental. The elution protocols were adapted to the column sizes. DNA content was measured in the MAX.16H5 fraction by fluorimetry using bisbenzimide H33258.

Chromatography	Column matrix	DNA added	DNA found	Factor[a]
Anion-exchange	Q-Sepharose HP	1 mg	<10 ng	$>10^5$
Hydrophobic interaction	Phenyl-Sepharose HP	1 mg	592 ng	$1.7 \cdot 10^3$
Gel filtration	Superdex 200	1 mg	507 μg	1.97

[a] Reduction factor calculated as [DNA added]/[DNA found].

TABLE III

PREPARATIVE-SCALE PURIFICATION OF mAb MAX.16H5

A batch of ascites fluid containing 16 g of total protein and about 7 g of mAb was purified by ammonium sulphate precipitation and the four column chromatographic steps as outlined in Table I and Experimental. Note the sample loss in the sterile filtration step caused by clogging of macromolecules in the filter. The yield was calculated as the percentage of mAb compared with that in ascites fluid. The purity was calculated as the percentage of mAb (as measured by ELISA) compared with total protein (as measured by protein determination) in each step of the procedure.

Step	Protein (g)	mAb (g)	Yield (%)	Purity (%)
Ascites fluid	16.00	6.94	100	43
$(NH_4)_2SO_4$ precipitate	10.08	6.29	91	62
Filtration (0.22 μm)	5.5	n.d.[a]	–	–
Q-Sepharose HP II	4.05	3.59	52	89
Phenyl-Sepharose	2.80	2.43	35	87
Superdex 200 pg	2.09	2.10	30	100

[a] Not determined.

and Fig. 7, lanes 1 and 2). The second run did not result in enhanced protein purification (Fig. 4). This step was carried out to obtain more complete removal of DNA as discussed above.

The subsequent HIC on phenyl-Sepharose HP 35/100 resulted in a single peak (Fig. 5). In contrast to analytical-scale chromatography, slight tailing of mAb MAX.16H5 was observed. Although no further protein purification was achieved (Table III, Fig. 7), this chromatographic step contributed to removal of DNA (Table II) and probably of pyrogens.

For gel filtration chromatography the material eluted from phenyl-Sepharose had to be concentrated by ultrafiltration.

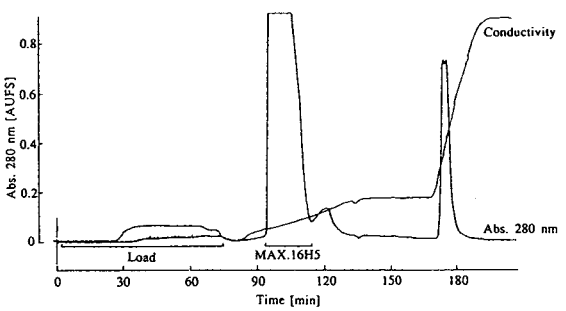

Fig. 3. Preparative-scale purification of mAb MAX.16H5 on BioPilot Q-Sepharose HP 35/100. About 800 mg of protein containing mAb MAX.16H5 previously purified by $(NH_4)_2SO_4$ precipitation were chromatographed on BioPilot Q-Sepharose HP 35/100 using a BioPilot system. The chromatographic system including column was made pyrogen-free by CIP as detailed under Experimental. The column was equilibrated with buffer A [40 m*M* NaCl–20 m*M* Tris–HCl (pH 7.5)] and sample was loaded at a flow-rate of 3.0 ml/min. Elution was done by pumping increasing percentages of buffer B [1 *M* NaCl–20 m*M* Tris–HCl (pH 7.5)] at a flow rate of 3.6 ml/min. The gradient (detailed under Experimental) is graphically displayed as the conductivity trace of the column eluate in the chromatogram. The elution position of MAX.16H5 is indicated.

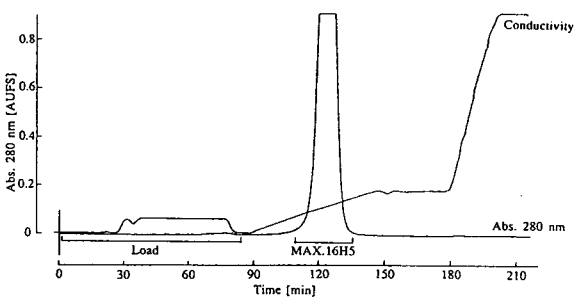

Fig. 4. Preparative-scale purification of mAb MAX.16H5 on BioPilot Q-Sepharose HP 35/100, second run. MAX.16H5 was chromatographed under identical conditions to those in Fig. 3 a second time on Q-Sepharose. The sample was obtained from a first preparative run on BioPilot Q-Sepharose dissolved in elution buffer containing about 100 m*M* NaCl. In order to facilitate binding to the column, MAX.16H5 was diluted three fold with sterile, pyrogen-free water before loading. The elution position of MAX.16H5 is indicated.

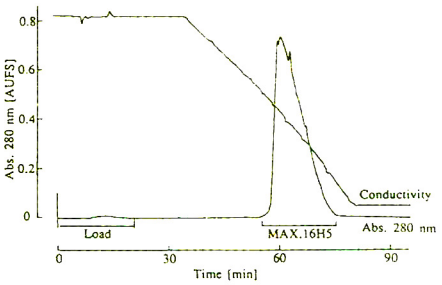

Fig. 5. Preparative-scale purification of mAb MAX.16H5 on BioPilot phenyl-Sepharose HP 35/100. About 700 mg of mAb MAX.16H5 previously purified on Q-Sepharose (two runs) were loaded on BioPilot phenyl-Sepharose HP 35/100 using buffer A [0.5 *M* $(NH_4)_2SO_4$–70 m*M* K_2HPO_4–KH_2PO_4 (pH 7.2)] at a flow-rate of 10 ml/min. Elution was carried out by pumping increasing percentages of buffer B [70 m*M* K_2HPO_4–KH_2PO_4 (pH 7.2)] at 10 ml/min. The gradient (detailed under Experimental) is graphically displayed as the conductivity trace of the column eluate in the chromatogram. The elution position of MAX.16H5 is indicated.

Gel filtration was performed on Superdex 200 Prep grade 35/600 or 60/600. The chromatograms usually revealed separation of mAb MAX.16H5 from contaminating proteins of M_r 65 000–70 000 and low-molecular-mass material (Fig. 6). In addition to purification nearly up to 100%, an exchange of the buffer to phosphate-buffered physiological NaCl solution was achieved by this step (Table III, Fig. 7).

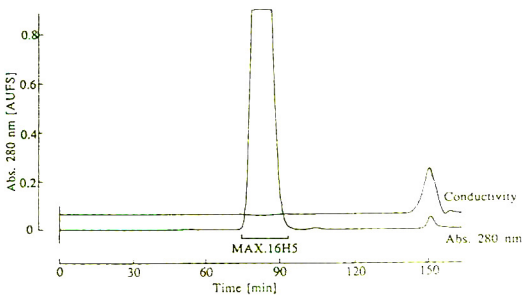

Fig. 6. Preparative-scale purification of mAb MAX.16H5 on BioPilot Superdex 200 Prep grade 60/600. About 900 mg of mAb MAX.16H5 previously purified on Q-Sepharose (two runs) and phenyl-Sepharose were chromatographed on BioPilot Superdex 200 Prep grade 60/600 using 75 m*M* NaCl–60 m*M* Na_2HPO_4–NaH_2PO_4 (pH 7.4) as elution buffer at a flow-rate of 11.7 ml/min. The elution position of MAX.16H5 is indicated. This preparation contained some contaminating material eluting at 103 min (M_r *ca.* 70 000) and 150 min (low-molecular-mass material).

Analytical characterization of the bulk final processed product (BFPP)

In the bulk final processed product, identity, purity and possible contaminations were studied. The identity was confirmed by IgG-specific ELISA and an HPLC method specifically designed to determine mAb, namely Pro Ana Mabs (Table IV). Both methods gave nearly identical results for IgG concentration. The identity as an anti-CD4 antibody and the biological activity were assessed by cytofluorimetric analysis (Table IV).

The purity was determined electrophoretically and chromatographically. A single band at about M_r 160 000 appeared in SDS-PAGE under non-reducing conditions (Fig. 7, lane 4, and Table

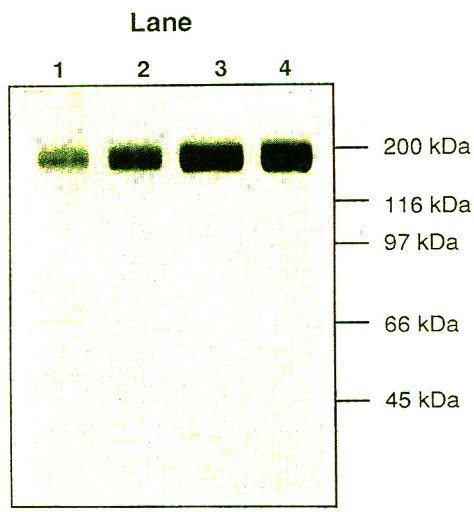

Fig. 7. SDS-PAGE of mAb MAX.16H5 at different stages of the purification schedule SDS-PAGE was carried out using a 7.5% gel, the Laemmli buffer system [7] and the MiniProtean electrophoresis system from Bio-Rad. Lanes: 1 = MAX.16H5 after $(NH_4)_2SO_4$ precipitation; 2 = MAX.16H5 after two runs on Q-Sepharose; 3 = MAX.16H5 after a further run on phenyl-Sepharose; 4 = MAX.16H5 after a further run on Superdex 200. An amount of 5 μg of protein was loaded on to each lane. Staining was done with Coomassie brilliant blue. Electrophoretic mobilities of marker proteins are indicated. kDa = Kilodalton.

TABLE IV

FINAL TESTING OF PURIFIED mAb MAX.16H5

Purified MAX.16H5 (BFPP) was checked for identity, purity and possible contamination using several methods as outlined under Experimental.

Feature	Method	Result
Identity	IgG-specific ELISA	0.925 mg/ml
	Pro Ana Mabs	1.14 mg/ml
	FACS analysis of $CD4^+$ cells	Cells stained
Purity	SDS-PAGE (non-reducing)	Single band
	SDS-PAGE (reducing)	Two bands
	IEF	Microheterogeneity pH 5.92–6.4
	HPSEC	Single peak
Contamination:		
Pyrogenicity	(1) Rabbit pyrogen test	Negative
	(2) Pyroquant 1 test	<0.03 endotoxin units
Sterility	Culture at 37°C for 5–6 days	Sterile
Abnormal toxicity	According to European Pharmacopoeia	Negative
Mouse DNA	Dot blot/hybridization assay	<8 pg per 20 mg
n-Hexane	GC and GC–MS	<0.5 mg/l[a]
Pristane	GC	<0.5 mg/l[a]
Viruses	Mouse antibody production test	Negative for 17 viruses listed under Experimental

[a] 1 mg/ml mAb.

IV). Under reducing conditions two bands representing heavy and light chains were observed (data not shown). IEF revealed a microheterogeneity of mAb MAX.16H5 giving five bands within the pH range 5.92–6.40, probably due to different patterns of glycosylation (Fig. 8). HPSEC resulted in a single peak (Table IV).

The presence of pyrogens was tested (i) by injection of mAb MAX.16H5 into rabbits and following their body temperature post-injection and (ii) by using the Limulus amoebocyte lysate test (Pyroquant 1 test). Both methods showed the absence of pyrogens in the BFPP (Table IV). The content of mouse DNA was determined by extraction of DNA from BFPP and by hybridization with radiolabelled specific DNA probes. In extracts corresponding to one therapeutic dose of MAX.16H5 (20 mg), DNA was not detected (Table IV). The absence of seventeen viruses in BFPP was assessed by the mouse antibody production test (Table IV). Pristane, which is injected into mice during the production period of ascites fluid and therefore could contaminate the mAb preparation, was not present in the BFPP as tested by GC (Table IV). Also, *n*-hexane, which was used for extraction of lipids during the preparative process, was not found in the BFPP by GC and GC–MS (Table IV).

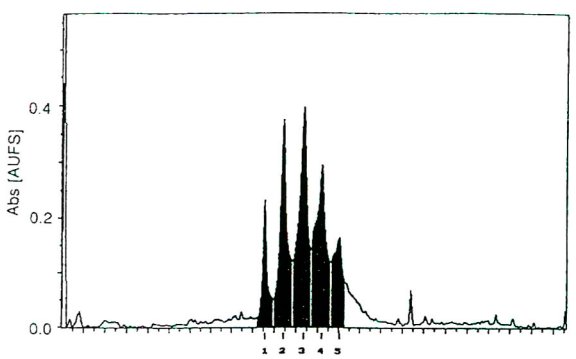

Fig. 8. Isoelectric focusing of purified mAb MAX.16H5. IEF was carried out using the Pharmacia PhastSystem employing a PhastGel with a gradient from pH 5.1 to 7. Densitometric analysis of the gel showed five major bands with isoelectric points at pH (1) 6.40, (2) 6.25, (3) 6.12, (4) 6.02 and (5) 5.92.

Finally, the sterility of the solution was checked by incubation at 37°C for several days and subsequent light microscopy of the solution (Table IV).

CONCLUSIONS

A method was established on an analytical scale and successfully scaled-up to the preparative scale that resulted in a highly purified product. As mAb MAX.16H5 preparations were free from contaminating compounds such as other proteins, mouse DNA, viruses, pyrogens and irritants, single case treatments of human patients suffering from autoimmune diseases could be carried out using these mAb preparations with encouraging results (reviewed in ref. 3).

ACKNOWLEDGEMENTS

The Max Planck Research Unit for Rheumatology/Immunology is funded by the German Ministry for Research and Technology (BMFT) by grant No. 01 VM 8702. This project was also supported by BMFT grant No. 01 ZU 8607 (to H.S.-K. and F.E.). H.S.-K. is recipient of a postdoctoral fellowship from the Deutsche Forschungsgemeinschaft (Schu 786/1-1). We thank Drs. D. Rohm and N. Kothe (Biotest Pharma, Dreieich, Germany) for the biochemical and pharmacological characterization of the bulk final processed product. Thanks are also expressed to Professor Dr. Gräf (Erlangen, Germany) for conducting the rabbit pyrogen tests and to Pharmacia (Freiburg, Germany) for supplying several FPLC columns for test runs. Mouse antibody production tests were carried out in the Zentralinstitut für Versuchstierzucht (Hannover, Germany).

REFERENCES

1 E. Harlow and D. Lane, *Antibodies. A Laboratory Manual*. Cold Spring Harbor Laboratory, Cold Spring Harbor, 1988.
2 *TIBTECH*, 8 (1988) G5.
3 F. Emmrich, H. Schulze-Koops and G. Burmester, in M.E. Davies and J.T. Dingle (Editors), *Handbook of Immunpharmacology*, Academic Press, London, in press.
4 M. Jonker, W. Slingerland, H. Niphuis, E. Golub, G.B. Thornton, L. Smit and J. Goudsmit, in W. Knapp, B. Dörken, W.R. Gilles, E.P. Rieber, R.E. Schmidt, H. Stein and A.E.G.Kr. von dem Borne (Editors), *Leukocyte Typing IV*, Oxford University Press, London, New York, Tokyo, 1989, p. 319.
5 A. Williams, personal communication.
6 C. Labarca and K. Paigen, *Anal. Biochem.*, 102 (1980) 344.
7 U.K. Laemmli, *Nature*, 227 (1970) 680.
8 B. Biesinger, I. Müller-Fleckenstein, B. Simmer, G. Lang, S. Wittmann, E. Platzer, R.C. Desrosiers and B. Fleckenstein, *Proc. Natl. Acad. Sci. U.S.A.*, 89 (1992) 3116.
9 A.P. Feinberg and B. Vogelstein, *Anal. Biochem.*, 132 (1983) 6.
10 G.M. Church and W. Gilbert, *Proc. Natl. Acad. Sci. U.S.A.*, 81 (1984) 1991.

Journal of Chromatography A, 661 (1994) 25–34
Elsevier Science B.V., Amsterdam

CHROMSYMP. 2895

Applications of amino acid derivatization with 6-aminoquinolyl-N-hydroxysuccinimidyl carbamate

Analysis of feed grains, intravenous solutions and glycoproteins

Steven A. Cohen*

Millipore Corporation, 34 Maple Street, Milford, MA 01757 (USA)

Kathryn M. De Antonis

Department of Chemistry, University of Rhode Island, Kingston, RI 02881 (USA)

ABSTRACT

Primary and secondary amines are rapidly labelled by 6-aminoquinolyl-N-hydroxysuccinimidyl carbamate to form highly fluorescent asymmetric urea derivatives which are readily amenable to analysis by liquid chromatography. Derivatization consists of a simple, one-step procedure, and the resulting labelled amines can be analyzed without further cleanup. The adducts are extremely stable with no discernible loss in response after storage for one week at room temperature, making the reagent an ideal candidate for pre-column amino acid analysis. Chromatographic methods for protein hydrolysates have been developed for the analysis of samples containing many unusual amino acids including a number of cysteine derivatives, collagen hydrolysates containing hydroxyproline and hydroxylysine, performic acid oxidized samples and glycoprotein hydrolysates containing glucosamine and galactosamine. Samples with potentially interfering matrix components such as hydrolyzed feed grains and intravenous solutions are readily analyzed and are quantified with average per cent relative standard deviations in the 1–2% range. Comparative data on these samples are in good agreement with either ion-exchange amino acid analysis or label information.

INTRODUCTION

Development of versatile, high-performance systems for amino acid analysis continues to be a subject of considerable interest [1–4]. We have recently developed a new method for amino acid analysis based on pre-column derivatization with the novel reagent 6-aminoquinolyl-N-hydroxysuccinimidyl carbamate (AQC) that provides dramatic improvements over existing methodologies [5]. Documented advantages include a rapid, simple derivatization protocol, excellent response linearity over at least two orders of magnitude, formation of highly stable urea derivatives, and detection limits below one picomole. The derivatization reaction has several key features that simplify analysis: (1) formation of amine or amino acid derivatives is extremely rapid, occurring within seconds, (2) excess reagent is hydrolyzed to 6-aminoquinoline (AMQ) in less than 2 min, thus preventing any unwanted side reactions and (3) fluorescence emission maxima of AMQ and AQC-derivatized amines

* Corresponding author.

0021-9673/94/$07.00
SSDI 0021-9673(93)E0821-B

are approximately 100 nm apart, allowing for selective detection of the desired analytes without significant reagent interference. Further studies with peptide and protein hydrolysates have shown the derivatization chemistry to be reproducible and provide excellent compositional analyses [6,7]. These results are comparable to the traditional ion-exchange method of analysis [8,9] with typical analyses providing average compositional errors of 3–8% with sample quantities ranging from 0.2–5.0 μg, approximately an order of magnitude smaller than that used for the traditional procedure.

Amino acid analysis using reversed-phase chromatography has been often cited for its versatility and flexibility [1,2,10–12], but there have been reports of problems due to interference by the sample matrix with samples such as hydrolyzed grains or with samples containing buffer salts. We have concentrated our most recent efforts on extending the capabilities of AQC-amino acid analysis from compositional analysis of peptides and proteins to a number of different sample types requiring modified sample preparation, and/or new chromatographic conditions for complete analysis. This report will describe the analysis of hydrolyzed grain samples, hydrolyzed food or feed samples including collagen-containing samples, glycoproteins and intravenous solutions. Chromatographic conditions for many common amino acids not present in standard hydrolysate samples have also been developed, and the key chromatographic parameters used for separation optimization will be described.

MATERIALS AND METHODS

Chemicals

AQC (Waters AccQ · Fluor reagent) and borate buffer were obtained as a kit from Millipore (Milford, MA, USA). Eluent A concentrate was also from Millipore. Water was supplied by a Milli-Q system purchased from Millipore (Bedford, MA, USA). Sodium acetate trihydrate (HPLC grade) and disodium ethylenediaminetetraacetic acid were from Baker (Phillipsburg, PA, USA); triethylamine (TEA) was purchased from Aldrich (Milwaukee, WI, USA). Amino acid standards were from Pierce (Rockford, IL, USA) or Sigma (St. Louis, MO, USA); proteins were purchased from Sigma. Intravenous solutions were from Laboratories Don Baxter (Freeamine III; Trieste, Italy) and Soluzione di L-Aminoacidi Selettivi All' 8%, Bieffe Medital (Modena, Italy); grain samples were from a collaborative study organized by DeGussa Inc.

Chromatography instrumentation

The HPLC system consisted of a 625 LC solvent delivery system equipped with a column heater, a 717 plus autosampler with heater/chiller accessory, a 470 scanning fluorescence detector, and a 486 variable-wavelength detector (all Waters components, Millipore, Milford, MA, USA). A Waters Millennium 2010 workstation was used to control system operation and collect and analyze data.

Protein hydrolysis

Samples dissolved in water or dilute HCl (0.1–5.0 μg) were pipetted into 50 × 6 mm test tubes, vacuum dried and batchwise hydrolyzed *in vacuo* with 200 μl of constant-boiling HCl with *ca.* 0.5 mg crystalline phenol as a scavenger [13]. The samples were heated at 114°C for 20 h, cooled to room temperature and dried to remove excess HCl. Amino acids were reconstituted with 20 μl of 20 m*M* HCl and derivatized as described below.

Intravenous solutions

Samples were diluted 200-fold with water and α-aminobutyric acid was added as an internal standard to give a final concentration of 0.1 m*M*. The diluted sample was derivatized as described below.

Grain samples

Feed grains were milled to a uniform size and 296 mg weighed into a screw top test tube. A 50-ml volume of 6 *M* HCl was added and the sample sealed after flushing with nitrogen for 5 min. Some samples were oxidized with performic acid prior to hydrolysis according to previously published methods [14]. After hydrolysis 20 ml of internal standard Nle (0.19 mg/ml) was

added, the volume reduced to 2 ml, and then 50 ml of 0.2 *M* sodium citrate pH 2.20 was added.

Sample derivatization

In a typical analysis, 10–20 μl of sample were buffered with 0.2 *M* sodium borate, pH 8.8 containing 5 m*M* disodium EDTA (total volume 80 μl). The derivatization reaction was then initiated by the addition of 20 μl of AQC solution (3 mg/ml in acetonitrile). Grain samples were diluted to 200 μl with borate and derivatized with 50 μl of reagent. The reaction was terminated within 2 min due to reagent hydrolysis [5] and reversal of tyrosine phenol modification to the unmodified form accelerated by heating at 55°C for 10 min. The heating step was occasionally automated with a heated 717 plus autosampler at 40°C for 90 min. From this sample, 5–20 μl were then analyzed by HPLC.

Chromatographic analysis

Separations were carried out on a 150 × 4.6 mm AccQ · Tag C_{18} reversed-phase column (Millipore). Two eluent systems (eluents 1 and 2) used a concentrated eluent formulation before final dilution. Concentrate was made by dissolving 190.4 g sodium acetate trihydrate (Baker HPLC grade) in 1 l of water, adding 23.7 ml of triethylamine and titrating the solution with 50% phosphoric acid. The concentrate contained 10 ml of a 1 g/l solution of disodium EDTA and 0.1% sodium azide as a preservative. Eluent 1 used concentrate at pH 5.02 and working eluent was made with 100 ml of concentrate and 1000 ml of water. Eluent 2 used concentrate at pH 5.10 and contained 100 ml of concentrate and 800 ml of water. Eluent 3 was a ready-to-use formulation containing 19.04 g sodium acetate and 970 μl of TEA titrated to pH 5.80. EDTA and azide were added at one-tenth the concentration of the concentrate described above. Eluent B was acetonitrile and eluent C was water.

RESULTS AND DISCUSSION

Sample derivatization

Samples buffered at pH 8.8 are rapidly derivatized in a single step by the addition of the AQC solution. Within 2 min excess reagent is hydrolyzed to produce 6-aminoquinoline, N-hydroxysuccinimide and CO_2 [5]. The derivatization reaction for amines is shown in Fig. 1. A highly favorable blue shift in the fluorescence emission maximum of the AQC-labelled amino acids *versus* the hydrolysis product AMQ [5] enables direct injection of the derivatized mixture without any further sample workup.

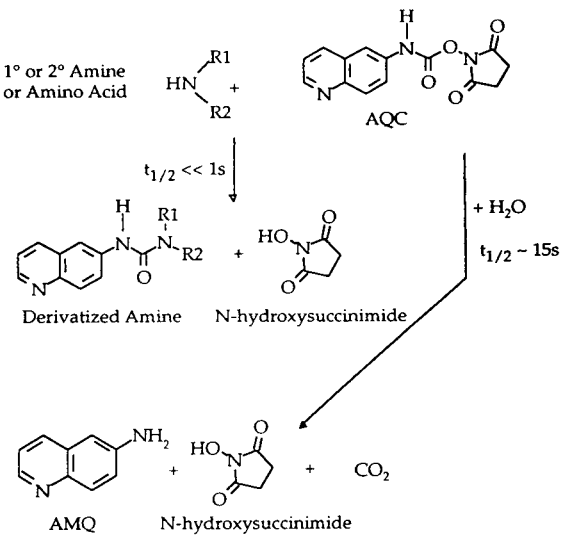

Fig. 1. Derivatization of primary (1°) and secondary (2°) amines with AQC. Also shown is the hydrolysis reaction of excess reagent.

Analysis of intravenous (i.v.) solutions

Chromatography of i.v. solutions employed eluent 1 and a multi-step gradient profile given in Table I (system 1). A typical analysis is shown in Fig. 2 where detection was accomplished by both fluorescence and UV at 254 nm to facilitate tryptophan detection. Analytical reproducibility is a priority concern with a pharmaceutical sample such as an i.v. solution. Table II presents a summary of 10 replicate derivatizations of an i.v. solution and a comparison of the recoveries with the sample label information. Data were generated in two laboratories using AQC derivatization, one system using both fluorescence and UV detection, the second being equipped

TABLE I

GRADIENT TABLES FOR THREE CHROMATOGRAPHY SYSTEMS

Eluent A is described in the text, eluent B was acetonitrile, and eluent C was water. Separation used only eluents A and B, with the water used for column flushing at the end of each analysis using 60% acetonitrile in water. After washing the column for 4 min it was re-equilibrated in 100% eluent A for 9 min. The total run time for system 1 was 45 min, 50 min for system 2 and 63 min for system 3. The gradient profile for each step was either linear (L) or a step (S) segment. * is initial conditions.

System 1			System 2			System 3		
Time (min)	MeCN (%)	Curve	Time (min)	MeCN (%)	Curve	Time (min)	MeCN (%)	Curve
0	0	*	0	0	*	0	0	*
0.5	1	S	0.5	1	S	1	1	S
18	5	L	16	3	L	16	3	L
19	9	L	23	8	L	25	6	L
29.5	18	L	36	19	L	35	14	L
33	18	L	38	19	L	40	14	L
						50	18	L

only with a fluorescence detector. Recoveries were extremely reproducible with average relative standard deviations (R.S.D.s) of approximately 1.4%. Interlaboratory comparison indicated that the method was capable of generating similar results with two completely different laboratory systems, and completely independent sample preparation. All data were generated by fluorescence detection except for the analysis of Trp, whose fluorescence response is weak due to internal quenching, which used UV detection.

Analysis of grain samples

Oxidation with performic acid produces two additional amino acids, methionine sulfone and cysteic acid, from methionine and cyst(e)ine respectively. Complete resolution of these derivatives and the normal hydrolysate amino acids

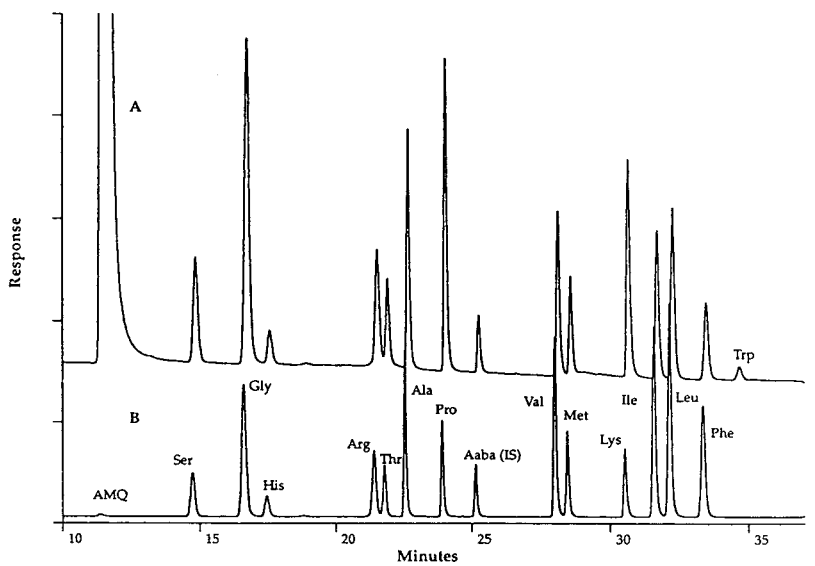

Fig. 2. Analysis of the Baxter Freeamine III intravenous solution. Sample preparation and chromatography are described in the text and Table I. The column was thermostatted at 37°C. Detection was by UV at 254 nm, full scale = 0.2 AU (A) and by fluorescence with excitation at 250 nm and emission at 395 nm, full scale = 2 V (B).

TABLE II

ANALYSIS OF INTRAVENOUS SOLUTIONS

ND = Not determined.

Amino acid	Baxter i.v. solution			Bieffe i.v. solution		
	Label value (mg/100 ml)	Laboratory 1 (% Label value)[a]	Laboratory 2 (% Label value)[b]	Label value (mg/100 ml)	Laboratory 1 (% Label value)[a]	Laboratory 2 (% Label value)[b]
Ser	500	97.2	104.4	430	95.7	99.5
Gly	1190	95.3	101.8	950	103.6	100.5
His	240	115.8	106.6	298	105.8	100.8
Arg	810	103.5	108.4	780	103.3	106.4
Thr	340	109.1	107.4	580	108.3	104.6
Ala	600	100.7	103.4	550	104.6	103.3
Pro	950	104.6	104.4	580	105.4	101.9
Val	560	106.4	104.7	1065	108.4	101.0
Met	450	108.7	106.0	50	144.8 (114.8)[d]	82.2
Lys	870	102.0	106.3	760	101.7	103.7
Ile	590	106.4	104.3	709	106.4	102.7
Leu	770	104.9	103.8	1184	107.3	103.6
Phe	480	109.2	102.4	27	118.1	99.6
Trp	130	100.7[c]	64	15	ND	ND

[a] Average of 10 injections.
[b] Average of 3 injections.
[c] Concentration based on UV data.
[d] Met data reported based on peak area and peak height measurements (in parentheses).

required modification of the original conditions. The key peak pair was alanine and methionine sulfone which could be resolved through a combination of gradient, eluent and column temperature changes. Thus, increasing the pH and eluent ionic strength slightly with eluent 2 and decreasing the column temperature from 37 to 31°C yielded the separation shown in Fig. 3. The gradient profile (system 2) is given in Table I. These chromatographic conditions have also proved useful for the analysis of collagen-type samples containing hydroxyproline and hydroxylysine (Fig. 4).

Replicate analyses of hydrolyzed grain samples exhibit highly reproducible amino acid yields (average R.S.D. = 1.1%) which are well-correlated with results obtained by ion-exchange amino acid analysis with post-column derivatization by *ortho*-phthalaldehyde (Table III). Comparative data in Table III have been normalized to the recovery of leucine, with the data from the AQC-derivatized samples then expressed as a percentage of the ion-exchange (IEX) results. The formula below was used to calculate the yield determined by AQC derivatization relative to the ion-exchange analysis:

$$\text{Per cent yield amino acid} = \frac{\text{AQC yield amino acid/AQC yield Leu}}{\text{IEX yield amino acid/IEX yield Leu}} \cdot 100\%$$

Glycoprotein analysis

The analyses of derivatized glycoprotein hydrolysates are shown in Fig. 5. Different classes of glycoproteins are represented by lactoferrin, α_1-acid glycoprotein and fetuin, which contain N-linked, O-linked and both types of oligosaccharides, respectively. The significance of these different classes with respect to amino acid analysis is the presence of either N-acetyl galactosamine ($GalNH_2$) in the O-linked glycoproteins or N-acetyl glucosamine ($GlcNH_2$) in the N-linked oligosaccharides which upon hydrolysis yield their respective hexosamines. These form

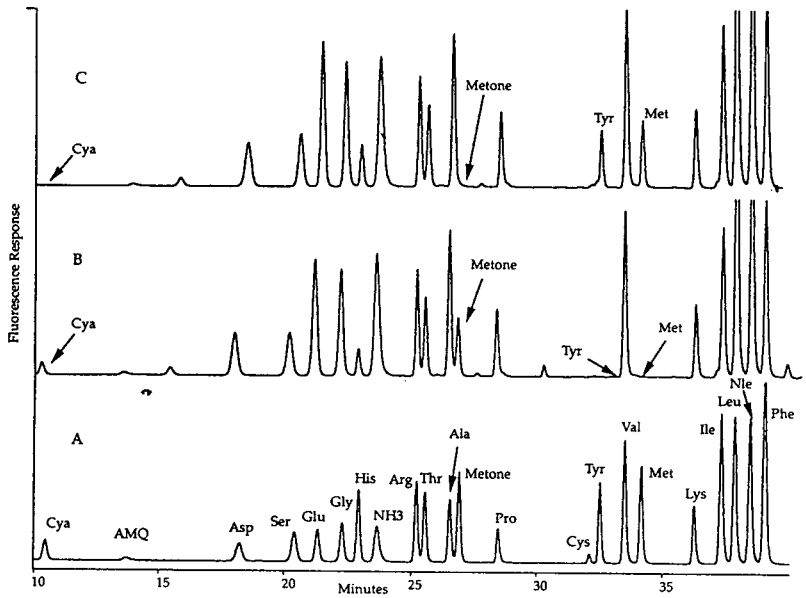

Fig. 3. Analysis of a standard containing cysteic acid (Cya) and methionine sulfone (Metone) (A), and a hydrolyzed grain sample with (B) and without (C) performic acid oxidation prior to hydrolysis. Eluent and gradient conditions are described in the text and Table I. The column was thermostatted at 31°C. Norleucine (Nle) was used as an internal standard.

stable derivatives with AQC which must be resolved from the normally present amino acids to allow for good quantitation. It is worth noting that such hydrolysates should not be used to quantitate the amino sugars as recoveries after hydrolysis are significantly less than quantitative [15].

The chromatography using eluent 3 and the

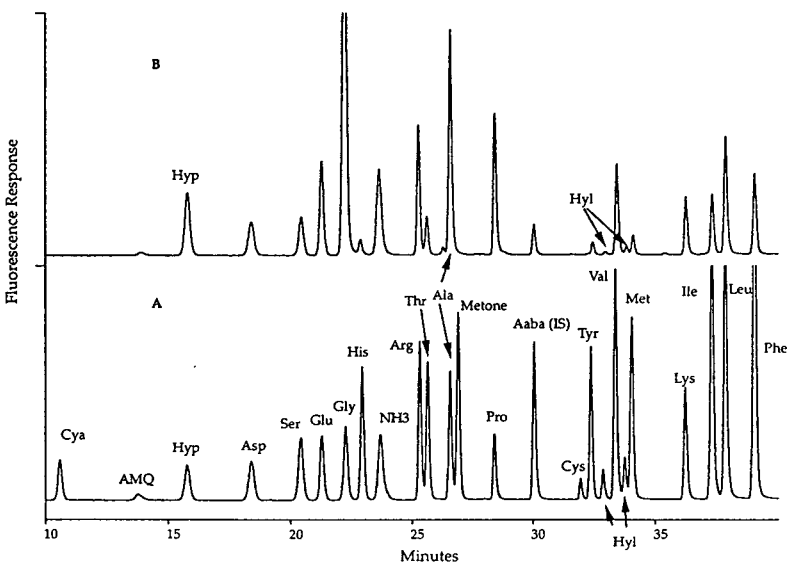

Fig. 4. Analysis of a collagen standard (A) and a sample containing collagen (B). The internal standard was α-aminobutyric acid (Aaba). Conditions as in Fig. 3.

TABLE III

REPRODUCIBILITY DATA FOR FEED GRAIN SAMPLE

	Retention time reproducibility		Amount reproducibility R.S.D. (%) (n = 10)[a]	Comparison with ion-exchange[b]
	n	R.S.D. (%)		
Cya	10	1.29	1.31	1.33
Asp	20	0.92	1.86	0.98
Ser	20	0.61	1.72	0.93
Glu	20	0.46	1.70	0.96
Gly	20	0.37	1.72	0.87
His	20	0.32	1.75	1.01
Arg	20	0.25	1.27	1.00
Thr	20	0.24	1.44	0.98
Ala	20	0.23	0.88	1.00
Metso	10	0.22	1.21	0.86
Pro	20	0.16	0.88	
Tyr	10	0.07	1.75	1.19
Val	20	0.10	0.62	0.96
Lys	20	0.09	2.62	1.01
Ile	20	0.09	0.42	1.05
Leu	20	0.09	0.20	1.00
Phe	20	0.10	0.28	1.06
Average R.S.D. (%)		0.33	1.27	

[a] Data for Cya and Metone used performic acid oxidized samples, other data were from unoxidized samples.

[b] Ion-exchange data were kindly provided by Mike Kennedy, Cargill, Inc. (Minnetonka, MN, USA). See the text for the calculation method used.

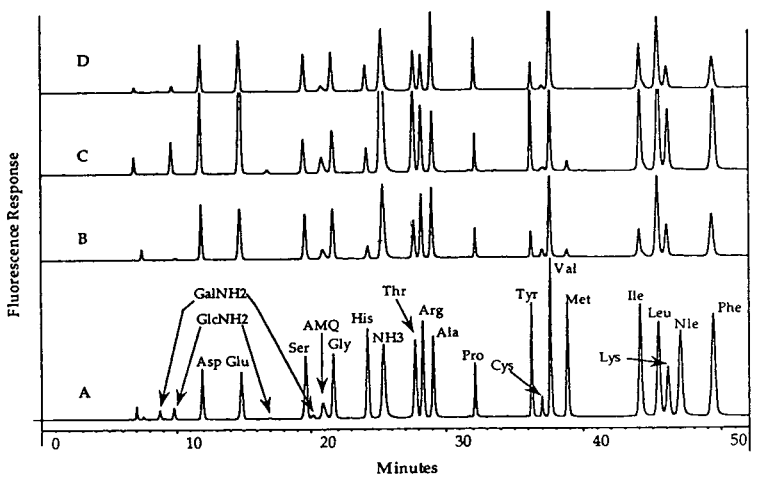

Fig. 5. Analyses of derivatized glycoprotein hydrolysates. Eluent and gradient conditions are described in the text and Table I. The column was thermostatted at 37°C. The samples are standard mixture with glucosamine and galactosamine (A), lactoferrin (B), α_1-acid glycoprotein (C) and fetuin (D).

gradient described in Table I (system 3) resulted in some significant changes in relative retention of key amino acids. At the higher pH of the mobile phase, the acidic amino acids Asp and Glu are retained much less relative to other amino acid derivatives as the side chain becomes deprotonated. Conversely, AMQ has much greater retention and elutes between Ser and Gly. This would make UV detection impractical as the reagent peak would interfere with Gly quantitation, but poor fluorescence emission for AMQ at the amino acid derivative emission maximum at 395 nm makes it feasible to use conditions under which AMQ elutes between components of interest. Other changes in elution order observed include reversal of Arg and Thr, Cys and Tyr, and elution of Lys after Ile and Leu.

Derivatization of standard solutions of either $GalNH_2$ or $GlcNH_2$ resulted in the appearance of a major peak and a minor peak. This complicated the analysis of $GlcNH_2$ containing samples as the smaller peak interfered with Ser if the samples were analyzed with the lower eluent pH separation system used for either i.v. solutions or grain samples. However, glycoproteins with N-linked carbohydrates could be analyzed with the system using eluent at pH 5.02 as both the major and minor peaks were resolved from the other amino acid derivatives (data not shown). One possible source of the multiple derivatives for the aminosugars is resolution of anomeric forms. This hypothesis is consistent with previous studies on glycoprotein analysis using OPA derivatization [16].

Compositional analysis of the glycoprotein lactoferrin is shown in Table IV. Error data were calculated according to the procedure described by Strydom *et al.* [3] and provide an unbiased measure of compositional accuracy. With highly purified proteins and sample amounts of 2–5 μg, typical analytical procedures give average errors of *ca.* 10% [3]. The data in Table IV were obtained from *ca.* 1.6 μg of hydrolyzed protein and give an excellent analysis with an average error of 7.1%.

Analysis of alkylated cysteine derivatives

Because cysteine and cystine are not quantitatively recovered after standard hydrolysis proce-

TABLE IV

COMPOSITIONAL ANALYSIS OF LACTOFERRIN

The hydrolyzed sample contained approximately 1.6 μg; 5% was analyzed by HPLC.

Amino acid	Literature composition (residues/mol)	Calculated composition (residues/mol)	Error (%)
Asp	77	74.42	3.35
Glu	71	77.74	9.50
Ser	50	48.95	2.09
Gly	46	54.17	17.77
His	9	8.81	2.06
Thr	31	31.75	2.43
Arg	46	45.56	0.95
Ala	63	60.30	4.29
Pro	35	37.49	7.11
Tyr	20	20.57	2.85
Val	49	46.49	5.12
Met	6	4.56	24.05
Ile	16	18.17	13.57
Leu	61	57.65	5.49
Lys	46	43.94	4.49
Phe	31	28.64	7.61
Average error (%)			7.05

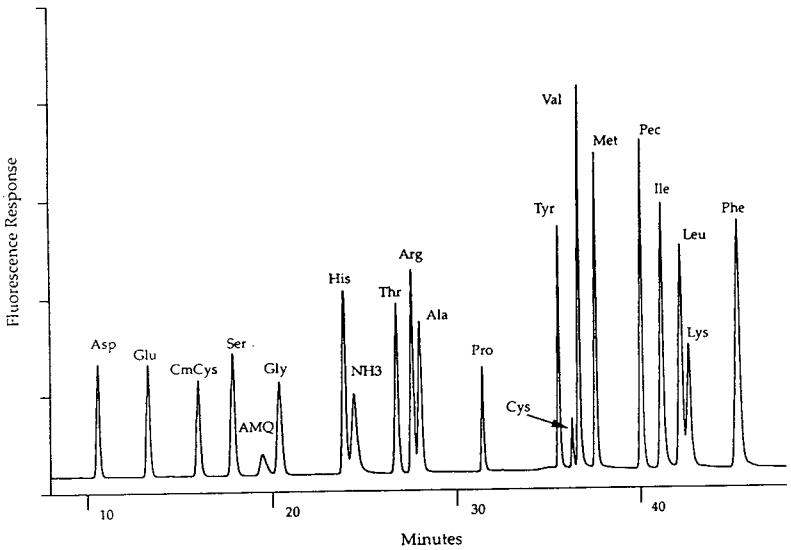

Fig. 6. Analysis of a hydrolysate standard plus the alkylated cysteine derivatives carboxymethyl cysteine (CmCys) and pyridylethyl cysteine (Pec). Conditions as in Fig. 5.

dures, chemical modification of these amino acids to more stable derivatives is usually performed. Previously, we have shown analysis of cyst(e)ine modified with the disulfide interchange reagent dithiodipropionic acid, and in this paper we have described the analysis of grain samples oxidized with performic acid. These are both destructive techniques in that the protein cannot be used for subsequent analytical procedures such as peptide mapping or N-terminal sequence analysis after the modification. Alkylation of the sulfhydryl group is an established procedure for non-destructive cyst(e)ine modification that yields acid-stable derivatives. Two of the more common reagents are iodoacetic acid [17] and 4-vinyl pyridine [18] which react with cysteine to form carboxymethyl cysteine and pyridylethyl cysteine, respectively. Using the conditions described for the analysis of glycoproteins (gradient system 3 and eluent 3), the AQC derivatives of these modified amino acids are easily resolved from the other amino acids allowing for quantitation of all the amino acid components (Fig. 6).

CONCLUSIONS

Derivatization of amino acids with AQC is a simple, highly reproducible, accurate procedure that is easily adapted for a wide variety of samples including feed grains, intravenous solutions, and glycoproteins. Derivative yields are essentially unaffected by the presence of metallic salts and high concentrations of carbohydrates present in these samples. Flexible chromatographic systems have allowed the development of conditions that resolve a number of amino acids in addition to those present in standard protein hydrolysates. This versatile reagent will undoubtedly be useful in a number of important amino acid analysis applications. Recent work in our laboratory suggests that the range of applications can be routinely expanded to a number of interesting target molecules such as amine drugs and peptides [19].

REFERENCES

1 S.A. Cohen and D.J. Stydrom, *Anal. Biochem.*, 174 (1988) 1–16.
2 J.A. White and R.J. Hart, in M.L. Leo (Editor), *Food Analysis by HPLC*, Marcel Dekker, New York, 1992, pp. 53–74.
3 D.J. Strydom, G.E. Tarr, Y.-C.E. Pan and R.J. Paxton, in R.H. Angeletti (Editor), *Techniques in Protein Chemistry III*, Academic Press, San Diego, CA, 1992, pp. 261–271.
4 D. Atherton, in T. Hugli (Editor), *Techniques in Protein Chemistry*, Academic Press, San Diego, CA, 1989, pp. 273–283.

5 S.A. Cohen and D.P. Michaud, *Anal. Biochem.*, (1993) 211 (1993) 279–287.
6 S.A. Cohen, K.M. De Antonis and D.P. Michaud, in R.H. Angeletti (Editor), *Techniques in Protein Chemistry IV*, Academic Press, San Diego, CA, 1993, pp. 289–298.
7 D.J. Strydom and S.A. Cohen, in R.H. Angeletti (Editor), *Techniques in Protein Chemistry IV*, Academic Press, San Diego, CA, 1993, pp. 299–306..
8 S. Moore and W.H. Stein, *J. Biol. Chem.*, 176 (1948) 367–388.
9 S. Moore, D.H. Spackman and W.H. Stein, *Anal. Chem.*, 30 (1958) 1185–1190.
10 R.F. Pfeifer and D.W. Hill, *Adv. Chromatogr.*, 22 (1983) 37–69.
11 R.S. Ersser and J.F. Davey, *Med. Lab. Sci.*, 48 (1991) 59–71.
12 L.B. Smillie and M. Nattriss, in C. Mant and R.S. Hodges (Editors), *High-Performance Liquid Chromatography of Peptides and Proteins: Separation, Analysis and Confromation*, CRC Press, Boca Raton, FL, 1991, pp. 847–858.
13 S.A. Cohen, T.L. Tarvin and B.A. Bidlingmeyer, *Am. Lab.*, August (1984) 490–59.
14 C.W. Gehrke, P.R. Rexroad, R.M. Schisla, J.S. Absheer and R.W. Zumwalt, *J. Assoc. Off. Anal. Chem.*, 70 (1987) 171–174.
15 R.G. Spiro, *Methods Enzymol.*, 28 (1972) 3–43.
16 F. Altmann, *Anal. Biochem.*, 204 (1992) 215–219.
17 A.M. Crestfield, S. Moore and W.H. Stein, *J. Biol. Chem.*, 238 (1963) 2413–2421.
18 J.F. Cavins and M. Friedman, *Anal. Biochem.*, 35 (1970) 489.
19 K.M. De Antonis, P.R. Brown, Y.-F. Cheng and S.A. Cohen, *J. Chromatogr. A*, 661 (1994) 279.

Journal of Chromatography A, 661 (1994) 35–42
Elsevier Science B.V., Amsterdam

CHROMSYMP. 2878

Kinetic study of the adsorption of human serum albumin on immobilized antibody using the split-peak effect in immunochromatography

James Renard and Claire Vidal-Madjar*

Laboratoire de Physico-Chimie des Biopolymères, CNRS, Université Paris Val de Marne, UM 27, 2 Rue Henry Dunant, 94320 Thiais (France)

ABSTRACT

The split-peak effect was used to determine the association rate constant of the antigen–immobilized antibody reaction. The amount of immobilized human serum albumin antibody on the chromatographic support was varied in order to find the optimal conditions to reduce the mass transfer contribution in the stagnant mobile phase fluid and measure the effective association rate constant of human serum albumin with the immobilized antibody. Kinetic studies as a function of flow-rate demonstrate the validity of the method consisting in determining the association rate constant from measurements performed on columns of various capacities. These experiments show that limitations due to mass transfer to the surface of the adsorbent are minimized at high flow-rates and for a low density of immobilized ligand.

INTRODUCTION

Studies of the reaction between antigens and antibodies are becoming increasingly important because of the development of immunoreactions. This type of interaction is utilized in various techniques, such as enzyme-linked immunosorbent assay (ELISA) or immunochromatography [1]. These techniques, based upon biospecific recognition, measure the interaction of antibody with immobilized antigen (or *vice versa*). However, it is not enough to know if an antigen–antibody reaction occurs, it is also important to analyse the kinetic steps of this reaction in order to optimize the separation methods based upon this mode of interaction. Moreover, a comprehensive approach to the kinetic process is necessary for the quantitative analysis of kinetic chromatographic immunoassays [2,3].

Reliable and fast methods of carrying out such immunochemical reaction studies are needed. An instrument based upon surface plasma resonance detection of the adsorbed amount was recently introduced for this type of study [4,5], but its sophistication makes its use difficult for routine investigations. Immunochromatography, which uses standard high-performance liquid chromatographic (HPLC) instruments, is well suited for this kind of measurement. Until now the technique has mainly been used as a powerful tool to isolate and purify a single substance from a complex mixture [1] or for rapid immunoassay tests in quantitative analysis [2,3].

Kinetic measurements generally use frontal elution chromatography. Analytical solutions based on the Thomas model [6] are often applied to interpret the chromatographic kinetic experiments [7–9]. The main difficulty with the chromatographic method for kinetic measurements is that several mass transfer processes are at work in non-linear conditions: the mass transport phenomena and the sorption processes. Numeri-

* Corresponding author.

0021-9673/94/$07.00
SSDI 0021-9673(93)E0771-L

cal procedures have also been applied to analyse the frontal elution curves and estimate the kinetics of biospecific adsorption of a protein with an immobilized monoclonal antibody [10]. The intraparticle mass transfer diffusion mechanisms could be neglected because non-porous particles were used.

The applications of high-performance immunochromatography for kinetic studies of the antigen–antibody interaction were first described by Sportsman and co-workers [11,12], but the unusual behaviour observed was not well understood. Experiments based upon the "split-peak" effect in linear elution conditions were presented by Walters and co-workers [13,14] to measure the adsorption kinetics on immunoadsorbents. In this method, part of the solute injected elutes from the column as a non-retained peak, while the rest is irreversibly adsorbed and does not elute from the column on the time scale of the experiment. The amount injected was kept as small as possible in order to avoid column overloading effects.

In previous papers, we have shown that the split-peak method may be used in non-linear elution conditions. A model based upon second-order Langmuir kinetics relates the amount injected to the column capacity and to the apparent adsorption rate constant [15]. The method was applied to a study of the adsorption kinetics of human serum albumin (HSA) on a C_6 reversed-phase support [16,17]. In spite of a packing with pores of small size from which the protein is excluded, the column capacity was still too large and the measurements did not allow us to distinguish between diffusion- and adsorption-limited processes. In the present work, we shall show that kinetic studies on adsorbents of low capacity enable reduction of the contributions for mass transfer into the mobile phase fluid and measurement of the effective adsorption rate constant of an antigenic protein (HSA) onto the immobilized antibody.

THEORY

We assume that the immobilized ligand X interacts with the adsorbate according to the chemical equilibrium:

$$A + X \underset{k_d}{\overset{k_a}{\rightleftharpoons}} AX \tag{1}$$

where k_a and k_d are the association and dissociation rate constants. The binding rate equation is a Langmuir second-order kinetic law:

$$\frac{\partial q}{\partial t} = k_a c(q_x - q) - k_d q \tag{2}$$

where c is the concentration of solute in solution and q and q_x are, respectively, the amount adsorbed and the maximum capacity per unit volume of adsorbent.

Thomas [6] has shown that an analytical expression predicts the breakthrough curve on the basis of the following assumptions: adsorption isotherm of the Langmuir type, negligible axial dispersion and no rate-limiting steps due to transport to the adsorbent surface. Several analytical models were further developed to account for this last effect [7–9]. Starting from Goldstein solution [18] giving the equation for the zonal elution peak in mass-overload conditions, we have shown [15] that the split-peak effect is described by an analytical expression relating the adsorption yield to the amount injected, to the experimental parameters (flow-rate F, column length L) and to the kinetic constants (k_a, k_d and q_x). The model assumes negligible axial dispersion of the solute, a non-porous adsorbent or an adsorbent with small pores into which the protein molecule cannot penetrate.

If irreversible adsorption occurs on the time scale of the experiment ($k_d = 0$), the fraction of non-retained compound f is given by [15]:

$$f = \frac{Q_x}{nQ_i} \cdot \ln[1 + (e^{nQ_i/Q_x} - 1)\, e^{-n}] \tag{3}$$

where Q_i is the sample size, Q_x the maximum column loading capacity and n the number of transfer units characterizing the rate-limiting mass transfer step and the adsorption step.

If the rate for the sorption step is similar to the rate for slow mass transfer, it can be shown [8,9] that $1/n$ may be expressed as a sum of different increments:

$$\frac{1}{n} = \frac{1}{n_{mt}} + \frac{1}{n_k} \tag{4}$$

where n_k represents the contribution of binding kinetics and n_{mt} represents the contribution of the mass exchange into the stagnant fluid. n_k is a function of the effective second-order rate constant for the binding process and of the maximum loading capacity:

$$n_k = \frac{Q_x k_a}{F} = q_x k_a \cdot \frac{(1-\varepsilon)}{\varepsilon} \cdot \frac{L}{u} \quad (5)$$

where u is the interstitial mobile phase velocity and ε is the column void fraction.

The n_{mt} contribution depends upon the particle size, the pore structure of the packing and the column geometry. It is a complicated function of the flow-rate. For a given mobile phase velocity and a given chromatographic system (instrument, column geometry, nature of the packing), the n_{mt} parameter is independent of the density of immobilized ligand, and the effective adsorption rate constant, k_a, may be determined from the variation of n with q_x. The aim of the present work is to show that the split-peak method may be applied to determine the binding rate constant from the kinetic studies performed on supports on which various amounts of antibody are immobilized.

EXPERIMENTAL

Materials

Human serum albumin (ref. A 1887), rabbit polyclonal antibodies to human albumin (ref. A 0659) and tresyl chloride (ref. T 7907) were purchased from Sigma (St. Louis, MO, USA). LiChrospher SI 60 (10 μm diameter, 60 Å pore size) was from Merck (Darmstadt, Germany).

Apparatus

The chromatographic experiments were carried out using an HPLC system consisting of a dual-pump system (LC-9A; Shimadzu, Kyoto, Japan), a sample injector (7125; Rheodyne, Berkeley, CA, USA) equipped with a 20-μl loop and an optical scanning UV detector set at 280 nm (Spectra Focus; Spectra-Physics, San Jose, CA, USA). Spectra Focus software on an IBM PS2 personal computer controls the detector, performs on-line data acquisition via an OS/2 interface and reprocesses peak integrations.

Procedure

Immunoadsorbent. The rabbit polyclonal antibody was immobilized on the LiChrospher 60-Å silica support using the tresyl activation method [19]. The tresylated silica was synthesized according to the procedure described by Cabrera and Wilchek [19]. The antibody was immobilized on the support as follows: 1 g of activated silica was added to 4 ml of a solution of antibody in 1 *M* phosphate buffer and the mixture was shaken at ambient temperature for 5 h. The support was further washed with 0.1 *M* Tris–HCl buffer, pH 8.5, to remove unreacted tresyl groups. Four different supports were prepared by varying the concentration of antibody in the phosphate buffer solution used for immobilization (Table I).

Chromatography. The supports were vacuum slurry packed into polyether ether ketone (PEEK) columns (30 mm × 4.6 mm I.D.). The column temperature was maintained at 20 ± 0.1°C using a thermostated bath (CB 11C; Heto, Birkerod, Denmark). The mobile phase was phosphate-buffered saline (PBS; 10 m*M* phosphate buffer, pH 7.4, 150 m*M* NaCl); the HSA samples were dissolved in the eluent. After column saturation with HSA injections, protein desorption was achieved using 0.1 *M* citric acid buffer at pH 1.6.

RESULTS

Successive injections of HSA on the polyclonal anti-HSA columns were performed until saturation of the support was achieved. Fig. 1 illustrates the progressive overloading of the column after repeated injections of 2 μg of HSA. With the first injections an impurity is eluted while HSA is totally adsorbed onto the column. Then, after several injections, because of column saturation and kinetic effects, the amount of the first peak increases until it reaches a plateau. The percentage of the impurity corrective factor, given in relative detector response units, is calculated from the ratio of the area of the first peak observed on the antibody column to that measured when the same HSA solution is injected on a diol column. It is about 10% of the total HSA signal. The method does not give the actual impurity level in the sample, but this

TABLE I

VARIATION IN THE KINETIC PARAMETERS WITH THE DENSITY OF IMMOBILIZED ANTIBODY

Column	Antibody in reacting solution (g/l)	Q_x (μg)	F (ml/min)	$1/n$	$1/n_k$	k_a ($l\ g^{-1}\ s^{-1}$)
A	0.16	9	0.5	0.13 ± 0.01	0.08	12 ± 2
			1.0	0.23 ± 0.02	0.18	10 ± 2
			1.5	0.30 ± 0.03	0.25	11 ± 2
B	0.42	27	0.5	0.08 ± 0.01	0.03	10 ± 4
			1.0	0.11 ± 0.01	0.06	10 ± 3
			1.5	0.13 ± 0.01	0.08	12 ± 2
C	2.30	39	0.5	0.08 ± 0.01	0.03	7 ± 4
			1.0	0.09 ± 0.01	0.04	11 ± 4
			1.5	0.11 ± 0.01	0.06	11 ± 3
D	2.50	41	0.5	0.07 ± 0.01	0.02	10 ± 5
			1.0	0.09 ± 0.01	0.04	10 ± 4
			1.5	0.10 ± 0.01	0.05	12 ± 4

information is enough to correct for the unretained fraction: at each injection, the unretained HSA amount is calculated by subtracting the area corresponding to the impurity response (area of the first peak).

Fig. 1 shows, for comparison, the diagrams observed at two different flow-rates: 0.5 and 1.5 ml/min. The first signal corresponds to a non-retained impurity response, and it is only the increase in the HSA response that is analysed. At the higher flow-rate, the increase in the first peak occurs for lower amounts injected. To determine the adsorption rate constant, the split-peak behaviour is quantitatively analysed according to eqn. 3, by studying the variation in the unretained fraction as a function of the amount injected.

Fig. 2 shows the plot of $1/f$ *vs.* Q_i, where f is the ratio of the cumulative amounts injected to the cumulative amounts which are not irreversibly adsorbed and Q_i is equal to the cumulative amounts injected. This figure also shows the results of the experiments performed at a given flow-rate on columns of various binding capacities. A non-linear least-squares fit was used to adjust eqn. 3 to the experimental data. The method gives the two parameters necessary to describe the adsorption model: the column capacity for HSA, Q_x, and the number of transfer units, n.

The four columns studied differ in the density of the polyclonal antibody immobilized on the silica support and therefore in the column capacity, Q_x, for HSA (Table I). In order to check the possibility of non-specific adsorption, a column was packed with a silica support prepared exactly as described for coupling the antibody, but in this case no protein was added to the reacting solution. No peak area increase was noticed when repeated injections of HSA were performed on this column. Moreover, under similar elution conditions, the area of the non-retained HSA peak is equal to that observed with a diol column or with an antibody column at saturation. Therefore the non-specific HSA adsorption on the matrix used for the antibody immobilization may be considered to be negligible.

For each column, the number of transfer units determined at different flow-rates is listed in Table I. The reported errors on the parameter determination are given for a 95% confidence interval. Fig. 3 illustrates the variation of L/n as a function of the interstitial mobile phase velocity. This diagram may be analysed as classically where the theoretical plate height is plotted as

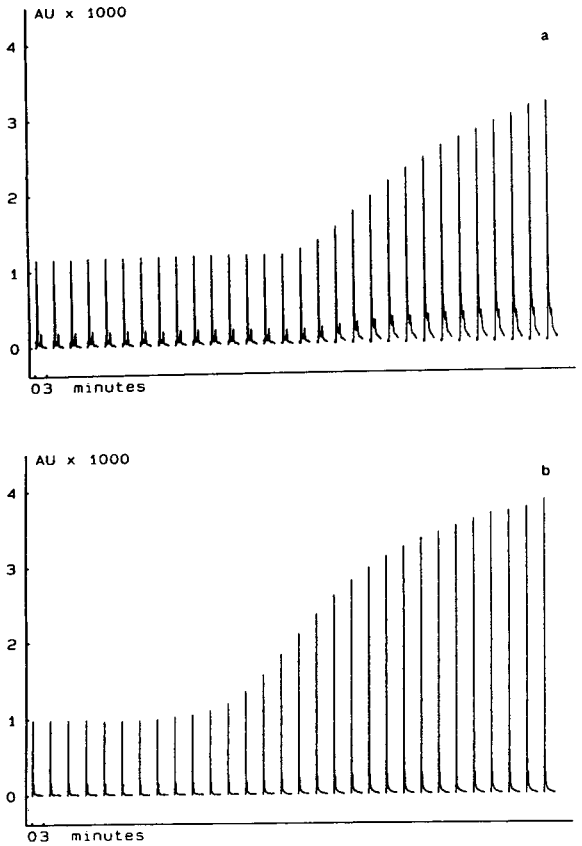

Fig. 1. Successive injections of HSA on a polyclonal HSA antibody support. Eluent: 10 m*M* phosphate buffer pH 7.4–150 m*M* NaCl. Injected volume: 20 μl. HSA concentration: 0.1 g l^{-1}. Data acquisition rate: 24 readings per s. $T = 20°C$. Column: D (30 × 4.6 mm, dead volume: 0.3 ml). (a) $F = 0.5$ ml min^{-1}; (b) $F = 1.5$ ml min^{-1}.

a function of the mobile phase velocity. L/n increases with increasing flow-rate, and this effect may be explained by mass transfer phenomena due to slow adsorption and/or to slow diffusion into the stagnant mobile phase fluid.

DISCUSSION

Fig. 4 shows that for each flow-rate studied the reciprocal of the global mass transfer unit, n, varies linearly with the reciprocal of q_x, the column capacity per volume of adsorbent. This result agrees well with eqns. 3 and 4 describing $1/n$ as a sum of various contributions. At a given

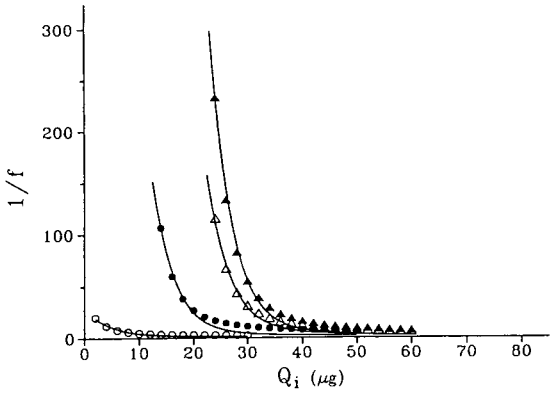

Fig. 2. Variation in the non-retained fraction f with the amount of HSA injected. Same experimental conditions as in Fig. 1 and $F = 1.5$ ml min^{-1}. Columns: ○ = A; ● = B; △ = C; ▲ = D.

mobile phase velocity, the model predicts a linear variation of $1/n$ *vs.* $1/q_x$, with the same n_{mt} contribution for the columns used. In this case, similar values for the contribution of the mass transfer in the stagnant mobile phase are to be expected, since the columns tested on a single instrument are of identical geometrical design and packing: they differ only in the density of immobilized antibody on the silica support. For each flow-rate, the value of $1/n_{mt}$ may be determined by extrapolating the straight lines to $1/q_x = 0$. Since the extrapolated values are similar for the three flow-rates studied (Fig. 4), the

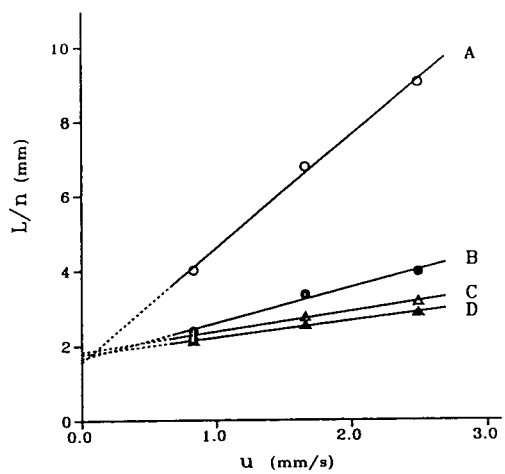

Fig. 3. Variation in the number of transfer units with the interstitial mobile phase velocity. Same experimental conditions as in Fig. 1. Columns: ○ = A; ● = B; △ = C; ▲ = D.

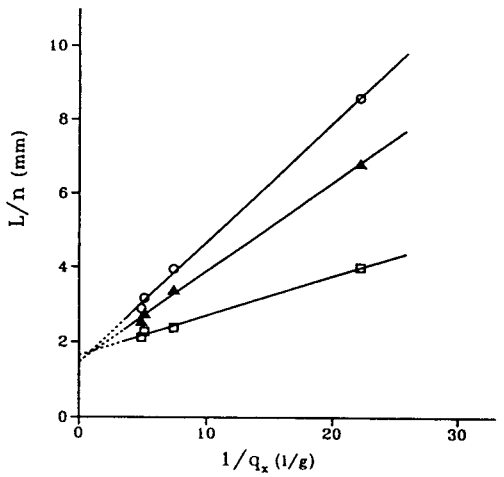

Fig. 4. Variation in the number of transfer units with the column capacity. Same experimental conditions as in Fig. 1. Interstitial mobile phase velocity: ○ = 0.5 ml min^{-1}; ▲ = 1.0 ml min^{-1}; □ = 1.5 ml min^{-1}.

variation of n_{mt} with the mobile phase velocity, u, may be considered negligible.

Similarly, a linear variation of L/n with u is found (Fig. 3). An important variation in the number of unit transfers, n, is observed for the column of lower HSA capacity. On the other hand, L/n is almost independent of flow-rate with the column packed with the adsorbent of higher density of immobilized antibody. The higher the straight-line slope, the lower is the density of immobilized antibody. The values of L/n extrapolated at $u = 0$ are similar for all the columns studied and correspond to a constant contribution to the overall mass transfer, independent of the density of the immobilized ligand.

Since n_{mt} is proportional to the theoretical plate height of an unadsorbed tracer [13], such behaviour may be independently examined by studying, as a function of the mobile phase velocity, the band broadening of the non-retained HSA elution peak. Fig. 5 shows that the variation in the theoretical plate height H with u is negligible. Also, as expected for all the columns studied, the efficiencies of the unretained HSA peak are close, within the range of experimental errors. They are about ten times higher than the optimal value for a 10 μm particle size support. The poor efficiencies generally observed in the HPLC of proteins [20] are the result of several complex mechanisms involving slow mass transfers due to diffusion into the stagnant fluid of the small pores of the packing, that between the silica particles, or the extra column contributions.

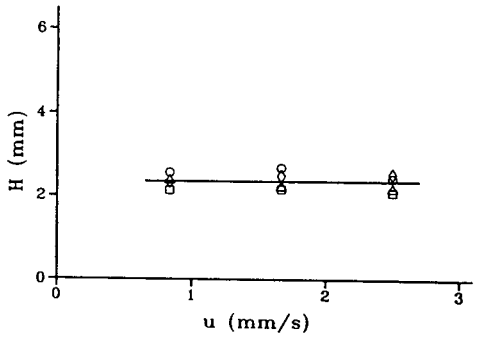

Fig. 5. Variation in the theoretical plate height of the unretained HSA peak with the interstitial mobile phase velocity. Same experimental conditions as in Fig. 1. Columns: ○ = A; ◇ = B; □ = C; △ = D.

These results demonstrate that, within experimental errors, n_{mt} may be considered a constant for all the columns and in the range of flow-rates studied. This contribution may be determined by extrapolating the straight lines L/n *vs.* u (Fig. 3) or L/n *vs.* $1/q_x$ (Fig. 4) to zero abscissa. In agreement with the assumption of a constant n_{mt} contribution, the intercepts with the ordinate axis are similar for the straight lines of both figures. The mean n_{mt} value is 20 ± 3.

Subtracting n_{mt} from the global mass transfer unit term, n, leads to the contribution for binding kinetics, n_k. Table I lists the n_k values determined for each column and each flow-rate studied. These results show that the contribution of mass transfer in the stagnant fluid film to the global mass transfer process is minimized when the kinetic experiments are performed at high flow-rates and with low amounts of immobilized antibody. The error made in neglecting the n_{mt} contribution with the column of lower capacity is about 20% at the higher flow-rates. The mass transfer in the stagnant fluid is a large part of the total $1/n$ value with the columns of larger capacity (columns C and D).

The effective adsorption rate constant was

calculated for each column and each flow-rate studied (Table I). Within experimental errors the results are in good agreement, and the mean value obtained for the effective adsorption rate constant is $k_a = 10.5$ l g^{-1} s^{-1} ($7.2 \cdot 10^5$ M^{-1} s^{-1}). It is of similar magnitude as that found in other kinetic studies of protein–protein interactions [4,5]. However, because of the heterogeneous nature of the polyclonal antibody used, the association rate constant characterizes an average adsorption process.

The mass transfer into the stagnant mobile phase fluid has several causes (nature of the column packing or extra-column effects), and this contribution could be reduced by a systematic study of the experimental conditions leading to this effect. Under the present HPLC experimental conditions, the transport process to the adsorbent can be faster than the rate constant of the immunoreaction. In some cases, with a high flow-rate and a low column capacity, direct measurement of the kinetic contribution is possible if this effect can be neglected or accounted for. The measurements are then performed in conditions in which non-linear effects are important considerations in the theoretical models.

CONCLUSIONS

The present work describes an easy immunochromatographic method based upon peak-area measurements to determine the association kinetic rate constant of the antigen–immobilized antibody system. The reverse interaction could be determined just as easily by immobilizing the antigen and studying the split-peak effect by injecting the antibody sample. So far very few kinetic measurements have been determined as a function of the density of immobilized ligand. Our results clearly demonstrate that this type of study enables determination of the sorption rate constant for the antigen–immobilized antibody interaction. Experiments performed at various flow-rates confirm the validity of this type of approach.

Selecting the appropriate experimental chromatographic conditions enables characterization of the kinetics of the antigen–antibody reaction at the solid–liquid interface. The rate-controlling step may not be diffusion into the stagnant fluid if the experiments are carried out at a high flow-rate on a support on which low amounts of antibody (or antigen) are immobilized. The characteristics of the packing material are also important in order to reduce the extra mass transfer contribution: a regular packing of beds with uniform and small size distribution must be achieved, and non-porous supports or supports with pores small enough to exclude the antigen or the antibody must be selected.

In the present work, we studied the interaction of HSA with an immobilized polyclonal antibody in order to define the optimal conditions for kinetic measurements. The advantage of immobilizing the antibody is that several systematic studies on the same column may be performed in order to demonstrate the feasibility of the method with chromatographic columns having capacities as low as a few micrograms. The amount of antibody consumed is minimal and equal to the amount immobilized. This problem is an important consideration when using expensive and rare monoclonal antibody samples.

REFERENCES

1 M. de Frutos and F.E. Regnier, *Anal. Chem.*, 65 (1993) 17A.
2 A. Riggin, F.E. Regnier and J.R. Sportsman, *Anal. Chem.*, 63 (1991) 468.
3 S.A. Cassidy, L.J. Janis and F.E. Regnier, *Anal. Chem.*, 64 (1992) 1973.
4 E. Stenberg, B. Persson, H. Roos and C. Urbaniczky, *J. Colloid Interface Sci.*, 143 (1991) 513.
5 R. Karlsson, A. Michaelsson and L. Mattsson, *J. Immunol. Methods*, 145 (1991) 229.
6 H.C. Thomas, *J. Am. Chem. Soc.*, 66 (1944) 1664.
7 N.K. Hiester and T. Vermeulen, *Chem. Eng. Prog.*, 48 (1952) 505.
8 F.H. Arnold and H.W. Blanch, *J. Chromatogr.*, 355 (1986) 13.
9 Q.M. Mao, A. Johnston, I.G. Prince and M.T.W. Hearn, *J. Chromatogr.*, 548 (1991) 147.
10 A.I. Liapis, B. Anspach, M.E. Findley, J. Davies, M.T.W. Hearn and K.K. Unger, *Biotechnol. Bioeng.*, 34 (1989) 467.
11 J.R. Sportsman and G.S. Wilson, *Anal. Chem.*, 52 (1980) 2013.
12 J.R. Sportsman, J.D. Liddll and G.S. Wilson, *Anal. Chem.*, 55 (1983) 771.

13 D.S. Hage, R.R. Walters and H.W. Hethcote, *Anal. Chem.*, 58 (1986) 274.
14 L.A. Larew and R.R. Walters, *Anal. Biochem.*, 164 (1987) 537.
15 A. Jaulmes and C. Vidal-Madjar, *Anal. Chem.*, 63 (1991) 1165.
16 H. Place, B. Sebille and C. Vidal-Madjar, *Anal. Chem.*, 63 (1991) 1222.
17 C. Vidal-Madjar, H. Place, L. Boulkanz and A. Jaulmes, *J. Chromatogr.*, 548 (1991) 81.
18 S. Goldstein, *Proc. R. Soc. London Ser. A*, 219 (1953) 151.
19 K. Ernst-Cabrera and M. Wilchek, *J. Chromatogr.*, 397 (1987) 187.
20 R.R. Walters, *J. Chromatogr.*, 249 (1982) 19.

Journal of Chromatography A, 661 (1994) 43–50
Elsevier Science B.V., Amsterdam

CHROMSYMP. 2889

Review

Advances in the high-performance liquid chromatographic determination of phenylthiocarbamyl amino acids

I. Molnár-Perl

Institute of Inorganic and Analytical Chemistry, L. Eötvös University, P.O. Box 32, H-1518 Budapest 112 (Hungary)

ABSTRACT

Some of the general problems commonly encountered in the analysis of phenylthiocarbamyl amino acids are described. This review includes experiences associated with the preparation and storage of derivatives prior to analysis and those originating from the analytical procedure itself. The issue of the quantification of the phenylthiocarbamyl derivatives of tryptophan and cyst(e)ine, together with all other amino acids from the same hydrolysate, is also discussed. The possible reproducibility of the measurements, as a function of the conditions applied is considered.

CONTENTS

1. Introduction 43
1.1. Literature overview 44
2. Sample preparation and storage 44
2.1. Derivatization reaction 44
2.1.1. Storage of derivatives 45
2.2. Hydrolysis 45
2.3. The status of "difficult" amino acids 46
2.3.1. Tryptophan 46
2.3.2. Cystine/cysteine 46
2.3.3. Glutamine, asparagine 47
2.4. Applicability to non-protein compounds 47
3. Chromatographic conditions 47
3.1. Columns 47
3.2. Eluents, gradient programmes 47
3.3. Quantification conditions 49
4. Acknowledgement 49
References 49

1. INTRODUCTION

Since the 1970s, the developments in high-performance liquid chromatography (HPLC) and the increased choice of reversed phases have extended its competitiveness with other chromatographic methods such as the classical ion-exchange chromatography (IEC) and gas chro-

0021-9673/94/$07.00
SSDI 0021-9673(93)E0808-8

matography (GC) in the field of amino acid analysis. The main advantage of the IEC technique, which involves the direct elution of amino acid-containing samples, was offset in the amino acid analysis by greater time and cost requirements. HPLC also now seems to be superior to GC because in the latter instance the highly selective and necessarily quantitative derivatization procedures for all essential amino acids are time consuming methods consisting of two steps (acylation and esterification), the samples to be derivatized must be cleaned up to a much higher level than is needed in HPLC procedures and the derivatives, prior to and during their GC elution and quantification, must be present in almost water-free conditions.

1.1. Literature overview

In this paper, of the numerous possible precolumn derivatization procedures, the advances in the HPLC of amino acids as their phenylthiocarbamyl (PTC) derivatives [1–65] are followed in detail. PTC derivatives can be prepared from all essential amino acids, containing both primary and secondary amino groups, they can be obtained in quantitative yield over a wide concentration range, even at the low picomole level, they can be monitored by UV detection, before dissolution they can be stored in a refrigerator for an unlimited time, in dissolved form they are stable enough to make testing of the reproducibility of their derivatization and elution conditions possible and the automation of the procedure has been achieved, including the steps of hydrolysis, derivatization and the subsequent elution procedure.

After the first pioneering work [1], the required conditions for the precolumn derivatization method were published in 1984 [2–6]. A number of modifications and improvements have been suggested both at the basic research level [7–37], including comparative studies with other precolumn derivatization procedures for HPLC [32–37], and also in applications of the method [38–65] to the determination of free amino acids [38–47] present in various biological matrices, such as in pig plasma [38], human plasma [39,40–42,46], rat brain [41,45], urine [43] and microbially colonized sandstone [47]; the determination of the PTC derivatives of the important non-protein constituents of biological matrices, present in free forms [48,49], such as acidic opines [48], galactosamines and glucosamines [49], phosphorylated or sulphated amino acids [50], and the characteristic compounds in hydrolysates of special proteins [51–56], such as *trans*-hydroxyproline from collagen [51], hexitolamino acids from glycated proteins [52], methyl-substituted amino acids [53,54] (mono- and dimethylarginine, mono- and trimethyllsine and methylhistidine) from myelin basic protein [53], methylhistidine from actin [54], cross-linked glutamyllysine from complex biological systems, including tissue homogenates [55], and the losses of amino sugars in glycoproteins, monitoring the extent of Maillard reactions [56]; and the determination of PTC amino acids even in foods and feedstuffs [57–62] and in faeces [63]. Derivatization of the free acids in apple extract [57], in wine [58,59] and the components of hydrolysates obtained from molasses, infant formula, milk and isolated whey protein [60], peas and lentils [61], soya, sorghum, corn and peanut meals and their mixtures [62] has been reported.

2. SAMPLE PREPARATION AND STORAGE

In protein hydrolysates, amino acids to be derivatized are present in hydrochloric acid-containing solutions. Thus, after evaporating the excess of HCl acid, the samples are ready for derivatization.

Free amino acids present mostly in biological matrices are deprotonated by applying cation-exchange chromatographic clean-up [39], centrifugation [41], ultrafiltration [42] or treatment with sulphosalicylic acid [44,45], completed with centrifugation [45]. Electrochemical detection, with its higher selectivity in comparison with UV detection, makes easier and shortens the preparation of the sample; only mild and simple treatment of the sample with absolute ethanol is needed prior to derivatization [43].

2.1. Derivatization reaction

The derivatization reaction consists of two steps. The first, known as the redrying or coupling step, is performed under alkaline condi-

tions, in order to eliminate the last traces of water and to ensure that the amino groups of acids are in the "free" condition. The mainly used "coupling buffers" [1–4,6–10,12–25,27–30,32–37] contain ethanol–water–triethylamine (2:2:1, v/v/v) or (in other papers [5,11,26, 31]) acetonitrile–pyridine–triethylamine–water (10:5:2:3, v/v).

The second step, the real derivatization with phenyl isothiocyanate (PITC), is a very simple, fast and quantitative reaction requiring 5 min at ambient temperature; to be on the safe side, the suggested reaction time is 20 min. The composition of the mainly used reagent, following the coupling step with ethanol–water–triethylamine, is ethanol–triethylamine–water–PITC (7:1:1:1, v/v), and in other proposals [5,11,26,31] PITC is added to the above pyridine-containing coupling agent.

The most important and also the most time-consuming step of the derivatization procedure is the removal of the excess of PITC. For this purpose, according to the earlier work [1–6], a high vacuum is needed in supplying the end pressure of <60 mTorr (1 Torr = 133.322 Pa). This special requirement can be comfortably achieved by applying the Waters Pico Tag work station. Most workers use this apparatus as an evaporator in PTC derivatization; as an oven for protein hydrolysis it suffers from considerable limitations (see Section 2.2).

Later, in order to eliminate the excess of PITC [15,17,37] and those of its substitutes (1-naphthyl isothiocyanate [19] and 4-nitroisothiocyanate [25]), extraction procedures were recommended instead of the high-vacuum conditions, with diethyl ether [15], heptane [17,37], cyclohexane [19] or hexane [25] as extractant. The complete automation of the PTC derivatization procedure with the Varian Model 9095 autosampler also involves an extraction step instead of the high-vacuum removal of PITC.

2.1.1. Storage of derivatives

With regard to the stability of derivatized solid samples, in our experience they can be stored in vacuum-sealed flasks, or even in flasks closed with a ground-glass stopper, in a freezer for at least 6 months without any change; longer storage time are under study in our laboratory.

Regarding the stability of dissolved PTC derivatives, in general, they are considered to be stable compounds. Concerning the exact "lifetime" of the individual PTC amino acids there are contradictory experiences [2,10,14,16,26,27]: the statement that no loss could be detected after 3 days (in the cold) proved to be incorrect [10,16,26]. On keeping the dissolved PTC amino acids at 5–8°C their stability lasted 16 h [10], whereas others [16,26] reported a *ca.* 5% loss after storage for 48 h at 4°C. As a result of an exhaustive study in the author's laboratory [27], in which 21 PTC amino acids, dissolved in 0.05 *M* sodium acetate, were kept in a refrigerator at 4°C and tested immediately after preparation and after 0.5, 7, 18, 26, 44, 73, 102 and 190 h), revealed that the maximum time during which the dissolved derivatives retained their initial amounts was <7 h. After 18 h losses of serine (4%), histidine (7%), alanine (3%), arginine (9%), cyst(e)ine (5%) and ornithine (3%) could be determined. After 190 h the maximum loss for cyst(e)ine (30%), and the minimum loss for hydroxyproline was demonstrated.

2.2. Hydrolysis

It is very well known that hydrolysis is a crucial point in the amino acid analysis of protein hydrolysates: it is the limiting parameter for the reliable preparation of the sample for the chromatographic method. According to Pickering and Newton [65], in a paper entitled "Amino acid hydrolysis: old problems, new solutions", they stated that "With new instrumentation, amino acid hydrolysis is becoming a fast and automated process. But the problems of degradation, conversion, contamination and incomplete hydrolysis must be solved".

Prior to PTC derivatization, as the hydrolysis agent (with the only known exception of methanesulphonic acid (MSA) [13]) hydrochloric acid has been used, partly in the liquid phase and partly in the gas phase. In liquid-phase hydrolysis the acid is added directly to the sample tube, whereas in vapour-phase hydrolysis the dried sample-containing tubes are sealed in a larger vessel containing the acid. The gas-phase hydrolysis methods are regarded as preferable because their use excludes contamination of the

sample by the non-volatile impurities of the acid. When a limited amount of protein-containing sample is available, vapour-phase hydrolysis is the best choice.

2.3. The status of "difficult" amino acids

During hydrolysis, undesirable degradation, conversion and resistance of selected constituents must be taken into account [65,66]. Degradation of tryptophan, methionine, cystine, tyrosine, serine and threonine of >50%, >50%, >30%, >20%, >10% and >5% has been reported; the conversion of asparagine and glutamine to the corresponding acids proved to be quantitative. Because of the resistance of the peptide bonds between Ala–Ala, Val–Val, Ile–Ala and others, their incomplete hydrolysis necessitates a prolonged hydrolysis time. A number of remedies for the above phenomena have been proposed [67–79].

2.3.1. Tryptophan

For the determination of tryptophan [67–76], hydrolyses by alkali [67,68], by sulphur-containing organic acids [13,69–71] and by hydrochloric acid + additives [72–76] have been proposed. Alkaline hydrolyses (performed with NaOH [67], $Ba(OH)_2$ [67–68] or LiOH [68]), being extremely laborious and providing the quantification of tryptophan only, with an 80–90% recovery of the theoretical value, can be regarded as the worst solution to the problem. Sulphur-containing organic acids (non-volatile compounds such as *p*-toluenesulphonic acid [69], methanesulphonic acid [13,70] and mercaptoethanesulphonic acid [71]) lead to a number of shortcomings in the subsequent derivatization and chromatographic separation of the acids in hydrolysates. The most promising procedures are the classical hydrochloric acid hydrolyses in the presence of additives (thioglycolic acid [72], phenol [73], β-mercaptoethanol [74], ethanedithiol [75], thioglycolic acid + trifluoroacetic acid + indole [76] and tryptamine [28,29], providing the quantification of tryptophan simultaneously with all other amino acids; of the suggested additives, only the last two [28,29,76] proved to be satisfactory in vapour-phase hydrolyses.

Applying the combined additives [76], a >75% tryptophan yield from lysozyme, myoglobin and papain, monitored by conventional IEC, has been reported. Performing vapour-phase hydrolysis in the presence of tryptamine, with subsequent PITC derivatization, a >80% tryptophan recovery could be obtained, measured with different hydrolysis parameters, with a number of proteins and without any disturbing effect on the determination of the other amino acids [28,29]. The same results were achieved in vapour-phase hydrolysis in the author's laboratory using a CEM MDS-2000 microwave system with a protein hydrolysis accessory set (160°C, 110 psi, 65% power) (data will be presented at the 9th Danube Symposium on Chromatography, Budapest, Hungary, August 23rd–27th, 1993).

2.3.2. Cystine/cysteine

The determination of cystine/cysteine as their PTC derivatives proved to be an extremely complex problem, and in many papers this determination is not considered [30]. In those cases where it is also necessary to know the amount of cyst(e)ine, mainly the classical performic acid oxidation is applied, as detailed recently [61]. As a result of a 16-h reaction time, storing the tubes in an ice-bath at 5°C in a refrigerator, from cystine and cysteine the same product, *i.e.*, cysteic acid, and from methionine methionine sulphone are formed. The common, but very time-consuming and tedious (involving multiple reaction steps) procedure, suffers from a number of limitations [61,65]. With complex protein matrices, the performic acid oxidation results in substantial destruction of histidine (25%) and tyrosine (87%). Therefore, if cyst(e)ine, histidine and tyrosine determinations are required simultaneously, two separate hydrolyses need to be performed [61], with and without performic acid oxidation. Further possibilities for the determination total of cystine and cysteine, after reductive alkylation, in the form of the PTC derivatives of carboxymethylcysteine [16,77], pyridylethylcysteine [78] and sulphopropylcysteine [79] have been reported.

Our study (partly published [30] and discussed

[80], and partly to be presented very shortly) on the individual determination of all six possible racemates (L-, D- and DL-cystine and -cysteine) demonstrated that (i) the interaction of all six racemates and PITC results in two main and two trace PTC derivatives and the ratios of the derivatives are characteristic of the initial compound; and (ii) the total molar responses of the two main PTC derivatives are the same before and after hydrolysis and are independent of the original racemate form of cyst(e)ines. Thus, if the elution procedure permits the separation of the two main derivatives (their elution should be ensured by the gradient programme generally to be before isoleucine), the determination of the total cyst(e)ine does not need any previous pretreatment. The utility of this approach has been shown by the determination of the cyst(e)ine content in the hydrolysates of various proteins [30].

2.3.3. *Glutamine, asparagine*

Under hydrolysis conditions the glutamine and asparagine contents of proteins will be converted quantitatively into the corresponding acids. Thus, the PTC derivatives of aspartic and glutamic acid represent the total of the corresponding free acids and acid amides, respectively.

The treatment of several proteins with [bis-(trifluoroacetoxy)iodo]benzene (BTI) showed a possible way to determine separately their asparagine and glutamine contents through the determination of their corresponding 2,3-diaminopropionic and 2,4-diaminobutyric acids [32]. A rapid and quantitative conversion (30 min, 100%) has been reported for glutamine, but the reaction of asparagine could not be completed (2 h, 65%).

2.4. *Applicability to non-protein compounds*

Selected applications of the PTC derivatization of non-protein compounds [48–56] revealed without exception that these components did not need extra derivatization conditions. Only the elution parameters had to be adjusted to the separation of the particular derivatives present.

3. CHROMATOGRAPHIC CONDITIONS

This compilation contains various proposals given in selected papers cited above. The main differences regarding the size and filling of columns, the composition and pH values of eluents, the time of elution, and the number of components separated are presented (Table 1).

3.1. *Columns*

Table 1 indicates that the most advantageous conditions (short elution time, separation of the maximum number of amino acids) can be obtained by the use of the Waters Pico-Tag columns with any length (column filling of 3-μm particle size). A short column (15 cm × 3.9 mm I.D.) provides the resolution of 18 amino acids in 12 min [2,4,6,8,13–15,32], whereas on a longer column 29 amino acids have been determined in 20 min [16]. For laboratories with limited means even non-special columns can give results [27–30]. In our laboratory, two packings have been tested, and both proved to be satisfactory (for details, see Section 3.2).

3.2. *Eluents, gradient programmes*

The composition and pH of the eluents and the gradient programme have a considerable impact on the optimum resolution of the PTC amino acids in general and, in particular, on the "hardly" separable PTC derivatives such as those of histidine, threonine, alanine, proline and arginine, or phenylalanine and ammonia or ornithine and tryptophan. In order to overcome the poor resolution of these components, the use of a gradient programme with eluents [5], triethylamine (TEA) as an additive to eluent A, in different concentrations, and/or the optimization of the pH of the eluent for any given working conditions have been advised. In work at Waters, TEA has been applied in a small amount (0.05 ml/l [16] and 0.5 ml/l [2,4,6,8,13–15,32]), and its beneficial effect also up to 2.5 ml/l has been reported [11].

In our studies [27] (i) carried out with two different columns (Hypersil ODS bonded phase, Nucleosil 5 C_{18}, 5 μm), (ii) performed in parallel

TABLE 1

HPLC CONDITIONS SUGGESTED FOR THE ANALYSIS OF PTC AMINO ACIDS

Column (cm × mm I.D.)	Particle size (μm)	Product of	pH	Temperature (°C)	Eluents[a]		No. of amino acids measured	Analysis time (min)[b]	Ref.
					A	B			
15 × 3.9	3	Waters, Pico Tag	6.4	38	0.14 *M* NaOAc + 0.5 ml/l TEA	ACN–H_2O (6:4)	18	12	2, 4, 6, 8, 13–15, 32
25 × 4.6	5	IBM, DuPont, Altex	6.8	52	0.1 *M* NH_4OAc	ACN–MeOH–H_2O (44:10:46 and others)	16	35	5, 35
25 × 4.6	5	Waters, Pico Tag and others	6.4	46	0.7 *M* NaOAc + 2.5 ml/l TEA	H_2O; C = ACN–H_2O (80:20)	23	30	10
10 × 4.6	3	Thomson Instrument, Newark, DE	6.4 6.4	36	0.5 *M* NaOAc + 2.25 ml/l TEA	Solvent A: ACN–MeOH (5:4:1)	17	20	11
30 × 3.9	3	Pico Tag	6.4	40	0.14 *M* NaOAc + ACN (60 ml/l) + TEA (0.5 ml/l) + EDTA (1 ml of 10 m*M*)	ACN–H_2O (8:2)	16	25	17
15 × 3.9	3	Waters, Pico Tag	6.4	?	0.14 *M* NaOAc–ACN (9.4:0.6) + 0.05 ml/l TEA	ACN–H_2O (6:4)	18	14	39
15 × 3.9	3	Waters, Pico Tag	5.7	33	0.14 *M* NaOAc + 0.7 ml/l TEA	ACN–H_2O (6:4)	20	16	62
30 × 3.9	?	Waters, Pico Tag	6.4	46	0.14 *M* NaOAc–ACN (9.4:0.6) + 0.05 ml/l TEA	ACN–H_2O (6:4)	29	20	16, 17
25 × 4.6	5	Hypersil (?)	6.5	55	0.15 *M* NaOAc	ACN	16	20	31
25 × 4.6	5	Dynamex C_{18} (Rainin, Emeryville, CA, USA)	5.7	45	0.1 *M* NaOAc + 0.5 ml/l TEA	ACN–H_2O (6:4)	18	45	41
25 × 4.6	5	Hypersil (Jones, Hengoed, UK)	6.4	?	0.01 *M* NaOAc	0.01 *M* NaOAc–ACN (6:4)	17	60	43
25 × 4.6	5	Vydac C_{18} (?)	5.0–6.8	40–60	0.05 *M* NH_4OAc	0.023 *M* NH_4OAc–ACN–H_2O (44:46:10)	17	50	26
12.5 × 4.6 + 10 × 4.0 (guard column)	3	Spherisorb ODS	6.8	37	0.0125 *M* Na phosphate	ACN–0.0125 *M* Na phosphate (6:4)	21	25	36
15 × 4.0	5	Micro Pak SP-C_{18}	4.8	?	NaOAc (conc. ?)	ACN–NaOAc (conc. ?) (7:3)	18	20	37
15 × 4.6	5	Hypersil (Shandon)	7.2	Ambient	0.05 M NaOAc or	0.1 *M* NaOAc (NH_4OAc)–			
2 × 2.6 (guard column)		Nucleosil (Macherey–Nagel)			0.05 *M* NH_4OAc	ACN–MeOH (46:44:10)	21	22	27, 30

[a] ACN = acetonitrile; MeOH = methanol; TEA = triethylamine; NaOAc = sodium acetate; NH_4OAc = ammonium acetate.

[b] Time from injection to elution of the last PTC derivative.

with sodium and ammonium salt-containing eluents of six pH values (5.6, 6.0, 6.4, 6.8, 7.2 and 7.6) and (iii) completed by TEA for eluent A of pH 7.2 in various concentrations (0.005, 0.05, 1, 2, 3 and 4 ml/l), the following results were obtained. (i) Concerning the two types of columns, under strictly identical elution conditions, no differences were found. (ii) The studies with eluents of lower pH, *i.e.* <7, showed disadvantageous changes; the retention times of the first nine components, eluting in the order aspartic acid, glutamic acid, hydroxyproline, serine, glycine, histidine, threonine, alanine and proline, increase in parallel with decreasing pH of the eluent, becoming increasingly closer to each other. At pH 7.2 and 7.6 optimum resolution could be obtained for the 21 PTC amino acids. Thus, in order to ensure a longer column lifetime, as the working pH a lower value of 7.2 was chosen. (iii) The effect of the presence of TEA proved to be of secondary importance. Although its presence increased the detector response of cyst(e)ine by 5–10%, at the same time the proline and arginine peaks became inseparable.

With regard to the column lifetime, in contrast to literature data [37], we have excellent experiences with both columns: on a 15 cm × 4.6 mm I.D. column filled with Hypersil, completed by a 2-cm long guard column, more than 1000 injections have been performed and it is still in satisfactory condition (the guard columns had to be changed after 50–150 injections, depending on the sample).

3.3. Quantification conditions

The reliability, repeatability and reproducibility of the determination of PTC amino acids are unambiguously accepted in the literature. Concerning the linearity of the detector responses and the statistical errors of measurements, different data can be found [13,14,16,22,27–30,34,36]. Linear detector responses have been reported with an error of <1.6% (R.S.D.) in wide concentration ranges: 20–500 pmol [14], 10–2000 pmol [13] and 10–5000 pmol [16]. These, excellent results were obtained with the use of Pico Tag columns [13,14,16]. Others [22,27–30,34,36], probably owing to the use of various, but not the special Pico Tag columns, reported higher error values, even in higher concentration ranges (R.S.D. <6.1% for 50–1000 pmol), while at the lower levels much higher error values were given [22] (R.S.D. 10% and 20% for 20 and 10 pmol, respectively).

4. ACKNOWLEDGEMENT

This work was supported by the Hungarian Academy of Sciences (Project No. OTKA I/3 2284 and I/4, T5053).

REFERENCES

1 D.R. Koop, E.T. Morgan, G.E. Tarr and M.J. Coon, *J. Biol. Chem.*, 257 (1982) 847.
2 B.A. Bidlingmeyer, S.A. Cohen and T.L. Tarvin, *J. Chromatogr.*, 336 (1984) 93–104.
3 T.H. Maugh, II, *Science*, 225 (1984) 42.
4 S.A. Cohen, T.L. Tarvin and B.A. Bidlingmeyer, *Am. Lab.*, 8 (1984) 49–51.
5 R.L. Heinrikson and S.C. Meredith, *Anal. Biochem.*, 136 (1984) 65–74.
6 S.A. Cohen, *BioTechniques*, 2 (1984) 273–275.
7 R.R. Granberg, *LC Mag.*, 2 (1984) 776, 778 and 780.
8 C.Y. Yang and F.I. Sepulveda, *Chromatographia*, 346 (1985) 413–416.
9 H. Scholze, *J. Chromatogr.*, 350 (1985) 453–460.
10 P.S.L. Janssen, J.W. van Nispen, P.A.T.A. Melgers, H.W.M. van den Bogaart, R.L.A.E. Hamelinck and B.C. Goverde, *Chromatographia*, 22 (1986) 345–350.
11 R.F. Ebert, *Anal. Biochem.*, 154 (1986) 431–435.
12 H.P.J. Bennett and S. Solomon, *J. Chromatogr.*, 359 (1986) 221–230.
13 S.A. Cohen, B.A. Bidlingmeyer and T.L. Tarvin, *Nature*, 320 (1986) 769–770.
14 B.A. Bidlingmeyer, T.L. Tarvin and S.A. Cohen, in K.A. Walsh (Editor), *Methods in Protein Sequence Analysis*, Humana Press, 1987, pp. 229–245.
15 J.L. Tedesco and R. Schafer, *J. Chromatogr.*, 403 (1987) 299–306.
16 S.A. Cohen and D.J. Strydom, *Anal. Biochem.*, 174 (1988) 1–16.
17 A.S. Inglis, N.A. Bartone and J.R. Finlayson, *J. Biochem. Biophys. Methods*, 15 (1988) 249–254.
18 K. Xu, S. Hao, G. Sur and L. Zhang, *Yaowu Fenxi Zazhi*, 8 (1988) 283–287.
19 A. Neidle, B.S. Miriam, S. Sacks and D.S. Dunlop, *Anal. Biochem.*, 180 (1989) 291–297.
20 B.C. Pramanik, C.R. Moomaw, C.T. Evans, S.A. Cohen and C.A. Slaughter, *Anal. Biochem.*, 176 (1989) 269–277.

21 F.E. Romantsev and V.N. Prozorovskii, *Zh. Anal. Khim.*, 44 (1989) 1100–1104.
22 D. Adherton, *Tech. Protein Chem.*, (1989) 273–283.
23 D.R. Dupont, P.S. Kelin and A.H. Chui, *Tech. Protein Chem.*, (1989) 284–294.
24 K.A. West and J.W. Crabb, *Tech. Protein Chem.*, (1989) 295–304.
25 S.A. Cohen, *J. Chromatogr.*, 512 (1990) 283–290.
26 A. Guitart, P.H. Orte and J. Cacho, *Analyst*, 116 (1991) 399–403.
27 M. Morvai, V. Fábián and I. Molnár-Perl, *J. Chromatogr.*, 600 (1992) 87–92.
28 I. Molnár-Perl, M. Pintér-Szakács and M. Khalifa, *J. Chromatogr.*, 632 (1993) 57–61.
29 I. Molnár-Perl and M. Khalifa, *Chromatographia*, 36 (1993) 43–46.
30 I. Molnár-Perl and M. Morvai, *Chromatographia*, 34 (1992) 132–136.
31 R. Mora, K.D. Berndt, H. Tsai and S.C. Meredith, *Anal. Biochem.*, 172 (1988) 368–376.
32 D. Fouques and J. Landry, *Analyst*, 116 (1991) 529–531.
33 T. Bergman, M. Carlquist and H. Joernvall, *Adv. Methods Protein Microsequence Anal.*, (1986) 45–55.
34 J.A. Saunders, J.M. Saunders, S. Morris and S.A. Wynne, *Chromatogram*, 9 (1988) 2–4.
35 G. McClung and W.T. Frankenberger, Jr., *J. Liq. Chromatogr.*, 11 (1988) 613–646.
36 P. Furst, L. Pollack, T.A. Graser, H. Godel and P. Stehle, *J. Chromatogr.*, 499 (1990) 557–569.
37 F. Lai, A. Mayer and T. Sheehan, *BioTechniques*, 11 (1991) 236–243.
38 P. Rasquin, R.J. Early and R.O. Ball, *Spectra 2000*, 126 (1987) 27–30.
39 L. Robitaille and L.J. Hoffer, *Can. J. Physiol. Pharmacol.*, 66 (1988) 613–617.
40 B.L. Rosenlund, *J. Chromatogr.*, 529 (1990) 258–262.
41 S. Gunawan, N.Y. Walton and D.M. Treiman, *J. Chromatogr.*, 503 (1990) 177–187.
42 B.L. Rosenlund, *J. Chromatogr.*, 529 (1990) 258–262.
43 R.A. Sherwood, A.C. Titheradge and D.A. Richards, *J. Chromatogr.*, 528 (1990) 293–303.
44 Q. Xia and G. Wu, *Shengwu Huaxue Yu Shengwu Wuli Xuebao*, 21 (1989) 465–469.
45 V. Fierabracci, P. Masiello, M. Novelli and E. Bergamini, *J. Chromatogr.*, 570 (1991) 285–291.
46 A.S. Feste, *J. Chromatogr.*, 574 (1992) 23–34.
47 J. Siebert, R.J. Palmer and P. Hirsch, *Appl. Environ. Microbiol.*, 57 (1991) 879–881.
48 M. Sato, S. Suzuki, Y. Yasuda, H. Kawauchi, N. Kanno and Y. Sato, *Anal. Biochem.*, 174 (1988) 623–627.
49 R. Gupta and N. Jentoft, *J. Chromatogr.*, 474 (1989) 411–417.
50 M.M.T. O'Hare, O. Tortora, U. Gether, H.V. Nielsen and T.W. Schwartz, *J. Chromatogr.*, 389 (1987) 379–388.
51 V. Semensi and M. Sugumaran, *LC·GC*, 4 (1986) 1108–1110.
52 D.J. Walton and J.D. McPherson, *Anal. Biochem.*, 164 (1987) 547–553.
53 P.R. Young and F. Grynspan, *J. Chromatogr.*, 421 (1987) 130–135.
54 M. Raghavan, C.K. Smith and C.E. Schutt, *Anal. Biochem.*, 178 (1989) 194–197.
55 E. Tarcsa and L. Fesus, *Anal. Biochem.*, 186 (1990) 135–140.
56 D.E.H. Palladino, R.M. House and K.A. Cohen, *J. Chromatogr.*, 599 (1992) 3–11.
57 D. Lanneluc-Sanson, C.T. Phan and R.L. Granger, *Anal. Biochem.*, 155 (1986) 322–327.
58 R.M. Marce, M. Calull, J. Guasch and F. Borrull, *Am. J. Enol. Vitic.*, 40 (1989) 194–198.
59 M. Calull, J. Fabregas, R.M. Marce and F. Borrull, *Chromatographia*, 31 (1991) 272–276.
60 J.A. White, R.J. Hart and J.C. Fry, *J. Autom. Chem.*, 8 (1986) 170–177.
61 S.R. Hagen, B. Frost and J. Augustin, *J. Assoc. Off. Anal. Chem.*, 72 (1989) 912–916.
62 R.G. Elkin and A.M. Wasynczuk, *Cereal Chem.*, 64 (1987) 226–229.
63 G. Sarwar, H.G. Botting and R.W. Peace, *J. Assoc. Off. Anal. Chem.*, 71 (1988) 1172–1175.
64 *Pico Tag Work Station Operator's Manual*, No. 86746, Millipore, Waters Chromatography, Milford, MA, 1988, Revision C.
65 M.V. Pickering and P. Newton, *LC·GC Int.*, 3 (1992) 22–26.
66 C.W. Gehrke, L.L. Wall, J.S. Absheer, F.E. Kaiser and R.W. Zumwalt, *J. Assoc. Off. Anal. Chem.*, 68 (1985) 811–821.
67 S. Delhaye and J. Landry, *Analyst*, 117 (1992) 1875–1877.
68 J. Landry and S. Delhaye, *J. Sci. Food Agric.*, 58 (1992) 439–441.
69 T.Y. Liu and Y.H. Chang, *J. Biol. Chem.*, 246 (1971) 2842–2848.
70 R.J. Simpson, M.R. Neuberger and T.Y. Liu, *J. Biol. Chem.*, 251 (1976) 1936–1940.
71 B. Penke, R. Ferenczi and K. Kovács, *Anal. Biochem.*, 60 (1974) 45–50.
72 R.B. Ashworth, *J. Assoc. Off. Anal. Chem.*, 70 (1987) 80–85.
73 K. Muramoto and H. Kamiya, *Anal. Biochem.*, 189 (1990) 223–230.
74 L.T. Ng, A. Pascaud and M. Pascaud, *Anal. Biochem.*, 167 (1987) 47–52.
75 P. Felker, *Anal. Biochem.*, 76 (1976) 192–213.
76 H. Yano, K. Aso and A. Tsugita, *J. Biochem.*, 108 (1990) 579–582.
77 P.S.L. Janssen, J.W. van Nispen, P.A.T.A. Melgers, H.W.M. van den Bogaart, T.L.A.E. Hamelinck and B.C. Goverde, *Chromatographia*, 22 (1986) 351–357.
78 K. Okazaki, T. Imoto and H. Yamada, *Anal. Biochem.*, 145 (1985) 87–90.
79 U.T. Ruegg and J. Rudinger, *Methods Enzymol.*, 47 (1977) 116–122.
80 I. Molnár-Perl, *Chromatographia*, 35 (1993) 345–346.

Journal of Chromatography A, 661 (1994) 51–54
Elsevier Science B.V., Amsterdam

CHROMSYMP. 2966

Ligand-exchange high-performance liquid chromatography of fluorine-containing phenylglycine and phenylalanine

S.V. Galushko*, I.P. Shishkina and V.A. Soloshonok

Institute of Bioorganic Chemistry and Oil Chemistry, Academy of Sciences of the Ukraine, 253660 Kiev-94 (Ukraine)

ABSTRACT

The relationships between the number of fluorine atoms, their position in the aromatic ring of fluorine-containing phenylglycine and phenylalanine and the selectivity of the separation of enantiomers on Chiral ProCu, Chiral ValCu and Chiral-1 (hydroxyproline) columns were studied. Optimum conditions for the separation of enantiomers were established.

INTRODUCTION

The replacement of hydrogen atoms by fluorine atoms in natural compounds in general and amino acids in particular is a very useful approach in the design of biologically active compounds [1].

Fluorine analogues of amino acids have high biological activity depending on the absolute configuration of the molecule. High-performance liquid chromatography (HPLC) has been used successfully to separate the enantiomers of fluoroamino acids, but only a few data concerning the effect of replacement of hydrogen atoms in molecules of amino acids by fluorine atoms on the retention and selectivity of the separation of enantiomers on chiral sorbents have been reported. The relationship between the number of fluorine atoms and the retention of enantiomers of alanine derivatives on different chiral columns has been studied [2]. The separation of some aromatic fluoroamino acids by ligand-exchange chromatography (LEC) has been described [3]. It has been shown that the introduction of fluorine atoms into the *ortho* and *para* positions of the phenyl ring has little effect on the capacity factors and the selectivity of separation of phenylserine isomers [4].

The aim of this work was to separate the enantiomers of different fluoro derivatives of phenylalanine and phenylglycine and to compare the selectivity of the separation of the enantiomers on different chiral sorbents.

EXPERIMENTAL

Chromatographic conditions

The experiments were performed on an LKB (Bromma, Sweden) liquid chromatographic system consisting of a Model 2150 HPLC pump, a Model 7410 injector, a Model 2140 rapid spectral detector set at 235 nm, a Model 2200 recording integrator and a Model 2155 column oven.

The columns used were (I) Chiral ProCu=Si100, (II) Chiral ValCu=Si100, both 5 μm (250 × 4.6 mm I.D.) (Serva, Heidelberg, Germany) and (III) Nucleosil Chiral-1, 5 μm (250 × 4.6 mm I.D.) (Macherey–Nagel, Düren, Germany). The mobile phases were 2–5 m*M*

* Corresponding author.

0021-9673/94/$07.00
SSDI 0021-9673(93)E1109-D

copper(II) sulphate solutions at a flow-rate of 0.75 ml/min.

Materials

Racemic fluorine-containing phenylglycines and phenylalanines were purchased from Fluka (Buchs, Switzerland). Individual enantiomers of fluorine-containing phenylglycines were prepared by biocatalytic separation of their corresponding racemic N-phenylacetyl derivatives [5], and enantiopure fluorinated phenylalanines were prepared by asymmetric synthesis using chiral nucleophylic glycine template [6].

Copper(II) sulphate was of analytical-reagent grade. Water was doubly distilled and filtered before HPLC use.

RESULTS AND DISCUSSION

The selectivity of the separation of the enantiomers of phenylalanine (Phe) and phenylglycine (PhGly) derivatives depends substantially on the structures of both the ligand and the enantiomers being separated (Table I). As can be seen from Table I, the introduction of a fluorine atom into the *ortho* position of the aromatic ring of PhGly increases the selectivity of enantiomer separation on all the sorbents studied. The introduction of a fluorine atom in the *meta* and *para* positions of PhGly leads to a considerable decrease in the selectivity of separation of enantiomers on column III and to a complete loss of selectivity on column I. Addition of methanol to the mobile phase (0–30%, v/v) has only a slight effect on the selectivity of enantiomer separation but leads to an appreciable increase in efficiency. Columns II and III allow the complete separation of enantiomers of fluoro derivatives of PhGly with a mobile phase containing 2.5–5 m*M* copper(II) sulphate (Fig. 1a and b) and 0–20% (v/v) methanol.

The introduction of a methylene group into the molecule on going from PhGly to Phe derivatives results in a significant increase in capacity factors (Table I). In this case the maximum selectivity can be achieved on column I. It should be noted that the replacement of one hydrogen atom by a fluorine atom in any position on the phenyl ring of Phe derivatives hardly affects the selectivity of separation of enantiomers (Table I). The replacement of hydrogen by two and five atoms of fluorine in the aromatic ring results in a decrease in retention of the enantiomers on columns I and II. An increase in the number of fluorine atoms in the aromatic ring affects differently the selectivity of separation of enantiomers. For column I the introduction of each F atom into the molecule of Phe

TABLE I

SEPARATION OF AROMATIC FLUORINE-CONTAINING AMINO ACIDS

$n = 4$. For k' and α values, S.D. = 0.2 and 0.1 respectively; $r = 0.987$.

Compounds	Column I		Column II		Column III	
	k'_L	α	k'_L	α	k'_L	α
4F-DL-α-PhGly	2.1	1.0	2.5	1.2	0.9	1.8
3F-DL-α-PhGly	1.9	1.0	2.2	1.2	0.9	1.8
2F-DL-α-PhGly	2.4	1.3	2.7	1.4	0.9	2.8
DL-α-PhGly	2.3	1.1	2.7	1.2	0.8	2.4
4F-DL-α-Phe	4.8	2.3	4.6	1.5	1.3	1.6
3F-DL-α-Phe	5.1	2.0	4.6	1.4	1.5	1.6
2F-DL-α-Phe	5.3	2.0	4.6	1.3	1.6	1.5
DL-α-Phe	4.6	2.3	3.6	1.3	1.4	1.6
$3CF_3$-DL-α-Phe	6.2	2.2	4.8	1.4	2.3	2.0
3-Di-F-DL-α-Phe	4.4	1.9	3.7	1.7	1.7	1.7
1,2,3,4,5-Penta-F-DL-α-Phe	2.3	1.2	2.7	1.2	1.5	1.6

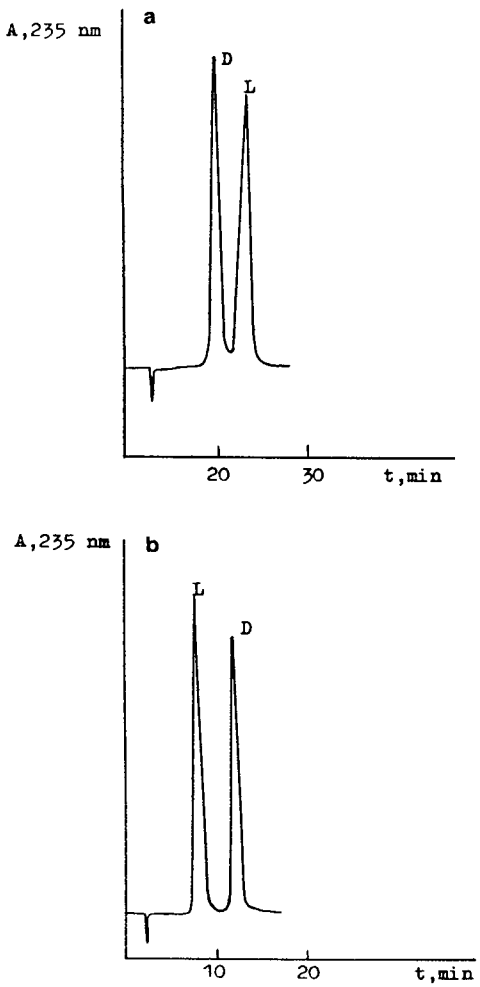

Fig. 1. Separation of enantiomers of (a) 4-fluoro-DL-α-phenylglycine and (b) 3-fluoro-DL-α-phenylglycine. Mobile phase, 5.0 m*M* $CuSO_4$; flow-rate, 0.75 ml/min; temperature, 35°C; detection wavelength, 235 nm. Column: (a) Chiral ValCu, 5 μm (250 × 4.6 mm I.D.); (b) Nucleosil Chiral-1, 5 μm (250 × 4.0 mm I.D.).

leads to a decrease in the selectivity of separation of 0.2, whereas for column III no effect is observed (Fig. 2). It has been found that a CF_3 group in the α-position in Phe exerts a considerable influence on both the retention and the selectivity of the separation of enantiomers [7]. Introduction of a CF_3 group into the phenyl ring of Phe has little effect on the retention and selectivity. It seems that only a slight interaction occurs between the CF_3 group in a *meta* position

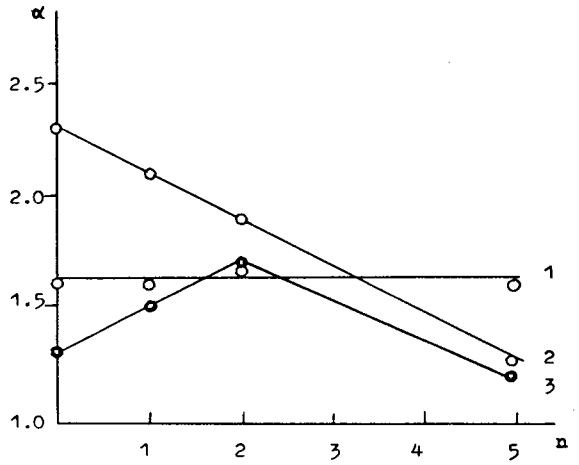

Fig. 2. Effect of the number of fluorine atoms in the molecule of phenylalanine (*n*) on selectivity of enantiomer separations (α). Column: 1 = Nucleosil Chiral-1, 5 μm (250 × 4.0 mm I.D.); 2 = Chiral ProCu, 5 μm (250 × 4.6 mm I.D.); 3 = Chiral ValCu, 5 μm (250 × 4.6 mm I.D.).

on the phenyl ring of Phe and the surface ligand of the sorbent.

A mobile phase containing 2.5–5 m*M* copper(II) sulphate and 0–20% (v/v) methanol is optimum for separating fluoro derivatives of phenylalanine (Fig. 3).

CONCLUSIONS

The replacement of hydrogen atoms with fluorine atoms in the aromatic ring affects the

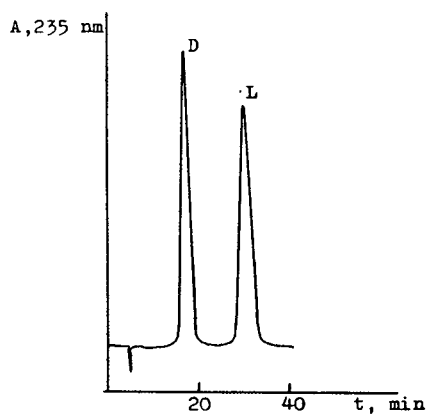

Fig. 3. Separation of enantiomers of 2-fluoro-DL-α-phenylalanine. Column, Chiral ProCu, 5 μm (250 × 4.6 mm I.D.); eluent and conditions as in Fig. 1.

selectivity of separation of enantiomers to a greater extent for phenylglycine derivatives than for phenylalanine derivatives.

Chiral ProCu=Si100 is to be preferred for the separation of monosubstituted derivatives of phenylalanine.

A Nucleosil Chiral-1 (hydroxyproline) column is to be preferred for the separation of monosubstituted derivatives of phenylglycine and pentafluoro derivatives of phenylalanine.

All columns studied have similar possibilities for the separation of enantiomers of 2,6-difluoro derivatives of phenylalanine.

REFERENCES

1 J.T. Welch, *Flourine in Bioorganic Chemistry*, Wiley, New York, 1991.
2 S.V. Galushko, I.P. Shishkina, I.I. Gerus and M.T. Kolycheva, *J. Chromatogr.*, 600 (1992) 83.
3 J.R. Gerson and M.I. Adam, *J. Chromatogr.*, 325 (1985) 103.
4 S.V. Galushko, I.P. Shishkina and V.A. Soloshonok, *J. Chromatogr.*, 592 (1990) 345.
5 V.F. Soloshonok, I.Yu. Galaev, V.G. Svedas, E.V. Kozlova, U.V. Kotik, I.P. Shishkina, S.V. Galushko, A.V. Rozhenko and V.P. Kukhar, *Bioorg. Khim.* 19 (1993) 103.
6 V.P. Kukhar, Yu.N. Belokon', V.A. Soloshonok, N.A. Svistunova, A.V. Rozhenko and N.A. Kuz'mina, *Synthesis*, 1 (1993) 117.
7 S.V. Galushko, I.P. Shishkina, V.A. Soloshonok and V.P. Kukhar, *J. Chromatogr.*, 511 (1990) 115.

Journal of Chromatography A, 661 (1994) 55–60
Elsevier Science B.V., Amsterdam

CHROMSYMP. 2896

Liquid chromatographic–mass spectrometric studies on the enzymatic degradation of gonadotropin-releasing hormone

M. Brudel, U. Kertscher, H. Berger and B. Mehlis*

Institute of Molecular Pharmacology, A.-Kowalke-Strasse 4, D-10315 Berlin (Germany)

ABSTRACT

Gonadotropin-releasing hormone (GnRH) derivatives are used in cancer therapy, but relatively little is known about their metabolic fate in the organism. This paper describes the application of high-performance liquid chromatography combined with electrospray mass spectrometry to identify the degradation products resulting from the incubation of two GnRH analogues, D-Phe^6–GnRH and DSer(OtBu)^6–desGly^{10}–GnRH–ethylamide (buserelin) with rat kidney membranes. Reversed-phase columns were applied with gradient elution using a flow-rate of *ca.* 2 μl/min to the mass spectrometer. Post- and precolumn stream splitting were employed to adjust the flow-rates for columns of 2 and 0.32 mm I.D. The pattern of peptide degradation products obtained with this method indicates that a defined proteolytic membrane enzyme system is responsible for these catabolic processes.

INTRODUCTION

Gonadotropin-releasing hormone (GnRH) derivatives are used in cancer therapy, but relatively little is known about their metabolic fate in the organism [1–3]. To increase their stability against proteolytic degradation and their biological activity, these synthetic "superactive" analogues have D-amino acids substituted for glycine in position 6 of the GnRH peptide chain (Fig. 1). Some analogues are additionally modified at the C-terminus of the peptide chain (*e.g.*, buserelin). Although stabilized in this way, these peptide analogues are known to be extensively degraded in the organism and thus inactivated.

pGlu-His-Trp-Ser-Tyr-Gly-Leu-Arg-Pro-GlyNH$_2$ (1 2 3 4 5 6 7 8 9 10) — GnRH, natural sequence

pGlu-His-Trp-Ser-Tyr-D-Phe-Leu-Arg-Pro-GlyNH$_2$ (1 3 6 10) — D-Phe^6-GnRH (PG)

pGlu-His-Trp-Ser-Tyr-D-Ser(OtBu)-Leu-Arg-Pro-NHEt (1 3 6 9) — Buserelin (SG)

Fig. 1. GnRH and analogues studied.

Recently, the kidney has been identified as the organ with special relevance concerning the pharmacokinetic fate of GnRH analogues [4]. In an attempt to minimize *in vivo* studies, we were able to demonstrate a close correlation between experiments with GnRH analogues in rats and with rat kidney membranes. Therefore, degradation experiments in this study were carried out by incubation of GnRH analogues with rat kidney membranes. Two GnRH analogues, D-Phe^6–GnRH and D-Ser(OtBu)^6–desGly^{10}–GnRH–ethylamide (buserelin) (where tBu = *tert.*-butyl), were used as representative molecules of the two types of superactive analogues mentioned above (Fig. 1). The objectives of this study were (i) to obtain more information on the pattern of degradation products of these peptides, (ii) to investigate the feasibility of on-line LC–MS experiments for this problem and (iii) a comparison of HPLC columns of 2 and 0.32 I.D. using stream splitting.

* Corresponding author.

0021-9673/94/$07.00
SSDI 0021-9673(93)E0830-N

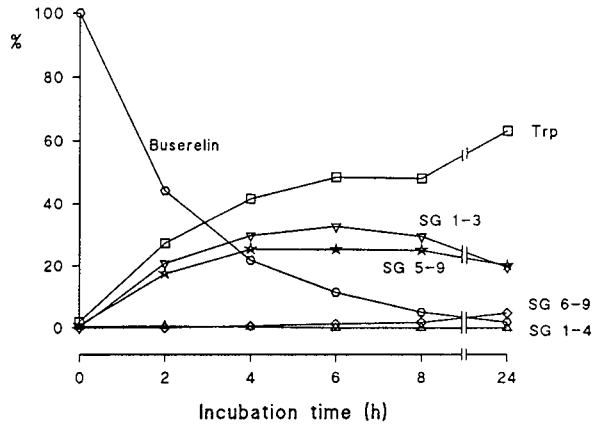

Fig. 2. Time course of the degradation of buserelin by rat kidney membranes and resulting degradation products measured by relative $[(Q/P)\cdot 100]$ chromatographic peak areas (UV detection at 215 nm; P = peak area of buserelin at zero time and Q = peak area at the corresponding incubation time).

LC–MS, especially with fast atom bombardment ionization, has already been applied for the study of peptide proteolysis [5,6]. We used electrospray ionization (ESI) mass spectrometry [7], which is a relatively new technique with great potential for this purpose. We report here the unambiguous identification of the degradation products of the two GnRH analogues produced by a selective enzyme system of the kidney membranes. The kinetics of the metabolites (Fig. 2) were also studied, but will be reported in detail in a separate publication.

EXPERIMENTAL

Materials

The peptides D-Phe^6–GnRH and buserelin and their partial sequences were obtained from Berlin-Chemie (Berlin, Germany) and Hoechst (Frankfurt, Germany), respectively. Trifluoroacetic acid (TFA) of HPLC gradient grade was obtained from Baker (Gross-Gerau, Germany). Acetonitrile (MeCN) of HPLC gradient grade and all other chemicals were purchased from Merck (Darmstadt, Germany).

Incubation and sample preparation

Membrane fractions of rat kidney were prepared as described previously [4] and incubated with 10–30 nmol/ml of peptide at 37°C in 20 m*M* phosphate or Tris buffer (pH 7.4) (100 m*M* NaCl, 0.1 mg/ml human serum albumin, *ca.* 20 mg kidney membrane per millilitre). Samples were taken at time intervals, the reaction stopped by heating and the samples were frozen at −20°C. In the off-line mode these samples were thawed, the peptides were adsorbed on C_{18} cartridges, eluted with MeCN–0.05% TFA (1:1) and the solvent evaporated by vacuum centrifugation. The residue was dissolved in the HPLC eluent, separated on a 4 mm I.D. column (see below) with fractionation, again evaporated and the residue dissolved in methanol–water (1:1) containing 1% acetic acid for mass spectrometric measurement. If TFA or pentafluoropropionic acid (PFP) was used (both 0.05%) instead of acetic acid in the off-line MS measurement, lower signal intensities were obtained. The signal ratio measured with the methanol–water system for acetic acid–PFP–TFA was 100:20:6 using buserelin (16.7 pmol/μl).

Chromatography

Peptides were separated in the off-line mode with 4 mm I.D. HPLC columns (Nucleosil 120 C_{18}, 5 μm, length 250 + precolumn 11 mm) using a Shimadzu LC-6A gradient system (RF-535 fluorescence detector, $\lambda_{ex} = 280$ nm, $\lambda_{em} = 365$ nm). Gradient elutions were run with (A) MeCN–water (5:95) and (B) MeCN–water (35:65), both containing 0.05% TFA, from 5% to 100% B within 25 min. For the isolation of the dipeptide pGlu-His ($t_R = 6$ min) the gradient was preceded by a 10-min isocratic elution period with MeCN–water (0.5:99.5). The systems used for the LC–MS experiments [Fig. 3, (A) columns of 2 mm I.D., (B) columns of 0.32 mm I.D.] consisted of an Applied Biosystems Model 140B dual-syringe pump and a Model 785A UV detector equipped with a micro flow cell (light path 0.1 mm, quartz capillary). The injectors were Rheodyne Model 7125 (20-μl loop) and Model 7520 (0.5-μl internal loop) and Valco Model C14W (60-nl internal loop). The split systems were made of Valco T (ZT1C) and quartz capillaries (75 and 50 μm I.D.) of appropriate length to achieve a stream splitting ratio of 100:1. With the precolumn split (Fig. 3B), a Lee (Frankfurt, Germany) visco jet micro mixer was applied. Separations were run with columns of

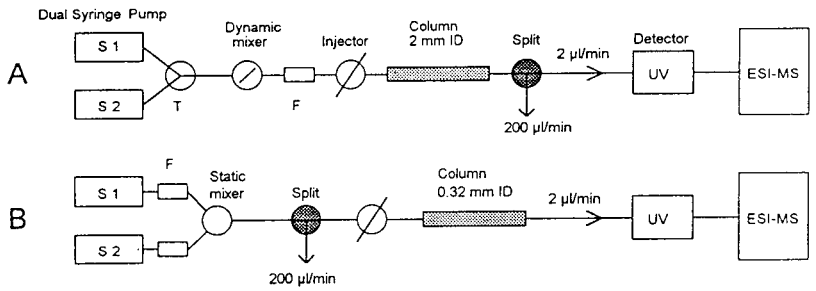

Fig. 3. HPLC set-up in the on-line mode for columns of 2 mm I.D. (variant A) and 0.32 mm I.D. (variant B) to deliver an eluent flow-rate of *ca.* 2 µl/min to the ESI mass spectrometer. Sample volumes were (A) 20 µl and (B) 60 nl or 0.5 µl.

Nucleosil 300 C_{18}, 5 µm (100 + 11 mm × 2 mm) (Macherey–Nagel, Düren, Germany) and Vydac 300A C_{18}, 5 µm (100 × 0.32 mm) (LC-Packings, Frankfurt, Germany).

Gradient elution in the on-line mode was performed with mobile phases of (A) MeCN–water (5:95) and (B) MeCN–water (1:1), both containing 0.05% TFA, from 5% to 60% B within 30–40 min. When large sample volumes (>60 nl) were applied to the capillary column, a 5-min equilibrium time with eluent A was inserted after sample injection before starting the gradient.

Mass spectrometry

The mass spectrometric equipment consisted of a TSQ 700 tandem quadrupole mass spectrometer (Finnigan MAT, Bremen, Germany) with an electrospray ion source (Analytica of Branford, Branford, CT, USA) operating in the positive-ion mode. Off-line ESI mass spectra were obtained by syringe infusion with a flow-rate of 1 µl/min of methanol–water (1:1) containing 1% acetic acid without sheath liquid, a drying gas temperature of 140°C and a high voltage of 2.8 kV. In the on-line mode the ESI ion source was operated at a sample flow-rate of about 2 µl/min, a 2-methoxyethanol sheath liquid flow-rate of 0.5 µl/min with a drying gas temperature of 210°C and a high voltage of 3.2 kV.

RESULTS AND DISCUSSION

Identification of degradation products

Incubation of the GnRH analogues PG and SG with rat kidney membranes results in a very similar pattern of HPLC peaks. As can be seen in Fig. 4, three major and two minor UV absorption peaks appear, two of them having no counterpart in the fluorescence trace (*i.e.*, no tryptophan). Using the off-line procedure, the peaks were fractionated and analysed by ESI-MS as described above. The results in Table I clearly demonstrate that both types of analogues, despite their structural differences at the C-terminus, are degraded in the same way, as depicted in Fig. 5 for buserelin. These results indicate that a selective proteolytic enzyme system is responsible for the metabolic events at the kidney membranes. By this method the structures of all degradation products (individual HPLC–UV peaks) were revealed. The weakness of this analytical procedure concerns the small hydrophilic molecules that elute together in or near the void volume of the RP chromatogram and are difficult to analyse by ESI-MS. Therefore, serine had to be identified by the dansylation procedure [8]. Obviously, the expected dipeptide pGlu-His appeared in the same fraction but could primarily not be detected by the LC–MS procedure. Therefore, the chromatographic conditions were changed to elution with a low MeCN content (see Experimental), resulting in the identification of pGlu–His.

On-line LC–MS studies

ESI-MS is an increasingly used method for detection in LC–MS experiments. As this method is ideally suited to the LC–MS of peptides, we tried to substitute an on-line LC–MS method for the laborious off-line procedure described above.

The feasibility of this approach was tested

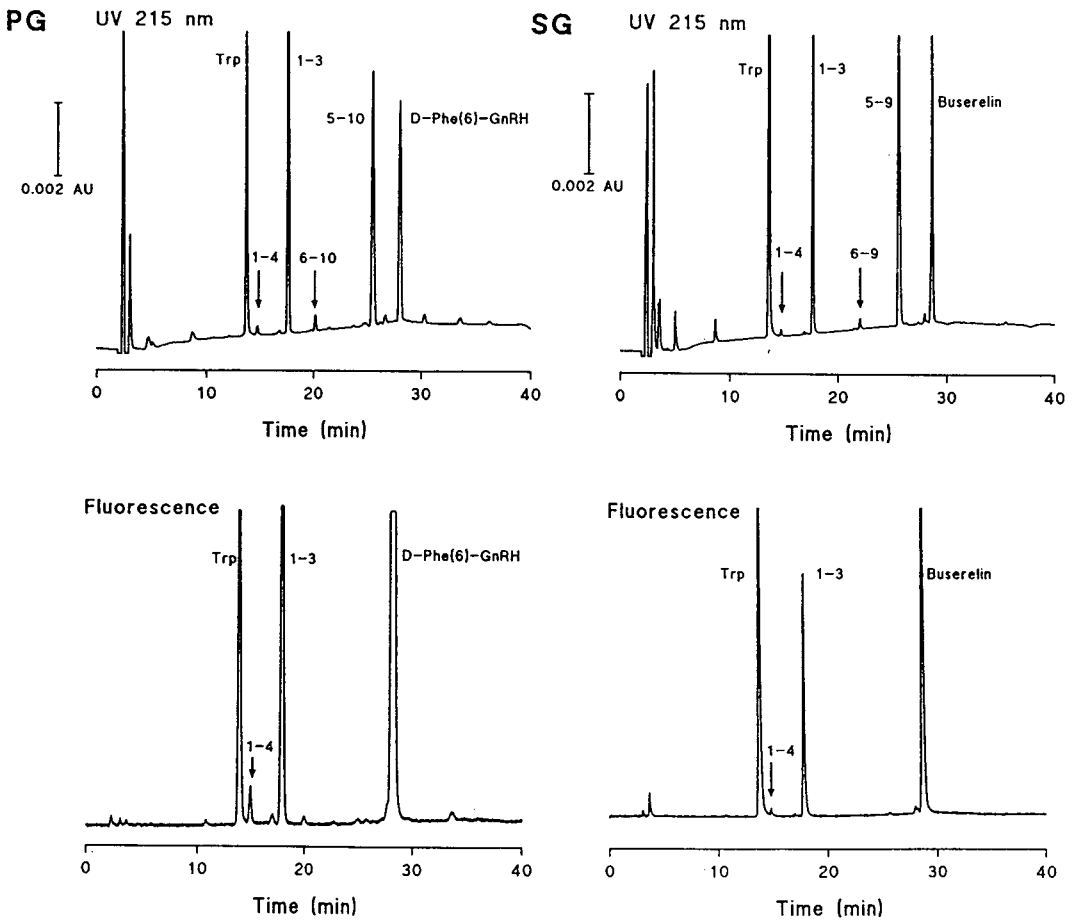

Fig. 4. HPLC separation of the degradation mixtures of D-Phe^6–GnRH (PG) and buserelin (SG), incubation time 3 h, with a Nucleosil 120 C_{18}, 5 μm column (250 + 11 mm × 4 mm) using UV and fluorescence detection. Gradient elution with acetonitrile–water–trifluoroacetic acid (see Experimental, off-line mode) was applied. Minor peaks with low retention times resulting from the kidney membrane matrix were not identified in the UV trace.

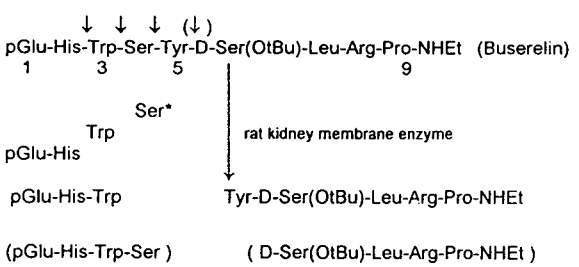

Fig. 5. Degradation pattern of buserelin produced by incubation with rat kidney membranes (minor products in parentheses). Primary and secondary splitting by the enzyme complex occurs around the serine residue. Serine was identified by the dansylation method [8].

using two known HPLC variants (Fig. 3A and B) using columns of 2 and 0.32 mm I.D., respectively. In set-up A, 2 mm were preferred to 4 mm I.D. columns to reduce sample and solvent consumption. Both variants were applied to the described peptide mixtures produced by the degradation of buserelin and to a test mixture of the same peptides prepared for quantitative comparison. Figs. 6 and 7 show two examples of these four sets of LC–MS experiments. As expected, the amount of peptide delivered at the same flow-rate to the MS system was the critical factor for the limit of detection.

In Fig. 6, a run with variant A is depicted with

TABLE I

STRUCTURAL ASSIGNMENT BY ESI-MS OF THE PEPTIDE DEGRADATION PRODUCTS OF D-Phe^6–GnRH AND BUSERELIN

Sequence assignment	Sequence No.	M_r (calc.)[a]	m/z[b]	
			MH^+	MH_2^{2+}
Trp	3	204.1	205.1	–
pGlu–His	1–2	266.1	267.0	–
pGlu–His–Trp	1–3	452.2	453.1	–
pGlu–His–Trp–Ser	1–4	539.2	540.2	–
Tyr–D-Phe–Leu–Arg–Pro–Gly–NH_2	PG 5–10	750.4	751.5	376.3
D-Phe–Leu–Arg–Pro–Gly–NH_2	PG 6–10	587.3	588.4	294.6
Tyr–D-Ser(OtBu)–Leu–Arg–Pro–NHEt	SG 5–9	717.4	718.4	359.7
D-Ser(OtBu)–Leu–Arg–Pro–NHEt	SG 6–9	554.3	555.5	–
D-Phe^6–GnRH	PG 1–10	1271.6	1272.8	636.9
Buserelin	SG 1–9	1238.6	1239.8	620.3

[a] Monoisotopic masses.
[b] m/z Values for the $[M + H]^+$ and $[M + 2H]^{2+}$ ions in the ESI mass spectra.

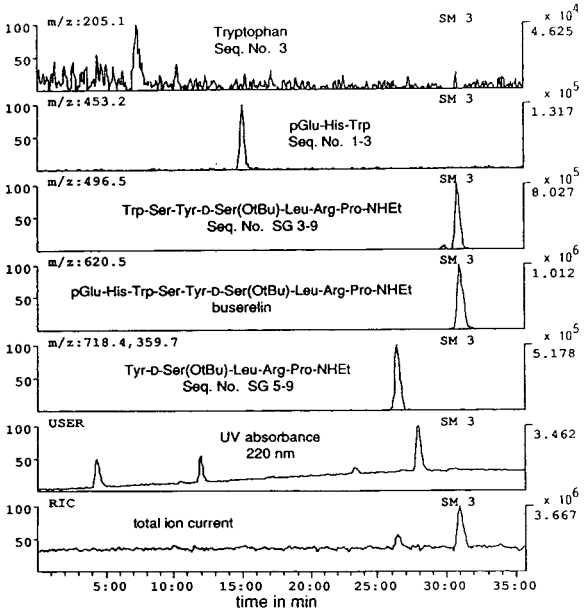

Fig. 6. LC–MS experiment with a test mixture (20 pmol/μl of each component) of buserelin SG 1–9 and the peptide sequences 3, 1–3, SG 5–9 (*cf.*, Table I) and SG 3–9 [Trp–Ser–Tyr–D-Ser(OtBu)–Leu–Arg–Pro–NHEt]. The separation was carried out with experimental set-up A (Fig. 3). The sample volume was 20 μl and the splitting ratio 250 to 2.1. The amount of each component introduced into the mass spectrometer was 3.4 pmol. The dead volume between the UV detector and the ESI ion source causes a delay of about 3 min of the mass chromatograms relative to the UV trace. The sequence SG 3–9 (not separated by the chromatographic system) is detected in the ion chromatogram of the $[M + 2H]^{2+}$ ion (m/z 496.5).

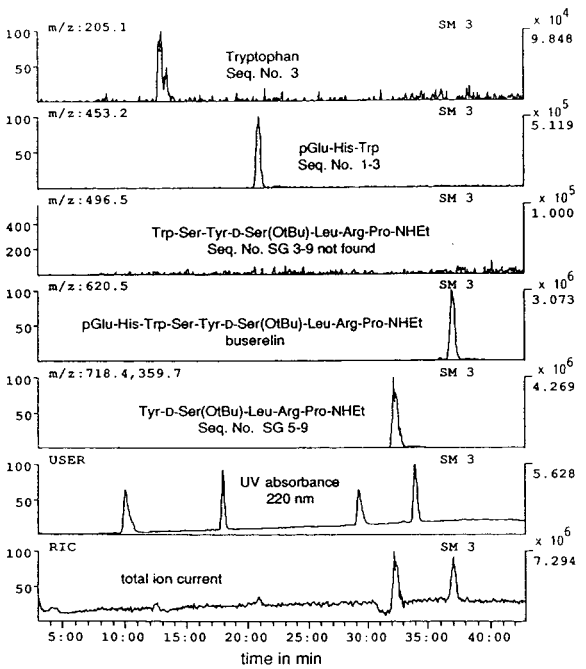

Fig. 7. LC–MS experiment with a degradation mixture of buserelin after incubation for 4 h with rat kidney membranes. Experimental set-up B (Fig. 3) was employed (sample volume 500 nl, eluent flow-rate to the ESI ion source 2.1 μl/min, delay time between mass chromatograms and UV trace *ca.* 3 min). The amount of each of the major components injected and delivered to the MS system was *ca.* 10 pmol. The sequence SG 3–9 was not detected in the respective ion chromatogram (m/z 496.5).

the peptide test mixture of known concentration (20 pmol/μl for each substance). Although 400 pmol of each peptide were injected, only 3.4 pmol per substance were delivered to the MS system (because of the postcolumn stream splitting), which is near the limit of detection. This mixture additionally contained the potential degradation product SG 3–9. We were not able to separate SG 3–9 from the starting peptide buserelin with our chromatographic system but both peptides were clearly detected by the MS system (Fig. 6, traces SG 1–9 and SG 3–9).

Fig. 7 shows a run with a degradation mixture using variant B. The amounts injected were *ca.* 10 pmol of each of the major components, which were also completely delivered to the MS system in this set-up. As can be seen from the ion current traces, peptides SG 1–3, SG 5–9, the starting material SG 1–9 and tryptophan were identified. However, the small amounts (<1 pmol) of SG 1–4 and SG 6–9, still detectable by the UV detector, are below the limit of mass spectrometric detection. The sequence SG 3–9 ($m/z = 496.5$) was not detected. Therefore, this peptide can be ruled out as a major degradation product.

CONCLUSIONS

Peptide metabolites resulting from the enzymatic degradation of the modified peptide structures of two GnRH analogues were unambiguously identified by combined HPLC and ESI-MS methods. A comparison of the off-line and on-line modes demonstrates that each of them has advantages in some respects.

The off-line mode is preferable if small amounts of unknown peptide have to be identified in the chromatogram. High enrichment factors can be attained and TFA can be replaced with acetic acid before the sample is introduced into the mass spectrometer, which results in higher sensitivity in this measurement.

The on-line mode is fast, reliable and less laborious than the off-line procedure. If only a very small amount of material is available (*e.g.*, cell fractions), the use of a 0.3 mm I.D. capillary column (variant B) is advantageous. Even with this small column, relatively high sample volumes can be used in the applied gradient system to increase the amount of peptide introduced into the mass spectrometer.

ACKNOWLEDGEMENTS

We thank Dr. J. Sandow (Hoechst) and Professor K.-D. Kaufmann (Berlin-Chemie) for kindly supplying the various peptides used. H. Apelt and D. Runald are thanked for their skilful technical assistance.

REFERENCES

1 A.S. Dutta, *Drugs Future*, 13 (1988) 43.
2 J. Kiesel, J. Sandow, K. Bertges, G. Jarabek-Sandow, H. Trabant and B. Runnebaum, *J. Clin. Endocrinol. Metab.*, 68 (1989) 1167.
3 H. Ueno and S. Matsuo, *J. Chromatogr.*, 566 (1991) 57.
4 H. Berger, N. Heinrich, E. Albrecht, U. Kertscher, J. Oehlke, M. Bienert, H. Schäfer, I. Baeger and B. Mehlis, *Regul. Pep.*, 33 (1991) 229.
5 R.B. van Breemen and R.G. Davis, *Anal. Chem.*, 64 (1992) 2233.
6 W.E. Seifert, Jr., W.T. Moore and R.M. Caprioli, in D.M. Desiderio (Editor), *Mass Spectrometry of Peptides*, CRC Press, Boca Raton, FL, 1991, p. 201.
7 E.C. Huang, T. Wachs, J.J. Conboy and J.D. Henion, *Anal. Chem.*, 62 (1990) 713A.
8 Y. Tapuhu, D.G. Schmidt, W. Lindner and B.L. Karger, *Anal. Biochem.*, 115 (1981) 123.

Journal of Chromatography A, 661 (1994) 61–75
Elsevier Science B.V., Amsterdam

CHROMSYMP. 2908

High-performance liquid chromatography of amino acids, peptides and proteins

CXXXIII☆. Peak tracking of peptides in reversed-phase high-performance liquid chromatography

A.J. Round, M.I. Aguilar and M.T.W. Hearn*

Department of Biochemistry and Centre for Bioprocess Technology, Monash University, Wellington Road, Clayton, Victoria 3168 (Australia)

ABSTRACT

A peak tracking algorithm for peptide analysis has been developed based on a normalised spectral overlay method which directly compares the UV spectra of any two chromatographic peaks. Additionally, the algorithm compares the spectrum of each peak in the first chromatogram with the spectra of every peak in the second chromatogram to determine the best cross-match. The sensitivity of the technique was further enhanced by incorporation of the primary and secondary derivative spectra for cross-match normalisation. The utility of the software was demonstrated by its application to the analysis of tryptic digests of porcine growth hormone. Peptide solutes could be identified and tracked in chromatograms generated with various column types, gradient times, mobile phase types and temperatures. These results therefore constitute the initial stages of development of a more robust approach to the optimisation of the resolution, detection and characterisation of peptides and proteins separated by HPLC techniques.

INTRODUCTION

Over the past 15 years high-performance liquid chromatography (HPLC) has emerged as a powerful tool for the analysis and purification of peptides and proteins [1]. However, it has only been during the last several years that strategies for systematic optimisation of HPLC separations of peptides have begun to be systematically investigated [2,3]. Reversed-phase HPLC (RP-HPLC) is the mode of chromatography which has been most extensively studied, and now represents the dominant technique for resolution of peptide samples. Various different strategies have been proposed to permit optimisation of the mobile phase composition for this mode of chromatography. These optimisation strategies can generally be grouped into two categories. The first category consists of interpretive optimisation methods, which base their predictions of the optimum mobile phase conditions on a model (or map) of the retention behaviour of the individual components in a mixture. In this approach, a limited set of "scouting" experiments are performed on a given sample under various chromatographic conditions, the resolution data fitted to a mathematical function by linear or non-linear regression techniques and a retention "map" is then generated to encompass the behaviour of the solutes under conditions not explicitly tested during the initial experiments [2–6]. The second category includes optimisation methods whereby an iterative search is per-

* Corresponding author.
☆ For Part CXXXII, see ref. 25.

0021-9673/94/$07.00
SSDI 0021-9673(93)E0874-T

formed. In these methods, the results from one experiment are used to predict the conditions for the next experiment (often using algorithms such as modified sequential simplex methods) [2,3,7–10]. The process is repeated until the optimum chromatographic conditions have been determined. These methods make no assumptions concerning the nature of the mathematical function used to interrogate the retention data and have the advantage that generally fewer experiments are required to locate the optimum chromatographic conditions.

In order to effectively utilise any of these optimisation methods, the location (but not necessarily the structural identity) of the solute components in successive chromatograms must be known. Thus, a fundamental requirement in the application of chromatographic optimisation methods to the characterisation of unknown solute mixtures is peak recognition. In order to quantitatively describe the influence of changes in the experimental chromatographic parameters on the retention of the individual solutes in a sample, the investigator must be able to identify and follow the relative movement of individual solute peaks as the experimental chromatographic conditions are varied. Since the actual identification of the solutes is not necessarily of immediate interest, but rather the determination of the relative location of individual peaks corresponding to the same solutes in two (or more) different chromatograms of the same mixture (as the chromatographic conditions are varied), this process is referred to as peak tracking.

With the advent of rapid-scanning photodiode array UV–Vis detectors, complete spectral information for any or all peaks in a chromatogram can now be acquired. Comparison of the spectral data from peaks in different chromatograms has great potential to facilitate peak identification and hence the development of HPLC optimisation systems. Algorithms for the numerical comparison of spectra have been successfully used in the past to distinguish between very similar compounds [11]. The present study is based on a modification of one such algorithm, utilising the spectral information from each peak in a chromatogram to perform normalised spectral overlay comparisons (NSOC) for all of the normal (zero-order) UV spectra as well as the first-order and second-order derivatives of these spectra. The algorithm developed has been validated by the matching between any two chromatograms (derived under different chromatographic conditions) the spectral absorbance of peaks derived from samples of a tryptic digest of recombinant porcine growth hormone, regardless of whether or not the compositional identity of the peaks is known. The software compares the spectra from each peak in the first chromatogram with every peak in the second chromatogram to determine the best match. In this way each peak from the first chromatogram can be assigned to its best matching peak in the second chromatogram.

EXPERIMENTAL/MATERIALS AND METHODS

Chemicals and solvents

Acetonitrile (MeCN), methanol (MeOH) and isopropanol (*i*-PrOH) were ChromAR HPLC grade from Mallinckrodt Australia (Melbourne, Australia); trifluoroacetic acid (TFA) was obtained from Pierce (Rockford, IL, USA). Water was quartz-distilled and deionised by passage through a Milli-Q water purification system (Millipore, Bedford, MA, USA).

Recombinant porcine growth hormone (Met-Asp-Gln-pGH, r-pGH) was obtained from American Cyanamid (Princeton, NJ, USA).

Dithiothreitol (DTT), iodoacetic acid (IAA) and N-tosyl-L-phenylalanine chloromethyl ketone (TPCK) trypsin were purchased from Sigma (St. Louis, MO, USA), Fluka (Buchs, Switzerland) and Worthington (Freehold, NJ, USA), respectively. All other reagents were analytical grade or the best available grade.

Tryptic digest of r-pGH

The tryptic digest of recombinant porcine growth hormone (r-pGH) was performed using the following method: 1 mg growth hormone was dissolved in 250 μl guanidine hydrochloride (GdHCl) buffer [6*M* GdHCl, 200 m*M* Tris, 2 m*M* ethylenediaminetetraacetic acid (EDTA), pH 8.0] and incubated at 37°C for 30 min. After cooling, DTT (1 mg/30 μl GdHCl buffer) was added and the solution flushed with a stream of

nitrogen gas. Following incubation at 37°C for 3 h the solution was allowed to cool, and IAA (1.9 mg/70 μl 1 *M* Tris–HCl, pH 8.0) was added. The mixture was then incubated in the dark at room temperature for 15 min, after which 10 μl mercaptoethanol was added, followed by 5 μl TPCK trypsin (10 μg/5 μl 1 *M* HCl). The protein was recovered by adding 3.15 ml methanol (chilled at −20°C), stored overnight at −20°C and centrifuged at 2000 *g* for 20 min at 4°C. The supernatant was poured off and the pellet resuspended in 400 μl chilled methanol. The suspension was recentrifuged as above and the pellet resuspended in 400 μl of fresh 100 m*M* NH_4HCO_3–2 mM $CaCl_2$ solution. An additional aliquot of TPCK trypsin was then added to the solution, which was then incubated for 24 h at room temperature. Digestion was stopped by acidification with 2 *M* HCl.

Reversed-phase high-performance liquid chromatography

Reversed-phase chromatographic analyses of r-pGH tryptic digests were performed using a Hewlett-Packard HP1090M HPLC system consisting of a DR5 solvent delivery system, a thermostatically controlled column compartment, an automated injection and sampling system and a HP1090 diode-array detector. This instrument was connected to a HP79994A ChemStation Analytical Workstation computer coupled to a ThinkJet printer and a HP7470 plotter.

Table I summarises the chromatographic conditions utilised in this study. Three linear gradient mobile phase systems were employed for the separation of the tryptic fragments (as listed in Table I). With each of these mobile phase systems, two types of ligands chemically bonded to the stationary phase packed into steel columns were used. The first was a 25 cm × 0.46 cm Bakerbond Analytical WidePore C_{18} reversed-phase column, and the second column was a 25 cm × 0.46 cm Bakerbond Analytical WidePore C_4 reversed-phase column (J.T. Baker, Phillipsburg, NJ, USA). Certain combinations of mobile and stationary phases created high back-pressures, necessitating the use of a range of solvent flow-rates, as illustrated in Table I.

Data processing

For all analyses, spectra were acquired at time intervals of 0.320 s over a wavelength range from 200 to 350 nm. Chromatographic peak spectral absorbances were also recorded at both 215 nm and 274 nm, with a reference wavelength of 350 nm in both cases. Raw data was stored on both a 20 MByte Hard and 1.44 MByte Floppy disks by the ChemStation for subsequent processing by the peak tracking software.

The peak tracking software was written using

TABLE I

CHROMATOGRAPHIC CONDITIONS USED TO ESTABLISH DATABASE OF CHROMATOGRAMS

Solvent system	Mobile phase solvents	Stationary phase[a] ligand	Flow-rate (ml/min)
1	(A) 0.1% TFA in water	C_4	1.0
	(B) 0.09% TFA 90% acetonitrile	C_{18}	1.0
2	(A) 0.1% TFA in water	C_4	0.8
	(B) 0.09% TFA 90% methanol	C_{18}	0.6
3	(A) 0.1% TFA in water	C_4	0.6
	(B) 0.09% TFA 90% *i*-propanol	C_{18}	0.4

[a] A linear gradient from mobile phase A to mobile phase B at different gradient times (30, 45, 60, 90, 120 min) and temperatures (25, 37, 50, 65, 80°C) was employed with the two RP-sorbents.

the high-level PASCAL interpreter command language available on the ChemStation. The software functions as a "stand-alone" program which allows access to, and manipulation of, the chromatographic and spectroscopic data previously stored on either the floppy or the hard disk media.

Chromatographic database

The initial task in the development of our new optimisation procedures and peak tracking algorithms was the creation of a large database of chromatograms and their associated spectra. This database consists of chromatograms of tryptic digests of r-pGH run under a wide variety of chromatographic conditions. These conditions consisted of the mobile phase and stationary phase ligand systems listed in Table I, with separations performed at 5 different linear gradient times (30, 45, 60, 90, 120 min) and 5 different temperatures (25, 37, 50, 65, 80°C). Together these combinations create 150 different chromatographic conditions. As each tryptic digest produces at least 20 peptide fragments, this represents a spectral database of several thousand solute spectra. This database was used to extensively test and validate the peak tracking software.

RESULTS AND DISCUSSION

(A) Development of the peak tracking software

Peak tracking software description. A number of methods have been previously described which perform peak tracking based on analysis of relative peak areas [5,6,12], wavelength ratios [13] or retention values [14]. These methods have limitations, especially when peaks overlap or samples vary in the relative concentration of the individual components. The introduction of linear photodiode array detection (PDAD) for HPLC instrumentation increased the potential for peak tracking considerably, since full spectra for each solute peak in a chromatogram can be compared. Drouen *et al.* [15] performed comparisons of spectra "by eye", and reported difficulties in distinguishing between similar spectra. This is not surprising since a visual interpretation of pattern similarities in spectra would be a highly subjective exercise. More recently, peak tracking methods based on combinations of spectral recognition and peak areas have been investigated [16,17]. These methods require prior knowledge of the spectrum of an individual solute obtained under analogous conditions and/or the use of sophisticated computer software such as neural networks.

We describe here a strategy based on an objective comparison of spectra by computer software. The UV spectra of peptides and proteins are characteristic of their constituent amino acids, especially with regard to their aromatic amino acids (phenylalanine, tyrosine and tryptophan). These amino acids have absorption maxima between 250 to 300 nm, but the spectra are rather broad and overlapping. It is therefore difficult to distinguish between peptides containing these aromatic amino acids simply from their zero-order derivative spectra. However, these problems can be overcome by derivatisation of the zero-order spectra which increases the resolution between spectral differences. Second-order derivative spectral analysis as a static method (derivative spectroscopy) has been widely used to assess solvent accessibility and conformational information for peptides and proteins containing aromatic amino acids [18]. In particular, the second-order derivative of a spectrum transforms peaks and shoulders of the corresponding zero-order derivative spectrum into well defined maxima/minima. The enhanced resolution between different spectra after derivatisation forms the basis of our new peak tracking software.

The flowchart shown in Fig. 1 provides a simplified explanation of the steps carried out by this peak tracking algorithm. Basically, the algorithm performs a detailed analysis and cross-correlation comparison of the zeroth-order, first-order and second-order derivatives of the UV spectra obtained from each solute peak. The software takes a chromatogram and compares the spectra (*i.e.* zero-, first- and second-order derivative spectra) of the first peak in that chromatogram with the spectra (*i.e.* zero-, first- and second-order derivative spectra) of every peak in a second chromatogram to determine the best matching correlation. The software then takes the second peak in the first chromatogram and compares its spectra to the spectra of every

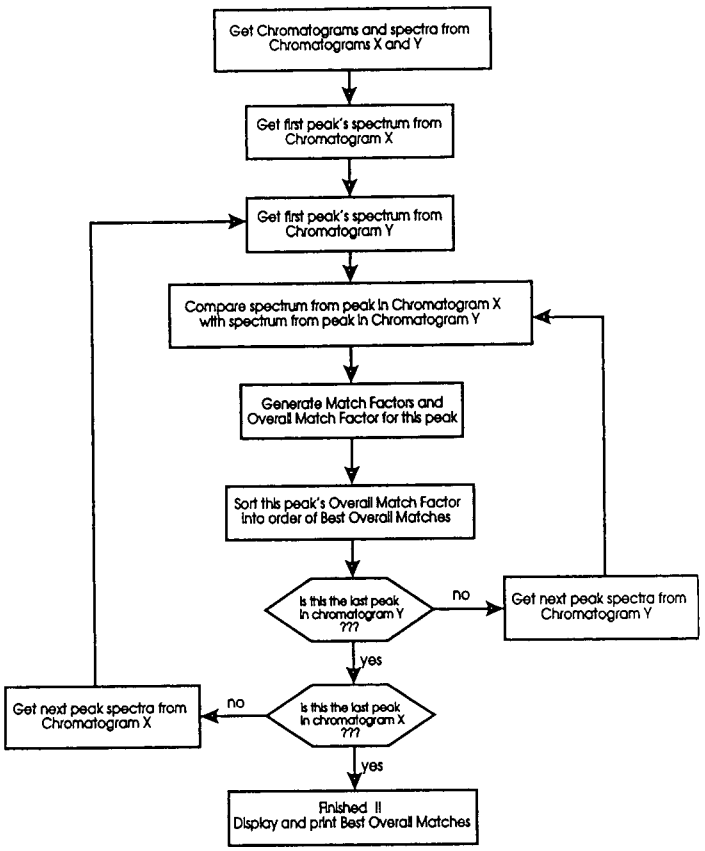

Fig. 1. Flowchart illustrating peak tracking procedure.

peak in the second chromatogram, again finding the best matching correlation. The process is repeated until each peak from the first chromatogram is assigned to its best matching peak in the second chromatogram.

To perform this matching procedure, the spectra are subjected to a process known as normalised spectral overlay comparison. The normalised spectral overlay comparison process is based on the numerical point-by-point comparison of two UV spectra by the COMPARE command implemented on the ChemStation [19]. The procedure is illustrated in Fig. 2 with the comparison of two typical spectra. Fig. 2a shows the two spectra to be compared. These spectra are first normalised at the point of maximum absorbance and then digitally superimposed. The absorbance values for spectrum 2 are then plotted against the corresponding absorbance values for spectrum 1 at each wavelength, as shown in Fig. 2b (solid line). A linear regression is then applied to the resulting scatterplot. The regression line calculated is shown in Fig. 2b (dashed line). The square of the correlation coefficient derived from this linear regression is defined as the match factor for the two spectra according to the following expression,

$$\text{Match factor} = 1000 \cdot r^2 = \frac{1000[\Sigma xy - (\Sigma x \, \Sigma y)]^2}{\left[\Sigma x^2 - \left(\frac{\Sigma x \, \Sigma x}{n}\right)\right]\left[\Sigma y^2 - \left(\frac{\Sigma y \, \Sigma y}{n}\right)\right]} \quad (1)$$

The x and y values are the measured absorbances in the first and second spectrum respectively at the same wavelength, n is the number of data points used in the comparison (typically >100), Σ is the sum of the data, and r^2 is the square of the linear regression correlation coefficient.

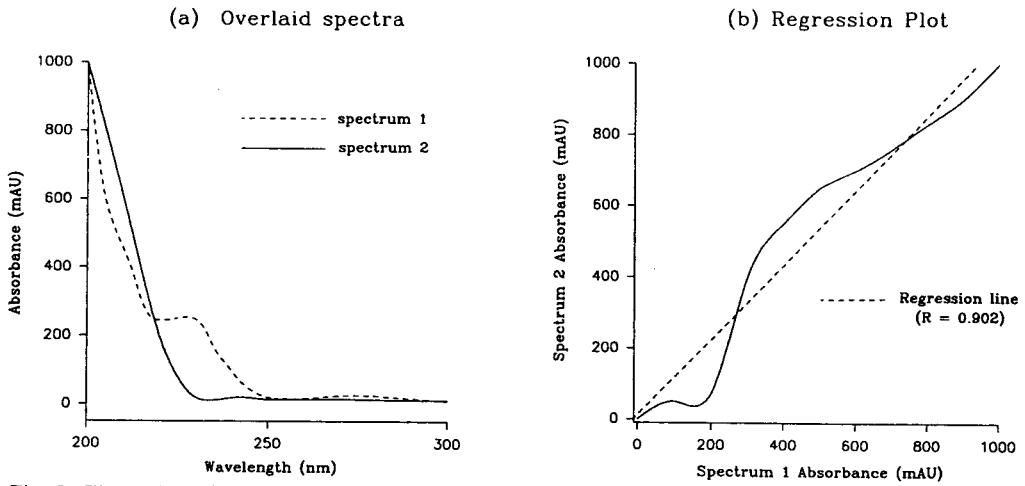

Fig. 2. Illustration of the normalised spectral overlay comparison procedure.

Individual match factors are determined by this overlay comparison process independently for each of the zero-order, first-order and second-order derivative spectra. An *overall match factor (O.M.F.)* concept was then applied to each peak comparison based on the optimum combination of each of the zero-, first- and second-order derivative UV spectra match factor scores. This combination enhanced the accuracy of the peak tracking procedure compared to the use of zero-order derivative spectra alone. The combination of match factors required to maximise the accuracy of peak tracking was initially established by statistical examination of the individual match factor scores for each of the zero-order, first-order and second order derivative spectra. Appropriate weighting factors for the zero-order, first-order and second-order derivative spectra were derived from this analysis.

Table II illustrates a typical example of the

TABLE II

TYPICAL EXAMPLE OF THE RANGE OF INDIVIDUAL MATCH FACTOR SCORES OBTAINED WHEN PEAK TRACKING IS PERFORMED BETWEEN TWO CHROMATOGRAMS DESIGNATED M AND N

The data below illustrate only a small portion of the total data analysed and show only five match factor scores for each of the two peaks investigated.

Peak number from chromatogram M	Peak number from chromatogram N	Zero-order derivative spectra match factor	First-order derivative spectra match factor	Second-order derivative spectra match factor	Correct matching peak
1	3	999.473	986.344	690.558	yes
1	6	999.245	987.802	615.727	
1	5	988.271	862.140	239.036	
1	2	976.217	962.382	642.526	
1	4	986.276	862.656	223.382	
2	2	998.889	982.509	742.898	yes
2	9	997.421	970.649	623.631	
2	8	992.723	967.411	658.823	
2	7	991.461	977.483	773.512	
2	10	993.149	929.182	680.812	

range of individual match factor scores obtained when peak matching is performed between two chromatograms (designated as chromatograms M and N) using unweighted zero-order, first-order and second-order derivative spectra. It can be seen in Table II that peaks 3 and 6 of chromatogram M have very similar zero-order derivative spectra match factor scores (999.473 and 999.245, respectively) when their spectra are compared to the spectrum of peak 1 from chromatogram N. Using just the zero-order derivative spectra match factors, it could be concluded that peak 3 is a slightly better match for peak 1 from chromatogram M than peak 6, although the confidence limits for this assignment would be low since the two scores are so close. It can be noted at this point that the correct matching peak for peak 1 from chromatogram M, as determined by independent structural analysis, is peak 3 from chromatogram N. An O.M.F. score based on just the first-order derivative spectra match factor scores would have incorrectly matched peak 6 to peak 1. Similarly, an unweighted combination of both the zero-order and first-order derivative spectra match factors would also have resulted in an incorrect match. Examination of the second-order derivative spectra match factors for these peaks, reveals that peak 3 has a significantly higher score than peak 6 and an O.M.F. score based solely on the second-order derivative spectra match factor score would yield a correct match. However, this situation does not always arise, as can be seen in the analysis of peak 2 from chromatogram M in Table II. In this case, an O.M.F. score based solely on the second-order derivative spectra match factor score would have resulted in an incorrect match.

While in general, the zero order match factors usually provided good peak matching, as illustrated for peaks 1 and 2 in Table II, the accuracy of the peak tracking procedure can be enhanced by incorporation of a weighted contribution of the first- and second-order derivative spectra match factors. Detailed analysis of several spectral comparisons of this sort demonstrated that a weighted combination of each of the individual match factors is needed to create an accurate O.M.F. score. The largest weighting was assigned to the zero-order derivative spectra match factor score (0th DSMF) with smaller contributions from the first- (1st DSMF) and second-order (2nd DSMF) derivative spectra match factor scores. The weighting of the individual match factors also allowed increased baseline noise levels associated with derivative spectra to be taken into account, since taking the derivative of a spectrum also multiplies the noise inherent in the baseline of the spectrum.

Considering the factors outlined above, the relative contribution of the first derivative spectra ($dA/d\lambda$) match factor was given 1/10th the weight of the zero-order derivative spectra match factor; the relative contribution of the second derivative spectra ($d^2A/d^2\lambda$) was then given $(1/10\text{th})^2 = 1/100\text{th}$ the weight of the first derivative spectra match factor. Thus, the final equation for the overall match factor (O.M.F.) score has the form:

$$\text{O.M.F.} = \frac{\text{0th DSMF} + 10\%\ \text{1st DSMF} + 0.1\%\ \text{2nd DSMF}}{1.101} \quad (2)$$

The peaks with the highest overall match factor are selected as the best matching peaks and should thus represent the same solute in both chromatograms.

Reproducibility of peak tracking software and chromatographic equipment. The reproducibility of individual match factors determines the statistical limits for similarity between any two spectra, and thus defines the sensitivity of the spectral matching. According to classical linear regression theory, a match factor of 1000 would characterise a perfect match according to eqn. 2, whereas a value of 0 would indicate the spectra are totally dissimilar. Values >990 (*i.e.* $r^2 > 0.99$) would indicate *statistical* identity, values between 900 to 990 would indicate *statistical* similarity, whilst values <900 (*i.e.* $r^2 < 0.90$) would indicate the spectra are *statistically* different. Since the characteristic UV spectra of peptides between 200–300 nm arises from the peptide backbone carbonyl bond and the aromatic side-chain residues, a fairly high degree of spectral similarity is expected for peptide solutes (*i.e.* match factors >900). However, additional factors will also

influence the degree of spectroscopic identity. For example, experimental errors in chromatographic equipment such as pump flow-rates, temperature instabilities, UV lamp deterioration, electrical interference and even mechanical vibrations all contribute to levels of detector baseline spectral noise above those envisaged in the ideal theoretical models upon which the *statistical* values for match factors are based. Two spectra and their corresponding solute peaks can only be considered different when the mean and standard deviation for the O.M.F. between them differs significantly from those obtained by repeatedly matching identical spectra. Thus, reproducibility of the peak tracking method (with respect to the software, detector and chromatographic hardware) was determined in order to obtain more appropriate cut-off values for matching criteria than the purely statistical values quoted above.

One system to determine such cut-off scores is by repetitive matching of identical chromatograms. Thus, by repetitively injecting the tryptic digest sample of r-pGH, recording the chromatograms under identical conditions and applying the peak tracking procedure, information was acquired on the reproducibility of spectra and the minimum cut-off scores needed to determine whether two spectra are associated with the same solute peak or different solute peaks. The r-pGH tryptic digest mix was therefore chromatographed three times under identical chromatographic conditions (*i.e.* same mobile phases, stationary phase, gradient time, flow-rate, and temperature). The chromatograms recorded were designated A, B and C, and are shown in Fig. 3. Chromatograms A, B and C were then subjected to the peak tracking procedure whereby each chromatogram was compared to the other two chromatograms (*i.e.* A to B and C, B to C and A, and C to A and B). Table III shows part of the output from one of those comparisons. For each of the six pairs of chromatograms compared, the mean of the highest O.M.F. scores was calculated and used to construct Table IV. These values in turn were used to calculate the overall mean of the highest O.M.F scores (999.79 ± 0.27 as shown in Table IV). Note that in this case, all the highest O.M.F. scores were obtained from peaks which are

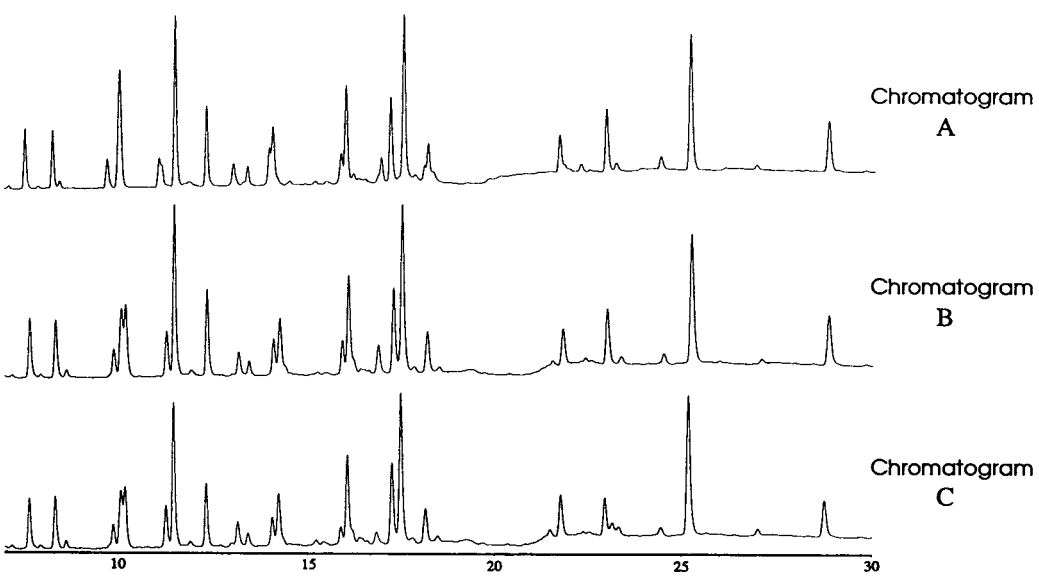

Fig. 3. Chromatograms of r-pGH tryptic digest used to determine the reproducibility of the peak tracking procedure. Each chromatogram was recorded using the same chromatographic conditions.

TABLE III

HIGHEST OVERALL MATCH FACTOR (O.M.F.) SCORES FOR THE PEAKS IN CHROMATOGRAM B WHEN COMPARED TO THE PEAKS IN CHROMATOGRAM C BY THE PEAK TRACKING METHOD

These scores give an indication of the reproducibility of O.M.F. scores, since the two chromatograms (B and C) were recorded under identical chromatographic conditions.

Peaks matched[a] by highest O.M.F. score	Score obtained (*i.e.* highest O.M.F. score)
B1 to C1	999.98
B2 to C2	999.97
B3 to C3	999.75
B4 to C4	999.99
B5 to C5	999.97
B6 to C6	999.66
B7 to C7	999.91
B8 to C8	999.98
B9 to C9	999.96
B10 to C10	999.99
B11 to C11	999.68
B12 to C12	999.31
B13 to C13	999.25
B14 to C14	999.98
B15 to C15	999.58
Mean ± S.D. of highest O.M.F. score	999.80 ± 0.25

[a] Since chromatographic conditions are identical between chromatograms B and C, all peaks are correctly matched.

correctly matched. The overall mean of the highest O.M.F. scores gives a minimum cut-off score above which two peaks from different chromatograms are very likely to arise from the same solute.

These cut-off values for O.M.F. scores should be very reliable since they were obtained under near-ideal circumstances in which the chromatographic conditions were identical. Actual applications of this peak tracking method will involve variation in at least one of the chromatographic conditions, which would be expected to lead to deterioration in match factor stabilities. That is, when chromatograms are recorded under different chromatographic conditions, lower match factor scores would be anticipated. Thus, using the data summarised in Table IV, it can be concluded that peak comparisons having O.M.F.

TABLE IV

VARIATION OF O.M.F. SCORES UNDER INVARIANT CHROMATOGRAPHIC CONDITIONS

Chromatograms compared	Highest O.M.F.[a] scores (mean ± S.D.)	Range of highest O.M.F. scores
A → B	999.77 ± 0.31	998.95–999.97
B → A	999.77 ± 0.31	998.95–999.97
A → C	999.81 ± 0.26	999.14–999.98
C → A	999.81 ± 0.26	999.14–999.98
B → C	999.80 ± 0.25	999.25–999.99
C → B	999.80 ± 0.25	999.25–999.99
Overall average	999.79 ± 0.27	

[a] Represents the average O.M.F. scores derived from individual peak pairs with highest O.M.F. scores, representing correctly matched peaks between the two chromatograms (*i.e.* corresponding to the same peptide solutes in both chromatograms).

scores greater than 999.79 ± 0.27 can be considered to be correctly matched with a high degree of confidence.

The results obtained also allow the limits of the reproducibility of the peak tracking method to be defined with respect to the software and hardware used. Any peaks with O.M.F. scores above 999.79 ± 0.27 can be considered to be identical. Therefore if any one peak is matched with two or more peaks with an O.M.F. score above 999.79 ± 0.27 then as far as the sensitivity of the equipment and the software is concerned, those peaks are identical and an unambiguous identification of the correct matching peak cannot be made.

Special features of peak tracking software. The peak tracking software has a number of special features which allow the user to selectively manipulate the way the software is applied to different problems. The software has been designed to incorporate the following features:

(1) The user can select which section of a chromatogram they wish to search for matching peaks. That is, selected portions of one chromatogram can be compared with selected portions of another chromatogram. This feature is especially useful in cases where only a small area of the chromatogram is of interest, or if the

identity of only a few of the peaks is uncertain. This feature allows the user to selectively exclude solvent breakthrough peaks.

(2) The wavelength range over which spectra are compared can be selected by the user. Peptides (such as those derived from growth hormone) often lack chromophores with UV absorbance above 300 nm and hence the operator might select a wavelength range from 200 to 300 nm. Alternatively, for peptides or proteins containing a heme group or some other chromophore, the operator might select an extended wavelength range for comparisons, anywhere from 200 to 600 nm.

(3) The integrator threshold value (the absorbance value above which a peak is detected) can be adjusted to exclude small "noise" peaks from the comparison process.

(4) Automatic spectral baseline subtraction. Concern has been expressed in the past [20,21] that spectroscopic peak matching methods assume that the spectral characteristics of the solute components do not change significantly with varying experimental conditions. In light of the known background absorbance of TFA at relatively high concentrations [22], these concerns seem well founded. For example, if the differences between the UV spectra for a given solute induced by variations in the background absorbance of the mobile phase are larger than the differences between the UV spectra of different solutes recorded under identical conditions, then clearly the application of multi-channel PDAD UV detection will be of limited use. This concern has been directly addressed in the software by automatically subtracting baseline spectra from each peak spectra to obtain a "pure" peak spectra free from baseline (background) absorbances. This procedure results in peak spectra which are independent of the mobile phase absorbances arising in the particular chromatographic system used to obtain the chromatogram.

(5) The overall match factor is based not simply on the UV spectra, but also on the first- and second-order derivatives of these spectra, adding a further level of sensitivity to matching when the underivatised UV spectra may seem similar.

(6) The software automatically ranks the 5 best matching peaks so that if a mismatch occurs, the next best candidate for a matching peak can be found in the 5 best matching peaks. This feature also allows a quick analysis of the degree of similarity between peptide spectra being compared.

(7) Visual presentation of spectra can be made either to the computer screen or to hard-copy devices. This option may prove useful in cases when human judgement is desired or required. The human eye and brain still remains the unsurpassed instrument for pattern recognition.

(8) Automatic retention time checking can be enabled for chromatograms recorded under identical chromatographic conditions. This option does not form part of the actual peak matching decision making process, rather it is a feature which indicates in the final report peaks which fall within a 10% time window of the peaks with which they are being compared. This feature should prove especially useful in applications such as quality control testing of different batches of synthetic peptides separated by RP-HPLC.

(9) Spectral data is "smoothed" using a 7-point Savitzki-Golay smoothing algorithm [23] to reduce the influence of baseline noise in spectra. The use of "weightings" in the calculation of the O.M.F. score also attempts to reduce noise influences in the comparison process.

(B) Application of the peak tracking software

The general application of the peak tracking procedure to match peaks between any two chromatograms will be described on the basis of the following selected example. The example was chosen to illustrate not only the ability of the software to correctly match peaks, but also to illustrate some of the shortcomings in the method and to discuss ways to avoid them.

Two typical examples of chromatograms of tryptic digest maps of r-pGH were selected from the database of more than 150 recorded chromatograms (see Fig. 4). The two chromatograms (designated as chromatograms X and Y in the following discussion) were generated under significantly different chromatographic conditions.

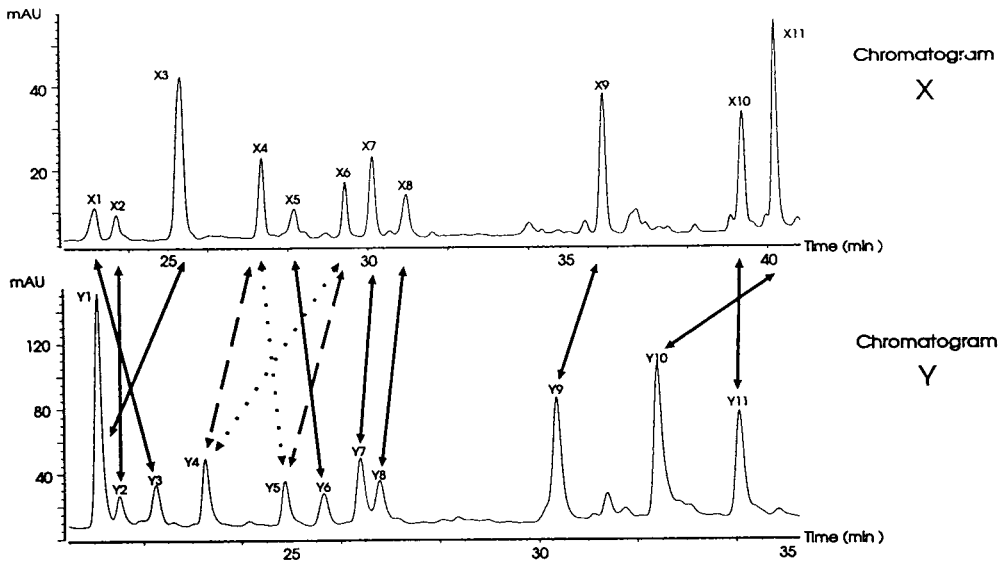

Fig. 4. Graphical representation of the peak tracking method applied to match peaks between two different chromatograms. ⟷ Peaks correctly matched by peak tracking method; ←– – –→ correct matching peaks (but incorrectly matched by peak tracking); ←· · ·→ peaks matched incorrectly by peak tracking method.

Chromatogram X was recorded using solvent system 1 (aqueous TFA–acetonitrile —see Table I) using a 120-min gradient elution (0–100% B) at a flow-rate of 1.0 ml/min with a C_{18} sorbent at 37°C. Chromatogram Y was recorded using solvent system 3 (aqueous TFA–propanol —see Table I) using a 90-min gradient elution (0–100% B) at a flow-rate of 0.6 ml/min with a C_{18} sorbent at 37°C.

The identity and position of the individual peaks in each chromatogram were confirmed by fraction collection of the separated r-pGH tryptic fragments, independently determining their composition by amino acid analysis, and re-injection of purified isolated fragments under the chromatographic conditions used here. However, the peak tracking strategy as such assumes no prior knowledge of the number of components nor their identities, hence chromatograms of "unknown" mixtures can be analysed in an analogous manner.

Peak self-matching. In part A of this discussion, the reproducibility of the O.M.F. scores were established (that is, the reproducibility of the O.M.F. scores with respect to the software and hardware used). Another factor which needs to be considered is the selectivity of the peak matching process; that is, the stability of the method against false positive matches. To establish the selectivity of the method, each solute peak in a chromatogram was matched against every other peak in that same chromatogram to determine how similar the peak spectra are within a chromatogram, and hence estimate the number of potential mismatches. A mismatch in this context is defined as a solute peak spectra for which more than one match candidate (*i.e.* other than itself) was found with a O.M.F. score within the cut-off limits established in part A. That is, any peaks with O.M.F. scores of 999.79 ± 0.27 are considered to be identical within the reproducibility limits of the peak tracking method.

Table V summarises the results obtained when just such an analysis was performed on chromatogram Y (*i.e.* the peaks from Chromatogram Y have been compared to themselves). Table V shows that although some peaks have quite high O.M.F. scores with other peaks (*i.e.* other than themselves with the expected perfect match factors of 1000.00) within the same chromatogram, only two of the peaks, Y4 and Y5, have

TABLE V

SUMMARY OF THE O.M.F. SCORES OBTAINED FOR FIVE BEST MATCHING PEAKS WHEN THE PEAKS IN CHROMATOGRAM Y ARE COMPARED TO THEMSELVES BY THE PEAK TRACKING METHOD

Values in bold have exceptionally high overall match factor.

Peaks Y[a]	Peaks Y										
	Y1	Y2	Y3	Y4	Y5	Y6	Y7	Y8	Y9	Y10	Y11
Y1	1000.00										
Y2		1000.00				966.56	993.42	995.14	998.89	991.27	
Y3			1000.00		983.95	998.86					
Y4	959.33		983.09	1000.00	**999.60**	976.82				985.11	996.18
Y5	955.30		983.95	**999.60**	1000.00	978.65					995.01
Y6			998.86			1000.00					
Y7		993.42					1000.00	999.12	995.74		
Y8		995.14					999.12	1000.00	997.60	987.43	
Y9		998.89					995.74	997.60	1000.00	990.88	
Y10		991.27	975.47	985.11			983.38	987.43	990.88	1000.00	978.93
Y11	975.26			996.18	995.01						1000.00

[a] Peaks Y: peak numbers from chromatogram Y.

O.M.F. values which fall within the previously established confidence limits of the reproducibility of the method (*i.e.* 999.79 ± 0.27). Thus, when the sensitivity of the peak tracking method is taken into account, these two peaks are basically indistinguishable, and we can can expect the peak tracking method to have problems identifying them accurately. Since these two peaks have such high O.M.F. scores, this must mean that they have very similar spectra.

Amino acid analysis of the chromatographic fractions corresponding to peaks Y4 and Y5 from chromatogram Y revealed that they have identical amino acid composition corresponding to the peptide pGH [141–152] (QTYDKFDTNLR) and would therefore be expected to exhibit identical spectra. As indicated in Fig. 4, peaks Y4 and Y5 from chromatogram Y and their respective corresponding peaks X4 and X6 from chromatogram X have significantly different elution positions. The cause of the different retention behaviour of these peptides with apparently identical amino acid composition is currently being investigated, but by analogy with other xxYDKxx containing peptides may correspond to the β-rearranged form of the aspartic acid at position xDx.

To summarise, because of the exceptionally high O.M.F. scores (which fall within the absolute sensitivity limits of the peak tracking method) and the corresponding spectral similarity between peaks Y4 and Y5, these peaks are unlikely to be able to be accurately distinguished by the peak tracking software. In other words, the software provides a pre-warning for matches assigned by the peak tracking method for peaks Y4 and Y5.

Peak cross-matching. Table VI summarises the results obtained after application of the peak tracking software to the two selected chromatograms. The peaks from chromatogram X were matched to peaks in chromatogram Y. The peaks from chromatogram Y with the 5 highest O.M.F. values for each of the peaks in chromatogram X are presented. Fig. 4 graphically illustrates the matching of peaks from chromatogram X to chromatogram Y as selected by the peak tracking algorithms. As indicated in Fig. 4 and Table VI, 9 of the 11 solute peaks in chromatogram Y were correctly matched to their corresponding solute peaks in chromatogram X. Fig. 4 and Table VI also indicate that 2 of the 11 peaks were not correctly matched. Peak X4 was incorrectly matched to peak Y5 when it should have been matched to peak Y4. Similarly, peak X6 was

TABLE VI

SUMMARY OF THE O.M.F. SCORES FOR THE FIVE BEST MATCHING PEAKS FROM CHROMATOGRAM Y WHEN COMPARED TO EACH PEAK IN CHROMATOGRAM X BY THE PEAK TRACKING METHOD

Values in italics: peaks correctly matched by the peak tracking method. Values in bold: peaks incorrectly matched by the peak tracking method. Value between parentheses: correct matching peaks (but incorrectly matched by the peak tracking method).

Peaks Y[a]	Peaks X[b]										
	X1	X2	X3	X4	X5	X6	X7	X8	X9	X10	X11
Y1			*999.54*								
Y2	974.66	*997.17*			965.67		991.46	994.23	998.45		991.25
Y3	*998.00*			983.38	997.20	982.75					
Y4	974.36		964.43	(999.22)	973.30	**997.81**				995.93	987.27
Y5	976.13		960.98	**999.33**	975.78	(997.63)				995.23	
Y6	997.86				*998.72*						
Y7		989.99					*999.58*	997.70	995.07		
Y8		990.12					998.21	*999.10*	996.76		986.25
Y9		994.65					993.68	996.96	*999.80*		990.54
Y10		987.06					980.45	986.39	990.14	975.16	*999.79*
Y11			979.72	994.85		993.60				*999.54*	

[a] Peaks Y: peak numbers from chromatogram Y.
[b] Peaks X: peak numbers from chromatogram X.

incorrectly matched to peak Y4 when it should have been matched to peak Y5.

Thus, as predicted, peaks Y4 and Y5 were indeed mismatched in this example. It is not surprising that peaks Y4 and Y5 were incorrectly matched, since even the slightest differences in chromatographic baseline noise will subtly alter the spectral characteristics of these peaks and make these peptide peaks especially susceptible to mismatching. It should be noted, however, that the correctly matched (but *not* best matching) peaks in these cases (values between parentheses in Table VI) were in fact the second-best matching peaks (*i.e.* had the second highest O.M.F. scores) and have very similar O.M.F. scores to the incorrectly matched (but best matching) peaks (values in bold in Table VI) in both cases.

This example has therefore illustrated an important feature point in this peak tracking method. When all components differ sufficiently in their spectral characteristics, a close match between the spectra, expressed by the O.M.F score, is adequate for unambiguous identification purposes (as illustrated by 9 of the 11 peaks correctly matched in the above example). However, when two or more components in the mixture being investigated have very similar spectral characteristics (O.M.F. scores within the reproducibility limits of the equipment and software), as was the case for the solutes corresponding to peaks Y4, Y5, X4 and X6, an additional source of peak matching information is required. This extra information could be supplied by comparing the relative areas or heights of the peaks. Close examination of Fig. 3 demonstrates that just such an analysis would easily have matched peaks X4 to Y4 and X6 to Y5, since they have different area ratios to each other.

In the rare situation where two different components in a sample have identical spectral characteristics as well as equal peak areas/heights, the present version of the software will not distinguish between them and the outcome will involve three possible peak matching solutions. The first would be to assume that no cross-over of peak elution order occurs as the chromatographic conditions are changed. This seems the most reasonable since peptide homo-

logues will usually respond in a similar fashion to changes in the selectivity of the solvent system. The second option would be to assume that peak cross-over has occurred, and the third option would be to assume that the peaks co-eluted (this latter option would be obvious since there would be a "missing" peak in the chromatogram). Each of these three possible solutions can then be considered independently from analysis of the log $\bar{k}$ *versus* $\bar{\psi}$ plots, or from the slope of log $\bar{k}$ *versus* $1/T$ plots [24].

CONCLUSIONS

The described peak tracking procedure is capable of monitoring the positions of each peptide solute peak between any two chromatograms of a solute mixture recorded under different chromatographic conditions. The process is based on the analysis of each peak's characteristic UV–Vis spectrum to generate an overall match factor (O.M.F.) representing the similarity between any two peptide peaks from the different chromatograms.

Using this new peak tracking method, the peptide solutes derived from a tryptic map of r-pGH can be identified and tracked across various chromatographic conditions, including changes in stationary phases, mobile phase solvents, gradient times, temperatures and solvent flow-rates. As shown in the selected example, the peak tracking software can effectively deal with changes in peak elution orders and relative peak areas. The nine correctly matched peaks in the selected example illustrate that when the solute peaks in the mixture differ sufficiently in their spectral characteristics from each other, a close match between spectra, as expressed by an O.M.F. score, is sufficient for unambiguous identification. However, when components with very similar spectra are present in a mixture, additional information such as the relative areas/heights of the peaks must be used in order to perform an unambiguous identification. Further work is underway to incorporate into the peak tracking software an algorithm to perform peak area matching for these difficult cases. Another area which needs to be investigated is the problem of mixed component spectra due to poorly resolved peaks. This problem could be addressed by the use of principle component analysis to de-convolute the complex impure spectra into their component spectra. In the present method, no attempt is made to match peaks whose spectra reveal that they are impure (*i.e.* co-eluting or poorly resolved peaks).

The peak tracking method described in this paper is not limited to tracking peaks from tryptic digests of proteins such as the r-pGH tryptic digests. The method should be generally applicable to any peptide mixture, or indeed any mixture of organic molecules. In fact, peptide fragments, because of their rather nondescript and similar spectra, probably represent a more difficult scenario to deal with than many other types of chromatographic samples of comparable compositional complexity but with considerably greater spectral variety. This peak tracking procedure should thus assist in the development of new HPLC optimisation protocols, providing a basis for improved strategies for the monitoring and control of the analysis and purification of biological macromolecules, particularly peptides and proteins produced by chemical synthesis or recombinant DNA techniques, and from enzymatic and chemical digestions.

ACKNOWLEDGEMENT

The support of the Australian Research Council is gratefully acknowledged.

REFERENCES

1 M.T.W. Hearn (Editor), *HPLC of Proteins, Peptides and Polynucleotides —Contemporary Topics and Applications*, VCH, Deerfield, FL, 1991.
2 J.C. Berridge, *Techniques for the Automated Optimization of HPLC Separations*, Wiley-Interscience, New York, 1985.
3 P.J. Schoenmakers, *Optimization of Chromatographic Selectivity —A Guide to Method Development (Journal of Chromatography Library*, Vol. 35), Elsevier, Amsterdam, 1986.
4 S.D. Patterson, *J. Chromatogr.*, 592 (1992) 43.
5 A.G. Wright, A.F. Fell and J.C. Berridge, *J. Chromatogr.*, 458 (1988) 335.
6 H.J. Issaq and K. McNitt, *J. Liq. Chromatogr.*, 5 (1982) 1771.

7 J.C. Berridge and E.G. Morrissey, *J. Chromatogr.*, 316 (1984) 69.
8 A.S. Kester and R.E. Thompson, *J. Chromatogr.*, 310 (1984) 372.
9 J.C. Berridge, *J. Chromatogr.*, 244 (1982) 1.
10 A.G. Wright, A.F. Fell and J.C. Berridge, *Chromatographia*, 24 (1987) 533.
11 D.H. Hill, T.R. Kelly and K.J. Langner, *Anal. Chem.*, 59 (1987) 350.
12 M. Otto, W. Wegscheider and E.P. Lankmayr, *Anal. Chem.*, 60 (1988) 517.
13 A.C.J.H. Drouen, H.A.H. Billiet and L. de Galan, *Anal. Chem.*, 56 (1984) 971.
14 Y. Zhang, H. Zou and P. Lu, *J. Chromatogr.*, 515 (1990) 13.
15 A.C.J.H. Drouen, H.A.H. Billiet and L. de Galan, *Anal. Chem.*, 57 (1985) 962.
16 H-J.P. Sievert, S-L. Wu, R. Chloupek and W.S. Hancock, *J. Chromatogr.*, 499 (1990) 221.
17 P.J.M Coenegracht, H.J. Metting, E.M. van Loo, G.J. Snoeijer and D.A. Doornbos, *J. Chromatogr.*, 631 (1993) 145.
18 B. Grego, E. Nice and R.J. Simpson, *J. Chromatogr.*, 352 (1986) 359.
19 A. Drouen, *The COMPARE Command Information Note*, Hewlett-Packard, Waldbronn, Publication Number 12-5952-3725, 1987.
20 J.K. Strasters, H.A.H. Billiet, L. de Galan and B.G.M. Vandeginste, *J. Chromatogr.*, 499 (1990) 499.
21 J.K. Strasters, F. Coolsaet, A. Bartha, H.A.H. Billiet and L. de Galan, *J. Chromatogr.*, 499 (1990) 523.
22 G. Winkler, P. Wolschann, P. Briza, F. Heinz and C. Kunz, *J. Chromatogr.*, 347 (1985) 83.
23 A. Savitzky and M.J.E. Golay, *Anal. Chem.*, 36 (1964) 1627.
24 A.W. Purcell, M.I. Aguilar and M.T.W. Hearn, *J. Chromatogr.*, 593 (1992) 103.
25 Q.M. Mao, I.G. Prince and M.T.W. Hearn, *J. Chromatogr.* 646 (1993) 81.

Journal of Chromatography A, 661 (1994) 77–82
Elsevier Science B.V., Amsterdam

CHROMSYMP. 2904

Determination of peptide hydrophobicity parameters by reversed-phase high-performance liquid chromatography

S. Rothemund*, E. Krause, A. Ehrlich and M. Bienert

Institute of Molecular Pharmacology, Alfred-Kowalke-Strasse 4, 10315 Berlin (Germany)

E. Glusa

Institute of Pharmacology and Toxicology, Medical School Erfurt, Erfurt (Germany)

P. Verhallen

Schering AG, Berlin (Germany)

ABSTRACT

The log k_w values of fourteen potential fibrinogen receptor antagonist peptides (RGDX) determined by reversed-phase HPLC were correlated to hydrophobic parameters of the amino acid side-chain log P in position X of the tetrapeptides. Comparing the polymer columns with LiChrosorb RP-8, the correlation coefficient using a polyethylene column is higher (0.94) than that for RP-8 (0.88), which demonstrates the importance of a homogeneous hydrophobic surface and makes this method very suitable for the determination of the overall hydrophobicity of shorter peptides. The hydrophobicity parameters log k_w of the RGDX peptides (−1.15 to 2.19) were used to investigate the influence of molecular parameters of X on the potency of RGDX in inhibiting platelet aggregation. The results confirm the importance of hydrophobicity for the contribution of X to the biological activity of RGDX.

INTRODUCTION

In addition to the steric and electronic properties, hydrophobicity has a strong influence on the biological activity of drugs. Many studies of quantitative structure–activity relationships (QSAR) are based on the relation between bioactivity and hydrophobicity [1,2]. As suggested by Hansch and Fujita [3], this influence may be due to the transport processes and/or hydrophobic ligand–receptor interactions. Usually, the partition coefficient between 1-octanol and water (log P) is accepted as a hydrophobic parameter and a reference system because of its analogy with biomembranes [4]. An important limitation of QSAR studies of peptides is the lack of reliable sets of structural descriptors. However, the traditional shake-flask method for log P determination causes experimental problems [5] and therefore alternative methods for estimating hydrophobicity indices have been investigated [6,7].

Reversed-phase HPLC has been used for this purpose, and several studies have described a correlation between log P (n-octanol/water) and

* Corresponding author.

0021-9673/94/$07.00
SSDI 0021-9673(93)E0839-M

the logarithm of the capacity factors (log k') by using alkyl-bonded silica as the stationary phase [8]. In more recent studies the hydrophobicity parameters derived by polycratic methods have shown a better correlation with log P than chromatographic retention data obtained under monocratic conditions [9,10]. In order to suppress the effect of the organic co-solvent, one approach is to use the isocratic capacity factors (log k') extrapolated to 100% water (log k_w). Linear plots of log k' *vs.* organic modifier content were obtained by using methanol as the organic modifier [11]. However, the presence of residual surface silanols of alkyl-bonded silica phases causes interactions with basic groups, leading to additional non-hydrophobic interactions with peptides [12].

Organic polymer-based stationary phases [13,14] as well as polymer-coated silica phases [15,16] have been shown to be excellent alternatives to alkyl-bonded silica. The polymer phases are stable with eluents from pH 1 to 14, and the homogeneous non-polar surface leads to a retention behaviour different to that of the alkyl-bonded silica phases [17,18].

An attractive approach for the pharmacological inhibition of platelet aggregation is focused on small molecule antagonists derived from RGD sequences. Charon *et al.* [19] studied the influence of different amino acids of RGDX tetrapeptides on platelet aggregation. These results show an increasing inhibitory potency with an increasing hydrophobicity in position X.

The aim of the present study was to compare the chromatographic hydrophobicity parameters of RGDX tetrapeptides using alkyl-bonded silica, poly(styrene–divinylbenzene) and polyethylene [20] as stationary phases. Furthermore, a relation between the determined log k_w values and the bioactivity of the peptides in a platelet aggregation test, using multiple regression, was established.

EXPERIMENTAL

HPLC conditions

The HPLC system consisted of two pumps (Jasco Model 880), a UV detector (Shimadzu SPD-6A) operated at 220 nm and a Rheodyne Model 7125 injection valve (20 μl). Chromatograms were recorded with a data system from Nuclear Interface. For isocratic elution mixtures of methanol and 0.05 M KH_2PO_4 (pH 7.0) were used as mobile phase. The flow-rate was set at 0.5 ml/min using the polyethylene column and at 1 ml/min using PLRP-S or LiChrosorb RP-8. All measurements were made at ambient temperature. Sample concentration of peptides was 1 mg/ml.

Capacity factors (k') were calculated from the retention time, $k' = (t_R - t_0)/t_0$. Data for t_0 were obtained by injecting a liquid mixture with a volume composition different from that of the eluent.

Column

A commercial Merck LiChrosorb RP-8 (5 μm) column (125 × 3 mm I.D.) and a PLRP-S (8 μm) column (150 × 4.6 mm I.D.) containing poly(styrene–divinylbenzene) from Polymer Laboratories were used without further treatment. Polyethylene was supplied by E. Merck, (Darmstadt, Germany), sieved to 20–40 μm irregular particles and was packed into a stainless-steel column (150 × 4.6 mm I.D.) as described previously [21].

Peptide synthesis and purification

The peptides RGD-Nal [3-(1-naphthyl)-alanine], RGD-Hph (homo-phenylalanine), RGD-Cha (cyclohexyl-alanine), RGD-Fpa (4-fluoro-phenylalanine), RGD-Bpa (4-bromo-phenylalanine), RGDS(Bzl) (O-benzylserine), RGDY(Bzl) (O-benzyltyrosine) and RGD-Cpa (4-chloro-phenylalanine) were synthesized by the classical mixed anhydride method with final deprotection by catalytic hydrogenolysis. RGDN, RGDS, RGDK, RGDH, RGDY, RGDF and RGDW were synthesized by a solid-phase method using the Fmoc strategy. Purification of crude peptides was carried out by preparative reversed-phase chromatography on a polyethylene column (450 × 25 mm, 40–60 μm). The peptides gave correct values in amino acid analysis and fast atom bombardment MS and were analysed by HPLC.

Measurement of platelet aggregation

Platelets were isolated from human venous blood drawn into 1:10 volume of acid citrate.

The platelet-rich plasma was prepared by centrifugation (10 min, 150 *g*). Briefly, platelets at a final concentration $2.5–3.0 \cdot 10^8$ /ml were incubated with varying concentrations of peptides. After 3 min aggregation was induced by the addition of ADP, adrenaline, collagen and plasma activating factor (PAF). Aggregation was measured at 37°C using a dual-channel aggregometer (Payton).

IC_{50} values were estimated from the concentration–response curves.

RESULTS AND DISCUSSION

Determination of log k_W values

The capacity factors of fourteen RGDX tetrapeptides were determined using LiChrosorb RP-8, PLRP-S and polyethylene. The measurements were performed in methanol concentrations of 0–40% (v/v). To suppress the silanol activity of the alkyl-bonded silica column, 0.05 *M* NaH_2PO_4 buffer (pH 7.0) was used as eluent. Plots of log k' against the methanol concentration in the eluent using polyethylene, PLRP-S and LiChrosorb RP-8 are shown in Figs. 1, 2 and 3, respectively.

The increase in log k' with decreasing methanol concentration was very close to linear with all stationary phases. Consequently, the log k' values could be extrapolated linearly to 100% water content, yielding log k_W values of the peptides shown in Table I. The elution orders of the tetrapeptides on the polymer phase and RP-8 were identical, indicating that the dominant retention mechanism was hydrophobic in nature. The deviations in terracing of the log k_W values emphasize the individual retention behaviour of each stationary phase. The capacity factors using poly(styrene–divinylbenzene) show increasing retention for peptides with aromatic amino acids in position X owing to the additional $\pi-\pi$ interactions. As expected, RGDY(Bzl) with two

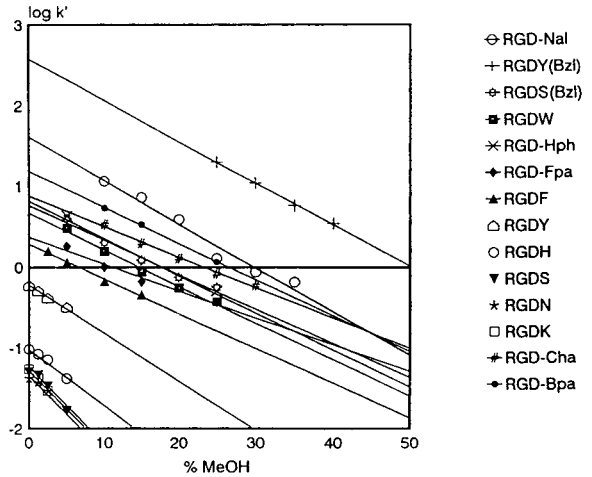

Fig. 2. Change in the capacity factors of RGDX peptides with increasing content of methanol in water (0.05 *M* phosphate, pH 7.0) on PLRP-S.

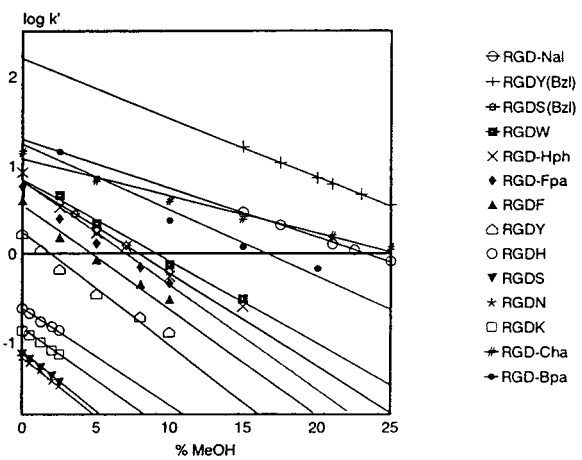

Fig. 1. Change in the capacity factors of RGDX peptides with increasing content of methanol in water (0.05 *M* phosphate, pH 7.0) on polyethylene.

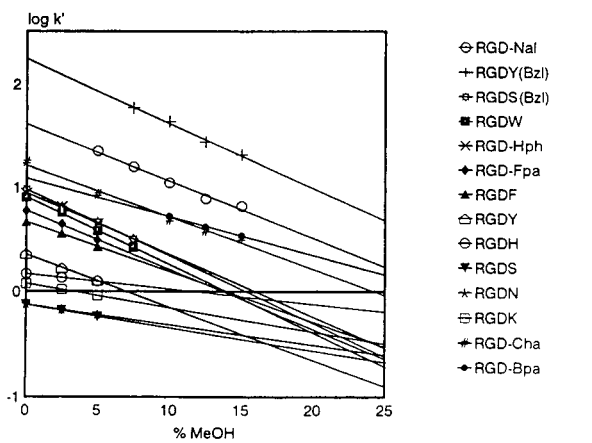

Fig. 3. Change in the capacity factors of RGDX peptides with increasing content of methanol in water (0.05 *M* phosphate, pH 7.0) on LiChrosorb RP-8.

TABLE I

LOG k_w VALUES DETERMINED BY USING DIFFERENT STATIONARY PHASES (POLYETHYLENE, PLRP-S AND LICHROSORB RP-8) AND THE CORRELATION WITH 1-OCTANOL/WATER PARTITION COEFFICIENTS LOG P [22] OF THE AMINO ACID SIDE-CHAIN IN POSITION X AND HYDROPHOBICITY SCALES $z1$ [23]

n.d., not determined.

Sequence	Log k_w polyethylene	Log k_w PLRP-S	Log k_w LiChrosorb RP-8	Log P amino acid side-chain [22]	$z1$ amino acid [23]
RGDN	−1.15	−1.33	−0.12	−0.60	2.88
RGDS	−1.13	−1.26	−0.12	−0.04	2.48
RGDK	−0.87	−1.26	0.08	−0.99	3.76
RGDH	−0.63	−1.00	0.17	0.13	3.46
RGDY	0.15	−0.23	0.35	0.96	−3.58
RGDF	0.52	0.25	0.67	1.79	−3.62
RGD-Fpa	0.70	0.37	0.78	n.d.	−4.70
RGD-Hph	0.81	0.82	0.95	2.10	n.d.
RGDS(Bzl)	0.82	0.76	0.98	2.34	−4.76
RGDW	0.84	0.67	0.91	2.25	−4.02
RGD-Cha	1.08	0.88	1.21	2.72	−5.15
RGD-Bpa	1.25	1.19	1.09	n.d.	−5.13
RGD-Nal	1.30	1.48	1.61	3.15	−6.21
RGDY(Bzl)	2.19	2.53	2.27	2.72	−6.02
$r(z1)$	0.93	0.91	0.85	0.96	1.00
r (log P)	0.94	0.93	0.88	1.00	0.96

separated aromatic rings shows the highest retention on PLRP-S.

Comparison of the overall tetrapeptide hydrophobicity (log k_w) and calculated amino acid side-chain parameters

In order to verify the determined hydrophobicity parameters of the RGDX tetrapeptides, the log k_w values were compared with calculated hydrophobicity parameters of the different natural and non-natural amino acids in position X (Table I).

The log P values represent the 1-octanol/water partition coefficients of the amino acid chains determined by Fauchère *et al.* [22] using the shake-flask method of acetyl-amino acid amides. The z-scales [23] of the amino acids were derived by principal component analysis of a matrix, consisting of twelve properties (NMR, TLC, Van der Waals volume, MW) for 55 coded and non-coded amino acids and are related to hydrophobicity ($z1$), bulk ($z2$) and electronic properties ($z3$).

The data for the correlation coefficient r show a sufficient correlation (0.91–0.94) between the log k_w values, measured on polymer-based phases, and the hydrophobic side-chain parameters in position X, especially for the polyethylene stationary phases (0.93–0.94). However, the correlation coefficients obtained with LiChrosorb RP-8 (0.85–0.88) were lower than those of polyethylene and PLRP-S.

The good correlation of log k_w values with the peptide hydrophobicity demonstrates that the polyethylene stationary phase is a useful tool for assessing the overall hydrophobicity of shorter peptides. Polyethylene has a homogeneous hydrophobic adsorption surface and therefore does not require additional inhibition of polar peptide–solid phase interactions.

Quantitative structure–activity relationship (QSAR) studies using HPLC log k_W values

A set of eleven RGDX peptides with different side-chain hydrophobicity in position 4 was synthesized and used in QSAR studies. The biological activity of these peptides was investigated by measuring the inhibition of platelet aggregation. The inhibitory potencies of the peptides were expressed as the IC_{50} values and are shown in Table II.

Modelling using the multiple regression of the set resulted in a parabolic model in the biological test. The important factor in this model is the hydrophobicity parameter log k_W of the amino acid side-chain in position X, estimated on polyethylene:

$$\log IC_{50} = -0.398 \log k_W + 0.157 (\log k_W)^2 + 1.931$$
$$(0.059) \quad (0.048) \quad (0.074)$$
$$n = 11, \mathrm{SE} = 0.17, r^2 = 0.85, F = 22.7 \quad (1)$$

Eqn. 1 gives the best fit with observed bioactivities, assuming that a parabolic dependence of log IC_{50} on the hydrophobicity of amino acids in position X of RGDX peptides contributes to the activity. Obviously, a hydrophobic amino acid side-chain in the C-terminal position of RGDX peptides enhances the binding to platelet glycoprotein GPIIb/IIIa receptors. Correlation coefficients of log P, $z1$ and log k_W determined on C_{18} PLRP-S are in each case lower than that of polyethylene ($r^2_{C8} = 0.82$, $r^2_{\mathrm{PLRP\text{-}S}} = 0.82$, $r^2_{z1} = 0.77$, $r^2_{\log P} = 0.73$, $r^2_{\mathrm{polyethylene}} = 0.85$).

The results demonstrate that the incorporation of amino acids with a hydrophobicity similar to tryptophan leads to an optimized inhibitory activity. Incorporation of amino acids exhibiting both lower and higher hydrophobicity resulted in analogues with diminished receptor binding. On the basis of these results further improvements of the antagonistic potency were achieved by preventing the enzymatic degradation. Thus, des-NH_2-RGDW (Table II) was the most active compound in this series.

TABLE II

IC_{50} VALUES DETERMINED BY PLATELET AGGREGATION TEST

Sequence	IC_{50} (μmol/l) platelet-aggregation assay
RGDN	322 ± 38
RGDS	447 ± 45
RGDH	203 ± 30
RGDF	38 ± 13
RGD-Fpa	53 ± 14
RGD-Hph	60 ± 20
RGDS(Bzl)	90 ± 18
RGDW	32 ± 8
RGD-Bpa	80 ± 25
RGD-Nal	33 ± 12
RGDY(Bzl)	63 ± 19
des-NH_2-RGDW	1.4 ± 0.35

CONCLUSION

Polymer-based stationary phases can be used for the determination of the overall hydrophobicity of RGDX peptides just like silica-based reversed-phase columns. The measured log k_W values of the tetrapeptides correlate with calculated hydrophobic amino acid side-chain parameters (log P, $z1$), especially for using polyethylene as stationary phases. Both the absence of residual polar groups (silanols) and the homogeneous hydrophobic adsorption surface of polyethylene contribute to the improved compatibility between log k_W values and hydrophobicity parameters.

Furthermore, a parabolic model based on peptide log k_W of the tetrapeptides was established to describe the structure–activity relationship of RGDX peptides.

The results demonstrate the applicability of reversed-phase HPLC capacity factors as hydrophobic parameters for quantitative structure–activity relationship of shorter peptides.

REFERENCES

1 V. Pliska and M. Charton, *J. Rec. Res.*, 11 (1991) 59.
2 H. Iwamura, M. Assao, M. Akamatsu and T. Fujita, *J. Med. Chem.*, 30 (1987) 1873.

3 C. Hansch and T. Fujita, *J. Am. Chem. Soc.*, 86 (1964) 1616.
4 H. Kubinyi, *Prog. Drug Res.*, 23 (1979) 97.
5 J.C. Dearden and G. Bresnen, *Quant. Struct. Act. Relat.*, 7 (1988) 133.
6 S.D. Black and D.R. Mould, *Anal. Biochem.*, 193 (1991) 72.
7 R.F. Rekker, in W.Th. Nauta and R.F. Rekker (Editors), *The Hydrophobic Fragmental Constant (Pharmacochemistry Library*, Vol. 1), Elsevier, Amsterdam, 1977.
8 E.J. Haky and A.M. Young, *J. Liq. Chromatogr.*, 7 (1984) 675.
9 D.J. Minick, D.A. Brent and J. Frenz, *J. Chromatogr.*, 461 (1989) 177.
10 B. Testa, A. Bechalany, T. Röthlisberger and N.El Tayar, *J. Chromatogr.*, 473 (1989) 115.
11 B. Testa, A. Tsantili-Kakoulidou, N.El Tayar and A. Bechalany, *J. Chromatogr.*, 541 (1991) 221.
12 E.B. Klaas, C. Horvath, W.R. Melander and A. Nahum, *J. Chromatogr.*, 203 (1981) 65.
13 Z. Iskandarani and D.J. Pietrzyk, *Anal. Chem.*, 53 (1981) 489.
14 T. Hanai, Y. Arai, M. Hirukawa, K. Noguchi and Y. Yanagihara, *J. Chromatogr.*, 349 (1985) 323.
15 G. Schomburg, A. Deege, J. Köhler and U. Bien-Vogelsang, *J. Chromatogr.*, 282 (1983) 27.
16 G. Schomburg, J. Köhler, H. Figge, A. Deege and U. Bien-Vogelsang, *Chromatographia*, 18 (1984) 256.
17 R.M. Smith, *J. Chromatogr.*, 291 (1984) 372.
18 J.V. Dawkins, N.P. Gabbott, L.L. Lloyd, J.A. McConville and F.P. Warner, *J. Chromatogr.*, 452 (1988) 145.
19 M.N. Charon, A. Poggi, M.B. Donati and G. Marguerie, in J.E. Rivier and G.R. Marshall (Editors), *Proc. 11th Amer. Pept. Symp., 1990, La Jolla*, ESCOM, Leiden, 1990, pp. 82–83.
20 E. Krause, D. Smettan, F. Loth and H. Herma, *J. Chromatogr.*, 520 (1990) 263.
21 E. Krause and M. Bienert, *J. Liq. Chromatogr.*, 15 (1992) 1773.
22 J.L. Fauchêre, M. Charton, L.B. Kier, A. Verloop and V. Pliška, *Int. J. Pept. Protein Res.*, 32 (1988) 269.
23 J. Jonsson, L. Eriksson, S. Hellberg, M. Sjöström and S. Wold, *Quant. Struct. Relat.*, 8 (1989) 204.

Journal of Chromatography A, 661 (1994) 83–92
Elsevier Science B.V., Amsterdam

CHROMSYMP. 2964

Recombinant human insulin

III[☆]. High-performance liquid chromatography and high-performance capillary electrophoresis control in the analysis of step-by-step production of recombinant human insulin

V.E. Klyushnichenko*, D.M. Koulich, S.A. Yakimov, K.V. Maltsev, G.A. Grishina, I.V. Nazimov and A.N. Wulfson

Shemyakin and Ovchinnikov Institute of Bioorganic Chemistry, Russian Academy of Sciences, ul.-Mikluho-Maklaya 16/10, 117871 GSP Moscow V-437 (Russian Federation)

ABSTRACT

The production of recombinant human insulin consists of five main stages, accompanied by considerable transformation of molecules, concerning size, secondary structure and the presence of charged groups. The application of different methods, *i.e.*, size-exclusion, ion-exchange and reversed-phase high-performance liquid chromatography (HPLC) and high-performance capillary electrophoresis (HPCE) (capillary zone electrophoresis and micellar electrokinetic capillary chromatography), to the analysis of insulin, insulin-related and non-insulin-related substances was studied. A combined HPLC–HPCE system for the step-by-step control of recombinant human insulin production technology is suggested. The advantages and shortcomings of these methods are discussed.

INTRODUCTION

Insulin is an important protein in practical medicine, and it is advisable to carry out its production by microbiological methods. Recombinant human insulin (Fig. 1) is formed in the course of fermentative splitting of proinsulin, which is in turn is obtained from fusion protein, isolated from "inclusion bodies" of the producer's ground recombinant cells. Recombinant strains of *Escherichia coli* with transformed plasmid are used as the producer [1,2]. In the given case, we used a strain with a built-in plasmid nucleotide sequence, expressing fusion protein, which consists of linear proinsulin and protein A fragments, linked with the N-terminus by means of a methionine residue. The cultivation of a saturated biomass of recombinant cells ensures the beginning of fusion protein production, the expression and step-by-step transformation of which lead to insulin. Insulin intended for the production of medicaments must be of high

* Corresponding author.

[☆] For Part II, see ref. 27. Abbreviations used: SE-, IO- and RP-HPLC = size-exclusion, ion-exchange and reversed-phase high-performance liquid chromatography; HPCE = high-performance capillary electrophoresis; CZE = capillary zone electrophoresis; MECC = micellar electrokinetic capillary chromatography; rHI = recombinant human insulin; rHP = recombinant human proinsulin; drHP = denatured recombinant human proinsulin; rHP = SSO_3 = recombinant human proinsulin-S-sulphonate; rPFP = recombinant proinsulin fusion protein; HMP = high-molecular-mass proteins; TP = theoretical plates.

0021-9673/94/$07.00
SSDI 0021-9673(93)E1108-C

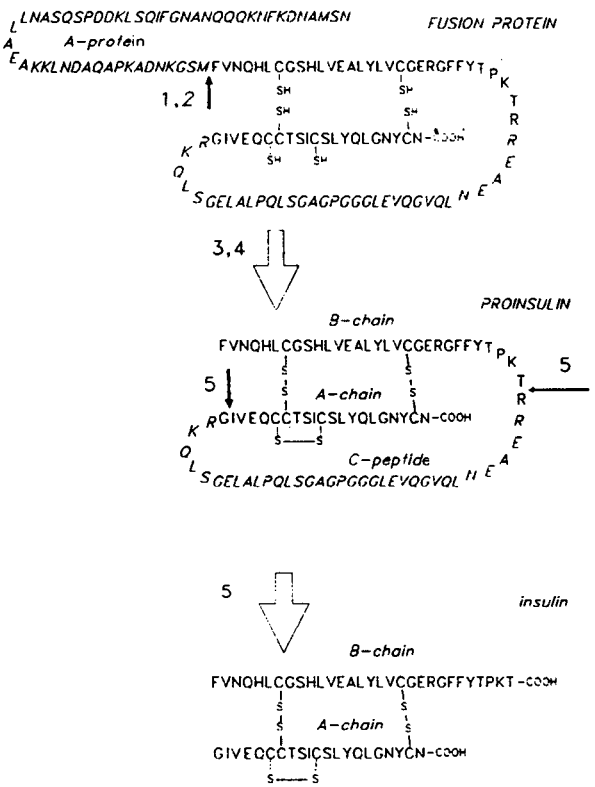

Fig. 1. Transformation of fusion protein molecules into insulin molecules: 1 = rPFP; 2 = rPFP splitting according to methionine residue (M) under the influence of BrCN into linear proinsulin and A-protein fragment; 3,4 = formation of rHP as a result of SH-group sulphitolysis, followed by the closure of S–S bonds in the process of S–SO_3 group reduction; 5 = C-peptide restriction out of rHP molecule, accompanied by the formation of rHI.

purity and contain, for example, not more than 0.1% of proinsulin, not more than 1% of high-molecular-mass proteins, including insulin oligomers, and not more than 1% of desamido-(A_{21})-insulin [3,4]. The separation of insulin and peptides closely related to it is a difficult task because of the small difference in their conformation and charge [3,5]. The use of RP-HPLC for the fine purification of recombinant, human, bovine, porcine rat and other insulin and insulin-related proteins on well known commercial columns has been suggested earlier [3,5–13]. Proinsulin-S-sulphonate (see below), proinsulin, separate A- and B-chains and their S-sulphonates have also been characterized with the help of RP- and IE-HPLC [14,15].

High-performance capillary electrophoresis (HPCE) is very promising analytical method applicable in many branches of chemistry [16], including biochemistry [17]. The most useful and successfully technique of HPCE for the analysis of biopolymers is capillary zone electrophoresis (CZE) [18]. In spite of problems connected with the adsorption of species on the capillary walls, good results in the analysis of peptides and proteins by CZE have been achieved [19,20]. CZE is considered to be promising for the analysis of recombinant proteins in biotechnology [20–24], where its advantages such as economy [21] and high resolving power [22] are especially important.

EXPERIMENTAL

For SE-HPLC the columns used were TSK G 3000 SW (300 × 7.5 mm I.D.) (TOSOH) and Protein Pack 60 (30 × 0.75 mm I.D.) (Waters–Millipore); elution was performed at a flow-rate of 0.5 ml/min.

Chromatography was carried out using a Varian 8500 pump with a Waters U6K injector, DuPont Model 852001-902 spectrophotometer and Waters Model 740 integrator. For IE-HPLC the columns used were Armsorb-Si-500 poly-Amin (150 × 4 mm I.D.). Armsorb-Si-500 DEAE (150 × 4 mm I.D.), (Armchrom, Yerevan, Armenia), Protein Pac DEAE 5 PW (250 × 4.6 mm I.D.) (Waters,) and Nucleogen DEAE 4000-7 (150 × 4 mm I.D.) (Machery–Nagel), For RP-HPLC the columns used were Armsorb-Si-300 C_8 P(DM) (150 × 4 mm I.D.), Armsorb-Si-300 C_8 RP-PR (300 × 4 mm I.D.), (ErONEM Archrom), Nucleosil 300-7 Protein RP (150 × 4 mm I.D.), Nucleosil C_{18} (150 × 4 mm I.D.) (Machery–Nagel) and μBondaPak C_{18} (300 × 3.9 mm I.D.) (Waters), Chromatography was carried out using a Waters Model 510 pump with a Waters U6K injector, a Waters Model 490E spectrophotometer and a Waters Model 740 integrator.

For the separation we used specimens of insulin, proinsulin, denatured proinsulin, proinsulin-S-sulphonte, fusion protein (obtained from IBC RAS) and for identification a human insulin standard specimen (Atlanta, Cat. No. 83/500,

Chemie- und Handelsgesellschaft, Heidelberg, Germany). The reagents used were: acetonitrile, methanol, sodium hydroxide, sodium chloride, sodium sulphate, sodium phosphate, phosphoric acid, acetic acid (all of the highest purity available), water purified on a Milli-Q system (Millipore), sodium dodecyl sulphate (Serva) and guanidine hydrochloride (Merck). Before chromatography, the eluents were filtered through nitrocellulose and GVWP filters (pore diameter 0.45 μm; Millipore) and degassed for 20 min.

For HPCE we used a PACE 2010 system, with fused-silica capillaries of I.D. 100 μm, length 87 cm, effective length 80 cm, and I.D. 100 μm, length 52 cm, effective length 40 cm (Beckman).

Sodium dodecyl sulphate-polyacrylamide gel electrophoresis (SDS-PAGE) was carried out in vertical polyacrylamide gel (thickness 0.7 mm, T = 15%) according to Laemmli [25], at a constant voltage of 220 V. Mass spectrometric analysis was carried out on an MSBX-252Cf instrument. Amino acid analyses were carried out using well known methods [26].

RESULTS AND DISCUSSION

Total scheme of protein transformation

The production of recombinant human insulin includes five main steps, in the course of which considerable transformations of the molecule take place (Table I and Fig. 1). These changes were analysed by SE-, RP- and IE-HPLC and HPCE (CZE and MECC), the process being accompanied by a study of applicability and informativity of chromatographic and electrophoretic methods.

rPFP, produced by recombinant cells and expressed in the first step, which is human proinsulin with open and chaotically closed six cysteine SH groups [2], specifically splits according to the methionine residue under the influences of BrCN into linear ("denatured") proinsulin and A-protein fragment (stage 2).

As a result of the denatured proinsulin sulphitolysis reaction, cysteine SH groups are converted into SSO_3 groups of proinsulin-S-sulphonate (stage 3). Subsequently, proinsulin-S-sulphonate is reduced and renatured in the presence of β-mercaptoethanol (stage 4); the "curling up" of the proinsulin molecule on the closure of the S–S bridges takes place. The final stage 5, under the influence of trypin, is the formation of insulin, the structure and properties of which do not differ from those of human hormone [2,4].

The authenticity of insulin obtained according to the given method at the Institute of Bioorganic Chemistry of the Russian Academy of Sciences was corroborated by HPLC with a standard specimen, SDS-PAGE (insulin appears in the form of a single stripe, corresponding to M_r 5800 ± 500), analysis of the N-terminal amino acid sequence and complete amino acid composition, and mass spectrometry (the insulin molecular mass was found to be 5808.2). The physiological activity of the protein proved to satisfy modern requirements, *i.e.*, more than 27 u/mg [4].

As purity of intermediate products is necessary for the correct performance of the technological steps, this work was devoted to developing the control system for the main stage of recombinant human insulin production with the help of different highly effective chromatographic and electrophoretic methods. The necessity to use separate types of HPLC and HPCE and their combinations for the complete analysis of technological products in each step has been demonstrated. The use of specially developed (in cooperation with Armchrom) laboratory-made Armsorb HPLC columns for proteins was studied. Parameters for the column support were obtained and conditions for carrying out chromatography were established such that the resolution and selectivity in the separation of protein products were comparable to those obtained on foreign commercial analogues.

HPLC analysis

It is necessary to use size-exclusion HPLC along with reversed-phase and ion-exchange chromatography because in the process of transformation of the initial FP into insulin considerable change in the size and structure of the molecules take place (Table I). In using known methods and developing new ones, we were limited by the conditions of preventing oxidation and denaturation of protein molecules and the

TABLE I
MAIN STEPS AND INTERMEDIATE AND FINAL PRODUCTS OF RECOMBINANT HUMAN INSULIN PRODUCTION TECHNOLOGY

Steps No.	Step	Step products[a]	Molecular mass ($\times 10^{-3}$)	Using of HPLC and HPCE methods for product analysis				
				IE	RP	SE	CZE	MECC
1	Fusion protein isolation	*rPFP*	17.0			+	+	
		Dimeric rPFP	34.0					
		HMP	40–70					
2	Proinsulin denaturation	*Denatured proinsulin*	9.0			+		
		rPFP	17.0					
		HMWP	70.0					
3	Proinsulin sulphiting	*Proinsulin-S-sulphonate*	9.5		+		+	
		Incompletely sulphited proinsulin	9.0					
		rPFP	17.0					
		Fusion protein-S-sulphonate	17.5					
4	Proinsulin renaturation	*Proinsulin*	9			+	+	
		Structural analogues and oligomers	9 18–36					
5	Insulin production	*Insulin*	5.8		+	+	+	+
		Insulin-like proteins	5.7					
		Deamidated insulin	5.75					
		Proinsulin	9					
		HMWP	6–36					

[a] Main products in italics.

corrosive resistance of the instruments. Conditions were found under which all the main products of insulin production technology are separated (Fig. 2). It should be noted that, although proinsulin, proinsulin-S-sulphonate and denatured proinsulin (*i.e.*, open proinsulin with free SH groups of cysteine residues) have close molecular masses, they differ considerably in conformation and charge [14,15]. It is these differences that explain the possibilities for their separation, and although the mechanism of separation is not purely size exclusion in character, a sufficiently high resolution between protein peaks was achieved (Fig. 2). Detailed information about the SE-HPLC of insulin-containing products can be found elsewhere [27].

In the first step, when the FP is expressed, the content of the main product with reference to oligomers and high-molecular-mass proteins (*E. coli* metabolites) is analysed by the given size-exclusion system (Table I), and rPFP elution on the RP-IE columns is characterized by low

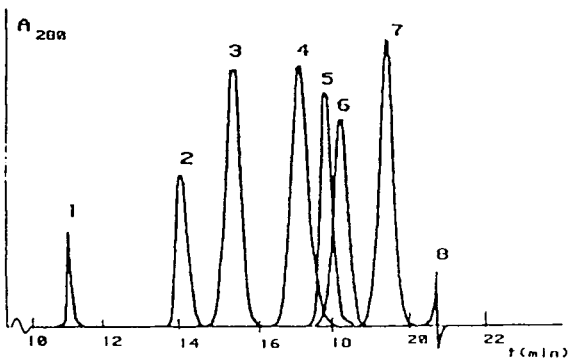

Fig. 2. Superposed chromatograms of insulin-containing proteins, performed on a TSK G 2000 SW column (600 × 8 mm I.D.) with 0.1 *M* sodium phosphate–0.2 *M* Na_2SO_4–5% acetonitrile (pH 7.0), flow-rate 1 ml/min. In the analysis of technological products the following proteins, corresponding to every stage in Table I, are present: 1 = HMP; 2 = rPFP dimer; 3 = rPFP; 4 = rHP-SSO_3; 5 = drHP; 6 = rHP; 7 = rHI; 8 = salts.

selectivity of separation and partial protein sorption on the columns. The protein appears in the form of a broad peak and it is difficult to detect the presence of impurities. When analysing the products of BrCN splitting of rPFP (into linear proinsulin and A-protein fragment), we obtain information concerning the completeness of the reaction and the amount of high-molecular-mass impurities in the reaction mixture. The use of RP and IE chromatography in the step of rPFP splitting is also not effective, because, first, these proteins do not process a considerable difference in charge and, second, although linear proinsulin is eluted in the form of separate narrow peak on an RP column, its comparison with non-splitting rPFP is difficult. In this step, SE chromatography is most effective. In the proinsulin sulphitolysis reaction, we found the reaction to be complete made and found in the reaction mixture high-molecular-mass impurities, which are products of protein oligomerization and which are not easily separated from monomers in IE-HPLC. After renaturation of proinsulin and in the final step of insulin production, an analysis is made in order to determine to content of high-molecular-mass impurities, the level of which should not exceed 0.1%, and which are not detected by RP-HPLC owing to the coincidence of their retention times with those of related proteins. It should be noted that the dynamics of performing the reactions can also be analysed with the help of the given size-exclusion system.

A more effective separation of insulin, proinsulin and proinsulin-S-sulphonate from the accompanying impurities is ensured by RP- and IE-HPLC, carried out on commercial and domestic columns. Anion-exchange HPLC was used for the analysis of proinsulin-S-sulphonate. The presence of SSO_3 groups in this protein leads to its affinity to the anion-exchange support. Fig. 3 shows the separation of proinsulin-S-sulphonate from incompletely sulphonated proinsulin in the form of separate peaks. The sorbent Armsorb-Si-500 poly-Amin is a wide-pore silica (pore diameter 500 Å), modified by a polymer-inoculated phase, carrying amino groups. Columns with this support are characterized by high effectiveness ($N = 7000$ TP per

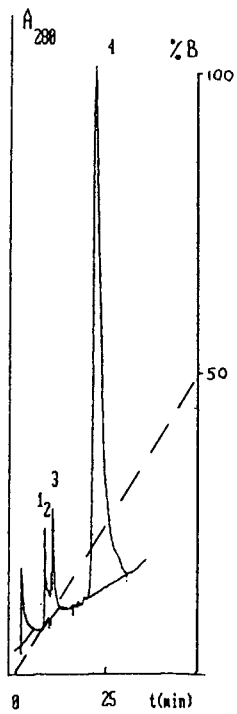

Fig. 3. Chromatogram of reaction mixture of rHP-SSO_3 production (4). Peaks 1–3 represent incompletely sulphonated proinsulin. Column, Armsorb-Si-500 poly-Amin; eluents, (A) 0.02 *M* sodium phosphate–MeOH (90:10) (pH 7.5); (B) 1 *M* sodium phosphate–MeOH (90:10) (pH 6.2); flow-rate, 1 ml/min. The percentage of eluent B in the mobile phase is shown by the dashed line.

column for insulin), resolution between peaks (in the given case $R_{s3,4} = 2$) and selectivity ($\alpha_{3,4} = 1.5$) (Fig. 3). In addition, Armsorb-SI-500 poly-Amin is distinguished by stability, chemical resistance and a sufficiently high loading ability.

The resolution between peaks did not change substantially when proinsulin-S-sulphonate was applied to the column in amounts of 2 μg–2 mg. The dependence of the peak area on the amount of sample applied within the specified limits turned out to be linear, which also testified to the high loading ability and high quality of the sorbent surface. After carrying out 1500 analyses (during a year), the resolution and loading ability were same as with a new column. The column was used in the pH range 2.5–8.0 with different organic solvents and salts, with did not affect its physico-chemical properties. The separation of proinsulin-S-sulphonate and incompletely sulphonated proinsulin, carried out on Armsorb-Si-500 poly-Amin columns, was similar to that on commercial columns as far as resolution and selectivity are concerned.

On renaturation (reduction of SSO_3 groups and closure of S–S bridges), along with the formation of proinsulin, the formation of its linear molecular analogues (in the case of incorrect closure of S–S bonds) and oligomers in intramolecular S–S binding is possible. It has been shown above that the determination of oligomers is carried out by means of SE-HPLC, and the analysis of proinsulin proper and the presence of analogues by means of RP-HPLC, selective to these variations in the structure of protein molecules (see Fig. 4 and ref. 3). The separation of proinsulin and insulin and their close analogues is caused by the difference in the hydrophobic properties of these proteins and was carried out on reversed-phase columns. Among several modifications of column supports, the best results were achieved on an Armsorb-Si-300-C_8 P(DM) column (Fig. 4) (wide-pore silica, modified by γ-glycidyl groups with inoculated C_8 phase). Several eluent systems used for the chromatography of proteins and peptides were tested and high resolution was achieved with systems such as acetonitrile–water with TFA, acetonitrile–water with sodium phosphate, acetonirtile–water with NH_4OAc and methanol–water with NH_4OAc. The separation was accompanied by good resolution of the insulin, desamidoinsulin and proinsulin peaks ($R_{s1,2} = 2{,}3$; $R_{s1,3} = 3.8$), owing to the high selectivity, which is especially important in the final steps of purification in the process of the identification of small amounts of these impurities (Fig. 4).

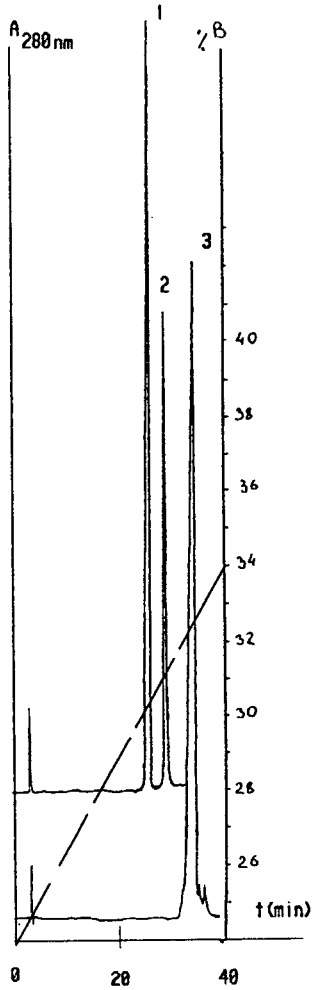

Fig. 4. Analysis of isolated fractions: rHP (peak 3); insulin (peak 1). Peak 2 = desamidoinsulin. Column, Armsorb-Si-300 p (DM); eluents, (A) CH_3CN–1 *M* NH_4OAc (10:90) (pH 7); (B) CH_3CN–1 *M* NH_4OAc (50:50) (pH 7); flow-rate, 0.8 ml/min. The percentage of eluent B in the mobile phase is shown by the dashed line.

For the analysis of insulin medicaments, it is necessary that the column effectiveness should not be less than 4000 TP/m and the resolution

between insulin and desamidoinsulin not less than 1.8 [4]. In the given case the column effectiveness is 7000 TP per column of length 15 cm. The resolution between peaks (insulin–desamidoinsulin and insulin–proinsulin) is similar to that with commercial columns, and satisfies the necessary requirements (Table II) [4]. The columns were tested for loading ability, stability and chemical resistance with the help of the above-mentioned method with similar results.

HPCE analysis

In order to determine the advisability of including HPCE in a set of techniques using during the process of production of recombinant human insulin (rHI), we carried out investigations of its applicability in all stages of this process. The main technique used was CZE, but some interesting results was obtained with MECC.

Analysis of recombinant human proinsulin fusion protein (rPFP) by CZE gave interesting results. As mentioned above, the same analysis by SE-HPLC demonstrated three peaks (Table I, Fig. 2). We identified first the monomer and dimer of rPFP and other oligomers generated by chaotic formation of disulfide bonds, which were not separated by SE-HPLC because they have similar dimensions. However, CZE demonstrated many peaks (Fig. 5a). Probably this phenomenon can be explained from the position of charge heterogenity of the oligomers with different numbers of disulphide bonds and different conformations.

It is obvious that the presence of oligomers hinders any analysis. In order to achieve monomerization we treated a sample of rPFP with 2-mercaptoethanol (ME). The fact that monomerization carried by this procedure out is exhaustive was proved by CZE of chromatographically refined renatured rPFP (rPFP) monomerized by ME (Fig. 5b). Monomerization of rPFP allowed us to obtain good results in the analysis of mixture of rPFP and contaminated proteins of host cells (Fig. 5c). ME gave a separate peak because it was injected with the sample, but addition of ME to the buffer solution is impossible owing to its high UV adsorption at the wavelength used. The same approach was demonstrated by Patrick and Lagu [28] in the analysis of rPFP by SE-HPLC.

MECC separation of rPFP monomerized by ME resulted in wide peak broadening, which excluded the possibility of any analysis.

We consider that rPFP, which is able to form many isomers differing in many, charge and conformation, is a useful model for studying of the laws and driving forces of CZE and MECC separations.

Insulin-containing proteins devoid of free cysteine groups are readily separated by both CZE (Fig. 6a) and MECC (Fig. 6b). Recombinant human proinsulin (rHP) was in all instances

TABLE II
COMPARISON OF RESOLUTIONS (R_s) OF DIFFERENT SERIAL COMMERCIAL (NOS. 1–3) AND DEVELOPED (ARMSORB) RP COLUMNS FOR THE SEPARATION OF INSULIN, DESAMIDO-(A_{21})-INSULIN AND PROINSULIN

Column	R_s	
	Insulin–desamidoinsulin	Insulin–proinsulin
No. 1: C_{18} (250 × 4.6 mm I.D.)	0.4–1.11	3.0–4.85
No. 2: C_{18} (300 × 3.9 mm I.D.)	1.8	–
No. 3: C_{18} (250 × 4.6 mm I.D.)	1.8	–
Armsorb-Si-300-C_8-RP-PR (I50 × 4 mm I.D.)	2.3	6.5
Armsorb-Si-300-C_8-(P)DM (I50 × 4 mm I.D.)	2.2	6.3

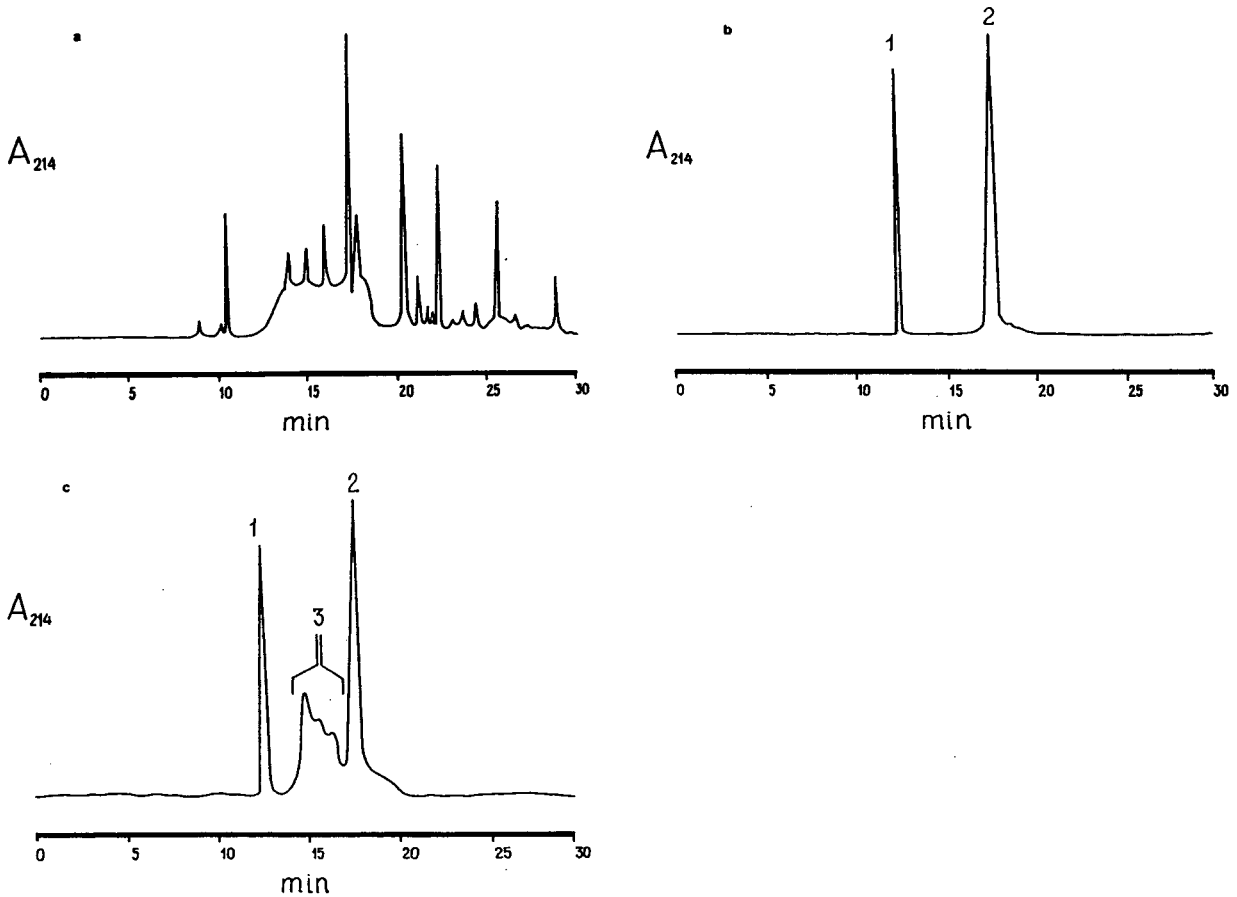

Fig. 5. CZE of recombinant human proinsulin fusion protein (rPFP). (a) Separation of oligomers of rPFP; (b) analysis of pure renatured rPFP (rPFP-r) treated with 2-mercaptoethanol (ME). ME was added to the sample tube in stoichiometric amounts and mixed. Analysis was performed immediately without further treatment. Peaks were identified by migration times of standards: 1 = ME; 2 = rPFP. (c) Analysis of rPFP in mixture with contaminating proteins of host cell. Peak 3 = contaminating proteins. Analysis was performed using the Beckman PACE 2010 system. Conditions: fused-silica capillary supplied by Beckman, I.D. 100 μm, length 87 cm, effective length 80 cm; voltage, 10 kV; temperature, 28°C; buffer, 0.1 *M* borate (pH 9.3); concentration of protein in sample, 1 mg/ml; electrophoretic injection, 5 s/+5 kV; detection, UV absorbance at 214 nm.

satisfactorily separated from recombinant human insulin (rHI). rPFP was badly separated from rHP by CZE but satisfactorily by MECC.

During the investigations we typically met in CZE the problem of protein adsorption on the capillary walls. Optimization of the separation conditions allowed us to minimize the adsorption and to achieve an efficiency of 200 000 TP and a selectivity $\alpha = 1.8$ for the separation of rHP and RHI by CZE (Fig. 7a). This results are an order of magnitude higher for this pair them with RP-HPLC.

In spite of the impossibility of protein adsorption during analysis by MECC, the efficiency of separtion of rHP and rHI by this technique was lower than that using CZE. The causes of this phenomenon and methods for optimizing MECC separations of proteins are under investigation.

An important application of the CZE analysis of rHI is in the certification of pharmaceutical insulin according to pharmacopoeial requirements. Other groups have worked in this area [20–23]. Nielsen *et al.*, [23], in a significant

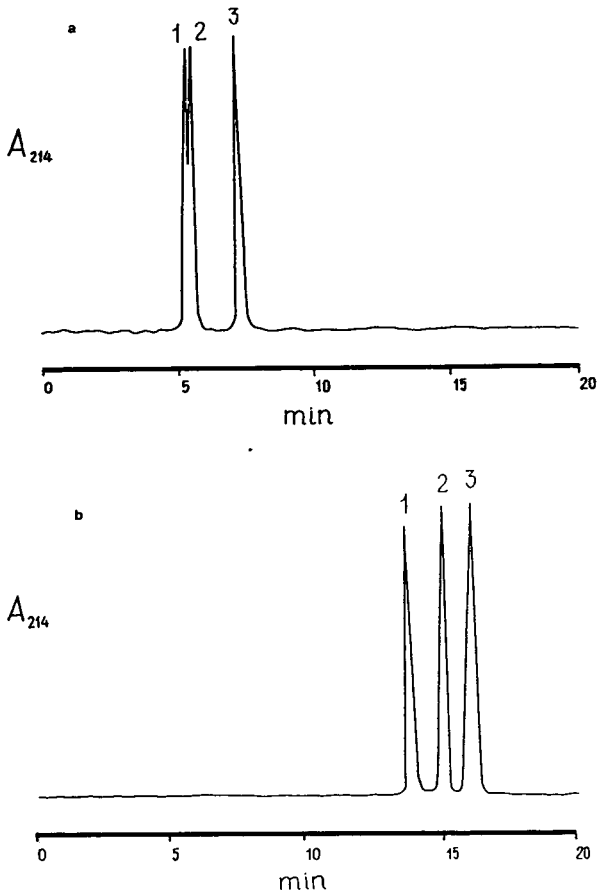

Fig. 6. Separations of renatured recombinant human proinsulin fusion protein (rPFP-r), recombinant human proinsulin (rHP) and recombinant human insulin (rHI) by (a) CZE and (b) MECC. Peaks were identified by migration times of standards: 1 = rPFP-r; 2 = rHP; 3 = rHI. Analysis was performed using the Applied Biosystems 270A CE system. Conditions: fused-silica capillary supplied by Beckman, I.D. 100 μm, length 52 cm, effective length 40 cm; voltage, 18 kV; temperature, 28°C; buffer, (a) 0.1 *M* borate (pH 9.3) and (b) 0.1 *M* borate–0.1 *M* SDS (pH 9.3); concentration of protein in sample, 1 mg/ml; electrophoretic injection, 5 s/+5 kV; detection, UV absorbance at 214 nm.

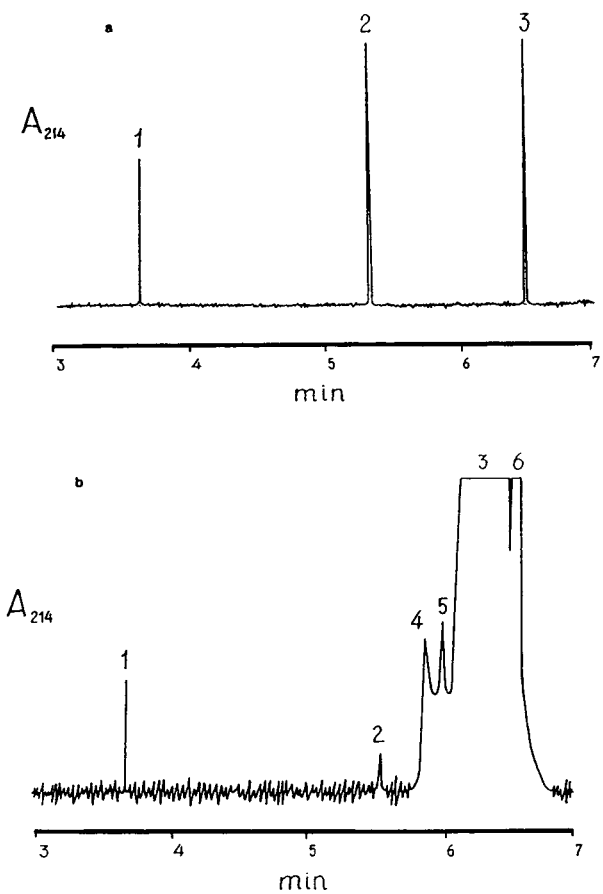

Fig. 7. Separation of recombinant human proinsulin (rHP) and recombinant human insulin (rHI) by CZE under optimum conditions. (a) Model separation. Peaks were identified by migration times of standards: 1 = marker of electroosmotic flow; 2 = rHP; 3 = rHI. (b) Determination of minor impurity of rHP in rHI. Peaks: 1–3 as in (a); 4 = diarginine-(B31–B32)-insulin; 5 = arginil-(AO)-insulin; 6 = desamido-(A21)-insulin (peaks 5 and 6 were identified according to ref. 23). Analysis was performed using the Applied Biosystems 270A CE system. Conditions: fused-silica capillary supplied by Beckman, I.D. 100 μm, length 52 cm, effective length 40 cm; voltage, 20 kV; temperature, 28°C; buffer, 0.03 *M* Na_2HPO_4 (pH 11.2); (a) concentration of protein 0.3 mg/ml, electrophoretic injection 0.1 s/+5 kV; (b) concentration of rHP 0.02 mg/ml, electrophoretic injection 8 s/+5 kV; detection, UV absorbance at 214 nm.

paper, described the separation of rHI and the main products of its acid degradation, satisfactorily efficiency and selectivity being achieved.

Proinsulin is also included in the list of pharmacopeial impurities and its concentration is limited more stricly to 0.1%. The efficiencies of seveal thousand TP demonstrated by HPLC in the analysis of proteins lead to the impossibility of determining this minor impurity owing to the low statistical authenticity of the results. Today slow and expensive immunoassays and PAGE with overloaded track are used for the determination rHP in rHI [4]. This separation by HPCE

has not yet been discussed in the literature. CZE separation under optimized conditions allowed us to determine less than 0.1% of rPH in rPI (Fig. 7b).

In conclusion we want to discuss briefly the potential of CZE. The various advantages of HPCE have often been discussed in the literature, and the combination of practicalness, economy and high resolving power would without doubt ensure a leading role for this method in separation science, if it were not for one great disadvantage, *i.e.*, HPCE is applicable only in the analytical mode. all reports of micropreparative HPCE separations are connected with complicated equipment and a narrow range of application. This is the reason why we cannot today consider HPCE to be a really powerful and independent method. However, in combination with other methods, HPCE can show superior results [22].

The combination of HPCE and HPLC is very easy, because the methdos are similar both in theory and in practice.

The application of different methods of SE-, IE- and RP-HPCE and HPCE (CZE and MECC) for the analysis of insulin, insulin-related and non-insulin-related substances have been studied in this work. A combined system of HPLC and HPCE for the step-by-step control of recombinant human insulin production technology has been suggested. The advantages and shortcomings of these methods have been discussed. Chromatographic columns with commercial and specially developed domestic supports for SE-, RP- and IE-HPLC have been used and their effective application for the analysis of products and semiproducts at every stage of the technology concerned has been demonstrated. The combination of optimized methods of SE-, RP-, and IE-HPLC and CZE and MECC can form the basis of a production control system.

REFERENCES

1 I.S. Johnson, *Science*, 219 (1983) 632–637.
2 Yu.A. Ovchinnikov, V.A. Efimov and O.G. Chakhmakhcheva, *Dokl. Akad. Nauk SSSR*, 270 (1983) 743–747.
3 E.P. Kroeff, R.A. Owens, E.L. Campbell, R.D. Johnson and H.I. Marks, *J. Chromatogr.*, 461 (1989) 45–61.
4 *United States Pharmacopeia, Revision XX*, United States Pharmacopeial Convention, Rockville, MD. 1984, pp. 2177–2179; *British Pharmacopoeia 1988*, H.M. Stationary Office, London, 1988, pp. 312–313.
5 A. Peter, G. Szepesi, L. Balaspiri and K. Burger, *J. Chromatogr.*, 408 (1987) 43–52.
6 B.S. Welinder, H.H. Sorensen and B. Hansen *J. Chromatogr.*, 361 (1986) 357–367.
7 S. Linde and B.S. Welinder, *J. Chromatogr.*, 548 (1991) 195–206.
8 S. Linde and B.S. Welinder, *J. Chromatogr.*, 536 (1991) 43–55.
9 S. Linde, J.H. Nielsen, B. Hansen and B.S. Welinder, *J. Chromatogr.*, 462 (1989) 243–254.
10 F.L. Lloyd and P.H. Coran, *J. Chromatogr.*, 240 (1982) 445–454.
11 A. McLeod and S.P. Wood, *J. Chromatogr.*, 285 (1984) 319–331.
12 J. River and R. McClintock, *J. Chromatogr.*, 268 (1983) 112–119.
13 D.J. Smith, R.M. Venable and J. Collins, *J. Chromatogr. Sci.*, 23 (1985) 81–88.
14 D. Kalant, J.C. Crawhall and D.I. Posner, *Biochem. Med.*, 34 (1985) 230–240.
15 O.L. Guevara De, G. Estrada, S. Antonio, L. Guereca, F. Zqamudio and F. Bolivar, *J. Chromatogr.*, 349 (1985) 91–98.
16 W.G. Kuhr, *Anal. Chem.*, 62 (1990) 403R–411R.
17 B.L. Karger, A.S. Cohen and A. Guttman, *J. Chromatogr.*, 492 (1989) 585–614.
18 Z. Deyl and R. Struzinsky, *J. Chromatogr.*, 569 (1991) 63–123.
19 H.H. Lauer and D. McManigill, *Anal. Chem.*, 58 (1986) 166–170.
20 P.D. Grossman, J.C. Colburn, H.H. Lauer, R.G. Nielsen, R.M. Riggin, G.S. Sittampalam and E.C. Rickard, *Anal. Chem.*, 61 (1989) 1186–1194.
21 E. Wenisch, C. Tauer, A. Jungbauer, H. Katinger, M. Faupel and P.G. Righetti, *J. Chromatogr.*, 516 (1990) 133–146.
22 A. Vinther, S.E. Bjorn, H.H. Sorensen and H. Soeberg, *J. Chromatogr.*, 516 (1990) 175–184.
23 R. Nielsen, G.S. Sittampalam and E.C. Rickard, *Anal. Biochem.*, 177 (1989) 20–26.
24 S.-L. Wu, G. Teshima, J. Cacia and W. Hancock, *J. Chromatogr.*, 516 (1990) 115–122.
25 L.A. Osterman, *Methods of Protein and Nucleic Acid Research. VI. Electrophoresis, Isoelectric Focusing and Ultracentrifugation*, Springer, Berlin, 1984, pp. 7–98.
26 Yu.A. Ovchinnikov, *Bioorganicheskaya Khimiya*, Prosveschenie, Moscow, 1987, pp. 34–41.
27 V.E. Klyushnichenko and A.N. Wulfson, *Bioorg. Khim.*, 19 (1993) 174–181.
28 J.S. Patrick and A.L. Lagu, *Anal. Chem.*, 64 (1992) 507–511.
29 R. Palmieri, *Application Data DS-749*, Beckman, Palo Alto, CA, 1989.

Journal of Chromatography A, 661 (1994) 93–99
Elsevier Science B.V., Amsterdam

CHROMSYMP. 2907

Synthesis and analysis of oxidation and carbonyl condensation compounds of tryptophan

T. Simat*, K. Meyer and H. Steinhart

Institut für Biochemie und Lebensmittelchemie, Graduiertenkolleg Biotechnologie, Universität Hamburg, Grindelallee 117, D-20146 Hamburg (Germany)

ABSTRACT

Modified methods of synthesizing the oxidative degradation products N-formylkynurenine, oxyindolylalanine diastereomers and dioxyindolylalanine diastereomers (DiOia) and the carbonyl condensation products 1-methyl-1,2,3,4-tetrahydro-β-carboline-3-carboxylic acid and 1-pentyl-1,2,3,4-tetrahydro-β-carboline-3-carboxylic acid are described. These methods produce compounds with purities sufficiently high to allow them to be used as reference substances for analytical purposes and as samples for toxicological investigations. The obtained substances were characterized by ^{1}H-NMR, ^{13}C-NMR, IR and UV spectroscopy. The purities of the substances were verified by RP-HPLC and UV detection. An RP-HPLC method was developed which allowed the separation of the synthesized products, 5-hydroxytryptophan, 3-hydroxykynurenine and tryptophan. As an application, a sample of eosinophilia–myalgia syndrome (EMS)-related tryptophan was examined. Low contents of the oxidation products were found, together with the known peaks A–E.

INTRODUCTION

The essential amino acid tryptophan (Trp) is exceptional in its diversity of biological functions. In particular, it is the precursor of the neurotransmitter serotonin. The formation of Trp-derived antinutritional and potentially toxic compounds occurs during processing and storage of food and feedstuffs (Fig. 1). Elucidation of the degradation conditions is important for the evaluation of pharmaceuticals, food and feedstuffs.

The *oxidative degradation* of Trp reduces the nutritional value of proteins. *Carbonyl condensation* reactions of Trp with aliphatic aldehydes (Pictet–Spengler reaction) produce 1,2,3,4-tetrahydro-β-carboline-3-carboxylic acids (THCC), which have neurophysiological activity [1,2].

The occurrence of eosinophilia–myalgia syndrome (EMS; generalized myalgia and increased eosinophil count) in 1989 was correlated to the intake of L-Trp as antidepressant which contained 0.01% 1,1′-ethylidenebis(L-tryptophan). This L-Trp dimer was determined as the causative agent of this autoimmune disease, which afflicted 1500 people [3] and caused 27 fatalities in the USA [4]. Hitherto, most investigations have focused on the decrease in Trp or the formation of only single degradation products.

The aims of our studies were:

(1) The synthesis of high-purity compounds for use as reference substances.

(2) The development of an HPLC separation of the major known Trp oxidation and carbonyl condensation derivatives that might be formed from free or peptide-bound Trp.

MATERIALS AND METHODS

Chemicals

3-Hydroxykynurenine (3-OH-Kyn, Sigma), kynurenine (Kyn, Fluka) and 5-hydroxytryptophan (5-OH-Trp, Merck) were purchased

* Corresponding author.

0021-9673/94/$07.00
SSDI 0021-9673(93)E0873-S

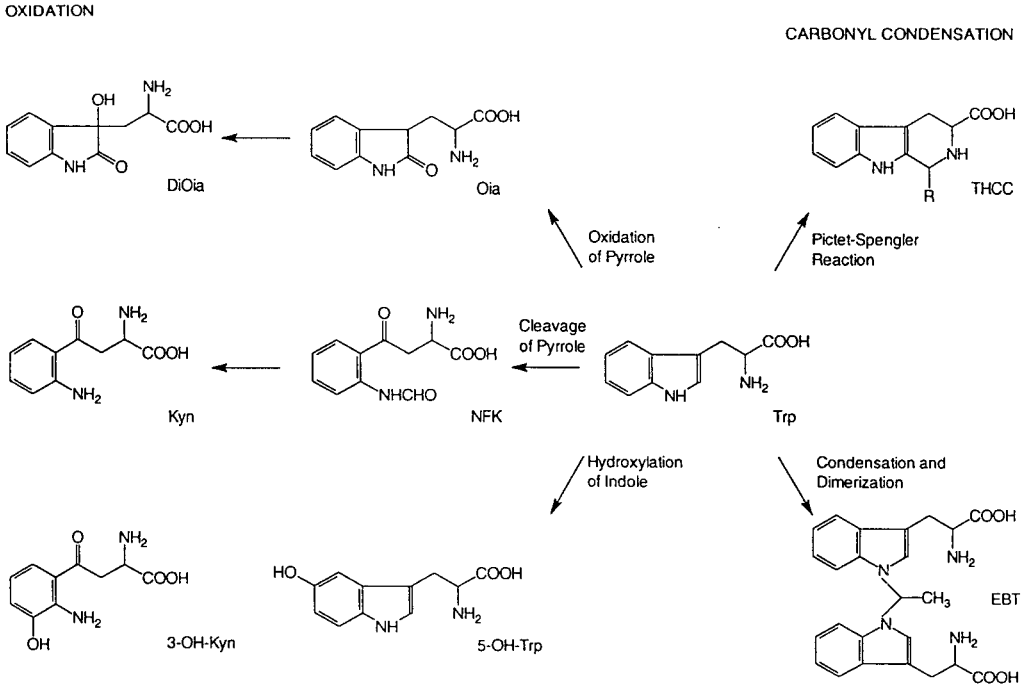

Fig. 1. Formation of Trp-derived antinutritional and potentially toxic compounds.

from commercial distributors. L-Tryptophan was donated by Degussa (Hanau, Germany). A sample of an EMS case-related L-Trp lot was donated by the Centers for Disease Control (Atlanta, GA, USA).

Synthesis of reference substances

Oxindolylalanine was synthesized as described in refs. 5 and 6 by treating 5 g of Trp suspended in 25 ml of acetic acid with a mixture of 4.5 ml of dimethylsulphoxide and 12.5 ml of concentrated HCl. The mixture was stirred for 70 min at room temperature. Oxyindolylalanine diastereomers (Oia) precipitate after adjusting the pH to 5.8 (isoelectric point), yielding 4.05 g of Oia (75%). A higher purity was obtained by ion-exchange chromatography. Conditions were as follows: column, DOWEX 1 × 2-200 (100 × 26 mm I.D.); eluent A, water (200 ml); eluent B, 2 *M* acetic acid (200 ml); linear gradient 0–100% eluent B; flow-rate 2 ml/min.

^{1}H-NMR (400 MHz, ^2H_2O): Diastereomer A: 7.47 (mc, 2H, H-5 and H-6), 7.29 (mc, 1H, H-4 or H-7), 7.14 (mc, 1H, H-4 or H-7), 4.62 (t, 1H, α-H), 2.78 (dd, 1H, β-H_a), 2.54 (dd, 1H, β-H_b). $J_{\alpha,\beta} = 6.4$, $J_{\beta a,\beta b} = 15.1$ Hz. Diastereomer B: 7.47 (mc, 2H, H-5 and H-6), 7.29 (mc, 1H, H-4 or H-7), 7.14 (mc, 1H, H-4 or H-7), 4.50 (t, 1H, α-H), 2.83 (dd, 1H, β-H_a), 2.45 (dd, 1H, β-H_b). $J_{\alpha,\beta} = 7.1$, $J_{\beta a,\beta b} = 15.1$ Hz. The H-3 protons were exchanged by deuterium and therefore they were not detected.

Dioxindolylalanine was prepared by aerating a solution of Oia adjusted to pH 10–12 with triethylamine [6] for several hours. The product was isolated by ion-exchange chromatography (conditions as above), followed by the removal of the solvent yielding a mixture of diastereomers in a 70:30 ratio.

^{1}H-NMR (400 MHz, ^2H_2O): Diastereomer A, 70%: 7.63 (d, 1H, H-4 or H-7), 7.52 (t, 1H, H-5 or H-6), 7.32 (t, 1H, H-5 or H-6), 7.18 (d, 1H, H-4 or H-7), 4.33 (dd, 1H, α-H), 2.62 (dd, 1H, β-H_a), 2.40 (dd, 1H, β-H_b). $J_{4,5} = 7.4$, $J_{5,6} = 7.4$, $J_{6,7} = 7.4$, $J_{\alpha,\beta a} = 3.7$, $J_{\alpha,\beta b} = 9.6$, $J_{\beta a,\beta b} = 15.7$ Hz. Diastereomer B, 30%: 7.58 (d, 1H, H-4 or H-7), 7.50 (t, 1H, H-5 or H-6), 7.29 (t, 1H, H-5 or H-6), 7.15 (d, 1H, H-4 or H-7), 4.43 (dd,

1H, α-H), 2.60 (dd, 1H, β-H_a), 2.46 (dd, 1H, β-H_b). $J_{4,5} = 7.4$, $J_{5,6} = 7.4$, $J_{6,7} = 7.4$, $J_{\alpha,\beta a} = 3.4$, $J_{\alpha,\beta b} = 9.8$, $J_{\beta a,\beta b} = 15.7$ Hz.

N-Formylkynurenine (NFK) was synthesized by formylation of a solution of 0.75 g of Kyn in 1.65 ml of formic acid using a mixture of 0.72 ml of formic acid and 0.36 ml of acetic anhydride [7]. After 2 h the mixture was poured into diethyl ether and the precipitate was isolated and recrystallized from ethanol yielding 0.56 g of NFK (66%).

^{1}H-NMR (250 MHz, ^2H_2O): 8.64 (bs, 1H, Aryl-NH), 8.19 (s, 1H, Formyl-H), 8.02 (d, 1H, H-3), 7.63 (t, 1H, H-5), 7.30 (t, 1H, H-4), 7.24 (d, 1H, H-6), 4.46 (t, 1H, α-H), 3.88 (d, 2H, β-H). $J_{3,4} = 8.0$, $J_{3,5} = 1.0$, $J_{4,5} = 7.7$, $J_{4,6} = 1.0$, $J_{5,6} = 8.2$, $J_{\alpha,\beta} = 4.4$ Hz.

1-Methyl- (MeTHCC) and *1-pentyl-1,2,3,4-tetrahydro-β-carboline-3-carboxylic acid (*PeTHCC*)* [8,9] were obtained by acid-catalysed cyclization of Trp with acetaldehyde and hexanal, respectively. For MeTHCC 2 g of Trp were suspended in 9 ml of 0.00625 *M* H_2SO_4 and 2 ml of acetaldehyde were added. The mixture was stirred for 6 h at room temperature, then the precipitate was filtered and recrystallized from water yielding 1.4 g of MeTHCC (62%). *cis*-Isomer can be separated by fractionated crystallization from water.

^{1}H-NMR (400 MHz, MeO^{2}H + 1% TFA): 7.95 (bs, 1H, H-9), 7.58 (d, 1H, H-5), 7.46 (d, 1H, H-8), 7.25 (t, 1H, H-7), 7.16 (t, 1H, H-6), 4.88 (q, 1H, H-1), 4.49 (dd, 1H, H-3), 3.56 (ddd, 1H, H-4a), 3.22 (ddd, 1H, H-4b), 1.87 (d, 3H, 1-Me). $J_{1,1\text{-Me}} = 6.6$, $J_{1,4a} = 1.4$, $J_{1,4b} = 1.5$, $J_{3,4a} = 5.7$, $J_{3,4b} = 12.2$, $J_{4a,4b} = 16.4$, $J_{5,6} = 8.1$, $J_{5,7} = 1.4$, $J_{6,7} = 7.7$, $J_{6,8} = 1.0$, $J_{7,8} = 8.0$ Hz.

For PeTHCC 1 g of Trp and 0.67 ml of hexanal were suspended in 20 ml of 0.0125 *M* H_2SO_4 and 10 ml of methanol. The mixture was heated for 4 h and than neutralized with 25% ammonia. The precipitate was collected, yielding 0.35 g of PeTHCC (25%).

^{1}H-NMR (400 MHz, MeO^{2}H + 1% TFA): 7.91 (bs, 1H, H-9), 7.53 (d, 1H, H-5), 7.40 (d, 1H, H-8), 7.15 (t, 1H, H-7), 7.07 (t, 1H, H-6), 4.80 (q, 1H, H-1), 4.40 (dd, 1H, H-3), 3.55 (ddd, 1H, H-4a), 3.20 (ddd, 1H, H-4b), 2.40 (mc, 1H, H-10a), 2.05 (mc, 1H, H-10b), 1.65 (mc, 2H, H-11), 1.50 (mc, 4H, H-12 and H-13), 1.00 (t, 3H, H-14). $J_{1,4a} = 1.2$, $J_{1,4b} = 2.5$, $J_{1,10a} = 1.7$, $J_{1,10b} = 7.2$, $J_{3,4a} = 5.1$, $J_{3,4b} = 12.3$, $J_{4a,4b} = 16.4$, $J_{5,6} = 7.8$, $J_{5,7} = 1.0$, $J_{6,7} = 7.5$, $J_{6,8} = 1.0$, $J_{7,8} = 8.2$, $J_{13,14} = 7.1$ Hz.

The structures of the synthesized reference substances were confirmed by UV, IR, ^{1}H and ^{13}C-NMR spectroscopy. Their purity as determined by RP-HPLC and UV detection (260 nm) was higher than 98%.

The synthesis of *1,1'-ethylidenebis(L-tryptophan)* according to the only published method, that of Smith *et al.* [10], failed. The formation conditions of EBT and a new simple procedure for synthesis will be published shortly.

RESULTS AND DISCUSSION

The desired compounds were obtained in sufficient amounts by using previously published methods of synthesis, which were varied and optimized in order to yield reference substances in high purities. With these compounds it was possible to establish an HPLC separation method (for conditions, see Table I) giving high resolution of all substances of interest (Figs. 2 and 3). Using this method it was possible to determine the oxidation and carbonyl condensation compounds of Trp in a single-step analysis.

In an EMS-related Trp sample (Figs. 4 and 5), we identified the oxidation products dioxindolylalanine diastereomers (DiOia), Oia, Kyn and, confirming the findings of Toyo'oka *et al.* [11], 5-OH-Trp. NFK could not be identified in this Trp sample. In addition, we detected MeTHCC and the known peaks A–E as described in ref. 12. The identification of the detected compounds was achieved by standard addition of synthesized authentic material as well as by comparison of UV–VIS spectra (200–400 nm) obtained by diode-array detection.

The concentrations of DiOia (25 ppm for each diastereomer), Oia (90 ppm in total for both diastereomers), Kyn (20 ppm) and 5-OH-Trp (120 ppm) were determined by external standard and related to Trp. The concentrations of MeTHCC (40 ppm) and peak E (110 ppm) were similar to those found by Müller *et al.* [12].

In comparison with the described material, a

TABLE I

HPLC CONDITIONS

Stationary phase		Nucleosil 120 3-C_{18}, 250 × 4 mm		
Mobile phase		0.1% TFA	MeOH	MeCN
Gradient	0 min	95%	5%	0%
	−10 min	86%	14%	0%
	−30 min	46%	14%	40%
Flow		1 ml/min		
Temperature		35°C		
Injection volume		20 μl		
Detection		UV, 260 nm		
		Fluorescence, excitation 290 nm, emission 356 nm		
		Diode-array detection, 260 nm; UV–VIS spectra, 200–400 nm		
Standards		10 μg/ml (Oia, DiOia 20 μg/ml)		

control sample of Trp donated by Degussa was similarly analysed. The pattern of the detected oxidation products did not differ (Figs. 6 and 7). Their amounts, however, were smaller than in the EMS-related sample, in particular the concentration of 5-OH-Trp (<5 ppm) showed a considerable difference. Furthermore, peak E was absent in this Trp sample.

During the RP-HPLC monitoring of the syntheses much information about the conditions of formation and the stability of the described compounds was collected. This information will influence in further analytical work:

(1) NFK is deformylated with the formation of Kyn in alkaline and acidic solutions.

(2) Oia is oxidized in alkaline solutions of pH > 12, mainly to Kyn, and at pH 10–12 to DiOia.

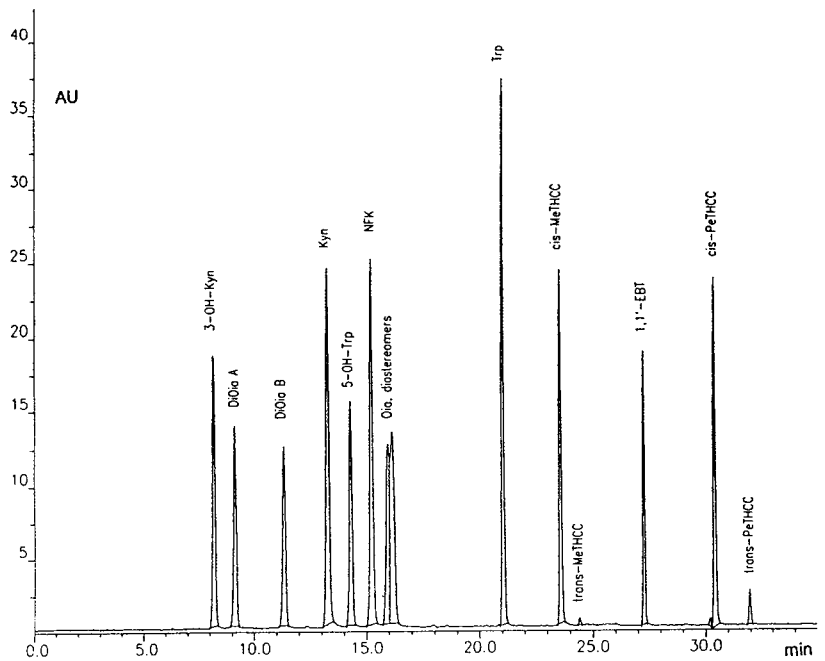

Fig. 2. HPLC chromatogram of a standard mixture (UV detection).

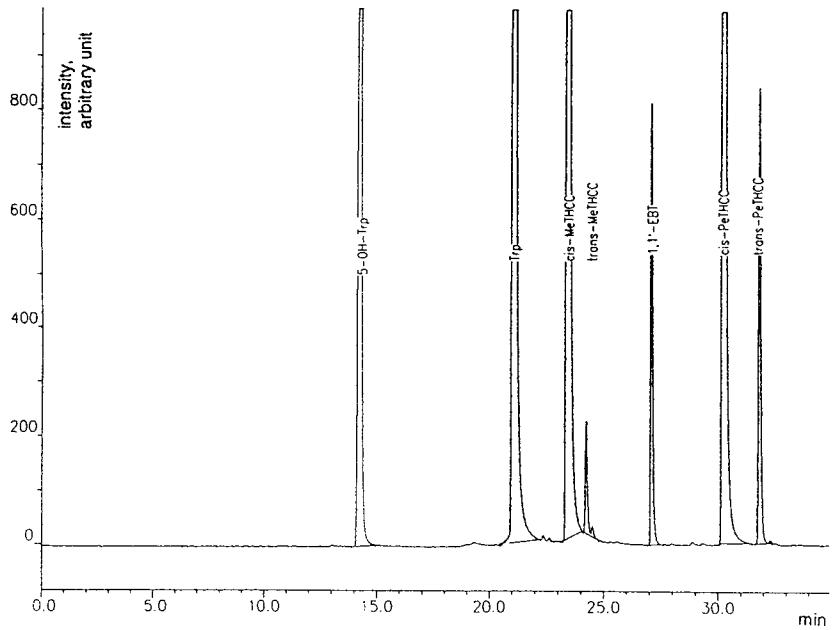

Fig. 3. HPLC chromatogram of a standard mixture (fluorescence detection).

These results imply that the formation of different oxidation products depends not on the oxidizing agent [O_2, $h * \nu_{(sens)}$, irradiation, peroxides] but on the pH value. It seems that the formation and degradation of EBT is fundamentally dependent on the reaction conditions, espe-

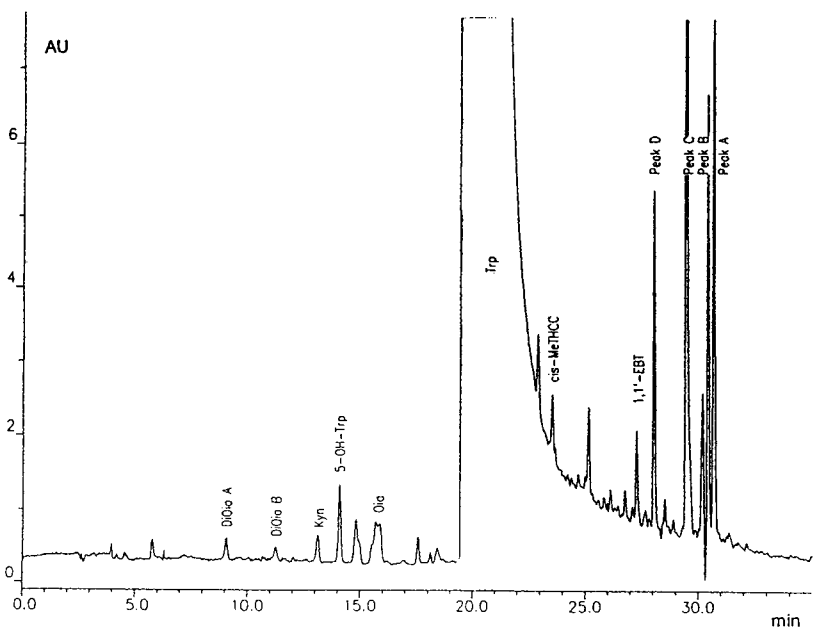

Fig. 4. HPLC chromatogram of an EMS-related Trp sample (UV detection), overloaded, 10 mg/ml.

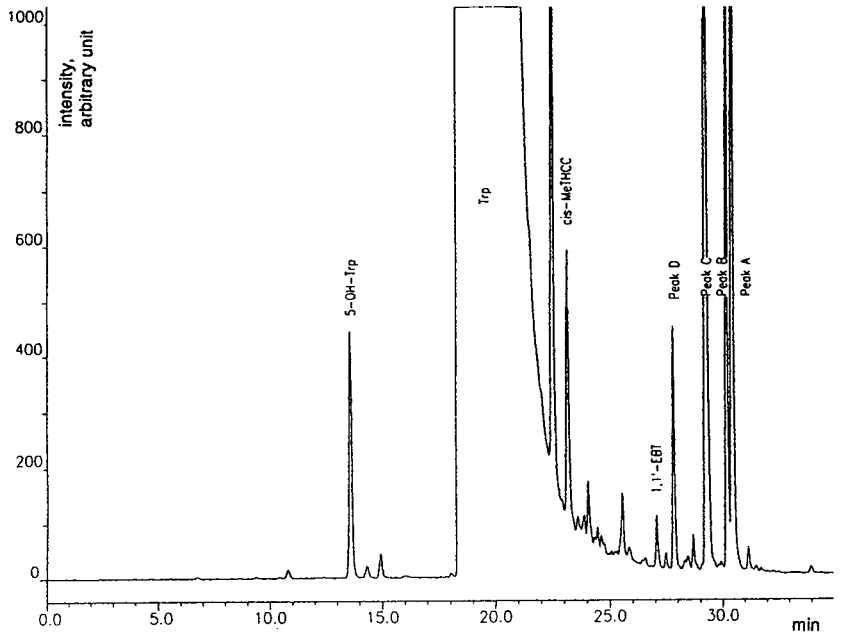

Fig. 5. HPLC chromatogram of an EMS-related Trp sample (fluorescence detection), overloaded, 10 mg/ml.

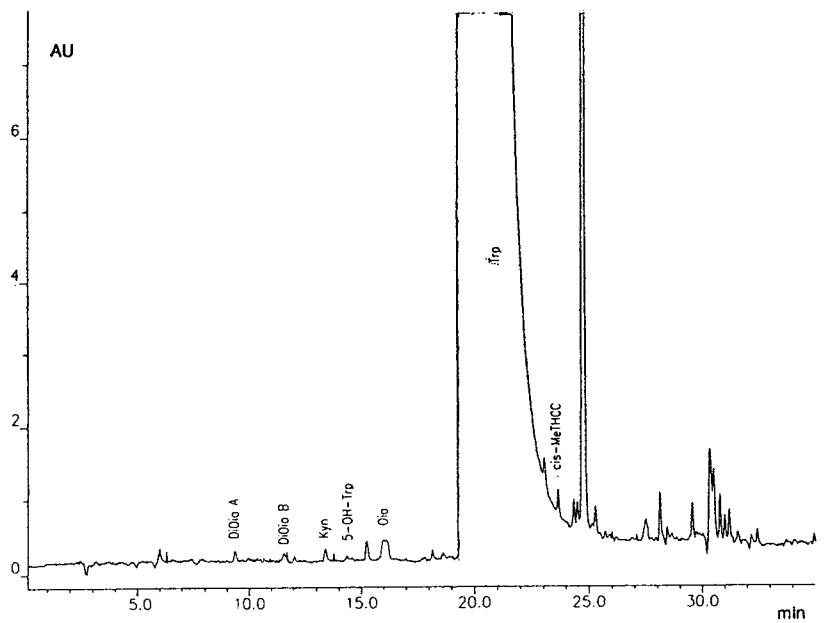

Fig. 6. HPLC chromatogram of a Trp control sample (UV detection), overloaded, 10 mg/ml.

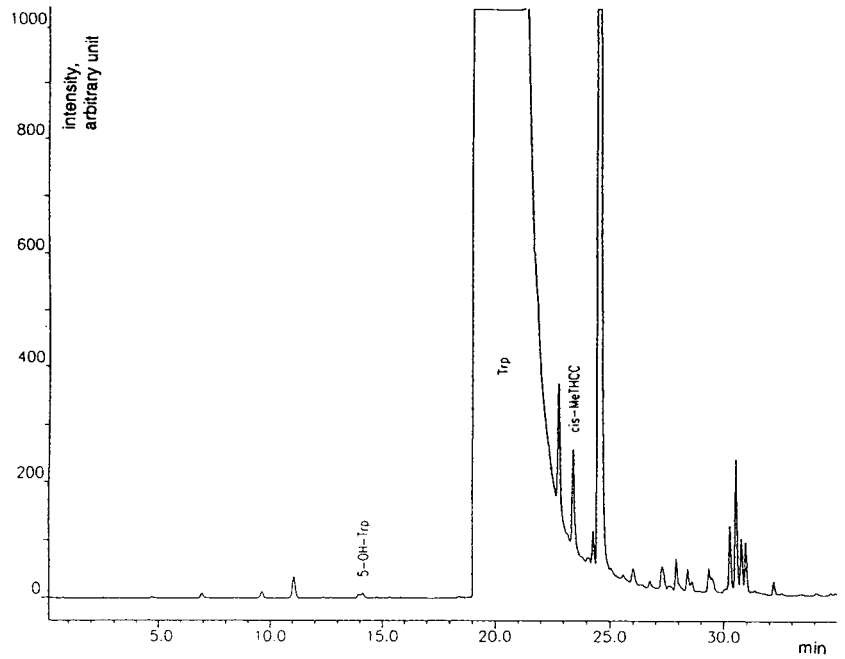

Fig. 7. HPLC chromatogram of a Trp control sample (fluorescence detection), overloaded, 10 mg/ml.

cially temperature and acid concentration. By varying these parameters it was possible to obtain EBT by a simple procedure.

FUTURE PROSPECTS

(1) Further examination of the conditions for the formation and degradation of EBT.

(2) Synthesis and determination of the stability of further oxidation products, for example 5-OH-Trp analogues.

(3) Determination of degradation products of peptide-bound Trp in different model systems (oxidation and carbonyl condensation model systems).

REFERENCES

1 H. Rommelspacher, H. Honecker, M. Barbey and B. Meinke, *Naunyn-Schmiedeberg's Arch. Pharmacol.*, 310 (1979) 35–41.
2 N.S. Buckholtz, *Life Sci.*, 27 (1980) 893–903.
3 US Centers for Disease Control, *J. Am. Med. Assoc.*, 262 (1989) 3116.
4 US Centers for Disease Control, *Morb. Mortal. Wkly. Rep.*, 39 (1990) 589–591.
5 G. Kell, *Dissertation*, University of Hamburg, 1988.
6 W.E. Savige, *Aust. J. Chem.*, 28 (1975) 2275–2287.
7 C.E. Dalgliesh, *J. Chem. Soc.*, (1952) 137–141.
8 A. Brossi, A. Focella and S. Teitel, *J. Med. Chem.*, 16 (1973) 418–420.
9 H.R. Snyder, C.H. Hansch, L. Katz, S.M. Parmerter and E.C. Spaeth, *J. Am. Chem. Soc.*, 70 (1948) 219–221.
10 M.J. Smith, E.P. Mazzola, T.J. Farrell, J.A. Sphon, S.W. Page, D. Ashlez, S.R. Sirimanne, R.H. Hill and L.L. Needham, *Tetrahedron Lett.*, 32 (1991) 991–994.
11 T. Toyo'oka, T. Yamazaki, T. Tanimoto, K. Sato, M. Sato, M. Toyoda, M. Ishibashi, K. Yoshihira and M. Uchiyama, *Chem. Pharm. Bull.*, 39 (1991) 820–822.
12 A. Müller, E. Busker, K. Günther and B. Hoppe, *Bioforum*, 14 (1991) 350–354.

Journal of Chromatography A, 661 (1994) 101–104
Elsevier Science B.V., Amsterdam

CHROMSYMP. 2938

Determination of tryptophan and ten of its metabolites in a single analysis by high-performance liquid chromatography with multiple detection

U. Caruso*
University Department of Pediatrics I, G. Gaslini Institute, Largo G. Gaslini 5, 16147 Genova (Italy)

B. Fowler
University Children Hospital, Basle (Switzerland)

G. Minniti and C. Romano
University Department of Pediatrics I, G. Gaslini Institute, Largo G. Gaslini 5, 16147 Genova (Italy)

ABSTRACT

Tryptophan is an essential amino acid whose metabolism involves several pathways. Defects, either inherited or functional, in its transport mechanism or catabolism are related to a large variety of clinical abnormalities. This paper presents a relatively simple and rapid method to determine quantitatively tryptophan and several of its metabolites in biological fluids using reversed-phase high-performance liquid chromatography and multiple detection.

INTRODUCTION

Tryptophan (Trp) is an essential amino acid whose metabolism involves several different pathways. Two are of fundamental importance in man:

(1) Trp is hydroxylated by a tetrahydrobiopterin-dependent enzyme leading to the production of the neurotransmitter serotonin and of 5-hydroxy-indoleacetic acid.

(2) The kynurenine pathway leads to nicotinic acid and to the synthesis of NAD^+ [1]; this main breakdown requires the activity of the pyridoxal-requiring enzyme kynureninase [2].

Moreover, gut bacterial activity causes decomposition of unabsorbed Trp, producing indole compounds [2]. The determination of Trp and its metabolities is of interest in the study of all clinical conditions related to either a block or an enhancement of any of these pathways. This can be due either to a defect in enzyme activities (*i.e.* defects in tetrahydrobiopterin biosynthesis, kynureninase deficiency, vitamin B_6 deficiency) or to a transport defect (Hartnup disease). The assay of 5-hydroxy-Trp and of the catecholamines is well established and it is not the object of this work [3]. We report a simple chromatographic method for the determination of Trp and ten of its closely related metabolites (four indole derivatives, three kynurenine-type compounds and xanthurenic, 3-hydroxy-anthranilic and

* Corresponding author.

0021-9673/94/$07.00
SSDI 0021-9673(93)E0948-T

kynurenic acids) using reversed-phase high-performance liquid chromatography (HPLC) and combined UV–fluorimetric detection.

EXPERIMENTAL

Materials

Trp and other standards were obtained from Sigma (St. Louis, MO, USA); potassium phosphate, sulphosalicylic acid (analytical reagent grade), water and solvents (HPLC grade) were obtained from Merck (Darmstadt, Germany), as was the chromatographic column.

Sample preparation

Some compounds are easily degraded by increasing temperature, by light or by low pH [4]; therefore, the standard solutions and biological samples were promptly treated and then assayed, or stored under conditions of light exclusion at −20°C until analysis, which was then performed as soon as possible. Proteins must be immediately removed from plasma and other protein-containing fluids by precipitation with an equal volume of 5% sulphosalicylic acid in water. This method allows the measurement of total Trp. When measurement of free Trp is needed, other methods such as ultracentrifugation or ultrafiltration can be used for deproteinization. As a rule, protein removal is not necessary for urine, but the absence of proteins should be checked. Antioxidants such as sodium metabisulphite or ascorbic acid can be added. Plasma and urine are collected in the basal condition (fasting) and/or after a provocative test (*i.e.* oral Trp load) [2].

HPLC equipment

Analyses were carried out using a Hewlett-Packard (HP) 1090-L liquid chromatograph, equipped with an HP1040-M diode-array detector connected on line with an HP1046-A spectrofluorimetric detector. Signals were acquired with a Pascal workstation (Series 9000, software revision 5.21) which allows, together with the management of analytical conditions, a real-time view of UV absorbance (spectra and traces) and fluorescence emission, data storage and reduction. The injector was a manual Rheodyne valve with a 50-μl loop. The stationary phase was LiCrospher 100 RP-18 (5 μm particle size) in a LiChroCART 124-4 cartridge 12 cm long × 4.6 mm I.D.

Analytical conditions

The mobile phase was made up of two eluents: A, phosphate buffer (0.02 *M* KH_2PO_4–H_3PO_4) pH 5.4; B, acetonitrile–methanol–water (50:10:40, v/v/v). The flow-rate was 1 ml/min. The gradient was as follows: isocratic elution with eluent A for 6 min, then a ramp to 25% eluent B until 20 min and to 75% B until 35 min. The column was cleaned with eluent B for 5 min, then conditioned with 20 ml of eluent A. UV absorption was monitored at the wavelengths 254, 280 and 365 nm, band width 16 nm, using

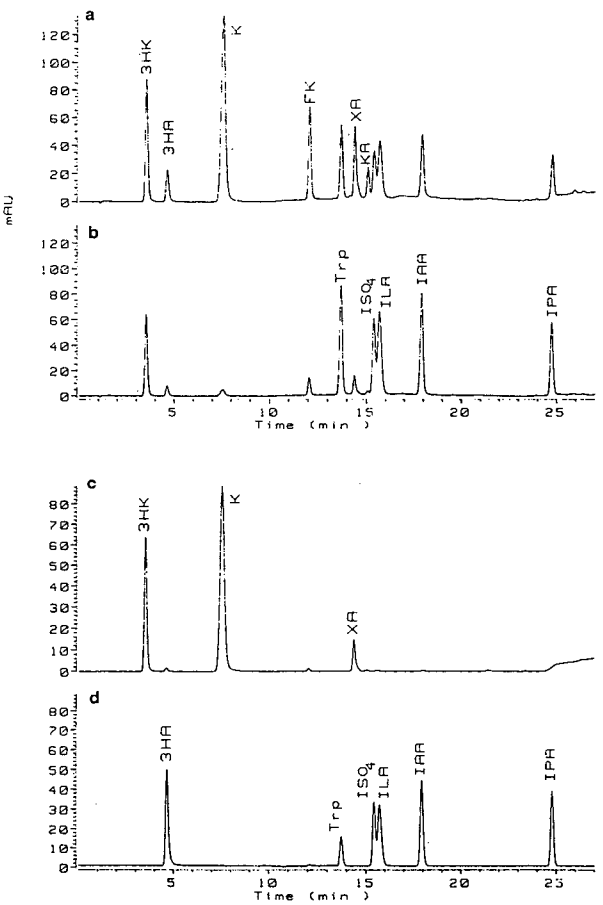

Fig. 1. The four chromatograms [UV at (a) 254, (b) 280, (c) 365 nm and (d) fluorescence] obtained from a standard mixture of the eleven compounds (concentration: 0.5 m*M*).

550 nm, band width 80 nm, as the reference wavelength; additionally UV spectra from 190 to 450 nm were stored. The fluorescence excitation was set to 340 nm and the emission to 440 nm; after 13.5 min, excitation and emission were changed to 280 and 340 nm, respectively.

RESULTS

The results of the analytical run were obtained as four chromatograms: UV absorbance at 254, 280 and 365 nm and fluorescence emission.

Eleven compounds, of relevant biochemical and clinical significance, were well separated and identified (Fig. 1, Table I).

Quantitation of each compound was possible using peak areas, and calibration curves were obtained from standard solutions at concentrations of 10, 50, 100 and 500 μmol/l. The choice of the chromatogram used for each peak for quantitative measurements depended on considerations of sensitivity and peak resolution (see Discussion).

The responses were linear in the measured range; as an example Table II reports data on linearity for Trp. The sensitivity of the method is enough to determine usual levels in plasma for the majority of the compounds. The lower response limit is about 2.5 μmol/l for Trp as well as for the other metabolites.

DISCUSSION

Methanol is generally used with different buffers as the organic modifier in reversed-phase liquid chromatography of Trp metabolites [4–6]. In our experience this method is not reliable (even using different gradient profiles) for a full separation of all compounds. Trp/XA and ISO_4/KA/ILA are poorly separated. While the use of both fluorescence and UV at 365 nm can resolve the problem well for Trp and XA (the first is fluorescent and does not absorb at 365 mm: see Table I), in the last triplet this method is not reliable because the contribution of the signal at 365 nm in the KA peak is very low and ISO_4 and ILA (both fluorescent) absorb considerably also at 254 and 280 nm. The introduction of acetonitrile into the organic eluent can overcome this disadvantage, yielding an acceptable resolution of all the peaks.

As a result of this procedure, each compound is well separated and can be measured in at least one of the four chromatograms. The choice of

TABLE I

RETENTION TIMES AND RELATIVE ABSORBANCES AT DIFFERENT WAVELENGTHS OF THE ELEVEN METABOLITES

The underlined signals are used for quantitation. For some compounds more than one signal can be used (see text).

Compound		t_R (min)	Fluorescence ($\lambda_{ex.}/\lambda_{em.}$)	UV signals[a] (nm)		
				254	280	365 nm
3-Hydroxykynurenine	3HK	3.9	None	41.2	27.2	31.6
3-Hydroxyanthranilic acid	3HA	8.09	340/440	69.1	23.4	7.4
Kynurenine	K	8.63	None	58.0	2.8	39.2
Formyl-kynurenine	FK	12.99	340/440	79.6	18.5	1.9
Tryptophan	Trp	14.6	280/340	34.4	65.6	None
Xanthurenic acid	XA	14.7	None	57.7	21.7	20.6
Kynurenic acid	KA	15.45	None	84.0	13.0	3.0
Indoxyl-sulphate	ISO_4	16.47	280/340	34.7	65.3	None
Indol-lactic acid	ILA	17.13	280/340	32.6	67.4	None
Indol-acetic acid	IAA	22.35	280/340	32.1	67.9	None
Indol-propionic acid	IPA	28.6	280/340	31.5	68.5	None

[a] The numbers indicate the relative mAU for the three wavelengths (percentage of the sum of the three absolute absorbances).

TABLE II

DATA ON RESPONSE LINEARITY AND MINIMUM DETECTION LEVEL FOR Trp USING UV (280 nm) AND FLUORESCENCE (FL) EMISSION (EXCITATION 280 nm, EMISSION 340 nm) SIGNALS

The equation of the calibration curve is $y = a + bx + cx^2$. r^2 = linear regression coefficient.

x		y response (area)	
		FL (280/340 nm)	UV (280 nm)
10	μmol/l	30.4	194.8
50	μmol/l	173.3	970.1
100	μmol/l	367.8	2192.1
500	μmol/l	1835.2	10938.0
A		−4.52	−30.9
B		3.68	21.7
C		$5.69e^{-6}$	$5.61e^{-3}$
r^2		0.99996	0.99988
Minimum detectable (μmol/l)		Below 5	Below 1

the signal used for quantitation is based on either specificity or sensitivity considerations. The fluorescence trace with excitation at 280 nm is particularly useful for the identification of Trp and indole derivatives.

The UV spectra acquired during the run are a relevant additional help in peak identification. However, special care must be taken comparing the spectra from biological samples with those from authentic compounds, since the elution is in gradient mode and the UV spectra are critically affected by the actual percentage of methanol and acetonitrile in the mobile phase: even the slightest alteration in the retention time can lead to a substantial modification of the UV spectra.

In conclusion, the present method is reliable for the simultaneous determination of several biochemically linked compounds, using a relatively simple and rapid procedure.

Its clinical applications are considerable because of the wide clinical relevance of Trp and Trp-related compounds. Their involvement in several clinical conditions and pathologies, such as Hartnup disease, B_6 deficiency, dermatological changes, cancers and mental disturbances, is well known [2,4].

REFERENCES

1 A.H. Mehler, in T.M. Devlin (Editor), *Textbook of Biochemistry with Clinical Correlations*, Wiley–Liss, New York, 1992, p. 491.
2 H.L. Levy, in C.R. Scriver, A.L. Beaudet, W.S. Sly and D. Valle (Editors), *The Metabolic Basis of Inherited Disease*, McGraw-Hill, New York, 1989, p. 2515.
3 D.A. Richards and A.C. Titheradge, *Biomed. Chromatogr.*, 2 (1987) 115.
4 P.M.M.M. Van Haard and S. Pavel, *J. Chromatogr.* 429 (1988) 59.
5 A.M. Krstulovic and C. Matzura, *J. Chromatogr.* 163 (1979) 72.
6 J.B. Tarr and J. Arditti, *New Physiol.*, 88 (1981) 621.

Journal of Chromatography A, 661 (1994) 105–112
Elsevier Science B.V., Amsterdam

CHROMSYMP. 2936

Sensitive determination of N-terminal prolyl peptides by high-performance liquid chromatography with laser-induced fluorescence detection

Toshimasa Toyo'oka*, Mumio Ishibashi and Tadao Terao

Division of Drugs, National Institute of Health Sciences, 1-18-1 Kamiyoga, Setagaya-ku, Tokyo 158 (Japan)

ABSTRACT

Short-chain peptides with an N-terminal proline (Pro–Gly, Pro–Ile, Pro–Gly–Gly, Pro–Leu–Gly–NH_2, and Pro–Thr–Pro–Ser–NH_2, etc.) were determined by HPLC with laser-induced fluorescence (LIF) detection. The peptides were quantitatively labelled with 4-(N,N-dimethylaminosulphonyl)-7-fluoro-2,1,3-benzoxadiazole (DBD-F) at 50°C after 1 h in a 0.1 *M* borax (pH 9.3)–acetonitrile mixture. The rate of reaction decreases inversely with the molecular weight of the peptides. The mean value of fluorescent emission of the resulting DBD–peptides and DBD–peptide amides was 573 nm (excitation, 453 nm). The proline peptides, including bioactive peptides such as Pro–Leu–Gly–NH_2 (release inhibitor of melanocyte-stimulating hormone), Pro–Thr–Pro–Ser–NH_2 (IgA_1 proteinase inhibitor) and Pro–Asp–Val–Asp–His–Val–Phe–Leu–Arg–Phe–NH_2 [FMRF amide-like (Phe–Met–Arg–Phe–NH_2) neuropeptide], were well separated by reversed-phase HPLC with water–acetonitrile containing 0.1% trifluoroacetic acid (TFA). The acetonitrile concentration in the mobile phase had a profound effect upon the retention times, and the capacity factors (k') were dependent on the hydrophobicity of the peptides. The structure of DBD–Pro–Leu–Gly–NH_2 was identified by LC–atmospheric pressure chemical ionization MS. The chromatographic detection limits ($S/N = 2$) of the peptides with a 15-mW argon-ion laser at 488 nm were in the 6–28 fmol range. The detection limits were improved to 2–5 fmol with a microbore column. The detectability was two orders of magnitude higher than with a conventional fluorescence detector using xenon arc lamp.

INTRODUCTION

A number of fluorogenic labelling reagents, *e.g.* 5-N,N-dimethylaminonaphthalenesulphonyl chloride (Dns-Cl), 4-nitro-7-fluoro-2,1,3-benzoxadiazole (NBD-F), fluorescamine, *o*-phthalaldehyde (OPA) and 2,3-naphthalenedicarboxyaldehyde (NDA), have been developed for the amino functional group [1,2]. Many of these reagents are currently used for the determination of various amines, such as biogenic amines, and amino acids. The following characteristics of the labelling reagent are required: (1) the reagent and its hydrolysate exhibit no or negligible fluorescence, (2) the reagent reacts with target compound selectively and rapidly, (3) the resulting derivative is sufficiently stable and fluoresces strongly and (4) the derivative preferably has fluorescence characteristics at long wavelengths (excitation, more than 400 nm; emission, more than 500 nm).

The fluorescence properties are important for the analysis of real samples, because other interfering substances in the samples that fluoresce at 300–400 nm will prevent accurate and reproducible determinations.

In previous papers, we described the synthesis of fluorescence labelling reagent, 4-(N,N-dimethylaminosulphonyl)-7-fluoro-2, 1, 3-benzoxadiazole (DBD-F) [3], and evaluated the reactivity of the reagent toward thiols and amines [4]. Secondary amines such as proline react more rapidly with the reagent than a primary amine such as alanine, whereas the reaction with thiol compound proceeds quantitatively under the

* Corresponding author.

0021-9673/94/$07.00
SSDI 0021-9673(93)E0941-M

selected conditions. A reaction product with alcohols was not found. Therefore, the reactivity of DBD-F with functional groups seems to be in this order: $-SH > -NH > -NH_2 \gg -OH$. Reagents (fluorescamine, OPA and NDA, etc.) [5–7] reported have been used as the labelling reagents for primary amines. Primary and secondary amino groups have been derivatized with fluorescein isothiocyanate, Dns-Cl and NBD-F, etc. [8–10]. Only a few reagents, such as 4-nitro-7-chloro-2,1,3-benzoxadiazole (NBD-Cl), react predominantly with secondary amines [11]. Since the derivatization conditions with NBD-Cl are quite rigorous, the derivatives decompose in the course of the reaction. In contrast, the DBD derivatives obtained from secondary amine are stable in the reaction medium [12,13]. The sensitivity of detection of the derivatives with conventional fluorescence detection using a xenon arc lamp is limited to sub-pmol level [4]. To achieve better sensitivity, excitation by a laser source has recently been developed. Laser-induced fluorescence (LIF) detection offers some definite potential advantages over conventional light sources [14,15], *i.e.* production of a very high photon flux (high excitation energy), improvement of the signal-to-noise ratios and the possibility of an accurate positioning and focusing of the beam. The purpose of present paper is highly sensitive determination of N-terminal prolyl peptides including bioactive amides by HPLC with LIF detection.

EXPERIMENTAL

Materials and reagents

DBD-F was obtained from Tokyo Kasei (Tokyo, Japan). L-Proline (Pro), hydroxy-L-proline (OH-Pro), L-prolyl-glycine (Pro–Gly), L-prolyl-glycyl-glycine (Pro–Gly–Gly), L-prolyl-L-leucine (Pro–Leu), L-prolyl-L-isoleucine (Pro–Ile), L-prolyl-L-leucyl-glycine (Pro–Leu–Gly), L-prolyl-L-leucyl-glycinamide (Pro–Leu–Gly–NH_2) (release inhibitor of melanocyte-stimulating hormone) [16], L-prolyl-L-threonyl-L-prolyl-L-serinamide (Pro–Thr–Pro–Ser–NH_2) (IgA_1 proteinase inhibitor) [17] and L-prolyl-L-asparaginic acidyl-L-valyl-L-asparaginic acidyl-L-histidyl-L-valyl-L-phenylalanyl-L-leucyl-L-arginyl-L-phenylalaninamide (Pro–Asp–Val–Asp–His–Val–Phe–Leu–Arg–Phe–NH_2) [FMRF amide-like (Phe–Met–Arg–Phe–NH_2) neuropeptide] [18] were purchased from Sigma (St. Louis, MO, USA). Ethylenediaminetetraacetic acid disodium salt (Na_2EDTA) was also used as received (Dojindo, Kumamoto, Japan). Trifluoroacetic acid (TFA), acetonitrile and water were of HPLC grade (Wako, Tokyo, Japan). All other chemicals were of analytical-reagent grade and were used without further purification.

HPLC

The high-performance liquid chromatograph consisted of two LC-9A pumps (Shimadzu) and an SCL-6B system controller (Shimadzu). Sample solutions were injected by an SIL-6B autoinjector (Shimadzu). The analytical column was an Inertsil ODS-2 (150 × 4.6 mm I.D., 5 μm) (GL Sciences, Tokyo, Japan) and a TSK-gel PTH-Pak (250 × 2.0 mm I.D., 5 μm) (Tosoh, Tokyo, Japan). The column was maintained at 40°C with a 655A-52 column oven (Hitachi, Tokyo, Japan). A Shimadzu RF-550 fluorescence monitor equipped with a 12-μl flow cell was employed for the detection. The wavelengths of excitation and emission were fixed at 450 and 560 nm, respectively. A Tosoh LF-8010 monitor, equipped with a 5-μl flow cell and an interference filter at 540 ± 20 nm, was employed for the LIF detection. The peak areas obtained from the fluorescence and LIF monitors were determined with a C-R4A Chromatopac (Shimadzu). All mobile phases were degassed with an on-line degasser (DGU-3A, Shimadzu). The flow-rate of the eluent for the conventional column and microbore column was 1.0 ml/min and 0.2 ml/min, respectively.

LC–MS

The apparatus used was a Hitachi L-6200 HPLC instrument equipped with an Inertsil ODS-2 (150 × 4.6 mm I.D., 5 μm) column and connected to a Hitachi M-1000 mass spectrometer [atmospheric pressure chemical ionization (APCI) system] [19,20]. The vaporizer temperature was 280°C, and the drift voltage was 160 V. The separation of DBD–Pro–Leu–Gly–NH_2, DBD-OH and DBD-F was carried out with a

mobile phase of water–acetonitrile (7:3) containing 0.1% TFA at a flow-rate of 1.0 ml/min.

Time course of the reaction of peptide or peptide-amide with DBD-F

A 0.1-ml aliquot of DBD-F (10 m*M*) in acetonitrile [or dimethyl formamide (DMF)] and 0.2 ml of peptide or peptide-amide (2.5 μM) in 0.1 *M* borax (pH 9.3) containing (or without) 1 m*M* Na_2EDTA were mixed in a 1.5-ml mini-vial (GL Science). The vials were tightly capped and heated at 50°C for 4 h. At fixed time intervals, one vial was taken out from dry heat block, and cooled in ice-water (0–5°C). Then a 627 μl of water were added to 40 μl of the reaction mixture. An aliquot (10 μl, corresponding to 1 pmol) of the diluted solution was automatically injected into the Inertsil ODS-2 column, and the LIF peak area of the resulting diastereomer was determined with an integrator. The reagent blanks without peptide or peptide-amide were treated in the same manner.

For the fluorescent spectra measurements, 50 μl of the reaction solution before dilution were injected onto the column, monitored with a conventional fluorescence detector, and the peak corresponding to the derivative was collected from outlet of the detector (*ca.* 2-ml portion).

Separation of peptide and peptide-amide derivatives

To 0.5 ml (low nmol to pmol) of a test solution in 0.1 *M* borax containing 1 m*M* Na_2EDTA placed into a 1.5-ml mini-vial were added 0.25 ml of 10 m*M* DBD-F in acetonitrile. The vials were tightly capped and heated at 50°C for 1 h in the dark. After cooling in ice-water (0–5°C), a suitable volume of water was added to the reaction mixture, an aliquot of the diluted solution was chromatographed and the fluorescence peak area of the derivative obtained from the LIF detector was determined with an integrator. The reagent blanks without peptide or peptide-amide were treated in the same manner.

RESULTS AND DISCUSSION

Fluorescence characteristics of the derivatives

Fig. 1 shows the labelling reaction of proline with DBD-F. DBD-F is not itself fluorescent; however, the derivatives with amines fluoresce at relatively long wavelengths. Initially, the fluorescence excitation and emission maxima of DBD derivatives were determined in acetonitrile–water containing 0.1% TFA, which has been widely used as an eluent for peptide separations by reversed-phase HPLC. As shown in Table I, the maximal wavelengths of excitation and emission were *ca.* 453 nm and *ca.* 573 nm, respectively. The results suggest that the fluorescence is independent of the peptides or amides. Although the excitation maximum (453 nm) is not well suited to the light emission of argon ion at 488 nm, it is possible to achieve sensitive detection of the peptides and their amides with the laser source.

Derivatization

The reactivity to N-terminal prolyl peptides was compared with N-terminal prolyl peptide-amides in aqueous acetonitrile (pH 9.3) containing 1 m*M* Na_2EDTA at 50°C. Figs. 2 and 3 show the time course of the reaction of the peptides and the peptide-amides, respectively. Judging from the curves in Fig. 2, the reaction rate seems to be dependent on the molecular

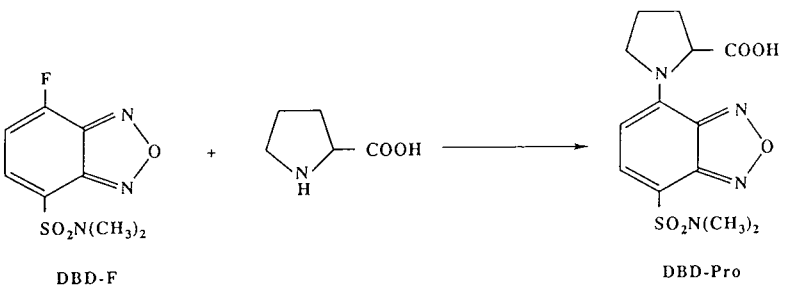

Fig. 1. The reaction of DBD-F and proline.

TABLE I

FLUORESCENCE PROPERTIES OF DBD-PEPTIDES IN WATER–ACETONITRILE (7:3) CONTAINING 0.1% TFA

Derivative	λ_{max} (nm)	
	Excitation	Emission
Pro	453	574
Pro–Gly	452	574
Pro–Gly–Gly	453	576
Pro–Leu–Gly	452	572
Pro–Leu	454	572
Pro–Ile	454	573
Pro–Leu–Gly–NH_2	453	573
Pro–Thr–Pro–Ser–NH_2	453	573
Pro–Asp–Val–Asp–His–Val–Phe–Leu–Arg–Phe–NH_2	452	568

mass, Pro > Pro–Gly > Pro–Gly–Gly. A similar phenomenon was also observed in the comparison of peptide-amides (Pro–Thr–Pro–Ser–NH_2 *versus* Pro–Asp–Val–Asp–His–Val–Phe–Leu–Arg–Phe–NH_2) (Fig. 3). However, the rates to Pro–Leu–Gly–NH_2 and Pro–Thr–Pro–Ser–NH_2 are essentially the same. Therefore, the rate seems to be a function not only of molecular weight, but also of hydrophilicity. Differences in the reactivities of peptides and peptide-amides were not observed. Even though a 2000-fold

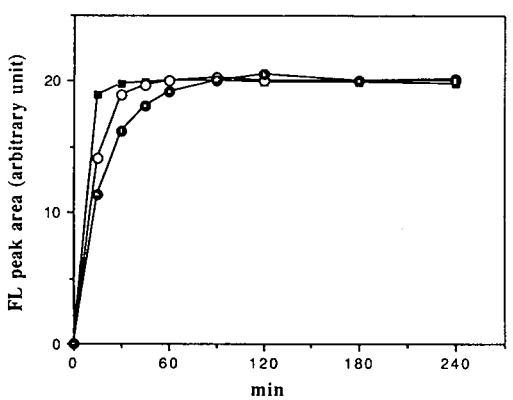

Fig. 2. Time course of the derivatization reaction of N-terminal prolyl peptides with DBD-F. □ = Pro; ○ = Pro–Gly; ● = Pro–Gly–Gly. Eluent, water–acetonitrile (7:3) containing 0.1% TFA; fluorescence (FL) detection, 560 nm (excitation at 450 nm). Other HPLC conditions are given in the Experimental section.

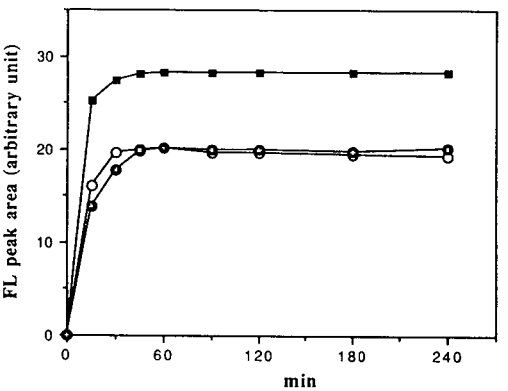

Fig. 3. Time course of the derivatization reaction of N-terminal prolyl peptide-amides with DBD-F. ○ = Pro–Thr–Pro–Ser–NH_2; □ = Pro–Leu–Gly–NH_2; ● = Pro–Asp–Val–Asp–His–Val–Phe–Leu–Arg–Phe–NH_2. HPLC conditions as in Fig. 2.

excess of the reagent relative to the peptides and peptide-amides was added to the reaction solution, a peak due to DBD-OH was not apparent on the chromatograms obtained with the LIF detector. The negligible fluorescence of DBD-OH is a predominant consideration for the determination of peptides and peptide-amides because a large amount of the labeling reagent must be added to the sample solution to drive the reaction to completion. As described in a previous paper [21], when the derivatization reaction of amino acids with NBD-F, which has a similar structure to DBD-F, is carried out without EDTA in the medium, the yield of some derivatives is reduced compared with the reaction in the presence of EDTA. EDTA probably inhibits intramolecular and/or intermolecular chirate formation between amino acids, such as Asp and His, and metals such as Cu^{2+} and Ni^{2+}. Therefore, a small amount of EDTA was added to the reaction medium to scavenge the metal ions. Fig. 4 shows that the reaction rates without EDTA are slightly slower than the rates in the presence of EDTA. The results suggest that the contribution of metal ions to the reaction of peptides and/or peptide-amides is not significant. To improve the solubility of peptides and/or peptide-amides in biological specimens, the reaction in DMF–water was substituted for the acetonitrile–water mixture. As depicted in Fig. 5, the required heating time is slightly reduced;

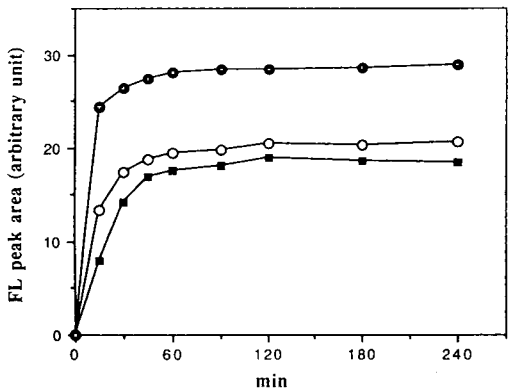

Fig. 4. Time course for the derivatization reaction of N-terminal prolyl peptides and the amides with DBD-F in acetonitrile–water without Na_2EDTA. ○ = Pro–Gly; ■ = Pro–Leu–Gly; ● = Pro–Leu–Gly–NH_2. HPLC conditions as in Fig. 2.

however, the curves obtained from the reaction in aqueous DMF are almost superimposable on the curves obtained from the reaction in aqueous acetonitrile. Therefore, both solvents can be used as reaction medium by combination with alkaline solution. Thus, 50°C for 1 h in aqueous acetonitrile (pH 9.3) containing 1 m*M* Na_2EDTA is recommended for the derivatization of peptides and the corresponding amides.

Structural elucidation of the derivatives with LC–MS

The structure of DBD–Pro–Leu–Gly–NH_2 was identified by LC–APCI-MS. Figs. 6 and 7

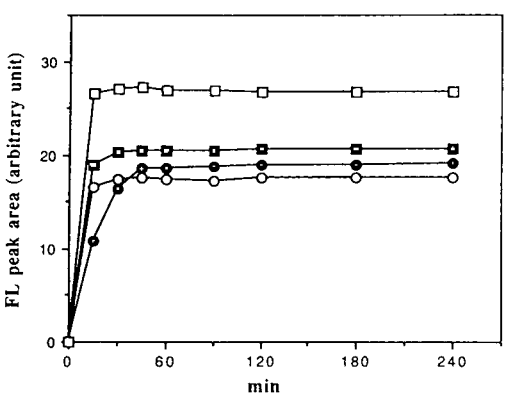

Fig. 5. Time course for the derivatization reaction of N-terminal prolyl peptides and the amides with DBD-F in DMF–water. ■ = Pro; ○ = Pro–Gly; ● = Pro–Leu–Gly; □ = Pro–Leu–Gly–NH_2. HPLC conditions as in Fig. 2.

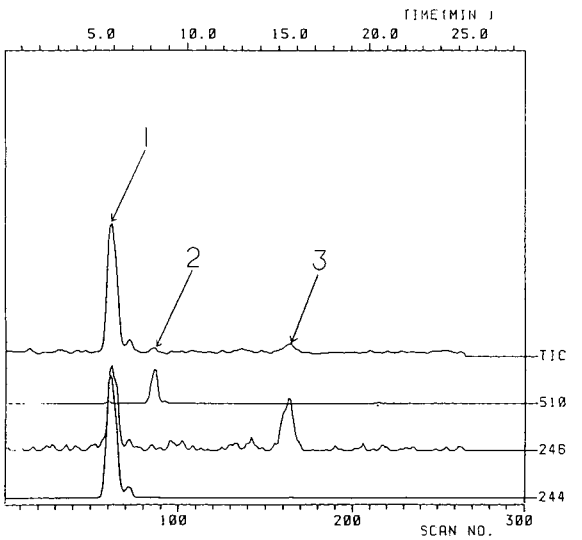

Fig. 6. Mass chromatograms of DBD derivatives. 1 = DBD-OH; 2 = DBD–Pro–Leu–Gly-NH_2; 3 = DBD-F. TIC = Total ion current.

show the mass chromatogram and mass spectra of the derivative, the hydrolysate (DBD-OH) and the reagent (DBD-F). From the analysis with a UV detection at 220 nm, the derivative, DBD-OH and DBD-F elute at 8.5, 6.0 and 15.5 min, respectively. In the APCI-MS system, quasimolecular ions $[M + H]^+$ of the compounds were observed as base peaks: $m/z = 510$ for DBD–Pro–Leu–Gly–NH_2, $m/z = 244$ for DBD-OH and $m/z = 246$ for DBD-F.

HPLC separation of the derivatives

The separation of the DBD derivatives obtained from peptides and peptide-amides with an N-terminal proline was studied with reversed-phase chromatography with aqueous acetonitrile containing 0.1% TFA. Figs. 8 and 9 show the correlation between acetonitrile concentration in the mobile phase and capacity factor (k'). The acetonitrile concentration in the eluent influences the retention times of the derivatives and larger k' values are obtained with a lower concentration of acetonitrile. In the case of the peptides, C-terminal glycyl peptides elute faster than leucine or isoleucine. Therefore, the elution order is dependent on the kind of C-terminal amino acid, but independent of molecular mass.

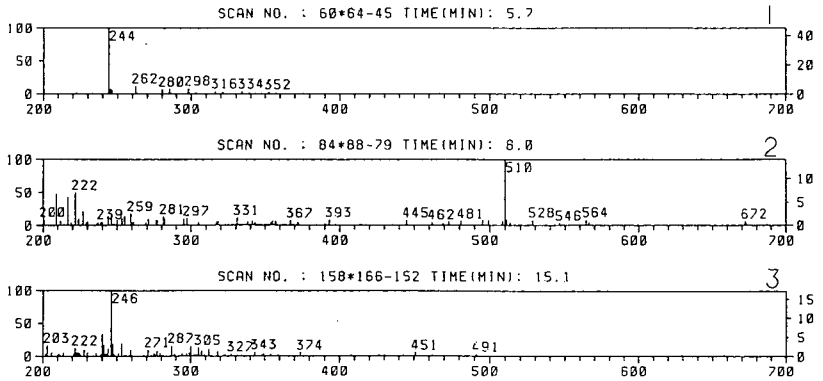

Fig. 7. Mass spectra scanned at the peak tops of the mass chromatograms (see Fig. 6).

In other words, the order might be defined by the hydrophobicity of the peptides. Similar results were obtained with the separation of peptide-amides (Fig. 9). A high degree of dependency on acetonitrile concentration was observed with decapeptide-amide (Pro–Asp–Val–Asp–His–Val–Phe–Leu–Arg–Phe–NH_2). The peptide-amide with high hydrophobicity such as Pro–Leu–Gly–NH_2 is strongly influenced by the concentration of acetonitrile in the mobile phase; however, a hydrophilic peptide-amide, such Pro–Thr–Pro–Ser–NH_2, is not significantly changed over a relatively wide concentration range. Consequently, the acetonitrile concentration should be carefully controlled to obtain precise and accurate results.

Figs. 10 and 11 show typical chromatograms of DBD derivatives obtained from peptides and peptide-amides. Six DBD–peptides and three DBD–peptide amides were completely separated by isocratic elution with a water–acetonitrile mixture in the presence of 0.1% TFA. The detection limits (signal-to-noise ratio of 2) of DBD–peptides, calculated from the chromatogram, were from 7 fmol (Pro–Gly–Gly) to 28 fmol (Pro–Leu), while those of DBD–peptide-amides were between 6 fmol (Pro–Thr–Pro–Ser–NH_2) and 83 fmol (Pro–Asp–Val–Asp–His–Val–Phe–Leu–Arg–Phe–NH_2). The detection limits were about two orders of magnitude lower than those with conventional fluorescence detection. The detectability improved with the use of

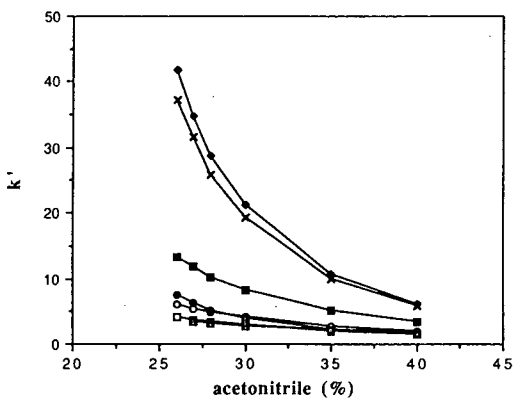

Fig. 8. The effect of acetonitrile concentration in the mobile phase on the retention time of DBD–peptides. ■ = Pro; ○ = Pro–Gly; □ = Pro–Gly–Gly; ◆ = Pro–Leu; × = Pro–Ile; ● = Pro–Leu–Gly; △ = OH-Pro. HPLC conditions as in Fig. 2, except for the eluent composition.

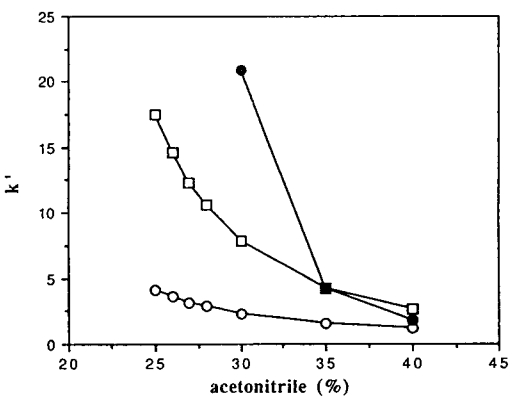

Fig. 9. The effect of acetonitrile concentration in the mobile phase on the retention time of DBD–peptide amides. □ = Pro–Leu–Gly–NH_2; ○ = Pro–Thr–Pro–Ser–NH_2; ● = Pro–Asp–Val–Asp–His–Val–Phe–Leu–Arg–Phe–NH_2. HPLC conditions as in Fig. 2, except for the eluent composition.

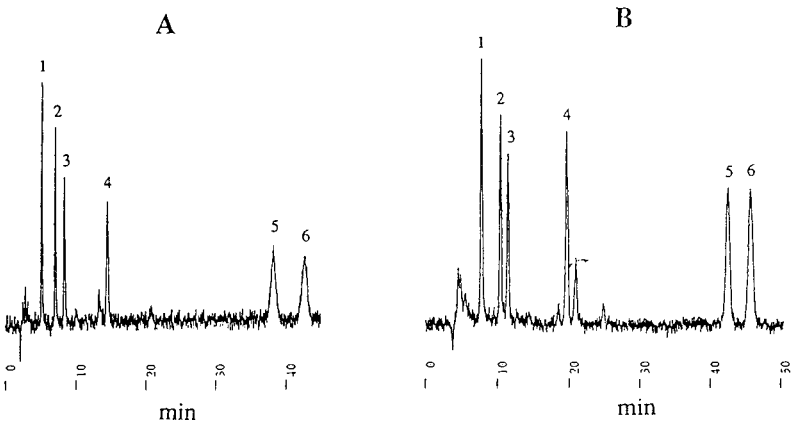

Fig. 10. Chromatograms of DBD–peptides using a reversed-phase column with LIF detection. (A) Inertsil ODS-2, each peak corresponding to 100 fmol. (B) TSK-gel PTH-Pak, each peak corresponding to 50 fmol. Peaks: 1 = Pro–Gly–Gly; 2 = Pro–Gly; 3 = Pro–Leu–Gly; 4 = Pro, 5 = Pro–Ile; 6 = Pro–Leu. Eluents: A = water–acetonitrile (74:26) containing 0.1% TFA; B = water–acetonitrile (70:30) containing 0.1% TFA. Flow-rate: A = 1.0 ml/min; B = 0.2 ml/min. Detection: A = 15 mW; B = 10 mW. Other HPLC conditions are given in the Experimental section.

a microbore column of 2.0 mm diameter relative to a conventional column with a 4.6 mm diameter. The chromatograms obtained with the microbore column are shown in Figs. 10B and 11B. The detection limits of DBD–peptides were 2.7 fmol (Pro–Gly–Gly), 3.4 fmol (Pro–Gly), 4.3 fmol (Pro–Leu–Gly), 3.6 fmol (Pro), 5.1 fmol (Pro–Ile) and 5.1 fmol (Pro–Leu), whereas those of DBD–peptide amides were 2.6 fmol (Pro–Thr–Pro–Ser–NH_2), 2.3 fmol (Pro–Leu–Gly–NH_2) and 14 fmol (Pro–Asp–Val–Asp–His–Val–Phe–Leu–Arg–Phe–NH_2). The low sensitivity for the decapeptideamide might be due to the quantum yield of the derivative.

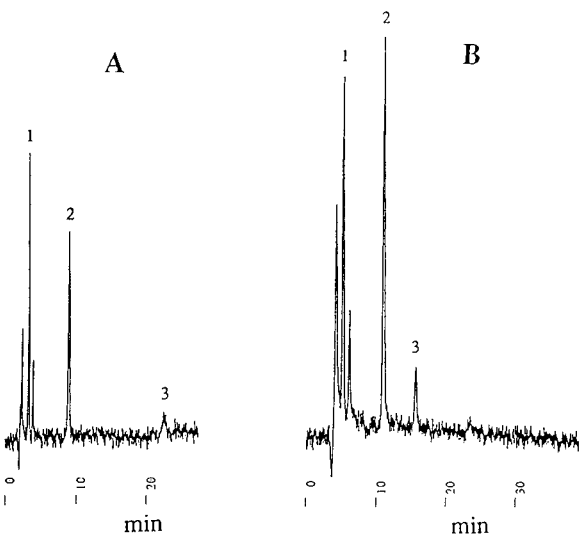

Fig. 11. Chromatograms of DBD–peptide amides using a reversed-phase column with LIF detection. (A) Inertsil ODS-2, each peak corresponding to 100 fmol. (B) TSK-gel PTH-Pak, each peak corresponding to 50 fmol. Peaks: 1 = Pro–Thr–Gly–Ser–NH_2; 2 = Pro–Leu–Gly–NH_2; 3 = Pro–Asp–Val–Asp–His–Val–Phe–Leu–Arg–Phe–NH_2. Eluents: A = water–acetonitrile (70:30) containing 0.1% TFA; B = water–acetonitrile (65:35) containing 0.1% TFA. Flow-rate: A = 1.0 ml/min; B = 0.2 ml/min. Detection: 15 mW. Other HPLC conditions are given in the Experimental section.

In conclusion, ultra trace analysis at the low fmol level is possible with DBD-F using the recommended procedure, even though the excitation and emission wavelengths do not match the light emission of the laser source and the interference filter wavelengths. The sensitivity may be improved with a suitable interference filter (570 nm) and an increase in the output laser power. Hence, the proposed procedure using DBD-F may be applicable to sensitive determination of peptides and/or peptide amides in biological specimens. Further study is under way.

ACKNOWLEDGEMENTS

The authors thank Mr. T. Takahashi, Hitachi Instruments Engineering Co., for LC–MS measurement. Thanks are also due to Dr. C.R.

Warner, Food and Drug Administration, Washington, DC, USA for reviewing the manuscipt.

REFERENCES

1 H. Lingeman, W.J.M. Underberg, A. Takadate and A. Hulshoff, *J. Liq. Chromatogr.*, 8 (1985) 789.
2 K. Imai and T. Toyo'oka, in R.W. Frei and K. Zech (Editors), *Selective Sample Handling and Detection in High-performance Liquid chromatography (Journal of Chromatography Library*, Vol. 39A), Elsevier, Amsterdam, 1988, p. 209.
3 T. Toyo'oka, T. Suzuki, Y. Saito, S. Uzu and K. Imai, *Analyst*, 114 (1989) 413.
4 T. Toyo'oka, T. Suzuki, Y. Saito, S. Uzu and K. Imai, *Analyst*, 114 (1989) 1233.
5 P. Bohlen, S. Stein, J. Stone and S. Udenfriend, *Anal. Biochem.*, 67 (1975) 438.
6 P.E. Hare, *Methods Enzymol.*, 47 (1977) 3.
7 B.K. Matuszewsky, R.S. Givens, K. Srinivasachar, R.G. Carlson and T. Higuchi, *Anal. Chem.*, 59 (1987) 1102.
8 K. Muramoto, H. Kamiya and H. Kawauchi, *Anal. Biochem.*, 141 (1984) 446.
9 C. De Jong, G.J. Hughes, E. Van Wieringen and K.J. Wilson, *J. Chromatogr.*, 241 (1982) 345.
10 Y. Watanabe and K. Imai, *J. Chromatogr.*, 239 (1982) 723.
11 L. Johnson, S. Lagerkvist, P. Lindroth, M. Ahnoff and K. Martinsson, *Anal. Chem.*, 54 (1982) 939.
12 T. Toyo'oka, M. Ishibashi, Y. Takeda, K. Nakashima, S. Akiyama, S. Uzu and K. Imai, *J. Chromatogr.*, 588 (1991) 61.
13 T. Toyo'oka, M. Ishibashi and T. Terao, *Analyst*, 117 (1992) 727.
14 E.S. Yeung and M.J. Sepaniak, *Anal. Chem.*, 52 (1980) 1465A.
15 R.B. Green, *Anal. Chem.*, 55 (1983) 20A.
16 R. Walter, R.F. Ritzmann, H.N. Bhargava and L.B. Flexner, *Proc. Natl. Acad. Sci. U.S.A.*, 76 (1979) 518.
17 S.G. Wood, M. Lynch, A.G. Plaut and J. Burton, *J. Med. Chem.*, 32 (1989) 2407.
18 S. Robb, L.C. Packman and P.D. Evans, *Biochem. Biophys. Res. Commun.*, 160 (1989) 850.
19 M. Sakairi and H. Kambara, *Anal. Chem.*, 60 (1988) 774.
20 H. Kodama, H. Nakamura, K. Sugahara and Y. Numajiri, *J. Chromatogr.*, 527 (1990) 279.
21 H. Miyano, T. Toyo'oka, K. Imai and T. Nakajima, *Anal. Biochem.*, 150 (1985) 125.

Journal of Chromatography A, 661 (1994) 113–119
Elsevier Science B.V., Amsterdam

CHROMSYMP. 2959

Column-switching liquid chromatographic method for the simultaneous determination of iothalamic acid and creatinine in biological fluids

Tokuichiro Seki* and Yoshimasa Orita

College of Bio-Medical Technology, Osaka University, 1-1, Machikaneyama-cho, Toyonaki-shi, Osaka 560 (Japan)

Shigeo Yamamoto and Naohiko Ueda

1st Department of Internal Medicine, Osaka University Medical School, 2-2, Yamadaoka, Suita-shi, Osaka 565 (Japan)

Yuzo Yanagihara and Kohji Noguchi

Asahi Chemical Industry Co. Ltd., 1-3-2, Yakoo, Kawasaki-ku, Kawasaki-shi, Kanagawa 210 (Japan)

ABSTRACT

A column-switching liquid chromatographic method for the simultaneous determination of iothalamate and creatinine in human serum and urine was developed. Iothalamate and creatinine were separated on a weakly acidic ion-exchange column (C1) by ion-exclusion chromatography and iothalamate excluded from the column was purified by gel chromatography on a hydrophilic gel column (C2) and then by ion-exchange chromatography on a weakly basic ion-exchange column (C3). Creatinine that was eluted from C1 after iothalamate was transferred to a hydrophilic gel column (C4) and then to a strongly acidic ion-exchange column (C5). The mobile phase for C1–C4 was a pH 3.8 propionate buffer (propionic acid–NaOH = 0.35 + 0.035 mol/kg in water) and a pH 5.6 propionate buffer (propionic acid–NaOH = 0.04 + 0.035 mol/kg in water) was used for C5. Diluted serum and urine samples could be injected directly on to C1, as the matrix of C1 is hydrophilic and C1 is backflushed after the transfer of the creatinine fraction from C1 to C4. Iothalamate and creatinine in the eluates were determined by measuring their ultraviolet absorption at 245 and 234 nm, respectively. The precision (R.S.D.) of the chromatographic method was 1.6% ($n = 7$) and 0.36% ($n = 6$) for diluted serum and urine with iothalamate concentrations of 1.0 and 10.0 μmol/l, respectively, and 0.85% ($n = 7$) and 0.55% ($n = 7$) for diluted serum and urine with creatinine concentrations of 5.77 and 272 μmol/l, respectively.

INTRODUCTION

[^{125}I]iothalamate clearance has been used for the determination of the glomerular filtration rate as an alternative of inulin clearance [1–3]. However, with radioactive compounds there are problems of discarding radioactive waste and the administration of radioactive materials to humans. To avoid these problems, high-performance liquid chromatographic (HPLC) methods for the determination of non-radioactive iothalamate in human serum and urine have been developed [4–8]. Most of these methods required sample pretreatment such as deproteinization or extraction with an organic solvent. Chromatographic systems utilized for the determination of serum creatinine include ion-exchange [9–16], reversed-phase [17,18] and ion-pair chromatography [19] with pretreatment such as deproteinization. Analyses of serum

* Corresponding author.

0021-9673/94/$07.00
SSDI 0021-9673(93)E1092-E

creatinine by multi-dimensional HPLC have also been reported [9,17,18,20]. Urinary creatinine has been determined by ion-exchange [10,13], ion-pair [19,21] and reversed-phase chromatography [22].

We have developed a method for on-line sample pretreatment based on ion-exclusion chromatography. The method has been applied to the determination of catecholamines [23], vanillylmandelic acid [24], homovanillic acid [24] and iothalamate [25] in biological fluids. In this paper, the simultaneous determination of iothalamate and creatinine in human serum and urine is described.

Iothalamate in a sample is excluded from a column of a weakly acidic ion exchanger with a hydrophilic matrix (C1) and the excluded iothalamate is switched to a column of hydrophilic gel and then to a column of anion exchanger using a sodium propionate buffer as the mobile phase. Creatinine eluted from C1 after iothalamate is purified further by gel and cation-exchange chromatography by column switching. As the same mobile phase is used for filtration of a sample through C1 and for backflushing of C1 after the transfer of creatinine from C1 to a hydrophilic gel column, C1 could be used repeatedly and the whole process could be automated.

EXPERIMENTAL

Materials

DIP Conray injection, a solution for drip infusion pyelography, containing 50.07 g of iothalamic acid, 3-(acetylamino)-2,4,6-triiodo-5-[(methylamino)carbonyl)]benzoic acid, in the form of N-methyl-D-glucamine iothalamate in 220 ml of the solution, was purchased from Daiichi Seiyaku (Tokyo, Japan) and creatinine of special grade was purchased from Wako (Osaka, Japan). Other chemicals were of analytical-reagent grade from Yashima Pharmaceutical (Osaka, Japan).

Stock standard solutions of iothalamate and creatinine (1 and 10 mmol/l, respectively) were prepared in 0.01 mol/l propionic acid solution and were diluted with mobile phase A described below to give working standard solutions of various concentrations.

Apparatus

The liquid chromatographic system equipped with automatic column-switching valves consisted of four Model 880-PU constant-flow pumps (Jasco, Tokyo, Japan), a Model SP-024-2 dual-head pump (Jasco), a Model KSST-60J automatic injector (Kyowa Seimitsu, Tokyo, Japan), five columns [Asahipak ES-502C, a weakly acidic ion-exchange column, 10×0.76 cm I.D.; Asahipak GS-320H, a hydrophilic gel column, 25×0.76 cm I.D.; Asahipak ES-502N, a weakly basic ion-exchange column, 10×0.76 cm I.D.; Asahipak GS-220H, a hydrophilic gel column, 25×0.76 cm I.D.; all of particle size 9 ± 0.5 μm (Showa Denko, Tokyo, Japan); and Dowex 50W-X8, a strongly acidic ion-exchange column, 5×0.46 cm I.D., particle size 20–30 μm (Dow Chemical, Midland, MI, USA)], a Model 821-09 automatic six-way valve (Jasco), four Model MVA-4U7H automatic four-way valves (Sanuki Kohgyo, Tokyo, Japan), two Model 870-UV spectrophotometers (Jasco) and two Model RC-125 recorders (Jasco). These components were assembled as shown in Fig. 1.

The sample injection and switching events were controlled by using nine timer units (T1–T9). The first timer unit (T1), controlling the automatic injector and a four-way valve (V4), is equipped with a Model KS-1500 programmable timer (Koizumi Computer, Kobe, Japan), which repeats on and off modes of electric supply (100 V a.c.), at preset time intervals, to the relay circuit of T1 and to those of T2–T9. Each timer unit of T2–T9 is equipped with a motor timer with a maximum graded time of 6, 12 or 30 min (Models SYS-6M, -12M and -30M; Omron Electronics, Kyoto, Japan), and also with a relay circuit. When the preset time of the motor timer is over, the 100 V a.c. supply to the motor timer is shut off and the circuit is reset when the supply of 100 V a.c. from T1 is off. Timer units T2 and T3 control valve V2, T4 controls V4, T5 controls V1, T6 and T7 control V3 and T8 and T9 control V5 (Table I).

Mobile phases

A pH 3.8 propionate buffer (propionic acid–NaOH = 0.35 + 0.035 mol/kg in water) (mobile phase A) was used as the mobile phase for C1–C4, and a pH 5.6 propionate buffer (propi-

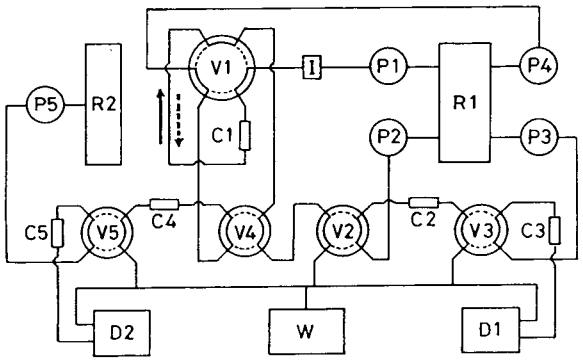

Fig. 1. Diagram of the column-switching equipment. R1 and R2 = mobile phase reservoir containing mobile phase A and B, respectively; I = automatic injector; P1–P3 and P5 = 880-PU; P4 = dual-head pump; C1 = Asahipak ES-502C column (10 × 0.76 cm I.D., 30°C); C2 = Asahipak GS-320H column (25 × 0.76 cm I.D., 50°C); C3 = Asahipak ES-502N column (10 × 0.76 cm I.D., 50°C); C4 = Asahipak GS-220H column (25 × 0.76 cm I.D., 30°C); C5 = Dowex 50W-X8 column (5 × 0.46 cm I.D., 40°C, packed in the laboratory); V1 = six-way automatic valve (full line and broken line represent rotor positions B and A of the valve, respectively); V2–V5 = four-way automatic valve (full line and broken line represent rotor positions L and R, respectively; D1 and D2 = spectrophotometers measuring absorbance at 245 and 234 nm, respectively; W = waste. When the rotor position of V1 is B and that of V2–V5 is L, mobile phases flow through the channels drawn with full lines, and when the rotor position of V1 is A and that of V2–V5 is R, mobile phases flow through the channels drawn with broken lines. The arrow drawn with a full line indicates the direction of flow of mobile phase A pumped by P1 when the rotor position of V1 is B. When the rotor position of V1 is A, mobile phase A pumped by P1 and P4 passes through the channels of V1 drawn with a broken line, and the mobile phase A pumped by P4 flows in the direction indicated by the arrow drawn with a broken line.

onic acid–NaOH = 0.04 + 0.035 mol/kg in water) (mobile phase B) was used for C5. Water of ultra-pure grade, obtained by using reverse osmosis (ROpure 40, Barnstead, Boston, MA, USA), ion-exchange and charcoal adsorption (NANOpure II, Barnstead) in series, was used to prepare mobile phases. They were filtered through a membrane filter (Type HV, pore size 0.45 μm; Millipore, Bedford, MA, USA) and degassed before use. The flow-rate of these mobile phases was 1.2 ml/min.

Sample preparation

Samples in plastic vials were kept frozen at −70°C and thawed before use. Serum (0.2 ml) was mixed with 1.8 ml of 2.5% (w/v) propionic acid solution. Urine (0.2 ml) was mixed with 1.8 ml of 2.5% propionic acid solution and then mixed with 3 ml of mobile phase A. The diluted sample was filtered through a disposable membrane filter (Shodex DT MX-13K, pore size 0.2 μm; Showa Denko) and poured into a vial. It was placed in the rack of the automatic injector and analysed within 10 h after preparation. For the determination of recovery, one volume of serum was diluted with nine volumes of 2.5% propionic acid solution containing iothalamate and creatinine to give a diluted serum sample with an iothalamate concentration of 1.0 μmol/l and creatinine concentration increased by 5.0 μmol/l, and one volume of urine was diluted with nine volumes of 2.5% propionic acid solution containing iothalamate and creatinine and fifteen volumes of mobile phase A to give a diluted urine sample with an iothalamate concentration of 10.0 μmol/l and creatinine concentration increased by 300 μmol/l (Table II).

Column switching and detection

The rotors of valves V1–V5 were positioned at B and L (full line in Fig. 1). Mobile phase A pumped by P1 flowed through the cation-exchange column (Asahipak ES-502C, C1) to waste, and mobile phase A pumped by P4 flowed through the hydrophilic gel column (Asahipak GS-220H, C4). When the switch of the programmable timer of T1 was turned on, T2–T9 came on, and sample (300 μl) was injected on to C1 from which anionic compounds together with iothalamate were excluded. The iothalamate fraction was transferred from C1 to Asahipak GS-320H (C2) via V2 by column switching. Next, creatinine was transferred to Asahipak GS-220H (C4) by switching the rotor position of V4 to R. When the transfer of creatinine fraction to C4 was over, the rotor position of V1 was changed to A to disconnect C1 and C4, and at the same time to backflush C1 by the mobile phase A pumped by P4. The creatinine fraction transfered to C4 was eluted with mobile phase A pumped by P1 and transferred to the Dowex 50W-X8 column (C5) via V5. The iothalamate fraction was transferred from C2 to Asahipak ES-502N (C3) via V3 and eluted from C3 with mobile phase A pumped by P3. Creatinine was eluted from C5 with mobile phase B pumped by

TABLE I

TIMING AND SEQUENCE OF EVENTS OF AUTOMATED COLUMN SWITCHING FOR THE DETERMINATION OF IOTHALAMATE AND CREATININE

Time (min)	On–off of timers of the timer units									Rotor position of valves					Event
	T1	T2	T3	T4	T5	T6	T7	T8	T9	V1	V2	V3	V4	V5	
0	On	On	On	On	On	On	On	On	On	B	L	L	L	L	Sample injection on to C1
3.8	On	Off	On	On	On	On	On	On	On	B	R	L	L	L	Connection of C1 and C2. Transfer of iothalamate fraction from C1 to C2
5.7	On	Off	Off	On	On	On	On	On	On	B	L	L	L	L	Disconnection of C1 and C2. End of transfer of iothalamate fraction from C1 to C2
6	On	Off	Off	Off	On	On	On	On	On	B	L	L	R	L	Connection of C1 and C4. Transfer of creatinine fraction from C1 to C4
8	On	Off	Off	Off	Off	On	On	On	On	A	L	L	R	L	Backflushing of C1 with P4. End of transfer of creatinine fraction from C1 to C4
11.6	On	Off	Off	Off	Off	On	On	Off	On	A	L	L	R	R	Connection of C4 and C5. Transfer of creatinine fraction from C4 to C5
14	On	Off	Off	Off	Off	On	On	Off	Off	A	L	L	R	L	Disconnection of C4 and C5. End of transfer of creatinine fraction from C4 to C5
14.2	On	Off	Off	Off	Off	Off	On	Off	Off	A	L	R	R	L	Connection of C2 and C3. Transfer of iothalamate fraction from C2 to C3
17.5	On	Off	Off	Off	Off	Off	Off	Off	Off	A	L	L	R	L	Disconnection of C2 and C3. End of transfer of iothalamate fraction from C2 to C3
47	Off	Reset	Reset	Reset	Reset	Reset	Reset	Reset	Reset	B	L	L	L	L	End of blackflushing of C1
55	On	On	On	On	On	On	On	On	On	B	L	L	L	L	Injection of next sample

TABLE II

RECOVERY OF IOTHALAMATE AND CREATININE ADDED TO DILUTED SERUM AND URINE

Sample	Analyte	Concentration of analyte added (μmol/l)	Recovery (%)[a]
Serum (10-fold dilution)	Iothalamate	1.0	100.2 ± 1.6
	Creatinine	5.0	102.1 ± 2.19
Urine (25-fold dilution)	Iothalamate	10.0	100.5 ± 0.36
	Creatinine	300	99.6 ± 1.78

[a] Mean ± R.S.D. ($n = 7$).

P5. After 47 min from sample injection, the programmable timer of T1 was off, T2–T9 were reset, the rotor position of V1 became B and backflushing of C1 ended, and at the same time the rotor position of V4 became L. Eight minutes later, the timer of T1 was on, and next sample was injected (Table I). Iothalamate and creatinine were determined from their peak heights on the chromatogram obtained with ultraviolet detection at 245 and 234 nm, respectively.

RESULTS AND DISCUSSION

Sodium propionate buffers were used as the mobile phases because they are stable, easy to

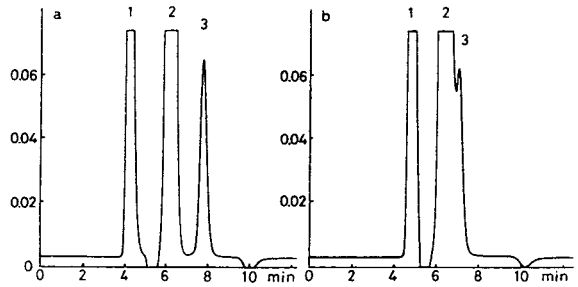

Fig. 2. Elution of (1) iothalamate, (2) uric acid and (3) creatinine from C1. (a) Elution pattern from a new column and (b) from the column after 70 serum samples had been injected. Ordinate, absorbance at 245 nm; abscissa, retention time.

prepare and do not allow microorganisms to grow. Among the propionate buffers of various concentrations and pH tried, mobile phase A gave the best result for the purification of iothalamate. As iothalamate is anionic and creatinine is cationic at pH 3.8, they were separately eluted from the weakly acidic cation-exchange column (C1) as shown in Fig. 2. Iothalamate could be separated from most impurities by filtration through the hydrophilic gel column (C2), and after elution from C3 no endogenous UV-absorbing peak was found at the retention time of iothalamate in the elution patterns of blank serum and urine samples (Fig. 3). Most impurities present in the creatinine fraction eluted from C1 could be removed by filtration through the hydrophilic gel column (C4), and the creatinine fraction eluted from C4 was transferred to C5 as shown in Fig. 4. The creatinine fraction transferred from C4 to C5 could not be eluted with mobile phase A, as the ion-exchange capacity of Dowex 50W-X8 column is higher than that of Asahipak ES-502C (C1).

With the use of the mobile phase of pH 5.6, in which the net charge of creatinine is decreased, elution of creatinine was successful (Fig. 5). Creatine was eluted from C1 with iothalamate and did not interfere with the determination of creatinine. The rate of conversion of creatine to creatinine in aqueous solution is maximum at pH 4 [26]. However, the conversion was 0.9% after 10 h when a solution of creatine in mobile phase A at concentration of 200 μmol/l was incubated at 20°C. As the concentration of creatine in serum is of the same order as that of creatinine and in urine is much lower [27], the increase in the concentration of creatinine in diluted serum and urine samples before analysis due to the dehydration of creatine present in diluted samples will be less than 1% of the concentration of creatinine in diluted samples.

The change in the efficiency of C1 was checked after 70 injections of serum samples on to C1. The retention time of iothalamate increased and that of creatinine decreased, as shown in Fig. 2b. However, after the timing of the switching of valves was adjusted, separation of iothalamate and creatinine from other UV-

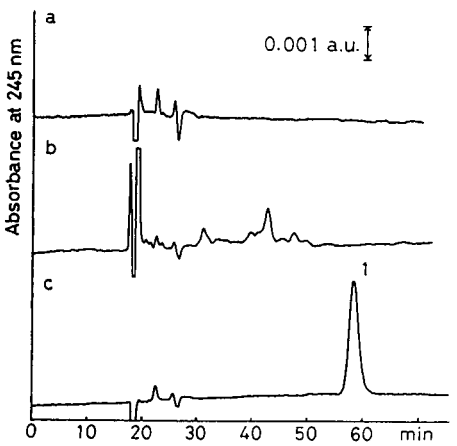

Fig. 3. Elution of samples from C3. (a) Diluted serum (10-fold dilution, (b) diluted urine (25-fold dilution) and (c) standard solution of iothalamate (peak 1, 1.0 μmol/l). Ordinate, absorbance at 245 nm; abscissa, retention time.

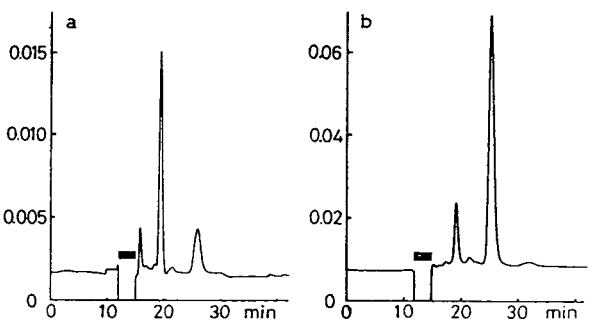

Fig. 4. Elution from C4 of the creatinine fraction transferred from C1 to C4. (a) Diluted serum sample and (b) diluted urine sample. Ordinate, absorbance at 245 nm; abscissa, retention time. The black horizontal bars represent the creatinine fractions transferred from C4 to C5.

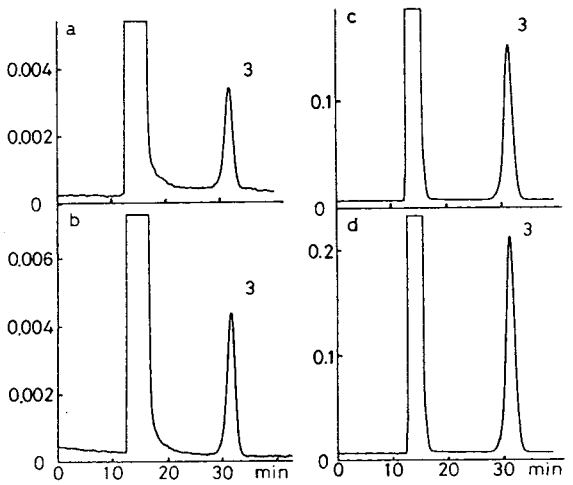

Fig. 5. Elution of creatinine (peak 3) from C5. (a) Standard solution (4.0 μmol/l); (b) diluted serum sample (calculated concentration 5.77 μmol/l); (c) standard solution (200 μmol/l); (d) diluted urine sample (calculated concentration 272 μmol/l). Ordinate, absorbance at 234 nm; abscissa, retention time.

absorbing peaks was satisfactory, as shown in Figs. 3, 5 and 6. Adjustment of the times of switching of the valves is as follows. First, the switching times of V2, V4 and V1 are adjusted so that the peaks of iothalamate and creatinine

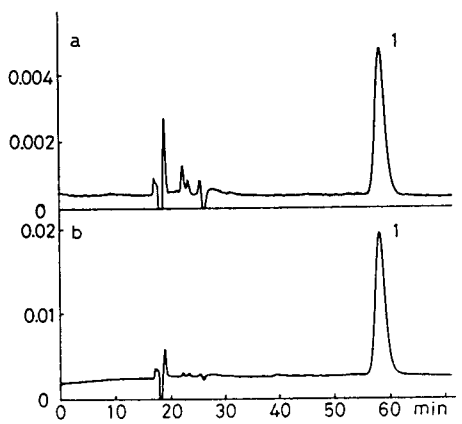

Fig. 6. Elution of samples containing iothalamate (peak 1). (a) Diluted serum sample prepared from serum taken from a patient 150 min after intravenous administration of 1.0 ml of DIP Conray injection containing 227.6 mg (388.5 μmol) of iothalamate (calculated concentration 1.31 μmol/l); (b) diluted urine sample prepared from urine collected from the same patient between 135 and 165 min after the intravenous administration of iothalamate (calculated concentration 5.03 μmol/l). Ordinate, absorbance at 245 nm; abscissa, retention time.

disappear from the chromatogram monitoring the eluate from C1. Then the switching times of V3 and V5 are adjusted so that the peaks of iothalamate and creatinine in the chromatograms monitoring the eluates from C2 and C4 disappear. Chromatograms showing the transfer of creatinine fraction from C4 to C5 are shown in Figs. 4a and b.

The sensitivity of this method was high enough to determine the concentration of iothalamate and creatinine in diluted serum and urine samples. The limit of detection was 0.1 μmol/l for iothalamate and 0.3 μmol/l for creatinine at a signal-to-noise ratio of 3. the relationship between the peak height (x) and the concentration of the analyte (y) was linear. In the ranges 0.5–20 μmol/l for iothalamate and 2–400 μmol/l for creatinine in mobile phase A, the equations were $y = 0.302x - 0.0155$ ($r = 0.9999$) and $y = 1.313x + 0.383$ ($r = 0.9999$), respectively.

The recovery of iothalamate and creatinine added to serum and urine is shown in Table II. The within-day relative standard deviation (R.S.D.) for iothalamate in diluted pooled serum (1.0 μmol/l of iothalamate) was 1.6% ($n = 7$) and in diluted pooled urine (10.0 μmol/l) it was 0.36% ($n = 6$). The within-day R.S.D. for creatinine in diluted pooled serum (calculated concentration 5.77 μmol/l) was 0.85% ($n = 7$) and in diluted pooled urine (calculated concentration 272 μmol/l) it was 0.55% ($n = 7$).

The creatinine concentration obtained by the present method (y) was compared with that obtained by the modified Jaffé method [28] (rate

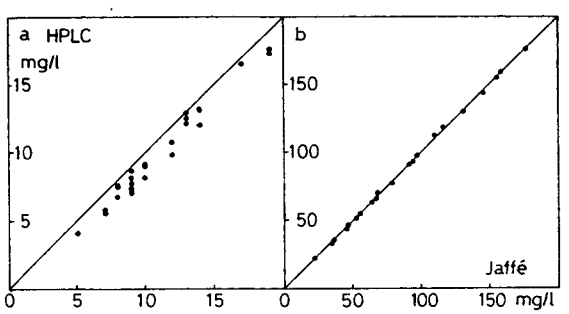

Fig. 7. Comparison between the concentration of creatinine in serum determined by the present method and Jaffé's method. Ordinate, concentration determined by the present method (y); abscissa, concentration determined by Jaffé's method (x). (a) Lower and (b) higher concentration ranges. The diagonal line represents $x = y$.

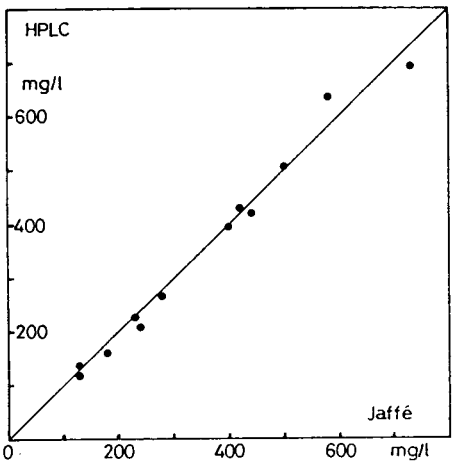

Fig. 8. Comparison between the concentration of creatinine in urine determined by the present method and Jaffé's method. Ordinate, concentration determined by the present method (y); abscissa, concentration determined by Jaffé's method (x). The diagonal line represents $x = y$.

assay) (x). In the concentration range 5–19 mg/l, the serum creatinine value obtained by the present method was lower than that obtained by the Jaffé method. The regression line was $y = 1.005x - 1.22$ ($n = 29$, $r = 0.9879$) and in the higher concentration range of 22–177 mg/l, $y = 1.0013x - 0.724$ ($n = 21$, $r = 0.9997$) (Fig. 7). The urinary creatinine concentration obtained by the present method was also lower than that of Jaffé method, $y = 1.0175x - 10.4$ ($n = 12$, $r = 0.9916$) (Fig. 8).

These results indicate that this column-switching liquid chromatographic method is suitable for the determination of creatinine and iothalamate in human serum and urine.

ACKNOWLEDGEMENTS

This work was supported by the special fund of Osaka University for education and research, and a grant for protection against the intractable disease "progressive renal disease" by the Ministry of Health and Welfare of Japan.

REFERENCES

1 F.T. Maher, N.G. Nolan and L.R. Elveback, *Mayo Clin. Proc.*, 46 (1971) 690.
2 N.T. Ott and D.M. Wilson, *Mayo Clin. Proc.*, 50 (1975) 664.
3 N. Tessitore, C. Lo Schiavo, A. Corgnati, G. Previato, E. Valvo, A. Lupo, S. Chiaramonte, P. Messa, A. D'Angelo, M. Zatti and G. Maschino, *Nephron*, 24 (1979) 41.
4 S. Boschi and B. Marchesini, *J. Chromatogr.*, 224 (1981) 139.
5 T. Preuksaritanout, M.-L. Chen and W.L. Chiou, *J. Chromatogr.*, 306 (1984) 89.
6 A.F. Weber, D.W. Lee, K. Opheim and A.L. Smith, *J. Chromatogr.*, 337 (1985) 434.
7 M.M. Reidenberg, B.J. Lorenzo, D.E. Drayer, J. Kluger, T. Nestor, J.C. Regnier, A. Kowal and I. Berkersky, *Ther. Drug Monit.*, 10 (1988) 434.
8 F. Gaspari, L. Maniadri, P. Ruggeneti and G. Remuzzi, *J. Chromatogr.*, 570 (1991) 435.
9 E. Wiedemann, E. Hägele, J. Siedel and J. Ziegohorn, *Fresenius' Z. Anal. Chem.*, 324 (1986) 334.
10 G.P. Xue, R.C. Fishlock and A.M. Snoswell, *Anal. Biochem.*, 171 (1988) 135.
11 B. Kågedal and B. Olsson, *J. Chromatogr.*, 527 (1990) 21.
12 T.G. Rosano, R.T. Ambrose, A.H.B. Wu, T.A. Switt and P. Yadegari, *Clin. Chem.*, 36 (1990) 1951.
13 A. Harmoninen, P. Sillanukee and H. Jokela, *Clin. Chem.*, 37 (1991) 563.
14 S. Kawaguchi, N. Hirai and M. Fukamachi, *J. Chromatogr.*, 567 (1991) 11.
15 S. Osawa, in T. Kawai, Y. Ohba, T. Kanno, K. Kawano, K. Ueda and E. Etsumi (Editors), *Quality Control in the Clinical Laboratory '91*, Excerpta Medica, Amsterdam, 1991, p. 29.
16 P. Schneiderka, V. Pacáková, K. Štulík, M. Kloudová and K. Jelínková, *J. Chromatogr.*, 614 (1993) 221.
17 A. Zhiri, O. Houot, M. Wellamn-Bednawska and G. Siest, *Clin. Chem.*, 31 (1985) 109.
18 G. Werner, V. Schneider and J. Emnert, *J. Chromatogr.*, 525 (1990) 109.
19 R. Paroni, C. Arcelli, I. Fermo and P.A. Bonini, *Clin. Chem.*, 36 (1990) 830.
20 A. Puhlmann, T. Dulffer and V. Kobold, *J. Chromatogr.*, 581 (1992) 129.
21 E. Palmisano, T. Rotuno, A. Guerrieri and P.G. Zambonin, *J. Chromatogr.*, 493 (1989) 35.
22 R.F.A. Ginman and J.S. Colliss, *Clin. Chem.*, 31 (1985) 331.
23 T. Seki, Y. Yanagihara and K. Noguchi, *J. Chromatogr.*, 515 (1990) 435.
24 T. Seki, K. Yamaji, Y. Yanagihara and K. Noguchi, in K. Miyai, T. Kanno and E. Ishkawa (Editors), *Progress in Clinical Biochemistry, International Congress Series 991*, Excerpta Medica, Amsterdam, 1992, p. 321.
25 T. Seki, Y. Orita, Y. Yanagihara and K. Noguchi, in K. Miyai, T. Kanno and E. Ishikawa (Editors), *Progress in Clinical Biochemistry, International Congress Series 991*, Excerpta Medica, Amsterdam, 1992, p. 163.
26 B.K. Cannan and A. Shore, *Biochem. J.*, 22 (1928) 920.
27 J. Woo and D.C. Cannon, in J.B. Henry (Editor), *Clinical Diagnosis and Management by Laboratory Methods*, Saunders, Philadelphia, 1984, p. 135.
28 J.G.H. Cook, *Clin. Chim. Acta*, 32 (1971) 485.

Journal of Chromatography A, 661 (1994) 121–126
Elsevier Science B.V., Amsterdam

CHROMSYMP. 2890

Thermospray liquid chromatography–mass spectrometry of flavonol glycosides from medicinal plants

Piergiorgio Pietta*

Dipartimento di Scienze e Tecnologie Biomediche, Sez. Chimica organica, Via Celoria 2, 20133 Milan (Italy)

Roberto Maffei Facino and Marina Carini

Istituto di Chimica Farmaceutica, Viale Abruzzi 42, 20131 Milan (Italy)

Pierluigi Mauri

ITBA-CNR, Via Ampère 57, 20131 Milan (Italy)

ABSTRACT

High-performance liquid chromatography interfaced with thermospray mass spectrometry is described for the identification of various flavonol glycosides from *Ginkgo biloba*, *Calendula officinalis* and *Tilia cordata*. Thermospray ionization gave parent species with few and diagnostic fragment ions, thus allowing structure elucidation as well as discrimination between different glycosylation sites.

INTRODUCTION

Phytochemical preparations of medicinal plants are commercially available and used medically for different purposes. TLC and HPLC are generally applied for their analysis. However, identification problems arise when reference standards are not available, and this is often the case for plant extracts. When screening flavonoid glycoside-containing drugs, HPLC with "on-line" ultraviolet detection is normally applied to obtain preliminary information on the analytes' structure [1]. Moreover, semipreparative isolation of unknown flavonoid glycosides followed by hydrolysis and liquid or gas chromatography of the resulting aglycones and sugars provides further data to aid identification [2]. Nevertheless, this approach is time-consuming and laborious. On the contrary, LC–MS represents a fast and reliable method to analyse these non-volatile compounds. Of the different modes, thermospray (TSP) using ammonium acetate as buffer provides mass spectra of flavonoid glycosides nearly identical to those obtained by D/chemical ionization–MS using ammonia [3]. This "soft-ionization" technique produces molecular ions suitable for mass measurements and limited fragment ions, from which the aglycone and the sugar moiety can be determined [4,5]. Extending our study [6] on methods for plant extracts analysis, TSP–MS has been applied to flavonol di- and triglycosides from *Ginkgo biloba*, *Calendula officinalis* and *Tilia cordata* (Fig. 1), and the results are presented in this paper.

EXPERIMENTAL

Materials

Ginkgo biloba leaves, *Calendula officinalis* flowers and *Tilia cordata* leaves were obtained

* Corresponding author.

0021-9673/94/$07.00
SSDI 0021-9673(93)E0806-6

PEAK	COMPOUND	R_1	R_2	R_3
I	K-3-O- 6-(P-COUM)-GLU -RHA	H	H	6-(P-COUMAROYL)-GLUCOSYL-RHAMNOSIDE
II	Is-3-O-2^G-RHA-RUTINOSIDE	RHAMNOSIDE	OCH_3	2^G-RHAMNOSYLRUTINOSIDE
1	Q-3-O-GLU-7-O-RHA	RHAMNOSIDE	OH	GLUCOSIDE
2	K-3-O-GLU-7-O-RHA	RHAMNOSIDE	H	GLUCOSIDE
3	Q-3,7-DI-O-RHA	RHAMNOSIDE	OH	RHAMNOSIDE
4	K-3,7-DI-O-RHA	RHAMNOSIDE	H	RHAMNOSIDE

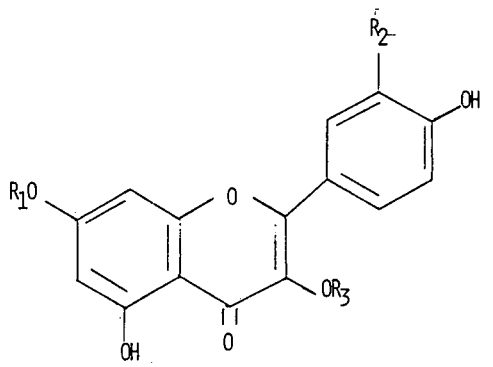

Fig. 1. Structures of the investigated flavonol glycosides. K = kaempferol; Is = isorhamnetin; Q = quercetin.

from Milanfarma)Milan, Italy) and Galke (Gittelde/Harz, Germany). Kaempferol-3-O-[6‴-O-(*p*-coumaroyl)-α-D-glucopyranosyl-(1→4)-α-L-rhamnoside] (I) and isorhamnetin-3-O-2^G-rhamnosyl-rutinoside (II) were isolated from a purified extract of *Ginkgo biloba* [7] and *Calendula officinalis* [8], respectively.

Sample preparation

Compounds I and II were dissolved in methanol (100 μg/ml) and 10 μl were flow injected into the MS apparatus.

Powdered *Tilia* leaves (2 g) were suspended in 50% methanol (20 ml) and left overnight at room temperature. After filtration, the solution was evaporated to dryness *in vacuo* and the residue dissolved in methanol (2 ml). A 20-μl aliquot was injected into the HPLC column.

HPLC conditions

The HPLC apparatus consisted of a Model HP 1090 chromatograph equipped with a Model 1040 photodiode-array detector (Hewlett-Packard, Waldbronn, Germany). The column was an Aquapore RP-300 (4.6 × 220 mm, Applied Biosystems, San José, CA, USA) and the eluents were 2-propanol–tetrahydrofuran–water (10:5:85) and 2-propanol–tetrahydrofuran–ammonium acetate pH 4.5 (10:5:85). The flow-rates were 1.8 and 1.2 ml/min, respectively.

Mass spectrometry

A Hewlett-Packard 5989 mass spectrometer was used together with a Hewlett-Packard thermospray LC–MS interface. The ion source temperature was 220°C, and the vaporizer temperature was held at 100°C. The temperature of the aerosol in the source's jet chamber was 220°C. Full-scan spectra in the range *m/z* 260–800 in the positive-ion (PI) mode were recorded, except for II, which was taken in the negative-ion mode. Polypropylene glycol was used for mass calibration.

RESULTS AND DISCUSSION

Flavonol glycosides are thermolabile compounds, and the ability to detect their pseudomolecular ions depends on the vaporizer temperature. Using quercetin-3-O-galactoside as a model compound, a relatively high pseudomolecular ion (m/z 465) was obtained by setting the vaporizer temperature at 100°C, although the ion corresponding to the aglycone (m/z 303) produced the base peak of the spectrum. Thus, this vaporizer temperature was chosen for all experiments. The mass spectra of I from *Ginkgo biloba* and II from *Calendula officinalis* confirmed the fragmentation behaviour shown by quercetin-3-O-galactoside. In the PI mass spectrum of I, in addition to the [M + H] ion (m/z 742), fragments that are characteristic of the deacylated flavonoid disaccharide (m/z 433) and of the aglycone (m/z 287) are present (Fig. 2). The fragmentation in the negative-ion mode of the trisaccharide II from *Calendula officinalis* is shown in Fig. 3. The molecular ion [M − H] (m/z 769), the fragment ions originated by loss of the first rhamnose (m/z 623), of the second rhamnose unit (m/z 477) and of glucose to yield the aglycone (m/z 315) are present. To our knowledge, these results represent the first evidence of the potential of TSP for the identification of flavonol acylated diglycoside and flavonol triglycosides.

Owing to the presence in *Tilia cordata* of flavonol derivatives differing in the position of glycosylation, such as quercetin-3-O-glucoside-7-O-rhamnoside (1), kaempferol-3-O-glucoside-7-O-rhamnoside (2), quercetin-3,7-O-dirhamnoside (3) and kaempferol-3,7-O-dirhamnoside (4), it has been interesting to evaluate the data achievable by LC–TSP. Fig. 4 shows a typical reversed-phase chromatogram of an extract of *Tilia cordata* leaves, using 2-propanol–tetrahydrofuran–water (10:5:85) at a flow-rate of 1.8 ml/min. The products of interest were peaks 1–4, whereas peaks 5–8 were not considered since they can be easily identified by co-chromatography with standards and "on-line" UV spectroscopy [7]. For LC–MS analysis of the glycosides 1–4 water in the eluent was replaced by

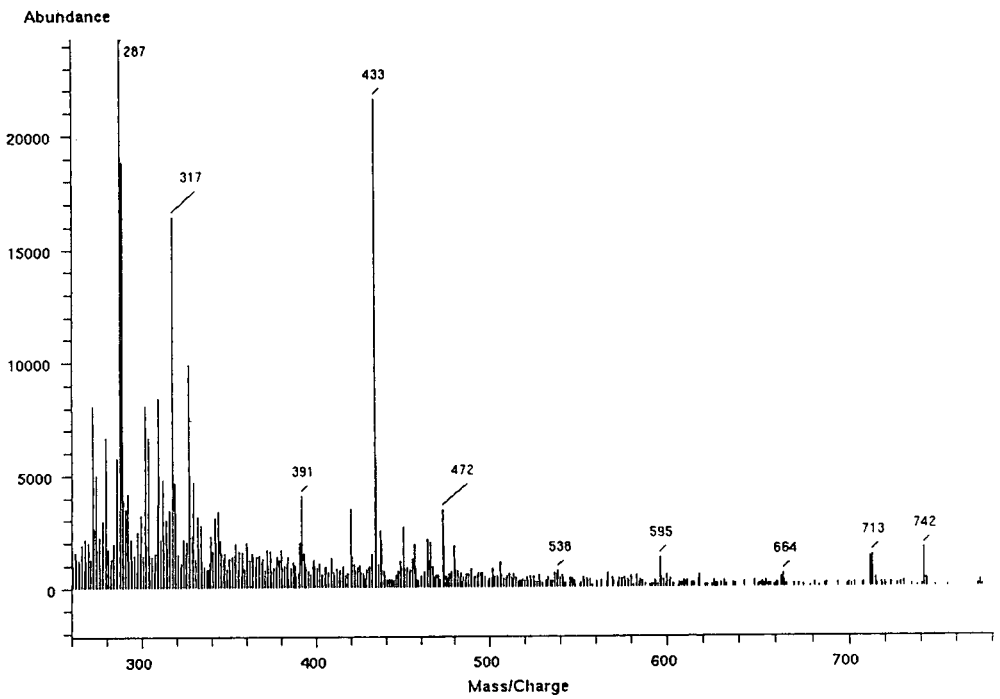

Fig. 2. Mass spectrum of kaempferol-3-O-(6‴-O-*p*-coumaroyl)-glucosyl-rhamnoside (I) from *Ginkgo biloba*.

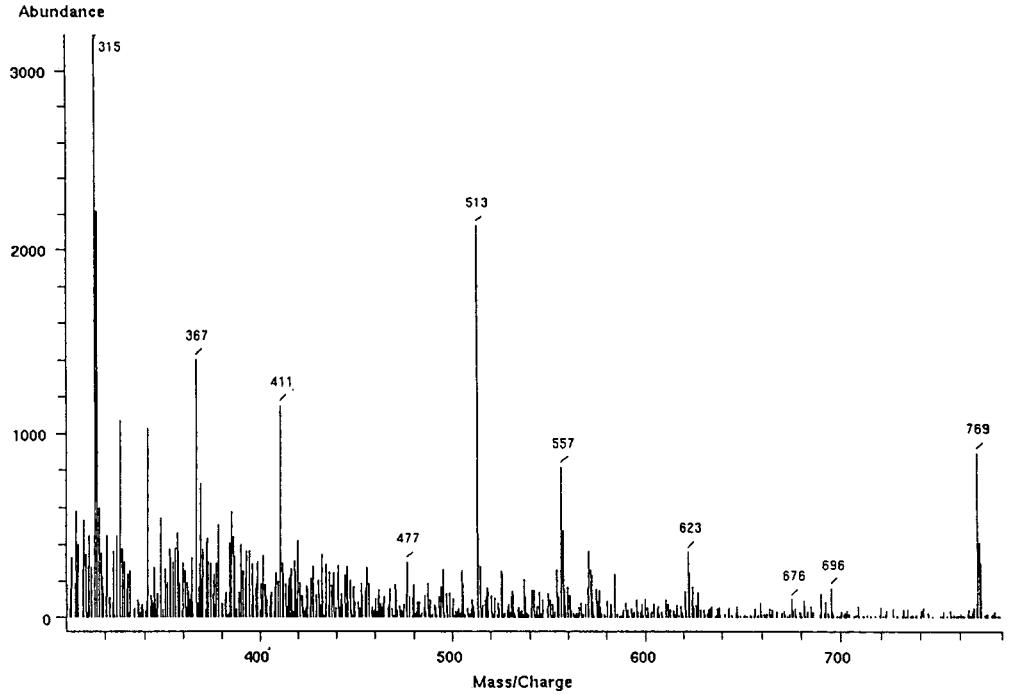

Fig. 3. Mass spectrum of isorhamnetin-3-O-2-rhamnosyl-rutinoside (II) from *Calendula officinalis*.

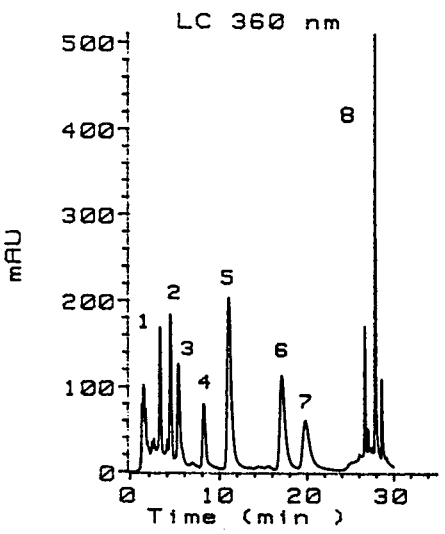

Fig. 4. HPLC of *Tilia cordata*. Column: Aquapore RP-300 (4.6 × 220 mm). Eluent: 2-propanol–tetrahydrofuran–water (10:5:85). Flow-rate: 1.8 ml/min. Peaks: 1–4, see Fig. 1; peak 8 = tiliroside.

0.08 *M* ammonium acetate and the flow-rate was reduced to 1.2 ml/min. After the elution of these peaks, the mobile phase was gradually changed to 100% methanol to rinse the column for a new run. "On-line" photodiode-array detection indicated clearly that compounds 1 and 3 and 2 and 4 was quercetin and kaempferol derivatives, respectively (Fig. 5). Subsequent TSP–MS gave further data (Table I) useful for the identification of these glycosides. As expected, peaks 2 and 3 yielded low protonated molecular ions, both the fragments derived from the parent ion by loss of the 3-O-glucose or the 7-O-rhamnose, and intense aglycone ions. On the contrary, the mass spectra of peaks 2 and 4 presented, together with the small molecular ions, only one intermediate fragment originated by removal of rhamnose from the 3- or 7-position, and abundant aglycone ions. As examples, the spectra of 2 and 4 are shown in Figs. 6 and 7. From these data peaks 1, 2 and 4 can be confirmed as the

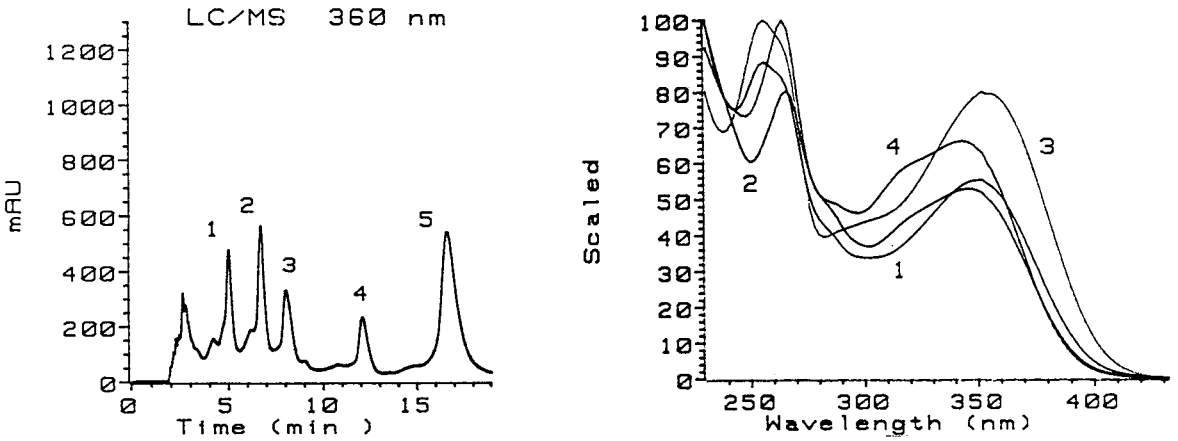

Fig. 5. HPLC of *Tilia cordata* for LC–MS analysis. Column: Aquapore RP-300 (4.6 × 220 mm). Eluent: 2-propanol–tetrahydrofuran–0.08 *M* ammonium acetate pH 4.5 (10:5:85). Flow-rate: 1.2 ml/min. Peaks: 1–4, see Fig. 1; peak 5 = isoquercitrin.

TABLE I

MAIN IONS IN THE TSP SPECTRA OF THE GLYCOSIDES 1–4 FROM *TILIA CORDATA*

		MW	M + H$^+$	Q-glu + H$^+$	Q-rha + H$^+$	K-glu + H$^+$	K-rha + H$^+$	Q + H$^+$	K + H$^+$
Q-3-glu-7-rha	(1)	610	611	465	449			303	
K-3-glu-7-rha	(2)	594	595			449	433		287
Q-3,7-di-rha	(3)	594	595		449			303	
K-3,7-di-rha	(4)	578	579				433		287

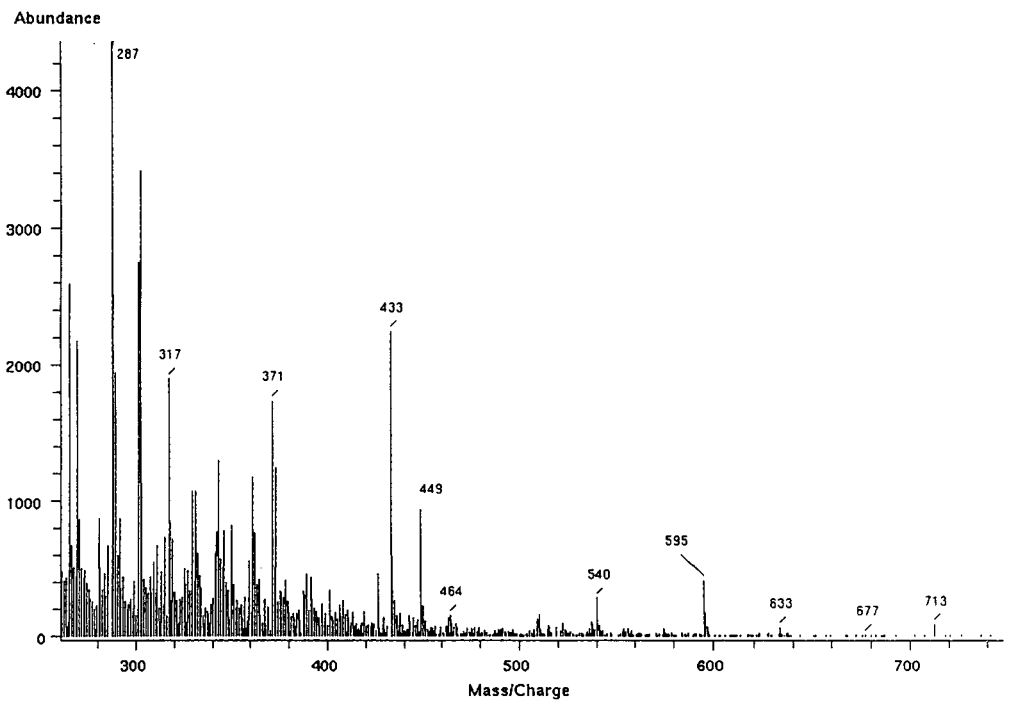

Fig. 6. Mass spectrum of kaempferol-3-O-glucoside-7-O-rhamnoside (2).

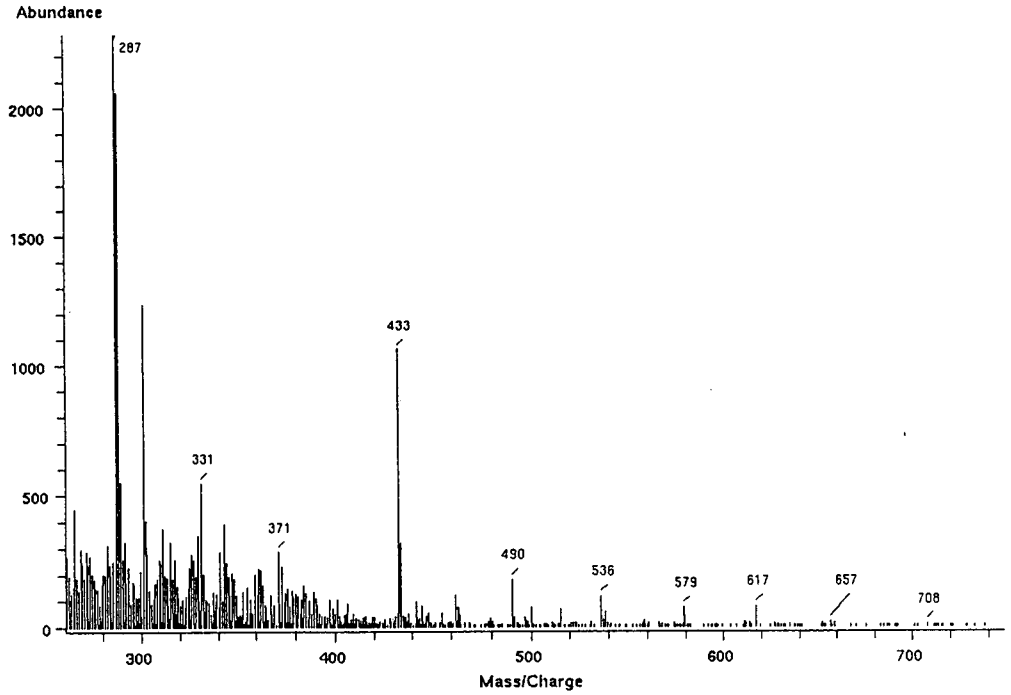

Fig. 7. Mass spectrum of kaempferol-3,7-O-dirhamnoside (4).

previously reported flavonol glycosides [8], while peak 3 can reasonably be assumed to be the analogue quercetin-3,7-O-dirhamnoside.

It may be concluded that TSP is of high value for the analysis of flavonol glycosides occurring in plant extracts, since this ionization technique provides information on molecular ions, sugar sequence and glycosylation site. Moreover, photodiode-array detection can be performed simultaneously, thus obtaining confirmatory data based on ultraviolet spectra.

ACKNOWLEDGEMENTS

The authors are grateful to Dr. B. Raverdino (HP, Geneva) for his valuable advice and to CNR-PF "CHIMICA FINE" for providing funds.

REFERENCES

1 P.G. Pietta, P.L. Mauri, A. Bruno and A. Rava, *J. Chromatogr.*, 553 (1991) 223.
2 P.G. Pietta, A. Bruno, P.L. Mauri and A. Rava, *J. Chromatogr.*, 593 (1992) 165.
3 D. Schaufelbeger, B. Domon and K. Hostettmann, *Planta Med.*, 50 (1984) 398.
4 E. Schröder and I. Merfort, *Biol. Mass Spectrom.*, 4 (1991) 11.
5 M. Maillard, J.L. Wolfender and K. Hostettmann, *Planta Med.*, 58 (1992) A591.
6 P.G. Pietta, P.L. Mauri, R. Maffei-Facino and M. Carini, *Pharm. Biomed. Anal.*, 10 (1992) 1041.
7 P.G. Pietta, P.L. Mauri, A. Bruno and L. Zini, *J. Chromatogr.*, 638 (1993) 357.
8 L. Horhammer, L. Stich and H. Wagner, *Arch. Pharm. Biol.*, 294 (1961) 685.

Journal of Chromatography A, 661 (1994) 127–136
Elsevier Science B.V., Amsterdam

CHROMSYMP. 2920

Evaluation of the analysis of cholesterol oxides by liquid chromatography

B.H. Chen* and Y.C. Chen

Department of Nutrition and Food Science, Fu Jen University, Taipei 242 (Taiwan)

ABSTRACT

Several extraction, separation and detection methods for cholesterol oxidation products (COPS) were developed and evaluated using liquid chromatography. The results showed that extraction of COPS from lard by cold saponification at 25°C or a Sep-Pak C_{18} cartridge resulted in higher recoveries than those given by a silica gel Sep-Pak cartridge. With HPLC, by using a cyano-bonded column and hexane–2-propanol (95:5, v/v) as the mobile phase at a flow-rate of 1.0 ml/min, and a C_{18} column with a gradient flow system with acetonitrile–methanol (55:45, v/v), it was possible to separate eight and nine COPS within 17 and 60 min, respectively. All the COPS with one, two and three double bonds could be detected by UV spectrophotometry at 212, 234 and 280 nm, respectively. UV detection had a 1000 times higher sensitivity than refractive index detection. Ten COPS were separated from heated lard using a cyano-bonded column, and five of them were identified.

INTRODUCTION

Cholesterol, an important biological compound that is widely distributed in various kinds of foods, readily undergoes oxidation in air under a variety of conditions to produce a large number of oxidation products. To date more than 60 cholesterol oxidation products (COPS) have been characterized in nature [1], some of which have been shown to be cytotoxic mutagenic and carcinogenic [2–5]. The major COPS in foodstuffs include 25-hydroxycholesterol, cholesta-3β,5α,6β-triol, 5,6α-epoxycholesterol, 5,6β-epoxycholesterol, 7α-hydroxycholesterol, 7β-hydroxycholesterol, 7-ketocholesterol and cholesta-4,6-dien-3-one [6].

Owing to the presence of low concentrations of COPS in food, their extraction and determination have been difficult. The major problems associated with extraction of COPS are as follows: (1) most COPS are present in trace amount (ppm or ppb) in foods, which makes extraction difficult; (2) some COPS are present in esterified form, which make quantification difficult; and (3) some COPS are susceptible to oxidative loss and degradation during extraction.

Saponification has often been employed to remove neutral triacylglycerol, sterol ester and water-soluble impurities during extraction of COPS from foods [6–13]. Park and Addis [7] used cold saponification (25°C) to extract COPS from tallow and found that a 100% recovery could be achieved. Since then, this technique has been used by many workers to extract COPS from foods [10–13]. Although cold saponification could prevent the formation of COPS artifacts, the saponification time was too long (18–20 h). Some workers therefore used hot saponification to facilitate the extraction of COPS from foods [14]. However, it has been found that hot saponification might degrade 7-ketocholesterol to form artifacts [14].

In view of these problems, several workers used silica gel- or C_{18}-packed columns to extract COPS from foods [15–22]. Compared with

* Corresponding author.

0021-9673/94/$07.00
SSDI 0021-9673(93)E0893-Y

saponification methods, the application of columns for extraction of COPS was faster and could prevent the formation of COPS artifacts. However, some impurities such as triacylglycerol and free fatty acids might be co-eluted with COPS from the column and thus interfere with the separation. Also, the COPS present in esterified forms could not be determined. To solve these problems, the selection of an appropriate solvent system to remove impurities without affecting the elution of COPS was extremely important.

Methods for the separation of COPS have been developed from early thin-layer chromatography (TLC) [1,23,24] to capillary gas–liquid chromatography (GLC) [7–13,15,18,20,25,26] and high-performance liquid chromatography (HPLC) [17,19,20,24,27,28]. TLC can readily separate some side-chain and B-ring hydroxycholesterols but not cholesterol hydroperoxides [23]. Although the separation of COPS by TLC is lengthy and tedious, TLC can still be used to confirm the identity of COPS based on their distinctive colour development after spraying with acid and observation under UV radiation [1]. Capillary GLC has been found to resolve some B-ring oxidation products and geometric isomers, but it may also thermally destroy cholesterol and B-ring hydroperoxide to form artifacts [13,25]. HPLC is a milder method than GLC for separating COPS. Although the separation power of HPLC is theoretically inferior to that of GLC, it can still provide an ideal means for sample recovery and purification. Interestingly, Tsai and Hudson [27] reported that HPLC not only provided superior resolution of COPS over TLC and GLC, but also simplified the quantification procedure and introduced fewer artifacts.

The purpose of this study was to evalute several COPS extraction and separation methods using liquid chromatography. Lard was used as a reference sample for evaluation.

EXPERIMENTAL

Materials

Commercial deodorized lard was purchased from a local supermarket. Approximately 2.0 kg of lard were melted at 65°C in a water-bath and then divided into two portions of 0.5 and 1.5 kg; the former was used for method evaluation and the latter for heating.

Cholesterol and ten COPS standards, 25-hydroxycholesterol (25-OH), cholesta-3β,5α,6β-triol (triol), 5,6α-epoxycholesterol (5,6α-EP), 5,6β-epoxycholesterol (5,6β-EP), 7α-hydroxycholesterol (7α-OH), 7β-hydroxycholesterol (7β-OH), 6-ketocholestanol (6-keto), 7-ketocholesterol (7-keto), cholesta-4,6-dien-3-one (4,6-dien-3-one) and cholesta-3,5-diene (3,5-diene) were purchased from Sigma (St. Louis, MO, USA).

HPLC-grade solvents such as hexane, 2-propanol, methanol, acetonitrile, ethyl acetate, chloroform and 1,4-dioxane were purchased from Merck (Taiwan) and filtered through a 0.2-μm membrane filter under vacuum prior to use. Silica gel 60 TLC plates (20 × 20 cm) with a thickness of 300 μm were made using a Camag spreader (Muttenz, Switzerland). TLC plates were activated at 110°C for 2 h prior to use. The spray reagent N,N-dimethyl-*p*-phenylenediamine was obtained from Aldrich (Milwaukee, WI, USA).

Instrumentation

The HPLC instrument consisted of an SSI 222D digital pump (Scientific Systems, State College, PA, USA) an SSI 231 gradient controller, a Linear 206 rapid-scanning UV–Vis photodiode-array detector (Linear Instruments, Reno, NV, USA) and a Jasco Model 830 RI detector. A sensitivity of 0.32 AUFS was used. The data were stored and processed with an Axxiom 727 dual-channel chromatography system (Axxiom Chromatography, Calabasas, CA, USA). A LiChrospher CN column (25 cm × 4.6 mm I.D.) and a Phenomenex C_{18} column (25 cm × 4.6 mm I.D.) packed with material of the same particle size (5 μm) were used. Silica gel and Sep-Pak C_{18} cartridges were purchased from Waters (Milford, MA, USA).

Separation of COPS standards by TLC

A ternary solvent system of hexane–ethyl acetate–methanol (70:35:10, v/v/v) was used to confirm the identities of cholesterol and seven

COPS (3,5-diene, 4,6-dien-3-one, 5,6α-EP, 7-keto, 25-OH, 7β-OH and triol). The colour development of cholesterol and COPS under UV radiation was described in a previous paper [29].

Separation of COPS standards by HPLC

A mixture of cholesterol and ten COPS standards was dissolved in 2-propanol and hexane–2-propanol (95:5, v/v) for HPLC separation on the C_{18} column and the CN-bonded column, respectively. Concentrations of the COPS ranging from 10 to 200 ppm were prepared and injected into the HPLC system to obtain the chromatograms shown in Figs. 1, 3, 4 and 5. Acetonitrile–methanol (55:45, v/v) and UV and refractive index (RI) detection were used with the C_{18} column. The flow-rate was maintained at 0.5 ml/min for the first 25 min, then increased linearly to 3.0 ml/min within 35 min. Before the next injection the flow-rate was linearly reduced to 0.5 ml/min. The wavelength for UV detection was set at 212, 234 and 280 nm; 212 nm was used to detect most COPS, 234 for 7-keto and 3,5-diene and 280 nm for 4,6-dien-3-one. For the CN column, hexane–2-propanol (95:5, v/v) at a flow-rate of 1.0 ml/min and UV and RI detection were used. In addition, each COPS was scanned between 190 and 350 nm by employing a photodiode-array detector. The separation efficiency of these methods was determined by the capacity factor, k':

$$k' = \frac{\text{elution time of COPS} - \text{elution time of solvent}}{\text{elution time of solvent}}$$

It has been well established that k' could be affected by the solvent strength, and the best k' value should be between 1 and 10 [30]. In addition, the reproducibility of retention time was determined by injecting COPS standards five times, and the relative standard deviation (R.S.D.) of the retention time was calculated. 6-Keto was used as an internal standard.

Extraction of COPS from lard

Lard was used as a reference sample to evaluate the recovery of COPS by three extraction methods, using cold saponification, a Sep-Pak C_{18} cartridge and a silica gel Sep-Pak cartridge. HPLC was used to determine the extraction recoveries. A cyano-bonded column and a mobile phase of hexane–2-propanol (95:5, v/v) at a flow-rate of 1.0 ml/min and RI detection were used.

Cold saponification. A mixture of cholesterol, COPS standards and 100 μg of an internal standard (6-keto) was added to 1 g of melted lard in a flask. Saponification was carried out by adding 10 ml of methanolic KOH (1 *M*) to lard and allowing the mixture to stand in the dark for 18 h at room temperature. Distilled water (10 ml) was added to the solution and the mixture was poured into a separating funnel. The unsaponifiable fraction was extracted with 10 ml of hexane three times and the hexane layers were collected and combined. The combined hexane solution was further washed with 10 ml of KOH (1 *M*) and 10 ml of water, then passed through a Whatman No. 1 filter-paper containing anhydrous sodium sulphate to remove excess water. The filter-paper was washed with 20 ml of hexane to remove any residual unsaponifiable materials. The combined filtrate was then evaporated under vacuum (40°C) to remove the solvent and the residue was dissolved in an appropriate solvent for HPLC analysis.

Sep-Pak C_{18} cartridge. A Sep-Pak C_{18} cartridge was activated with 10 ml of deionized water followed by 10 ml of methanol before extraction was conducted. Melted lard (1 g) was dissolved in 1 ml of ethyl acetate–methanol (1:1, v/v) to reduce the viscosity of the lard, and a mixture of cholesterol, COPS standards and 100 μg of internal standard (6-keto) was added to the solution. The solution was poured into a Sep-Pak C_{18} cartridge, and most of the cholesterol and triacylglycerol were eluted with 1 ml of ethyl acetate–methanol (1:1, v/v). COPS and the remaining impurities were then eluted with 10 ml of methanol and 6 ml of ethyl acetate–methanol (1:1, v/v). The eluate containing COPS was then evaporated under vacuum (40°C) to remove the solvent and the residue was dissolved in an appropriate solvent for HPLC analysis.

Silica gel Sep-Pak cartridge. A silica gel Sep-Pak cartridge was activated with 10 ml of hexane before extraction was conducted. Melted lard (1 g) was dissolved in 1 ml of hexane to reduce the

viscosity of the lard, and a mixture of cholesterol, COPS standards and 100 μg of internal standard (6-keto) was added to the solution. The solution was poured into a silica gel Sep-Pak cartridge, and most of the cholesterol and triacylglycerol were eluted with 10 ml of hexane. COPS were then eluted with 20 ml of acetone, and the eluate was evaporated under vacuum (40°C) to remove the solvent and the residue was dissolved in an appropriate solvent for HPLC analysis.

Recovery data were subjected to analysis of variance (PROC ANOVA) and Duncan's multiple range test procedures of the statistical analysis system [31].

Determination of COPS in heated lard by TLC and HPLC

In order to demonstrate the best extraction and separation efficiencies of the developed methods, *ca.* 1.5 kg of lard heated at 180°C for 200 h was used as a reference sample for evaluation. COPS in heated lard were extracted using a Sep-Pak C_{18} cartridge and analysed using the cyano-bonded column with RI detection. COPS were identified by comparison of the retention times of unknowns with those of reference standards, addition of COPS standards to the sample for co-chromatography and collection of eluates for TLC analysis for further identification.

RESULTS AND DISCUSSION

LC separation and detection

Fig. 1 shows the HPLC of cholesterol and eight COPS standards using the cyano-bonded column with UV detection at 212, 234 and 280 nm. Only cholesterol and five COPS standards (4,6-dien-3-one, 25-OH, 7-keto, 7β-OH and 6-keto) were detected at 212 nm. Triol, 5,6α-EP and 5,6β-EP were not detected because of absence of π-electrons. 3,5-Diene was not separated probably because of its low polarity, so that it overlapped with the solvent peak. When the UV detection wavelength increased from 212 to 234 nm, only 4,6-dien-3-one and 7-keto were detected. In addition, 4,6-dien-3-one was the only COPS detected at 280 nm. By comparing the detector responses of each COPS on the HPLC trace, it was found that 4,6-dien-3-one has the maximum absorption at 280 nm, 7-keto at 234 nm and the other COPS containing one double bond at 212 nm.

However, the UV scanning spectra of cholesterol, 7β-OH and 25-OH were found to have maximum absorption between 200 and 205 nm

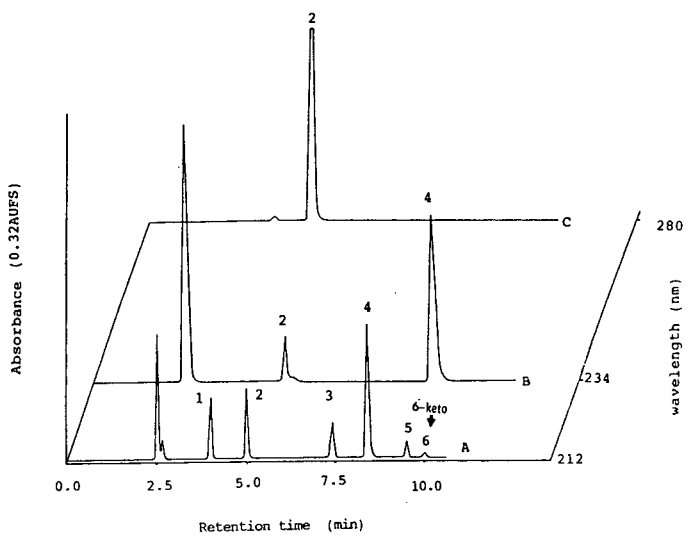

Fig. 1. HPLC of cholesterol and COPS standards on a cyano-bonded column with multiple wavelength scanning and UV detection. Solvent system, hexane–2-propanol (95:5, v/v); flow-rate, 1.0 ml/min. Peaks: (A) 1 = cholesterol, 2 = 4,6-dien-3-one, 3 = 25-OH, 4 = 7-keto, 5 = 7β-OH, 6 = 6-keto; (B) 2 = 4,6-dien-3-one, 4 = 7-keto; (C) 2 = 4,6-dien-3-one.

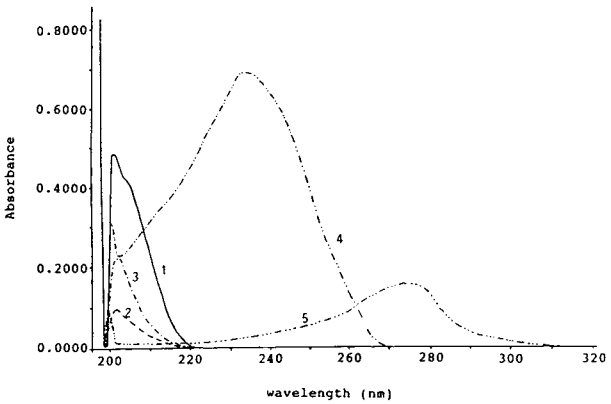

Fig. 2. UV spectra of cholesterol and COPS standards. 1 = Cholesterol; 2 = 7β-OH; 3 = 25-OH; 4 = 7-keto; 5 = 4,6-diene.

(Fig. 2). The selection of 212 nm rather than 205 nm for the detection of cholesterol, 7β-OH and 25-OH by HPLC is due to the fact that the latter was more readily subject to interference by the presence of solvents such as ethyl acetate, chloroform and 1,4-dioxane, which could lead to inaccurate quantification of COPS.

Fig. 3 shows the HPLC of cholesterol and eight COPS standards with RI detection. All compounds were adequately resolved within 17 min by employing the solvent system hexane–2-propanol (95:5, v/v) at a flow-rate at 1.0 ml/min. This solvent system was chosen based on a report by Nourooz-Zadeh [20], who used the same mobile phase at a flow-rate of 0.4 ml/min to separate cholesterol and eight COPS. However, baseline drift occurred during separation, which was accomplished within 60 min. By increasing the flow-rate to 1.0 ml/min it was possible to minimize the baseline drift and decrease the separation time to 17 min.

The separation efficiency of this method was determined by the capacity factors (k'); the k' values were cholesterol 1.51, 4,6-dien-3-one 2.05, 5,6α-EP 2.46, 5,6β-EP 2.63, 25-OH 2.76, 7-keto 3.01, 7β-OH 3.23 and triol 5.14. It is well established that the k' value should be between 2 and 10 to achieve an ideal separation [30]. However, in practice, eluting a sample within the k' range 1–20 is a more realistic goal [30]. Teng [28] used a silica gel-packed column to separate cholesterol and eleven COPS. Separation was achieved within 120 min. Obviously the drastically reduced separation time of COPS when using a cyano-bonded column is due to the interaction force between COPS and Si–$(CH_2)_3CN$ being smaller than that between COPS and Si–OH. In order to demonstrate the reproducibility of this method, a solution of COPS in hexane–2-propanol (95:5, v/v) was injected into the HPLC column five times. The R.S.D. with respect to the retention times of COPS was 0.00–1.00%.

The linearity responses of cholesterol and all COPS standards with UV detection at 212 nm or with RI detection on the cyano-bonded column were very high ($r^2 = 0.997$–0.999). The graph was obtained by plotting peak-area ratios against concentration ratios, and the peak-area ratios of cholesterol and COPS to the internal standard

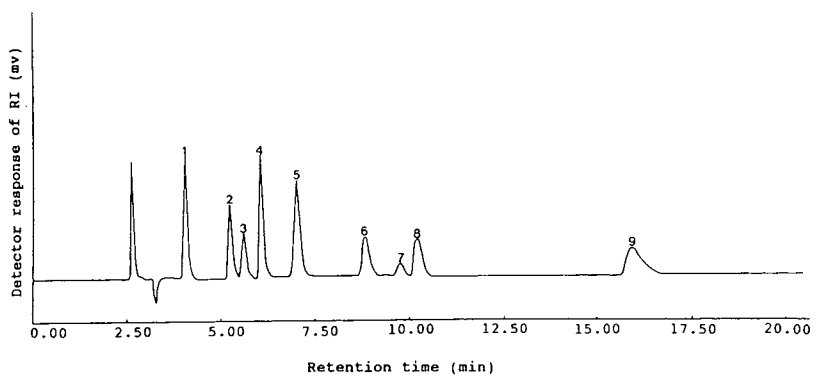

Fig. 3. HPLC of cholesterol and eight COPS standards on a cyano-bonded column with RI detection. Solvent system, hexane–2-propanol (95:5, v/v); flow-rate, 1.0 ml/min. Peaks: 1 = cholesterol; 2 = 4,6-dien-3-one; 3 = 5,6α-EP; 4 = 5,6β-EP; 5 = 25-OH; 6 = 7-keto; 7 = 7β-OH; 8 = 6-keto; 9 = triol.

were determined at four different concentration ratios of 0.5, 1.0, 1.5 and 2.0. However, the linearity response of 4,6-dien-3-one drastically decreased from 0.992 (r^2) to 0.747 (r^2) when the detection wavelength was changed from 234 to 280 nm. According to Beer's law, the absorption error can increase sharply with very dilute and very concentrated solutions. Hence the increased absorption of 4,6-dien-3-one at 280 nm could decrease the linearity response. 7-Keto with UV detection at 234 nm also showed the same phenomenon. To solve these problems, an appropriate range of concentrations (50–200 μg/ml) should be chosen so that high linearity (r^2 = 0.912) can be achieved.

Fig. 4 shows the HPLC of cholesterol and eight COPS standards detected at 212, 234 and 280 nm using the C_{18} column. A binary solvent system of acetonitrile–methanol (55:45, v/v) at a flow-rate of 0.5 ml/min was developed to resolve cholesterol and six COPS (4,6-dien-3-one, 3,5-diene, 25-OH, 7-keto, 7β-OH and 6-keto). Triol, 5,6α-EP and 5,6β-EP were not detected because of the absence of π electrons. However, 3,5-diene was the last eluted at 120 min. To decrease the retention time the flow-rate was maintained at 0.5 ml/min for the first 25 min and then increased linearly to 3.0 ml/min. The elution time of COPS could be reduced to within 60 min. Ansari and Smith [24] used a binary solvent system of acetonitrile–water (90:10, v/v) at a flow-rate of 1.0 ml/min to separate cholesterol and nine COPS. Although separation was accomplished within 60 min, baseline drift occurred and the resolution was poor. Also, cholesterol was eluted before 3,5-diene. This difference in elution order of cholesterol and 3,5-diene is due to their relative solubility in the solvent system used. 3,5-Diene had the strongest adsorption to the C_{18} packing material, so it was the last to be eluted. However, the separation time could be shortened to within 30 min if 3,5-diene was excluded from this experiment. As 3,5-diene is not commonly present in foods, its detection may be ignored because of its low cytoxicity [6]. Hence the application of a C_{18} column to separate common COPS in foods can still be adopted as a reference method.

Fig. 5 shows the HPLC of cholesterol and nine COPS standards on the C_{18} column with RI detection. All compounds were adequately resolved within 60 min using the same solvent system and flow-rate as described above. The k' values were triol 1.00, 25-OH 2.19, 7β-OH 2.59,

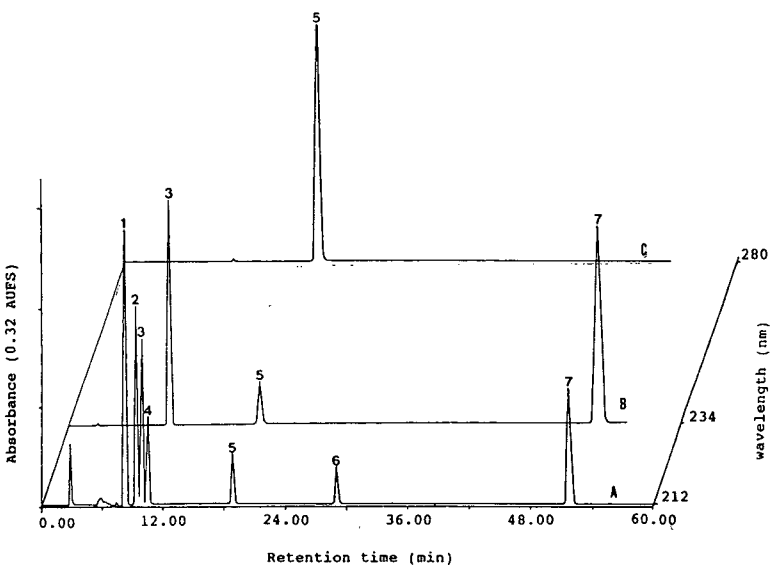

Fig. 4. HPLC of cholesterol and COPS standards on a C_{18} column with UV detection at 212, 234 and 280 nm. Solvent system acetonitrile–methanol (55:45, v/v); flow-rate, 0.5–3.0 ml/min. Peaks: (A) 1 = 25-OH, 2 = 7β-OH, 3 = 7-keto, 4 = 6-keto, 5 = 4,6-dien-3-one, 6 = cholesterol, 7 = 3,5-diene; (B) 3 = 7-keto, 5 = 4,6-dien-3-one, 7 = 3,5-diene; (C) 5 = 4,6-dien-3-one.

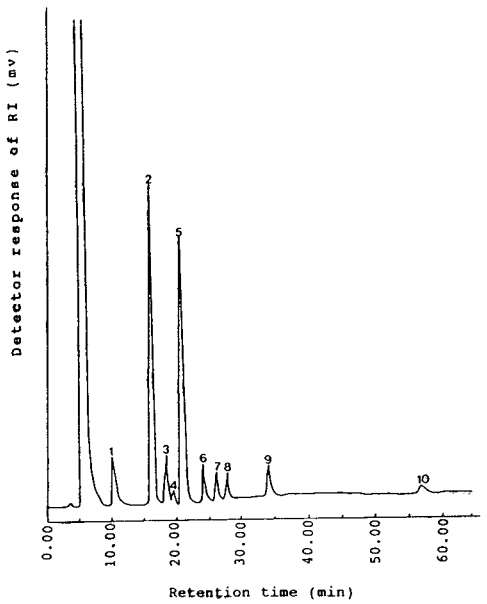

Fig. 5. HPLC of cholesterol and COPS standards on a C_{18} column with RI detection. Solvent system, acetonitrile–methanol (55:45, v/v); flow-rate, 0.5–3.0 ml/min. Peaks: 1 = triol; 2 = 25-OH; 3 = 7β-OH; 4 = 7-keto; 5 = 6-keto; 6 = 5,6α-EP; 7 = 5,6β-EP; 8 = 4,6-dien-3-one; 9 = cholesterol; 10 = 3,5-diene.

7-keto 2.79, 6-keto 3.12, 5,6α-EP 3.79, 5,6β-EP 4.19, 4,6-dien-3-one 4.59, cholesterol 5.78 and 3,5-diene 10.17. Compared with a normal-phase column, the elution time of COPS on the C_{18} column increased substantially from 17 to 60 min. However, a satisfactory separation could still be achieved because the k' values were in the range 1–11.

The linearity responses of cholesterol and standard COPS on the C_{18} column with UV detection at 212 nm and RI detection were very high ($r^2 = 0.980$–0.998). The r^2 values for 4,6-dien-3-one detected at 280 nm and for 7-keto and 3,5-diene detected at 234 nm were 0.950, 0.966 and 0.913, respectively. The linearity response of 4,6-dien-3-one on the C_{18} column with UV detection at 280 nm was much higher than that at 280 nm on the cyano-bonded column. This difference is due to the fact that the former was obtained by choosing a lower concentration range. On comparing the separation efficiency of the cyano-bonded column and C_{18} columns, the former was found to be superior in terms of retention time and resolution. Nevertheless, using this column to separate COPS has some drawbacks. First, 3,5-diene was eluted too fast and overlapped with the solvent peak. Second, the presence of residual triacylglycerol after extraction could form a large peak on the HPLC trace and thus interfere with the separation of cholesterol and some COPS. Also, UV detection of COPS was found to be 1000 times more sensitive than RI detection, the detection limits being 10 ng/g and 10 μg/g, respectively.

6-Keto was found to be a suitable internal standard because its structure is similar to that of other COPS, it did not interfere with the separation of the other compounds, it was completely eluted from the column and it was chemically inert towards other compounds. In addition, the linearity responses (r^2) for 6-keto on both columns with UV or RI detection was found to be between 0.992 and 0.999.

Extraction procedures

Table I gives the recoveries of cholesterol and COPS obtained by the three different extraction methods. Extraction by cold saponification and application of the Sep-Pak C_{18} cartridge were found to give higher recoveries than those obtained with the silica gel cartridge. Compared with the recoveries of the other COPS using cold saponification, triol was the lowest (86.9%), because hexane was used instead of diethyl ether to extract the COPS. The lower solubility of triol in hexane relative to diethyl ether resulted in a low recovery of triol. Hexane was adopted instead of diethyl ether because the latter has a strong odour and is volatile, which makes extraction difficult, and it can interfere with the UV detection of COPS. 3,5-Diene had the lowest recovery (95.4%) among the COPS extracted with the C_{18} cartridge. This is probably because a small portion of 3,5-diene was eluted together with triacylglycerol at the beginning by the ethyl acetate–methanol (1:1, v/v) solvent system used. It is also possible that a small portion of 3,5-diene has the strongest adsorption to the C_{18} packing material and thus its complete elution from the cartridge was not possible. Nevertheless, the recovery of 3,5-diene was still high in comparison with those of the other COPS ex-

TABLE I

RECOVERIES OF CHOLESTEROL AND COPS OBTAINED BY THREE DIFFERENT EXTRACTION METHODS

Means of quadruplicate analyses ± standard deviation.

Compound	Extraction method		
	Saponification[a]	C_{18}	Silica gel
3,5-Diene	102 ± 0.2[b]	95.4 ± 0.5[c]	50.2 ± 5.4[d]
4,6-Dien-3-one	101 ± 1.2[b]	100.8 ± 4.3[b]	52.1 ± 3.3[c]
Cholesterol	112 ± 3.2[b]	111.6 ± 5.8[b]	78.5 ± 1.6[c]
5,6α-EP	96.8 ± 1.1[b]	98.5 ± 2.4[b]	82.3 ± 1.4[c]
5,6β-EP	95.7 ± 3.2[b]	96.7 ± 1.5[b]	80.7 ± 0.2[c]
25-OH	100 ± 0.3[b]	99.4 ± 1.1[b]	81.2 ± 3.9[c]
7-Keto	108.9 ± 4.2[b]	110.7 ± 2.8[b]	99.7 ± 4.3[c]
7β-OH	99.6 ± 2.2[b]	101.2 ± 2.1[b]	90.2 ± 2.8[c]
6-Keto	101.1 ± 2.1[b]	103.8 ± 2.5[b]	95.2 ± 2.7[c]
Triol	86.9 ± 3.1[b]	97.7 ± 0.7[c]	70.3 ± 3.1[d]

[a] Conducted at room temperature for 18–20 h.
[b–d] Means within a row having different superscripts are significantly different ($P < 0.5$).

tracted with the silica gel cartridge. Most COPS had low recoveries when extracted with the silica gel cartridge, especially 3,5-diene and 4,6-dien-3-one (50.2 and 52.1%, respectively). This is probably due to the low polarity of 3,5-diene and 4,6-dien-3-one (which has the weakest adsorption to silica gel), and in turn this caused the elution of a small portion of both compounds together with triacylglycerol with the hexane solvent system used. For triol, the recovery is low (70.3%) because it has the strongest adsorption to silica gel and hence its complete elution from the cartridge was not possible. By comparison of the extraction efficiencies of the three methods, it was concluded that the application of a C_{18} cartridge and cold saponification was superior to a silica gel cartridge, and the use of a C_{18} cartridge was faster than cold saponification.

Determination of cholesterol oxides in heated lard

In order to demonstrate the extraction and separation efficiencies with the C_{18} cartridge and cyano-bonded column, lard heated at 180°C for 200 h was used as a reference sample. Fig. 6 shows the HPLC of COPS in this lard. Fig. 7 shows the HPLC of COPS in heated lard using co-chromatography with added standards. Only cholesterol and five COPS (4,6-dien-3-one, 5,6α-EP, 7-keto, 7β-OH and triol) were identified. No 6-keto was found in fresh lard. 6-Keto was present in heated lard is because it was added as an internal standard. The quantitative changes in COPS during heating of lard have been described in another paper [29].

In conclusion, the extraction and separation of

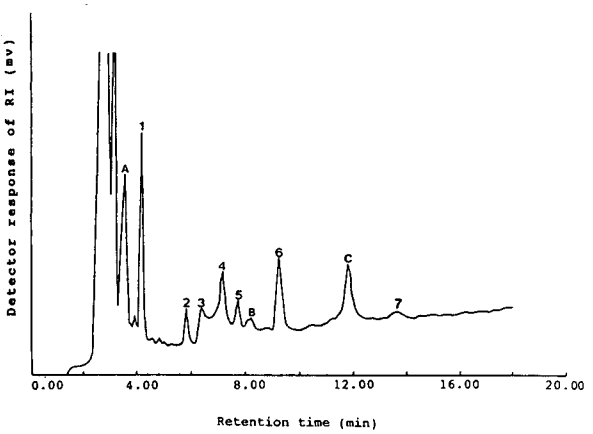

Fig. 6. HPLC of COPS in lard heated at 180°C for 200 h with RI detection. Solvent system, hexane–2-propanol (95:5, v/v); flow-rate, 1.0 ml/min. Peaks: 1 = cholesterol; 2 = 4,6-dien-3-one; 3 = 5,6α-EP (5,6β-EP); 4 = 7-keto; 5 = 7β-OH; 6 = 6-keto; 7 = triol; A,B,C = unknowns.

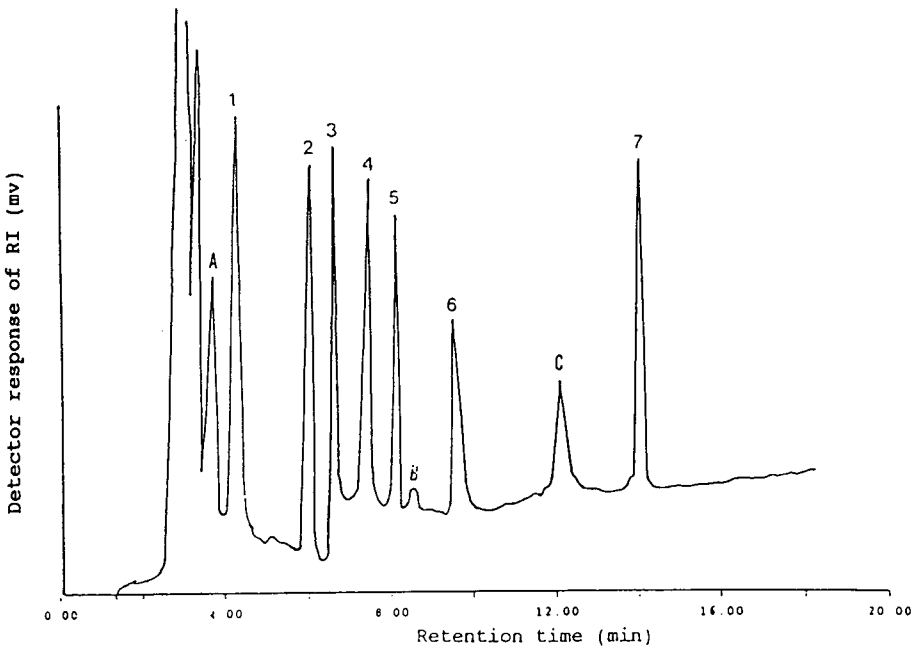

Fig. 7. HPLC of COPS in heated lard by co-chromatography with added standards with RI detection. Solvent system, hexane–2-propanol (95:5, v/v); flow-rate, 1.0 ml/min. Peaks: 1 = cholesterol; 2 = 4,6-dien-3-one; 3 = 5,6α-EP (5,6β-EP); 4 = 7-keto; 5 = 7β-OH; 6 = 6-keto; 7 = triol; A,B,C = unknowns.

COPS using a Sep-Pak C_{18} cartridge and a cyano-bonded column with UV detection were found to be the most efficient in terms of retention time and sensitivity. Further research is necessary to determine what unknown COPS may present in heated lard.

ACKNOWLEDGEMENT

This study was supported by a grant (DOH81-TD-100) from the National Health Bureau, Taiwan).

REFERENCES

1 L.L. Smith, *Cholesterol Autoxidation*, Plenum Press, New York, 1981.
2 S.K. Peng, P. Tham, C.B. Taylor and B. Mikkelson, *Am. J. Clin. Nutr.*, 32 (1979) 1033.
3 C.B. Taylor, S.K. Peng, N.T. Werthessen, P. Tham and K.T. Lee, *Am. J. Clin. Nutr.*, 32 (1979) 40.
4 H. Imai, N.T. Werthessen, V. Subramanyam, P.W. Lequesne, A.H. Soloway and M. Kanisawa, *Science*, 207 (1980) 651.
5 G.A.S. Ansari, R.D. Walker, V.B. Smart and L.L. Smith, *Food Chem. Toxicol.*, 20 (1982) 35.
6 E.T. Finocchiaro and T. Richardson, *J. Food Protect.*, 46 (1983) 917.
7 S.W. Park and P.B. Addis, *J. Agric. Food Chem.*, 34 (1986a) 653.
8 S.W. Park and P.B. Addis, *J. Food Sci.*, 51 (1986) 1380.
9 S.W. Park and P.B. Addis, *J. Food Sci.*, 52 (1987) 1500.
10 B.D. Sander, P.B. Addis, S.W. Park and D.E. Smith, *J. Food Protect.*, 552 (1989) 109.
11 B.D. Sander, D.E. Smith, P.B. Addis and S.W. Park, *J. Food Sci.*, 54 (1989) 874.
12 J.E. Pie, K. Spahis and C. Seillan, *J. Agric. Food Chem.*, 38 (1990) 973.
13 P.S. Yan and P.J. White, *J. Am. Oil Chem. Soc.*, 67 (1990) 927.
14 G. Maerker and J. Unruh, *J. Am. Oil Chem. Soc.*, 63 (1986) 767.
15 L.S. Tsai and C.A. Hudson, *J. Food Sci.*, 49 (1984) 1245.
16 L.S. Tsai and C.A. Hudson, *J. Food Sci.*, 50 (1985) 229, 237.
17 I.L. Kou and R.S. Holmes, *J. Chromatogr.*, 330 (1985) 339.
18 S.R. Missler, B.A. Wasilchuk and C. Merritt, *J. Food Sci.*, 50 (1985) 595.
19 S.W. Park and P.B. Addis, *J. Food Sci.*, 50 (1985) 1437.
20 J. Nourooz-Zadeh, *J. Agric. Food Chem.*, 38 (1990) 1667.

21 W.W. Nawar, S.K. Kim and M. Vajdi, *J. Am. Oil Chem. Soc.*, 68 (1991) 496.
22 M.P. Zubillaga and G. Maerker, *J. Food Sci.*, 56 (1991) 1194.
23 J.I. Teng, M.J. Kulig, L.L. Smith, G. Kan and E.V. Lier, *J. Org. Chem.*, 38 (1973) 119.
24 G.A.S. Ansari and L.L. Smith, *J. Chromatogr.*, 175 (1979) 307.
25 E.T. Finocchiaro, K. Lee and T. Richardson, *J. Am. Oil Chem. Soc.*, 61 (1984) 877.
26 S.W. Park and P.B. Addis, *Anal. Biochem.*, 52 (1985b) 275.
27 L.S. Tsai and C.A. Hudson, *J. Am. Oil Chem. Soc.*, 58 (1981) 931.
28 J.I. Teng, *LC·GC*, 9 (1991) 214.
29 Y.C. Chen, C.P. Chiu and B.H. Chen, *Food Chem.*, in press.
30 J.W. Dolan, *LC·GC*, 9 (1991) 466.
31 *SAS/STAT Guide for Personal Computers, Version 6ed*, SAS Instruments, Cary, NC, 1985.

Journal of Chromatography A, 661 (1994) 137–142
Elsevier Science B.V., Amsterdam

CHROMSYMP. 2886

Determination of catecholamines by automated pre-column derivatization and reversed-phase column liquid chromatography with fluorescence detection

Jan Kehr

CMA/Microdialysis AB, Roslagsvägen 101, 104 05 Stockholm (Sweden)

ABSTRACT

A highly selective and sensitive method for fluorescence determination of catecholamines (CAs) after automated derivatization with 1,2-diphenylethylenediamine (DPE)/potassium ferricyanide-based reagent is described. The reaction is specific for catechol compounds and was shown to be very reliable for analysis of CAs (noradrenaline, adrenaline, dopamine) in plasma and urine. However, in spite of its high sensitivity the method has not yet achieved wide application, probably because of a rather complicated manual derivatization and reaction times of 40–60 min. The present method describes an optimized automated procedure utilizing the CMA/200 refrigerated microsampler. Usually, 10-μl samples cooled at 4°C were mixed with 13.5 μl of acetonitrile–ferricyanide reagent and then with 7.5 μl DPE–bicine as a second reagent; 29 μl were aspirated into the sampling loop and heated to 80°C. After 6.5 min reaction time, samples were injected onto a 100 × 4 mm column packed with Nucleosil C_{18}, 3 μm particle size. CAs (including internal standards α-methyl-noradrenaline and isoproterenol) were separated within 8 min using 0.05 *M* acetate buffer pH 7.0–40% acetonitrile–8% methanol at a flow-rate of 1 ml/min. The detection limits for CAs were 2–5 fmol, which is about 2–4 times better than electrochemical detection used under similar chromatographic conditions. Furthermore, fluorescence detection is more reliable for routine use in clinical laboratories because the detector is much simpler to maintain. The method could be used for automated analysis of CAs in plasma and urine extracts and for microdialysis perfusates.

INTRODUCTION

Since the first reports on the use of electrochemical detection for liquid chromatographic determinations of catecholamines (CAs) and their metabolites [1,2], this technique has become widely used and modified for analysis of monoamines in tissue and body fluids. The main advantages of electrochemical detection of catechol and indol compounds in HPLC are high sensitivity, relatively inexpensive apparatus and the possibility of automation.

On the other hand, the electrochemical detector reacts to all compounds that can be oxidized at a given potential of the working electrode. This increases the risk of interferences in the chromatogram and necessitates troublesome maintenance of the detector. Polishing the electrode often means several hours of delay while waiting for the baseline signal to stabilize.

Recently, a fluorescence (FL) method for CA detection based on derivatization with 1,2-diphenylethylenediamine (DPE) was described [3–12]. The high fluorescence yield of this reaction allows detection of 2–10 fmol of CAs even on standard-bore (4 mm I.D.) columns. CAs can be derivatized either before injection onto the reversed-phase column [4–6,8–11] or after separation on the ion-exchange system [7]. Pre-column derivatization is preferable to the post-column approach, which requires extra pumps, coils or other reactors, causing dispersion of peaks and delay in the analysis. Furthermore, separation of precolumn-derivatized DPE–CAs on the reversed-phase system allows the use of gradient elutions [10,11] and reduces the problems associ-

0021-9673/94/$07.00
SSDI 0021-9673(93)E0809-9

ated with accumulation of interferences on the column. The most serious limitation of the pre-column method is the need for several manual pipetting steps and an incubation time of 45–60 min. The long reaction times, large final volumes of derivatized samples and the need for expensive fluorescence detectors are probably the main reasons why this method has not yet gained wider attention.

This paper reports a method for the automated pre-column derivatization of CAs with two reagent solutions by using an HPLC autosampler with a heated loop. The optimal parameters for reagent composition, their sequence, reaction time and temperature are discussed.

EXPERIMENTAL

Chemicals

The catecholamines noradrenaline (NA), adrenaline (A) and dopamine (DA) were obtained from Sigma (St. Louis, MO, USA). Isoproterenol (IP) and α-methyl-noradrenaline (α-MNA) were purchased from Research Biochemicals (Natick, MA, USA), potassium ferricyanide (PFC), acetonitrile, methanol and sodium acetate were from Merck (Darmstadt, Germany). Meso-DPE (*R,S*-form) was a kind gift from Dr. F. Boomsma (University Hospital, Rotterdam, Netherlands) or later obtained in either *R,R*-(+) or *S,S*-(−) form from Aldrich (Steinheim, Germany).

Apparatus

The liquid chromatographic pump was either a Spectra-Physics SP-8800 pump (San Jose, CA, USA) or a Pharmacia LKB 2249 gradient pump (Uppsala, Sweden). The mobile phase was degassed on-line by using a CMA/260 degasser (CMA/Microdialysis, Stockholm, Sweden). Automated derivations and injections were performed using a CMA/200 refrigerated microsampler. An LC-22C temperature controller (Bioanalytical Systems, W. Lafayette, IN, USA) was used to heat the sampling loop of the CMA/200. Derivatized CAs were detected either by a Smidadzu RF-535 spectrofluorometer (Kyoto, Japan) or later by a CMA/280 fluorescence detector (CMA/Microdialysis). The excitation and emission wavelengths of the former were set to 350 nm and 480 nm, respectively. The CMA/280 detector operates at fixed wavelengths with excitation and emission maxima at 330–365 nm and 440–530 nm, respectively. Chromatograms were recorded and integrated using an SP-4290 integrator (Spectra-Physics). Separations were performed on a 100×4 mm cartridge column (H. Knauer, Berlin, Germany) packed with Nucleosil 120 C_{18}, 3 μm particle size, protected with a 5×4 mm guard column packed with the same material.

Derivatization and chromatography

The manual derivatizations were performed as described previously [8]. Briefly, 40 μl of CA standard sample (NA, A and DA at $1 \cdot 10^{-8}$ *M* each), stored in 0.01 *M* hydrochloric acid, were pipetted into a plastic Eppendorf tube, followed by 50 μl of acetonitrile, 10 μl of bicine buffer, 20 μl of DPE and 4 μl of PFC. Concentrations of these stock solutions were: 1.75 *M* bicine buffer, pH 7.05, adjusted with 10% NaOH; 0.1 *M* DPE in 0.1 *M* HCl; and 20 m*M* PFC in water. The mixture was incubated in a water bath shielded against light at 37°C for 45 min and then 50-μl volumes were injected onto the column.

For automated derivatizations, different combinations of DPE, PFC, acetonitrile and bicine were tested. Two pairs of reagents (R1, R2 and R3, R4) were prepared by mixing different volumes (shown in parentheses) of the stock solutions: R1, acetonitrile–PFC (25:2); R2, DPE–bicine (2:1); R3, bicine–PFC (5:2); and R4, acetonitrile–DPE (5:2). For derivatizations of CAs, a pair of reagents, R1 then R2, R2 then R1, R3 then R4 or R4 then R3, was placed into the autosampler. Normally, 10 μl of samples were mixed with 13.5 μl of R1 and 7.5 μl of R2, or alternatively 4 μl of R3 and 17.5 μl of R4. It is supposed that no reaction was activated at this stage since samples and reagents were stored at +4°C in the CMA/200 autosampler. After mixing in the vials, each sample was aspirated into the heated loop and allowed to remain there for a preset period of time. The optimal reaction time found was 6.5 min at 80°C.

The mobile phase for isocratic separations consisted of 0.05 *M* sodium acetate buffer, pH

7.0, 40% acetonitrile and 8% methanol, as reported elsewhere [8]. The flow-rate was 1.0 ml/min.

RESULTS AND DISCUSSION

The optimal temperature of the reaction loop for DPE derivatization of NA, A and DA is shown in Fig. 1. As seen, for a fixed 5 min reaction time the maximal fluorescence yields (expressed as peak heights) for all CAs were achieved at 80°C. At this temperature, the optimal reaction time was found to be 6.5 min (Fig. 2). Here, the variation of reaction times from 5 to 8 min did not have such a profound effect on the FL yields as increasing the temperature. Thus it may be expected that higher temperature can shorten the reaction time significantly, while still maintaining the same sensitivity as for manual derivatization at room temperature or 37°C. Indeed, almost identical peak heights were measured for the CA standard sample derivatized automatically as compared with that derivatized manually: NA 92%, A 87%, DA 106%, and internal standards α-MNA 73%, IP 73% (expressed as a percentage of 80°C/6.5 min reaction *vs.* 37°C/45 min reaction).

Previously, it was assumed that a high temperature could affect the reaction yields and reduce the stability of fluorescence derivatives [12], yet no systematic study has been made on the effects of temperature on reaction kinetics.

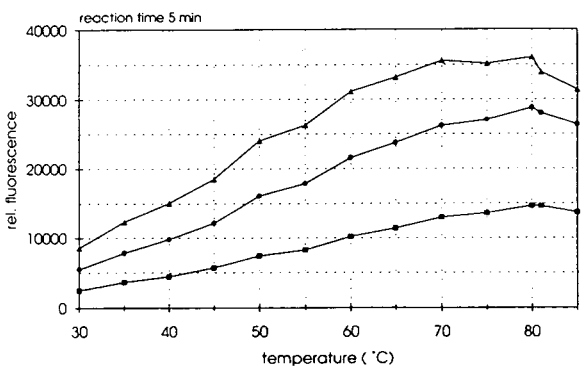

Fig. 1. Effect of reaction temperature on the fluorescence yields of DPE–catecholamine derivatives. ▲ = NA; ○ = A; □ = DA.

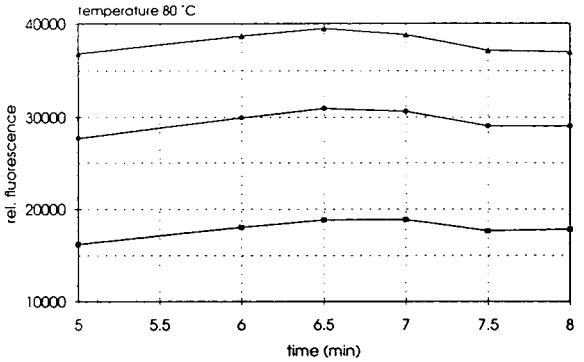

Fig. 2. Effect of reaction time on the fluorescence yields of DPE–catecholamine derivatives. ▲ = NA; ○ = A; □ = DA.

More detailed studies were devoted to finding the optimal chemical conditions for the DPE reaction, such as pH, effect of accelerator (glycine, acetonitrile) and oxidant (PFC). Recently, the structure of the final DPE–adrenaline fluorophore was described [13]. It is postulated that, in the first step, CAs are oxidized to the corresponding adrenochromes by PFC. Also, coulometric oxidation is possible, which allows derivatization of hydroxymethylated CAs to their *o*-quinones [7]. Adrenochromes then react with DPE to form corresponding, highly fluorescent 2-aryl(4,5-dihydropyrrolo)[2,3-*f*]benzoxazoles [13].

Fig. 3A shows a typical chromatogram of 10 μl of a standard mixture of CAs, including internal standards α-MNA and IP, at concentrations of 0.1 pmol/10 μl each. Automated derivatization was performed at 80°C for 6 min with R1 and R2 as described in the Experimental section. The highest signal was observed for α-MNA; for CAs the largest peak was NA, whereas A and DA produced only 79% and 45% of the NA peak height. However, the extreme fluorescence intensity of DPE fluorophores allows detection to as low as 5 fmol of each catecholamine, as illustrated in Fig. 3B. It should be noted that electrochemical detection on a glassy carbon electrode can detect only 10–20 fmol of CAs under the same chromatographic conditions. A derivatized blank (water) sample is shown in Fig. 3C. No detectable peaks were observed in this sample, which suggests that the small peak

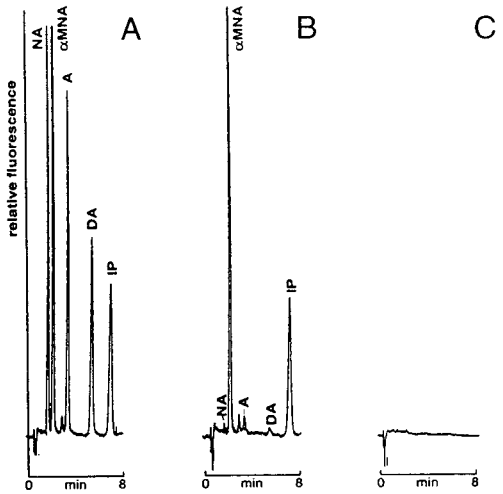

Fig. 3. (A) A typical chromatogram of 10 μl of CA standards at concentrations of 0.1 pmol/10 μl each. Internal standards α-methyl-noradrenaline (α-MNA) and isoproterenol (IP) were also included. (B) The limits of detection. A 10-μl aliquot of standard mixture contained $5 \cdot 10^{-10}$ M (5 fmol) NA, A and DA each and $1 \cdot 10^{-8}$ M internal standard. (C) A blank (10 μl water) sample was derivatized as described above.

eluted at 2.9 min, shown in Fig. 3A and B, is an impurity present in the internal standard (α-MNA).

The internal standard (α-MNA or IP) should be used for plasma or urine samples, which must undergo preseparation on solid phase (alumina or ion-exchange) cartridges or by liquid–liquid extraction [8]. In these cases the recoveries of extracted CAs can vary from 60 to 100%. For analysis of microdialysis samples, no preseparation steps are normally needed, and thus internal standards can be omitted. However, it is advisable to correct for any possible variations in derivatization yields and the precision of sample pipetting by adding the internal standard to one of the reagents. The best signal for internal standards without any interferences or multiple peaks was observed when α-MNA and IP were added to R2 (see Fig. 3B).

Another important factor affecting the final number and shape of peaks is the reagent composition and the sequence of mixing for each pair of reagents. The chromatograms in Fig. 4A–D illustrate the effect of the composition of

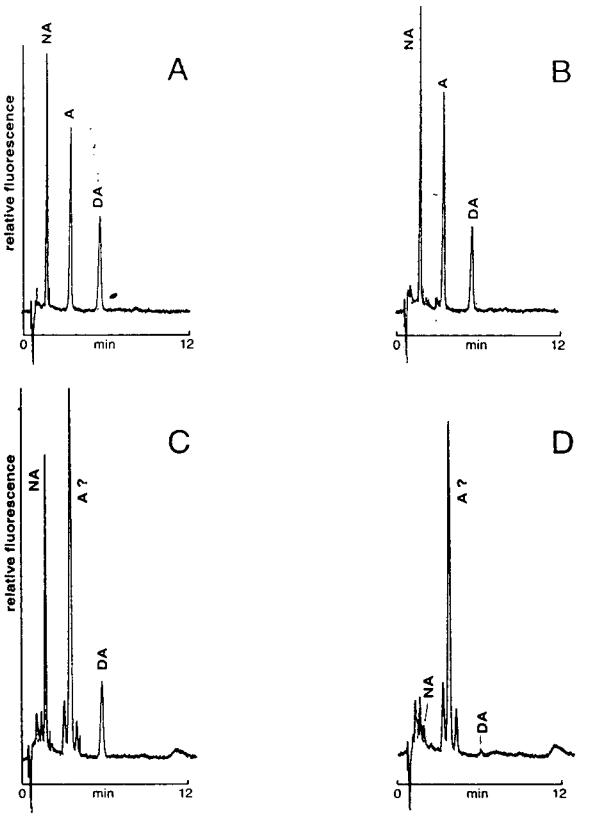

Fig. 4. Effects of reagent composition and mixing sequences on reaction yields of DPE-derivatized catecholamines. A 20-μl aliquot of $1 \cdot 10^{-8}$ M CA standards was derivatized with two pairs of reagents. For chromatograms B and D, the mixing order of reagents was reversed. Standards and reagents were kept at +4°C; the derivatization was performed at 65°C for 5 min: (A) 27 μl of acetonitrile–PFC + 15 μl of bicine–DPE, the optimal derivatization; (B) 15 μl of bicine–DPE + 27 μl of acetonitrile–PFC; (C) 7 μl of bicine–PFC + 35 μl of acetonitrile–DPE; (D) 35 μl of acetonitrile–DPE + 7 μl of bicine–PFC.

each reagent and the mixing order of the reagents on derivatization yields. The best results were achieved with R1 and R2, mixed in this sequence with a $1 \cdot 10^{-8}$ M CA standard (Fig. 4A). When the derivatization order was reversed, *i.e.* R2 was pipetted first followed by R1, a similar chromatogram was obtained, but with several small unidentified peaks. These data suggest that no significant chemical reaction occurs during pipetting of the reagents, since samples and reagents are stored at +4°C. The reaction starts when the mixture is aspirated into

the heated sampling loop. R1 and R2 are stable and give reproducible signals for at least 24 h. It is recommended that fresh reagents are prepared daily in order to prevent any source of impurities or carry-over from the samples.

R3 and R4 gave quite different chromatograms (Fig. 4C and D). When mixing the standard sample with R3 followed by R4, a large A peak was measured, compared with almost unchanged NA and DA peaks. At the same time, as many as five "degradation" peaks were eluted in the vicinity of the NA and A peaks. Reversing the derivatization order to R4 then R3 led to almost complete disappearance of NA and DA peaks, while there remained a large peak corresponding to the retention time of A. This peak, although not so high, also appears in a blank (water) sample derivatized by the same procedure. In both cases, several by-product peaks were eluted at the beginning of the chromatogram. It was concluded that the R3 + R4 pair is less 'safe' in terms of peak purity than R1 + R2. Because of many interfering peaks it is not possible to use internal standards such as α-MNA.

The main difference between R3,R4 and R1,R2 pairs is most probably the chemical stability of the mixed components themselves, rather than alternation of the reaction steps in the derivatization formula.

The chemical environment in which catecholamine samples are stored also plays a significant role in the derivatization efficiency, as documented in Fig. 5A and B. In both cases derivatizations were performed with R1 + R2 at 80°C/6.5 min as described in the Experimental section. Derivatization of 10 μl of a standard sample of CAs at concentrations of $5 \cdot 10^{-8}$ *M* each, which was stored in 0.3 m*M* glutathione, yielded dramatically suppressed peak heights for all compounds, except for A, with which some unknown products co-eluted (Fig. 5A). Glutathione is often used as an antioxidant during preparation of plasma samples for CA measurements. Obviously, it inhibits the effect of PFC in oxidizing CAs to their corresponding *o*-quinones.

Similarly, low pH can block the reaction, as shown for the CA standard stored in 0.1 *M* hydrochloric acid (Fig. 5B). Lowering the concentration of HCl in CA standards to 0.01 *M* produced normal peak heights, as seen in Fig. 3A. The effect of the pH of the bicine buffer on the fluorescence intensity of CA derivatives has been detailed previously [8]. The highest FL yields are achieved at pH 6.5–7.0. This means that samples stored in strong acids should be neutralized before derivatization, or the pH of the DPE–bicine reagent should be increased to shift the final pH of the reaction mixture to the optimal range.

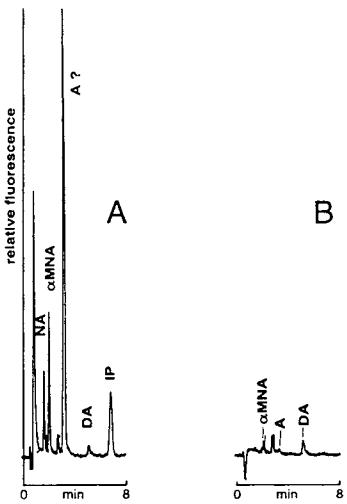

Fig. 5. Effect of antioxidants and acids present in the CA extracts on derivatization yields of NA, A, DA and internal standards α-MNA and IP. A 10-μl aliquot of standard containing $5 \cdot 10^{-8}$ *M* catecholamines and internal standards was stored in: (A) 0.3 m*M* glutathione solution or (B) 0.1 *M* HCl. Derivatizations were performed as described in Fig. 4A.

CONCLUSION

The present method for fluorescence detection of derivatized CAs possesses several advantages over electrochemical detection. Probably the main difference is easier maintenance and superior reliability of the FL method for routine use. High sensitivity and the possibility of using gradient elutions or microbore columns make the technique very suitable for automated analysis of CAs in plasma and urine extracts and for moni-

toring the neurotransmitters NA and DA in microdialysis samples.

REFERENCES

1 P.T. Kissinger, R.M. Riggin, R.L. Alcorn and L.D. Rau, *Biochem. Med.*, 13 (1975) 299.
2 I.N. Mefford, *J. Neurosci. Methods*, 3 (1981) 207.
3 H. Nohta, A. Mitsui and Y. Ohkura, *Anal. Chim. Acta*, 165 (1984) 171.
4 A. Mitsui, H. Nohta and Y. Ohkura, *J. Chromatogr.*, 344 (1985) 61.
5 H. Nohta, A. Mitsui and Y. Ohkura, *J. Chromatogr.*, 380 (1986) 229.
6 H. Nohta, A. Mitsui, Y. Umegae and Y. Ohkura, *Biomed. Chromatogr.*, 2 (1987) 9.
7 H. Nohta, E. Yamaguchi, Y. Ohkura and H. Watanabe, *J. Chromatogr.*, 467 (1989) 237.
8 F.A.J. van der Hoorn, F. Boomsma, A.J. Man in 't Veld and M.A.D.H. Schalekamp, *J. Chromatogr.*, 487 (1989) 17.
9 F.A.J. van der Hoorn, F. Boomsma, A.J. Man in 't Veld and M.A.D.H. Schalekamp, *J. Chromatogr.*, 563 (1991) 348.
10 F. Boomsma, G. Alberts, F.A.J. van der Hoorn, A.J. Man in 't Veld and M.A.D.H. Schalekamp, *J. Chromatogr.*, 574 (1992) 109.
11 G. Alberts, F. Boomsma, A.J. Man in 't Veld and M.A.D.H. Schalekamp, *J. Chromatogr.*, 583 (1992) 236.
12 Y. Umagae, H. Nohta and Y. Ohkura, *Anal. Chim. Acta*, 208 (1988) 59.
13 H. Nohta, M.-K. Lee and Y. Ohkura, *Anal. Chim. Acta*, 267 (1992) 137.

Journal of Chromatography A, 661 (1994) 143–151
Elsevier Science B.V., Amsterdam

CHROMSYMP. 2918

Correlative retention time peak identification method for glycated haemoglobin in high-performance liquid chromatography

Masahito Ito*, Junkichi Miura, Mitsuo Ito, Fuminori Umesato, Kenji Yasuda and Yoshinori Takata

Instrument Division, Hitachi Ltd., Katsuta 312 (Japan)

Bernd Stanislawski

Diagnostica Forschung, E. Merck, D-6100 Darmstadt (Germany)

ABSTRACT

A convenient peak identification method in stepwise elution was investigated and correlation among the retention times of peaks in ion-exchange chromatography of glycated haemoglobin was assessed. By using a correlation method, accuracy of peak identification among columns with degradation and product deviations can be maintained. The correlative retention time identification procedure is treated theoretically.

INTRODUCTION

In chromatographic separations, peaks are usually identified by measuring the retention times. Data processors are usually equipped with a function to assign and print the component names for the peaks appearing in the time windows set up in advance. However, retention time variations often occur in HPLC [1], which could disturb peak identification. To minimize the variations, the column temperature, flow-rate and quality control of the stationary and mobile phases are important considerations for chromatographers. However, small variation cannot be avoided because of degradation of the stationary phase and also reproducibility. Even when retention times vary, it is known that correlation among the retention times of peaks seems to be conserved in the ion-exchange chromatography of glycated haemoglobin [2,3].

Glycated haemoglobins are classified as HbA_{1a} (A_{1a}), HbA_{1b} (A_{1b}), labile HbA_{1c}(l-A_{1c}), HbA_{1c} (A_{1c}), etc. The concentration of A_{1c} is one of the indices of diabetes. Human haemoglobins consist not only of glycated haemoglobin but also of non-glycated haemoglobins such as HbF and HbA_0 [4,5].

In this paper, focusing discussion on the analysis of glycated haemoglobin, correlation among the retention times of peaks is considered. A method of peak identification based on the correlation is presented. This method is similar to a peak identification method based on the relative retention times with internal standards [6,7]. The relative retention method is based on the assumption that each retention time varies is proportion to the retention time of the internal standard. With stepwise elution, some peaks will be identified incorrectly, because this assumption

* Corresponding author.

0021-9673/94/$07.00
SSDI 0021-9673(93)E0886-Y

is not always valid. The relative retention time is a kind of linear transformation on a common time axis for each peak. On the other hand, the present method, based on the correlation among the retention times of peaks, can treat each peak individually. In other words, this method has linear transformations of retention times, the number of which is the same as that of the peaks to be identified.

A general equation for the retention mechanism can be applied theoretically [8,9]. This supports the correlation among the retention times of peaks in glycated haemoglobin analysis.

THEORY

Retention model of ion-exchange chromatography

In the ion-exchange chromatography of haemoglobin, as the valence of potassium ion in the mobile phase is 1, the capacity factor of the ith peak (k'_i) can be expressed as

$$k'_i \sim \frac{V_s}{V_m} \cdot K_i Q^{n_i} X^{-n_i} \quad (1)$$

where V_s and V_m are the total volumes of the stationary (s) and mobile (m) phases in the column, K_i is the conventional selectivity constant, Q is the ion-exchange capacity of the stationary phase, X is the concentration of potassium ion in the mobile phase and n_i is the effective valence of ith haemoglobin molecule, Hb_i. The conventional selectivity constant is defined as $K_i = X^{n_i}(Hb_i)/\{(K)^{n_i}[Hb_i]\}$, where (K) is the concentration of potassium ion in the stationary phase, (Hb_i) is that of Hb_i in the stationary phase and [Hb_i] is that of Hb_i in the mobile phase [8].

The selectivity between the ith and jth peaks, a_{ij}, is defined as

$$\alpha_{ij} = k'_j / k'_i \quad (2)$$

By combining eqns. 1 and 2, the following equation is obtained:

$$\alpha_{ij} \sim \frac{K_j}{K_i} \cdot Q^{n_j - n_i} X^{-(n_j - n_i)} \quad (3)$$

If the n_j value is very close to n_i, the α_{ij} values will not be influenced by the ion-exchange capacity of the stationary phase (Q) and the concentration of potassium ion in the mobile phase (X), and then α_{ij} is almost constant.

HbF and A_{1c} with isocratic elution

In isocratic elution, the retention time of the ith peak, t_{R_i}, can be expressed as

$$t_{R_i} = t_0 k'_i + t_0 \quad (4)$$

where t_0 is mobile phase hold-up time.

The retention time of the jth peak (t_{R_j}) can be expressed as a function of the retention time of the ith peak (t_{R_i}) using α_{ij}:

$$t_{R_j} = f(t_{R_i}) = \alpha_{ij} t_{R_i} + (1 - \alpha_{ij}) t_0 \quad (5)$$

When α_{ij} = constant is assumed, t_{R_j} can be represented by a linear form of t_{R_i}. In addition, the mobile phase hold-up time (t_0) is a function of flow-rate, column length and available column cross-section; t_0 can be regarded as a constant when degradation of the stationary phase or reproducibility occurs, because these three variables are regarded as constant.

For example, the jth and ith peaks can be considered as HbF and A_{1c}, respectively. If $\alpha_{A_{1c}F}$ is constant, the retention time of HbF (t_{RF}) can have a correlation with the retention time of A_{1c}($t_{RA_{1c}}$) as follows;

$$t_{RF} = \alpha_{A_{1c}F} t_{RA_{1c}} + (1 - \alpha_{A_{1c}F}) t_0 \quad (6)$$

The value of $\alpha_{A_{1c}F}$ is the inverse of $\alpha_{FA_{1c}}$. Although the selectivity α is generally defined as $\alpha_{FA_{1c}}$, $\alpha_{A_{1c}F}$ is used in this paper. Thus, $\alpha_{A_{1c}F}$ varies between 0 and 1.

HbF and A_{1c} with stepwise elution

This method can be evolved with stepwise elution of glycated haemoglobin. The programme for stepwise elution is shown in Fig. 1. The first mobile phase A carries a solute to a migration distance q_A in a total elution period τ_A; τ_A is the sum of the time corresponding to the volume of the instrumentation causing a stepwise delay (τ_Z) [8], the programme period of the

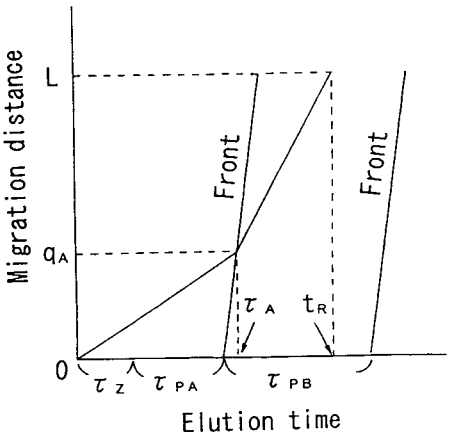

Fig. 1. Migration distance *versus* elution time with stepwise elution. L = column length; q_A = migration distance by mobile phase A; t_R = retention time; τ_A = total elution period of mobile phase A; τ_Z = stepwise delay time; τ_{PA} and τ_{PB} = programme period with mobile phases A and B.

mobile phase A (τ_{PA}) and the time corresponding to the migration distance of the ith solute with mobile phase A $[(\tau_Z + \tau_{PA})/k'_i(X_A)]$, where $k'_i(X_A)$ is the capacity factor of the ith solute [9]. The third term is equal to the elution period of mobile phase B from the column inlet to the ith solute. When the value of $k'_i(X_A)$ is sufficiently larger than 1 ($k'_i > 10$), τ_A can be regarded as constant approximately; $\tau_A = \tau_Z + \tau_{PA}$.

Using $k'_i(X_A)$, τ_A can be expressed as

$$\tau_A = [1 + k'_i(X_A)]q_A/v \quad (7)$$

where X_A is the concentration of the gradient-forming ion in the first mobile phase A and v is the velocity of the mobile phase. This equation is similar to eqn. 4. Then the second mobile phase B carries the analyte through the remaining column length $(L - q_A)$ for the remaining retention time $(t_{R_i} - \tau_A)$. In the same way, using the capacity factor for the mobile phase B $[k'_i(X_B)]$, $t_{R_i} - \tau_A$ can be expressed as

$$t_{R_i} - \tau_A = [1 + k'_i(X_B)](L - q_A)/v \quad (8)$$

The retention time of the ith solute in stepwise elution (t_{R_i}) can be calculated from eqns. 7 and 8 as

$$\begin{aligned} t_{R_i} &= \frac{k'_i(X_A) - k'_i(X_B)}{1 + k'_i(X_A)}\tau_A + [1k'_i(X_B)]t_0 \\ &= \frac{1 + k'_i(X_B)}{1 + k'_i(X_A)} \cdot t_0 k'_i(X_A) \\ &\quad + \left[1 - \frac{1 + k'_i(X_B)}{1 + k'_i(X_A)}\right]\tau_A + \frac{1 + k'_i(X_B)}{1 + k'_i(X_A)} \cdot t_0 \\ &= C_1(X_A, X_B)k'_i(X_A) + C_0(X_A, X_B) \end{aligned} \quad (9)$$

where $C_1(X_A, X_B)$ and $C_0(X_A, X_B)$ are substituted coefficients which are introduced for a convenient expression and $t_0 = L/v$. Considering eqn. 4, the retention time ratio for different concentrations of mobile phase $[\beta_i(X_A, X_B)]$ in the isocratic elution mode is defined as

$$\beta_i(X_A, X_B) = [1 + k'_i(X_B)]/[1 + k'_i(X_A)] \quad (10)$$

When the value of k'_i is sufficiently larger than 1 ($k'_i > 10$), substitution of k'_i using eqn. 1 in eqn. 10 approximately gives the equation

$$\beta_i(X_A, X_B) \sim k'_i(X_B)/k'_i(X_A) = (X_A/X_B)^{n_i} \quad (11)$$

Generally, the retention time ratio $[\beta_i(X_A, X_B)]$ is nearly constant with variation of the ion-exchange capacity in the stationary phase. Then $C_1(X_A, X_B)$ and $C_0(X_A, X_B)$ are also constant, and t_{R_i} can be represented by the linear form of $k'_i(X_A)$, when eqn. 9 is considered.

In our analysis of glycated haemoglobin, A_{1c} is eluted with both the mobile phases A and B using stepwise elution. The retention time of $A_{1c}(t_{RA_{1c}})$ can be described as

$$t_{RA_{1c}} = C_1(X_A, X_B)k'_{A_{1c}}(X_A) + C_0(X_A, X_B) \quad (12)$$

where

$$C_1(X_A, X_B) = \beta_{A_{1c}}(X_A, X_B)t_0$$

and

$$\begin{aligned} C_0(X_A, X_B) &= [1 - \beta_{A_{1c}}(X_A, X_B)]\tau_A \\ &\quad + \beta_{A_{1c}}(X_A, X_B)t_0 \end{aligned}$$

Both $C_1(X_A, X_B)$ and $C_0(X_A, X_B)$ can be regarded as the functions of $\beta_{A_{1c}}(X_A, X_B)$. $\beta_{A_{1c}}(X_A, X_B)$ is the retention time ratio of A_{1c} in the isocratic elution mode.

On the other hand, HbF is eluted only with

the mobile phase A. From eqn. 4, the retention time of HbF (t_{RF}) can be expressed as

$$t_{RF} = t_0 k'_F(X_A) + t_0 \quad (13)$$

Combination of eqns. 12 and 13 gives

$$t_{RF} = \frac{t_0}{C_1(X_A, X_B)} \cdot \alpha_{A_{1c}F}(X_A) t_{RA_{1c}} + \left[1 - \frac{C_0(X_A, X_B)}{C_1(X_A, X_B)} \cdot \alpha_{A_{1c}F}(X_A)\right] t_0$$

$$= \frac{\alpha_{A_{1c}F}(X_A)}{\beta_{A_{1c}}(X_A, X_B)} \cdot t_{RA_{1c}} + [1 - \alpha_{A_{1c}F}(X_A)] t_0 - \frac{1 - \beta_{A_{1c}}(X_A, X_B)}{\beta_{A_{1c}}(X_A, X_B)} \cdot \alpha_{A_{1c}F}(X_A) \tau_A \quad (14)$$

where $\alpha_{A_{1c}F}(X_A)$ is the selectivity between HbF and A_{1c} in mobile phase A.

If both $\alpha_{A_{1c}F}(X_A)$ and $\beta_{A_{1c}}(X_A, X_B)$ are constant with variation in the ion-exchange capacity among the stationary phases, t_{R_F} correlates with $t_{RA_{1c}}$ even in the stepwise elution mode.

In the case of $\beta_{A_{1c}}(X_A, X_B) \sim 1$, t_{RF} can be approximated as follows:

$$t_{RF} \sim \alpha_{A_{1c}F}(X_A) t_{RA_{1c}} + [1 - \alpha_{A_{1c}F}(X_A)] t_0 + [1 - \beta_{A_{1c}}(X_A, X_B)] \alpha_{A_{1c}F}(X_A)(t_{RA_{1c}} - \tau_A) \quad (15)$$

Compared with eqn. 6, the effect of the second mobile phase B appears in the third term of eqn. 15.

l-A_{1c} and A_{1c} with stepwise elution

Both l-A_{1c} and A_{1c} are eluted with mobile phases A and B using stepwise elution. By using eqn. 9, the retention times of l-A_{1c}($t_{Rl\text{-}A_{1c}}$) and A_{1c}($t_{RA_{1c}}$) are expressed as follows:

$$t_{Rl\text{-}A_{1c}} = C_{1l\text{-}A_{1c}}(X_A, X_B) k'_{l\text{-}A_{1c}}(X_A) + C_{0l\text{-}A_{1c}}(X_A, X_B) \quad (16)$$

$$t_{RA_{1c}} = C_{1A_{1c}}(X_A, X_B) k'_{A_{1c}}(X_A) + C_{0A_{1c}}(X_A, X_B) \quad (17)$$

where $C_{1l\text{-}A_{1c}}(X_A, X_B)$, $C_{0l\text{-}A_{1c}}(X_A, X_B)$, $C_{1A_{1c}}(X_A, X_B)$ and $C_{0A_{1c}}(X_A, X_B)$ are constants. By using $\alpha_{A_{1c}l\text{-}A_{1c}}(X_A)$, the selectivity between l-A_{1c} and A_{1c} in mobile phase A, combination of eqns. 16 and 17 give

$$t_{Rl\text{-}A_{1c}} = \frac{C_{1l\text{-}A_{1c}}(X_A, X_B)}{C_{1A_{1c}}(X_A, A_B)} \cdot \alpha_{A_{1c}l\text{-}A_{1c}}(X_A) t_{RA_{1c}} - \frac{C_{1l\text{-}A_{1c}}(X_A, X_B) C_{0A_{1c}}(X_A, X_B)}{C_{1A_{1c}}(X_A, X_B)} \cdot \alpha_{A_{1c}l\text{-}A_{1c}}(X_A) + C_{0l\text{-}A_{1c}}(X_A, X_B) \quad (18)$$

Both $t_{Rl\text{-}A_{1c}}$ and t_{RF} can be represented with a linear form of $t_{RA_{1c}}$ in the stepwise elution mode. Then t_{RF} or $t_{Rl\text{-}A_{1c}}$ can be estimated by using $t_{RA_{1c}}$, employing the capacity factors as more important retention values than retention times. In other words, retention times can be regarded as secondary retention values.

In the isocratic elution mode, by employing eqns. 2 and 4, t_{RF} is related to $t_{RA_{1c}}$ (eqn. 6). In a similar way, in the stepwise elution mode of HbF and A_{1c}, the algorithm can be explained as follows: (1) $t_{RA_{1c}}$ is transformed into $k'_{A_{1c}}(X_A)$ by using t_0, τ_A and $\beta_{A_{1c}}(X_A, X_B)$; (2) $k'_{A_{1c}}(X_A)$ is changed into $k'_F(X_A)$ by using $\alpha_{A_{1c}F}(X_A)$; and (3) t_{RF} is obtained from $k'_F(X_A)$ by using t_0. The retention time correlation of l-A_{1c} and A_{1c} can be explained by a similar algorithm.

EXPERIMENTAL

Materials

All reagents were of analytical-reagent grade and purchased form Wako (Osaka, Japan). Human whole blood samples were obtained from Mito General Hospital, Hitachi (Katsuta, Japan).

Apparatus

The HPLC system was a Hitachi Model L-9100 glycated haemoglobin analyser. It had two analytical modes: high-speed mode and high-resolution mode. The two modes used the same mobile phases as follows: mobile phase A = 64 m*M* potassium phosphate buffer (pH 6.2); mo-

bile phase B = 75 m*M* potassium phosphate buffer (pH 6.2); and mobile phase C = 207 m*M* sodium phosphate buffer (pH 6.1).

In the high-speed mode, a 35 mm × 4.6 mm I.D. column packed with weak cation-exchange polymethacrylate resin was used. The mobile phase hold-up time (t_0) was about 0.2 min, the diameter of the resin particles was 3.5 μm and the ion-exchange capacity was about 0.3 mequiv./g. The time course of the stepwise elution was as follows: 0.0–0.6 min with A, 0.6–1.6 min with B, 1.6–2.0 min with C and 2.0–3.3 min with A. The flow-rate was adjusted to 1.4 ml/min. Samples were injected at 3.3-min intervals.

In the high-resolution mode, an 80 mm × 4.6 mm I.D. column packed with the same resin in the high-speed mode was used. The mobile phase hold-up time (t_0) was about 0.6 min. The time course of the elution was follows: 0.0–3.0 min with B, 3.0–3.9 min with C, 3.9–6.5 min with A and 6.5–7.0 min with B. The flow-rate was set to 1.0 ml/min. Samples were injected at 7.0-min intervals.

Other conditions for the two modes were identical. The column temperature was 40°C. The absorbance was measured at 415 nm, using the absorbance at 530 nm as a reference. Samples were whole blood diluted 160-fold with water. The injection volume was 10 μl by the complete-fill mode.

Methods

In order to simulate the retention time variations, the concentration of potassium ion in mobile phases A and B was varied, maintaining a constant ratio of potassium ion concentrations in mobile phases A and B. In the high-speed mode, the concentration of potassium ion in mobile phases A and B was varied from 94% to 106% and in the high-resolution mode from 94% to 111% of the standard concentration. These concentration ranges represent almost the limits to obtain satisfactory separations.

The integrator was set to have a delayed start time of 0.2 min after the injection time in the high-speed mode and 0.5 min in the high-resolution mode.

RESULTS AND DISCUSSION

High-speed mode

A chromatogram obtained using the high-speed mode is shown in Fig. 2a. It has six assigned peaks: A_{1a}, A_{1b}, HbF, l-A_{1c}, A_{1c} and HbA_0. There is a small valley between l-A_{1c} and

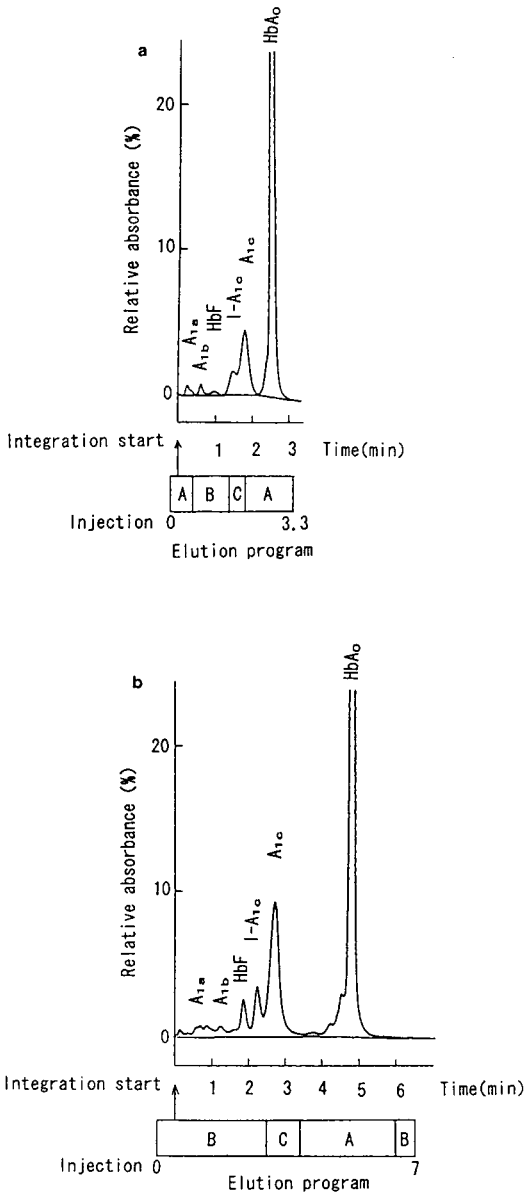

Fig. 2. Representative chromatograms of glycated haemoglobins obtained with stepwise elution. (a) High-speed mode; (b) high-resolution mode.

A_{1c}. Mobile phase A elutes mainly A_{1a}, A_{1b} and HbF. Mobile phase B elutes predominantly l-A_{1c} and A_{1c}. Mobile phase C elutes mainly HbA_0 drastically. The difference in time between a mobile phase change being detected at the detector and the switching of the mobile phases at the pump was about 0.5 min. The ordinate axis (relative absorbance) is normalized as the peak height of A_{1c} corresponding to the percentage of A_{1c} in total haemoglobin.

Simulation of stationary phase variation

In the high-speed mode, retention time variation was simulated by using three pairs of mobile phases A and B with different concentrations. The retention time of A_{1c} ($t_{RA_{1c}}$) was changed on purpose between 1.2 and 1.8 min for the simulation. The retention times of A_{1b} and HbF are correlated with $t_{RA_{1c}}$ in Fig. 3a, although mobile phase B influenced only A_{1c}. The retention time of HbF (t_{RF}) can be fitted to the linear form of the retention time of A_{1c}($t_{RA_{1c}}$):

$$t_{RF} = 0.65t_{RA_{1c}} - 0.11 \quad (19)$$

This corresponds to eqn. 14. The coefficients for the other peaks are given in Table I.

High-resolution mode

A chromatogram obtained using the high-resolution mode is shown in Fig. 2b. The sample was obtained for a diabetic patient. The separation between l-A_{1c} and A_{1c} in this mode was much better than that in the high-speed mode and the tail of the HbF peak reached the baseline.

In the high-resolution mode, mobile phase B elutes the solutes between A_{1a} and A_{1c}. In other words, the influence of mobile phase A on the elution of these solutes will be negligible. The difference in time between a mobile phase change detected at the detector and the switching of the mobile phases at the pump was about 1.0 min. The high-resolution mode showed good correlations between the retention times (Fig. 3b). The coefficients for the peaks are given in Table I.

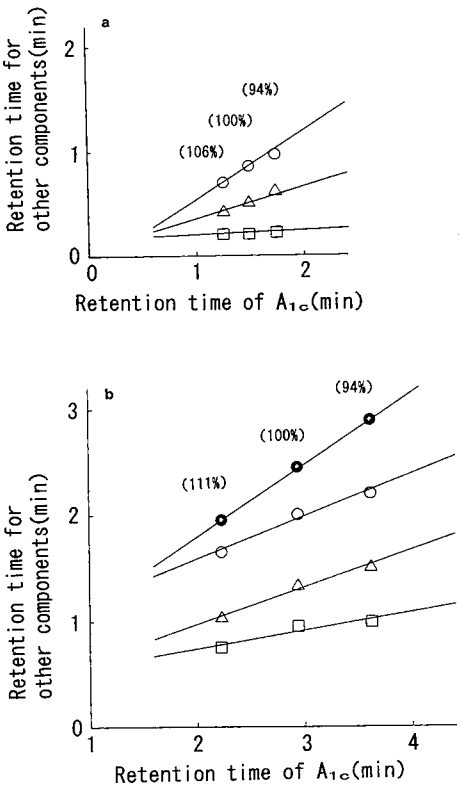

Fig. 3. Correlation of retention times between A_{1c} and the others with stepwise elution. The values in parentheses are the concentrations of mobile phases A and B as a percentage of that of the standard. □ = A_{1a}; △ = A_{1b}; ○ = HbF; ● = l-A_{1c}. (a) High-speed mode; (b) high-resolution mode.

TABLE I

FITTED LINEAR EQUATION FOR RETENTION TIME CORRELATION

High-speed mode
$t_{RA_{1a}} = 0.04t_{RA_{1c}} + 0.16$
$t_{RA_{1b}} = 0.30t_{RA_{1c}} + 0.06$
$t_{RF} = 0.65t_{RA_{1c}} - 0.11$
$t_{Rl\text{-}A_{1c}} = 1.03t_{RA_{1c}} - 0.39^a$
High-resolution mode
$t_{RA_{1a}} = 0.17t_{RA_{1c}} + 0.40$
$t_{RA_{1b}} = 0.35t_{RA_{1c}} + 0.27$
$t_{RF} = 0.40t_{RA_{1c}} + 0.79$
$t_{Rl\text{-}A_{1c}} = 0.68t_{RA_{1c}} + 0.43$

[a] The coefficients were obtained using several columns with retention time $t_{RA_{1c}}$ between 1.40 and 2.01 min.

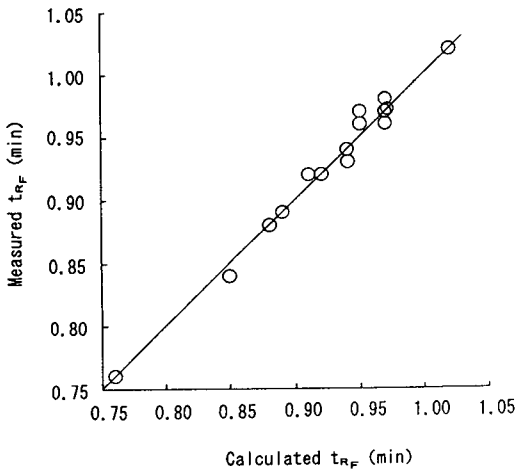

Fig. 4. Relationship between measured retention time of HbF and the calculated value in the high-speed mode. The retention times were calculated by using eqn. 19.

Correlation in the different stationary phases

In the high-speed mode, t_F measured on several different columns correlated with the calculated retention time from eqn. 19 as shown in Fig. 4. The correlation coefficient was found to be as 0.99 for fifteen columns. The difference between the measured and the calculated retention times was 0.03 min at most. This shows that the simulation for changes in mobile phases is almost equivalent to that for variations in the ion-exchange capacity in the stationary phase. Provided that the composition of the mobile phase is well controlled, even if the stationary phase has a slightly different nature, the retention times will correlate well with each other.

Some chromatographic values can be examined in detail. Both the selectivity of two solutes in the mobile phase A [$\alpha_{A_{1c}F}(X_A)$] and the retention time ratio of A_{1c} between two mobile phases [$\beta_{A_{1c}}(X_A, X_B)$] are considered to be almost constant owing to the small relative standard deviations (R.S.D.) among stationary phases (Table II). This constancy is the essential reason for the retention time correlation as estimated in eqn. 14.

Table III shows the variation of the capacity factors. The values in Table II were calculated from these factors. From eqn. 11, by using measured capacity factors, $k'_{A_{1c}}(X_A)$, $k'_{A_{1c}}(X_B)$, $k'_F(X_A)$ and $k'_F(X_B)$, and the concentration ratio (X_A/X_B), the effective valences of HbF (n_F) and A_{1c} ($n_{A_{1c}}$) can be estimated. Both n_F and $n_{A_{1c}}$ were *ca.* 4 (Table III). This is the reason why $\alpha_{A_{1c}F}(X_A)$ is almost constant despite variations in the stationary phase (eqn. 3). On the other hand, it is the constancy of $\beta_{A_{1c}}(X_A, X_B)$ that makes both $k'_{A_{1c}}(X_A)$ and $k'_{A_{1c}}(X_B)$ sufficiently higher than 1 (eqn. 11).

The R.S.D. of $k'_{A_{1c}}(X_B)$ was 15.4% (Table III). Hence the R.S.D. of the ion-exchange

TABLE II

RETENTION TIME, SELECTIVITY AND RETENTION TIME RATIO BETWEEN MOBILE PHASES

No.	Column[a]	$t_{RA_{1c}}$(min)	$\alpha_{FA_{1c}}(X_A)$	$\alpha_{FA_{1c}}(X_B)$	$\beta_{A_{1c}}(X_A,X_B)$	$\beta_F(X_A,X_B)$
1	Used column G[b]	1.40	2.60	2.12	0.51	0.65
2	Used column K[b]	1.44	2.61	2.11	0.53	0.68
3	New column K	1.62	2.65	2.20	0.52	0.66
4	New column G	1.77	2.60	2.16	0.49	0.62
5	New column K	1.85	2.64	2.21	0.50	0.62
6	New column B	1.90	2.56	2.22	0.53	0.64
7	New column B	2.01	2.66	2.25	0.48	0.60
Mean		1.713	2.617[c]	2.181[d]	0.509	0.639
S.D.		0.233	0.035	0.053	0.020	0.027
R.S.D. (%)		13.62	1.34	2.42	3.84	4.28

[a] G, K and B represent the resin lots. Columns with the same name, such as 6 and 7, have different packings.
[b] The stationary phase had experienced more than 3000 injections.
[c] $\alpha_{A_{1c}F}(X_A) = 1/\alpha_{FA_{1c}}(X_A) = 0.382$.
[d] $\alpha_{A_{1c}F}(X_B) = 1/\alpha_{FA_{1c}}(X_B) = 0.459$.

TABLE III

CAPACITY FACTOR AND EFFECTIVE VALENCE OF HEMOGLOBIN

The results were obtained using isocratic elution. The value of t_0 was measured as 0.2 min by using a non-retention peak from blood.

No.	Column	$k'_{A_{1c}}(X_A)$	$k'_{A_{1c}}(X_B)$	$n_{A_{1c}}$	$k'_F(X_A)$	$k'_F(X_B)$	n_F
1	Used column G[a]	11.20	5.20	4.8	4.30	2.45	3.5
2	Used column K[a]	11.50	5.60	4.5	4.40	2.65	3.2
3	New column K	13.50	6.60	4.5	5.10	3.00	3.3
4	New column G	12.67	5.75	5.0	4.88	2.67	3.8
5	New column K	16.65	7.75	4.8	6.30	3.50	3.7
6	New column B	15.00	7.46	4.4	5.86	3.36	3.5
7	New column B	15.96	7.21	5.0	6.00	3.21	3.9
Mean		13.78	6.51	4.71	5.26	2.98	3.56
S.D.		2.15	1.00	0.25	0.80	0.40	0.26
R.S.D. (%)		15.6	15.4	5.3	15.2	13.4	7.2

[a] The stationary phase had experienced more than 3000 injections.

capacity (Q) in the stationary phases can be estimated to be as small as *ca.* 4%, because $k'_{A_{1c}}(X_B)$ is proportional to the fourth power of Q (eqn. 1).

Further, the fitted parameters can be examined. The fitted first differential coefficient for HbF is 0.65 in eqn. 19, while the estimated value, which is calculated from eqn. 14 using the values in Table II, is 0.75. This difference can be explained as the difference between $\beta_{A_{1c}}(X_A, X_B)$ in the isocratic elution and stepwise elution modes. Actually, the value of $\beta_{A_{1c}}(X_A, X_B)$ with stepwise elution was to be about 15% larger than that with isocratic elution, because the influence of the third mobile phase C from the preceding sample analysis still remains in the succeeding analysis (eqn. 10).

The high-resolution mode can almost be regarded as isocratic elution with mobile phase B. The fitted first differential coefficient was 0.40 (Table I). This can be estimated as $\alpha_{A_{1c}F}(X_B)$ from eqn. 6 theoretically. From Table II, the selectivity in mobile phase A [$\alpha_{A_{1c}F}(X_A)$] is 0.38, whereas that in mobile phase B [$\alpha_{A_{1c}F}(X_B)$] is 0.46. In the high-resolution mode, the first differential coefficient will be an intermediate value between $\alpha_{A_{1c}F}(X_A)$ and $\alpha_{A_{1c}F}(X_B)$, since elution with mobile phase B should become slightly weaker owing to the remaining influence of the preceding mobile phase A.

Peak identification

The above-discussed correlation can be utilized in peak identification in HPLC. An example of the application of this method is shown in the chromatogram in Fig. 5. The first step of the method is a search for the largest peak as A_{1c} in the region with retention times shorter than 2.0

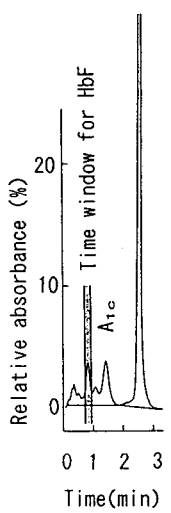

Fig. 5. Time window for peak identification with calculated retention time of HbF in the high-speed mode. The retention time of A_{1c} ($t_{RA_{1c}}$) was 1.37 min. By using the time window (0.77 ± 0.10 min) calculated from eqn. 19, the peak with a retention time of 0.78 min was identified as HbF. The shaded zone is the time window for HbF.

min. In Fig. 5, the retention time of A_{1c} ($t_{RA_{1c}}$) is regarded as 1.37 min. Next, the retention time of HbF (t_{RF}) can be calculated and is estimated as 0.77 min from eqn. 19. Then the time window for the peak identification can be adjusted to 0.77 ± 0.10 min. This width of the window (± 0.10 min) is allowed for compensation for the variation in the mobile phase. There is also the retention time variation caused by peak overlap. This can be estimated to be 0.02 min at most by simulating overlapped Gaussian peaks. The time window could identify the peak at a retention time of 0.78 min with HbF. This method is useful for the identification of other important components such as A_{1a}, A_{1b} and l-A_{1c}, and is also effective in the high-resolution mode.

CONCLUSION

Retention time correlation is preserved in stepwise elution in glycated haemoglobin analysis. This is based on the conservation of the selectivity and the retention time ratio in the two mobile phases in the event of stationary phase variations. The accuracy of peak identification can be improved by calculating the retention time relationship for each chromatogram instead of using time windows fixed in advance.

ACKNOWLEDGEMENTS

The authors wish to thank Mr. Hidetoshi Hara, Ms. Kazuko Terunuma (Mito General Hospital, Hitachi, Ltd., Katsuta, Japan), and Ms. Masako Mizuno (Hitachi Research Laboratory, Hitachi, Ltd., Hitachi, Japan) for developing the glycated haemoglobin analyzer.

REFERENCES

1. E. Grushka and I. Zamir, *High Performance Liquid Chromatography*, Wiley, New York, 1989, pp. 529–561.
2. M. Mizuno, K. Tochigi, M. Ito and J. Miura, *Bunseki Kagaku*, 40 (1991) 395.
3. M. Mizuno, K. Tochigi, M. Ito and J. Miura, *Bunseki Kagaku*, 40 (1991) 907.
4. R. Fluckiger and H.B. Mortensen, *J. Chromatogr.*, 429 (1988) 279.
5. E. Bisse and H. Wieland, *J. Chromatogr.*, 434 (1988) 95.
6. S.H. Ashoor and M.A. Osman, *J. Chromatogr.*, 393 (1987) 329.
7. R. Gill, A.C. Moffat, R.M. Smith and T.G. Hurdley, *J. Chromatogr. Sci.*, 24 (1986) 153.
8. P. Jandera and J. Churacek, *J. Chromatogr.*, 91 (1974) 207.
9. W. Markowski and W. Golkiewicz, *Chromatographia*, 25 (1988) 339.

Journal of Chromatography A, 661 (1994) 153–159
Elsevier Science B.V., Amsterdam

CHROMSYMP. 2883

On-line solid-phase extraction with automated cartridge exchange for liquid chromatographic determination of lipophilic antioxidants in plasma

Maria Hedenmo* and Britt-Marie Eriksson

Bioanalytical Chemistry, Astra Hässle AB, S-431 83 Mölndal (Sweden)

ABSTRACT

A fully automated liquid chromatographic method is described based on a Prospekt solid-phase extraction unit for the analysis of lipophilic indenoindolic antioxidants in plasma. Plasma samples, mixed with internal standard, were injected onto C_8-cartridges. After washing, the samples were eluted and transferred to a C_8-analytical column, where separation was performed. The eluent was monitored by electrochemical detection. Owing to the nature of the drugs investigated care had to be taken to avoid adsorption losses in vials and capillaries. The method, which was found to give excellent recoveries (100.9%, $n = 8$) and repeatability (R.S.D. ± 1.7%), is time-saving compared to a previously used assay with sample work-up by liquid–liquid extraction.

INTRODUCTION

The fully automated sample handling system Prospekt was first described in 1987 by Nielen *et al.* [1] and so far only a few papers regarding applications using this system have been published [1–3]. We found the Prospekt system attractive as it allows a complete on-line analysis with disposable extraction cartridges at reasonable cost. The cartridge is automatically replaced for every new sample, which means that plasma samples can be injected directly into the chromatographic system without giving problems with blockage by protein precipitate. A similar system OSP-2 with automated cartridge exchange is commercially available from E. Merck [4–6]. Automated techniques are also available using the robotic Zymark system [7] and the ASPEC system from Gilson [8,9].

In systems where the extraction cartridge is an integrated part of the liquid chromatograph, the flow through the cartridge is constant and well defined. This should lend to better reproducibility compared with conventional liquid–solid extraction systems.

In this study we have used the Prospekt system for analysing an indenoindolic antioxidant, H 290/51, in plasma samples in connection with pharmacokinetic studies, and the method has been evaluated against a procedure employing liquid–liquid extraction.

EXPERIMENTAL

Chemicals and reagents

H 290/51, H 290/39 and H 290/58 as hydrochlorides, and H 261/54 (Fig. 1) were synthesized at Medicinal Chemistry, Astra Hässle AB (Mölndal, Sweden). Hydrochloric acid was of analytical grade, Merck (Darmstadt, Germany) and tris(hydroxymethyl)aminomethane (Tris), analytical grade, was of Fluka quality (Buchs, Switzerland). Acetonitrile and methanol were of

* Corresponding author.

0021-9673/94/$07.00
SSDI 0021-9673(93)E0807-7

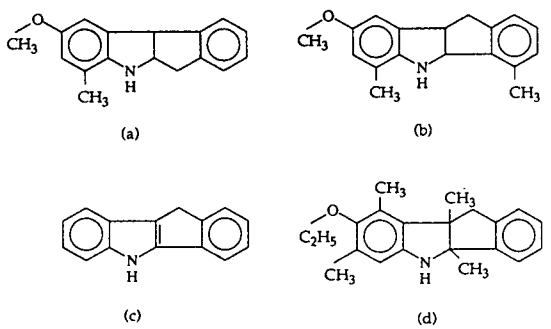

Fig. 1. Structural formulas of (a) H 290/51, (b) H 290/39, (c) H 261/54 and (d) H 290/58.

HPLC grade from Rathburn (Walkerburn, UK) and ethanol (95%) came from Kemetyl (Stockholm, Sweden). Water was purified through an ELGA purification system, ELGA (Wycombe Bucks, UK).

Chromatographic system

A schematic representation of the chromatographic system is shown in Fig. 2. It comprised a Gynkotek Model 480 pump, (Munich, Germany), a CMA/200 refrigerated autosampler (CMA Microdialysis, Stockholm, Sweden), a Spark Holland Prospekt module with a microprocessor, a cartridge transport system, three six-port valves and a solvent delivery unit (SDU) (Emmen, Netherlands), with the capability of delivering up to six solvents. Glass vials (0.3 ml) from Chromacol (London, UK) and plastic vials (0.3 ml) from CMA Microdialysis (Stockholm, Sweden) have been used. Plastic tips, Finntip for pipettes, came from Labsystems Oy (Helsinki, Finland). The solid-phase extraction cartridges (10 × 2 mm I.D.) contained 20 mg of Analytichem C_8, C_{18} or CN packings (30–40 μm) and were distributed by Spark Holland. The analytical columns (150 × 4.6 mm I.D.) Kromasil C_8 (5 μm) and Hypersil CN (5 μm) came from Eka Nobel (Bohus, Sweden) and Shandon (Astmoor, UK), respectively.

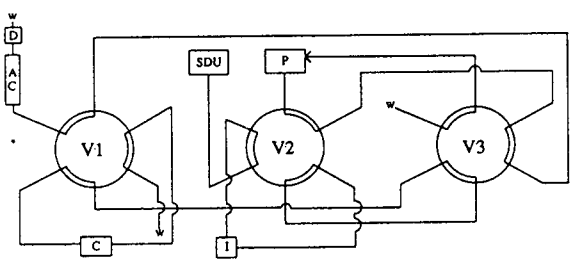

Fig. 2. Schematic representation of the chromatographic system. V1, V2, V3 = valves belonging to the Prospekt unit; SDU = solvent delivery unit; P = pump; I = injector; C = cartridge; AC = analytical column; D = detector; w = waste.

The mobile phase, pH 8.5, contained Tris (50 m*M*), hydrochloric acid (12 m*M*) and 65% of acetonitrile. The three solutions used for conditioning and loading of the cartridge were (1) 100% methanol, (2) 5% of methanol in water and (3) Tris (50 m*M*), hydrochloric acid (12 m*M*), pH 8.5, with 15% of acetonitrile. Prior to use the solutions and the mobile phase were ultrasonicated for degassing. The flow-rate over the analytical column was 1.0 ml/min and the eluent was monitored by a Waters M460 electrochemical detector (Millipore, Milford, MA, USA) at a potential of +0.70 V. Data was collected and processed by a Multichrom chromatographic data system (VG Data Systems, Altrincham, UK).

Sample preparation procedure

The frozen plasma samples were thawed at room temperature, mixed and placed on ice. Aliquots of 100 μl of the samples were pipetted into 1.5-ml glass vials and 100 μl of the internal standard solution of H 290/39 in Tris buffer pH 8.5 with 15% acetonitrile were added. The samples were mixed and centrifuged for 5 min at 3000 *g*. After centrifugation the samples were transferred to glass vials (0.3 ml) and placed in the autosampler. Aliquots of 20–50 μl of the samples were injected.

Plasma reference samples were prepared by mixing 100 μl of a solution containing H 290/51 and H 290/39 in Tris buffer pH 8.5 with 15% of acetonitrile, and 100 μl of drug-free plasma.

Solid-phase extraction procedure

The extraction cartridge connected to valve 1 (see Fig. 2) was activated with 2 ml of solvent 1 (100% methanol) followed by 2 ml of solvent 2

(5% methanol in water) and *ca.* 4 ml of solvent 3 (Tris buffer pH 8.5 with 15% acetonitrile). During the time of activation the autosampler was prepared for injection. Prior to injection the flow-rate over the cartridge was changed from 2 ml/min to 0.5 ml/min. By a signal from the microprocessor the sample was injected into the solid-phase extraction system. The plasma sample was applied to the cartridge and most of the plasma matrix was removed with solvent 3. After 1.5 min of loading valve 1 was switched, and the mobile phase eluted the compounds backwards onto the analytical column for separation and detection. At the same time data collection started. After 5 min of elution, valve 1 switched back and washing of the capillaries started with 3 ml of solvent 2, followed by 4 ml of solvent 1. The procedure is summarized in Table I.

We have used valve 2 to be able to make direct injections onto the analytical column. This was done to check the condition of the analytical column and to determine recoveries of the extraction procedure. By switching valve 2 the sample goes directly from the injector to the analytical column for separation and detection, see Fig. 2.

By switching valve 3 it is possible to utilize the solvent delivery unit for washing of the analytical column after long series of plasma samples to prevent deterioration.

RESULTS AND DISCUSSION

Acid-labile conjugate

H 290/51 can also exist as an acid-labile conjugate in authentic plasma samples. It was therefore necessary to keep the pH above 8 in order not to hydrolyse the conjugate and get falsely increased results. This was examined by adding buffer at pH 2, pH 7 and pH 9 to authentic rabbit plasma samples. The samples were allowed to stand for 20 min before the internal standard in Tris buffer (pH 8.5) was added. The samples were then analysed according to the described method. The results were similar at pH 7 and 9, whereas at pH 2 there was a three-fold increase in concentration. In plasma samples containing less conjugate, such as dog and rat plasma, the increase was not as pronounced as in rabbit plasma. In one strain of rabbits the conjugate existed to a large extent, up to 10 times the concentration of free drug. It was then difficult to stabilize the conjugate and the thawed samples were injected immediately and not allowed to stand in the injector. All

TABLE I

SOLID-PHASE EXTRACTION PROCEDURE

Time (min:s)	Switch valve No.	Solvent	Flow (ml/min)	Comment
00:00		1	2.0	Change of cartridge Activation of cartridge with 100% methanol
01:00		2		Activation of cartridge with 5% methanol in water
02:00		3		Conditioning of cartridge with Tris buffer pH 8.5 containing 15% acetonitrile
03:50			0.5	Adjusting flow-rate through cartridge
04:00				Injection of sample
05:30	1			Start of elution backwards onto the analytical column Start of data collection
10:30	1	2	2.0	End of elution Washing of cartridge and capillaries with 5% methanol in water
12:00		1		Washing with 100% methanol
14:00			0.0	End of washing

aqueous buffer solutions used had a pH of 8.5 to avoid hydrolysing any acid-labile conjugate.

Adsorption

At a pH above 8 adsorption losses in vials have to be taken into consideration. As can be seen in Table II adsorption was significant in plastic vials for both H 290/51 (3.5 μM) and H 290/39 (3.5 μM). The figures show adsorption losses in plastic vials compared with glass vials. The amount adsorbed increased with increasing pH but the presence of plasma decreased the adsorption losses considerably. No adsorption could be seen in glass vials containing a buffer of pH 8.5 with 7.5% of acetonitrile.

Adsorption may also occur in the capillaries between the injector and the cartridge. Adding more than 20% of acetonitrile to solvent 3 to avoid adsorption in the capillaries decreased the recovery of the solid-phase extraction procedure to below 90%, while with 15% acetonitrile, as used in the method, the adsorption was inhibited without lowering the recovery. One way to demonstrate adsorption effects in the capillaries is to switch valve 2 1 min before elution starts. The mobile phase with its high percentage of acetonitrile (65%) will desorb the amount that has been adsorbed in the injector and onto the capillary walls between the injector and valve 2.

We have demonstrated this by using a Tris buffer at pH 8.5 without acetonitrile as solvent 3. The amount adsorbed can be seen in the chromatogram (Fig. 3) as two minor peaks eluting approximately 1 min before the main components. The sample in the chromatogram contained H 290/51 (3.5 μM) and H 290/39 (3.5 μM). The sample was loaded onto a C_8-cartridge with Tris buffer pH 8.5 for 2 min.

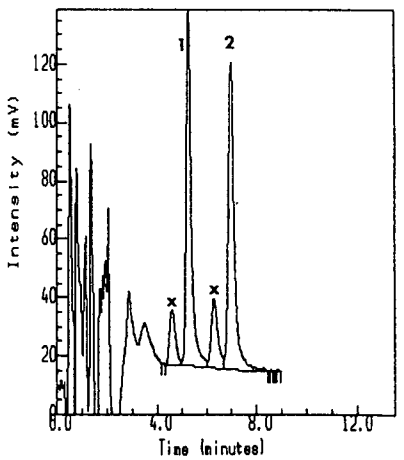

Fig. 3. Adsorption in capillaries when using Tris buffer pH 8.5 without acetonitrile as loading solution (solvent 3). 1 = H 290/51; 2 = H 290/39; × = substance adsorbed in capillaries between injector and valve 2.

TABLE II

ADSORPTION LOSSES IN PLASTIC VIALS COMPARED WITH GLASS VIALS

Buffer solutions contained 7.5% of acetonitrile. Plasma samples contained 7.5% of acetonitrile after dilution with buffer solution (1:1).

pH	H 290/51		H 290/39	
	Solution	Plasma	Solution	Plasma
7	13%	8%	41%	12%
9	21%	8%	54%	13%
10	24%	15%	63%	21%
9[a]	39%	16%	80%	23%

[a] No acetonitrile added.

In a previously used liquid–liquid extraction method, using 5% butan-2-ol in hexane at alkaline pH, followed by evaporation and reconstitution in an acidic solution, the chromatographic system consisted of a Hypersil CN analytical column and a mobile phase at pH 7 with 40% of acetonitrile. Under these conditions no adsorption occurred in vials or capillaries. When using the Prospekt unit, where plasma is directly injected into the chromatographic system, we had to use a pH above 8 because of the earlier mentioned acid-labile conjugate. To prevent adsorption in the chromatographic system we increased the amount of acetonitrile in the mobile phase by 20%. The analytical column was changed from Hypersil CN to Kromasil C_8 to obtain reasonable retention times.

The original Prospekt unit contained a Marathon autosampler, that we exchanged for a CMA/200 autosampler because of its insufficient washing capability for this particular application. The Marathon washes the needle and the loop, using alternately one out of four vials containing

washing solution, and the washing volume was not variable. These lipophilic compounds were adsorbed in the needle and to the rotorseal in the injection valve giving contamination between samples. The CMA/200 sucks washing solution from a separate bottle and there is no risk of contamination of the solution. The washing volume is also variable.

The CMA/200 autosampler cannot fully communicate with the Prospekt microprocessor as the Marathon does, but it is possible to give the CMA/200 a signal to start loading sample and to keep the sample in the loop until it receives an injection signal, by using the Prospekt's auxiliary outputs.

More lipophilic compounds

We have also tested the described method to see if it was possible to handle compounds even more inclined to adsorb in capillaries and vials. H 261/54 which is a dihydroindenoindole (see Fig. 1) gave severe adsorption in capillaries also for plasma samples. Increasing the amount of acetonitrile in solvent 3 to 20% still gave adsorption on capillary walls for H 261/54 along with a decreasing recovery of H 290/51 which was used as internal standard. We changed the internal standard to H 290/58 (see Fig. 1), which is more strongly retarded on C_8 cartridges compared with H 290/51, and could then increase the amount of acetonitrile in solvent 3 to 30% and avoid adsorption in capillaries with a maintained recovery of 99%.

Stability

The stock solutions of H 290/51 (60 μM) and the internal standard H 290/39 (60 μM) dissolved in 95% ethanol were stable in a refrigerator for at least five months. The working standard solutions of H 290/51 (3.5 μM) and H 290/39 (3.5 μM) diluted 17 times in Tris buffer pH 8.5 were stable in a refrigerator for more than 3 days when kept from light. Authentic plasma samples stored at − 70°C were stable for up to one year. In the injector with a refrigerated sample tray, authentic plasma samples and standard addition samples were stable for at least 24 h, except for samples from one strain of rabbits, as mentioned earlier.

Solid-phase extraction cartridges

The recovery of H 290/51 on C_8, C_{18} and CN cartridges was investigated as a function of loading time, which is the time between injection of sample onto the cartridge and start of elution. The flow, the amount of acetonitrile in solvent 3 and the elution time were kept constant at 0.5 ml/min, 15% and 5 min, respectively. The recovery was constant for C_8 and C_{18} cartridges when varying the loading time from 0.5 to 2.5 min, but for the CN cartridges it rapidly decreased after 1 min. No change in plate count of the separation column could be seen for any of the cartridges investigated when varying the loading time. The pressure over the analytical column increased at an loading time of less than 1 min.

To ensure that sample work-up conditions do not have to be modified due to inter-batch variation of cartridges under routine analysis, three different batches of C_8 cartridges were tested for recovery and repeatability. There was no difference between the three batches. Since then we have used several batches of C_8 cartridges and not found any differences between them.

Optimization

The importance of the factors which were expected to influence the extraction recovery and the ruggedness of the method was investigated.

A statistical full factorial experimental design [10] was initially performed and the 4 factors studied were (1) amount of acetonitrile in the washing solution (solvent 3 in Table I), (2) flow-rate through the cartridge, (3) loading time, *i.e.* time between injection of sample onto the cartridge and start of elution and (4) elution time, *i.e.* time from start of elution of the cartridge till disconnection from the analytical column.

Each factor was studied at two levels, for factor (1) 10 and 20% of acetonitrile, factor (2) 0.5 and 1.0 ml/min, factor (3) 0.5 and 2.5 min and for factor (4) 1 and 5 min. For 4 factors there are sixteen (2^4) possible combinations of factor levels. The experiments were made in duplicate and moreover one of the recovery experiments was performed at a level in between, *i.e.* (1) 15%, (2) 0.75 ml/min, (3) 1.5

min and (4) 3 min. This was repeated four times to provide an indication of the repeatability of the procedure. A statistical analysis of variance (ANOVA) [10] was performed to evaluate the effects of the experimental variables. The elution time had no statistically significant effect on the recovery, while, as expected, a high amount of acetonitrile in the washing solution in combination with a long loading time and a high flow-rate resulted in low recoveries, 12% for H 290/51 and 53% for H 290/39.

We chose a flow-rate of 0.5 ml/min as it seemed to be advantageous in terms of chromatographic efficiency, calculated as number of theoretical plates. Referring to the tendency of the indenoindolic compounds to adsorb in the capillaries, a high concentration of acetonitrile, 15%, in the washing solution was preferable. The recovery was unaffected by a change in loading time from 0.5 to 2.5 min, giving a very robust method. Even a loading time of 4 min gave as high a recovery as 97%. The front peak was somewhat larger at a loading time of 0.5 min compared with 1.5 min as chosen.

Detection

The response of the electrochemical cell slowly decreased when injecting a long sequence of plasma samples. It was thus important to have an internal standard that behaved similar to H 290/51 and compensated for a minor decrease in response. It was possible to re-establish the response at its former level by polishing the working electrode surface with acetone. This was done every second day.

Quantitation and accuracy

The ratios of the peak height of the analyte to that of the internal standard in the plasma reference samples were measured and used for calculation of plasma concentration. The recoveries were calculated by comparing the peak height ratios of analyte to internal standard of plasma reference samples with those obtained for the same amount injected directly onto the analytical column.

The within-day variability was determined by performing replicate analyses of plasma samples containing 3.2 μM ($n = 10$), 55 nM ($n = 8$) and 20 nM ($n = 8$) of H 290/51 and 3.5 μM ($n = 26$) of H 290/39. The recoveries and coefficients of variation of H 290/51 were $104.1 \pm 0.8\%$, $100.9 \pm 1.7\%$ and $104.0 \pm 3.6\%$, respectively. The extraction yield of the internal standard calculated by direct comparison of peak heights in reference samples to those from direct injection onto the analytical column was $96.0 \pm 4.0\%$ ($n = 10$).

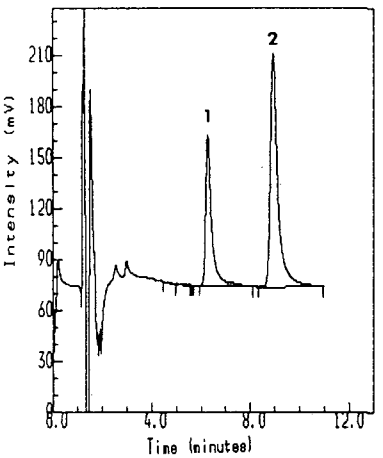

Fig. 4. Chromatogram of dog plasma sample. 1 = H 290/51: 1.75 μM and 2 = H 290/39 (internal standard): 3.5 μM. 20 μl of sample injected.

The within-cartridge variability ($n = 7$) was $101.7 \pm 0.5\%$ for a plasma sample containing 3.2 μM of H 290/51 and thus it was possible to

TABLE III

RESULTS FROM SOLID-PHASE EXTRACTION (SPE) METHOD COMPARED WITH LIQUID–LIQUID EXTRACTION (LLE) METHOD

The values are expressed as nmol/l ± R.S.D.

LLE method	SPE method	±R.S.D.(%)
349	370	4.1
491	526	4.9
900	960	4.6
3680	3860	3.4
4380	4680	4.7
5100	5500	5.3
8700	9000	2.4
9700	9840	1.0
14 100	14 400	1.5

re-use a cartridge at least 7 times without noticing any decrease in capacity. The analytical columns lasted for up to 1.5 months when using a mobile phase at pH 8.5.

The method was linear up to at least 50 μM and the limit of quantitation was estimated at 20 nM when injecting 10 μl of plasma. Fig. 4 shows a chromatogram of an authentic dog plasma sample containing 1.75 μM of H 290/51.

The method was evaluated by comparison analyses of dog plasma samples made with the earlier mentioned liquid–liquid extraction method. Good agreement between the two methods was found, as shown in Table III. The analyses with the liquid–liquid extraction method were performed one year earlier than those with the solid-phase extraction method.

CONCLUSION

Using the Prospekt solid-phase extraction unit for laboratory routine analyses is simple, straight forward and time-saving compared to regular liquid–liquid extraction procedures. The described method for determination of lipophilic indenoindolic compounds yielded high recoveries, good precision and accuracy.

ACKNOWLEDGEMENTS

We thank Mr. Sten Olov Jacobson for help with implementation of the Carnegie injector into the Prospekt system. We would also like to thank Dr. Bengt-Arne Persson for helpful reading of the manuscript.

REFERENCES

1 M.W.F. Nielen, A.J. Valk, R.W. Frei, U.A.Th. Brinkman, Ph. Mussche, R. de Nijs, B. Ooms and W. Smink, *J. Chromatogr.*, 393 (1987) 69.
2 J. Slobodnik, E.R. Brouwer, R.B. Geerdink, W.H. Mulder, H. Lingeman and U.A.Th. Brinkman, *Anal. Chim. Acta*, 268 (1992) 55.
3 G. Hotter, J. Ramis, G. Bioque, C. Sarmiento, J.M. Fernández, J. Roselló-Catafan and E. Gelpi, *Chromatographia*, 36 (1993) 33.
4 D. Chollet and P. Künstner, *J. Chromatogr.*, 577 (1992) 335.
5 D. Chollet and M. Salanon, *J. Chromatogr.*, 593 (1992) 73.
6 D. Chollet, P. Künstner and M. Wermeille, *J. Chromatogr.*, 629 (1993) 89.
7 T.L. Lloyd, T.B. Perschy, A.E. Gooding and J.J. Tomlinson, *Biomed. Chromatogr.*, 6 (1992) 311.
8 M.C. Rouan, J. Campestrini, J.B. Lecaillon, J.P. Dubois, M. Lamontagne and B. Pichon, *J. Chromatogr.*, 456 (1988) 45.
9 M.C. Rouan, F. Le Duigou, J. Campestrini, J.B. Lecaillon and J. Godbillon, *J. Chromatogr.*, 573 (1992) 59.
10 E. Morgan, *Chemometrics: Experimental Design*, Wiley, London, 1991.

Journal of Chromatography A, 661 (1994) 161–168
Elsevier Science B.V., Amsterdam

CHROMSYMP. 2939

Purification of human tumour necrosis factor by membrane chromatography

Janja Luksa, Viktor Menart, Stjepan Milicic and Breda Kus

Lek, Pharmaceutical and Chemical Company, Research and Development, Celovska 135, 61000 Ljubljana (Slovenia)

Vladimira Gaberc-Porekar

Institute of Chemistry, Hajdrihova 19, 61000 Ljubljana (Slovenia)

Djuro Josic*

Octapharma Pharmazeutika GmbH, Oberlaaer Str. 235, A-1100 Vienna (Austria)

ABSTRACT

The recombinant human tumour necrosis factor α from an extract of *Escherichia coli* was enriched to homogeneity according to specific activity and sodium dodecyl sulphate–polyacrylamide gel electrophoresis by purification using anion-exchange HPLC and hydrophobic interaction HPLC. Parallel experiments with the same separation methods, but carried out with membrane chromatography on compact discs, gave similar results in terms of yield and purity of the product. The active form of the protein is a trimer. The second isolation step, hydrophobic interaction chromatography, causes dissociation of the trimer into monomers and a partial loss of the biological activity of the protein. The phenomenon occurs on both the column and the disc. This in turn indicates strongly that the dissociation of the protein is a consequence of interaction between the sample and the hydrophobic ligand, and is not caused by non-specific interaction with the matrix.

INTRODUCTION

Tumour necrosis factor α (TNF-α) is secreted by macrophages and belongs to the cytokines, a group of molecules which includes also interferons and interleukins. These polypeptides with molecular masses of up to 25 000 are involved in the complex regulation of cellular growth and differentiation. They also play a key role in inflammation, immunity and haemopoiesis [1]. TNF-α has antitumour properties and it displays antiviral activity and *in vitro* cytotoxicity to certain transformed cell lines [2,3]. However, TNF is also implicated in the pathogenisis of cachexia (wasting), rheumatoid arthritus and inflammatory tissue destruction [4,5]. Because of these properties, the molecule is of considerable interest as a potential therapeutic agent and for purposes of diagnosis.

Human TNF-α is an unglycosylated polypeptide, containing 157 amino acids, with a molecular mass of 17 350. The active form of the molecule is a trimer [6]. Using recombinant DNA technology, the TNF gene was cloned. The recombinant protein was expressed in *E. coli* [7]. The biologically active protein can be purified by anion-exchange HPLC (HPAEC), followed by hydrophobic interaction HPLC (HPHIC) [8]. However, the recovery of biologically active TNF-α after HPHIC is low owing to partial dissociation of the trimer into monomers [9].

* Corresponding author.

0021-9673/94/$07.00
SSDI 0021-9673(93)E0946-R

High-performance membrane chromatography (MC) [10–14] was introduced chiefly for biopolymer separations. Several techniques of membrane construction exist. One strategy consists in bundling several thin membranes made of synthetic hollow fibres of cellulose, another involves compact, porous, disc-shaped membranes, made of silica gel or polymer supports, and a third option is a combination of these two strategies. Excellent results in biopolymer separations have been achieved especially with separation devices that consist of several bundled membranes and with compact discs made of poly(glycidyl methacrylate) [10–13].

Membranes have several important advantages over HPLC columns. The chromatographic separation is carried out on a wide, thin disc, so that there is only a low pressure drop even at high flow-rates [10,11]. The fact that separation can be carried out very quickly is due to the fast reaction kinetics in such systems [15,16]. Membrane chromatography has been successfully used for separations of enzymes [16,17], serum and membrane proteins [11,18] and even for the isolation of such large molecules as plasmid DNA [19]. This method allows a separation within a shorter period of time than a chromatographic column with the same capacity. Because of the structure of the support, its surface is reduced. Therefore, the possibility of non-specific interactions of the sample with the surface of the support is much lower [10,11]. A comparison between MC and HPLC of TNF-α was undertaken in order to find out whether the dissociation of TNF and consequently the loss of its biological activity take place during interaction with the hydrophobic ligand, or whether it is a consequence of non-specific interaction with the support material.

EXPERIMENTAL

Production of recombinant TNF-α

Synthetic gene human TNF-α with codons optimized for expression in *E. coli* in plasmid BBG4 was purchased from British Biotechnology (Oxford, UK). The gene was properly inserted into the expression vector pCYTEXPl, supplied by MEDAC (Hamburg, Germany). Intracellular expressison of biologically active TNF-α was achieved by growing cells at 28°C to an absorbance of 0.3–0.35, followed by incubation for a further 4–5 h at 41°C. In *E. coli* TG1 the high copy number of expression plasmid was maintained by addition of 50–70 μg/ml of ampicillin in Luria-Bretani medium made according to the laboratory manual [23]. With this system, a TNF expression level of about 1% total cellular protein in laboratory flask culture was reproducibly achieved.

An extract of bacterial cells was the starting material for the purification of human TNF-α. For this the cells were harvested, treated with a lysozyme solution (1 mg/ml) and subsequently sonicated (W358 sonicator; Ultrasonic, New York, USA). The clear supernatant after centrifugation, containing 1.3 mg/ml of protein, was subjected to chromatographic purification. The biological activity of TNF-α at the beginning was $5 \cdot 10^5$ U/mg of protein. The activity was based on its cytotoxic effect on transformed mouse fibroplasts, cell line L 929, measured according to the method of Marnenout *et al.* [20].

Chemicals

All chemicals were of analytical-reagent grade from Merck (Darmstadt, Germany) or Serva (Heidelberg, Germany). Water of HPLC grade was obtained either from Baker (Gross-Gerau, Germany) or from Merck. All chemicals required for electrophoresis were purchased from Pharmacia (Vienna, Austria).

Instrumental

A gradient liquid chromatographic system was used, consisting of two FPLC pumps, type P-500, an LCC-50 plus control unit, a UV monitor with a 280-nm filter, an REC 102 recorder and a FRAC-100 fraction collector (all from Pharmacia). Sample application loops with volumes between 0.5 and 10 ml were used. Equipment for electrophoresis was obtained from Hoefer Scientific (Vienna, Austria) or Pharmacia.

Chromatography on compact discs and on HPLC columns

For HPAEC, a Mono-Q column (50 × 5 mm I.D.) (Pharmacia) was used. A Quick Disk Q

compact disc 25 mm in diameter and 3 mm thick (Säulentechnik Knauer, Berlin, Germany) was used for anion-exchange (AE) MC. For HPHIC a phenyl-Superose column (50 × 5 mm I.D.) (Pharmacia) and a butyl-Sepharose fast flow column (60 × 8 mm I.D.) were used. Parallel HI-MC was carried out on a Quick Disk C4 unit 25 mm in diameter and 3 mm thick (Säulentechnik Knauer).

The buffers for HPAEC were (A) 10 m*M* Tris–HCl (pH 8.0) and (B) 10 m*M* Tris–HCl containing 1.0 *M* NaCl. For HPHIC, buffer A was 1.7 *M* ammonium sulphate in 0.1 *M* potassium phosphate (pH 7.0) and buffer B was 0.1 *M* potassium phosphate (pH 7.0). Both the column and the disc were regenerated with 0.1 *M* acetic acid. Other chromatographic conditions are given in the figure captions.

Electrophoresis

The dialysed and freeze-dried samples were dissolved in 62.5 m*M* Tris–HCl buffer (pH 6.8) containing 3% (w/v) sodium dodecyl sulphate (SDS), 5% (v/v) mercaptoethanol, 10% (v/v) glycerol and 0.0015 (w/v) bromophenol blue. In the other experiments, 20–50 μl of sample were taken from the collected fractions after HPLC or MC separation. These samples were subsequently mixed with a buffer that contained five times higher concentrations of the substances mentioned above. The amount of buffer used in the experiments was measured in such a way as to restore the original concentration after dilution by the sample. SDS–polyacrylamide gel electrophoresis (PAGE) was carried out by the Laemmli method [21] on a 15% separating gel with a 3% stacking gel. The amount of protein applied

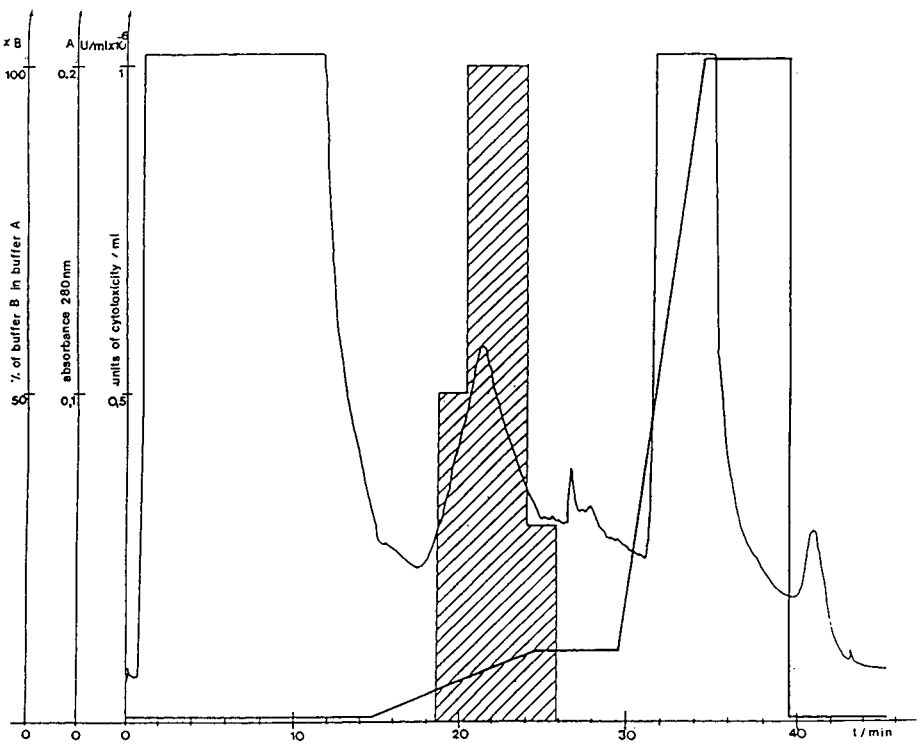

Fig. 1. First purification step: HPAEC of TNF-α. A 10-ml volume of extract from bacterial cells, containing 13 mg of protein and $6.5 \cdot 10^6$ units of TNF-α, were applied to a Mono-Q column and eluted with a sodium chloride gradient (see Experimental). Chromatographic conditions: flow-rate 1 ml/min; pressure, 15–20 bar; room temperature. The gradient is shown in the chromatogram. The fractions containing TNF activity are hatched. The presence of TNF-α in these fractions was also confirmed by subsequent dot blot analysis.

was between 10 and 75 μg per line, depending on the purity of the sample.

Dot blot analysis

The dot blot method was adopted from protocols for Western blotting [22,23]. A nitrocellulose membrane (Pharmacia) was spotted with samples (5 μl of each) from fractions which were collected after separation and dried. The remaining free groups of the membrane were blocked with excess of protein (3% bovine serum albumin in Tris-buffered saline, pH 7.4). Primary polyclonal rabbit anti-human recombinant TNF-α antibodies (Sigma, Deisenhofe, Germany), were bound to TNF-α from collected fractions. In a second step, goat anti-rabbit antibodies conjugated with horseradish peroxidase (Bio-Rad, Vienna, Austria) were bound and detected as blue spots by adding 4-cholor-1-naphthol solution.

RESULTS AND DISCUSSION

Figs. 1 and 2 show the two HPLC steps for the purification of recombinant human TNF-α, *i.e.*, HPAEC and HPHIC. The parallel experiments carried out with AE-MC and hydrophobic interaction (HI) MC are shown in Figs. 3 and 4, respectively. The purification steps agree with those presented by Lin and Yamamoto [8] in their purification scheme for TNF. The enrichment in the final product was from $5 \cdot 10^5$ units/mg of protein in the cell culture lysate to about $5 \cdot 10^7$ units/mg of protein after HPHIC. The initial concentration of TNF-α in the cell lysate was 1%, which means that the product was purified practically to homogeneity. This also agrees with the results that were obtained by Lin and Yamamoto [8].

Using membrane chromatography with compact discs as separation units, a considerable decrease in separation time was achieved, from

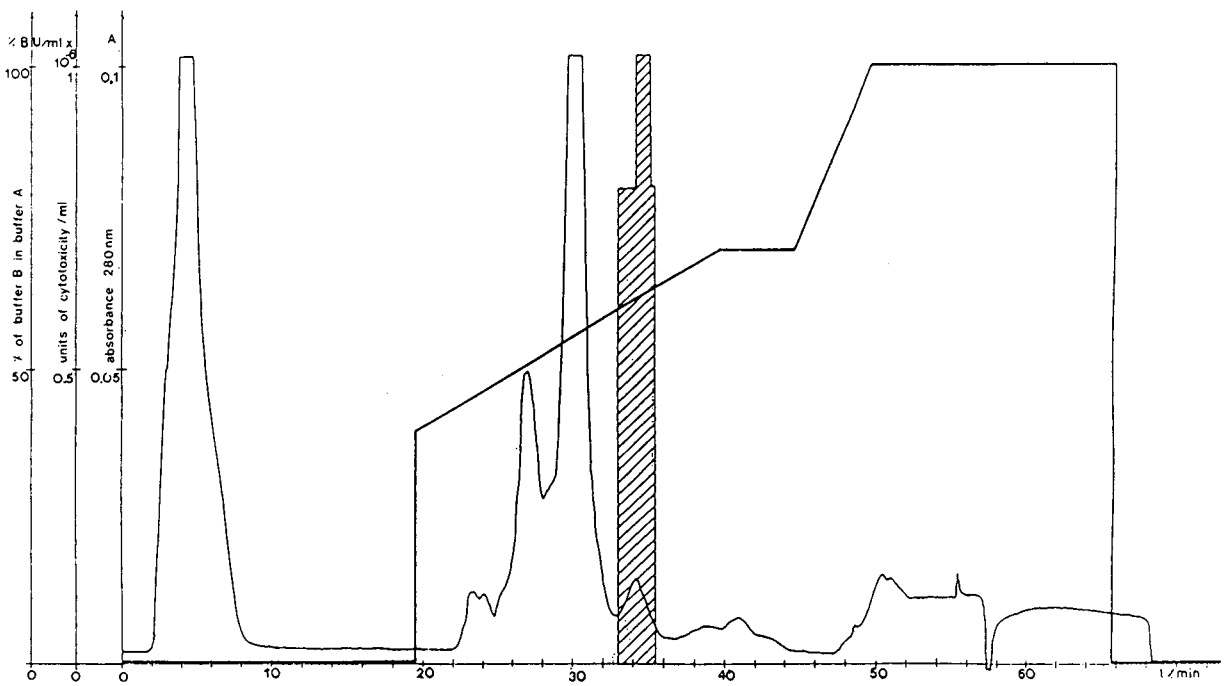

Fig. 2. Second purification step: HPHIC of TNF-α. A 10-ml volume of AE-HPLC product containing biologically active TNF-α was applied to a phenyl-Superose column and eluted by lowering the ammonium sulphate concentration (see Experimental). Chromatographic conditions: flow-rate, 0.5 ml/min; pressure, 15–20 bar; room temperature. The gradient is shown in the chromatogram. The fractions containing TNF activity are hatched.

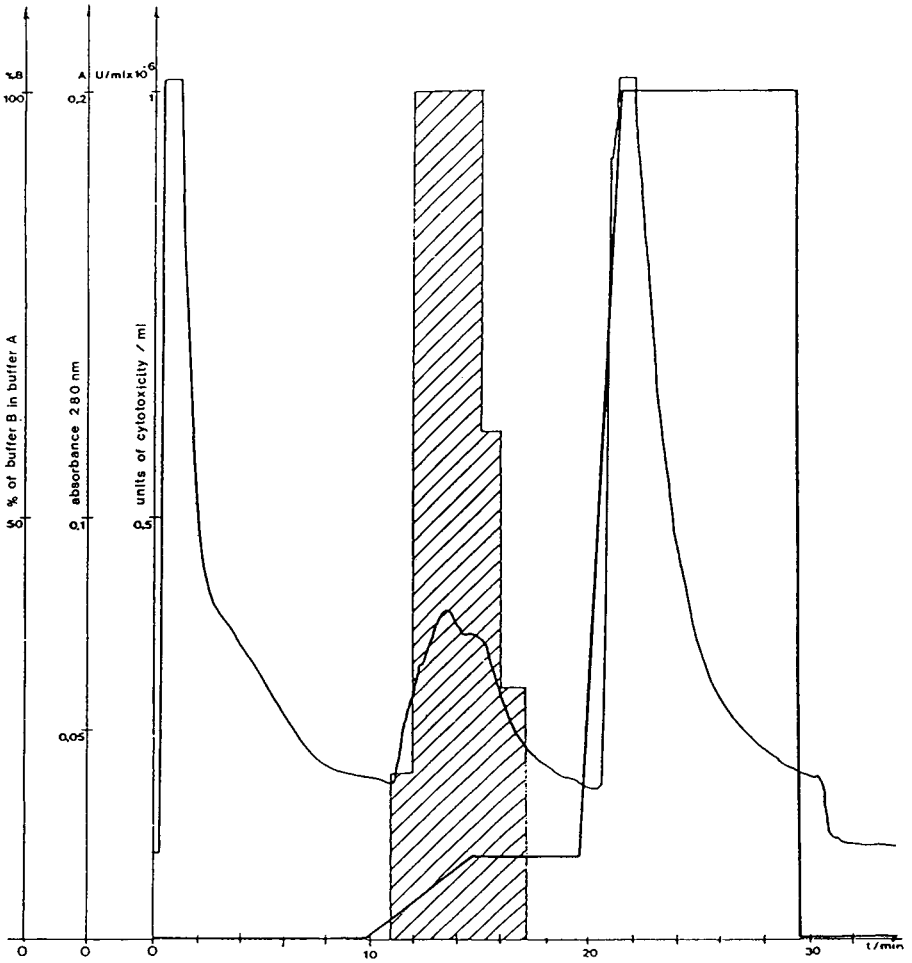

Fig. 3. AE-MC of TNF-α. The separation unit was a Quick Disk Q membrane. Chromatographic conditions: flow-rate, 3 ml/min; pressure, 5 bar; room temperature. Other conditions as in Fig. 1.

120 min in HPLC to about 60 min in MC. Fig. 5 shows the SDS-PAGE of samples with TNF-α activity from separations by HPLC and MC.

The HPAEC separation was performed on a Mono-Q column and the MC separation with a Quick Disk Q unit. The quaternary amine ligand density on a poly(glycidyl methacrylate) membrane (Quick Disk Q) is about 2.2 μM/g, which is two orders of magnitude lower than ligand density on a Mono-Q support (about 600–700 μM/g). However, the capacity of this anion-exchange membrane is about 30–40 g of BSA per gram of support, which is comparable to the capacity of Mono-Q material [11]. A similar relationship for ligand density exists between the butyl-Sepharose fast flow support (about 50 μM/ml) and a Quick Disk butyl membrane (0.85 μM/g). The separation and recovery of TNF-α on a butyl-Sepharose fast flow column (not shown here) was comparable to those on the phenyl-Superose column (Fig. 2). Because of the different geometry and mass transfer on a chromatographic column and on a membrane unit, a direct comparison of these two devices is difficult. In this paper, a comparison according to TNF-α purity and recovery of biologically active factor was made.

Although the chromatograms from HPLC

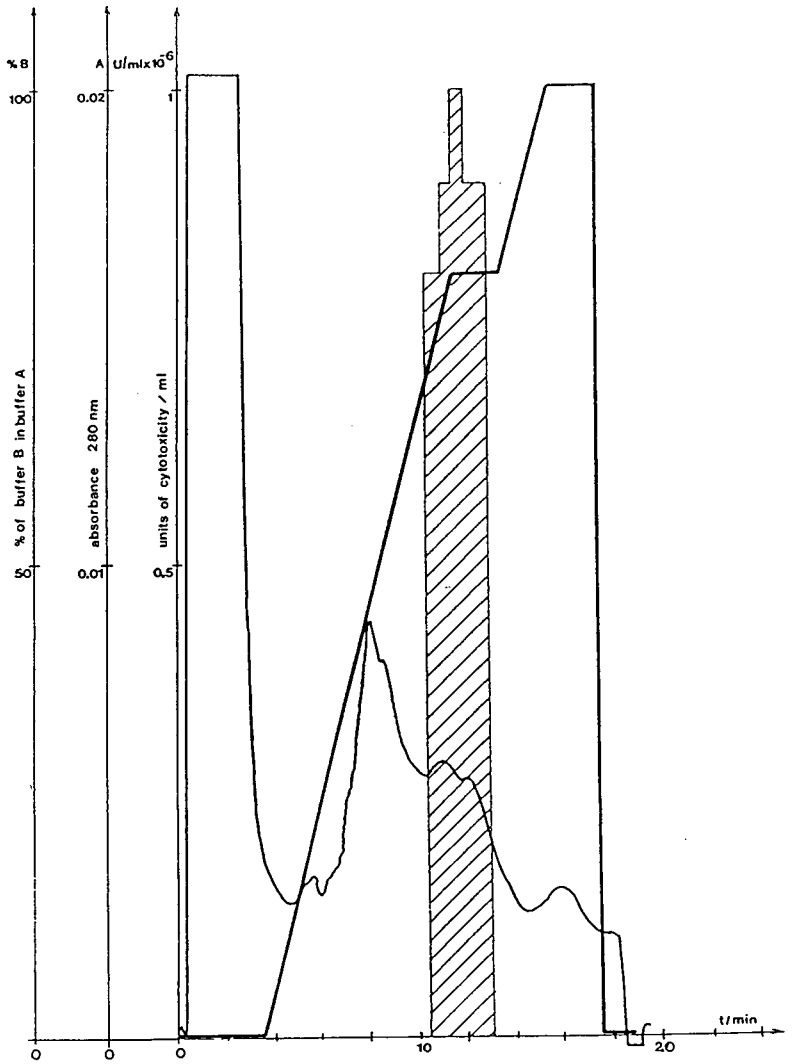

Fig. 4. HI-MC of TNF-α. The separation unit was a Quick Disk C4 (butyl) membrane. Chromatographic conditions: flow-rate, 3 ml/min; pressure, 5 bar; room temperature. Other conditions as in Fig. 2.

show superior peak resolution, the purity was comparable according to the electrophoretic presentation (*cf.*, Fig. 5): after HPAEC (lane 4), after AE-MC (lane 6), after HPHIC (lanes 2 and 3) and after HI-MC (lane 7). The specific activity of the final product was identical after purification by either HPLC or MC, *i.e.*, $5 \cdot 10^7$ units/mg protein.

The recovery of biologically active TNF was about 20% and therefore fairly low with both purification methods, HPLC and MC. A large loss in yield occurs in the second purification step, HPHIC, using both the column and the compact disc (membrane) methods. In order to establish what actually becomes of the TNF-α polypeptide, dot blot analyses of the biologically active fraction and of the other fractions from HPLC and MC were carried out. The results of the dot blot analysis are shown in Fig. 6. Apart from the peak where biological activity was found (hatched in Figs. 2 and 4), intense blue dots appear in fractions Acl–Ac5 also. These are

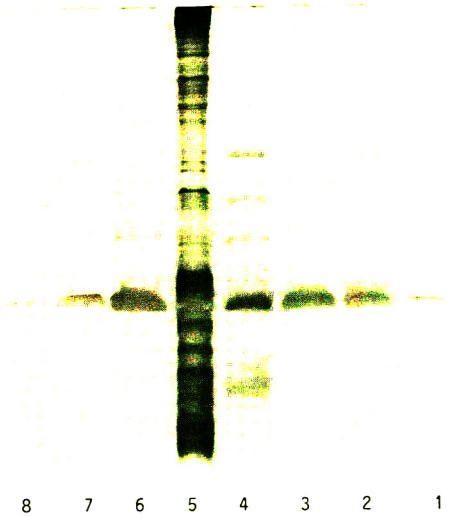

Fig. 5. SDS-PAGE of the fractions from anion-exchange HPLC and MC and from hydrophobic interaction HPHIC and MC. Lanes: 1 = myoglobin (marker protein for molecular mass 17 000); 2 = TNF-α purified by HPHIC column (C_4 functional group); 3 = TNF-α purified by HPHIC column (phenyl functional group); 4 = mixture of proteins obtained in HPAEC purification step; 5 = cell proteins of recombinant *E. coli* in extract; 6 = mixture of proteins obtained in AE-MC purification step; 7 = TNF-α purified by HI-MC compact disc (C_4 functional group); 8 = myoglobin.

the fractions that were obtained by rinsing the column with acidic acid. The protein in these fractions has lost its biological activity.

Kunitani *et al.* [9] investigated the behaviour of TNF-α in HPHIC. They found that the biologically active trimer dissociates on the column into biologically inactive monomers. They also found that the dissociation is reversible, *i.e.*, the monomers can be re-associated into the native, biologically active trimer. Re-association could not be achieved in our experiments, because the TNF-α monomers could not be eluted from either the column or the disc (membrane) unless strongly denaturing conditions (acetic acid) were applied. This causes a further decrease in biological activity in this fraction of recovered protein. However, Kunitani *et al.* [9] reported that an increase in sample volume favours the dissociation and therefore denaturation on the HPHIC column. The dissociation of TNF on a hydrophobic interaction column seems to be dependent on the form of the ligand. When butyl-Sepharose fast flow material was used, a similar separation performance and recovery to those on a phenyl-Superose column were

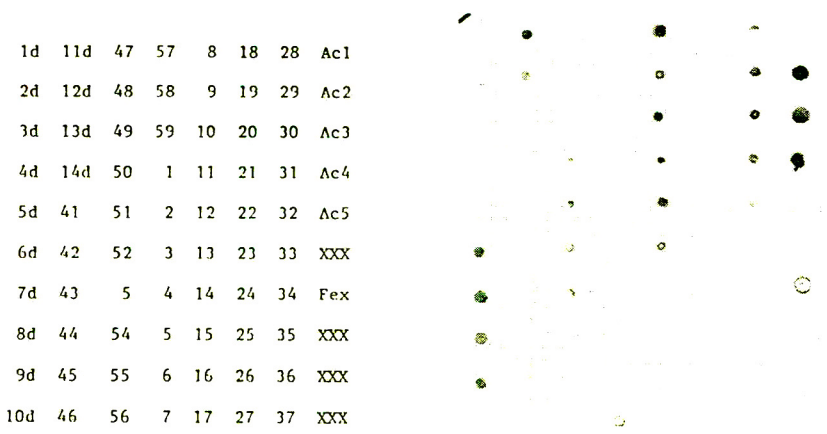

Fig. 6. Dot blot analyses of the fractions from hydrophobic interaction chromatography. 1d–14d = Fractions from Quick Disk Q separation. Fractions 6d–9d show also TNF-α activity in test with transformed mouse fibroblasts (see Experimental). These fractions correspond to the hatched region in Fig. 3 and lane 6 in SDS-PAGE in Fig. 5. 41–59 = Fractions from Quick Disk C4 separation. Fractions 51–54 show also TNF-α activity in biological test (see above). These fractions correspond to the hatched region in Fig. 4 and lane 7 in SDS-PAGE in Fig. 5. 1–37 = Fractions from HPHIC column. Fractions 8–13 show also TNF-α activity in biological test and correspond to the TNF-α peak in the chromatogram (hatched region in Fig. 2). Some TNF-α could be subsequently washed out with 0.1 *M* potasium phosphate buffer (spots 28–31). However, these fractions did not have biological activity. Fractions 8–13 correspond also to lane 2 in SDS-PAGE in Fig. 5. Ac1–Ac5 = Fraction collected during washing of hydrophobic compact disc (Quick Disk C4) with acetic acid. XXX = No sample.

achieved (see above). The large application volumes that were used here may explain the large amount of dissociated TNF-α. Apparently the interaction of the TNF-α takes place with the hydrophobic ligand, *i.e.*, the phenyl or butyl groups in HPHIC and the butyl groups in HI-MC. The surface of the support does not seem to be involved. The experiment with a disc, with contains hydroxy groups instead of quaternary amine groups, supports this assumption. In this experiment, the sample was applied under identical conditions on such a membrane unit, *i.e.*, means in 1.7 *M* ammonium sulphate. Neither retention nor loss of biological activity of TNF-α was observed (not shown here). Further, the identical behaviour of TNF-α in both HPLC and MC is in agreement with this conclusion. Despite the much smaller surface area of the support, due to the structural characteristics of the disc [10,11], the amount of dissociated TNF-α did not decrease when the separation was carried out by MC. The portion of dissociated TNF-α also could not be decreased by increasing the flow-rate, *i.e.*, by shortening the period of contact between the sample and the disc.

REFERENCES

1 L.J. Old, *Nature*, 326 (1987) 330.
2 E.A. Carswell, L.J. Old, R.L. Kassel, S. Green, N. Fiore and B. Williamson, *Proc. Natl. Acad. Sci. U.S.A.*, 72 (1975) 3666.
3 G.H.W. Wong and D.W. Goeddel, *Nature*, 323 (1986) 819.
4 B. Beutler and A.A. Cerami, *Rev. Biochem.*, 57 (1988) 505.
5 F.A. Wolheim, D. Heinegard, M. Palladino, T. Saxne and N. Tatal, *Arthritis Rheum.*, 30 (1987) 129.
6 P. Wingfield, R.H. Pain and S. Craig, *FEBS Lett.*, 211 (1987) 179.
7 L.J. Old, *Science*, 230 (1985) 630.
8 L.S. Lin and R. Yamamoto, in R. Burgess (Editor), *Protein Purification: Micro to Macro*, Alan R. Liss, New York, 1987.
9 M.G. Kunitani, R.L. Cunico and S.J. Staats, *J. Chromatogr.*, 443 (1988) 205.
10 J.A. Gerstner, R. Hamilton and S.M. Cramer, *J. Chromatogr.*, 596 (1992) 173.
11 Dj. Josic, J. Reusch, K. Löster, O. Baum and W. Reutter, *J. Chromatogr.*, 510 (1992) 59.
12 T. Tennikova, B.G. Belenkii and F. Svec, *J. Liq. Chromatogr.*, 13 (1990) 63.
13 B. Chompluvier and M.R. Kula, *J. Chromatogr.*, 539 (1991) 315.
14 O.-W. Reif and R. Freitag, presented at the *17th International Symposium on Column Liquid Chromatography, Hamburg, May 9–14, 1993.*
15 M. Unarska, P.A. Davies, M.P. Esnouf and B.J. Bellhouse, *J. Chromatogr.*, 519 (1990) 53.
16 H. Abou-Rebyeh, F. Körber, K. Schubert-Rehberg, J. Reusch and Dj. Josic, *J. Chromatogr.*, 566 (1991) 341.
17 V. Prpic, R.J. Uhing and T.W. Gettys, *Anal. Biochem.*, 208 (1993) 155.
18 Dj. Josic, F. Bal and H. Schwinn, *J. Chromatogr.*, 632 (1993) 1.
19 N. van Huguh, J.C. Motte, J.F. Pilette, M. Decleire and C. Colson *Anal. Biochem.*, 210 (1993) 1.
20 A. Marnenout, L. Fransen, J. Tavernier, J. Van der Heyden, R. Tizard, E. Kawashima, A. Shaw, M.J. Johnson, D. Seman, R. Mueller, M.-R. Ruysschaert, A. Van Vliet and W. Fiers, *Eur. J. Biochem.*, 152 (1985) 515.
21 U.K. Laemmli, *Nature*, 227 (1970) 680.
22 E. Harlow and D. Lane, in *Antibodies, a Laboratory Manual*, Cold Spring Harbor Laboratory, Cold Spring Harbor, NY, 1988, p. 471.
23 J. Sambrook, E.F. Fritsch and T. Maniatis, in C. Nolan (Editor), *Molecular Cloning, a Laboratory Manual*, Cold Spring Harbor Laboratory, Cold Spring Harbor, NY, 2nd ed., 1989, p. 18.

Journal of Chromatography A, 661 (1994) 169–174
Elsevier Science B.V., Amsterdam

CHROMSYMP. 2880

Determination of glycoalkaloids in potato tubers by reversed-phase high-performance liquid chromatography

Robert J. Houben and Kommer Brunt*

Netherlands Institute for Carbohydrate Research TNO, Rouaanstraat 27, 9723 CC Groningen (Netherlands)

ABSTRACT

A relatively fast and simple method for the determination of the glycoalkaloids α-solanine and α-chaconine in potato tubers is described. The glycoalkaloids are concentrated from potato samples by solid-phase extraction with a disposable C_{18} cartridge column. The recovery, determined by addition of glycoalkaloid standard to a potato sample, was found to be better than 90%. The relative standard deviation of the measured glycoalkaloid levels was less than 4%. For the reversed-phase (RP) HPLC analysis of basic compounds, *e.g.*, glycoalkaloids, too strong an interaction with the residual silanol groups of the stationary phase can be disadvantageous. In this work, acetonitrile–water was used as eluent with an RP-HPLC column with a reduced amount of residual silanol groups. The absence of buffer in the eluent increases the lifetime of the column and makes this system very suitable for the routine determination of glycoalkaloids.

INTRODUCTION

Glycoalkaloids are natural toxins, occurring in all parts of plants of the *Solanum* species [1]. These toxins are considered to form a natural resistance of the plant against parasites and diseases. In the potato plant, high concentrations of glycoalkaloids occur in the peel of the tuber (concentration about 300–600 mg/kg), in the sprouts (about 2000–4000 mg/kg) and in the flowers (3000–5000 mg/kg) [2]. The glycoalkaloid level averaged over the whole potato tuber is about 100 mg/kg. This relatively high level may even increase when the potato tuber experiences a kind of stress situation, *e.g.*, resulting from tuber injury or storing under non-ideal conditions [1,2].

Glycoalkaloids consist of a C_{27}-steroidal alkaloid skeleton (aglycone) to which one or more sugar groups are attached. In cultivated potatoes, α-solanine and α-chaconine, with solanidine as the aglycone, form about 95% of the total glycoalkaloid (TGA) content [2]. Glycoalkaloids are toxic to humans; the lethal dose is considered to be about 3–6 mg per kg body mass [3,4]. Therefore, commercial and especially new potato varieties are routinely screened in our institute for their glycoalkaloid content.

Chromatographic analysis of glycoalkaloids can be performed in a number of ways [4,5]. The intact glycoalkaloids can be analysed by gas chromatography (GC) after derivatization [6]. After hydrolysis of the glycoalkaloids, the aglycone skeleton can be examined by GC without the need for derivatization [7]. The disadvantage of this approach, however, is the high temperature necessary for analysing the compounds, which limits the lifetime of the GC column. For routine determinations of the glycoalkaloids present in potato tubers, high-performance liquid chromatography (HPLC) is probably the method of choice.

For the RP-HPLC of basic compounds, *e.g.*, glycoalkaloids, too strong an interaction between the compounds and the residual silanol groups of the stationary phase can be disadvantageous. This interaction leads to peak tailing and to an

* Corresponding author.

0021-9673/94/$07.00
SSDI 0021-9673(93)E0812-9

increase in retention time. The residual amount of silanol groups (the relative acidity of the column packing) greatly influences the retention behaviour of basic compounds [8]. Therefore, the analysis of basic compounds using standard RP-HPLC columns does not always give good results. Most of the HPLC methods described so far require the use of a relatively large amount of buffer in the eluent [9–12]. In this work, better results were obtained with an RP-HPLC column with a reduced amount of residual silanol groups (less acidic column). With this column, analyses for glycoalkaloids did not require the use of buffer in the eluent. The absence of buffer salts increases the lifetime of the column and also prevents the rapid deterioration of seals in the HPLC instrument. Therefore, this system is very suitable for the routine determination of glycoalkaloids in potato tubers.

EXPERIMENTAL

Solid-phase extraction

For concentrating the glycoalkaloids from the potato samples, solid-phase extraction (SPE) with a disposable Sep-Pak C_{18} column (Waters, Milford, MA, USA) was used. The glycoalkaloids were extracted from the potato sample by ion-pair extraction using 0.02 *M* sodium 1-heptanesulphonate (Sigma, St. Louis, MO, USA) in 0.17 *M* acetic acid (Merck, Darmstadt, Germany). For the preparation of solutions, distilled water that had been further purified with a Milli-Q system (Waters) was used. The SPE pretreatment was adapted from that of Carman *et al.* [9]. After thoroughly mixing the sample, insoluble constituents were removed by filtration. The pretreatment of the SPE column consisted of flushing with methanol (analytical-reagent grade; Labscan, Dublin, Ireland) followed by flushing with sodium 1-heptanesulphonate solution. The filtered potato sample was eluted through the SPE column and interfering constituents of the sample were removed by flushing with acetonitrile–water (20:80, v/v). The acetonitrile mixtures were prepared by mixing water or buffer with an azeotrope consisting of acetonitrile–water (83.7:16.3, v/v). The azeotrope mixture was obtained by distillation of HPLC effluents. Finally, the glycoalkaloids were eluted from the Sep-Pak column by applying acetonitrile–buffer (60:40, v/v). The buffer was prepared by dissolving 3 g of $(NH_4)_2HPO_4$ (Merck) in 1 l of water.

HPLC of glycoalkaloids

HPLC was performed using a Gilson (Middleton, WI, USA) Model 305 pump, a manometer, a Marathon (Spark, Emmen, Netherlands) autosampler with a 20-μl loop, an Applied Biosystems (San Jose, CA, USA) Model 757 UV detector operating at 202 nm and a Spectra-Physics (San Jose, CA, USA) SP 4600 integrator. Initially, a RoSil C_8 (3 μm) column (150 × 4.6 mm I.D.) (Bio-Rad, Richmond, CA, USA) with a Nucleosil 120-5 C_8 precolumn (30 × 4 mm I.D.) (Machery–Nagel, Düren, Germany) was used. The eluent consisted of acetonitrile–3 g/l $(NH_4)_2HPO_4$ buffer (45:55, v/v). However, the chromatographic conditions severely reduced the lifetime of this column system. Better results were obtained when using a Nucleosil 5 C_{18}-AB (5 μm) column (250 × 4 mm I.D.) with a Nucleosil 100-5 C_{18}-AB precolumn (30 × 4 mm I.D.) (Machery–Nagel). With this column system, glycoalkaloids were separated with acetonitrile–water (60:40, v/v) as the eluent at a flow-rate of 1 ml/min. For the determination of the glycoalkaloids, standards of α-solanine (purity >99%; Roth, Karlsruhe, Germany) and α-chaconine (purity >95%, Roth) dissolved in acetonitrile–buffer (60:40, v/v) were used. Quantitative analysis of the glycoalkaloid level was performed by using external standard solutions, which were directly injected into the chromatographic system.

RESULTS AND DISCUSSION

Fig. 1 shows the general structure of the glycoalkaloids α-solanine and α-chaconine present in potato tubers. For HPLC, the glycoalkaloids have to be concentrated from the sample. Further, they must be separated from interfering constituents present in the potato tuber. Fig. 2 illustrates the sample clean-up resulting from SPE. For this experiment, 10 ml of potato tuber extract were eluted through the SPE column, which was then flushed with 5 ml of water or 5 ml of acetonitrile–water (20:80, v/v). Final-

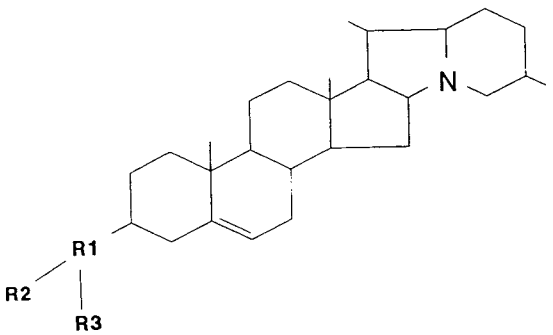

Fig. 1. General structure of the glycoalkaloids α-solanine and α-chaconine present in potato tubers. The sugar group consists of R1 = β-D-galactose, R2 = β-D-glucose and R3 = α-L-rhamnose for α-solanine and R1 = β-D-glucose and R2 = R3 = α-L-rhamnose for α-chaconine.

ly, the column was eluted with 3 ml of acetonitrile–buffer (60:40, v/v) and the eluate was subjected to HPLC.

As can be seen from Fig. 2, the glycoalkaloids can be efficiently separated from other constituents by flushing the SPE column with acetonitrile–water (20:80, v/v). Almost no sample clean-up was achieved by rinsing the column with water. This experiment indicates that complex chromatograms would be obtained without sample pretreatment, which would prevent the accurate determination of the glycoalkaloids. The relatively strong interaction between the SPE column and the glycoalkaloids results in an efficient sample clean-up, but also indicates that complete elution of the glycoalkaloids necessitates a relatively strong eluent. Table I gives the measured peak areas of α-solanine and α-chaconine after HPLC of a potato tuber sample in relation to the composition of the SPE eluent used. For this experiment, the SPE eluents consisted of mixtures of acetonitrile (ACN) with water or with buffer.

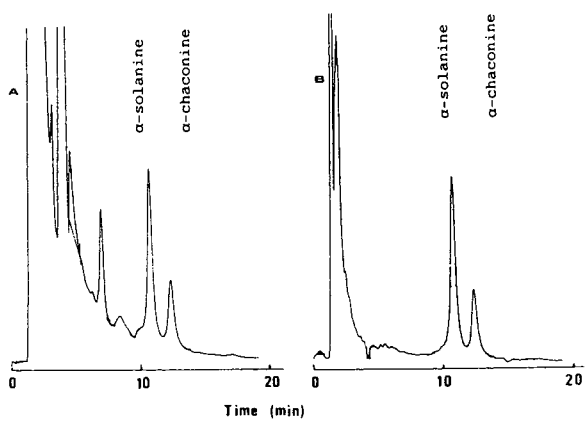

Fig. 2. Illustration of sample clean-up resulting from solid-phase extraction. (A) Washing SPE column with 5 ml of water; (B) washing SPE column with 5 ml of acetonitrile–water (20:80, v/v). The chromatograms were obtained with the RoSil C_8 column.

From Table I, it is clear that elution with a mixture of acetonitrile and buffer gives the highest recovery for the glycoalkaloids. The presence of buffer reduces the interaction between the glycoalkaloids and the silanol groups on the SPE packing. In this way, almost all of the glycoalkaloids are eluted from the SPE column in the first step. Only very small amounts of glycoalkaloids were recovered when using acetonitrile–water. To verify that the glycoalkaloids are completely eluted with acetonitrile–buffer (60:40, v/v), a known amount of glycoalkaloid standard was added to a potato tuber sample in which the glycoalkaloid level was known. For this experiment, the glycoalkaloid standard was dissolved in sodium 1-heptanesulphonate and 1, 2 or 5 ml of this standard solution was added to the potato sample. The samples were then treated and analysed as described above. In Table II are given the calculated recoveries after addition of the standard to the potato sample, which originally contained 72 mg/kg of α-solanine and 46 mg/kg of α-chaconine. As can be seen, the recovery of the glycoalkaloids is generally more than 90% under the SPE conditions used.

Initially, HPLC of glycoalkaloids was performed with a Rosil C_8 column. However, this column contained a relatively large amount of residual silanol groups on the silica packing. This type of column is routinely prepared by attaching C_8 chains to the silica packing by reaction with silanol groups [8,13]. However, because of steric hindrance usually only 30–40% of the silanols present on the packing are consumed in this reaction [8]. Even after end-capping, a relatively large number of silanol groups remain on the silica surface, which complicates the analysis of basic compounds. Because of the acidic character of the silanols, an ion-exchange process can occur between silanols and basic compounds, which can result in peak tailing and excessive retention times [8]. The retention mechanism of

TABLE I

PEAK AREAS OF α-SOLANINE AND α-CHACONINE WITH THREE DIFFERENT SPE ELUENTS

Average results of two individual analyses. Samples analysed with a RoSil column.

Compound	Eluent		
	ACN–water (45:55, v/v)	ACN–water (83.7:16.3, v/v)	ACN–buffer (60:40, v/v)
1st elution, 2 ml			
α-Solanine	0.54	1.8	10.8
α-Chaconine	0.25	1.8	8.4
2nd elution, 1 ml			
α-Solanine	0.75	1.9	0.75
α-Chaconine	0.45	3.0	0.81

the glycoalkaloids on standard RP-HPLC columns thus involves both hydrophobic interaction with the alkyl chain and ion-exchange interaction with residual silanol groups on the silica packing. The interaction with the silanol groups can be suppressed by addition of buffer to the eluent. In our experiments, a high-pH buffer was used, which prevents the protonation of the glycoalkaloids and thus interferes with the ion-exchange process. In this way, analyses were performed with an eluent consisting of acetonitrile–$(NH_4)_2HPO_4$ buffer (45:55, v/v). The relatively high pH of the buffer solution (*ca.* 8) severely reduces the lifetime of the column, however, probably because of dissolution of the silica packing. Another approach to prevent silanol interaction is to use a low-pH eluent (pH < 2.5), which prevents the ionization of the silanol groups [8]. RP-HPLC of glycoalkaloids with a low-pH buffer was recently described by Friedman and Levin [12]. They found an increased resolution with increasing acidity of the column. However, these findings are confusing because the columns were tested using a relatively large amount of buffer in the eluent, which masks the acidity of the column to a great extent. Further, a drawback of this approach is deterioration of the column because stripping of the alkyl ligands

TABLE II

RECOVERIES OF α-SOLANINE AND α-CHACONINE AFTER ADDITION OF GLYCOALKALOID STANDARD TO A POTATO TUBER SAMPLE

Average results of two individual analyses, samples analysed with a Nucleosil column.

Compound	Standard solution added (ml)	Recovery (%)		
		1st elution, 2 ml	2nd elution, 1 ml	Total
α-Solanine	1	74	13	87
	2	83	7	90
	5	81	9	90
α-Chaconine	1	83	14	97
	2	89	10	99
	5	86	19	105

from the silica surface may occur [8,13]. In conclusion, the determination of basic compounds with standard RP-HPLC columns often requires the use of low- or high-pH eluents, thus limiting the lifetime of the column.

The determination of glycoalkaloids by using polymer-based RP-HPLC columns (*e.g.*, with a polystyrene–divinylbenzene packing) with an acetonitrile–water eluent only gave good results for standards; for potato tuber samples, no good separation between the glycoalkaloids and the interfering compounds was obtained. The total lack of silanol groups on the polymer packing made this type of column insufficiently selective for application to glycoalkaloids. The results indicated that a relatively small amount of silanol groups may be necessary for the determination of basic compounds.

We concluded that the determination of glycoalkaloids requires a column with a reduced amount of silanol groups. The residual amount of silanols present on the column packing should be large enough to distinguish between glycoalkaloids and interfering constituents, but on the other hand low enough to be able to elute the glycoalkaloids without using buffers in the eluent. Good baseline resolution was obtained when using acetonitrile–water (60:40, v/v) as the eluent with a Nucleosil C_{18}-AB column (see Fig. 3). The absence of buffer in the eluent increases the lifetime of the column and diminishes problems caused by rapid wearing out of seals present in the pump and in the injector.

The standard deviation of the measured glycoalkaloid level was determined by repeatedly analysing a sample on one day and on several days. These analyses resulted in a relative standard deviation that was better than 4% for a sample containing 200 mg/kg of glycoalkaloids. Further, the glycoalkaloid levels determined with the described HPLC method were compared with those obtained with a spectrophotometric method. This method consisted of bisolvent extraction of glycoalkaloids from the sample followed by reaction with a mixture of phosphoric acid and paraformaldehyde and measurement of the absorbance at 600 nm [14,15]. As can be seen in Fig. 4, a good correlation was found between the two methods for 64 different potato tuber samples. The deviation from the ideal line (dashed line in Fig. 4) is most pronounced for a high glycoalkaloid level. This slight deviation is

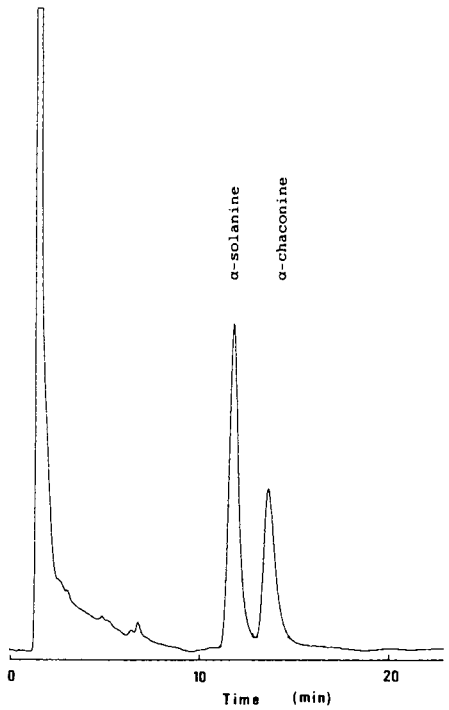

Fig. 3. Example of glycoalkaloid determination with an RP-HPLC column especially suitable for basic compounds. A Nucleosil 5 C_{18}-AB column was used with acetonitrile–water (60:40, v/v) as the eluent.

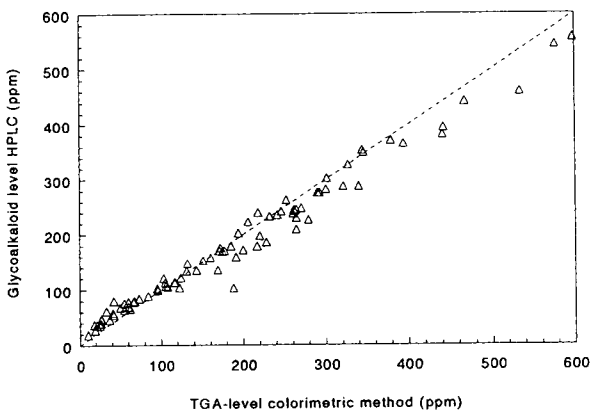

Fig. 4. Comparison between glycoalkaloid levels determined by the described HPLC method and a spectrophotometric method. TGA = total glycoalkaloids. For the 64 potato tuber samples, a correlation coefficient of 0.989 was found.

probably caused by the fact that the HPLC method only determines the glycoalkaloids α-solanine and α-chaconine, whereas the spectrophotometric method determines the total glycoalkaloid level. The high correlation coefficient (0.989) found between the two methods, however, confirms the accuracy of the method of analysis.

In conclusion, the relatively simple and fast method described for the determination of glycoalkaloids in potato tubers has the advantages of high precision and accuracy. Further, the chromatographic conditions with a column especially suitable for basic compounds are advantageous because of the long lifetime of the column. These conditions make routine determinations of glycoalkaloids possible.

REFERENCES

1 W.M.J. van Gelder, *Thesis*, Agricultural University of Wageningen, Wageningen, 1989, pp. 9–33.
2 S.J. Jadhav, R.P. Sharma and D.K. Salunkhe, *CRC Crit. Rev. Toxicol.*, 9 (1981) 21–101.
3 S.C. Morris and T.H. Lee, *Food Technol. Aust.*, 36 (1984) 118–124.
4 M. Friedman and L. Dao, *J. Agric. Food Chem.*, 40 (1992) 419–423.
5 D.T. Coxon, *Am. Potato J.*, 61 (1984) 169–183.
6 S.F. Herb, T.J. Fitzpatrick and S.F. Osman, *J. Agric. Food Chem.*, 23 (1975) 520–523.
7 R.R. King, *J. Assoc. Off. Anal. Chem.*, 63 (1980) 1226–1230.
8 D. Chan Leach, M.A. Stadalius, J.S. Berus and L.R. Snyder, *LC · GC Int.*, 1 (1988) 22–30.
9 A.S. Carman, Jr., S.S. Kuan, G.M. Ware, O.J. Francis, Jr., and G.P. Kirschenheuter, *J. Agric. Food Chem.*, 34 (1986) 279–282.
10 R.J. Bushway, E.S. Barden, A.W. Bushway and A.A. Bushway, *J. Chromatogr.*, 178 (1979) 533–541.
11 K. Saito, M. Horie, Y. Hoshino, N. Nose and H. Nakazawa, *J. Chromatogr.*, 508 (1990) 141–147.
12 M. Friedman and C.E. Levin, *J. Agric. Food Chem.*, 40 (1992) 2157–2163.
13 C.F. Poole and C.A. Schuette, *Contemporary Practice of Chromatography*, Elsevier, Amsterdam, 1984.
14 S.L. Wang, C.L. Bedford and N.R. Thompson, *Am. Potato J.*, 49 (1972) 302–308.
15 J. Sachse and F. Bachmann, *Z. Lebensm.-Unters.-Forsch.*, 141 (1969) 262–274.

Journal of Chromatography A, 661 (1994) 175–180
Elsevier Science B.V., Amsterdam

CHROMSYMP. 2925

Determination of aflatoxins in food by use of an automatic work station

Gunda Niedwetzki* and Günter Lach

Dr. Wiertz–Dipl.-Chem. Eggert–Dr. Jörissen GmbH, Handels- und Umweltschutzlaboratorium, Stenzelring 14b, 21107 Hamburg (Germany)

Klaus Geschwill

Zymark GmbH, Black & Decker-Strasse 17, 65510 Idstein/Ts. (Germany)

ABSTRACT

An automated HPLC method with postcolumn derivatization is described for the determination of aflatoxins B_1, B_2, G_1 and G_2 after an immunoaffinity column clean-up. It can be used for the determination of aflatoxins in a variety of foodstuffs such as nuts, nut-like products (pistachios, almonds, etc.) and dried fruit. The aflatoxins are extracted with methanol–water, followed by a filtration step. Dilution of the extract, mixing, immunoaffinity column clean-up, elution of the aflatoxins and optional on-line HPLC are performed by an automatic work station (Zymark BenchMate). The subsequent HPLC analysis includes a postcolumn derivatization step with iodine solution and fluorimetric detection. The method compared well with manual techniques and another automated method.

INTRODUCTION

Aflatoxins are extremely toxic secondary metabolites of the mould fungi *Aspergillus flavus* and *A. parasiticus*. The amount of aflatoxins represents a quality criterion for food and feedstuffs. As they belong to the most carcinogenic substances, there are very low legal limits for their occurrence in food. In Germany these limits are 4 μg/kg for the sum of aflatoxins B_1, B_2, G_1 and G_2 and 2 μg/kg for B_1 as a single component.

A variety of methods for the determination of aflatoxins have been described. A survey of the literature and a comparison between thin-layer chromatography (TLC), high-performance liquid chromatography (HPLC) and enzyme-linked immunosorbent assay (ELISA) were given by Werner [1].

In our laboratory, until 1991 aflatoxin analyses were performed by TLC, following published procedures [2,3]. Another TLC method has also been represented [4].

Since 1989 we have used HPLC with iodine postcolumn derivatization and immunoaffinity columns for sample clean-up. These columns contain a gel suspension of monoclonal antibodies covalently attached to a solid support. The antibodies are specific for aflatoxins B_1, B_2, G_1 and G_2. Various Clean-up [1,5,6] and HPLC [1,5–8] techniques have been published. The method used in our laboratory resembles most closely that the Trucksess *et al.* [5], which has been adopted as official first action by the AOAC as an AOAC–IUPAC method.

With the aim of rationalizing the immunoaffinity column clean-up for HPLC, we looked for possibilities of automation. Zymark provided

* Corresponding author.

0021-9673/94/$07.00
SSDI 0021-9673(93)E0891-W

an automatic work station, called BenchMate, which offers the options of pipetting, adding various reagents, weighing with an analytical balance, mixing solutions, performance membrane filtration, solid-phase extraction (SPE) (1- and 3-ml SPE columns can be used) and HPLC injection [9]. BenchMate procedures for sample preparation can be easily created and modified by the user. Another commercially available automated sample preparation system, called ASPEC, can also be used for aflatoxin analysis [10] and was compared with BenchMate.

An aflatoxin application for BenchMate had already been developed [11]. The procedure was adjusted to the requirements of our laboratory. Further research led to a simplification of our originally used procedure.

This paper describes automated HPLC analysis with postcolumn derivatization for the aflatoxins B_1, B_2, G_1 and G_2 after an immunoaffinity column clean-up. It can be used for the determination of aflatoxins in a variety of foodstuffs such as nuts, nut-like products (pistachios, almonds, etc.) and dried fruit (*e.g.*, figs).

EXPERIMENTAL

Field of application

The automated method can be applied to nuts and nut-like samples (pistachios, almonds, apricot kernels, peanuts, peanut butter, etc.), with the exception of walnuts, and to dried fruit (*e.g.*, figs). For other foods and for feedstuffs, manual techniques are performed because the sample clean-up is more complicated.

Principle

The aflatoxins, which are readily soluble in polar organic solvents, are extracted with methanol–water in a laboratory mixer, followed by a filtration sep. Dilution of the extract, mixing, immunoaffinity column clean-up, elution of the aflatoxins and optional on-line HPLC are performed by the BenchMate automatic work station (Zymark). The subsequent HPLC analysis includes a postcolumn derivatization step with iodine solution. Detection is carried out by spectrofluorimetry.

Reagents

Solvents were methanol (pure; *e.g.*, Riedel-de Haën Cat. No. 24228), LC-grade methanol and distilled water. The extraction solvent was pure methanol–distilled water (7:3, v/v). The LC mobile phase was LC-grade methanol–distilled water (1:1, v/v).

Postcolumn reagent. A 500-mg amount of iodine was dissolved in 10 ml of methanol, 1 l of water was added, the mixture was stirred for at least 10 min and filtered through a 0.45-μm filter. Fresh reagent was prepared every 2 days.

Aflatoxin standards. (1) Mixed aflatoxin stock standard solution (Sigma), containing 5 μg/ml each of aflatoxin B_1 and G_1 and 1.5 μg/ml each of aflatoxin B_2 and G_2. The flask contents [5 ml in benzene–acetonitrile (98:2)] were diluted with methanol (LC grade) to 50.0 ml giving 500 ng/ml of aflatoxins B_1 and G_1 and 150 ng/ml of B_2 and G_2). The solution was stored at −18°C.

(2) Mixed aflatoxin standard for standard addition: 40.0 ml of stock standard solution were diluted with methanol to 100.0 ml, giving 200 ng/ml of aflatoxins B_1 and G_1 and 60 ng/ml of B_2 and G_2. The solution was stored at −18°C.

(3) HPLC standard: 1.0 ml of stock standard solution was diluted with LC mobile phase to 100.0 ml, giving 5 ng/ml of aflatoxins B_1 and G_1 and 1.5 ng/ml of B_2 and G_2). This standard was kept in the dark at room temperature and prepared fresh weekly.

Apparatus

A blender with a 500-ml blender jar and cover, 18.5-cm filter-papers, prefolded, 0.45-μm membrane filters, diameter 50 and 30 nm, and borosilicate test-tubes (100 × 16 mm I.D.) were used.

The immunoaffinity columns were 1-ml AFLAPREP columns (Rhône-Poulenc) or 3-ml EasiExtract columns (Biocode). The specifications given by the manufacturers are as follows. AFLAPREP: when 4.0 ng of total aflatoxins are applied, a minimum of 80% of aflatoxin B_1 and G_1 and a minimum of 70% of aflatoxin B_2 and G_2 are recovered. The capacity of a column is 200 ng total aflatoxin, *i.e.*, larger amounts loaded result in decreased recoveries. EasiExtract: a minimum of 5.0 μg of aflatoxin B_1 is bound

when 10.0 μg are applied in 50 ml of 5% (v/v) methanol in phosphate-buffered saline. Greater than 80% of each aflatoxin is recovered when 3.5 ng of aflatoxins B_1, B_2, G_1 and G_2 are applied in 175 ml of diluted peanut butter extract (equivalent to 1 ppb of each aflatoxin).

A BenchMate automatic work station was provided by Zymark. A Baker SPE 10 system was used for manual immunoaffinity column handling. An HPLC system with a fluorescence detector and a data acquisition system was used. The LC column was Spherisorb S5 ODS-2 (250 mm × 4 mm I.D.). The postcolumn derivatization system consisted of a second LC pump, a zero-dead-volume T-piece, and a 320 cm × 0.5 mm I.D. PTFE reaction coil. Two column ovens were used with a temperature control module, heated to 35 and 70°C.

Sampling

Examples are as follows. For pistachios, a laboratory sample of about 50 kg was taken by sampling 10% of the bags following the random principle. The whole sampling material was mixed and divided into five subsamples of 10 kg. Three 10-kg subsamples of pistachios were ground in a 50-l cutter and a portion of each was analysed as described below. For figs, *ca.* 30 kg of sample were mixed and homogenized in a cutter after addition of 20% of water. Test portions were taken from various locations in the fig paste.

Extraction

The manual sample preparation prior to the BenchMate procedure was as follows. A 50-g homogenized sample was weighed into the blender jar and 100 ml of methanol–water (7:3, v/v) were added. The mixture was blended at high speed for 2 min, then filtered through a prefolded filter-paper. Approximately 12 ml of the extract were filled into a BenchMate test-tube.

Immunoaffinity column clean-up

The sample tubes, each provided with an immunoaffinity column on their caps, were placed in rack 1 of the BenchMate. Racks 2 and 3 were provided with empty "process" tubes and "final" tubes. In the BenchMate procedure, an aliquot of sample extract was pipetted, diluted with phosphate-buffered saline, mixed by cycling and then passed through the immunoaffinity column at a flow-rate of 4.2 ml/min. After washing the column with 20 ml of water, the aflatoxins were eluted with 1.5 ml of methanol at a flow-rate of 4.2 ml/min. Finally, 1.5 ml of water were added and the test solution was vortex mixed.

HPLC determination

The injections for HPLC can be performed on-line by the BenchMate directly after every sample clean-up. For an accelerated BenchMate clean-up and greater flexibility, an autosampler can be used. The test solutions in the BenchMate final tubes then have to be transferred into autosampler vials.

The HPLC conditions were as follows: column, Spherisorb S5 ODS-2 (250 mm × 4 mm I.D.), tempered at 35°C; precolumn RP-18 (4 mm × 4 mm I.D.); eluent, methanol–water (1:1, v/v); flow-rate, 0.85 ml/min; injection volume, 200 μl; detection, fluorescence with excitation at 360 nm and emission at 450 nm; derivatization, postcolumn derivatization with saturated iodine solution in water, flow-rate 0.2 ml/min, reaction coil 3.2 m × 0.5 mm I.D., temperature 70°C.

Fig. 1 shows a typical chromatogram of a

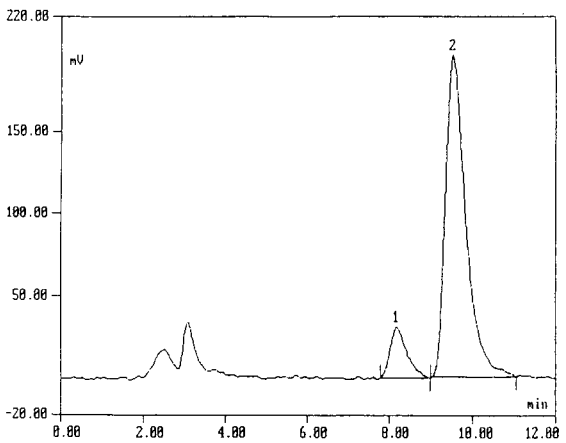

Fig. 1. Chromatogram of a naturally contaminated pistachio sample containing 8 μg/kg of aflatoxin B_1 and 0.5 μg/kg of aflatoxin B_2. Peaks: 1 = aflatoxin B_2; 2 = B_1.

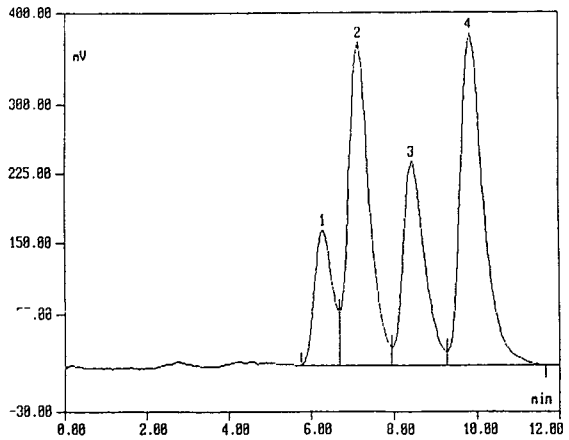

Fig. 2. Chromatogram of a standard solution containing 5 ng/ml each of aflatoxins B_1 and G_1 and 1.5 ng/ml each of aflatoxins B_2 and G_2. Peaks: 1 = aflatoxin G_2; 2 = G_1; 3 = B_2; 4 = B_1.

naturally contaminated pistachio sample with a content of 8 μg/kg of aflatoxin B_1 and 0.5 μg/kg of aflatoxin B_2, and Fig. 2 is a standard chromatogram for 5 ng/ml of aflatoxin B_1 and G_1 and 1.5 ng/ml of B_2 and G_2.

RESULTS AND DISCUSSION

For each sample matrix some recovery tests were carried out first by adding a mixed standard solution to the sample at the beginning of the preparation and processing the sample with and without standard addition. The amount of added standard was equivalent to 4 μg/kg of aflatoxin B_1 and G_1 and 1.2 μg/kg of aflatoxin B_2 and G_2. From the recovery results for spiked samples with low or no natural contamination, the repeatability of the method was calculated.

In a series of experiments, the same sample matrices as used for the BenchMate procedure were also processed manually in order to obtain comparative data about recoveries and repeatability. Because the volumes for the manual column clean-up are not as restricted as in the BenchMate procedure, the extracts to be treated manually were always diluted to a methanol concentration of 14% prior to immunoaffinity clean-up.

The following data (Table I) are based on the examination of 38 manually and 37 automatically

TABLE I

RECOVERIES AND RELATIVE STANDARD DEVIATIONS OF AFLATOXINS FOR NUT AND NUT-LIKE SAMPLES AFTER MANUAL (n = 38) AND AUTOMATIC (n = 37) CLEAN-UP WITH IMMUNOAFFINITY COLUMNS (AFLAPREP)

Clean-up	Parameter	Aflatoxin			
		B_1	B_2	G_1	G_2
Manual	Recovery (%)	73.6	55.7	78.2	32.1
	R.S.D. (%)	17.5	17.8	15.9	39.8
Automatic	Recovery (%)	74.5	64.2	83.7	34.7
	R.S.D. (%)	15.0	13.3	12.1	31.9

processed samples of pistachios, hazelnuts, brazil nuts, almonds, peanuts and apricot kernels by use of AFLAPREP columns. The recoveries obtained with the automated method are slightly better than those with the manual clean-up, although the methanol content of the automatically processed diluted extract (30%) is far higher than that of the diluted extract used for the manual method (14%).

The reason for better repeatability and higher recoveries is presumed to be the ability of the automatic work station to maintain slow and constant flow-rates for loading samples on to the immunoaffinity column and for the elution of the aflatoxins. Statistical data obtained in a collaborative trial of ten laboratories using HPLC with postcolumn derivatization have been reported [5]. The R.S.D. values for peanuts (and peanut butter in parentheses) were 16.4% (14.9%) for aflatoxin B_1, 23.1% (32.7%) for B_2, 6.2% (23.5%) for G_1 and 42.0% (79.1%) for G_2. These figures demonstrate the range of variation of results, which is normal for aflatoxin analysis. The repeatability obtained in our laboratory fits in the pattern of the published values.

We also carried out a study to compare AFLAPREP (Rhône-Poulenc) and EasiExtract (Biocode) aflatoxin immunoaffinity columns. Both types of column appear to be equally suitable for the clean-up of diluted pistachio sample extracts with a remaining methanol content of up to 15%. Higher methanol concen-

trations result is very low recoveries of aflatoxin B_2 and especially G_2 with the AFLAPREP column and in decreased recoveries of all aflatoxins with the EasiExtract column.

Comparison of BenchMate and ASPEC

The method developed for aflatoxin analysis using BenchMate was compared with that reported [10] using an ASPEC system.

The manual preparation of the test sample following our method is simpler and less time consuming than in the other method [10]; the latter involves mixing twice with an Ultra Turrax and has two manual dilution steps, whereas the dilution of the extract is automated in the BenchMate procedure, guaranteeing very precise dispensing volumes. The ASPEC procedure [10] includes a preconditioning step for the immunoaffinity columns. We omitted such a step, finding no differences in the results after clean-up with and without preconditioning of the columns.

The time needed per sample (double injection of sample, standard injections included) using the BenchMate procedure is 39 min, which is equivalent to 37 samples per day. If HPLC injection is carried out off-line, the preparation takes 20 min per sample, which means a throughput of 70 samples per day. Up to 50 samples can be put in a BenchMate rack and be processed unattended within 32 h. The ASPEC, on the other hand, has a sample carousel with which only 20 samples can be processed in an unattended operation time of 11 h. The time per sample (single injection, standard injections included) is 33 min, only slightly shorter than with BenchMate and double injection.

An obvious advantage of the ASPEC system is the greater working volume of the sample tubes of 50 ml in comparison with 12 ml for the BenchMate. The BenchMate can partly compensate for this restriction by the possibility of diluting concentrated extracts, also repeatedly by means of chained procedures. Hence higher volumes, *e.g.*, 50 ml of diluted extract, could be passed through the immunoaffinity column, but the time needed per sample would increase greatly. Owing to the higher sample tube volume, the ASPEC system allows the clean-up of samples which have been extracted with acetonitrile–water mixtures because immunoaffinity columns withstand only very low concentrations of acetonitrile, so that acetonitrile extracts must be more diluted than methanolic extracts. The BenchMate, in contrast, to achieve sufficient sensitivity in aflatoxin analysis, is suitable only for the clean-up of methanolic extracts.

The sensitivities of both methods are expected to be in the same range, calculated from the amount of sample per injection, although with the other method no detection limits were published [10]. With the equipment used, the BenchMate procedure gives detection limits equivalent to about 0.1 μg/kg for aflatoxins B_1 and G_1 and about 0.03 μg/kg for aflatoxins B_2 and G_2.

Advantages of automatic sample preparation over the manual technique

The automatic sample preparation gives better repeatability (see Table I) and reproducibility because of the precise control of flow-rates (column loading, rinsing, eluting) and volumes. Unattended sample preparation and HPLC injection (*e.g.*, overnight), including injection of calibration standards, can be performed, so that up to 4 h of manpower per day are saved in comparison with the manual technique. The BenchMate performs a gravimetric control of every preparation step which can be viewed afterwards.

Problems and limitations of automatic sample preparation

Restricted volumes of the sample and process tubes result in limitations on the construction of individual sample clean-up methods. It is very time consuming to pass high volumes of diluted extract through the column by means of chained procedures. Only sample matrices from which the aflatoxins can be extracted by methanol–water mixtures are suitable for the automatic procedure. Other extraction solvents (containing acetone or acetonitrile) have to be further diluted with water in order not to disturb the immunoaffinity process.

With BenchMate, only one sample at a time is processed, whereas manually up to six samples can be loaded on columns simultaneously by means of a Baker SPE system.

If any error occurs, the robot stops until it is attended to, which causes time losses. In on-line HPLC, this also means energy and material losses because the HPLC system is not switched off.

During a run nothing can be changed. Unnecessary injections cannot be skipped as would be possible with an autosampler. With versions I and II of the BenchMate work station there is no possibility of viewing and controlling the running procedure. Owing to matrix effects not all types of samples can be processed automatically, *e.g.*, nutmegs.

CONCLUSIONS

Sample preparation by use of immunoaffinity columns and a BenchMate automatic work station followed by HPLC is a suitable method for the determination of aflatoxins B_1, B_2, G_1 and G_2 in certain foodstuffs (nuts and nut-like products and dried fruit). It offers a numbers of advantages over other methods: lower detection limits than TLC and ELISA; greater confidence in the results than with all other methods because of the higher repeatability; very efficient clean-up; unattended sample preparation and optional on-line HPLC injection; economy of manpower in comparison with the manual technique; no need for large volumes of hazardous solvents; determination of all four aflatoxins simultaneously and over a wide range of concentrations (in contrast to the ELISA method).

In conclusion, the proposed method for the determination of aflatoxins by use of an automatic work station can be recommended for laboratories performing routine aflatoxin analyses. If necessary it can be combined with the manual immunoaffinity clean-up for certain sample matrices.

REFERENCES

1 G. Werner, *Agrobiol. Res.*, 44 (1991) 289–298.
2 Amtliche Sammlung von Untersuchungsverfahren nach § 35 LMBG, L. 00.00–2, German Official Collection of Analytical Methods (1981).
3 Eidgenössische Lebensmittelbuch-Kommission: Arbeitsgruppe "Toxine 2" der Eidgenössischen Lebensmittelbuch-Kommission, *Mitt. Geb. Lebensmittelunters. Hyg.* 73 (1982) 362–367.
4 P. Majerus and Z. Zakaria, *Z. Lebensm.-Unters.-Forsch.*, 195 (1992) 316–319.
5 M.W. Trucksess, M.E. Stack, S. Nesheim, S.W. Page and R.H. Albert, *J. Assoc. Off. Anal. Chem.*, 74 (1991) 81–88.
6 A.L. Patey, M. Sharman and J. Gilbert, *J. Assoc. Off. Anal. Chem.*, 74 (1991) 76–81.
7 B. Rudat and E. Thiry, *LaborPraxis*, (1991) 380–383.
8 W.E. Paulsch, E.A. Sizoo and H.P. van Egmond, *J. Assoc. Off. Anal. Chem.*, 71 (1988) 957–961.
9 A. Bruns, H. Waldhoff, A. Wilsch-Irrgang and W. Winkle, *J. Chromatogr.*, 592 (1992) 245–253.
10 M. Sharman and J. Gilbert, *J. Chromatogr.*, 543 (1991) 220–225.
11 L. Jordan and K.F. Donahue, presented at the *International Symposium on Laboratory Automation and Robotics, Boston, MA, 1991.*

Journal of Chromatography A, 661 (1994) 181–191
Elsevier Science B.V., Amsterdam

CHROMSYMP. 2898

High-performance liquid chromatographic method for the simultaneous detection of malonaldehyde, acetaldehyde, formaldehyde, acetone and propionaldehyde to monitor the oxidative stress in heart

Gerald A. Cordis

University of Connecticut School of Medicine, Farmington, CT 06030-1110 (USA)

Debasis Bagchi

Creighton University, Omaha, NE 68178-0230 (USA)

Nilanjana Maulik and Dipak K. Das*

University of Connecticut School of Medicine, Farmington, CT 06030-1110 (USA)

ABSTRACT

Lipid peroxidation (LPO) is the oxidative deterioration of polyunsaturated fatty acids (PUFA) with the production of lipid hydroperoxides, cyclic peroxides, cyclic endoperoxides, and finally fragmentation to ketones and aldehydes (including malonaldehyde, MDA). Estimation of LPO through MDA formation measured by assaying thiobarbituric acid (TBA) reactive products remains the method of choice to study the development of oxidative stress in tissues. However, MDA estimation by TBA reactive products is non-specific and often gives erroneous results. In this report we describe a method using high-performance liquid chromatographic separation to estimate MDA, formaldehyde (FDA), acetaldehyde (ADA), acetone, and propionaldehyde (PDA), the degradation products of oxygen-derived free radicals (ODFR) and PUFA, as presumptive markers for LPO. Oxidative stress was induced in the tissue by perfusing an isolated rat heart with hydroxyl radical generating system (xanthine + xanthine oxidase + $FeCl_3$ + EDTA). The coronary effluents were collected, derivatized with 2,4-dinitrophenylhydrazine (DNPH), and extracted with pentane. Aliquots of 25 μl in acetonitrile were injected onto a Beckman Ultrasphere C_{18} (3 μm) column. The products were eluted isocratically with a mobile phase containing acetonitrile–water–acetic acid (40:60:0.1, v/v/v), measured at three different wavelengths (307, 325 and 356 nm) using a Waters M-490 multichannel UV detector and collected for gas chromatography–mass spectrometry (GC–MS) analysis. The peaks were identified by co-chromatography with DNPH derivatives of authentic standards, peak addition, UV pattern of absorption at the three wavelengths, and by GC–MS. The retention items of MDA, FDA, ADA, acetone, and PDA were 5.3, 6.6, 10.3, 16.5, and 20.5 min, respectively. The results of our study indicated progressive increase of all five lipid metabolites as a function of the duration of ODFR perfusion. Hydroxyl radical scavengers, superoxide dismutase plus catalase, completely inhibited the formation of these lipid metabolites, demonstrating that the release of lipid metabolites from the isolated heart was indeed in response to oxidative stress. Since MDA, FDA, ADA, acetone, and PDA are the products of ODFR–PUFA interactions, this method allows proper estimation of LPO which monitors the oxidative stress developed during the reperfusion of ischemic myocardium.

* Corresponding author.

0021-9673/94/$07.00
SSDI 0021-9673(93)E0828-I

INTRODUCTION

Development of oxidative stress resulting from the generation of oxygen free radicals has been implicated in the pathogenesis of a variety of diseases including atherosclerosis, heart attack, stroke, shock lung, trauma, aging, malaria, and influenza [1,2]. These reactive oxygen species also play an important role in health hazards caused by industrial pollutants, environmental carcinogens, pesticides, cigarette smoke, and deterioration of foods. Oxidative stress can be detected either directly by estimating the presence of free radicals using electron spin resonance spectroscopy (ESR) or high-performance liquid chromatography (HPLC) or indirectly by monitoring the formation of the extent of lipid peroxidation and/or conjugated diene formation. Direct detection of free radicals is a difficult task, firstly, because of the extremely short lives of the free radicals (usually in the range of nanoseconds), and secondly, because of the sophistication in the methodologies. In addition, ESR is a very expensive instrument and not readily available in many laboratories. The measurement of lipid peroxidation, on the other hand, is extremely simple and therefore, the most popular method for the detection of oxidative stress.

Determination of malonaldehyde (MDA) is the most widely recognized method for the monitoring of lipid peroxidation in health related diseases [3]. Several methods are available for the detection of MDA. The most commonly used method consists of the measurement of thiobarbituric acid reactive products formed from the reaction of MDA and thiobarbituric acid (TBA) using spectrophotometric assay method [4,5]. Although this method is relatively simple, the significance of the results is often blunted because of the incorrect interpretation of the results. This is because of the non-specificity of the TBA reactions, TBA not only forms a colored complex with MDA, but it also reacts with many other compounds including ribose, biliverdin, amino pyrimidines, and sialic acid, which may also be present in biological samples [6]. This method was subsequently modified to quantitate the specific MDA–TBA adducts, but the method is not widely used because of the lengthy as well as extremely complex nature of sample preparation [7,8].

Recently we have described a rapid and simple technique for assaying MDA formed during the reperfusion of ischemic myocardium [9]. We now report that this technique can also be used to monitor the development of oxidative stress. Isolated rat heart was perfused with the free radical generating system to generate the reactive oxygen species. The extent of lipid peroxidation was measured by monitoring the formation of MDA and other lipid metabolites after derivatizing with 2,4-dinitrophenylhydrazine (DNPH) using HPLC. The identity of the reaction products obtained by HPLC of coronary perfusates was confirmed for the first time by gas chromatography–mass spectroscopy (GC–MS).

EXPERIMENTAL

Materials

Xanthine, xanthine oxidase, EDTA, TBA and DNPH were obtained from Sigma (St. Louis, MO, USA). Malonaldehyde-bis-dimethyl acetate was purchased from Aldrich (Milwaukee, WI, USA), while formaldehyde (FDA), acetaldehyde (ADA), acetone, and propionaldehyde (PDA) were from Sigma. High purity DNPH standards were prepared by stoichiometric derivatization and repeated crystalization from methanol.

All organic solvents were of HPLC grade (Burdick & Jackson, Muskegon, MI, USA). Water was purified with a Milli-Q system (Millipore, Marlborough, MA, USA). The mobile phase was filtered through a 0.22-μm Nylon-66 solvent filter (Rainin Instrument, Woburn, MA, USA). All other chemicals were of analytical grade.

Methods

Isolated rat heart preparation. Sprague Dawley male rats of about 250 g body weight were anesthetized with intraperitoneal pentobarbital (80 mg per kg). Hearts were removed and quickly mounted on a non-circulating Langendorff perfusion apparatus as described previously [10]. Retrograde perfusion was established at a pressure of 100 cmH_2O (1 $cmH_2O = 98.07$ Pa)

with oxygenated normothermic Krebs–Henseleit bicarbonate (KHB) buffer. Hearts were allowed to be equilibrated for 10 min at 37°C with non-circulating KHB buffer. The heart was then perfused for 45 min with the hydroxyl radical ($OH^{\cdot}$) generating system [xanthine (100 μM), XO (8 mU/ml), $FeCl_3$ (10 μM) and EDTA (100 μM) in the presence or absence of $OH^{\cdot}$ radical scavengers, superoxide dismutase (SOD) (50 U/ml) and catalase (50 U/ml)]. Perfusates were withdrawn before and during the perfusion with $OH^{\cdot}$ generating system for subsequent estimation of MDA and the lipid metabolites.

Spectroscopic assay for MDA as TBA-reactive materials. TBA-reactive materials were estimated by the well-established technique [11]. In short, 1 ml of the perfusate was mixed with 0.2 ml of 15% trichloroacetic acid, 1 ml of 0.75% TBA in 0.5% sodium acetate was then added and mixed, and finally the mixture was boiled for 15 min [11]. The red color of the TBA–MDA complex was read with a spectrophotometer using 535 nm wavelength.

Derivatization and extraction of lipid metabolites. The lipid metabolites extracted with the perfusate were derivatized using DNPH. For derivatization purpose, 310 mg of DNPH was dissolved in 100 ml of 2 *M* HCl, and 0.1 ml of this DNPH reagent (1.56 μmol) was added to 1.5 ml of the perfusate in a 20-ml screw-capped PTFE lined test tube. An aliquot of 0.5 ml of water was added to the tube, the contents were mixed for 15 min by vortexing, and then 10 ml of pentane was added to the mixture. The tubes were intermittently shaken for 30 min, and reactions were allowed to occur at room temperature. The organic phase was removed, and the aqueous phase was extracted with an additional 20 ml of pentane. The pentane extracts were combined, evaporated under a stream of nitrogen at 30°C and reconstituted in 200 μl of acetonitrile. This acetonitrile extract was directly injected onto the HPLC column. Generation of authentic standards, calibration curves, *r*-values, and response factors were calculated as described previously [9].

HPLC procedure. A 25-μl volume of the filtered (0.2-μm Nylon-66 membrane filters in Microfilterfuge tubes from Rainin Instrument) sample was injected onto a Beckman Ultrasphere ODS C_{18} (3-μm particle size, 7.5 cm × 4.6 mm I.D.) column (Rainin Instrument) in a Waters chromatograph (Milford, MA, USA) equipped with a Model 820 full control Maxima computer system, satellite Wisp Model 700 injector, Model 490 programmable multi-wavelength UV detector (4 channels), two Model 510 pumps, and a Bondapak C_{18} Guard-Pak precolumn. The DNPH derivatives were detected at 307, 325, and 356 nm simultaneously with 3 channels of the M-490 detector at a flow-rate of 1 ml/min with an isocratic gradient of acetonitrile–water–acetic acid (40:60:0.1, v/v/v) for a total run time of 24 min. The column was washed with acetonitrile–acetic acid (100:0.1, v/v) before each day's work to remove any bound reagent.

GC–MS. In order to confirm the identity of lipid metabolities in the effluents from the heart, GC–MS analyses were performed. The GC–MS system consisted of a Hewlett-Packard Model 5890 gas chromatograph (Fullerton, CA, USA) with a 15 m × 0.32 mm I.D. capillary column 0.25 μm film thickness (Supelco SPB-5, Bellefonte, PA, USA), which was connected directly to the mass spectrometer via a heated transfer line. The transfer line temperature was maintained at 250°C. The carrier gas was helium at an average linear velocity of 65.8 cm/s, and the injection temperature was 230°C. The injector was operated in the splitless mode. A temperature program was used which consisted of a starting temperature of 75°C which was increased to 175°C at increments of 25°C/min. Between 175 and 200°C, the temperature was increased at a rate of 5°C/min and finally to 300°C at increments of 25°C/min. The mass spectrometer was a Finnigan-MAT Model 50B quadrupole instrument (Palo Alto, CA, USA) in combination with an INCOS data system. The instrument was set on electron ionization mode. The ion source temperature was 180°C, and the ionization energy was 70 ev. The system was coupled to a Data General Model DG 10 computer (Southboro, MA, USA) and a Printronix Model MVP printer (Irvine, CA, USA). For GC–MS analysis, the hydrazine derivatives of MDA, FDA, ADA, acetone and PDA were dissolved in chloroform (50 ng/μl). Similarly, hydrazine-de-

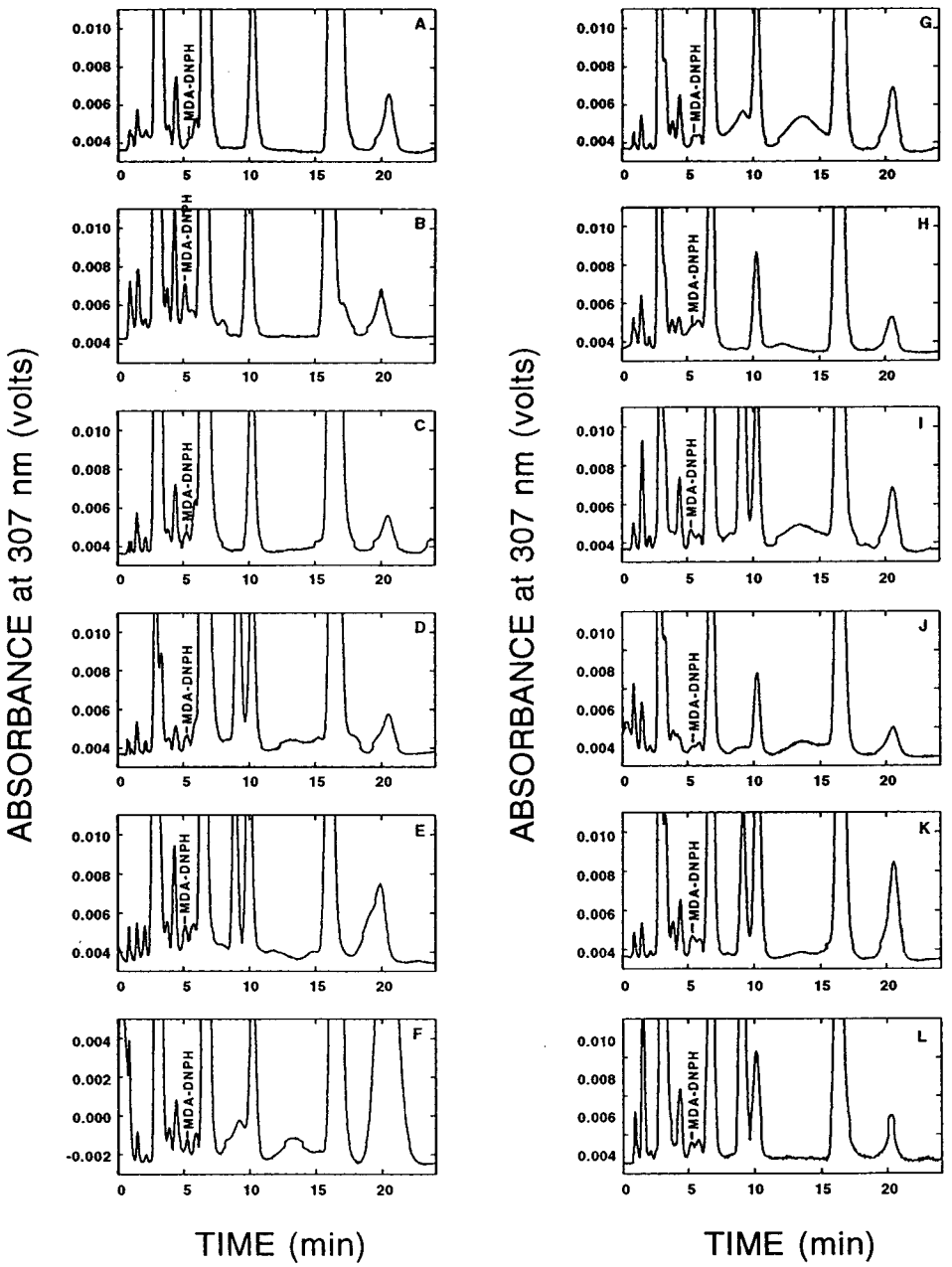

Fig. 1. Reversed-phase HPLC separation of MDA–DNPH from perfusates obtained from isolated rat hearts perfused with $OH^{\bullet}$ generating system in the presence and absence of SOD plus catalase. Perfusates were collected, derivatized and chromatographed as shown in Experimental. Absorbance was measured at 307 nm. (A) Baseline; (B) after 1 min perfusion with $OH^{\bullet}$; (C) after 10 min perfusion with $OH^{\bullet}$; (D) after 20 min perfusion with $OH^{\bullet}$; (E) after 30 min perfusion with $OH^{\bullet}$; (F) after 45 min perfusion with $OH^{\bullet}$; (G) baseline; (H) after 1 min perfusion with $OH^{\bullet}$ plus SOD and catalase; (I) after 10 min perfusion with $OH^{\bullet}$ plus SOD and catalase; (J) after 20 min perfusion with $OH^{\bullet}$ plus SOD and catalase; (K) after 30 min perfusion with $OH^{\bullet}$ plus SOD and catalase; (L) after 45 min perfusion with $OH^{\bullet}$ plus SOD and catalase.

rivatized heart perfusate samples were reconstituted in chloroform. Samples (2 μl) of standard and extracts were injected onto the GC–MS system. Following the full-spectrum identification of each of the hydrazones, a selective ion monitoring (SIM) program was developed, and additional spectra were obtained in the SIM mode.

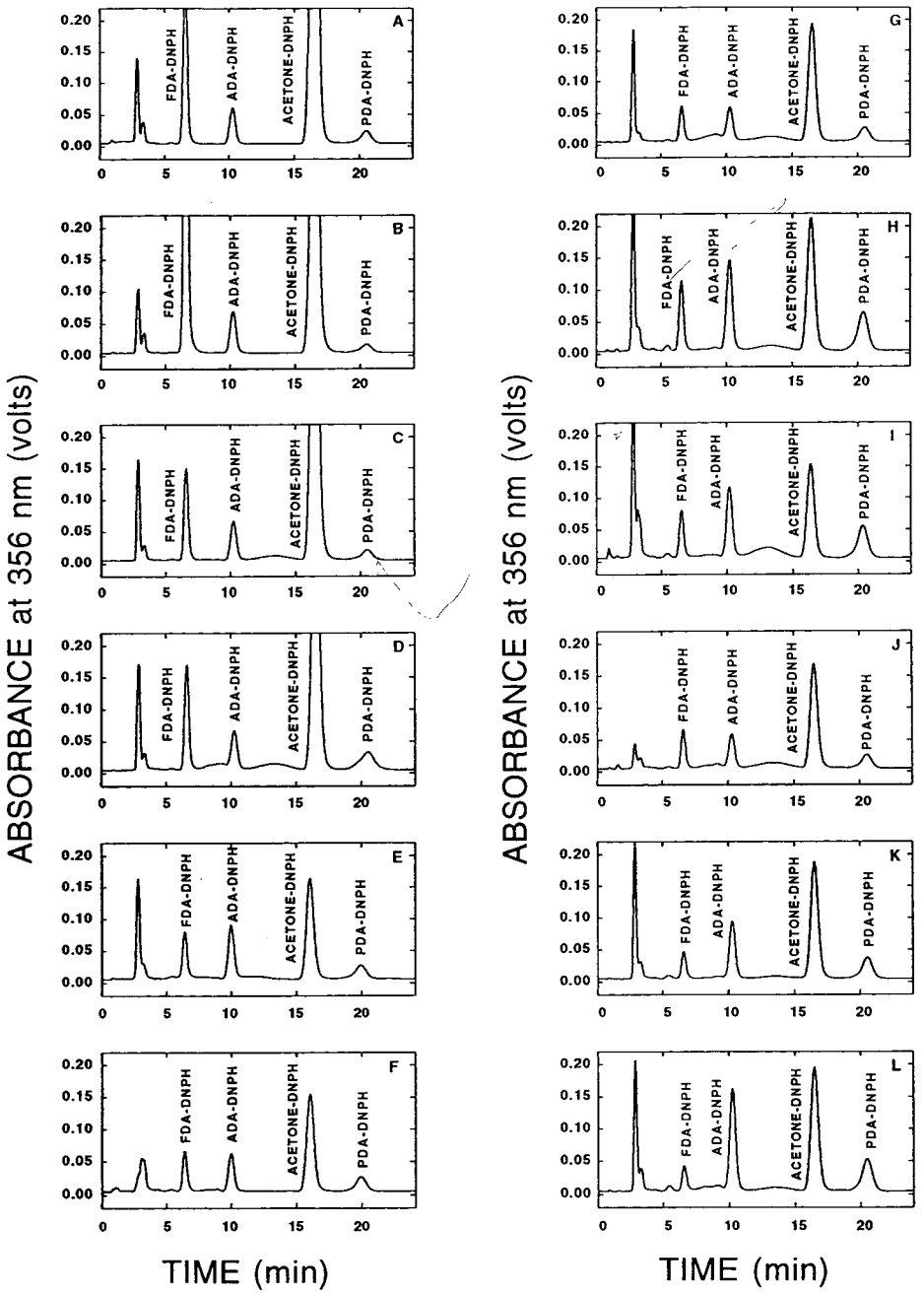

Fig. 2. Separation of FDA–DNPH, ADA–DNPH, acetone–DNPH and PDA–DNPH in rat heart perfusates under the same conditions as described in Fig. 1 except that the absorbance was measured at 356 nm (A) to (L), same as Fig. 1.

RESULTS

Separation and identification of lipid metabolites

The DNPH derivatives of authentic standards of FDA, ADA, MDA, acetone and PDA were separated using three different wavelengths: 307, 325, and 356 nm as described previously [9]. MDA gives absorption maxima at 307 nm whereas the absorption maxima for FDA, ADA, acetone and PDA is 356 nm. The retention times of MDA, FDA, ADA, acetone and PDA were 5.3, 6.6, 10.3, 16.5, and 20.5 min, respectively, making a total run time of 24 min.

Quantitative estimation of lipid metabolites in the perfusate

The perfusates obtained from the heart prior to and during the perfusion with $OH^{\cdot}$ generating system, were processed as described in Methodology, and the derivatized extracts were loaded onto the HPLC column equipped with programmable multi-wavelength UV detector. The results from the baseline (A), and after 1 min (B), after 10 min (C), after 20 min (D), after 30 min (E) and after 45 min (F) perfusion with $OH^{\cdot}$ are shown in Fig. 1 (307 nm) and Fig. 2 (356 nm). As shown in these figures, the peak for FDA, ADA, acetone and PDA are already present in the baseline samples, and they continue to be formed as the reperfusion progresses, thus causing an increase in the accumulated products. MDA peak is barely present in the baseline sample, it appears after the reperfusion, and like other lipid metabolite peaks, it continues to be formed as the duration of perfusion increases.

Each experiment was repeated by simultaneously perfusing the heart with $OH^{\cdot}$ scavengers, SOD plus catalase, in conjunction with $OH^{\cdot}$ radical generating system. As shown in Fig. 1 and Fig. 2, the peaks for the lipid metabolites either disappeared or reduced significantly after perfusing with SOD plus catalase. The exact values are shown in Table I.

In addition, spiking with the standards were also performed for each wavelength, 307 and 356 nm. Accuracy of the method was determined by standard addition technique. Addition of 50 pmol of each of the standards were accurately reflected in the peak heights. Within-run and inter-run variations were 1 and 5%, respectively.

Identification of the peaks by GC–MS

The identify of the peaks were confirmed by comparing the retention items with those of authentic standards using GC–MS. The MS data

TABLE I

PRODUCTION OF LIPID METABOLIC PRODUCTS DURING PERFUSION OF THE ISOLATED RAT HEART WITH THE $OH^{\cdot}$ GENERATING SYSTEM IN THE PRESENCE OR ABSENCE OF SOD PLUS CATALASE

Time of perfusion (min)	Perfusion agent	Amount ± S.E. ($n = 6$) (nmol/ml perfusate)				
		MDA–DNPH (307 nm)	FDA–DNPH (356 nm)	ADA–DNPH (356 nm)	Acetone–DNPH (356 nm)	PDA–DNPH (356 nm)
Baseline	$OH^{\cdot}$	0.068 ± 0.018	2.1113 ± 0.331	1.436 ± 0.177	5.015 ± 0.316	0.714 ± 0.183
	$OH^{\cdot}$ + SOD + catalase	0.053 ± 0.016	2.402 ± 0.433	1.534 ± 0.275	4.712 ± 0.431	0.684 ± 0.213
1	$OH^{\cdot}$	0.113 ± 0.030	12.684 ± 2.377	2.079 ± 0.404	8.670 ± 0.678	0.971 ± 0.258
	$OH^{\cdot}$ + SOD + catalase	0.090 ± 0.028	5.536 ± 0.809	1.753 ± 0.222	4.024 ± 0.300	0.766 ± 0.267
10	$OH^{\cdot}$	0.068 ± 0.010	6.698 ± 1.081	1.580 ± 0.216	8.651 ± 0.688	0.795 ± 0.133
	$OH^{\cdot}$ + SOD + catalase	0.053 ± 0.012	1.931 ± 0.205	1.444 ± 0.234	3.921 ± 0.213	0.593 ± 0.156
20	$OH^{\cdot}$	0.054 ± 0.005	2.189 ± 0.387	1.293 ± 0.206	5.999 ± 0.445	0.765 ± 0.136
	$OH^{\cdot}$ + SOD + catalase	0.033 ± 0.008	1.790 ± 0.221	0.756 ± 0.183	3.983 ± 0.412	0.581 ± 0.123
30	$OH^{\cdot}$	0.075 ± 0.022	2.573 ± 0.405	1.582 ± 0.345	6.973 ± 0.570	1.341 ± 0.266
	$OH^{\cdot}$ + SOD + catalase	0.065 ± 0.020	2.628 ± 0.417	1.267 ± 0.284	4.552 ± 0.131	0.826 ± 0.212
45	$OH^{\cdot}$	0.071 ± 0.023	2.217 ± 0.370	1.387 ± 0.248	6.752 ± 0.550	1.162 ± 0.078
	$OH^{\cdot}$ + SOD + catalase	0.050 ± 0.015	0.988 ± 0.156	0.856 ± 0.077	4.362 ± 0.420	0.525 ± 0.097

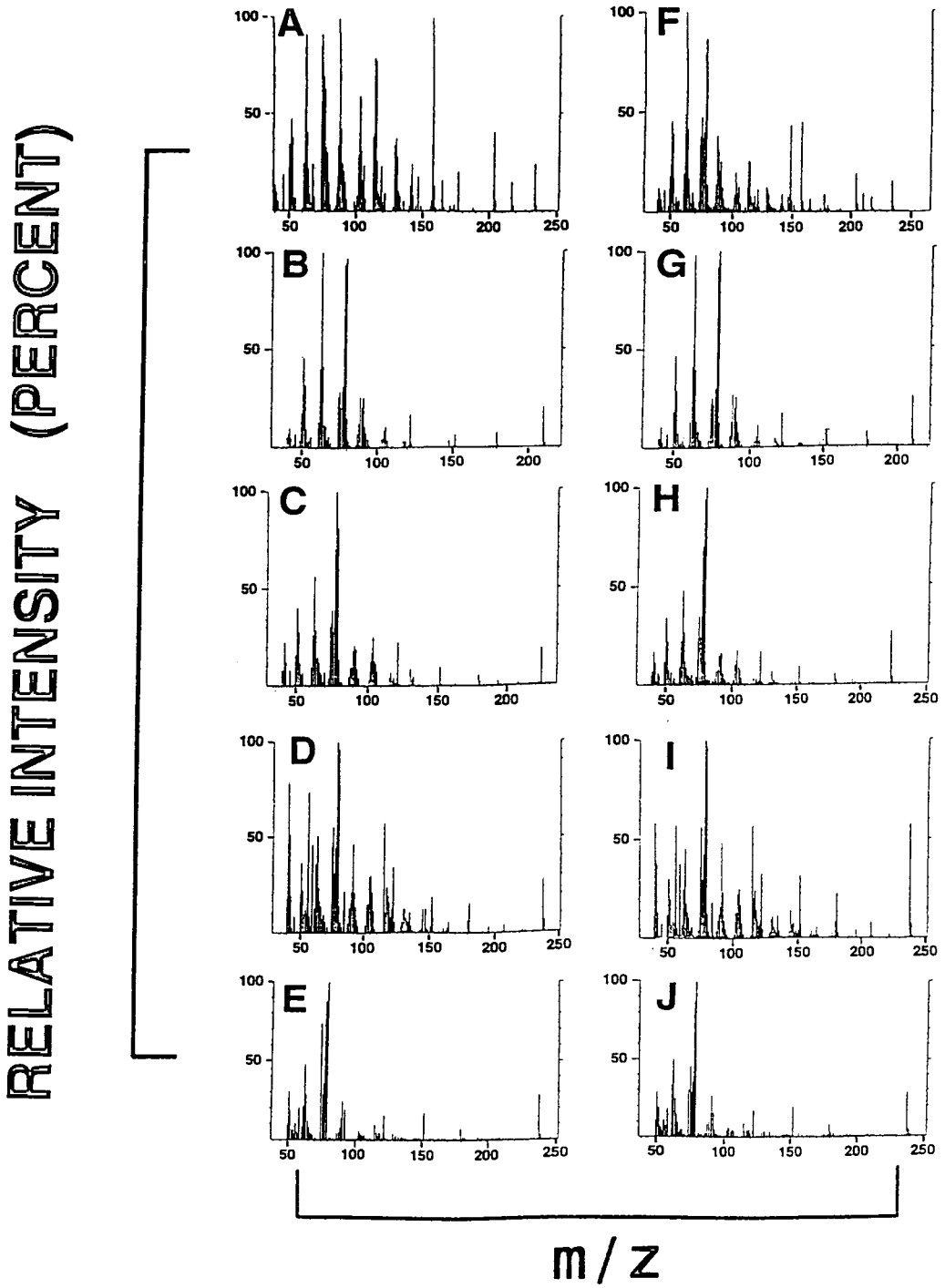

Fig. 3. Representative mass spectrum of the DNPH derivatives of the standards for the five lipid metabolites and for the five lipid metabolites in rat heart perfusates. Mass spectrum were obtained as described in Experimental. (A) MDA–DNPH standard; (B) FDA–DNPH standard; (C) ADA–DNPH standard; (D) acetone–DNPH standard; (E) PDA–DNPA standard; (F) MDA–DNPH in rat heart perfusate; (E) FDA–DNPH in perfusate; (H) ADA–DNPH in perfusate; (I) acetone–DNPH in perfusate; (J) PDA–DNPH in perfusate.

for the five lipid metabolites are presented in Fig. 3. The molecular ions (M^+) of the synthetic hydrazones of FDA, MDA, ADA, acetone, and PDA were found to be 210, 234, 224, 238, and 238, respectively (Fig. 3A–E). The same molecular ions and mass spectra were demonstrated in the extracts of heart perfusate samples following GC–MS (Fig. 3F–J).

Selective ion monitoring (SIM) was used to provide further confirmation of the identity of the five lipid metabolities in heart perfusate. Ion chromatograms for a mixture of hydrazones of the five reference standards and an extract of heart perfusate are presented in Fig. 4A–B. The ions which were selected in this display mode are 158 and 234 for MDA, 210 for FDA, 224 for ADA, 238 for acetone, and 238 for PDA. A comparison between Fig. 4A and B clearly indicates that mass ions produced by the five standards were associated with the components of heart perfusate that were separated by GC. These results provide further confirmation of the identification of the five lipid metabolites in the effluents obtained from the heart.

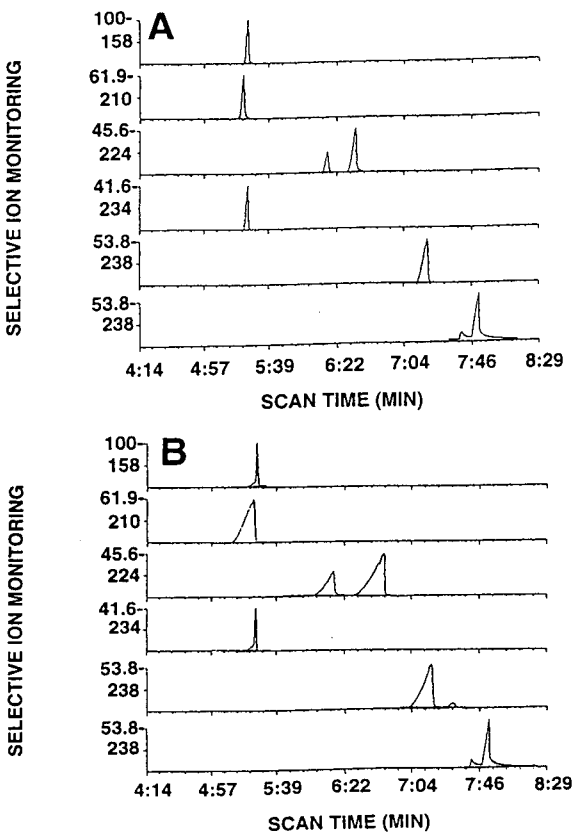

Fig. 4. Representative selective ion monitoring (SIM) for the DNPH derivatives of the standards for the five lipid metabolites and for the five lipid metabolites in rat heart perfusates. SIM obtained as shown in Experimental. (A) DNPH derivatives for standards of MDA (158, 234), FDA (210), ADA (224), acetone (238), and PDA (238). (B) DNPH derivatives of MDA (158, 234), FDA (210), ADA (224), acetone (238), and PDA (238) from rat heart perfusates.

TBA-reactive materials

The same perfusate samples were also estimated by assaying the TBA-reactive materials. The values for TBA-reactive materials are shown in Table II. As expected these values were much higher compared to those obtained for MDAs from the corresponding myocardial perfusate samples.

Correlation between the oxidative stress and the formation of lipid metabolite

To examine whether in fact these lipid metabolites truely reflect the development of oxidative stress during the perfusion with the $OH^{\cdot}$ generating system, we determined the correlation coefficient of the lipid metabolite accumulation versus the duration of $OH^{\cdot}$ perfusion. Accumulation of lipid metabolites was estimated in the perfusate obtained from heart as a function of the duration of perfusion with $OH^{\cdot}$ generating system. As shown in Fig. 5, excellent correlation was achieved for each lipid metabolite. Correlation coefficients for MDA, FDA, ADA, acetone and PDA were 0.994, 0.927, 0.997, 0.997, and 0.995, respectively, indicating the validity of monitoring these lipid metabolites for estimating oxidative stress development.

DISCUSSION

MDA and several other aldehydes and ketones, such as formaldehyde, acetaldehyde, acetone and propionaldehyde are the breakdown products of spontaneous fragmentation (β-cleavage) of peroxides derived from the free radical-polyunsaturated fatty acid (PUFA) interactions [11]. Formation of free radicals and peroxidation of PUFA are ongoing dynamic processes which

TABLE II

ESTIMATION OF MALONALDEHYDE PRODUCTION BY TBA REACTION IN HEART PERFUSATE DURING PERFUSION WITH $OH^{\cdot}$ GENERATING SYSTEM IN THE PRESENCE OR ABSENCE OF SOD PLUS CATALASE

Time of perfusion (min)	Perfusion agent	MDA–TBA ± S.E. ($n = 6$) (nmol/ml perfusate)
Baseline	$OH^{\cdot}$	0.15 ± 0.08
	$OH^{\cdot}$ + SOD + catalase	0.16 ± 0.06
1	$OH^{\cdot}$	0.16 ± 0.07
	$OH^{\cdot}$ + SOD + catalase	0.14 ± 0.07
10	$OH^{\cdot}$	0.88 ± 0.19
	$OH^{\cdot}$ + SOD + catalase	0.50 ± 0.16
20	$OH^{\cdot}$	1.45 ± 0.28
	$OH^{\cdot}$ + SOD + catalase	0.81 ± 0.19
30	$OH^{\cdot}$	2.35 ± 0.56
	$OH^{\cdot}$ + SOD + catalase	1.33 ± 0.37
45	$OH^{\cdot}$	2.67 ± 0.63
	$OH^{\cdot}$ + SOD + catalase	1.37 ± 0.24

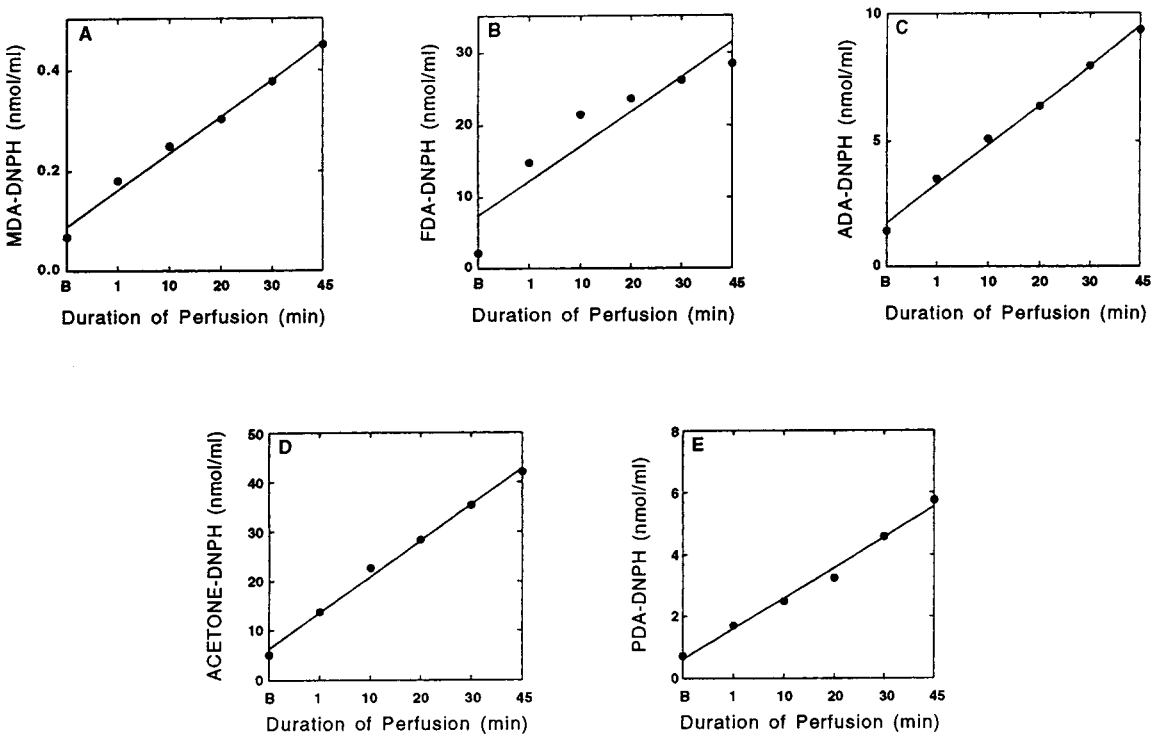

Fig. 5. Correlation of the accumulated lipid metabolites in the heart perfusates as a function of duration of perfusion with $OH^{\cdot}$ generation system. Accumulation of lipid metabolites was determined from the formation of each lipid metabolite over the total period of $OH^{\cdot}$ perfusion. (A) MDA–DNPH, correlation coefficient (r) = 0.994; (B) FDA–DNPH, $r = 0.927$; (C) ADA–DNPH, $r = 0.997$; (D) Acetone–DNPH, $r = 0.997$; (E) PDA–DNPH, $r = 0.995$.

occur in virtually all types of cells. Under normal conditions these processes are well regulated by the antioxidants and antioxidant enzymes which instantly detoxify the effect of free radicals. However, under the pathophysiological conditions as stated in the introduction, lipid peroxidation is enhanced because of the reduction in amount of tissue antioxidants in conjunction with the excessive amount of free radical production [12]. The fact that MDA represents one of the products of enzymatic PUFA oxygenation and an end product of auto-oxidative fatty peroxide decomposition and that extremely sensitive analytical methods are readily available to quantitate MDA, prompted the researchers to use MDA as presumptive marker for lipid peroxidation.

Several methods are available for the quantitation of MDA in biological tissues. These consist of direct detection or fluorometric detection of derivatized products using spectrophotometer [4,5,11] and spectrofluorometer [5,13], respectively. In addition, several methods using solvent extract followed by ion-pairing [14] or reversed-phase [15,16] HPLC and GC using nitrogen–phosphorus detection [17] or electron-capture detection [18] are also available. However, most of these methods are time-consuming and extremely sophisticated, and therefore, are not suitable for routine use in the laboratory. Among these methods, examination of TBA reactive products is the most popular and widely used to study the lipid peroxidation in biological samples. The success of the TBAR method depends on the accuracy of the determination of MDA content. However, as mentioned earlier, TBA reacts with many other compounds besides MDA, such as sugar alcohols, amino acids, glycerol and sialic acids, and as a result, it often overestimates the MDA content and yields erroneous results. This method was subsequently modified to determine MDA–TBA complex by HPLC, but the slowness as well as the complexity of the procedure could not make it easily adaptable for the routine assay of MDA.

The results of the present study demonstrate that at least five different lipid breakdown products (MDA, FDA, ADA, acetone and PDA) can be correlated with the lipid peroxidation after the development of oxidative stress in heart. In this method the carbonyls present in the myocardial tissue are converted into pyrazole and hydrazone derivatives by reacting with DNPH. This 2,4-dinitrophenyl hydrazine derivatization method in conjunction with HPLC and GC–MS was previously used to examine the lipid metabolites in the urine samples [19], and in conjunction with GC was used to examine MDA in a lipid peroxidation model system [20]. We have recently shown that this method can be used to monitor MDA formation during the reperfusion of ischemic myocardium [9]. However, we did not confirm the identity of the lipid products in this study. The present study, which is the extension of our previous observation, identified the aldehydes and ketone from the perfused myocardium by GC–MS and demonstrated an excellent correlation of the MDA values with the amount of oxidative stress, suggesting that this method is indeed suitable and highly efficient to monitor the development of oxidative stress in biological tissue such as heart.

In summary, we have shown that hydrazone derivatives of MDA and other lipid metabolites obtained from the heart subjected to oxidative stress can be assayed by HPLC as a marker for the measurement of the extent of lipid peroxidation. The simplicity, rapidity, and precision of the method should make it suitable for routine use.

ACKNOWLEDGEMENTS

This study was supported by Grants HL 22559 and HL 33889 from the US Public Health Service (National Institute of Health). We greatly appreciate the excellent secretarial assistance of Ms. Cathy Michanczyk and the computer assistance of Dr. Ion Moraru.

REFERENCES

1 D.K. Das, R.M. Engelman, D. Flansaas, H. Otani, J. Rousou and R.H. Breyer, *Basic Res. Cardiol.*, 82 (1987) 36.
2 J.M. Petruska, S.H.Y. Wong, W. Sanderman and B.T. Mossman, *Free Rad. Biol. Med.*, 9 (1990) 51.
3 H.S. Lee and A.S. Csallany, *Lipids*, 22 (1987) 104.
4 T.F. Slater, *Methods Enzymol.*, 105 (1984) 283.

5 R.P. Bird and H.H. Draper, *Methods Enzymol.*, 105 (1984) 299.
6 J.M.C. Gutterdge and T.R. Tickner, *Anal. Biochem.*, 91 (1978) 250.
7 H. Esterbauer, J. Lang, S. Zadravec and T.F. Slater, *Methods Enzymol.*, 105 (1984) 319.
8 L.W. Yu, L.L. Latriano, S. Duncan, R.A. Hartwick and G. Witz, *Anal. Biochem.*, 156 (1986) 326.
9 G.A. Cordis, N. Maulik, D. Bagchi, R.M. Engelman and D.K. Das, *J. Chromatogr.*, 632 (1993) 97.
10 H. Otani, R. Prasad, R.M. Jones and D.K. Das, *Am. J. Physiol.*, 257 (1989) H252.
11 H. Esterbauer, in D.C.H. Brien and T.F. Slater (Editors), *Free Radicals, Lipid Peroxidation and Cancer*, Academic Press, London, 1982, p. 101.
12 D.K. Das, R.M. Engelman, J.A. Rousou, R.H. Breyer, H. Otani and S. Lemeshow, *Basic Res. Cardiol*, 81 (1986) 155.
13 R. Santus, G. Huppe, J.-C. Maziere and L. Dabertret, *Biochim. Biophys. Acta*, 1084 (1991) 261.
14 W.A. Behrens and R. Madere, *Lipids*, 26 (1991) 232.
15 S.H.Y. Wong, J.A. Knight, S.M. Hopfer, O. Zaharia, C.N. Leach, Jr. and F.W. Sunderman, Jr., *Clin. Chem.*, 33 (1987) 214.
16 M.A. Carbonneau, E. Peuchant, D. Sess, P. Canioni and M. Clerc, *Clin. Chem.*, 37 (1991) 1423.
17 K.J. Dennis and T. Shibamoto, *J. Free Rad. Biol. Med.*, 7 (1989) 187.
18 M. Tomita, T. Okuyama, Y. Hatta and S. Kawai, *J. Chromatogr.*, 526 (1990) 174.
19 M.A. Shara, P.H. Dickson, D. Bagchi and S.J. Stohs, *J. Chromatogr.*, 576 (1992) 221.
20 E.N. Frankel and W.E. Neff, *Biochim. Biophys. Acta*, 754 (1983) 264.

Journal of Chromatography A, 661 (1994) 193–199
Elsevier Science B.V., Amsterdam

CHROMSYMP. 2965

Pre-column derivatization of biogenic amines and amino acids with 9-fluorenylmethyl chloroformate and heptylamine

Jochen Kirschbaum* and Bernd Luckas

Institute of Food Chemistry, University of Hohenheim, Pfaffenwaldring 55, D-70569 Stuttgart (Germany)

Wolf-Dieter Beinert

Fa. E. Merck, Frankfurter Strasse 250, D-64293 Darmstadt (Germany)

ABSTRACT

A rapid and fully automated pre-column derivatization method for the determination of primary and secondary biogenic amines and amino acids is described. The derivatization reagent 9-fluorenylmethyl chloroformate is used, together with heptylamine for removing the excess of reagent. The derivatization procedure is described in detail. Chromatographic separation and detection of biogenic amines only or of biogenic amines and amino acids is possible. Repeatability data and applications of the technique are presented.

INTRODUCTION

Biogenic amines and amino acids are natural compounds of different food products, such as fish, seafood, cheese and wine. During fermentation or spoilage biogenic amines are produced by decarboxylation of the corresponding amino acids. The latter are decomposed to different products [1–3]. Consequently, biogenic amines are indicators of food quality. Therefore, it is important to determine certain biogenic amines in the presence of amino acids in different food matrices. In 1981 Karmas [4] introduced the "biogenic amine index" (BAI) for quality control of fish and fish products.

$$\text{BAI} = \frac{(\text{mg/kg histamine} + \text{mg/kg putrescine} + \text{mg/kg cadaverine})}{(1 + \text{mg/kg spermidine} + \text{mg/kg spermine})}$$

BAI values > 10 indicate as a rule a clear reduction of quality. During ripening of cheese, biogenic amines are produced by decarboxylation of amino acids. The main products are tyramine, putrescine, cadaverine, tryptamine and β-phenylethylamine.

Most of the amines show neither natural UV absorption nor fluorescence. Therefore, chemical derivatization is necessary to obtain detectable derivatives of the amines after HPLC separation. Different derivatization reagents were tested for the analysis of amines, *e.g.* ninhydrin in amino acid analysers with post-column derivatization

* Corresponding author.

0021-9673/94/$07.00
SSDI 0021-9673(93)E1107-B

[5] and 5-dimethylaminonaphthalene-1-sulfonylchloride as well as *o*-phthaldialdehyde as pre-column derivatization reagents [6–12]. Recently, naphthalene-2,3-dicarboxaldehyde and 9-fluorenylmethyl chloroformate (FMOC-Cl) are introduced for analysis of amines with pre-column derivatization [13–17]. Primary and secondary amines react with FMOC-Cl to give the corresponding 9-fluorenylmethyl carbamates [18]. The fluorescent FMOC derivatives of biogenic amines and amino acids are reasonably stable. Therefore, the reaction is well suited for pre-column derivatization of both biogenic amines and amino acids.

EXPERIMENTAL

Apparatus

The following apparatus were used: D-6000 HPLC-manager version 2, revision 3 with Interface (Merck–Hitachi), degasser (Hitachi) with helium (5.0, Messer–Griesheim), L-6200A intelligent pump (Merck–Hitachi), T-6300 column thermostat (40°C column temperature) (Merck), AS-4000 intelligent autosampler (Merck–Hitachi), F-1050 fluorescence spectrophotometer (Merck–Hitachi) (excitation wavelength 265 nm, emission wavelength 315 nm), 250-4 Supersphere 60 RP-8 column (E. Merck)

Chemicals

Chemicals used were obtained from commercial sources, including: Fluka (Neu-Ulm, Germany), Merck (Darmstadt, Germany) and Sigma (Deisenhofen, Germany). All chemicals were of the highest purity available and were used without further purification. All HPLC solvents were obtained from Merck.

Preparation of standards

For the preparation of standards of biogenic amines and amino acids, 10 mg of each amino compound (or of the corresponding hydrochloride) were dissolved in 1000 ml of water. The resulting concentration of each amine (or its hydrochloride) was 10 μg/ml in the standard solution. Other concentrations were obtained by dilution of this standard solution, which was stored at −30°C.

Sample preparation

Wine and fruit and vegetable juices were injected directly into the HPLC system after filtration through a membrane (regenerated cellulose, 0.45 μm pore size, Sartorius G, No. 11606-13) and dilution (*e.g.* 1:5 or 1:20).

Samples of fish were chopped up and homogenized in a relationship of fish–0.1 *M* HCl (2:1, w/w). To 30 g paste (equivalent to 20.0 g fish) 40 ml 0.1 *M* HCl were added. After centrifugation and decantation of the supernatant solution, the residue was extracted twice with 40 ml 0.1 *M* HCl and once with 20 ml 0.1 *M* HCl. After filtration the extracts were made up to 100 ml with 0.1 *M* HCl and stored at − 30°C until HPLC analysis.

Samples of cheese were chopped up and homogenized in a relationship of cheese–0.1 *M* HCl (4:3, w/w). A 43.75-g amount of the paste (equivalent to 25.0 g cheese) were suspended with 40 ml 0.1 *M* HCl. After centrifugation the supernatant solution was filtered. The residue was extracted again twice with 20 ml 0.1 *M* HCl. The resulting combined extracts were made up to 100 ml with 0.1 *M* HCl and stored at − 30° until HPLC analysis.

Chromatographic conditions

Separation of biogenic amines only. Eluent A: 0.1 *M* sodium acetate, adjusted with NaOH to pH 4.4–acetonitrile (50:50). Eluent B: 100% acetonitrile. Gradient:

Time (min)	%B	Flow (ml/min)	Time (min)	%B	Flow (ml/min)
0	0	0.05	40	90	1.20
0.1	0	1.20	43	100	1.20
7	0	1.20	52	100	1.20
12	10	1.20	53	0	1.20
27	30	1.20	60	0	1.20
33	30	1.20	60.1	0	0.05

Separation of biogenic amines and amino acids. Eluent A: 0.1 *M* sodium acetate, adjusted

with NaOH to pH 4.4–acetonitrile (78:22). Eluent B: 100% acetonitrile. Gradient:

Time (min)	%B	Flow (ml/min)	Time (min)	%B	Flow (ml/min)
0	0	0.05	57	55	1.25
1	0	1.25	63	55	1.25
17	20	1.25	70	93	1.25
19	29	1.25	73	100	1.25
20	23	1.25	82	100	1.25
27	23	1.25	83	0	1.25
30	36	1.25	93	0	1.25
37	36	1.25	94	0	0.05
42	42	1.25			

Derivatization procedure

For derivatization, 50 μl sample (neutralization of strong acidic samples is sometimes necessary) were added to 200 μl borate buffer (0.2 *M* boric acid solution adjusted to pH 8.5 with 30% potassium hydroxide solution). After addition of 200 μl FMOC reagent (3 m*M* in acetone), the solution was mixed 3 min at room temperature. Then 50 μl heptylamine reagent (3 ml heptylamine and 15 ml acetonitrile, adjusted with 175 ml 0.1 *M* HCl to pH 7–8) were added to remove the excess of FMOC reagent. After 3 min of mixing, 80 μl of the reaction solution were diluted with 320 μl eluent A. Then 20 μl were injected for HPLC analysis. The procedure was used either in the manual mode or by utilizing a modified autosampler.

RESULTS AND DISCUSSION

Discussion of the derivatization conditions

Dependence of the derivatization on buffer and pH. 0.2 *M* Boric acid, adjusted to pH 8.5 with potassium hydroxide, was used for the derivatization buffer. Higher buffer concentrations sometimes led to separation of phases. The range of pH values, which was reported in earlier literature, was between pH 7.7 (derivatization of amino acids) [19] and pH 8.5 (derivatization of biogenic amines) [20]. Values of pH outside this range led to worse yields. Derivatization was therefore carried out at a pH of 8.5.

Dependence of the derivatization on concentration and solvent of the FMOC-Cl solution. When acetonitrile was used as the solvent for FMOC-Cl, a separation of phases occurred at high buffer concentrations. This could be avoided by use of acetone instead of acetonitrile. When the concentration of FMOC-Cl was too low (<2 m*M*), there was not enough FMOC-Cl for reaction, especially in samples in which many amino acids were present as well as biogenic amines. Histamine seemed to react particularly slowly, and in order to quantify, it was necessary either to separate the amino acids from the biogenic amines or to use higher FMOC-Cl concentrations (*e.g.* 5 m*M*).

If higher concentrations of FMOC-Cl were used, two problems appeared: (1) when the sample had low concentrations of amines and amino acids, the excess of FMOC-Cl was so high, that the FMOC derivative of heptylamine (which was used for reducing the excess of FMOC-Cl) was precipitated, and (2) an excess of FMOC-Cl caused interferences in the chromatographic separation at the retention time of spermidine and spermine.

Dependence of the derivatization on reaction time. Various reaction times (90 s–20 min) were tested for derivatization of the biogenic amines. The dependence of the peak heights of the amine derivatives on reaction time is shown in Fig. 1. Spermidine, spermine and β-phenylethylamine show optimum yields at a reaction time of 5 min whereas putrescine, histamine, cadaverine and tyramine have a maximum at 3 min. In the derivatization of the amino acids, a reaction time of more than 3 min led, particularly in the cases of glutamic acid and aspartic acid, to peaks which had a strong pronounced shoulder. Sometimes even double peaks were detected. Therefore, a reaction time of 3 min was chosen for derivatization of amino acids and biogenic amines.

Reactants to remove the excess of FMOC-Cl. Excessive FMOC-Cl had to be removed by extraction or reaction with an other amine, because disturbances appeared in the chromatog-

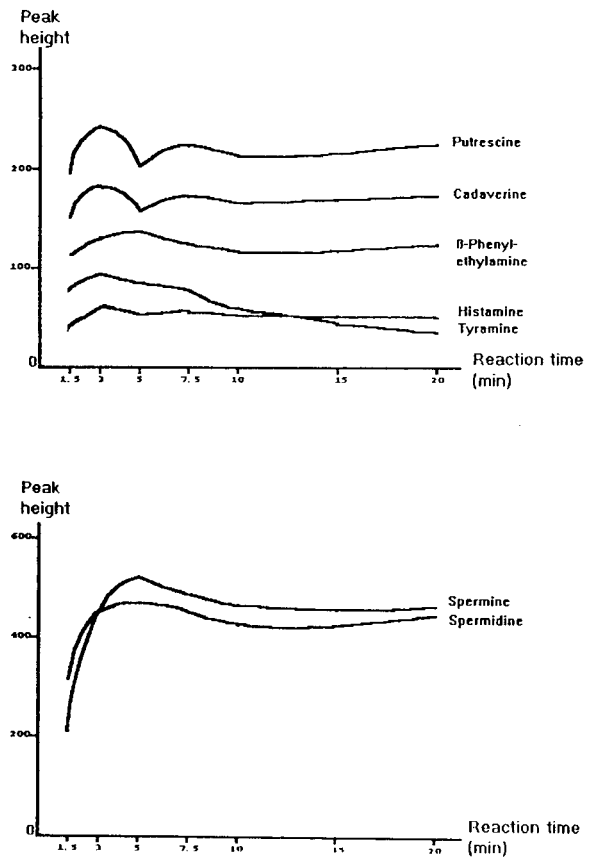

Fig. 1. Dependence of peak heights of FMOC derivatives on reaction time.

raphy, which made detection of tyramine and β-phenylethylamine impossible. Extraction with hexane removes FMOC-Cl from the water phase, but it also leads to the partial removal of most of the FMOC-amines. We also tested some amines, which react with FMOC-Cl after addition to the derivatization mixture. We obtained the best results with heptylamine, because no interferences were seen between its FMOC derivative and other FMOC-amines and -amino acids. When pure heptylamine was used, the pH would rise to such high values, that cleavage of the resulting FMOC derivatives took place. It was therefore necessary to adjust the pH of the heptylamine solution with 0.1 *M* HCl to a value in the range 7–8.

Influence of dilution after derivatization on chromatography. On injection into the HPLC system after derivatization and removal of the excess of FMOC-Cl it was found that the analysis was complicated by the presence of a greater number of interfering peaks from non-polar compounds. Most of these peaks could be suppressed by a fivefold dilution of the reaction mixture with starting eluent before injection. A loss of detection limit results from this dilution, but this factor is <5 because a better signal-to-noise ratio.

Discussion of eluents

Mixtures of aqueous buffers and acetonitrile were tested as eluents. We obtained best separations with 100 m*M* sodium acetate solution, which was adjusted with potassium hydroxide to pH 4.4, a column temperature of 45°C, and a flow-rate of 1.20–1.25 ml/min.

Chromatographic separation of biogenic amines

A mixture of seven amines (in the form of their hydrochlorides) was injected after derivatization for chromatographic separation of the biogenic amines. β-Phenylethylamine, putrescine, cadaverine, spermidine and spermine showed only one peak in their chromatograms (Fig. 2). Histamine and tyramine each gave two peaks, and in the case of histamine the peak with the retention time of 27.8 min clearly dominated. For tyramine the mono-substituted derivative (at the amino group) at a retention time of 9.0 min and the bis-substituted derivative (at the amino and at the hydroxy group) at 37.6 min were obtained. The yield of the bis-substituted derivative rose with higher concentrations, whereas the yield of the mono-substituted derivative decreased.

The presence of two derivatives showed no effect on the linearity for tyramine determination. We preferred to use the peak at 9.0 min in the chromatogram for quantitative analysis of tyramine, because of interferences with condensation products, which were eluted in the region of the second derivative.

For determination of calibration curves, standard solutions of 10 μg/ml, 5 μg/ml, 2.5 μg/ml and 1 μg/ml were derivatized and injected five times. The corresponding injection concentrations were 4 ng/20 μl, 2 ng/20 μl, 1 ng/20 μl

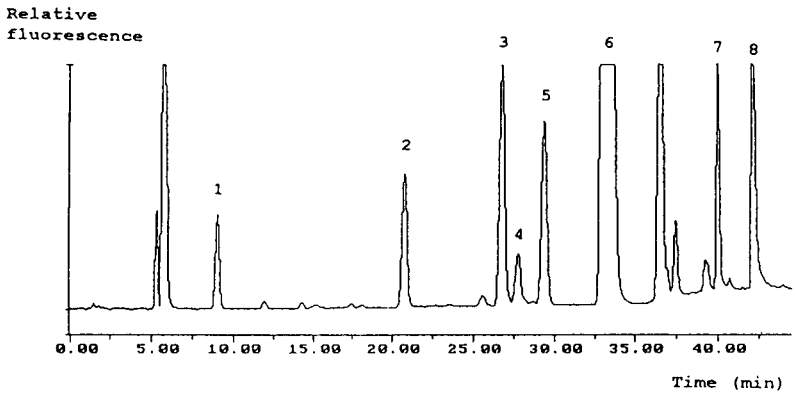

Fig. 2. HPLC chromatogram of a standard mixture (concentration 10 μg/ml) of biogenic amines after derivatization with FMOC-Cl and removing the excess of FMOC reagent with heptylamine. Peaks: 1 = tyramine; 2 = phenylethylamine; 3 = putrescine; 4 = histamine; 5 = cadaverine; 6 = heptylamine; 7 = spermidine; 8 = spermine.

and 0.4 ng/20 μl (calculated for the corresponding hydrochloride of the amine) (Table I).

In the last of these solutions the excess of FMOC-Cl became so high that condensation products were formed, which interfered with the chromatography of spermidine and spermine. Therefore, this concentration was neglected in the determination of correlation coefficients of spermidine and spermine.

The repeatability data determined in this analysis are shown in Table II.

A number of different food samples was successfully analysed for biogenic amine content using this procedure, *e.g.* wine, cheese, and fish (Fig. 3).

Chromatographic separation of amino acids and biogenic amines

A mixture of sixteen amino acids and seven biogenic amines (in the form of their hydrochlorides) was injected after derivatization with FMOC-Cl and removal of the excess of FMOC-Cl with heptylamine for chromatographic separation. The chromatogram (Fig. 4) showed a clear temporal separation of amino acids and biogenic

TABLE I

RESULTS OF THE LINEARITY TEST (ANALYSIS OF PEAK HEIGHT)

A = Correlation coefficient; B–E = relative standard deviations (%) of peak heights [injection concentrations: B 4.0 ng/20 μl ($n = 5$), C 2.0 ng/20 μl ($n = 5$), D 1.0 ng/20 μl ($n = 5$), E 0.4 ng/ 20μl ($n = 5$)].

Compound	A	B	C	D	E
Tyramine	0.9970	2.20	6.61	2.07	11.21
β-Phenylethylamine	0.9947	3.95	5.53	3.01	5.92
Putrescine	0.9971	2.91	4.88	5.64	15.51
Histamine	0.9954	2.98	1.40	4.94	5.17
Cadaverine	0.9965	3.20	5.52	6.65	10.97
Spermidine	0.9952	2.99	1.87	8.91	–
Spermine	0.9828	1.71	4.00	3.96	–

TABLE II

REPEATABILITY DATA (ANALYSIS OF RETENTION TIME AND OF PEAK HEIGHT)

A = Retention time (average) (min); B = standard deviation ($n = 20$); C = relative standard deviation (%) ($n = 20$); D = relative standard deviation (%) of peak heights ($n = 5$, injection concentration = 4 ng/20 μl).

Compound	A	B	C	D
Tyramine	9.00	0.016	0.18	2.20
β-Phenylethylamine	20.75	0.048	0.23	3.95
Putrescine	26.81	0.028	0.10	2.91
Histamine	27.79	0.036	0.13	2.98
Cadaverine	29.41	0.032	0.11	3.20
Spermidine	39.97	0.007	0.02	2.99
Spermine	42.09	0.019	0.05	1.71

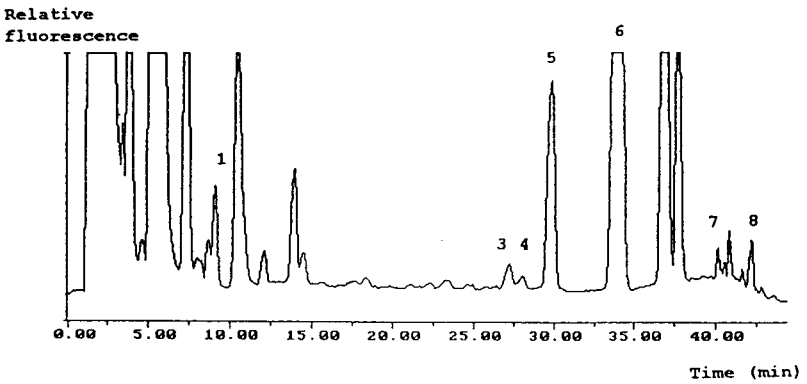

Fig. 3. HPLC chromatogram of salmon extract (with gradient for separation of biogenic amines). Peaks as in Fig. 2.

amines. Tyramine was the only representative of biogenic amines which eluted before the amino acid lysine.

Determination of calibration curves and repeatabilities were carried out analogous to the method described in the section *Chromatographic separation of biogenic amines*. The linearities and repeatabilities are as good as those for the chromatographic separation of biogenic amines [21].

Different food samples were successfully analysed for both biogenic amines and amino acids using this procedure, *e.g.* wine, fish and cheese (Fig. 5).

SUMMARY AND CONCLUSIONS

Primary and secondary amines react very fast with FMOC-Cl in slightly alkaline solution to give the corresponding fluorescent 9-fluorenylmethyl carbamates, which exhibit high stability. Therefore, selective determination of FMOC derivatives is possible by fluorescence detection after pre-column derivatization and reversed-phase HPLC separation. Disadvantages of this method are the fluorescence of FMOC-Cl and the fluorescence of hydrolysis products such as 9-fluorenylmethanol. Therefore, an additional step in the derivatization procedure is necessary

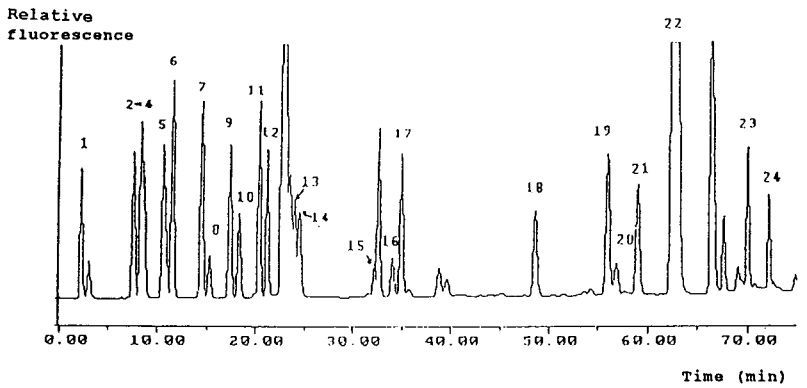

Fig. 4. HPLC chromatogram of a standard mixture (concentration 5 μg/ml) of biogenic amines and amino acids after derivatization with FMOC-Cl and removing the excess of FMOC reagent with heptylamine. Peaks: 1 = cysteic acid; 2 = aspartic acid; 3 = serine; 4 = glutamic acid; 5 = threonine; 6 = glycine; 7 = alanine; 8 = tyrosine; 9 = proline; 10 = methionine; 11 = valine; 12 = phenylalanine; 13 = isoleucine; 14 = leucine; 15 = histidine; 16 = tyramine; 17 = lysine; 18 = phenylethylamine; 19 = putrescine; 20 = histamine; 21 = cadaverine; 22 = heptylamine; 23 = spermidine; 24 = spermine.

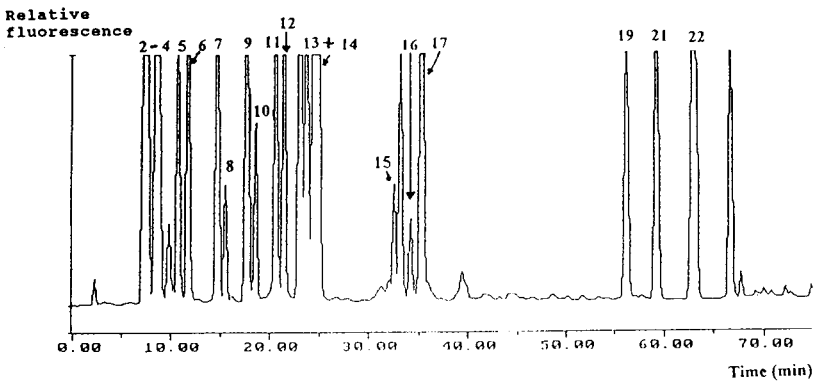

Fig. 5. HPLC chromatogram of cheese extract (with gradient for separation of biogenic amines and amino acids). Peaks as in Fig. 4.

for removing excess of reagent. There are two possibilities for this additional step: Extraction of excess reagent with *e.g.* hexane [18], or addition of an amine, *e.g.* adamantaneamine, which reacts with the excess of FMOC-Cl [19,20]. We prefer the second possibility using heptylamine as additional amine.

With this method we succeeded in detection of biogenic amines and amino acids. Additionally the determination of all biogenic amines (necessary for the calculation of the "biogenic amine index") is possible after HPLC separation of the FMOC derivatives and fluorescence detection. Yet, fluorescence detection is not sensitive enough for cystine, tryptophan, tryptamine and serotonine, because the fluorescence quantum yield is too low. However, UV detection at 265 nm is possible. The method allows full automatization with an autosampler such as the AS-4000 (Merck–Hitachi). Other advantages of the method are the good repeatabilities and good linearities for standards over a wide range of concentrations, and short run times.

REFERENCES

1 A. Askar and H. Treptow, *Biogene Amine in Lebensmitteln*, Eugen Ulmer Verlag, Stuttgart, 1986.
2 J. Stockemer, *Z. Lebensm.-Unters.-Forsch.*, 174 (1982) 108.
3 H.M.L.J. Joosten and J. Stadhouders, *Neth. Milk Dairy J.*, 41 (1987) 247.
4 E. Karmas, *Lebensm. Wiss. Technol.*, 14 (1981) 273.
5 P. Vandekerckhove and H.K. Hendrickx, *J. Chromatogr.*, 82 (1973) 379.
6 J.Y. Hui and S.L. Taylor, *J. Assoc. Off. Anal. Chem.*, 66 (1983) 853.
7 R. Schuster, *Hewlett-Packard HPLC Application Note, Publication No. 12-5954-90827*, Hewlett-Packard Intercontinental, Palo Alto, CA, 1985.
8 M. Roth, *Anal. Chem.*, 43 (1971) 880.
9 M.C. Garcia Alvarez-Coque, M.J. Medina Hernandez, R.M. Villanueva Camanas and C. Mongay Fernandez, *Anal. Biochem.*, 178 (1989) 1.
10 W.A. Jacobs, M.W. Leburg and E.J. Madaj, *Anal. Biochem.*, 156 (1986) 334.
11 T. Skaaden and T. Greibrokk, *J. Chromatogr.*, 247 (1982) 111.
12 E. Morier-Teissier, K. Drieu and R. Rips, *J. Liq. Chromatogr.*, 11 (1988) 1627.
13 M. Schollenberger and B. Luckas, presented at "*Euro Food Chem VI*", *Hamburg, 1991*, paper PE 25.
14 P. de Montigny, J.F. Stobaugh, R.S. Givens, R.G. Carlson, K. Srinivasachar, L.A. Sternson and T. Higuchi, *Anal. Chem.*, 59 (1987) 1096.
15 B.K. Matuszewski, R.S. Givens, K. Srinivasachar, R.G. Carlson and T. Higuchi, *Anal. Chem.*, 59 (1987) 1102.
16 S.M. Lunte, T. Mohabbat, O.S. Wong and Th. Kuwana, *Anal. Biochem.*, 178 (1989) 202.
17 P.J.M. Kwakman, H. Koelewijn, I. Kool, U.A.Th. Brinkman and G.J. de Jong, *J. Chromatogr.*, 511 (1990) 155.
18 S. Einarsson, S. Folestad, B. Josefsson and S. Lagerkvist, *Anal. Chem.*, 58 (1986) 1638.
19 *HPLC Analysis of Amino Acids by Automatic Pre-Column Derivatization with FMOC; Application Note*, Merck, Darmstadt, 1991.
20 B. Gustavsson and I. Betnér, *J. Chromatogr.*, 507 (1990) 67.
21 J. Kirschbaum and B. Luckas, *Vorsäulenderivatisierung von biogenen Aminen und Aminosäuren mit FMOC-Cl und Heptylamin, Final Report*, prepared for Fa. E. Merck, March 1993 (unpublished).

Journal of Chromatography A, 661 (1994) 201–205
Elsevier Science B.V., Amsterdam

CHROMSYMP. 2943

Determination of amines in wines by high-performance liquid chromatography with electrochemical coulometric detection after precolumn derivatization

Guido Achilli* and Gian Piero Cellerino

ESA srl, Piazza Maggiolini 3, 20015 Parabiago (Italy)

Gianvico Melzi d'Eril

Servizio di Analisi, IRCCS Fondazione "Istituto C. Mondino", Via Palestro 3, 27100 Pavia (Italy)

ABSTRACT

A sensitive and simple method for the simultaneous evaluation of histamine, tryptamine, tyramine, phenylethylamine, putrescine, cadaverine, 1,6-diaminohexane and tryptophan in wine was developed using HPLC and coulometric detection without clean-up pretreatment. After precolumn derivatization with *o*-phthaldialdehyde the compounds were separated on a reversed-phase column with gradient elution. To increase the selectivity of the method a coulometric array of sixteen electrodes at increasing potentials was used. The total analysis time was less than 35 min. The analytical performance of the methods is reported. The method was used to examine the levels of various amines in three different wines.

INTRODUCTION

Most amines found in wines come from the degradation of amino acids during malo-lactic fermentation [1]. Some of these amines generate distinct flavours which can affect the organoleptic quality of the wine. Other amines, such as histamine, tyramine, cadaverine and putrescine, can generate undesirable effects which include headache, vomiting and diarrhoea [2]. As a result, much attention has been given to the characterization and determination of amines in wine. However, the complexity of these natural products has made their identification and determination difficult. As amines are present in low concentrations in wines, they have been purified and preconcentrated by different methods [2,3], including *o*-phthaldialdehyde (OPA) derivatization with high-performance liquid chromatography (HPLC) followed by fluorescence detection [4] and derivatization of amines with dansyl chloride followed by electrochemical detection [4].

This paper reports the separation and the determination of eight amines (histamine, tryptamine, tyramine, phenylethylamine, putrescine, cadaverine, 1,6-diaminohexane and tryptophan) in a single run. It should be noted that tryptophan, an amino acid that is always present in wines, could present interference problems with the other amines. Separation and identification with the proposed method can be achieved without extraction or purification of the samples. This was done after their derivatization with OPA using gradient reversed-phase HPLC and electrochemical detection with an array of sixteen coulometric electrodes.

* Corresponding author.

0021-9673/94/$07.00
SSDI 0021-9673(93)E0971-V

EXPERIMENTAL

Chemicals

The two mobile phases used in the gradient runs were prepared by dissolving the appropriate chemicals in deionized water. Mobile phase A contained 0.1 *M* sodium acetate, 12.5% acetonitrile and 5% tetrahydrofuran (pH 6.5) and B contained 0.1 *M* sodium acetate, 25% acetonitrile and 30% tetrahydrofuran (pH 6.5). The mobile phases were filtered through a 0.22-μm PTFE lyophilic membrane (Millipore, Bedford, MA, USA) prior to use.

Acetonitrile (HPLC grade) and tetrahydrofuran, OPA, sodium acetate, mercaptoethanol and sodium tetraborate (all of analytical-reagent grade) were purchased from Sigma Chimica (Milan, Italy). The water used to prepare the mobile phases for the gradient runs was purified with a Milli-Q water-purification system (Millipore) and it was filtered through a 0.45-μm filter (Millipore). OPA solution was prepared by dissolving 27 mg of the compound in 1 ml of methanol. To this solution 5 μl of mercaptoethanol and 9 ml of 0.1 *M* sodium tetraborate (pH 9.3) were added. The final OPA solution was stored at room temperature and diluted 1:3 with sodium tetraborate (0.1 *M*, pH 9.3) just prior to use.

Apparatus

The chromatographic system used was a Coulochem Electrode Array System (CEAS) (ESA, Bedford, MA, USA). This instrument consisted of a refrigerated autosampler, two HPLC pumps capable of gradient operation and a detection system of four cell packs in series. These cell packs were contained with the column in a thermostatic compartment. Each pack contained four porous graphite working electrodes. Solutes were separated on a Model HR80 PTFE-lined column (80 × 4.6 mm I.D.) containing ODS, particle size 3 μm (ESA). The CEAS software monitored and controlled the autosampler, the two pumps, the detection system and the temperature of the column compartment.

Chromatographic method

A method capable of completely separating the eight compounds chosen was developed. It consisted of a gradient in which the organic modifier was altered during the run. The time line showing the gradient used in this separation is presented in Table I: the total flow-rate was 0.80 ml/min and the temperature of the column compartment was maintained at 37°C. The sixteen detector potentials were arranged in a symmetric array from 0 mV at electrode 1 to 1200 mV at electrode 16 with increments of 80 mV at each electrode. The indicated potentials refer to the solid-state palladium reference electrode built in the coulometric cells. Their absolute values were about 250 mV lower than the corresponding potential measured by using an Ag/AgCl reference electrode.

Standard and sample preparation

Pure standards of histamine, tryptophan, tryptamine, tyramine, phenylethylamine, putrescine, cadaverine and 1,6-diaminohexane were obtained from Sigma. Stock standard solutions were prepared by dissolving 10 mg of each component in methanol. These solutions were then subdivided into 1-ml portions and stored at −20°C. An eight-component working standard solution was prepared by combining and diluting with mobile phase A an aliquot of each of the stock standard solutions (final concentration 2 μg/ml). This method was used to measure the amines present in three wines: Gewürztraminer, Barolo and Port. The standards and the samples were kept refrigerated at 4°C up to the moment

TABLE I

GRADIENT PROFILE USED IN THE CHROMATOGRAPHIC SEPARATION

Time (min)	Phase A (%)	Phase B (%)
0	85	15
4.1	85	15
13	50	50
23	0	100
38	0	100
38.1	15	85
39	15	85

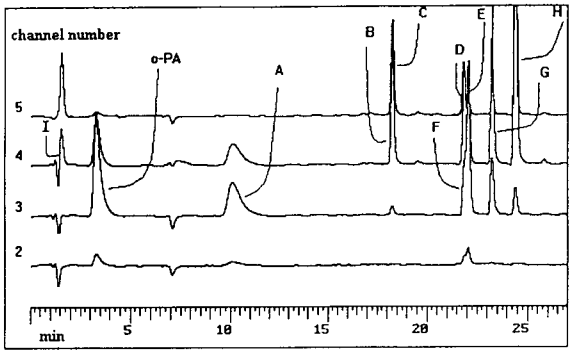

Fig. 1. Chromatogram of the OPA derivatives of (A) histamine, (B) tryptophan, (C) tryptamine, (D) tyramine, (E) phenylethylamine, (F) putrescine, (G) cadaverine and (H) 1,6-diaminohexane. Other peaks: injection void (I) and derivatizing reagent OPA. For clarity only four channels are presented. Electrode potentials: 2 = 80 mV; 3 = 160 mV; 4 = 240 mV; 5 = 320 mV. Full-scale sensitivity: 10 μA.

of derivatization. Prior to injection all samples were filtered through a 0.22-μm membrane (Millipore). The standards and samples, without any clean-up pretreatment, were then derivatized with OPA reagent and 20 μl were injected into the CEAS.

Precision

To investigate the within-run precision, twenty sets of the derivatized working standard mixture were injected and analysed under the conditions described above. Analysis of the same sample over a 10-day span (the sample was stored in aliquots at −20°C between assays) was used to measure the between-run precision.

RESULTS

Under the above conditions, a mixture containing the eight standards was separated and analysed. A typical separation of a 20-μl sample containing 25 ng of each of the eight components as external standard is shown in Fig. 1. Only four traces are shown, corresponding to electrodes 1–4. Although all sixteen channels were used, only a few signals are shown for the purpose of clarity. The total analysis time was less than 35 min. The detection characteristics of these eight standards are presented in Table II.

The retention time repeatability during the precision studies (carried out over a 10-day span) was found to be excellent (R.S.D. < 1.8%) for all standards. This was due to the strict control of both the gradient profile and the column temperature. The precision (within- and between-run), detection limits and dominant potentials are also reported (the dominant potential is that electrode potential where the maximum signal occurs for a given substance if eluted

TABLE II

CHROMATOGRAPHIC AND ELECTROCHEMICAL CHARACTERISTICS OF THE EIGHT EXTERNAL STANDARDS

25 ng of each component per injection of 10 μl.

Compound	Retention time (min)	Detection limit (mg/l)	Within-run R.S.D. (%)	Between-run R.S.D. (%)	Recovery[a] (%)	Dominant potential[b] (mV)
Histamine	10.05	0.016	2.2	3.2	93	80
Tryptophan	16.74	0.021	1.0	2.9	89	320
Tryptamine	17.14	0.018	1.8	3.5	96	320
Tyramine	18.23	0.016	0.7	3.2	92	320
Phenylethylamine	21.78	0.022	1.2	2.9	88	320
Putrescine	22.01	0.025	2.6	4.8	76	160
Cadaverine	23.19	0.021	2.1	5.2	89	160
1,6-Diaminohexane	24.34	0.012	3.1	3.9	103	160

[a] The recoveries are the means of three replicates from a sample of Gewürztraminer wine spiked with 10 ng of each of the eight amines.

[b] See text.

through a given coulometric array). Confirmation of peak identification was carried out in two steps. In the first, samples were spiked with the relevant standard. In the second, the ratio R between each standard was matched with the actual peaks of the samples (R is the ratio of the signal distribution between dominant and subdominant channels expressed as a percentage, where 1 corresponds to maximum match and 0 corresponds to no match) [5].

Several dilutions of the amine standards, having concentrations from 100 μg/ml to 10 ng/ml, were prepared and analysed to study the linearity of the method. The plots for the standards for all amines were linear throughout the range tested ($r = 0.997$, $p < 0.001$). The minimum detectable amounts (at a signal-to-noise ratio of 3:1) are reported in Table II. The recoveries for three replicates from a sample of Gewürztraminer wine are also reported in Table II. This sample was spiked with 10 ng of each of the eight amines and derivatized as described above.

The repeatability of the method was tested by repeated (twenty) injections of a standard solution containing 10 ng of each of the eight amines. The within-run variability (R.S.D.) ranged from 0.7 to 3.1%. The between-run variability was studied by analysing the same standard solution over a 10-day span. The R.S.D. ranged from 2.9 to 5.2%.

The standard mixture was used to examine the amine levels in three different wines: Gewürztraminer, a white, aromatic, rich-bodied wine, from Alto Adige, Italy; Barolo, a red, tannic, high-bodied wine aged 6 years in oak barrels, from Piemonte, Italy; and Port, an aged fortified wine, from Oporto, Portugal. These wines were selected since as a group they encompassed many different characteristics. The results are reported in Table III.

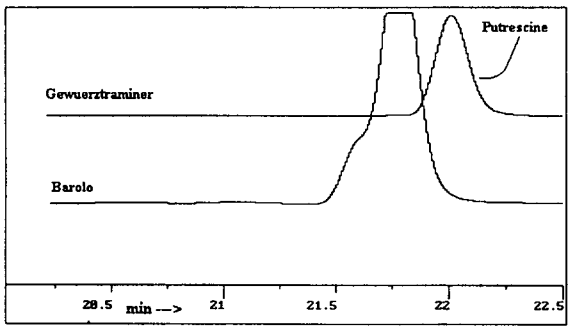

Fig. 2. Chromatograms of 20-μl samples of Barolo and Gewürztraminer wines after derivatization at 160 mV (channel 3). Full-scale sensitivity: 200 nA.

In Fig. 2, a comparison between a portion of the chromatogram of Barolo wine and one of Gewürztraminer wine is shown. The trace corresponds to the signal generated by electrode 3, which was set at 160 mV. The putrescine peak is visible in Gewürztraminer wine at a relatively high concentration whereas it is not present in Barolo wine. In addition, at this low potential a major unidentified peak is present in Barolo wine (not present in the external standard). This peak could interfere in the determination of

TABLE III

CONCENTRATIONS OF THE MEASURED COMPOUNDS IN THREE DIFFERENT WINES

Compound	Concentration (mg/l)		
	Gewürztraminer	Barolo	Port
Histamine	42.31	10.66	12.07
Tryptophan	9.52	0.74	–
Triptamine	0.40	2.94	1.09
Tyramine	25.49	5.65	1.95
Phenylethylamine	2.98	3.31	2.06
Putrescine	162.24	18.20	7.48
Cadaverine	0.28	0.76	0.31
1,6-Diaminohexane	0.25	0.12	1.59

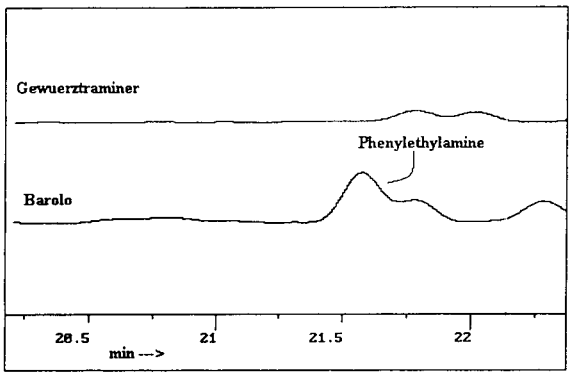

Fig. 3. Chromatograms of 20-μl samples of Barolo and Gewürztraminer wines after derivatization at 320 mV (channel 5). Full-scale sensitivity: 200 nA.

phenylethylamine. Fig. 3 shows the corresponding section of the chromatogram of electrode 5, which was set at 320 mV. At this electrode the signal of the unidentified substance shown in Fig. 2 disappeared. The substance was completely reacted by the coulometric electrodes placed before this electrode. As a result, it was possible to measure phenylethylamine without any interference at this channel.

DISCUSSION AND CONCLUSIONS

The use of CEAS for determining neurochemicals in tissues [6,7] and in cerebrospinal fluid [5] has been reported. More recently, a method for the evaluation of phenolic compounds in fermented beverages, fruit juices and plant extracts on the same analyser has been proposed [8].

In this work, we demonstrated that by combining reversed-phase chromatography with highly selective array electrochemical detection it is possible to determine a large number of amines in wines in a single run of 35 min. The derivatization procedure described allows for simple, rapid sample preparation at low cost and without any clean-up pretreatment. This method yields a high precision without preliminary separation of the different families of compounds which is necessary in other methods. The coulometric efficiency of each element of the array allows a complete voltammetric resolution of analytes as a function of their reaction potential. Some peaks may be resolved by the detector even if they are unresolved when they leave the chromatographic column. The detection limit is similar to that which was found with the measurement of dansyl derivatives followed by electrochemical detection [4]. However, it was better than the detection limit observed with OPA derivatization followed by fluorimetric detection [4]. In conclusion, the proposed method for the determination of amines in wines provides a simple, fast and reproducible sampling procedure with good selectivity and sensitivity over a wide concentration range.

REFERENCES

1 K. Mayer and G. Pause, *Mitt. Geb. Lebensmittelunters Hyg.*, 71 (1980) 38.
2 *P. Lehtonen, in Proceedings of the French Scientific Week*, French–Finnish Association for Scientific and Technical Research, Helsinki, 1989, pp. 305–313.
3 J. Almy, C.S. Ough and E.A. Crowell, *J. Agric. Food Chem.*, 31 (1983) 911.
4 G. Chiavari, G.C. Galletti and P. Vitali, *Chromatographia*, 27 (1989) 216.
5 V. Rizzo, G. Melzi d'Eril, G. Achilli and G.P. Cellerino, *J. Chromatogr.*, 536 (1991) 229.
6 K.J. Swartz and W.R. Matson, *Anal. Biochem.*, 185 (1990) 363.
7 C.N. Svendsen and D. Bird, *Neurosci. Lett. Suppl.*, 35 (1989) 49.
8 G. Achilli, G.P. Cellerino and G. Melzi d'Eril, *J. Chromatogr.*, 632 (1993) 111.

Journal of Chromatography A, 661 (1994) 207–213
Elsevier Science B.V., Amsterdam

CHROMSYMP. 2916

Analytical study of polyoxyethylene surfactants of high degree of condensation by normal-phase liquid chromatography on *p*-nitrophenyl-bonded silica

P.L. Desbène*

Laboratoire d'Analyse des Systèmes Organiques Complexes, Université de Rouen, Institut Universitaire de Technologie, 43 rue Saint Germain, 27000 Evreux (France)

B. Desmazieres

Institut Européen de Recherches Multidisciplinaires sur les Peptides, Université de Rouen, B.P. 118, 76134 Mont Saint Aignan Cédex (France)

ABSTRACT

Polyoxyethylene-based non-ionic surfactants resulting from the condensation of ethylene oxide with fatty alcohol cuts have been widely studied by high-performance liquid chromatography. Even though satisfactory analyses are obtained in normal-phase partition liquid chromatography (*e.g.*, using a diol stationary phase) and in reversed-phase partition liquid chromatography (*e.g.*, using C_8 bonded silica) for polyoxyethylenic (POE) surfactants with an average ethylene oxide (EO) number lower than 20 ($\bar{n} < 20$ EO), the analysis of the total distribution of the whole EO oligomers is impossible with more condensed POE surfactants ($\bar{n} > 20$ EO on C_{16} and C_{18} alcohols). In order to establish the total distribution of such surfactants, the potential offered by stationary phases with electron-acceptor characteristics used in normal-phase liquid chromatography was studied. The stationary phase selected was a *p*-nitrophenyl-bonded silica with an *n*-propyl spacer. Different mobile phases were tested. The results obtained indicated the possibility of determining the total distribution of polyoxyethylenic oligomers from 1 to more than 80 EO units with baseline resolution using this stationary phase and *n*-heptane–dichloromethane–methanol as the mobile phase, with either UV detection after derivatization of compounds that do not possess chromophoric groups or light-scattering detection, the latter technique having the great advantage of not requiring any derivatization.

INTRODUCTION

Various chromatographic methods have been proposed for the analysis of polyoxyethylenic surfactants. Most studies have been performed by normal-phase high-performance liquid chromatography (HPLC). The literature [1–5] suggests that adsorption chromatography will not give a satisfactory analysis of surfactants that have a wide distribution of polyoxyethylene (POE) units. The only HPLC technique that appeared to offer promise for the analysis of surfactants in terms of their ethylene oxide (EO) distribution is normal-phase chromatography using amino-bonded silica [6–9], cyano-bonded material [10–13] and more recently diol-bonded packings [14–16]. In particular, we have previously reported the analysis of non-ionic surfactants (KL6, KM11 and KM20) containing EO units of various lengths condensed with long-chain (C_{16} and C_{18}) aliphatic alcohols via normal-phase chromatography on diol-bonded silica [16,17]. In order to perform the analysis of these surfactants in crude oil phases, a specific and sensitive detector such as the electrochemical

* Corresponding author.

0021-9673/94/$07.00
SSDI 0021-9673(93)E0881-T

detector was required [18]. As this detection technique is difficult to apply in normal-phase chromatography, we optimized the reversed-phase analysis of these surfactants [19]. Other workers have studied the potential of reversed-phase chromatography [20,21]. Unfortunately, none of these chromatographic methods allows the analysis of polyoxyethylenic (POE) surfactants with a high degree of condensation such as KM25 ($\bar{n} = 25$ EO), condensed with a mixture of saturated fatty alcohols (C_{16} and C_{18}). Okada [22,23], using a combination of ion-exchange chromatography and complexation of metallic cations by POE chains, first analysed POE surfactants ($\bar{n} = 9$ EO) condensed with a C_{12} fatty alcohol. Moreover, using a temperature gradient [24], he performed the partial analysis of a non-ionic surfactant having a mean chain length of 25 EO units condensed again with a C_{12} saturated fatty chain. This technique allowed the separation of oligomers up to 41 EO units. However, the resolution of the peaks between $n = 6$ and 14 EO units was limited. Recently, we demonstrated [25], after optimization (nature of the stationary phase, nature and concentration of the complexing cation and its associated counter ion, nature and concentration of the organic co-solvent, pH of the aqueous phase and temperature of the separation), the possibility of analysing the total distribution of the POE surfactants with a high degree of condensation, such as KM25.

However, although this method allows the resolution of compounds with a degree of condensation corresponding to 60 oligomers, it has the disadvantage of a total resolution loss of the first units, *i.e.*, oligomers with a condensation of 1–6 EO units. Under such conditions, and with a view to obtaining a satisfactory resolution both of the first members of the distribution and of the oligomers of high degree of condensation, *i.e.*, more than 60 EO units, we undertook to study the potential offered by normal-phase partition stationary phases with the characteristic of interacting with the solutes by charge transfer. As the polyoxyethylenic surfactants we studied are potential electron donors, we chose a stationary phase functioning as an electron acceptor. The stationary phase selected for this study was a *p*-nitrophenyl-bonded silica with an *n*-propyl spacer.

EXPERIMENTAL

Reagents

KM25 non-ionic surfactant ($\bar{n} = 25$ EO) was of technical grade from Marchon France (Saint Mihiel, France). Cetalox AT non-ionic surfactant ($\bar{n} = 50$ EO) from Witco (Saint Pierre les Elbeuf, France) was also of technical grade. Igepal non-ionic surfactants Co-720 ($\bar{n} = 12$ EO), Co-890 ($\bar{n} = 40$ EO) and Co-990 ($\bar{n} = 100$ EO), obtained by condensation of *p*-nonylphenol with ethylene oxide, were supplied by Aldrich (Strasbourg, France). A surfactant standard with six EO units and a C_{18} moiety was purchased from Nikko Chemicals (Tokyo, Japan). All the solvents used (*n*-heptane, dichloromethane, chloroform, ethyl acetate, tetrahydrofuran, acetonitrile, 2-propanol and methanol) were of LiChrosolv HPLC grade (Merck, Darmstadt, Germany) and were filtered through a 0.45-μm FH filter (Millipore, Molsheim, France). Analyte compounds that do not possess chromophoric groups were derivatized to esters with 3,5-dinitrobenzoyl chloride according to a previously described method [16].

Instrumentation

Chromatographic separations were performed either on a 250 mm × 3 mm I.D. column filled with 5-μm Nucleosil *p*-nitrophenyl-bonded silica (Macherey–Nagel, Düren, Germany) or on a 250 mm × 4.6 mm I.D. column filled with 5-μm Ultraspher cyano-bonded silica (Beckman, Fullerton, CA, USA). Analyses were carried on using an HP 1090 low-pressure gradient liquid chromatograph (Hewlett-Packard, Palo Alto, CA, USA) fitted with a Rheodyne Model 7010 injector (5- or 20-μl loop). The detector was either a PU 4020 UV–Vis spectrophotometer (Pye Unicam, Cambridge, UK) fitted with an 8-μl cell (operated at 254 nm) or an ACS 950 light-scattering detector (ACS, Manchester, UK) using a 12 l min^{-1} flow-rate of dry air at 45°C.

RESULTS AND DISCUSSION

As non-ionic surfactants such as KM25 and Cetalox AT do not possess chromophoric groups, we optimized the analytical conditions after derivatizing these compounds to esters via reaction with 3,5-dinitrobenzoyl chloride. As a result of the wide range of polarity of these surfactant oligomers, owing to their high degree of condensation, isocratic analysis could not be considered. Hence only UV detection could be used during the optimization phase, as light-scattering detection, which is compatible with an elution gradient, had never been used to detect surfactants presenting such a high degree of condensation [26].

Different co-solvents were tested, with a view to finding the mobile phase composition giving the best possible resolution in unit time. The choice of co-solvents appeared to be relatively limited, as the mobile phase should present both a high elution strength because of the high polarity of the samples being analysed and a low viscosity in order to keep a high performance of the system.

With respect to these constraints and in order to optimize the system selectivity, we selected (see Table I) solvents belonging to each of the eight solvent groups defined by Snyder [27], with the exceptions of solvents of group 1 (too weak eluent), solvents of group 4 (too strong eluent) and solvents of the group 7 (too high cut-offs and incompatible with UV detection), *n*-heptane being used as the base solvent.

The solvents of groups 5 and 8, dichloromethane and chloroform, which are too weak eluents, were not used as co-solvents but were used as a third solvent in order to allow miscibility with *n*-heptane of solvents belonging to group 2, *i.e.*, methanol or 2-propanol. The solvents belonging to groups 3 and 6, tetrahydrofuran and ethyl acetate, give insufficient selectivities and are not suitable for resolving the complex mixtures studied.

Hence only solvents belonging to group 2 present suitable eluent strengths and selectivities. However, 2-propanol, previously used as a co-solvent in normal-phase partition chromatography with a diol-bonded silica stationary phase to analyse non-ionic POE surfactants with an intermediate average number of EO groups (*e.g.*, KM11, $\bar{n} = 11$ EO) [16], does not allow in the present instance the satisfactory resolution of oligomers more condensed than 25 EO units, as shown in Fig. 1.

In contrast, methanol, which is a sufficiently strong eluent and shows good selectivity, allows a satisfactory analysis of the 3,5-dinitrobenzoyl ester of KM25. However, owing to the non-miscibility of methanol and *n*-heptane, as previously reported, a third solvent is required. Hence, the total resolution of the KM25 dis-

TABLE I

SOLVENTS TESTED TO OPTIMIZE THE CHROMATOGRAPHIC SYSTEM

Solvent	Solvent group[a]	Viscosity at 20°C (cP)	Miscibility number, *M*
2-Propanol	2	2.37	15
Methanol	2	0.60	12
Tetrahydrofuran	3	0.45	17
Dichloromethane	5	0.42	
Ethyl acetate	6	0.45	19
Chloroform	8	0.57	19

[a] According to Snyder [27].

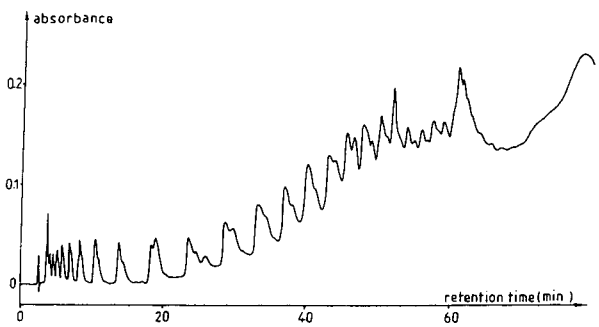

Fig. 1. Analysis of KM25 by normal-phase partition chromatography. Stationary phase, *p*-nitrophenyl bonded silica (250 mm × 3 mm I.D., $d_p = 5$ μm); mobile phase elution gradient from *n*-heptane–dichloromethane–2-propanol at 85:7.5:7.5 to 50:25:25 in 40 min, then isocratic elution at 50:25:25 for 50 min; flow-rate, 0.7 ml/min; temperature, 25°C.

tribution is possible with an elution gradient from the initial mobile phase [*n*-heptane–dichloromethane–methanol (90:5:5) to the final phase [*n*-heptane–dichloromethane–methanol (65:17.5:17.5)] (see Fig. 2).

This important point having been settled, we attempted to analyse non-ionic POE surfactants with a degree of condensation considerably higher than that of KM25, such as Cetalox AT ($\bar{n}$ = 50 OE).

As no pure standard of a POE surfactant with a high degree of condensation is commercially available, we performed, as a first step, the analysis of Cetalox AT in the presence of KM25. The broad EO distribution of the latter, between 1 and 50 EO, allows the precise attribution of the chromatographic peaks corresponding to the oligomers of Cetalox AT. The chromatogram obtained for a mixture of dinitrobenzoyl esters of KM25 (10^4 ppm, w/w) and Cetalox AT (10^4 ppm, w/w) is reported in Fig. 3. The analysis was performed as previously on a *p*-nitrophenyl-bonded silica stationary phase and using methanol as co-solvent in the mobile phase.

The analysis of this complex mixture with a high degree of condensation appears to be relatively satisfactory. It is possible to visualize oligomers between 1 and about 80 EO units. Moreover, the system allows a satisfactory separation of the first 30 oligomers. With more condensed oligomers, the efficiency of the chromatographic system is insufficient with respect to the selectivity obtained. In order to improve the resolution for highly condensed oligomers, we studied the influence of temperature. A temperature increase should lead to an improved efficiency of the chromatographic system owing to the decreased viscosity of the mobile phase. The chromatogram obtained at 45°C for a mixture of KM25 and Cetalox AT esters is reported in Fig. 4. The other operating conditions were kept identical with those previously reported.

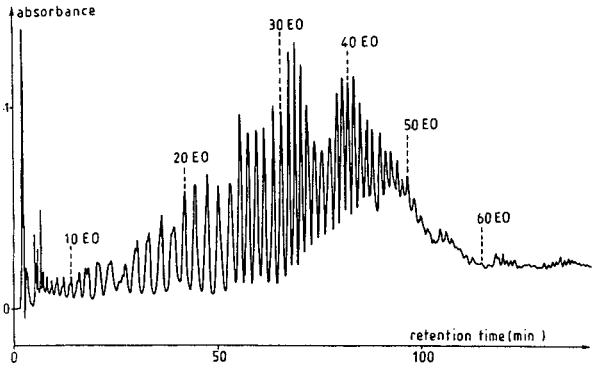

Fig. 3. Analysis of a mixture of non-ionic POE surfactants KM25 (10^4 ppm, w/w) and Cetalox AT (10^4 ppm, w/w) as esters by normal-phase partition chromatography. Conditions as in Fig. 1, except elution gradient from *n*-heptane–dichloromethane–methanol at 90:5:5 to 65:17.5:17.5 in 190 min, then isocratic elution at 65:17.5:17.5 for 30 min; flow-rate, 0.6 ml/min.

As evidenced by this chromatogram, it is possible, using these new operating conditions, to analyse correctly a highly condensed non-ionic POE surfactant. The resolution remains constant over the whole distribution of oligomers between 1 and >80 EO units.

Having established the optimum conditions for highly condensed non-ionic surfactants, *viz.*, a *p*-nitrophenyl-bonded silica stationary phase,

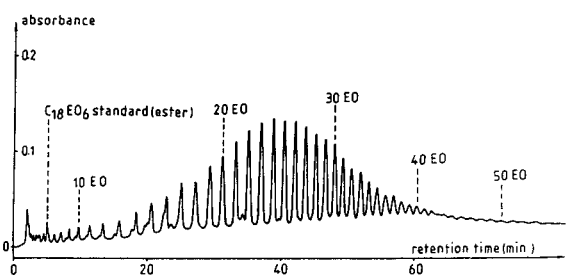

Fig. 2. Analysis of KM25 by normal-phase partition chromatography. Conditions as in Fig. 1, except final mobile phase composition *n*-heptane–dichloromethane–methanol at 65:17.5:17.5 and isocratic elution for 30 min.

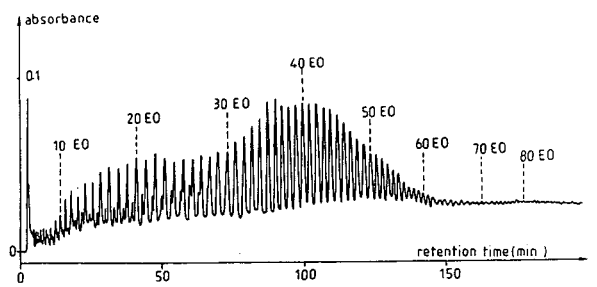

Fig. 4. Analysis of a mixture of non-ionic POE surfactants KM25 (10^4 ppm, w/w) and Cetalox AT (10^4 ppm, w/w) as esters by normal-phase partition chromatography. Conditions as in Fig. 3, except temperature, 45°C.

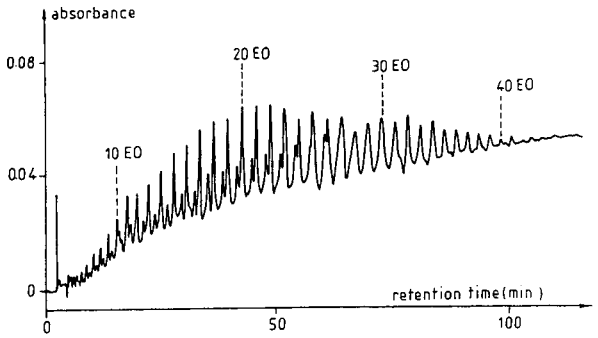

Fig. 5. Analysis of the non-ionic POE surfactant KM25, as the ester, at a 10^4 ppm (w/w) concentration by normal-phase partition chromatography. Conditions as in Fig. 4.

an elution gradient between an initial mobile phase of *n*-heptane–dichloromethane–methanol (90:5:5) and a final composition of *n*-heptane–dichloromethane–methanol (65:17.5:17.5) and a temperature of 45°C, we studied the separation of KM25 and Cetalox AT oligomers. The chromatograms obtained under these conditions are reported in Figs. 5 and 6 and their oligomer distributions as a function of EO number are given in Figs. 7 and 8.

The average numbers of EO units determined for both KM25 and of Cetalox AT are satisfactory, being 23 and 43 EO, respectively, compared with the values given by the manufacturers of 25 and 50 EO, respectively.

These satisfactory results led us to attempt the analysis of even more condensed non-ionic POE surfactants and we decided to study a mixture of Igepal Co-720, Co-890 and Co-990. These non-ionic surfactants result from the condensation of

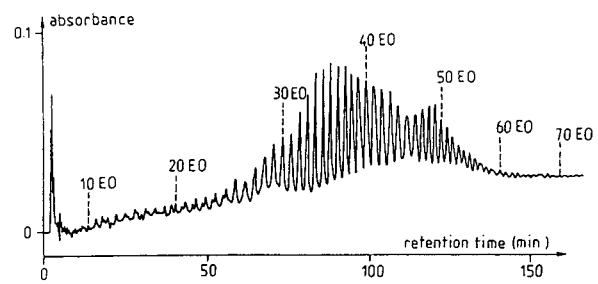

Fig. 6. Analysis of the non-ionic POE surfactant Cetalox AT, as the ester, at a 10^4 ppm (w/w) concentration by normal-phase partition chromatography. Conditions as in Fig. 4.

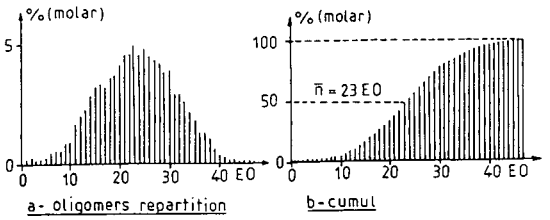

Fig. 7. Distribution histograms obtained from the chromatographic analysis of the non-ionic POE surfactant KM25, as the ester, reported in Fig. 5.

ethylene oxide with *p*-nonylphenol. Their mean EO numbers are $\bar{n} = 12$ EO for Igepal Co-720, 40 EO for Co-890 and 100 EO for Co-990. As they possess an aromatic group, these non-ionic surfactants can be detected without derivatization by UV spectrophotometry, unlike KM25 and Cetalox AT. The chromatogram obtained for the mixture of the three Igepal surfactants under the optimum conditions is reported in Fig. 9a.

Although this chromatographic system appears satisfactory for Igepal Co-720 ($\bar{n} = 12$ EO) and Co-890 ($\bar{n} = 40$ EO), it is insufficient to resolve

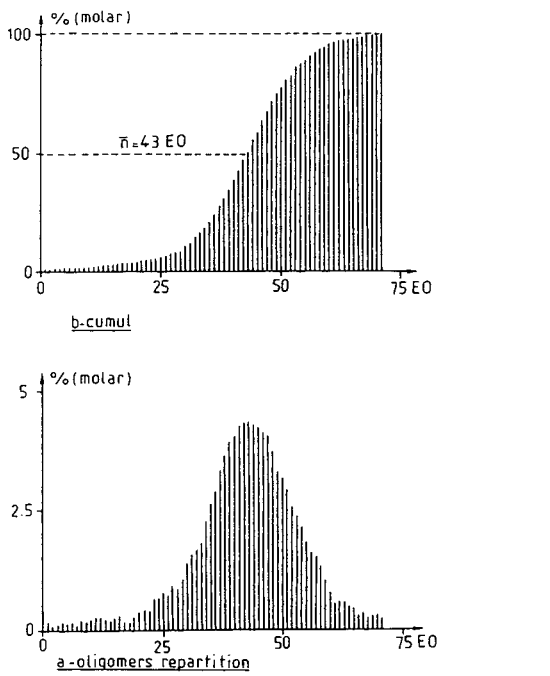

Fig. 8. Distribution histograms obtained from chromatographic analysis of the non-ionic POE surfactant Cetalox AT, as the ester, reported in Fig. 6.

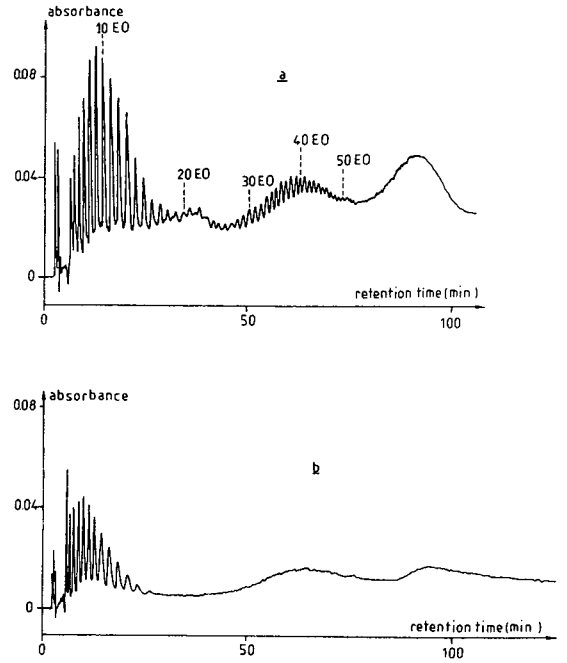

Fig. 9. Analysis of a mixture of the non-ionic POE surfactants Igepal Co 720, Co 890 and Co 990 by normal-phase partition chromatography at 45°C, using an elution gradient from *n*-heptane–dichloromethane–methanol at 90:5:5 to 65:17.5:17.5. Stationary phase: (a) *p*-nitrophenyl-bonded silica; (b) cyano-bonded silica.

the complex mixture constituting Igepal Co-990 ($\bar{n} = 100$ EO). It must be noted that the p-nitrophenyl-bonded silica stationary phase is clearly better adapted to the analysis of these complex compounds than the normal-phase partition stationary phases commonly used with non-ionic POE surfactants. For instance, Fig. 9b reports the analysis of this three-surfactant mixture under the same conditions using a cyano-bonded silica stationary phase.

To complete this study, as the procedure of derivatization of KM25 and Cetalox AT can be a drawback for some applications, we replaced UV detection with light-scattering detection, the other conditions remaining unchanged. Light-scattering detection appears relatively universal and is moreover compatible with gradient elution. Fig. 10 shows the chromatogram obtained with this detection technique in the analysis of a mixture of KM25 (5000 ppm, w/w) and Cetalox AT (10^4 ppm, w/w). This chromatogram indicates that the light-scattering detector is well adapted to the detection of non-ionic POE surfactants whatever their degree of condensation. However, the signal is slightly more noisy than with UV detection.

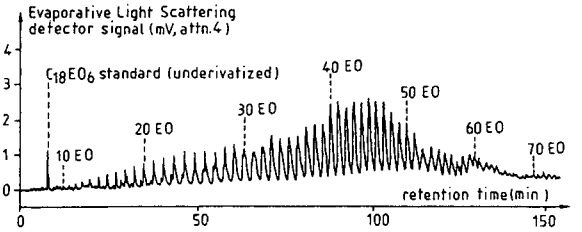

Fig. 10. Analysis of a non-ionic POE surfactant mixture containing KM25 at 5000 ppm (w/w) and Cetalox AT at 10^4 ppm (w/w) by normal-phase partition chromatography on *p*-nitrophenyl-bonded silica at 45°C. Detection system: light scattering. Other conditions as in Fig. 3.

CONCLUSIONS

A *p*-nitrophenyl-bonded silica stationary phase provides a satisfactory solution to the problem of non-ionic POE surfactant analysis. This phase, used in association with a ternary elution gradient with *n*-heptane–dichloromethane–methanol, allows the analysis, with a satisfactory and nearly constant resolution of the total oligomers of a POE surfactant containing a C_{16}–C_{18} base and from 1 to >80 EO units.

For non-ionic surfactants resulting from the condensation of ethylene oxide with *p*-nonyl phenol (Igepals), the results are less satisfactory as the correct resolution of this complex mixture is obtained only for the first 60 oligomers.

Finally, the evaporative light-scattering detector is well adapted to the detection of these compounds, whatever the degree of condensation.

REFERENCES

1 C.F. Allen and L.I. Rice, *J. Chromatogr.*, 110 (1975) 151.
2 K. Nakamura and I. Matsumoto, *Nippon Kagaku Kaishi*, 8 (1975) 1342.
3 M.C. Allen and D.E. Linder, *J. Am. Oil Chem. Soc.*, 58 (1981) 950.
4 J.D. McClure, *J. Am. Oil Chem. Soc.*, 59 (1982) 364.

5 A. Aserin, M. Frenkel and N. Garti, *J. Am. Oil Chem. Soc.*, 61 (1984) 805.
6 N. Cortesi, E. Moretti and E. Fredli, *Riv. Ital. Sostanze Grasse*, 57 (1980) 141.
7 B.F. Bogatzki and L.H. Lippmann, *Acta Polym.*, 34 (1983) 219.
8 M. Ahel and W. Giger, *Anal. Chem.*, 57 (1985) 1577.
9 M. Ahel and W. Giger, *Anal. Chem.*, 57 (1985) 2584.
10 A.C. Hayman and N.A. Parris, paper presented at the *1979 Pittsburgh Conference*, paper 24.
11 A.M. Rothman, *J. Chromatogr.*, 253 (1982) 283.
12 R.E.A. Escott, S.J. Brinkworth and T.A. Steedman, *J. Chromatogr.*, 282 (1983) 655.
13 J.A. Pilc and P.A. Sermon, *J. Chromatogr.*, 398 (1987) 375.
14 I. Zeeman, J. Silha and M. Bares, *Tenside Deterg.*, 23 (1986) 4.
15 I. Zeeman, *J. Chromatogr.*, 363 (1986) 223.
16 P.L. Desbène, B. Desmazieres, V. Even, J.J. Basselier and L. Minssieux, *Chromatographia*, 24 (1987) 857.
17 P.L. Desbène, B. Desmazieres, V. Even, J.J. Basselier and L. Minssieux, *Chromatographia*, 24 (1987) 588.
18 P.L. Desbène, B. Desmazieres, J.J. Basselier and A. Desbène-Monvernay, *J. Chromatogr.*, 465 (1989) 69.
19 P.L. Desbène, B. Desmazieres, J.J. Basselier and A. Desbène-Monvernay, *J. Chromatogr.*, 461 (1989) 305.
20 A. Marconi and W. Giger, *Anal. Chem.*, 59 (1987) 1709.
21 R.E.A. Escott and N. Mortimer, *J. Chromatogr.*, 553 (1991) 423.
22 T. Okada, *Anal. Chem.*, 62 (1990) 327.
23 T. Okada, *Anal. Chem.*, 62 (1990) 734.
24 T. Okada, *Anal. Chem.*, 63 (1991) 1043.
25 B. Desmazieres, F. Portet and P.L. Desbène, *Chromatographia*, 36 (1993) 307.
26 G.R. Bear, *J. Chromatogr.*, 459 (1988) 91.
27 L.R. Snyder, *J. Chromatogr. Sci.*, 16 (1978) 223.

Journal of Chromatography A, 661 (1994) 215–226
Elsevier Science B.V., Amsterdam

CHROMSYMP. 2919

Composition distribution separation of methyl methacrylate–methacrylic acid copolymers by normal-phase gradient elution high-performance liquid chromatography

Timothy C. Schunk

Analytical Technology Division, Eastman Kodak Company, Research Labs, Rochester, NY 14650-2136 (USA)

ABSTRACT

The characterization of copolymers requires the determination of chemical composition distribution in addition to molecular mass (M) distribution. Techniques commonly applied to copolymer analysis provide either average bulk composition or a convolution of M and composition distributions. The application of gradient elution adsorption chromatography, under appropriate conditions, allows the separation of copolymers based solely upon their chemical composition in a M-independent mode. Separation independent of M requires the elimination of size-exclusion effects with the porous adsorbent and the minimization of precipitation contributions. For separation over a wide copolymer composition range, the relative contributions of adsorption and precipitation retention mechanisms change with solvent composition. Under gradient elution conditions where adsorption retention dominates, composition fractionation can be combined with subsequent size-exclusion chromatography to provide a complete composition/M map of the copolymer.

INTRODUCTION

Synthetic polymers present many unique separations challenges because, unlike small organic molecules, they consist of a distribution of structurally different molecules [1,2]. Each macromolecule can differ in chain length and end groups; stereochemical and structural isomers are possible along with unique branching architectures. Copolymers are further complicated by the combination of these potential variables with varying ratios and sequence distributions of their comonomer units. Liquid chromatography of synthetic polymers is limited by the solution properties of macromolecules to narrow selections of solvents for each polymer type. The application of liquid chromatography to the separation of synthetic polymers is characterized by the balance between solvation and adsorption interactions and is often complicated by polymer solubility limitations in gradient elution separations [2].

Frequently synthetic polymers are described by single average values, such as average molecular mass, average chemical composition, average length between branch sites, etc. For many purposes these average values are sufficient. However, it is often the shape of a structural distribution not described by a single value which is most relevant to polymer properties. It is only after the joint structural distributions are deconvolved that this information is obtained. Separation by liquid chromatography thus becomes invaluable in elucidating these structural distributions [1,2].

The addition of selective detection systems to size-exclusion chromatography (SEC) can in some cases provide chemical composition information across the molecular size distribution [3,4]. However, SEC separates macromolecules

0021-9673/94/$07.00
SSDI 0021-9673(93)E0883-V

on the basis of solution hydrodynamic size rather than true molecular mass. The hydrodynamic size of copolymers in solution is a function of many variables including chemical composition and molecular chain length. At best, the chemical composition distribution information obtained from selective detection SEC is convolved with the molecular mass distribution of the copolymer sample [4]. Ideally it would be desirable to determine the chemical composition and molecular mass distributions independently.

HPLC compositional separation of copolymers has been documented by both precipitation and adsorption retention. Compositional separation of styrene–acrylonitrile (SAN) copolymers independent of column packing type has been demonstrated in tetrahydrofuran (THF)–isooctane gradients [5]. The comparison of the HPLC elution solvent concentration with turbidimetric titration solubility data indicated that the copolymers eluted immediately upon contacting mobile phase of sufficient strength to provide dissolution.

The compositional separation of styrene–methyl methacrylate (SMMA) copolymers in THF–methanol (90:10) in isooctane solvent gradient showed retention dependent upon the type of column packing. Non-polar bonded phase packings showed results similar to SAN precipitation separation. Separation on silica, however, provided retention in excess of the solubility limit [6]. These data indicated that retention occurred through a mixed mechanism of precipitation followed by adsorption interactions with the polar silica packing.

A primary difficulty lies in the selection of a gradient elution solvent pair capable of dissolving all copolymer compositions while possessing sufficient solvent strength range to allow both retention and displacement of the copolymer chains from the adsorbent. The compositional separation of ethyl methacrylate–butyl methacrylate (EMA–BMA) copolymers over the full composition range was obtained by Mori [7] with UV-absorbance detection at 233 nm. A shallow gradient of ethanol in 1,2-dichloroethane provided adsorption separation of increasing EMA content copolymers with increasing ethanol content. Although ethanol is a non-solvent for these copolymers, increasing ethanol content acted as a displacer for the adsorbed polymers.

Mourey [8] demonstrated compositional separations of several acrylate and methacrylate ester homopolymers and copolymers [SMMA and poly(methyl methacrylate–methyl acrylate) in toluene–2-butanone eluents]. Both of these solvents are good solvents for these copolymers; however, both are also opaque to UV radiation below 285 nm. Mourey employed an evaporative light-scattering detector to provide chromatographic elution response of the nonvolatile copolymers. In agreement with the observations of Mori [7], polymer retention was shown to increase with decreasing ester chain length for a series of methacrylate and acrylate ester homopolymers. Since all copolymer compositions studied were soluble in both solvents, the separation was clearly based on adsorption interactions with the silica packing.

The current experimental studies examine the retention mechanism of poly(methyl methacrylate–methacrylic acid) (PMMA–MAA) copolymers on narrow-pore silica. Evaluation of the relative contributions of adsorption and precipitation retention interactions are made through solubility data and the effect of injected sample mass on peak shape. Orthogonal separation of HPLC followed by SEC for the determination of the complete composition/molecular mass distribution map of a copolymer sample is evaluated.

EXPERIMENTAL

Copolymer compositional separations were performed on a Perkin-Elmer (Norwalk, CT, USA) Series 4 quaternary HPLC with an Applied Chromatography Systems (Cheshire, UK) evaporative light-scattering (ELS) detector Model 750/14 [temperature setting 30, pressure setting 40 p.s.i.g nitrogen (1 p.s.i.g = $69 \cdot 10^2$ Pa)]. All HPLC separations were performed on 250×4.6 mm 10-μm LiChrospher Si100 100-Å pore silica columns obtained from E.M. Science (Cherry Hill, NJ, USA). Linear gradient elution programs at 1.00 ml/min were produced with a strong solvent of either methanol (MeOH) or 5% glacial acetic acid (AcOH) in MeOH (v/v) in

the weak solvent toluene. Gradient conditions are specified in the discussion for individual experiments. Due to the potential for reaction between acetic acid and methanol, fresh solvent was prepared on a daily basis. Samples of each copolymer were dissolved in mobile phase solvent mixtures at least 10% higher than their solubility limit. Injection volume was 100 μl throughout. The non-linear concentration response of the ELS detector [9] for PMMA–MAA copolymers was calibrated with third-order polynomial fit for gradient elution separations of copolymer A (Table II) samples in 2 to 40% [AcOH–MeOH (5:95)] in toluene over 75 min. Third-order polynomial regression was applied to ELS detector peak height response for a series of standard concentrations to provide a calibration equation relating ELS detector response to instantaneous concentration across a chromatogram. No ELS detector response variation was observed as a function of polymer composition or molecular mass.

All solvents were used as received. HPLC-grade toluene and MeOH were obtained from J.T. Baker (Phillipsburg, NJ, USA). ACS reagent-grade glacial acetic acid was obtained from Eastman Kodak (Rochester, NY, USA).

The system gradient lag volume for calculation of elution solvent concentration was measured from the midpoint of a 2 to 100% [AcOH–MeOH (5:95)] in toluene, 5-min gradient. Solvent concentration was detected immediately prior to the column inlet by a Kratos Model 783 (Ramsey, NJ, USA) UV absorbance detector at 280 nm. An average of four determinations was used for calculation of the gradient lag and subsequent elution solvent concentration. Error propagation of measured values was used for the determination of data precision. Column void volume was measured as 2.6 min by isocratic elution of PMMA in 50% [AcOH–MeOH (5:95)] in toluene.

Copolymer compositional standards of PMMA–MAA were synthesized by solution polymerization in MeOH at 20% solids with AIBN (azobisisobutyronitrile, Eastman Kodak) initiator to approximately 10% conversion at 65°C. Monomers were obtained from Eastman Kodak and were vacuum distilled prior to use. Copolymers were isolated by precipitation into diethyl ether (J.T. Baker) followed by filtration and vacuum drying at 60°C.

Mole percent methacrylic acid incorporation was determined by potentiometric titration in MeOH–THF (3.8:96.2) with hexadecyltrimethylammonium hydroxide (Eastman Kodak) in MeOH–toluene (10:90). The combination glass electrode (Brinkmann Instruments, Westbury, NY, USA) containing tetramethylammonium chloride in MeOH was standardized with a benzoic acid primary standard (Fisher Scientific, Fairlawn, NJ, USA). Table I lists the composition of the copolymer standards determined by titration, as well as the polystyrene (PS) equivalent weight average molecular masses and polydispersities as determined by SEC.

TABLE I

LOW-CONVERSION PMMA–MAA COPOLYMERS

Mole% MAA incorporation by titration	% (w/w) conversion	Monomer feed composition mole% MAA	Weight average M (PS equiv.)	Polydispersity (M_w/M_n)
PMMA–4.0% MAA	12.9	5.0	156 000	1.67
PMMA–8.5% MAA	10.7	10	140 000	1.54
PMMA–17.5% MAA	8.2	20	153 000	1.54
PMMA–35.6% MAA	7.7	40	185 000	1.60
PMMA–61.2% MAA	7.7	70	179 000	1.82
PMMA–78.6% MAA	4.0	90	163 000	1.98
PMMA–85.5% MAA	13.4	90	234 000	1.97
PMAA	15.8	100	215 000	1.87

Molecular masses were determined by SEC in THF (HPLC grade without BHT, J.T. Baker) with a Waters Assoc., Div. of Millipore (Milford, MA, USA) Model R401 differential refractive index (DRI) detector. The methacrylic acid containing copolymers were methylated by reaction with diazomethane in THF solution prior to SEC to minimize adsorption interactions. Methylated samples were reduced to dryness under a N_2 stream and redissolved at 2.0 mg/ml and 200-μl aliquots injected for SEC. The samples were chromatographed on three Polymer Laboratories (Amherst, MA, USA) PLgel 10 μm 300 × 7.5 mm mixed bed columns. Third-order polynomial regression calibration of the columns was performed with narrow PS standards obtained from American Polymer Standards (Mentor, OH, USA).

Semipreparative gradient HPLC separation of copolymer A was performed with a 100-μl injection of a 100 mg/ml solution on a 2 to 40% [AcOH–MeOH (5:95)] in toluene gradient over 75 min. Two-minute fractions were collected with an ISCO (Lincoln, NE, USA) Model FOXY fraction collector and reduced to dryness under a N_2 stream. Fractions were then methylated as above, dried, and redissolved in either 0.80 or 5.0 ml of THF. SEC of the methylated fractions was performed with 200-μl injections on the PLgel columns described above in THF calibrated with narrow PMMA standards. PMMA narrow standards were obtained from American Polymer Standards Corp. ELS detection was used with a temperature setting of 50 and N_2 gas pressure of 20 p.s.i.g. ELS concentration response calibration was performed with a 198 000 dalton PMMA (Eastman Kodak) and third-order polynomial fit. Copolymer composition was calibrated with the elution times of a mixture of the first four samples in Table I plus the 198 000 dalton PMMA. The calibration equation was determined by third-order polynomial regression of the peak elution times from four repeat separations of the standards mixture.

Solubility limits of the PMMA–MAA copolymer samples of Table I were obtained in the same solvents as employed in the HPLC separations by a method similar to that used by Shalliker *et al.* [10]. Solutions of 1.0 mg/ml of each copolymer standard were prepared in a series of solvent concentrations. After standing overnight, a 100-μl aliquot of each solution was injected on a 5 to 100% [AcOH–MeOH (5:95)] in toluene, 30-min gradient. The ELS response peak areas were plotted *versus* solvent concentration and the midpoint determined by third-order polynomial fit. Solvent composition solubility midpoint precision was taken as one half of the range between 40 and 60% solubility points.

High-conversion PMMA–MAA copolymer samples were also prepared by three different polymerization methods (Table II). Sample A was prepared by solution polymerization at 20% solids in 60% acetone (J.T. Baker)–40% ethanol

TABLE II

HIGH-CONVERSION PMMA–MAA COPOLYMERS

Sample ID	Mole% MAA incorporation by titration	Weight average M (PS equiv.)	Polydispersity (M_w/M_n)
Copolymer A from solution polymerization	14.1	155 000	2.09
Copolymer B from batch suspension polymerization	14.1	38 900	1.91
Copolymer C from semi-continuous addition suspension polymerization	14.0	368 000	7.06

(Quantum Chemical, Tuscola, IL, USA) with benzoyl peroxide (Aldrich, Milwaukee, WI, USA) initiator. Sample B was prepared by batch suspension polymerization at 25% solids in water with lauroyl peroxide (Aldrich) initiator and 2% polyvinyl alcohol (PVA, Eastman Kodak) dispersant. Sample C was prepared by semicontinuous addition suspension polymerization under the same conditions as sample B with 1% PVA and monomer addition over two hours. Mole percent MAA incorporation and PS equivalent molecular mass of all three samples are shown in Table II. The ELS detector concentration response was calibrated with copolymer A sample (Fig. 7) by third order polynomial regression. The ELS detector response was also determined to be independent of M for PMMA narrow standards over the range from 2000 to 1 450 000 dalton.

RESULTS AND DISCUSSION

PMMA-MAA copolymers can be eluted in order of increasing mole percent MAA on 100-Å pore silica adsorbent with a MeOH–toluene gradient as shown in Fig. 1. Excessive peak broadening is observed with increasing MAA content of the copolymer samples. In fact, copolymers containing greater than 36% MAA could not be eluted. The addition of glacial acetic acid to the MeOH provided a strong displacer effect in reducing the elution volume of copolymers and narrowing the peak widths of the low-conversion samples to a more consistent value (Fig. 2). It was found that 5% AcOH was needed to provide consistent peak shape over the entire composition range from PMMA to PMAA (Fig. 3). This elution behavior change upon addition of acetic acid is indicative of the contribution of the strong adsorption interactions of the carboxylic acid functionality of MAA with the silica surface. This is consistent with the observations of Mori [11] on the improvement of elution profiles of methacrylate ester containing copolymers on the addition of a strongly hydrogen-bonding solvent to the eluent.

The influence of polymer molecular mass (M) on retention is demonstrated for two PMMA standards in Fig. 4. A 43 500 dalton PMMA with polydispersity $M_w/M_n = 2.00$ shows a highly asymmetrical elution profile under shallow gradient elution conditions. The low M components of this sample are resolved over a 9-min range, but the higher M components elute within 1 min.

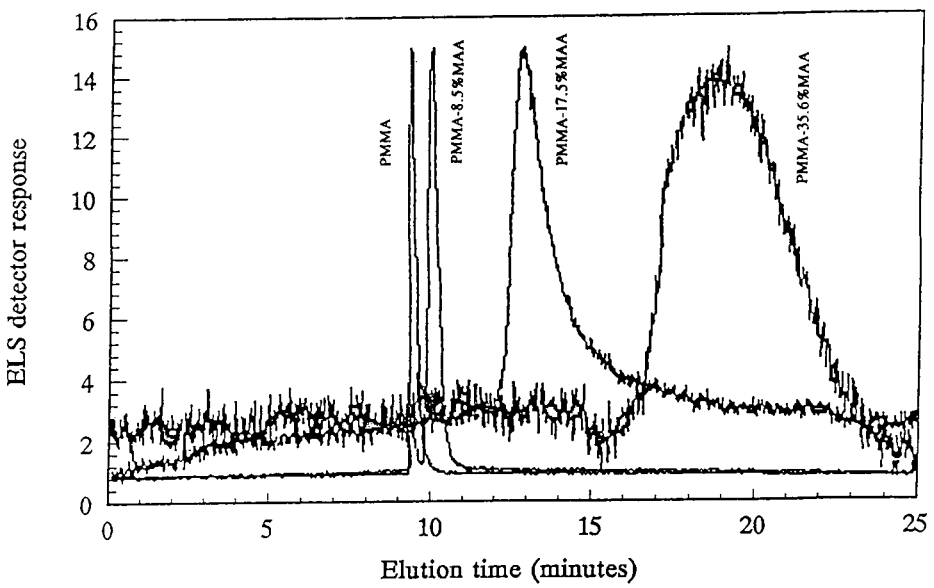

Fig. 1. Gradient elution separation of a mixture of low conversion PMMA–MAA copolymers on 100-Å pore silica. Linear gradient from 2 to 100% MeOH in toluene over 25 min. Injected sample 5 mg/ml each PMMA 198 000 dalton, PMMA–8.5% MAA, PMMA–17.5% MAA, and PMMA–35.6% MAA in MeOH–toluene (30:70).

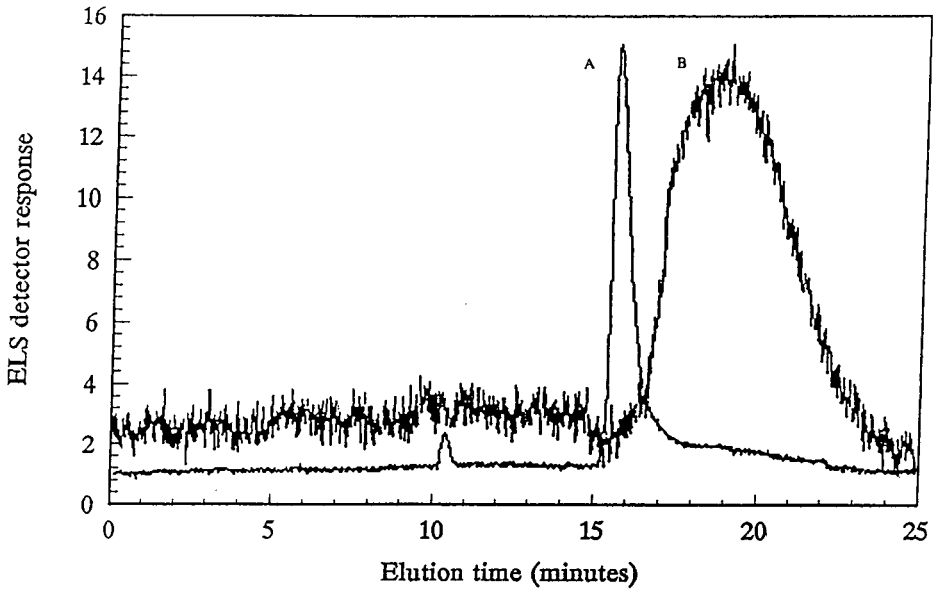

Fig. 2. Comparison of the elution profiles of 5 mg/ml injections of PMMA–35.6% MAA copolymer in MeOH–toluene (30:70) for gradients with (chromatogram A) and without (chromatogram B) 5% acetic acid in the MeOH strong solvent. Separations were performed with the same gradient slope and initial mobile phase concentration as Fig. 1.

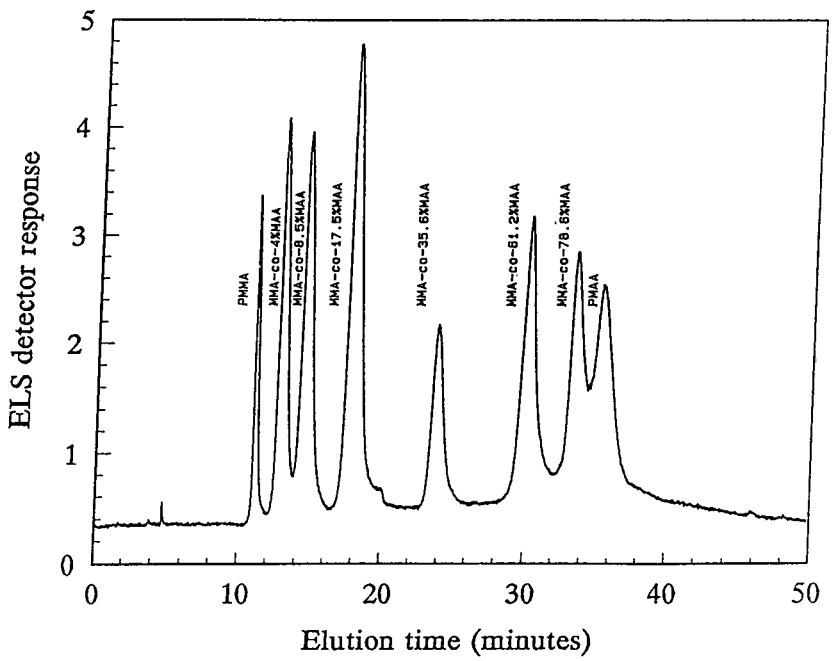

Fig. 3. Chromatogram of a mixture of PMMA–MAA copolymers plus PMMA and PMAA homopolymers. Injected sample 2 mg/ml of each polymer in 70% [AcOH–MeOH (5:95)] in toluene. Gradient conditions 2% to 100% in 55 min with [AcOH–MeOH (5:95)] strong solvent.

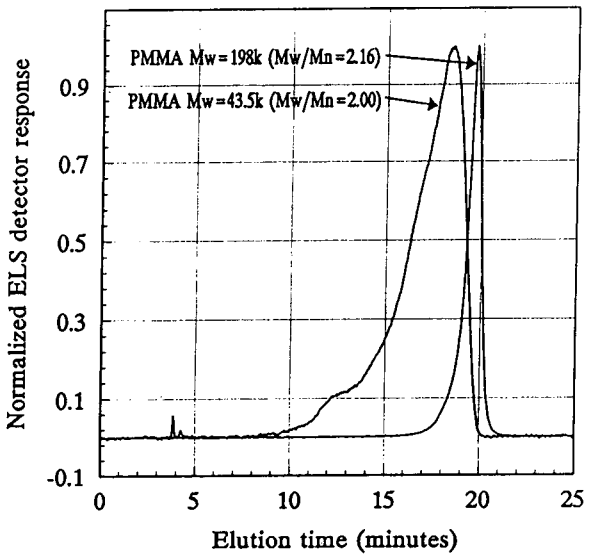

Fig. 4. Comparison of the profile of two different molecular mass PMMA samples. Gradient conditions 2 to 40% [AcOH–MeOH (5:95)] in toluene over 75 min. Each injected sample was 10 mg/ml in toluene.

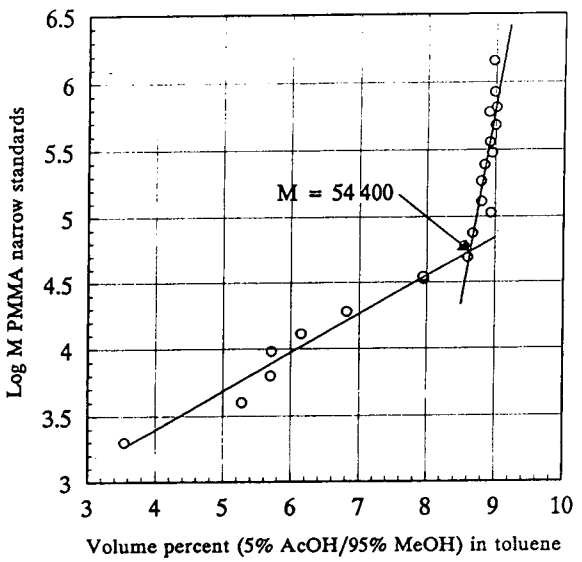

Fig. 5. Variation of the PMMA elution solvent concentration with molecular mass on 100-Å pore silica.

Elution of a PMMA standard of over four times higher molecular mass (198 000) and slightly higher polydispersity ($M_w/M_n = 2.16$) shows only minor peak asymmetry and elution over a narrow range at the same location as the high M tail of the 43 500 dalton PMMA. In a more quantitative format, the variation of PMMA peak elution volume in terms of eluent composition as a function of log M is shown in Fig. 5 for a series of narrow M standards. Note that for the 100-Å pore silica employed in these separations, the eluent composition required to elute PMMA becomes very nearly independent of M in excess of 54 400 dalton.

Based merely upon adsorption interactions, the increase in retention with increasing M is expected to be a monotonic function of M. Deviation from low M linearity has been documented as a function of the increasing contribution of polymer coil structure [12]. However, the behavior seen in Figs. 4 and 5 indicates a sudden deviation to elution nearly independent of M. This is attributable to the exclusion of the polymer molecules from the porous packing with a resultant dramatic decrease in available surface area [13]. This effect was clearly demonstrated by Shalliker *et al.* [10] for PS retention on C_{18}-bonded phase packings in dichloromethane–MeOH eluent. Under weak adsorption interactions, retention in excess of the solubility limit was observed at high M only for wide pore packings which did not provide exclusion of the polymer molecules.

PMMA is soluble in all proportions of the elution solvents, but is not eluted from silica by pure toluene. Therefore, it is concluded that PMMA is retained through adsorption interactions with the silica packing. Although the same molecular mass experimental data was not available for the copolymer samples studied, it is considered a reasonable assumption, based upon the results of other workers [11,14], that this molecular mass independent elution behavior applies to the PMMA–MAA copolymers eluted under adsorption conditions.

Retention mechanism

Since it is observed that the copolymer samples of PMMA–MAA having greater than approximately 8 mole% MAA are insoluble in the initial gradient solvent conditions, the separation mechanism falls into question. Mourey [8] has

shown that polyalkyl acrylates can be compositionally separated by adsorption chromatography on silica using 2-butanone–toluene gradients. Under these conditions all of the eluting sample components are soluble in all solvent ratios of the gradient solvents. This insures adsorption interactions are responsible for the compositional resolution between copolymers. Extensive work has also been published by Glöckner et al. (ref. 15 and refs. cited therein) employing gradient systems which are intentionally chosen to produce precipitation of the copolymer components in the solvent gradient. As the solvent strength of the elution solvent is gradually increased, the copolymer components redissolve and may then be eluted from the column under either of two possible mechanisms. Pure precipitation HPLC separation provides elution of the copolymer components immediately upon reaching the gradient conditions required for solubility [5,6,13]. On more strongly interacting adsorbents, such as bare silica, further adsorptive interactions may retard the elution of copolymer components after the solubility condition has been exceeded. Elution is observed only when the solvent reaches sufficient strength to displace the adsorptive interactions of the retained copolymer. Glöckner has verified that this behavior is effective in SMMA separation on silica by comparing the eluent concentration on copolymer elution to the solubility limit solvent concentration as determined by turbidimetric titration [6].

The comparison of turbidimetric titration results with HPLC elution solvent data must be done with care in the interpretation of retention mechanisms. Turbidimetric titration requires that the polymer behavior is compatible with the optical turbidity probe and data must be corrected for polymer dilution during the titration. Although time-consuming, the method used in the current study for the determination of copolymer solubility limits allows direct comparison in the HPLC solvent mixtures and does not require correction for polymer concentration effects.

The retention mechanism effective for the PMMA–MAA separation can be verified by solubility evaluation. Fig. 6 shows the eluent

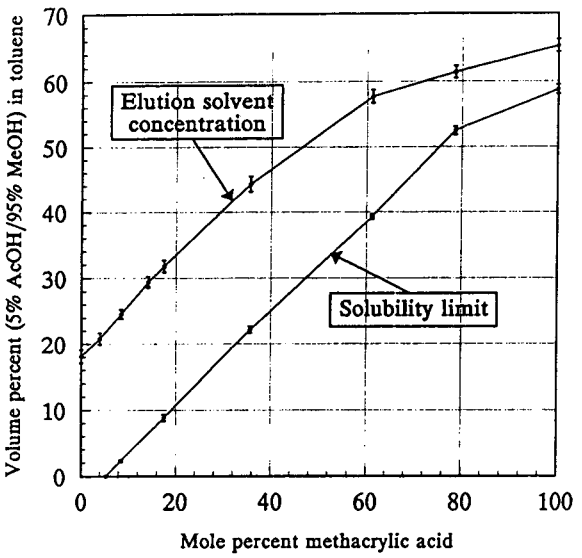

Fig. 6. Comparison of the elution solvent concentration and solubility limit for PMMA–MAA copolymers.

solvent composition corresponding to copolymer elution for the entire range of PMMA–MAA samples studied. Determination of the solubility limits of the same PMMA–MAA copolymer samples in the same solvents employed for gradient elution provided the values shown by the lower curve of Fig. 6. It is observed that for all PMMA–MAA compositions, the solvent concentration required for copolymer elution from the silica adsorbent is in excess of that required for solubilization.

Copolymer solubility in terms of the volume fraction of non-solvent (Φ_{NS}) at incipient precipitation has been described by Glöckner [15] as a function of polymer solution concentration (c^*_{polym})

$$\Phi_{NS} = A + B \log c^*_{polym}$$

where A and B are empirical constants. For the copolymer A sample with 14.1% MAA, the non-solvent (toluene) concentration necessary to precipitate the copolymer decreased from 95.8% to 87.2% on going from 1.0 to 58 mg/ml concentration $\{\Phi_{NS} = 0.9567 - 0.04812 \log [c^*_{polym}$ (mg/ml)]$\}$. When compared to the solubility limit in Fig. 6, this indicates that a range of strong solvent concentration is still required to elute

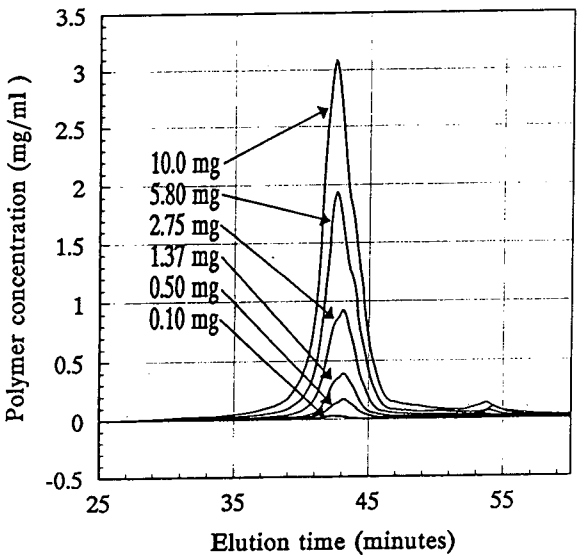

Fig. 7. Variation of the peak profile of PMMA–14.1% MAA (copolymer A) with injected sample mass. Gradient conditions 2 to 40% [AcOH–MeOH (5:95)] in toluene over 75 min.

copolymer A even at such extreme concentration as 100 mg/ml injected as shown in Fig. 7.

Arguments regarding the dominant polymer retention mechanism have also been made by evaluating the change in peak shape as a function of injected polymer mass. These effects were demonstrated by Schultz and Engelhardt [16] for PS under both precipitation and adsorption retention conditions. In THF–water eluent, precipitation dominates and polymer elution shifts to higher retention with increasingly fronting distortion for increasing injected sample mass. This is in opposition to the observed decrease in retention with increasing tailing distortion observed for overloaded adsorption retention. Fig. 7 shows the effect of a two-orders-of-magnitude increase in injected sample mass for copolymer A. Only a slight shift to earlier elution with no peak distortion indicates a wide linear adsorption isotherm range for this separation. No peak distortion characteristic of polymer precipitation was observed despite the noted decrease in solubility with increasing polymer concentration and the fact that this sample is insoluble in the initial gradient conditions for all injected concentrations.

Orthogonal separation

Previous studies have used a combination of SEC fractionation and subsequent HPLC compositional separation to determine the joint composition/molecular mass map of copolymer samples [17–19]. As stated previously, SEC separates based upon molecular size which can be a function of chemical composition. It would be preferable to separate the copolymer sample into a series of fractions based on a single physical property and subsequently determine the other. Gradient HPLC has a much broader linear sample mass range (Fig. 7) than SEC, so that a single HPLC fractionation can provide sufficient material for several SEC separations.

In the present study a high-conversion solution-polymerized PMMA–MAA copolymer (copolymer A, Table II) was separated into ten fractions by gradient elution HPLC. The gradient HPLC separation was calibrated by the elution times of a series of low-conversion copolymer standards (Table I). Subsequently, each fraction was characterized by SEC for polymer molecular mass distribution. The PMMA–MAA copolymers provide the capability of conversion to PMMA homopolymer by methylation with diazomethane. Absolute molecular mass distribution is then readily obtained by SEC separation and PMMA narrow standard calibration with total suppression of any remaining composition effects on molecular size.

The composition/molecular mass map can be represented by either a three-dimensional plot as in Fig. 8 or by a projection contour plot as in Fig. 9. Note that the large majority of the sample is in excess of the molecular mass independent limit as determined in Fig. 5. This provides good confidence that the HPLC gradient elution separation was based purely upon composition. In addition, the lack of peak profile distortion shown in Fig. 7 provides support that the composition/molecular mass map is not distorted by HPLC overload conditions. Note that the composition drift in the high-conversion copolymer map for the solution-polymerized sample is similar in distribution to that determined by Mori [17] for a high-conversion SMMA copolymer by HPLC of SEC fractions. The composition drift of copolymer A is shown in Fig. 10 by plotting

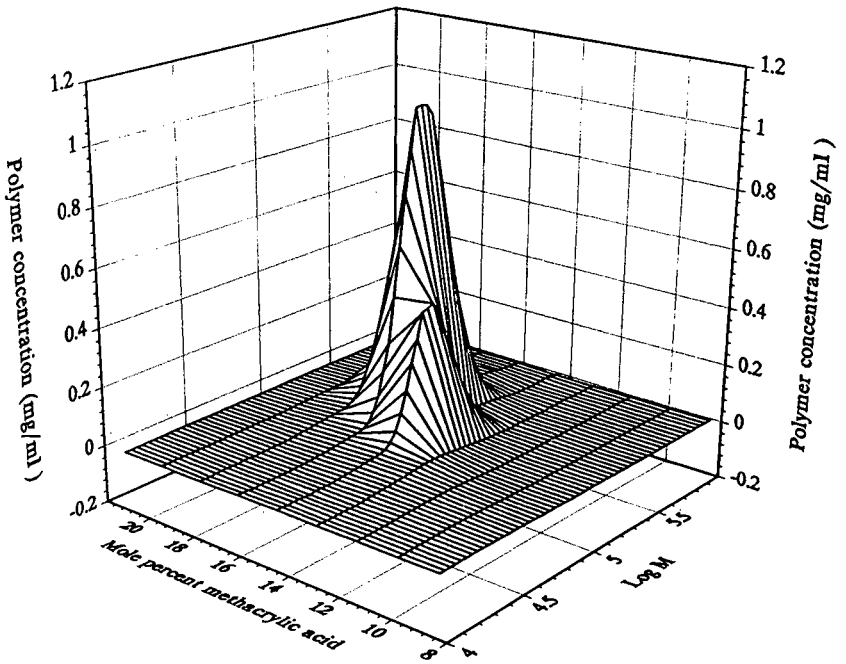

Fig. 8. Joint chemical composition and molecular mass distribution of a 10-mg sample of copolymer A separated into fractions by HPLC under the same conditions as Fig. 7. Molecular mass distributions of the methylated HPLC fractions were determined by SEC in THF.

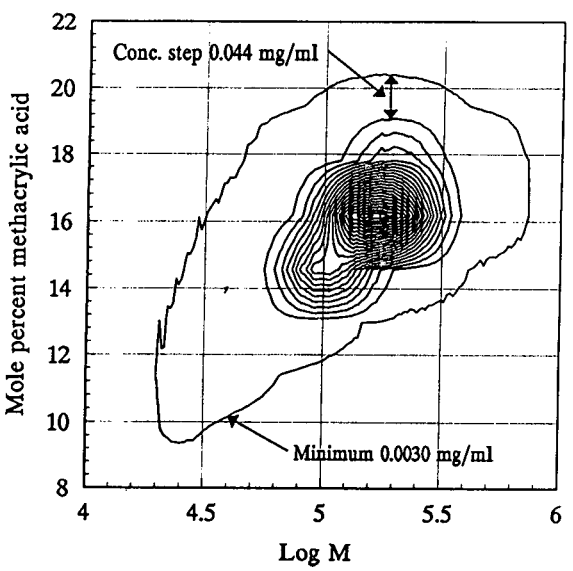

Fig. 9. Contour plot of the joint composition and molecular mass distribution of copolymer A corresponding to the data of Fig. 8.

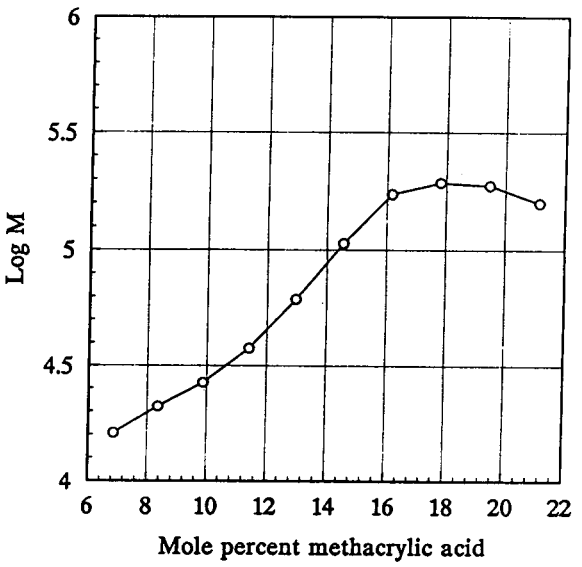

Fig. 10. Variation of the peak molecular mass as a function of chemical composition for the copolymer A HPLC fractions of Figs. 8 and 9.

the composition at the SEC peak maxima. The molecular mass gradually increases to a plateau with increasing MAA incorporation.

General applicability of composition distribution separation

The chemical composition distributions of three high-conversion PMMA–MAA copolymer samples prepared by three different polymerization techniques were compared. Figs. 11–13 show the composition profiles of the three copolymers described in Table II. Titration of the MAA content showed all three to have nearly equivalent average MAA incorporation at 14.1 mole%. SEC of the methylated samples provided evidence of widely differing molecular mass distributions (Table II). However, only HPLC composition separation demonstrates that all three samples also have significantly different composition distributions.

Copolymer A (Fig. 11) was produced by solution polymerization and has been thoroughly characterized in Figs. 8 and 9. Note that there is a consistent bias in the peak composition relative to that determined by titration in Figs. 11–13. This has also been observed in a wide variety of other PMMA–MAA copolymers characterized by this method. This has been attributed to the

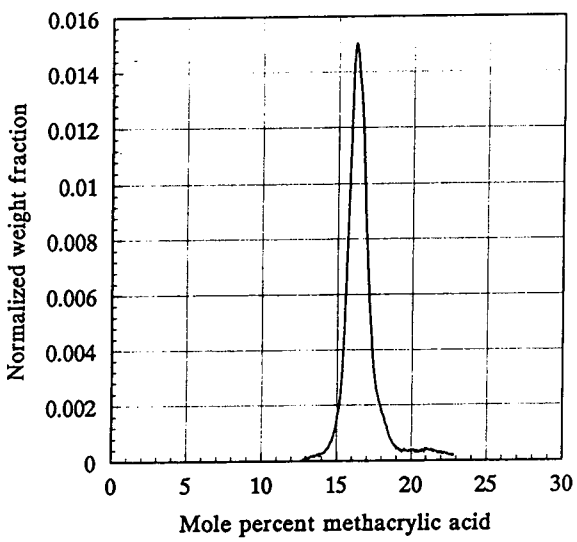

Fig. 11. The chemical composition distribution of a 5.0 mg/ml sample of copolymer A separated under the gradient conditions of Fig. 7.

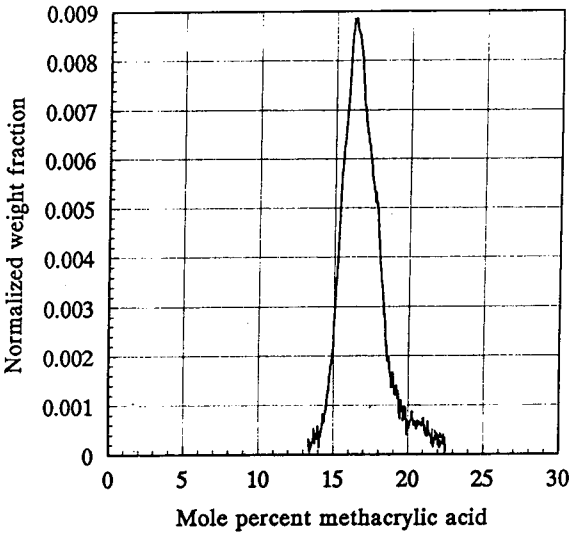

Fig. 12. The chemical composition distribution of a 5.0 mg/ml sample of copolymer B separated under the gradient conditions of Fig. 7.

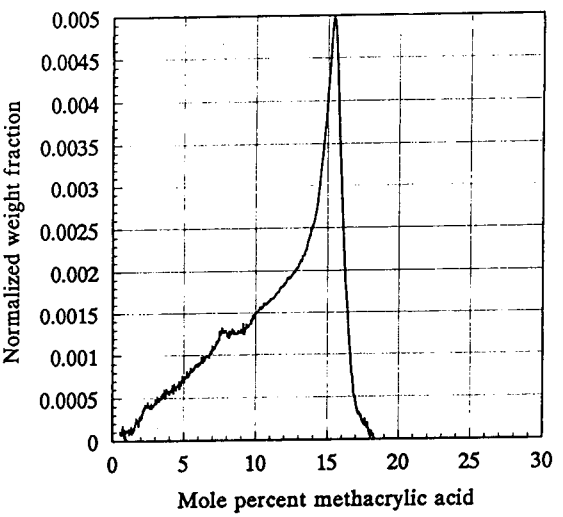

Fig. 13. The chemical composition distribution of a 5.0 mg/ml sample of copolymer C separated under the gradient conditions of Fig. 7.

manner in which the titration method provides an average value of MAA incorporation.

The composition distribution of the batch suspension-polymerized copolymer B sample is much broader than the solution-polymerized sample and tails to higher MAA incorporation (Fig. 12). The composition profile of this sample must be interpreted with additional caution,

however, because of its relatively low molecular mass. Despite the fact that the M_w of this sample is only 38 900 dalton, the peak composition agrees well with that of the other two samples. In addition, retention effects due to molecular mass would be expected to shift polymer elution to earlier time (Fig. 5). However, the broadening observed in Fig. 12 is predominantly toward higher retention, *i.e.*, higher percent MAA incorporation.

The copolymer C sample prepared by semi-continuous addition suspension polymerization is much higher in molecular mass and shows the most dramatic difference in composition distribution (Fig. 13). Composition tailing all the way to PMMA is observed. This sample was also observed to contain a small amount of insoluble gel which may be attributable to either very high M copolymer or some degree of crosslinking.

CONCLUSIONS

(1) The chemical composition separation of PMMA–MAA copolymers on silica has been shown to be predominantly through adsorption interactions. (2) Despite initial precipitation of higher mole% MAA copolymers, no elution is observed until well past the solubility limit. (3) A very wide linear adsorption range was observed for a 14.1 mole% MAA copolymer demonstrating that adsorption interactions dominate the polymer retention process after redissolution in the solvent gradient. (4) Molecular mass independent elution of PMMA was observed on 100-Å pore silica in excess of 54 400 dalton and inferred to occur for PMMA–MAA copolymers. (5) Orthogonal separation by HPLC followed by SEC provided a full composition/molecular mass map of a solution polymerized copolymer sample. Methylation of HPLC fractions prior to SEC provided for complete elimination of composition effects on M determination. (6) The general applicability of this composition separation was demonstrated in the composition distribution determination of PMMA–MAA copolymers prepared under different polymerization conditions.

REFERENCES

1 T.H. Mourey and T.C. Schunk, in E. Heftmann (Editor), *Chromatography (J. Chromatogr. Library*, Vol. 51B), Elsevier, New York, 1992, Ch. 22.
2 T.C. Schunk, *J. Chromatogr. A*, 656 (1993) 591.
3 L.H. Garcia-Rubio, in T. Provder (Editor), *Detection and Data Analysis in SEC (ACS Symposium Series*, No. 352), American Chemical Society, Washington, DC, 1987, Ch. 13.
4 S. Mori, *J. Chromatogr.*, 411 (1987) 355.
5 G. Glöckner and J.H.M. van den Berg, *Chromatographia*, 19 (1984) 55.
6 G. Glöckner and J.H.M. van den Berg, *J. Chromatogr.*, 352 (1986) 511.
7 S. Mori, *Anal. Chem.*, 62 (1990) 1902.
8 T.H. Mourey, *J. Chromatogr.*, 357 (1986) 101.
9 T.H. Mourey and L.E. Oppenheimer, *Anal. Chem.*, 56 (1984) 2427.
10 R.A. Shalliker, P.E. Kavanagh and I.M. Russel, *J. Chromatogr.*, 543 (1991) 157.
11 S. Mori and Y. Uno, *J. Appl. Polym. Sci.*, 34 (1987) 2689.
12 J.P. Larmann, J.J. DeStefano, A.P. Goldberg, R.W. Stout, L.R. Snyder and M.A. Stadalius, *J. Chromatogr.*, 255 (1983) 163.
13 G. Glöckner, *J. Appl. Polym. Sci.: Appl. Polym. Symp.*, 43 (1989) 39.
14 S. Mori, *Polymer*, 32 (1991) 2230.
15 G. Glöckner, *Gradient HPLC of Copolymers and Chromatographic Cross-Fractionation*, Springer-Verlag, New York, 1991.
16 R. Schultz and H. Engelhardt, *Chromatographia*, 29 (1990) 205.
17 S. Mori, *Anal. Chem.*, 60 (1988) 1125.
18 G. Glöckner and H.G. Barth, *J. Chromatogr.*, 499 (1990) 645.
19 G. Glöckner and J.H.M. van den Berg, *J. Chromatogr.*, 384 (1987) 135.

Journal of Chromatography A, 661 (1994) 227–238
Elsevier Science B.V., Amsterdam

CHROMSYMP. 2915

Quantitative polymer composition characterization with a liquid chromatography–Fourier transform infrared spectrometry–solvent-evaporation interface

T.C. Schunk*

Analytical Technology Division, Research Laboratories, Eastman Kodak Company, Rochester, NY 14650-2136 (USA)

S.T. Balke and P. Cheung

Department of Chemical Engineering and Applied Chemistry, University of Toronto, Toronto, Ontario M5S 1A4 (Canada)

ABSTRACT

Factors that are important to the quantitative analysis of polymer composition distribution by high-performance liquid chromatography (HPLC)–Fourier transform infrared (FT-IR) using a solvent-evaporation interface are investigated. These factors include the effects of the location and distribution of the deposited polymer films, as well as the morphology of the deposit. Consideration is given to the influence of these factors on the chromatographic resolution and FT-IR spectral quality. Size-exclusion separations of polystyrene and poly(methyl methacrylate) in tetrahydrofuran are used to demonstrate the impact of these effects on the quantitative use of the resulting FT-IR spectra. Results indicate that all absorbance bands are not uniformly affected by spectral distortions, but that compositional information can be obtained on simple blends. The effectiveness of a post-sample-collection solvent-annealing procedure is also considered.

INTRODUCTION

Size-exclusion chromatography (SEC) is well established for the characterization of molecular mass distributions of synthetic polymers. In addition to SEC, various forms of gradient high-performance liquid chromatography (HPLC) using adsorption, partition, precipitation, temperature-rising elution, and other "cross-fractionation" methods are being developed and applied to the characterization of synthetic polymer distributions other than molecular mass. These distributions include chemical composition, branching, stereochemistry, and end-group functionality [1,2]. Quantitative functional group-selective detection, such as Fourier transform infrared (FT-IR) spectrometry, is critical to the successful implementation of these fractionation methods.

The direct interfacing of HPLC and FT-IR has evolved from two directions: in-line flow cells and solvent evaporation prior to FT-IR spectral analysis. Low-volume flow cells offer continuous monitoring of the eluates with little loss of chromatographic resolution. Application has been limited, however, due to the strong infrared absorption inherent to HPLC eluents throughout much of the mid-infrared spectral range [3,4]. This interference also makes gradient elution HPLC impractical.

Solvent evaporation allows the use of the full

* Corresponding author.

0021-9673/94/$07.00
SSDI 0021-9673(93)E0882-U

mid-IR range without solvent spectral interference. Off-line FT-IR spectrometry can be performed with the advantage of increased sensitivity from unrestricted spectra signal averaging on samples that are in pure form with no diluting solvent. Solvent evaporation has gained favor recently over the flow-cell mode for both small molecule and polymer characterization [5–7].

HPLC–FT-IR detection of polymers using solvent evaporation has some commonality with small molecule detection. For example, several FT-IR optical configurations (transmission, external reflection, reflection-absorption, diffuse reflection, and diffuse transmittance) are possible after eluate deposition. A comparison by previous workers [8] for small-molecule spectroscopy indicates that conventional transmission FT-IR on flat subtrates yields the best information quality with the fewest spectral artifacts. There is no indication that small molecules and polymers differ significantly.

There are some important differences, however, between FT-IR detection using solvent evaporation for small molecules and polymers that are the focus of this study.

Resolution requirements. The emphasis of small-molecule analyses has been on minimum detectable quantity and minimum identifiable quantity [5] for well-resolved separations. However, quantitative polymer composition determination requires accurate representation of the entire polymer elution profile with minimum resolution loss. The term deposit distribution will be used to refer to the location of the eluates on the collection substrate relative to the infrared sampling beam. Deposit distribution is expected to be influenced by deposition conditions and instrumental configuration due to eluate remixing and deposit placement on the collection surface.

Deposited polymer morphology. A variety of spectral artifacts are possible when deposited eluates have size domains on the order of the wavelength of IR radiation [9]. Domains may be formed as a result of the deposition process and/or from eluate chemical effects. Considering that very few polymer blends are truly miscible on the molecular level, it is expected that morphological effects could be unique for polymeric materials. The term deposit morphology will be used to refer to domains within the polymer deposit on the scale of the infrared sampling wavelengths.

The above differences are generic to solvent evaporation interfaces and can be studied with a number of instrumental designs [9]. This investigation uses a commercial HPLC–FT-IR interface design based upon the work of Gagel and Biemann [10–12] and commercialized by Lab Connections Inc.

EXPERIMENTAL

The results described in this work were generated with an LC-Transform HPLC–FT-IR solvent evaporation interface manufactured by Lab Connections Inc. (Marlborough, MA, USA). The LC-Transform sample collection unit was connected to 55 p.s.i.g. N_2 gas supply (1 p.s.i.g. = $69 \cdot 10^2$ Pa) and solvent vapors were removed by a 4-in. (*ca.* 10 cm) fume exhaust. Samples were collected on 60 mm diameter × 2 mm thick rear-surface-aluminized germanium (Ge–Al) disks throughout. Initial gas flow and temperature conditions were established by visually inspecting the film deposits from 0.5-μl direct injection of polymer samples. The nebulizer gas flow was set to 2.5 ml/min and the sheath gas to 4 l/min. The height of the nebulizer tip above the collection disk was left constant at 10 mm for all experiments (Fig. 1A). The flow-rate of eluent split to the sample collection unit (nominally 70 μl/min) was estimated by collecting several repeat measurements of a time aliquot of eluent and measuring its volume by drawing into a 100-μl graduate syringe.

The operational temperature range of the nebulizer was determined to be 35–40°C for tetrahydrofuran (THF) at 70 μl/min. Operation at a higher setting of 45°C caused the solvent to evaporate too early, producing clogging in the nebulizer. When the interface temperature was set too low (30°C), a visible amount of solvent was observed on the collection disk that interfered with the formation of a stable deposit.

Rotation of the collection disk was delayed for five minutes after sample injection and was then

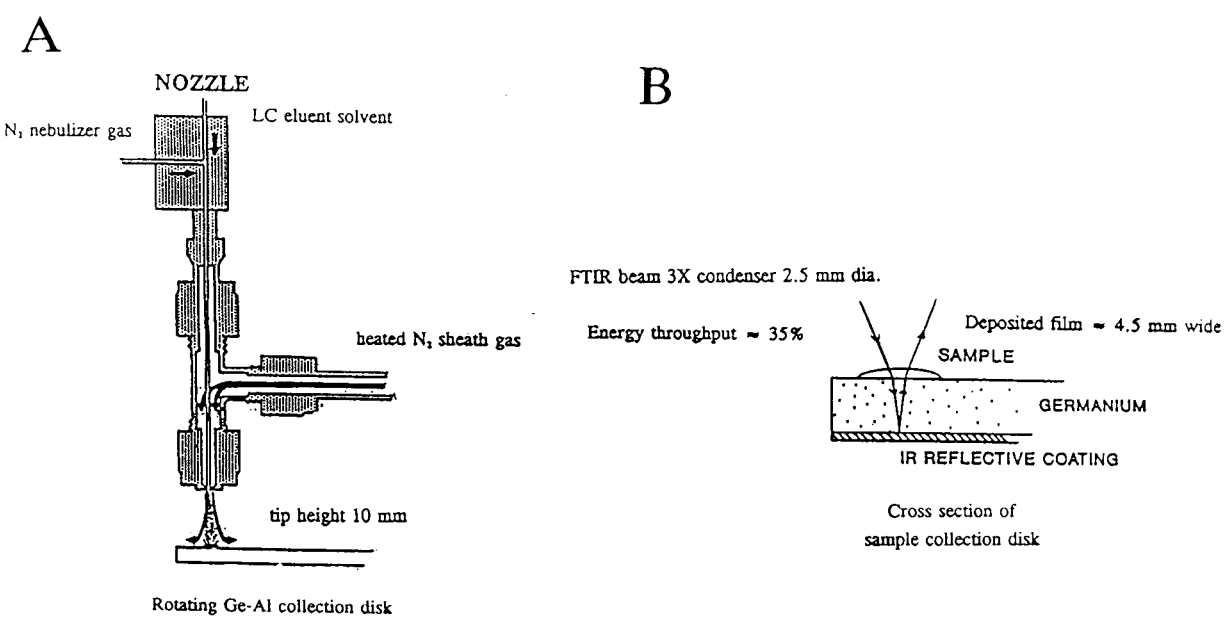

Fig. 1. (A) Diagram of the LC-Transform concentric flow nebulizer. (B) Ray diagram of the IR beam path through the sample deposit and rear-surface-aluminized-germanium collection disk.

rotated at 10°/min during polymer elution. This allowed up to five samples to be deposited on a single disk for the single SEC column separations. Disk rotation was delayed 15 min for three column separations. A disk rotation rate of 14.9°/min was used for the polystyrene (PS)–poly(methyl methacrylate) (PMMA) blend separation.

Separations were performed with a Perkin-Elmer (Norwalk, CT, USA) Series 4 HPLC operated at 1.0 ml/min. SEC separations were on either a single or three Polymer Laboratories (Amherst, MA, USA) PLgel 10-μm mixed bed 300×7.5 mm columns. Injections of 200-μl samples were made with a Perkin-Elmer ISS-100 autosampler. Each sample polymer solution was dissolved in THF containing 0.06% (v/v) toluene as a UV-absorbing flow marker. Sample concentrations were 1.0, 3.0, or 6.0 mg/ml for PS, 3.0 mg/ml for PMMA, and 1.5 mg/ml each for the PS–PMMA blend. THF eluent was redistilled from CaH_2 prior to use and was sparged with helium during use. PS NBS 706 was obtained from NIST (Washington, DC, USA) and PMMA broad standard 037B was obtained from Scientific Polymer Products, (Ontario, NY, USA). PS elution profiles were monitored by a Kratos Model 773 (Ramsey, NJ, USA) UV absorbance detector at 270 nm directly after the SEC column(s) and before the solvent flow divider. PMMA elution profiles were determined separately with a Waters Assoc., Division of Millipore (Milford, MA, USA) Model R401 differential refractive index (DRI) detector.

After polymer sample deposition, the Ge–Al collection disk was manually transferred to the FT-IR scanning module and a series of spectra collected while rotating the disk under the IR beam. FT-IR spectra were obtained on a dry-nitrogen-purged Nicolet 20SXB (Madison, WI, USA) spectrometer with the LC-Transform scanning module aligned in the sample chamber. A ray diagram of the optical path of the 2.5-mm IR beam through the sample deposit on the Ge–Al disk is shown in Fig. 1B. FT-IR spectra at 8 cm^{-1} resolution were collected by averaging 8 scans while the disk was rotated at 5°/min. A disk rotation rate of 10°/min was used for PS and PS–PMMA blend samples separated on three SEC columns.

Optical microcopy of the deposited polymer films on the Ge–Al collection disks was per-

formed with a Jenatech (Germany) binocular inspection microscope equipped with a Hitachi (Japan) VK-C360 color video camera. Micro-FT-IR spectrometry of selected polymer deposits was performed on a Digilab FTS60 FTIR spectrometer with a UMA 300A IR microscope in reflectance mode with a 10 μm beam diameter in 100-μm steps at 8 cm^{-1} resolution from 512 scans.

RESULTS AND DISCUSSIONS

Chromatographic resolution

Size-exclusion chromatography (SEC) separations of broad polymer standards were employed as model separations for the investigation of quantitative polymer FT-IR detection. Chromatographic peak dispersion associated with the solvent-evaporation interface was evaluated by comparing the polymer concentration elution profile as determined with an in-line detector (UV or DRI) with that reconstructed from the FT-IR data (FT-IR chromatogram). FT-IR and concentration chromatograms were aligned based upon their chromatographic peak maxima. The assumption of a linear Beer's law relationship between sample mass and FT-IR response area was made in plotting FT-IR chromatograms. This needs to be experimentally verified for the instrumental configuration employed.

The resolution loss for an FT-IR chromatogram of PS produced from the integrated intensity of the phenyl absorbance band at 698 cm^{-1} is shown in Fig. 2. Direct comparison can be made to the concentration chromatogram determined by a UV absorbance detector. A simple comparison of the peak base width from extrapolated inflection points gives a variance ratio of 1.36 FTIR:UV chromatograms (assuming an approximately Gaussian profile, base width = 4σ).

Aside from any dispersion effects in the connecting tubing leading to the interface nebulizer, two band-broadening effects should be specific to the deposition and sampling method employed. The finite diameter of the nebulized eluent spray impinging on the collection disk surface leads to the deposition of polymer over a specific area. As the collection disk is moved past this position, additional material must be laid down in the overlap region leading to some remixing and resolution loss. In addition, during FT-IR spectra collection the diameter of the IR beam sampling the eluate deposit has the effect of providing a spectrum which is a time average of a region of the sample deposit. This would also result in an effective resolution loss. These effects, however, could be altered by choice of the disk rotation rate and FT-IR spectral sampling time. In addition, compensation for both of these effects would assume that there is no sample-dependent effect on deposit distribution on the collection disk surface.

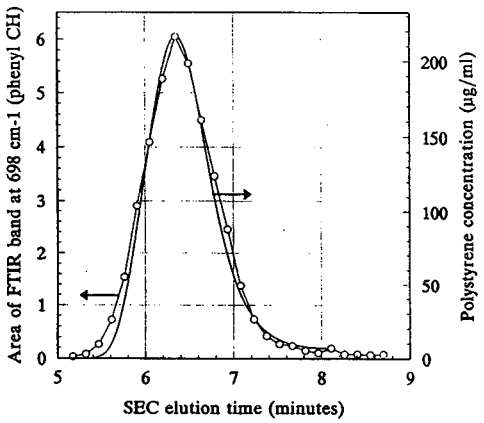

Fig. 2. SEC chromatograms of a 1.00 mg/ml polystyrene NBS 706 200-μl injection separation on one PLgel 10-μm mixed bed column at 1.0 ml/min THF, split flow 74 μl/min. Concentration chromatogram from the UV absorbance response at 270 nm (line). FT-IR chromatogram from the integrated area of the absorbance band at 698 cm^{-1} (data points) from the Ge–Al deposited sample.

Significantly different resolution loss behavior was observed, however, for a broad PMMA sample. An overlay plot of the PMMA SEC concentration chromatogram determined with an in-line DRI detector and the FT-IR chromatogram determined from the absorbance band area of the 1730 cm^{-1} carbonyl band is shown in Fig. 3. Surprisingly, the FT-IR chromatogram of PMMA is more narrow than the DRI concentration elution profile. This behavior may be explained by observation of the distribution of the deposited polymer film. The uppermost deposit on the Ge–Al disk in the photograph of Fig. 4 is the PMMA sample used to generate the

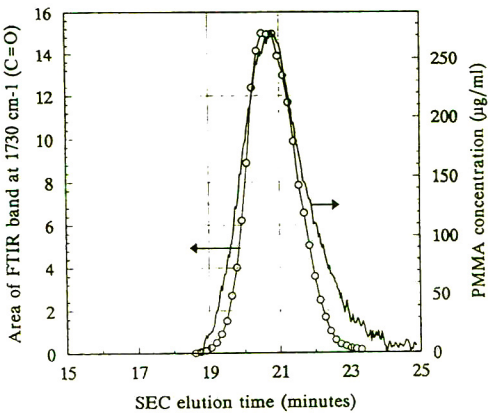

Fig. 3. SEC chromatograms of a 3.00 mg/ml poly(methyl methacrylate) 200-μl injection separation on three PLgel 10-μm mixed bed columns at 1.0 ml/min THF, split flow 103 μl/min. Concentration chromatogram from the DRI detector response (line). FT-IR chromatogram from the integrated area of the absorbance band at 1730 cm^{-1} (data points) from the Ge–Al deposited sample.

data of Figs. 3 and 5. Note that, although the deposited polymer stripe increases in width gradually at the beginning of deposition, the trailing portion of the deposit is split into two tails. At the tails of the polymer deposit a large percentage of the sample lies outside the 2.5 mm

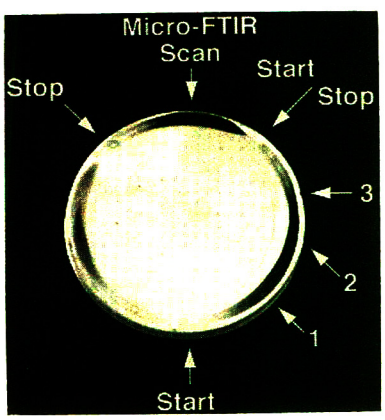

Fig. 4. Photograph of three polymer sample deposits on a Ge–Al collection disk. The upper deposit stripe is the PMMA sample described in Figs. 3, 5, 10, and 11. The right deposit stripe is the PS–PMMA blend sample described in Figs. 13–17. The arrows numbered 1, 2, and 3 correspond to the optical microscopy images of Fig. 17. Increasing elution time is counterclockwise.

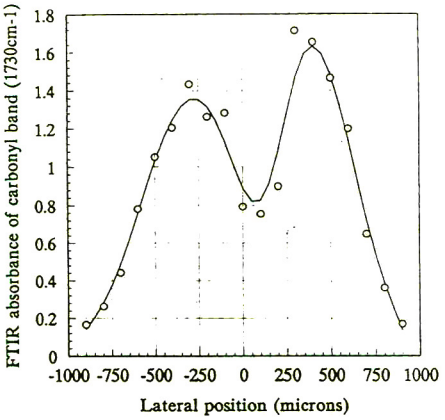

Fig. 5. Micro-FT-IR profile of the PMMA deposit location marked in Fig. 4. The IR beam diameter was 10 μm with 100-μm steps and 512 scans averaged at 8 cm^{-1} resolution.

IR beam diameter producing the erroneously narrow SEC profile described in Fig. 3. This deposit distribution is attributable to displacement of the wet film by the nebulizer gas jet during deposition and was confirmed to be present across the entire PMMA deposit by micro-FT-IR as shown in Fig. 5. This effect of analyte spot "washout" has also been described by Fraser *et al.* [13] and emphasizes the need for matching IR sampling beam diameter to analyte deposit width. From current data it cannot be determined whether this effect is due primarily to deposition conditions or has contributions from sample composition.

Spectral quality

The morphology of the deposited polymer can be investigated by optical microscopy. An example of the appearance of a polystyrene film is shown in Fig. 6. A wide range of particles are present in the film. Many of the larger particles have run together to form chains. It can be estimated from deposition conditions that the thickness of the deposited polymer corresponding to the SEC peak maximum is approximately 1.2 μm for a 1.00 mg/ml PS injection. In relation to the observed size of the deposited polymer features, it is not clear whether the irregular polymer morphology results from the nebulizer droplet evaporation or has contributions from interfacial tension between the hydro-

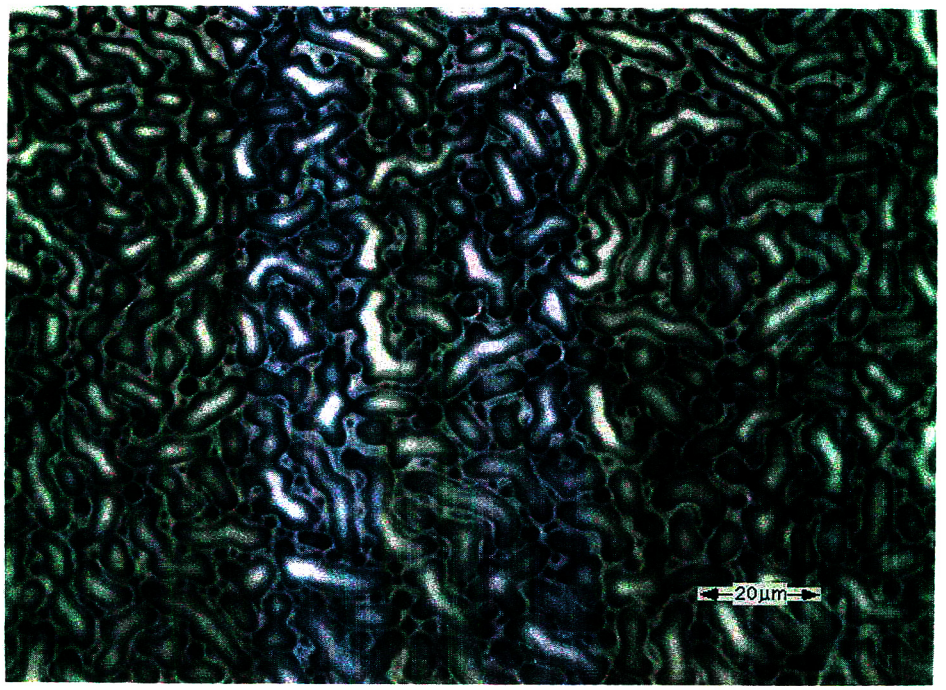

Fig. 6. Optical microscopy image of the deposit morphology of the polystyrene NBS 706 sample on the Ge-Al collection disk corresponding to Figs. 2, 7, and 8.

phobic polystyrene and the hydrophilic germanium surface.

A typical FT-IR spectrum of the deposited polystyrene film is shown in the upper trace of Fig. 7 obtained near the SEC peak maximum. A prominent feature of all the PS spectra collected was the large sloping background superimposed with the IR absorbance bands. This background is characteristic of the scattering of the IR radiation by the sample deposit. The range of particles sizes observed in Fig. 6 is consistent with the scattering observed in the mid-infrared wavelength range of 2.5 to 20 μm.

The intensity of the background scattering at 3600 cm^{-1} due to the irregular structure of the deposited PS follows the PS concentration profile as shown in Fig. 8. A correlation between polymer concentration and background scattering was observed for all PS-containing samples.

In an attempt to improve the quality of the FT-IR spectra obtained from the PS deposit, a solvent annealing procedure was used. The sample-containing disk was briefly exposed to the vapor above boiling dichloromethane. The visible appearance of the polymer deposit on the disk changed from a matte finish to a clear film showing visible light interference fringes. Low-

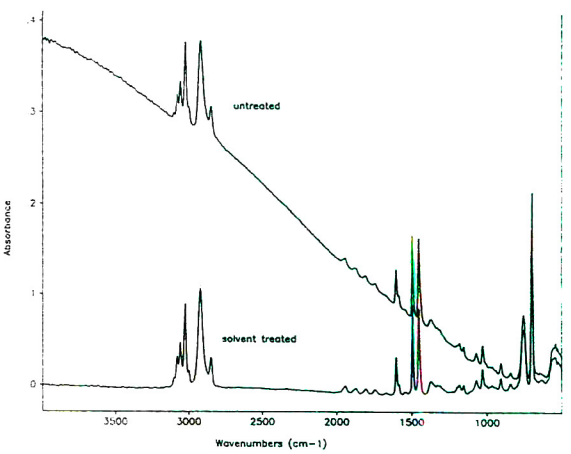

Fig. 7. Overlay FT-IR spectra of the polystyrene NBS 706 deposit corresponding to Figs. 2, 6, 8, and 9, before (upper trace) and after (lower trace) dichloromethane vapor annealing. FT-IR 8 scans, 8 cm^{-1} resolution.

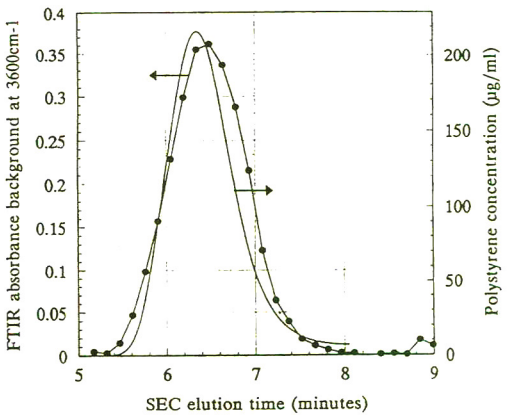

Fig. 8. SEC chromatogram of the same sample shown in Figs. 2 and 6. Comparison of the concentration chromatogram from the UV absorbance response at 270 nm (line) and the FT-IR background scattering intensity at 3600 cm^{-1} (data points).

power magnification of the leading edge of the polymer deposit after solvent annealing is shown in Fig. 9. The film became discontinuous at the edge, showing many large (>100 μm) domains. The gradation in the continuous film at the left of the image appears as colored interference fringes in visible light. The irregularity and fingering at the edges of the polymer domains is again indicative of some contribution of high interfacial tension to the structure of the PS film of the germanium surface.

The lower trace of Fig. 7 shows the FT-IR spectrum of the deposited PS film after solvent treatment. The absorbance bands are of similar intensity before and after solvent treatment, but the scattering background is absent after annealing. The FT-IR chromatogram of the PS deposit after solvent annealing showed little difference relative to the original deposit with the exception of a small decrease in SEC peak maximum response. Unfortunately, the manual annealing procedure was difficult to reproduce and it would be preferable to avoid the complexity of post-sample-collection treatments which could easily lead to chromatographic resolution loss.

The effect of polymer composition on deposit morphology is demonstrated by the appearance

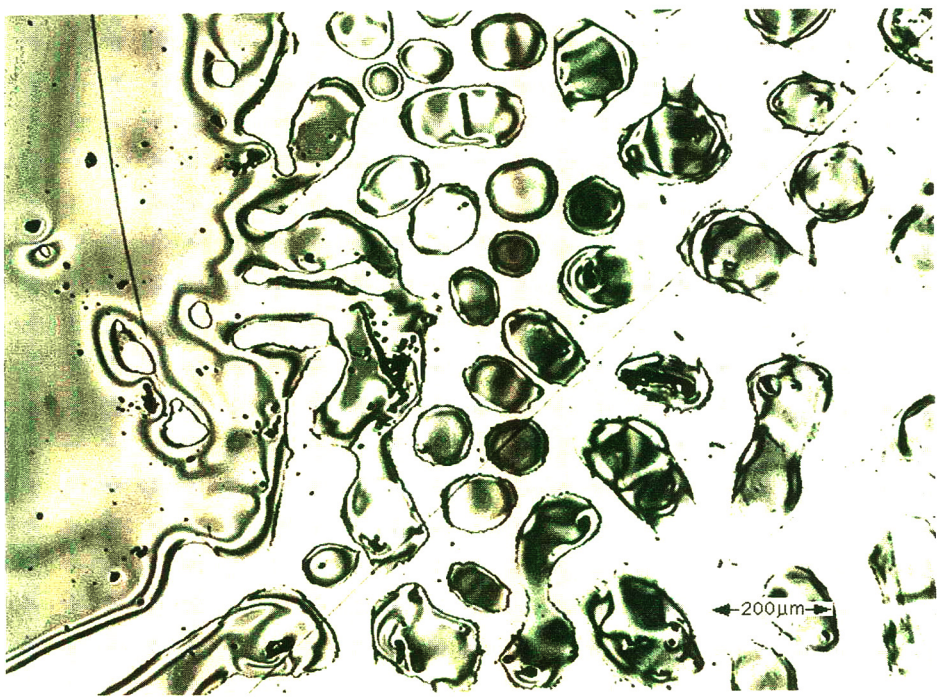

Fig. 9. Optical microscopy image of the dichloromethane vapor annealed polystyrene NBS 706 deposit corresponding to the lower trace of Fig. 7.

of the PMMA sample deposit. Optical microscopy of the PMMA film morphology gave the appearance of a random arrangement of irregular plates (Fig. 10). The FT-IR spectra of the PMMA film deposited on the Ge–Al disk (Fig. 11) did not show the scattering distortions associated with the PS samples.

The quality of the IR spectra and their utility for reconstructing SEC–FT-IR chromatograms was investigated by comparing FT-IR chromatograms from three characteristic IR absorbance bands for a three-column SEC separation of PS (Fig. 12). Band intensities were measured relative to local spectral baselines and were normalized based on the SEC response maximum. Some relative shifts in the SEC profiles described by the different bands can be noted, particularly on the high-retention side of the polymer distribution. The shorter wavelength bands do not show as good an agreement with the UV profile as does the strong 698 cm^{-1} band.

Band ratios across each SEC elution profile between SEC peak half height points were calculated as shown in Table I for comparison of the spectral quality. To investigate the possible effects of solid-state interactions and scattering distortions, the ratio of two different bands (3080 and 698 cm^{-1}) were calculated relative to the C–C band at 1600 cm^{-1}. The 698/1600 cm^{-1}

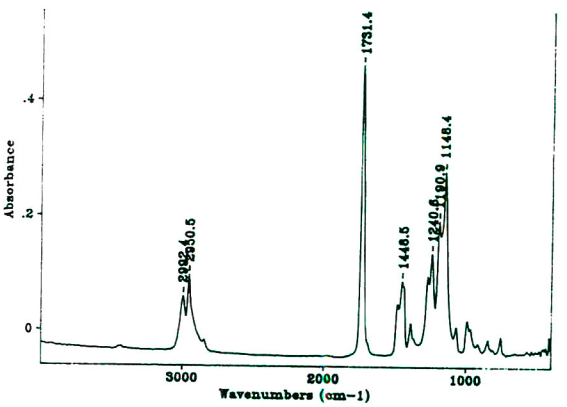

Fig. 11. FT-IR spectrum from 8 scans at 8 cm^{-1} resolution of the PMMA deposit corresponding to Fig. 10 near the maximum of the SEC chromatogram of Fig. 3.

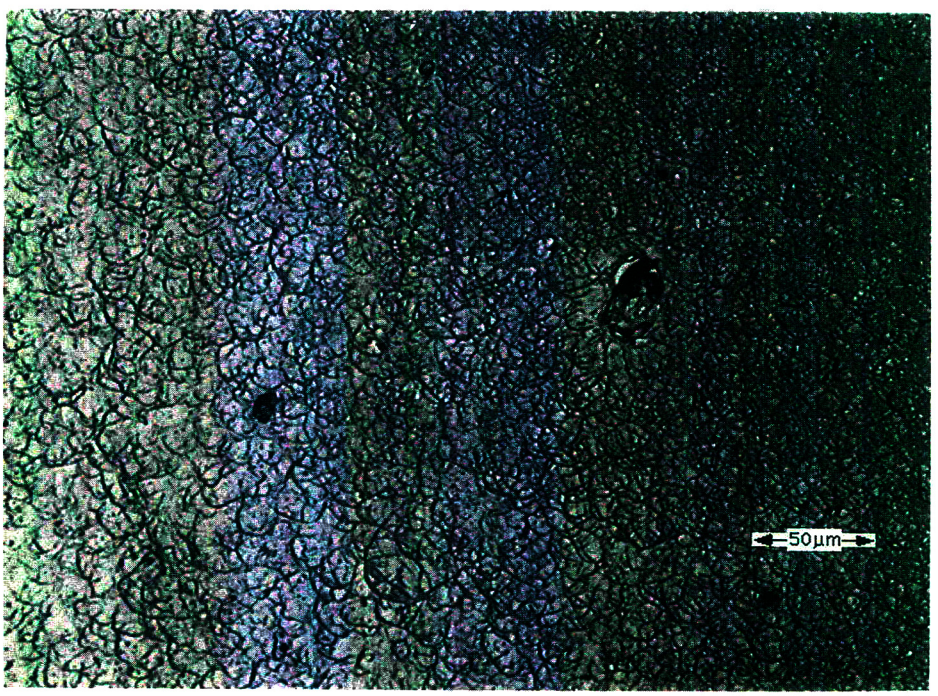

Fig. 10. Optical microscopy image of the morphology of the PMMA deposit on the Ge–Al collection disk corresponding to Figs. 3–5.

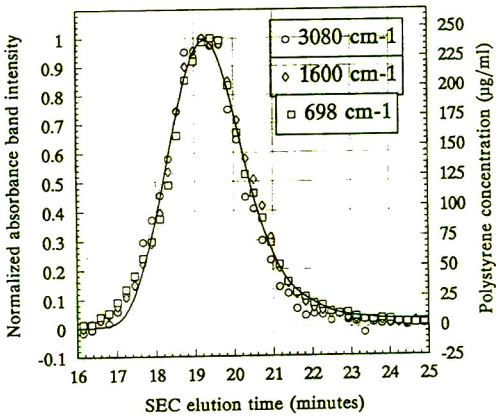

Fig. 12. SEC chromatograms of a 3.00 mg/ml PS NBS 706 200-μl injection separation on three PLgel 10-μm mixed bed columns at 1.0 ml/min THF, split flow 72 μl/min. Concentration chromatogram from the UV absorbance response at 270 nm (line). Data points represent the absorbance intensity of the FT-IR bands at 3080 (○), 1600 (◇), and 698 cm^{-1} (□) obtained from the Ge–Al disk-deposited sample.

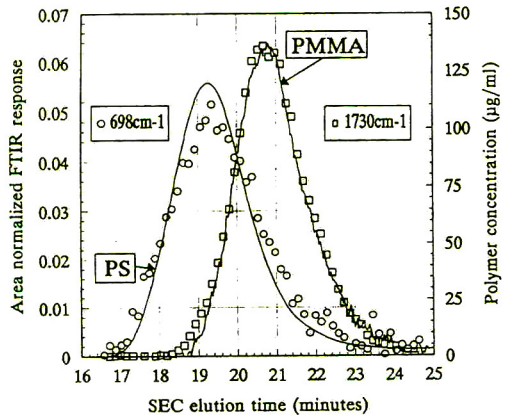

Fig. 13. SEC chromatograms of 1.5 mg/ml each PMMA (DRI response) and PS NBS 706 (UV absorbance 270 nm response) (lines) 200-μl injections on three PLgel 10-μm mixed bed columns at 1.0 ml/min THF measured separately. Data points represent the integrated area of the FT-IR absorbance bands at 698 (○) and 1730 cm^{-1} (□) obtained from a Ge–Al disk-deposited blend sample of these polymers with split flow at 94 μl/min and corresponding to Fig. 4.

ratio was relatively constant for all of the samples. Considerable variability was seen with the 3080/1600 cm^{-1} ratio, particularly for the samples before and after solvent annealing. This observation emphasizes the spectral distortions associated with the scattering of the IR radiation by the irregular deposit morphology.

Compositional distribution determination

Of most interest in the application of an HPLC–FT-IR solvent-evaporation interface is the determination of the variation in chemical composition across a polymer chromatogram. SEC separation of a blend of a broad PMMA and NBS 706 PS was used to investigate the capabilities for the determination of accurate polymer composition profiles.

The FT-IR chromatograms of the PS (698 cm^{-1} band) and PMMA (1730 cm^{-1} band) components of the blend are compared to the corresponding in-line detector concentration chromatograms in Fig. 13. The FT-IR chromatograms of PS and PMMA were normalized by SEC peak area for the uncalibrated concentration response. Although the chromatogram profiles agree fairly well, it is apparent that the PS profile shows more resolution loss than that of PMMA. The composition profile of the PS–

TABLE I

SAMPLE EFFECT ON FT-IR ABSORBANCE BAND RATIOS

Sample	3080/1600 cm^{-1}	S.D.	698/1600 cm^{-1}	S.D.
3.0 mg/ml PS	0.708	0.043 (n = 9)	5.02	0.22 (n = 9)
1.0 mg/ml PS	0.533	0.065 (n = 7)	4.83	0.19 (n = 7)
DCM[a] annealed 1.0 mg/ml PS	1.01	0.12 (n = 7)	4.76	0.43 (n = 7)
PS–PMMA blend	0.728	0.098 (n = 18)	4.79	0.39 (n = 18)

[a] DCM = dichloromethane.

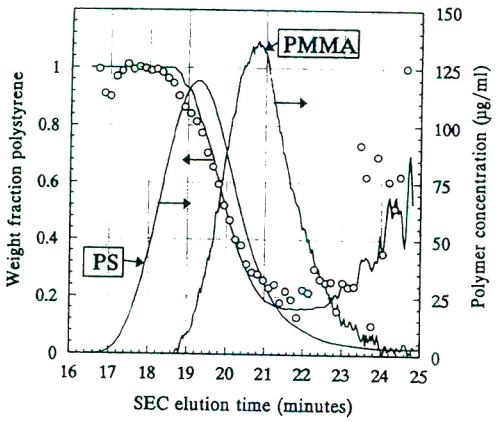

Fig. 14. SEC concentration chromatograms as described in Fig. 13. Comparison of the calculated weight fraction of PS from the concentration profiles (line) and from the FT-IR chromatogram data of Fig. 13 (data points).

PMMA blend was calculated as % (w/w) PS in Fig. 14 and compared to the UV and DRI concentration profiles. The FT-IR-determined blend composition is reasonably accurate in the middle of the chromatogram, but accuracy decreases in the wings of the chromatogram. It has not been determined which deposit distribution or morphological variations contribute most to the broadening of the PS portion of the FT-IR chromatogram.

Fig. 15 shows the FT-IR spectrum obtained near the middle of the blend chromatogram.

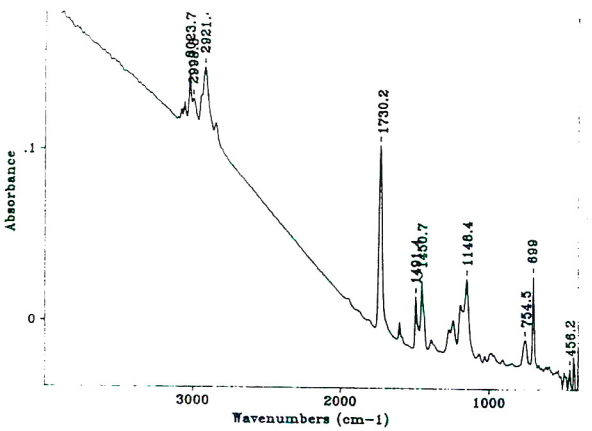

Fig. 15. FT-IR spectrum from 8 scans at 8 cm^{-1} resolution of the PS–PMMA blend deposit corresponding to Figs. 4, 13, and 14 obtained near the maximum of the SEC chromatogram (arrow position 2 on Fig. 4).

Note that the scattering background diminishes with increasing wavelength more rapidly than was observed for a pure PS deposit (Fig. 7). The presence of PMMA mixed with PS apparently produces fewer large scattering features than were present in a pure PS deposit.

The absorbance signal at 3600 cm^{-1} was used to map the background scattering intensity across the FT-IR chromatogram. Fig. 16 shows these data points in comparison to the spline fit smoothed FT-IR chromatograms at 698 cm^{-1} (PS) and 1730 cm^{-1} (PMMA). There is a clear correspondence between the scattering background intensity and the relative PS concentration.

A minimum in the scattering intensity occurs at the PMMA response maximum. This spectral response is consistent with the morphology of the polymer deposit as observed by optical microscopy. The optical micrographs of three locations on the blend deposit are shown in Fig. 17. Fig. 17A is quite similar to the morphology seen in Fig. 6 for a pure PS deposit. Fig. 17C appears similar to deposits observed for pure PMMA and Fig. 17B is intermediate.

Distortions present in the FT-IR spectra of the PS–PMMA blend were also evaluated by absorbance band ratios (Table I). There is reasonable agreement with values obtained from the pure PS deposit spectra. There are no obvious band-intensity distortions associated with the

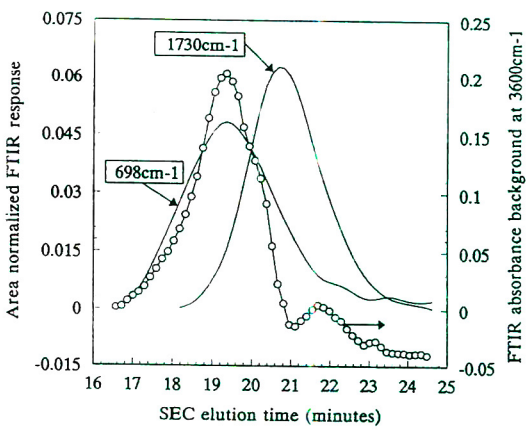

Fig. 16. Spline fit smoothed FT-IR chromatograms of the data points shown in Fig. 13. Comparison to the FT-IR scattering background intensity at 3600 cm^{-1} (data points).

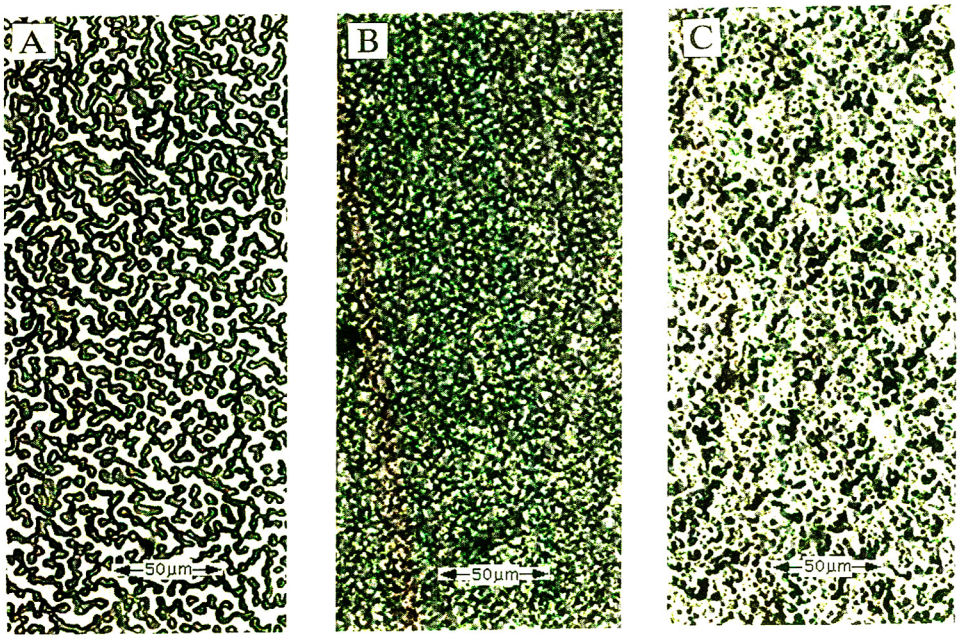

Fig. 17. Optical microscopy image of the morphology of the PS–PMMA blend deposit corresponding to the arrow positions of Fig. 4. (A) PS rich region at arrow position 1, (B) blend region at arrow position 2 (spectrum Fig. 15), and (C) the PMMA rich region at arrow position 3.

presence of PMMA blended with the PS in the deposit other than those due to scattering.

CONCLUSIONS

Several points for further investigation and performance improvements have been identified by the experimental evaluations described which are in general agreement with the findings of other researchers evaluating small molecule applications [5,8,13].

The novel FT-IR sampling configuration of transmission-reflection on a rear-surface-aluminized germanium disk was found to provide good signal-to-noise IR spectra which resembled conventional transmission spectra.

Lateral variations in polymer deposit distribution, particularly for sample "washout" from the center of the deposit, can result in significant chromatographic resolution distortions. This emphasizes the need to accurately match the deposit width with the IR beam diameter.

Irregular morphology of the deposited polymer films associated with a wide size distribution of features can produce intense IR-scattering backgrounds superimposed on the absorbance spectra.

Relative changes in IR band intensities accompany the IR-scattering effects, thus complicating quantitation.

Limited success with solvent annealing showed the elimination of the IR-scattering background, but was difficult to control experimentally and can lead to severe resolution distortion.

The determination of accurate composition profiles from the FT-IR spectral data of sample deposits relies on the maintenance of the chromatographic resolution. Reasonable compositional accuracy was found near the center of SEC distributions with increasing error at the wings.

ACKNOWLEDGEMENTS

Assistance in these experimental evaluations is gratefully acknowledged from J. Willis and J. Dwyer (Lab Connections Inc.) for interface operation; T.H. Mourey for manuscript im-

provements; L.E. Oppenheimer for optical microscopy; W.P. McKenna, S.A. Yeboah, and D. Margevich for FT-IR spectrometry, and S. Markel for micro-FT-IR spectrometry (all of Eastman Kodak Company).

REFERENCES

1 T.H. Mourey and T.C. Schunk, in E. Heftmann (Editor), *Chromatography*, (*J. Chromatogr. Library*, Vol. 51B), Elsevier, Amsterdam, 5th ed., 1992, pp. 475–512.
2 T.C. Schunk, *J. Chromatogr. A*, 656 (1993) 591.
3 C.W. Saunders and L.T. Taylor, *Appl. Spectrosc.*, 45 (1991) 900.
4 K. Nishikida, T. Housaki, M. Morimoto and T. Kinoshita, *J. Chromatogr.*, 517 (1990) 209.
5 A.J. Lange, P.R. Griffiths and D.J.J. Faser, *Anal. Chem.*, 63 (1991) 782.
6 A.H. Dekmezian, T. Morioka and C.E. Camp, *J. Polym. Sci.: Part B: Polym. Phys.*, 28 (1990) 1903.
7 A.H. Dekmezian and T. Morioka, *Anal. Chem.*, 61 (1989) 458.
8 R. Fuoco, S.L. Pentoney, and P.R. Griffiths, *Anal. Chem.*, 61 (1989) 2212.
9 P. Cheung, S.T. Balke, T.C. Schunk and T.H. Mourey, *J. Appl. Polym. Sci., Symp. Ed.*, in press.
10 J.J. Gagel and K. Biemann, *Anal. Chem.*, 58 (1986) 2184.
11 J.J. Gagel and K. Biemann, *Anal. Chem.*, 59 (1987) 1266.
12 J.J. Gagel and K. Biemann, *Mikrochim. Acta*, 11 (1988) 185.
13 D.J.J. Fraser, K.L. Norton and P.R. Griffths, in R.G. Messerschmidt and M.A. Harthcock (Editors) *Infrared Microspectroscopy: Theory and Applications*, Marcel Dekker, New York, 1988, pp. 197–210.

Journal of Chromatography A, 661 (1994) 239–243
Elsevier Science B.V., Amsterdam

CHROMSYMP. 2897

Retention behaviour of tributylphenol ethylene oxide oligomers on an alumina high-performance liquid chromatographic column

Esther Forgács and Tibor Cserháti*

Central Research Institute for Chemistry, Hungarian Academy of Sciences, P.O. Box 17, H-1525 Budapest (Hungary)

ABSTRACT

The retention behaviour of tributylphenol ethylene oxide oligomer surfactants was studied on an alumina HPLC column using ethyl acetate–*n*-hexane mixtures as eluents. The surfactants contained various numbers of ethylene oxide groups per molecule and tributylphenol isomers as hydrophobic moieties. The column separated the surfactants according to the length of the ethylene oxide chain and the position of butyl substituents in one run, demonstrating the good separation power of alumina. A significant linear correlation was found between the logarithm of the capacity factor of each surfactant and the concentration of ethyl acetate in the eluent, but the dependence of the retention on the ethyl acetate concentration was low. Stepwise regression analysis indicated that the number of ethylene oxide groups per molecule has a greater effect than the position of the butyl substituents in the tributylphenol moiety on the retention.

INTRODUCTION

The application of silica or silica-based supports in HPLC is limited by the low stability of silica at alkaline pH [1] and by the undesirable electrostatic interactions between the polar substructures of the solutes and the free silanol groups not covered by the hydrophobic ligand [2,3]. To decrease or eliminate the effect of residual acidic silanol groups, the eluent has to be buffered or various additives have to be added to the eluent to mask the effect of silanol groups [4]. The drawbacks mentioned above necessitated a search for supports other than silica, such as alumina [5], octadecyl-coated alumina [6], zirconia [7,8] and various polymer-based supports [9]. Owing to its higher isoelectric point and higher stability in the alkaline pH range, alumina partially or totally overcomes the difficulties arising from the low stability of silica [10], and therefore its application as a stationary phase for adsorption or after modification [11] for reversed-phase HPLC offers considerable advantages. The physico-chemical characteristics of alumina have recently been reviewed [12]. Good separations of various aromatic compounds [13,14], heroin derivatives, proteins [15] and drugs [16] have been achieved on alumina columns.

Many HPLC methods have been developed for the separation and determination of non-ionic surfactants [17,18]. As the separation power of ethylene oxide oligomer surfactants on common reversed-phase HPLC columns is relatively low, diol columns have also been used for the separation [19]. Non-ionic surfactants are generally separated on one HPLC column either according to the length of the ethylene oxide chain or according to the type of hydrophobic moiety. To carry out the separations in both senses, two different HPLC columns are needed [20]. Non-ionic surfactants have been separated according to the length of the ethylene oxide

* Corresponding author.

0021-9673/94/$07.00
SSDI 0021-9673(93)E0829-J

chain on a C_{18} HPLC column using typical reversed-phase eluents [21].

The objectives of this work were to study the retention behaviour of tributylphenol ethylene oxide oligomer surfactants on an alumina column, to elucidate the effects of various molecular substructures on the retention and to find the relationship between the retention parameters and solute characteristics.

EXPERIMENTAL

Alumina support material of 5-μm particle size was obtained from the Research Institute of the Hungarian Alumina Trust (Budapest, Hungary). A 25 cm × 4 mm I.D. column was filled in our laboratory using a Shandon (Pittsburg, PA, USA) analytical HPLC packing pump. The HPLC equipment consisted of a Liquopump Type 312 pump (LaborMIM, Budapest, Hungary), a CE-212 variable-wavelength UV detector (Cecil Instruments, Cambridge, UK), a Valco (Houston, TX, USA) injector with a 20-μl sample loop and a Model 740 integrator (Waters–Millipore, Milford, MA, USA). The flow-rate was 1 ml/min and the detection wavelength was set at 275 nm. Measurements were carried out at room temperature (22 ± 2°C). A sample of commercial tributylphenol ethylene oxide oligomer surfactants (Hoechst, Frankfurt, Germany) was dissolved in the eluent at a concentration of 0.5 mg/ml. The surfactant was a mixture of ethylene oxide oligomers (average number of ethylene oxide groups per molecule = 4) with the hydrophobic moiety containing a variety of tributylphenol isomers (probably 2,4,6-, 2,4,5- and 2,3,5-tributylphenol). This means that the commercial product contained a wide variety of solutes with similar chemical structures. The eluents were ethyl acetate–*n*-hexane mixtures, the ethyl acetate concentration being varied from 100 to 50 vol.% in steps of 10 vol.%. Each determination was run in quadruplicate.

Linear correlations between the logarithm of the capacity factors and the concentration of ethyl acetate were calculation:

$$\log k' = \log k'_0 + bC \quad (1)$$

where k' is the actual capacity factor of tributylphenol ethylene oxide oligomers at 0 % (v/v) ethyl acetate, k'_0 is the theoretical capacity factor of a tributylphenol ethylene oxide oligomer at 0% (v/v) ethyl acetate (pure *n*-hexane), b is the change in the logarithm of capacity factor caused by a 1% (v/v) change in ethyl acetate concentration in the eluent (related to the hydrophilic surface area of the solutes [3]) and C is the concentration (vol.%) of ethyl acetate in the eluent.

To elucidate the effects of various molecular substructures on the retention parameters (slope and intercept values of eqn. 1), the relationship between the retention parameters and the number of ethylene oxide groups per molecule (n) and the position (PI) of butyl substituents was determined. Calculations were carried out by stepwise regression analysis [22]. In the common multivariate regression analysis, the presence of independent variables that exert no significant influence on the dependent variable lessens the significance level of those independent variables which do significantly influence the dependent variable. To overcome this difficulty, the stepwise regression analysis automatically eliminates from the selected equation the insignificant independent variables. The number of accepted variables was not limited and their acceptance limit was set to the 95% significance level.

The linear correlation between the slope and intercept values of eqn. 1 was calculated to investigate that from a chromatographic point of view the tributylphenol ethylene oxide oligomers represent a homologous series of solutes on an alumina column [23].

RESULTS AND DISCUSSION

A tributylphenol ethylene oxide sample was separated into fifteen fractions on the alumina column (Figs. 1 and 2); the relative standard derivation was lower than 1.5% in each instance. The peaks were symmetrical and they were clustered in groups of three peaks. We assume that each "triad" represents tributylphenol derivatives with an identical ethylene oxide number, and the three members of the triad

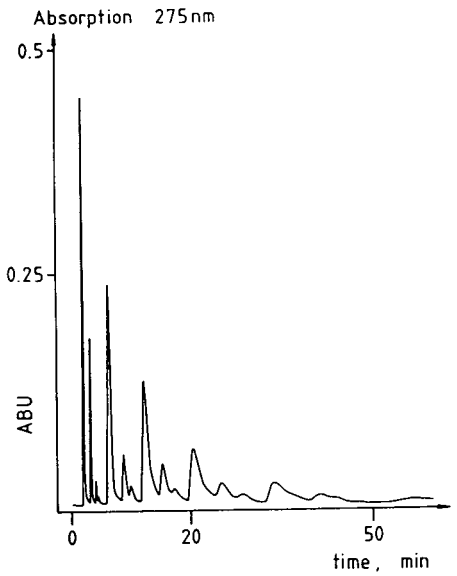

Fig. 1. Separation of tributylphenol ethylene oxide oligomer surfactants on an alumina column. Eluent, ethyl acetate–*n*-hexane (1:1, v/v); flow-rate, 1 ml/min; room temperature (22 ± 2°C); detection wavelength, 275 nm. ABU = Absorbance units.

represent the possible structural isomers of the tributylphenol moiety. These results indicate that the number of ethylene oxide groups and the

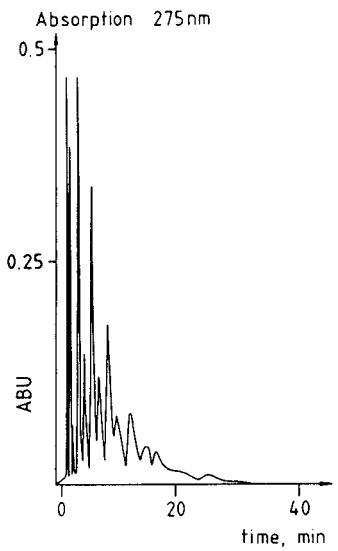

Fig. 2. Separation of tributylphenol ethylene oxide oligomer surfactants on an alumina column. Eluent, ethyl acetate; flow-rate, 1 ml/min; room temperature (22 ± 2°C); detection wavelength, 275 nm.

isomeric form of the hydrophobic moiety govern the retention of the surfactants on alumina. Steric considerations make it probable that the sterically less hindered 2,4,6-tributylphenol isomers are present in the greatest amount in the sample. Owing to the electron-withdrawing character of the substituents [24], we postulated the existence of 2,4,5- and 2,3,5-tributylphenol isomers. We must stress again that the assigment of positions to the various fractions is only hypothetical.

Although the strengths of the eluents are considerably different (ethyl acetate = 0.580 and ethyl acetate–*n*-hexane (1:1) = 0.295 (in arbitrary units) [25]), the differences in the retention times of the surfactants are still relatively low. Under these conditions changes in solvent strength do not have a considerable influence on the retention times of surfactants.

The linear correlations between the logarithm of the capacity factor and the ethyl acetate concentration in the eluent were significant for each fraction (Table I). However, as was qualitatively established from Figs. 1 and 2, the dependence of log k' on ethyl acetate concentration was considerably lower than with other HPLC systems [26].

The retention of surfactants increased with increasing length of the hydrophilic ethylene oxide chain. This indicates that the surfactants turn towards the stationary phase with their ethylene oxide chain, the hydrophobic moiety pointing away from the polar alumina surface. The specific hydrophilic surface area of surfactants containing the 2,4,6-tributylphenol hydrophobic moiety is smaller than that of surfactants containing the sterically more restricted 2,3,6-tributylphenol moiety. This finding can be hypothetically explained by the supposition that the symmetrical isomer is better solvated in the relatively hydrophobic mobile phase, drawing away the surfactant from the hydrophilic alumina surface.

The results of stepwise regression analysis are given in Table II. Both retention parameters of the tributylphenol ethylene oxide oligomer surfactants depended on the number of ethylene oxide groups per molecule and the position of the butyl substituents. The equations fit the

TABLE I

PARAMETERS OF LINEAR CORRELATIONS BETWEEN THE LOGARITHM OF CAPACITY FACTOR AND THE CONCENTRATION ON ETHYL ACETATE [C, % (v/v)] IN THE ELUENT: $\log k' = \log k'_0 + bC$

k' = Capacity factor of surfactants at C vol.% ethyl acetate concentration; k'_0 = theoretical capacity factor of a tributylphenol ethylene oxide oligomer at 0 vol.% ethyl acetate concentration, C = % (v/v) of ethyl acetate in the eluent and S_b = standard deviation of slope value.

Sample No.	Log k'_0	$-b \cdot 10^{-3}$	$S_b \cdot 10^{-3}$	r
1	−0.013	5.14	1.24	0.9899
2	0.189	5.01	1.39	0.9712
3	0.318	6.17	1.69	0.9805
4	0.526	5.52	1.48	0.9926
5	0.725	5.73	1.62	0.9845
6	0.862	6.85	1.66	0.9993
7	0.946	6.43	1.51	0.9752
8	1.061	6.43	1.52	0.9838
9	1.200	7.83	1.32	0.9974
10	1.293	8.03	1.65	0.9956
11	1.347	7.36	1.61	0.9726
12	1.458	8.49	1.45	0.9978
13	1.517	8.02	1.67	0.9802
14	1.615	8.11	1.61	0.9927
15	1.713	9.00	1.21	0.9832

experimental data well, the significance level being over 99.9% (see F values). The number of ethylene oxide groups per molecule (n) and the position of butyl substituents (PI) of solutes account for the 91.50% and 97.31% of the change in dependent variable (see r^2 values). The path coefficients indicate that the number of ethylene oxide groups per molecule has a greater effect on the retention than the position of the butyl substituents of the tributylphenol moiety (see $b_{1\%}$ and $b_{2\%}$ values). These results support our previous conclusions that the hydrophilic ethylene oxide chains of surfactants are in direct (probably electrostatic) interaction with the polar alumina surface, and the solvation state of the hydrophobic tributylphenol moiety only modifies the strength of the interaction.

A significant linear correlation was found between the slope and intercept value of eqn. 1:

$$b = 4.77 + 2.21 \cdot \log k'_0 \quad (2)$$

number of samples = 15; $r = 0.9336$; $S_b = 2.3 \cdot 10^{-1}$; $r_{99.9\%} = 0.7603$. The strong correlation indicates that from the chromatographic point of view the tributylphenol ethylene oxide oligomer surfactants can be considered as a homologous series of compounds. This result lends support to our previous conclusion that the retention of surfactants is mainly governed by the length of the ethylene oxide chains (identical in character in each oligomer) and that the isomeric form of the hydrophobic tributylphenol moiety has a secondary influence on retention.

TABLE II

RELATIONSHIP BETWEEN THE RETENTION PARAMETERS OF TRIBUTYLPHENOL ETHYLENE OXIDE OLIGOMERS AND NUMBER OF ETHYLENE OXIDE GROUPS PER MOLECULE (n) AND POSITION OF THE BUTYL SUBSTITUENTS (PI)

Results of stepwise regression analysis. Number of samples = 15.

Parameter	Equation[a]	
	A	B
a	3.56	$-3.41 \cdot 10^{-1}$
b_1	$7.80 \cdot 10^{-1}$	$3.56 \cdot 10^{-1}$
S_{b1}	$7.30 \cdot 10^{-1}$	$1.17 \cdot 10^{-2}$
b_2	$5.21 \cdot 10^{-1}$	$1.28 \cdot 10^{-1}$
S_{b2}	$1.27 \cdot 10^{-1}$	$3.02 \cdot 10^{-2}$
r^2	0.9150	0.9731
$b_{1\%}$	78.17	82.79
$b_{2\%}$	27.83	17.21
F	64.65	217.65

[a] (A) $b = a + b_1 n + b_2 PI$
(B) $\log k'_0 = a + b_1 n + b_2 PI$.

We conclude that the alumina support is especially suitable for the separation of tributylphenol ethylene oxide oligomer surfactants, separating the solutes both according to the length of the ethylene oxide chain and the position of the butyl substituents in one run.

ACKNOWLEDGEMENT

This work was supported by a grant for Cooperation in Science and Technology with Central and Eastern European Countries: "Enhanced removal and prevention of environmen-

tal pollution by attachment and immobilization of bacteria at surfaces".

REFERENCES

1 J.P.B. Brunell, *Pure Appl. Chem.*, 50 (1978) 1211.
2 A. Nahum and Cs. Horváth, *J. Chromatogr.*, 203 (1981) 53.
3 K.E. Bij, Cs. Horváth, W.R. Melander and A. Nahum, *J. Chromatogr.*, 203 (1981) 65.
4 N.E. Tayar, H. Waterbeend and B. Testa, *J. Chromatogr.*, 320 (1985) 305.
5 C.J. Laurent, H.A.H. Billiet and L. de Galan, *J. Chromatogr.*, 285 (1984) 161.
6 J.J. Sun and J.S. Fritz, *J. Chromatogr.*, 522 (1990) 95.
7 J.A. Blackwell and P.W. Carr, *J. Chromatogr.*, 549 (1991) 43.
8 J.A. Blackwell and P.W. Carr, *J. Chromatogr.*, 549 (1991) 59.
9 T. Takeuchi, W. Hu and H. Haraguchi, *J. Chromatogr.*, 517 (1990) 257.
10 R. Kaliszan, J. Petrusewitz, R.W. Blain and R.A. Hartwick, *J. Chromatogr.*, 458 (1988) 395.
11 J.J. Pesek, *Chromatographia*, 28 (1989) 565.
12 R. Poisson, J.P. Brunelle and P. Nortier, in A.B. Stiles (Editor), *Catalytic Supports, Supported Catalysis*, Butterworth, Boston, 1987, p. 11.
13 K.K. Unger, W. Messer and K.F. Krebs, *J. Chromatogr.*, 149 (1978) 1.
14 T. Cserháti, *Chromatographia*, 29 (1990) 593.
15 C.J.C.M. Laurent, H.A.H. Billiet, L. de Galan, F.A. Buytenhuys and F.P.B. van de Maeden, *J. Chromatogr.*, 287 (1984) 45.
16 H. Lingeman, H.A. van Muster, J.H. Beyben, W.J.M. Underber and A. Hulshoff, *J. Chromatogr.*, 352 (1986) 61.
17 T. Bán, E. Papp and J. Inczédy, *J. Chromatogr.*, 593 (1992) 227.
18 I. Zeman, *J. Chromatogr.*, 509 (1990) 201.
19 I. Zeman, *J. Chromatogr.*, 363 (1986) 223.
20 T. Okada, *J. Chromatogr.*, 609 (1992) 213.
21 Z.H. Wang and M. Fingas, *J. Chromatogr.*, 631 (1993) 251.
22 H. Hager, *Modern Regressionanalyse*, Salle Saulander, Frankfurt am Main, 1982, p. 135.
23 K. Valkó, *J. Liq. Chromatogr.*, 7 (1984) 1405.
24 C. Hansch and A. Leo, *Substituent Constants for Correlation Analysis in Chemistry and Biology*, Wiley, New York, 1979, p. 1.
25 L.R. Snyder and J.J. Kirkland, *Introduction to Modern Liquid Chromatography*, Wiley, New York, 1974, p. 286.
26 E. Forgács, K. Valkó and T. Cserháti, *J. Chromatogr.*, 631 (1993) 207.

Journal of Chromatography A, 661 (1994) 245–248
Elsevier Science B.V., Amsterdam

CHROMSYMP. 2935

Simultaneous determination of benzotriazole copper inhibitor and microbiocidal isothiazolinenones by high-performance liquid chromatography

A. Iob*, F. Al-Yousef, B.S. Tawabini, A.I. Mohammed and N.M. Abbas

Research Institute, King Fahd University of Petroleum and Minerals, Dhahran 31261 (Saudi Arabia)

ABSTRACT

A high-performance liquid chromatographic (HPLC) procedure for the separation and determination of the components of a formulation that contained sodium benzotriazole (copper inhibitor), 2-methyl-4-isothiazoline-3-one and 5-chloro-2-methyl-4-isothiazoline-3-one (microbiocide mixture) was developed. This mixture is used to protect and maintain a large water-chilling plant in Saudi Arabia. A UV spectrophotometric method was tried unsuccessfully as both sodium benzotriazole and the isothiazolinenones had λ_{max} at 275 nm, so an HPLC method was sought. Optimum conditions were established using a Hewlett-Packard RP C_8 column to be methanol–water (40:60) containing 0.05 *M* KH_2PO_4 as the eluent at a flow-rate of 1 ml/min. The relative standard deviation of the method at the 95% confidence level was found to be 0.8, 0.7 and 2.4% for the respective components at concentration levels of 35, 115 and 50 mg/l, respectively.

INTRODUCTION

Sodium benzotriazole (BZTR) and its derivatives are commonly used as copper inhibitors in coolant additives and as light stabilizers in photographic films and 2-methyl-4-isothiazoline-3-one (MIS) and 5-chloro-2-methyl-4-isothiazoline-3-one (CMIS) are extensively used as microbiocidal agents, disinfectants, etc., in cooling waters (chilling water). Mixtures of these products at certain levels are used in a large water-chilling plant in Saudi Arabia. This chilling plant serves as a cooling facility for a city which encompasses residential areas (>5000 apartments), schools and a local hospital. This facility needs rigorous maintenance procedures and additives are incorporated at the required concentration levels on a constant basis. Some of the common additives needed include dispersants, corrosion inhibitors and pH adjusters in addition to the copper inhibitors and microbiocidal mixture. The latter two are mainly used in the "closed-loop" water-chilling compressor section. The specification regarding these two additive solutions are sodium benzotriazole $\geq 0.1\%$ and isothiazolinone mixture $\geq 1.5\%$ (usually the 5-chloro product predominates, *i.e.*, *ca.* 1.15% with the other compound at 0.35%).

Having these additives at the specified concentrations is critical for the proper maintenance of the chilling plant and a method had to be developed to monitor the concentrations of all the additives. Several methods have been reported for the determination of isothiazolinones in variety of matrices, *e.g.*, HPLC and UV detection [1–3], spectrophotometric evaluation after reductive cleavage [4] and iodimetric determination after ring opening with $NaHSO_3$ [5]. Several HPLC techniques used for determination of benzotriazole and its derivatives have also been published [6–11] and have been used for the evaluation of benzotriazole in ethylene glycol coolants, photographic products, etc. However,

* Corresponding author.

0021-9673/94/$07.00
SSDI 0021-9673(93)E0942-N

there appears to be no method for evaluating mixtures of the isothiazolinone microbiocides and benzotriazole copper inhibitor simultaneously and particularly at the concentration levels indicated above.

This paper describes an HPLC method that was developed and successfully utilized for determining the three constituents in the chilling fluid additives formulation.

EXPERIMENTAL

Reagents

All solvents used for the chromatography were of HPLC grade from Baker. Benzotriazole was obtained from Fisher Scientific and the isothiazolinone mixture (1.15 and 0.35% in water) was supplied by the Chilling Plant Operation and Maintenance Office through a local vendor. Their total concentrations were confirmed in our laboratory by measuring their molar absorptivity at 275 nm.

Apparatus

UV spectra were recorded on a Varian Cary 2300 spectrophotometer. A Hewlett-Packard HP 1090 liquid chromatograph equipped with diode-array detector, HP-85B computing system, Model 3392A integrator and HP 9121 disk storage module was used for HPLC. The injection system was fitted with a 25-μl sample loop. HPLC columns tried included Hewlett-Packard silica-based amino-bonded, RP C_{18} and RP C_8 (200 × 4.6 mm I.D.).

RESULTS AN DISCUSSION

Preliminary work with a UV spectrophotometer indicated that the microbiocide mixture and the benzotriazole inhibitor showed an absorbance maximum at about 275 nm (Fig. 1). Fig. 1 indicated that multi-component analysis using wavelengths of 258 and 212 nm is a possibility. However, in real experimental work this was found to be unsuccessful, mainly because the concentration difference between the microbiocides and the copper inhibitor was greater than tenfold. The isothiazolinone concentration was too high compared with that of the benzotriazole and the results for benzotriazole were significantly affected.

An initial HPLC method development trial involved the use of an ion-pairing agent (PIC-A, *i.e.*, tetrabutylammonium phosphate) for the sodium benzotriazole (pK_1 for benzotriazole = 8.38) on the assumption that this reagent (eluent

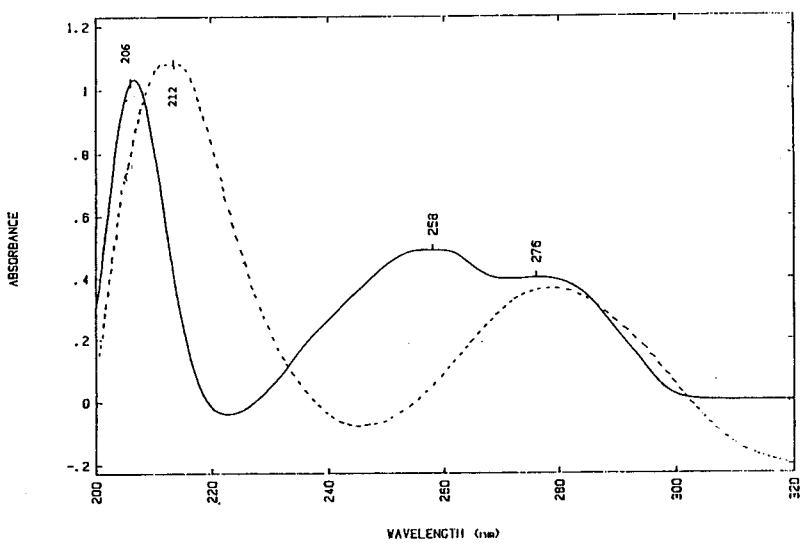

Fig. 1. UV spectra of *ca.* 10 mg/l of (solid line) benzotriazole and (dashed line) isothiazolinone mixture.

pH = 8) would not affect the two constituents of the microbiocide. However, even though the three constituents were clearly separated, the ion-pairing agent affected the concentration by varying the peak area and height of the 5-chloro-2-methyl-4-isothiazoline-3-one. Additionally, the benzotriazole peak was broad and tailing and introduced inconsistencies into the peak integration evaluations. The reason for this behaviour was not clear. Therefore, owing to time constraints, it was decided to use two HPLC techniques for determination of the constituents of the chilling fluid additives. In the first technique, the C_{18} column was used for the determination of the isothiazolinones and the amino-bonded column was used for the benzotriazole. However, it was time consuming and cumbersome to switch from one column and reagent system to another every time a sample needed to be analyzed. Therefore, it was decided to develop a method for determining the three constituents in a single analysis. After several trials with eluents and columns it was found that an RP C_8 column with methanol–water (40:60) containing 0.05 *M* KH_2PO_4 as the eluent achieved the separation of the constituents with good resolution. A typical chromatogram of a real example [diluted 100-fold with methanol–water (40:60)] is shown in Fig. 2.

As can be seen, the benzotriazole peak is small compared with the other two peaks. However, the peak area for each compound was found to be consistently reproducible. Calibration graphs for the three compounds are shown in Fig. 3.

The precision of the method was calculated by injecting known concentrations of the standards repeatedly (ten times). From the results, the standard deviations were evaluated and the relative standard deviations (R.S.D.s) at the 95% confidence level were calculated. The R.S.D.s were found to be 0.8, 0.7 and 2.4% for MIS, CMIS and BZTR, respectively.

Analysis of formulation samples over a period of 3 years indicated that on several occasions the materials supplied by some companies did not satisfy the specification. Some of the results found are given in Table I.

Based on these results, appropriate action

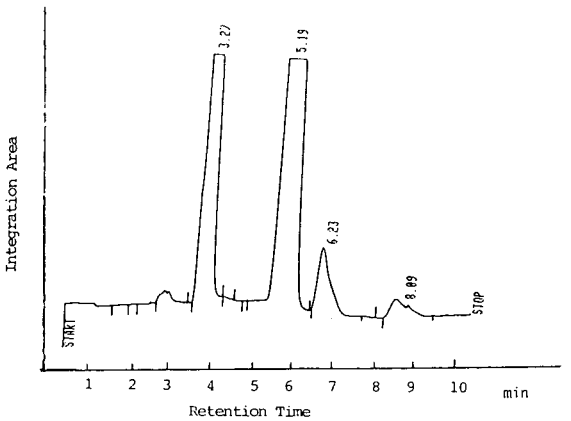

Fig. 2. HPLC of a real chiller fluid additive sample. Peaks at retention times of 3.27, 5.19 and 6.23 min correspond to MIS, CMIS and BTRZ, respectively. Column, RP C_8 (200 × 4.6 mm I.D.); eluent, methanol–water (40:60) containing 0.05 *M* KH_2PO_4; flow-rate 1 ml/min; UV detection at 275 nm.

(dilution, specific additions of the required ingredients) was taken before the product were used for the specified tasks.

CONCLUSIONS

The proposed HPLC method has effectively been used for evaluating the concentrations of microbiocide mixtures and copper inhibitor in chilling fluid additive formulations. This has permitted the chilling plant to save money and maintenance power, and helped to provide chilled water efficiently to the local population.

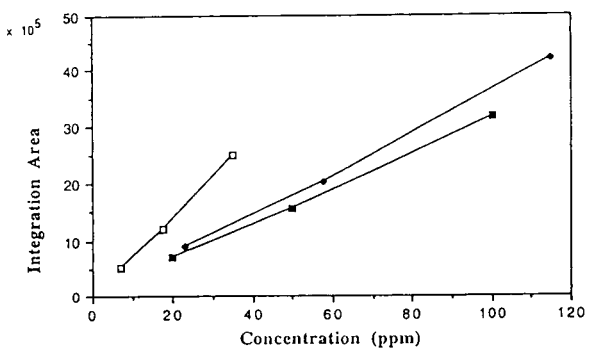

Fig. 3. Calibration graphs for (□) MIS, (◆) CMIS and (■) BZTR.

TABLE I

CONCENTRATIONS FOUND IN SOME COMMERCIAL CHILLING FLUID ADDITIVES

Sample	MIS (%)	CMIS (%)	BZTR (%)
Company 1 (1990)	0.58	1.34	1.4
Company 2 (1990)	0.15	0.33	0.52
Company 1 (May 1992)	0.35	1.15	<0.001
Company 2 (May 1992)	0.06	0.14	<0.001
Company 1 (Oct 1992)	0.35	1.09	0.1

ACKNOWLEDGEMENT

The authors extend their thanks to the Research Institute of King Fahd University of Petroleum and Minerals for providing the support for this work.

REFERENCES

1 R. Mattissek, B. Harper and R. Lehngutt, *Fresenius' Z. Anal. Chem.*, 322 (1985) 465–469.
2 R. Matissek and R. Lehnguth, *Fresenius' Z. Anal. Chem.*, 328 (1987) 108–111.
3 R. Matissek, R. Nagorka, M. Daase and I., Wengatz, *Fresenius' Z. Anal. Chem.*, 333 (1989) 806–809.
4 W.G. Geyer, *US Pat.*, 3 975 155 (1976); *C.A.*, 85 (1976) 155062a.
5 W. Beilfuss and G. Bestmann, *Arch. Pharm. (Weinheim, Ger.)*, 310 (1977) 216–222; *C.A.*, 87 (1977) 90774d.
6 W.R. Biggs and J.C. Fetzer, *J. Chromatogr.*, 260 (1983) 137–145.
7 T.M. Schmitt and E.S. Muzher, *Talanta*, 28 (1981) 777–779.
8 T. Koizumi, M. Ikeda, I. Imai and K. Yagishita, *Nisseki Rebyu*, 28 (1986) 151–156.
9 G.G. Hawn, P.A. Diehl and C.P. Talley, *J. Chromatogr. Sci.*, 19 (1981) 567–569.
10 M.M. Rhemrev-Boom and W.E. Hammers, *J. Photogr. Sci.*, 36 (1988) 53–56.
11 X. Zhou, L. Shen, Y. Ke, J. Zhang, Z. Chen and L. Liu, *Beijing Huagong Xueyuan Xuebao, Ziran Kexueban*, 18, No. 2 (1991) 70–74.

Journal of Chromatography A, 661 (1994) 249–256
Elsevier Science B.V., Amsterdam

CHROMSYMP. 2906

Low-molecular-mass p*I* markers for isoelectric focusing

K. Šlais*

Institute of Analytical Chemistry, Academy of Sciences of the Czech Republic, Veveří 97, CZ-611 42 Brno (Czech Republic)

Z. Friedl

Tessek Laboratory, Academy of Sciences of the Czech Republic, Veveří 97, CZ-611 42 Brno (Czech Republic)

ABSTRACT

Substituted aminomethylphenols are proposed as low-molecular-mass p*I* markers for the electrophoretic and chromatographic focusing of ampholytes. The important acid–base, spectroscopic and hydrophobic characteristics are presented for nineteen synthesized compounds. The low interaction between the suggested p*I* markers and proteins was verified by gradient ion-exchange chromatography of a mixture of some markers and alcohol dehydrogenase.

INTRODUCTION

Isoelectric focusing (IEF) is a technique for the separation, focusing and characterization of amphoteric analytes such as proteins [1,2]. The principle of the method involves the focusing of an amphoteric molecule at that point in the system where the pH value corresponds to its isoelectric point (p*I*).

To characterize the analyte, the pH at the place of its focusing should be known [1,3]. On gel plates, direct measurement by pH microelectrodes is possible. In preparative IEF variants, on-line or off-line pH measurement of the collected fraction can be considered. However, pH is most often evaluated with the help of reference substances. They may have different names, *e.g.*, p*I* markers [1,4], isoelectric point markers [5], IEF standards [6], IEF markers [7], pH markers [8,9], internal markers [10] or test substances for IEF. Their use may be universal: they are applicable on gel plates, in preparative channels and also in capillary modes of IEF. So far, native proteins have been used as p*I* markers [9,11,12]. Their p*I* values are determined mainly by IEF methods. For observing the focusing process, coloured proteins (*e.g.*, myoglobin, ferritin) or proteins stained with a suitable dye, *e.g.*, albumin stained with bromphenol blue [13], were used.

The native proteins, however, have some distinct disadvantages for use as p*I* markers. They tend to precipitate at pH values close to their p*I* and show instability as the substances themselves as aqueons solutions. Some protein standards consist of mixtures of related proteins; the high molecular mass of proteins makes their potential separation from the collected fractions of focused analytes difficult, and they cannot be used with reducing or denaturing agents such as urea, 2-mercaptoethanol or dithiothreitol [6]. So far, most analytical IEF has been carried out on gel plates; detection based on the protein staining is used almost exclusively in those methods. The low-molecular-mass analytes are washed out during the fixation step of this detection procedure. The newer capillary IEF method [14–18], preparative IEF methods and isoelectric focusing field flow fractionation (IEF FFF = IEF_4) [19]

* Corresponding author.

0021-9673/94/$07.00
SSDI 0021-9673(93)E0836-J

may also be applied to low-molecular-mass compounds. Detection methods based on the staining are not considered in such focusing methods. Further, in capillary IEF, off-line pH monitoring is possible using hydrodynamic or electroosmotic mobilization [20]; however, calibration with p*I* standards is necessary.

Suitable low-molecular-mass p*I* markers may help in avoiding some of the above disadvantages. A good p*I* marker should meet the following demands (see also ref. 9): it should be a good ampholyte [21–23], highly soluble in water and detectable by the method used, which in photometric detection usually means having a high absorptivity in the region where the focusing media are optically transparent and the analytes are detected, *i.e.*, at wavelengths of 270 nm and above.

Published tables [21–23] list few good low-molecular-mass ampholytes, only a few of them, including derivatives of tyrosine and 4-aminobenzoic acid, have satisfactory UV absorption at the wavelengths above 270 nm used for on-line detection of proteins and none of them absorbs in the visible region. As long as 20 years ago [8,10] the search for good low-molecular-mass ampholytes potentially applicable as reference substances in IEF was initiated. So far several have been reported, including methyl red [7,19], phenanthroline complexes [8] and some amphoteric triphenylmethane and azo dyes [10,19]. Methyl red has also been used for spectroscopic indication of the focusing solution pH [19] and for tracing the pH gradient in ion-exchange chromatography [24]. However, the low-molecular-mass p*I* markers so far used do not seem to meet all the necessary demands. Disadvantages are mainly based on their small number and the range of p*I* values covered. Moreover, their relatively high hydrophobicity causes their low solubility at the p*I* values, absorption on plastics and interactions with proteins; some of the dyes mentioned above have even been recomended for protein staining [25].

Here we propose the use of the aminomethylated nitrophenols of general formula **I** as p*I* markers. These compounds were prepared by aminomethylation of the phenolic substrates [26,27]. The purity of the reaction products was

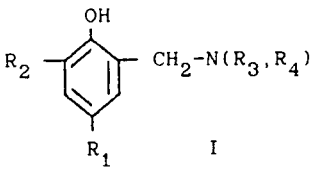

I

determinated by ion-exchange chromatography with a pH gradient and UV–Vis spectrophotometer with diode-array detection [28]. The acid–base properties were determined by potentiometric titration and numerical evaluation of the titration curves obtained.

THEORETICAL BACKGROUND FOR SELECTION OF SUGGESTED STRUCTURES

It is necessary for the sharp IEF of a low-molecular-mass amphoteric compound that it be a good ampholyte or, in other words, all the p*K* values adjacent to the p*I* value must be close to one another. The condition for the good ampholyte can be formulated as [22,29]

$$(pK_2 - pK_1) < 4 \quad (1)$$

For calculation of the width of the focused zone, it is more convenient to use the steepness of the dependence of the effective charge on pH at the isoelectric point of the compound, $[-dz/d(pH)]_{pI}$ [30,31]. Its relationship to the difference in p*K* is [29]

$$[-dz/d(pH)]_{pI} = \ln 10/[1 + (K_1/4K_2)^{0.5}] \quad (2)$$

A good ampholyte (and hence the proposed p*I* marker) then should have a $[-dz/d(pH)]_{pI}$ value above 0.045. The variance in the length units of the focused ampholyte zone, σ^2, is then [30,31]

$$\sigma^2 = RT/\{FE[-dz/d(pH)]_{pI}\, d(pH)/dx\} \quad (3)$$

where R, T and F have their usual meanings, E is the intensity of the electrical field and $d(pH)/dx$ is the steepness of the pH gradient.

For the design of the p*I* marker formula it is convenient if the p*K* values of both acidic and basic ionizable groups vary independently in a broad range. The phenolic group and aliphatic amino groups suit this concept. The interaction

of the respective groups within the molecule should also be considered when conbining the pK_a values of isolated groups [32,33]. Owing to the low molecular mass, the presence of two relatively independent charged groups at the p*I* of the compound and the presence of at least one hydrophilic amino group, the solubility of the compound in water can be expected to be sufficiently high even at pH values close to the p*I*. The presence of a nitro group leads to a high absorptivity also in the visible region.

EXPERIMENTAL

Materials

Compounds **1–19** (see Table I) were prepared from the commercially available nitrophenols by means of the Mannich reaction [26,27]. The appropriate amine (50 mmol) was added portionwise with cooling to 37% aqueous formaldehyde (60 mmol) in 25 ml of ethanol. After addition of substituted phenol (50 mmol), the reaction mixture was heated under reflux for 10 h [27,34]. The aqueous ethanol was removed under reduced pressure, the residue dissolved in 25 ml of methanol and to the resulting solution 5 ml of concentrated hydrochloric acid were added portionwise. After cooling, the products were separated by filtration or removal of the solvent under reduced pressure. The isolated hydrochlorides were recrystallized from methanol or aqueous ethanol. The purity of all compounds was checked by TLC and ion-exchange liquid chromatography with a pH gradient and UV–Vis diode-array detection [28].

Liquid chromatography

The conditions for ion-exchange chromatography with a wide pH gradient range were described previously [28]. A PU 4100M liquid chromatograph (Philips, Cambridge, UK) equipped with a Model 7125 injection valve (Rheodyne, Cotati, CA, USA) and a PU 4021 multi-channel detector (Philips) were used. The data collection and postrun evaluation were controlled by PU 6003 v. 3.0 diode-array detec-

TABLE I

STRUCTURES OF SUGGESTED p*I* MARKERS OF GENERAL FORMULA I

No.	R_1	R_2	$N(R_3, R_4)$[a]	M_r
1	NO_2	$CH_2N(R_3, R_4)$	PIP	406
2	$CH_2N(R_3, R_4)$	NO_2	PIP	406
3	NO_2	$CH_2N(R_3, R_4)$	MPIPE	509
4	$CH_2N(R_3, R_4)$	NO_2	MPIPE	509
5	$CH_2N(R_3, R_4)$	NO_2	HPIPE	569
6	NO_2	H	DEA	261
7	NO_2	H	PIP	273
8	NO_2	$CH_2N(R_3, R_4)$	MOR	435
9	CH_3	NO_2	MPIPE	338
10	CH_3	NO_2	HPIPE	368
11	$CH_2N(R_3, R_4)$	NO_2	MOR	410
12	Cl	NO_2	MPIPE	359
13	CH_3	NO_2	MOR	289
14	Cl	NO_2	HPIPE	389
15	NO_2	H	MOR	275
16	Cl	NO_2	MOR	309
17[b]	4-$CH_2N(R_3, R_4)$	2-Cl-6-NO_2	MPIPE	359
18[b]	4-$CH_2N(R_3, R_4)$	2-Cl-6-NO_2	HPIPE	389
19[b]	4-$CH_2N(R_3, R_4)$	2-Cl-6-NO_2	MOR	309

[a] PIP = 1-piperidyl; MPIPE = 1-(4-methylpiperazinyl); HPIPE = 1-(4-hydroxyethylpiperazinyl); DEA = diethylamino; MOR = 4-morpholinyl.

[b] Aminomethyl group in position 4- and substitutents R_1 and R_2 in position 2- and 6-, respectively.

tor software (Philips). The actual pH profile of the column effluent was monitored by a capillary flow-through pH electrode (Model OP-0745P; Radelkis, Budapest, Hungary) connected to a Model OP-208/1 pH meter (Radelkis) and a line recorder. A 150 × 2 mm I.D. Separon HEMA-BIO 1000 Q ion-exchange column (Tessek, Prague, Czech Republic) was used as received.

The alkaline buffer (A) was an aqueous solution of 10 m*M* each piperazine, L-histidine, ethylenediamine, 2-amino-2-(hydroxymethyl)-1,3-propanediol (Tris) and 20 m*M* ammonia solution. The pH of buffer A was adjusted to 10.0 with 2 mol l^{-1} potassium hydroxide solution. The acidic buffer (B) was 0.83 mol l^{-1} formic acid. Chemicals used for buffer preparation were obtained from Fluka (Buchs, Switzerland) and Merck (Darmstadt, Germany).

Alcohol dehydrogenase (yeast) No. 01106 (Reanal, Budapest, Hungary) was sampled in the alkaline buffer. In a sample volume of 10 μl, 0.8–1.2 mg of protein was loaded on the column.

Determination of absorptivity, $A^{1\%}_{1\ cm}$

The absorptivities of componds **1–19** in aqueous buffer solutions with pH corresponding to the marker p*I* value were determined with a Varian Techtron Series 634 UV–Vis spectrophotometer.

Determination of p*K*, p*I and* $[-dz/d(pH)]_{pI}$

The acid–base properties of the prepared compounds were evaluated by potentiometric titration using a Model MS 22 pH meter (Laboratory Instruments, Prague, Czech Republic), equipped with a Model 01-29 combined glass pH electrode (Crytur, Turnov, Czech Republic). The instrument was calibrated by means of commercial standard buffer solutions (Institute of Sera and Vaccines, SEVAC, Prague, Czech Republic). The temperature during titration was kept at 23°C. The titration curves obtained were evaluated both graphically and numerically to obtain p*K*, p*I* and $[-dz/d(pH)]_{pI}$ values of the p*I* marker. For the curve-fitting procedure, the program Eureka V. 1.0 (Borland, Scotts Valley, CA, USA) was used. The whole procedure for p*K* determination was verified by the determination of the p*K* of L-histidine monohydrochloride (Renal) as a standard. The differences between the determined and tabulated [35] p*K* values were less than 0.1 pH unit.

In fact, the titration enables one to calculate the isoionic point which might be different from the isoelectric point owing to the difference in mobilities of cationic and anionic forms of the ampholyte, which can amount to up to 5% [36,37]. It can be estimated that such a difference can make a difference between the isoionic and isoelectric point of only up to a few hundredths of a pH unit.

Determination of log P_{OW}

The partition coefficient between 1-octanol and water, P_{OW}, was determined spectroscopically by the shake-flask method as described previously [38]. The values presented correspond to the pH of the water-rich phase equal to the p*I* value of the respective marker. The pH of the water rich phase was adjusted with 0.1 mol l^{-1} phosphate buffer. The absorptivity of the water-rich phase was determined at its λ_{max} in the visible spectrum: the solution was equilibrated for 3 h at 23°C with a known amount of water-saturated 1-octanol and the absorptivity of the aqueous phase was measured again.

RESULTS AND DISCUSSION

Referring to the general structure **I** and the related structures in Table I, it is obvious that the compounds prepared include all the important groups necessary to meet the key properties of a good p*I* marker, namely the acid–base behaviour, hydrophilicity and light absorptivity. The hydrophilic amino groups are similar to those of common Good's buffers and the molecular masses are similar to those of the polyampholytic buffers used in IEF. The variation of the groups and their positions in formula **I** leads to changes in the acid–base properties of both phenolic and amino groups [39]. Consequently, the p*I* values of the prepared compounds cover a wide pH range (see Table II). Variations in the p*K* of ionizable groups also influence the $[-dz/d(pH)]_{pI}$ values of the respective compounds. It follows from Table II that except for compounds **6** and **7**, all of them can be considered as good

TABLE II

IEF, SPECTRAL AND LIPOPHILIC CHARACTERISTICS OF PROPOSED p*I* MARKERS

No.	p*I*	$\lvert(dz/dpH)_{pI}\rvert$	λ_{max} (nm)[a]	$A^{1\%}$ [b]	Log P_{OW}[c]
1	10.4	0.76	403	617	1.08
2	10.1	0.60	412	374	0.64
3	8.6	0.74	420	102	−0.02
4	8.5	0.72	419	131	−0.78
5	8.4	0.60	417	80	−1.30
6	8.1	0.01	392	744	0.38
7	8.0	0.02	392	661	0.62
8	7.9	0.45	403	698	0.43
9	7.9	0.27	425	165	0.79
10	7.7	0.19	423	119	0.31
11	7.5	0.43	416	115	−0.19
12	7.4	0.17	428	156	0.58
13	7.2	0.15	416	162	1.05
14	7.0	0.14	423	139	0.02
15	6.6	0.15	400	526	0.49
16	6.5	0.07	421	142	0.88
17	6.4	0.09	416	131	−0.94
18	6.2	0.10	415	133	−2.18
19	5.3	0.12	409	142	−0.16

[a] Wavelength of absorption maximum in UV–Vis spectrum of aqueous buffer solution at pH equal to the p*I* value.
[b] Absorptivity of a 1% aqueous buffer solution at pH equal to the p*I* value.
[c] Partition coefficient between 1-octanol and water at 25°C.

ampholytes. Nevertheless, even **7** can give a sharp peak in capillary IEF [40].

The suggested markers have satisfactory light absorptivity in both the UV and visible regions of the spectrum (see Table II). Therefore, a small amount of the marker in its focused zone is sufficient for its reliable detection and the pH gradient need not be influenced by the presence of the marker.

The p*I* markers can also be used for the approximate tracing of the pH gradient in ion-exchange chromatography (see Fig. 1). Here, compounds **4**, **11**, **17** and **19** (see Tables I and II) were chromatographed in a gradient decreasing from pH 10 to 4 on a strong anion exchanger. In Fig. 1a, the detection wavelength was close to the absorbtion maxima in the visible region of the marker spectra. In Fig. 1b, the wavelength common for detection of the proteins, *i.e.*, 280 nm, was selected. It should be noted that the pH of elution in ion-exchange chromatography need not always correspond to the isoelectric point of the analyte as interactions other than purely electrostatic ones can occur between the analyte and the stationary phase [41].

The important property of a suitable p*I* marker is its lowest possible interaction with the analytes, namely proteins. This property was checked by the ion-exchange chromatography of a mixture of some markers with proteins. Fig. 2 presents the chromatograms of compounds **4** and **11** (see Tables I and II) and alcohol dehydrogenase. Two peaks of the markers and a group of peaks corresponding to the enzyme was observed with detection at 280 nm (see Fig. 2b). With detection at the wavelength where only markers are detectable, *i.e.*, at 430 nm, almost no peaks can be detected in the elution range corresponding to the elution of the enzyme (see Fig. 2a); this means that less than 1% of marker can be bound to the sampled protein. This observation supports the statement that the tested markers are not irreversibly bound to the alcohol dehydrogenase proteins.

Good water solubility, high hydrophility and low interaction of the markers with the proteins

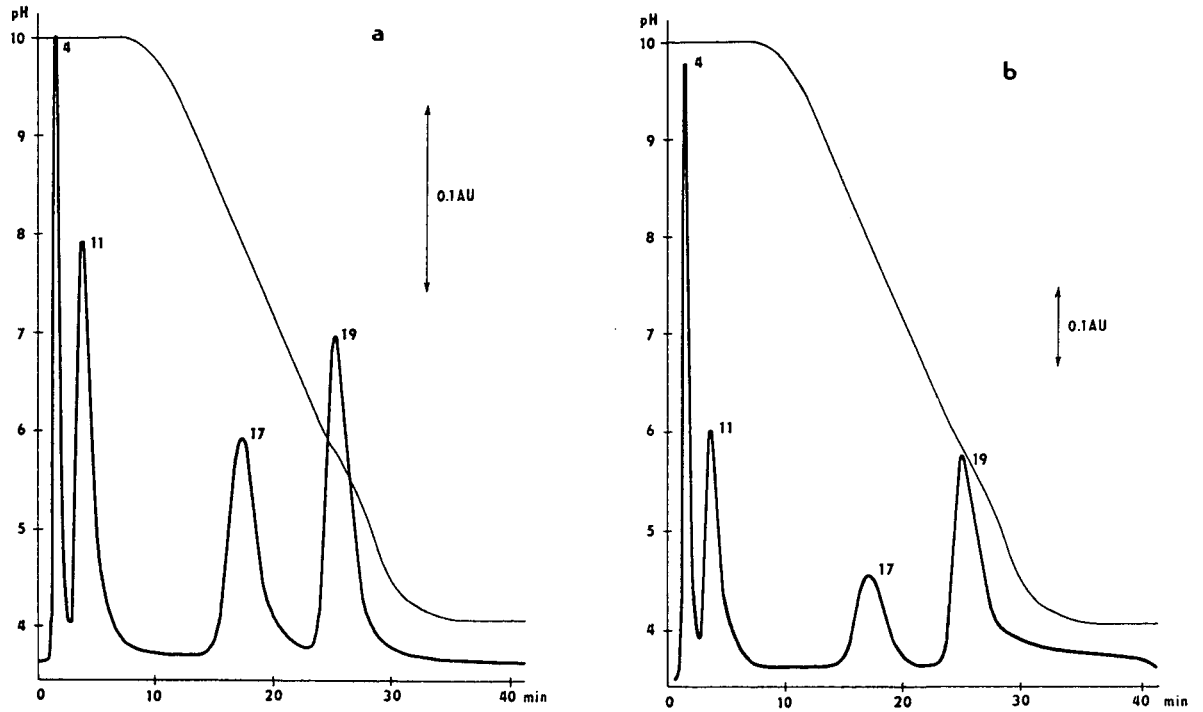

Fig. 1. Separation of selected p*I* markers by anion exchange liquid chromatography with a pH gradient. Column: 150 × 2 mm I.D. glass cartridge packed with Separon HEMA-BIO 1000 Q anion exchanger (Tessek); pH gradient from 0% of acidic buffer B in A (pH 10.0) to 13% B in A (pH 4.0) in 30 min. Detection wavelength (a) 430 nm and (b) 280 nm. Peak numbers correspond to the compound numbers in Tables I and II.

can further be illustrated by their behaviour during the focusing on the gel plates, *e.g.*, in the Pharmacia PhastSystem. When focusing the suggested markers with proteins, the development of visible sharp zones of the markers is possible. During the staining procedure, the nitrophenol markers are eluted from the plate in such a way that they are not detectable after staining. At the same time, the positions of the protein standards are the same irrespective whether they are sampled with or without the nitrophenol markers. The behaviour of the prepared compounds in the capillary and preparative electrophoretic focusing methods will be described elsewhere [40,42].

The high hydrophility of the compounds prepared follows from the low values of their partition coefficients between 1-octanol and water, P_{OW} (see Table II). Here, log P_{OW} of the p*I* markers are given as determined at the pH of the water-rich phase corresponding to p*I* of the marker; for methyl red (not included in Table II), an approximate value of log P_{OW} was calculated to be 3.5. For comparison, log P_{OW} values reported for some other ampholytes [43] are alanine −2.94, N-phenylglycine 0.62, 4-aminobenzoic acid 0.68 and 2-aminobenzoic acid 1.21.

The high hydrophility of the suggested markers can also be supported by the observation that common plastics (*e.g.*, PVC, Perspex) and skin are not observably coloured by aqueous solutions of the suggested markers.

CONCLUSION

Coloured ampholytes based on aminomethylnitrophenols are suggested as p*I* markers for free fluid formats of IEF. The suggested general formula offers wide variations of acid–base properties of the compounds. It can be expected that the utilization of other amino groups and/or other substituents on the aromatic ring can further increase the scope of p*I* values.

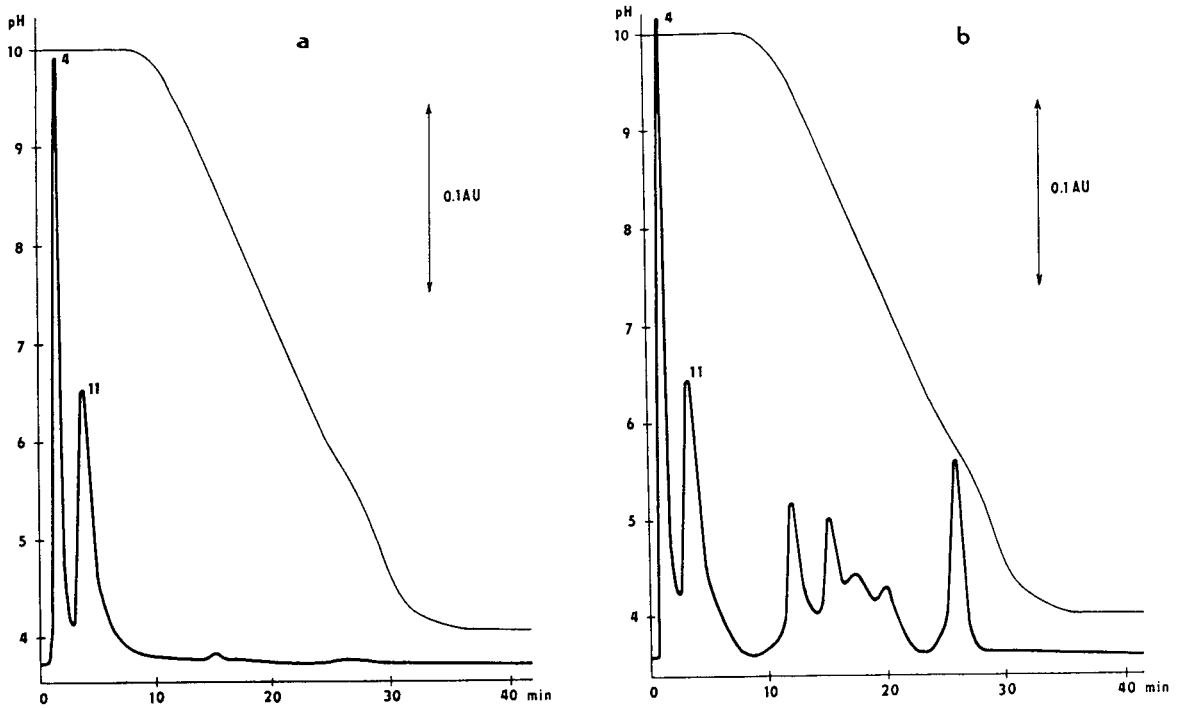

Fig. 2. Separation of a mixture of p*I* markers with alcohol dehydrogenase by anion-exchange liquid chromatography with a pH gradient. Detection wavelength: (a) 430 nm and (b) 280 nm. Sample amount: alcohol dehydrogenase 300 μg, p*I* markers 6 μg each. Experimental conditions as in Fig. 1.

A change in the spectroscopic properties of the marker would undoubtedly need a profound modification of the structure. A more detailed specification and testing of these compounds as p*I* markers in IEF are in progress.

REFERENCES

1 N. Catsimpolas, *Sep. Sci.*, 10 (1975) 55.
2 H. Svensson, *Acta Chem. Scand.*, 15 (1961) 425.
3 W.J. Gelsema and C.L. de Ligny, *J. Chromatogr.*, 130 (1977) 41.
4 *Serva Main Catalog*, Serva, Heidelberg, 1991–92, p. 414.
5 *Multiphor II System, Product Description*, Pharmacia–LKB Biotechnology, Uppsala, 1992, p. 18.
6 *Catalog R*, Bio-Rad, Richmond, CA, 1992, p. 286.
7 *Biochemicals and Organic Compounds for Research*, Sigma, St. Louis, MO, 1993, p. 1663.
8 E.T. Nakhleh, S.A. Samra and Z.L. Awdeh, *Anal. Biochem.*, 49 (1972) 218.
9 P.G. Righetti and T. Caravaggio, *J. Chromatogr.*, 127 (1976) 1.
10 A. Conway-Jacobs and L.M. Lewin, *Anal. Biochem.*, 43 (1971) 394.
11 B.J. Radola, *Biochim. Biophys. Acta*, 295 (1973) 412.
12 P.G. Righetti, G. Tudor and C. Ek, *J. Chromatogr.*, 220 (1981) 115.
13 W. Thormann, *J. Chromatogr.*, 389 (1987) 75.
14 S. Hjertén and M. Zhu, *J. Chromatogr.*, 346 (1985) 265.
15 S. Hjertén, K. Elenbring, F. Kilár, J.L. Liao, A.J.C. Chen, C.J. Siebert and M.D. Zhu, *J. Chromatogr.*, 403 (1987) 47.
16 S.M. Chen and J.E. Wiktorowicz, *Anal. Biochem*, 206 (1992) 84.
17 J.R. Mazzeo and I.S. Krull, *Anal. Chem.*, 63 (1991) 2852.
18 W. Thormann, J. Čáslavská, S. Molteni and J. Chmelík, *J. Chromatogr.*, 589 (1992) 321.
19 J. Chmelík, *J. Chromatogr.*, 539 (1991) 111.
20 F. Kilár, *J. Chromatogr.*, 545 (1991) 403.
21 M. Bier and T. Long, *J. Chromatogr.*, 604 (1992) 73, and references cited therein.
22 H. Svensson, *Acta Chem. Scand.*, 16 (1962) 456.
23 P.G. Righetti and C. Tonani, in F. Dondi and G. Guiochon (Editors) *Theoretical Advancement in Chromatography and Related Separation Techniques*, Kluwer, Dordrecht, 1992, p. 581.
24 M. Janeček and K. Šlais, *Chromatographia*, 36 (1993) 246.
25 *Catalogue, Handbook of Fine Chemicals*, Aldrich, Heidenheim, 1992–93, pp. 346, 639 and 640.

26 M. Tramontini, *Synthesis*, (1973) 703.
27 A. Sucharda-Sobczyk and S. Ritter, *Pol. J. Chem.*, 52 (1978) 1555.
28 K. Šlais and Z. Friedl, *Chromatographia*, 33 (1992) 231.
29 H. Rilbe, *Ann. N.Y. Acad. Sci.*, 209 (1973) 11.
30 J.C. Giddings and H. Dahlgren, *Sep. Sci.*, 6 (1971) 345.
31 J.C. Giddings, *Unified Separation Science*, Wiley-Interscience, New York, 1991, p. 180.
32 H. Martinek and P. Wolschann, *Bull. Soc. Chim. Belg.*, 90 (1981) 37.
33 A. Sucharda-Sobczyk and L. Sobczyk, *J. Chem. Res. (S)*, (1985) 208.
34 R.A. Magarian and W.L. Nobles, *J. Pharm. Sci.* 56 (1967) 987.
35 R.C. Weast (Editor), *Handbook of Chemistry and Physics*, CRC Press, Boca Raton, FL, 68th ed., 1987, pp. D-159 and C-699.
36 J.T. Edward and D. Waldron-Edward, *J. Chromatogr.*, 20 (1965) 563.
37 M. Bier, R.A. Mosher and O.A. Palusinski, *J. Chromatogr.*, 211 (1981) 313.
38 J.F.K. Huber, C.A.M. Meijers and J.A.R.J. Hulsman, *Anal. Chem.*, 44 (1972) 111.
39 N.A. Shishkina, K.A. Derstuganova, L.A. Kudryavceva, V.E. Belskii, B.E. Ivanov, *Izv. Akad. Nauk SSR, Ser. Khim.* 25 (1976) 1259.
40 J. Chmelík, K. Šlais, F. Matulík, J. Čáslavská, W. Thormann, presented at *HPLC' 93, 17th International Symposium on Column Liquid Chromatography, Hamburg, May, 1993.*
41 K. Šlais, *J. Microcol. Sep.*, 3 (1991) 191.
42 J. Pospíchal, M. Deml and P. Boček, *J. Chromatogr.*, 638 (1993) 179.
43 A. Leo, C. Hansch and D. Elkins, *Chem. Rev.*, 71 (1971) 525.

Journal of Chromatography A, 661 (1994) 257–264
Elsevier Science B.V., Amsterdam

CHROMSYMP. 2913

Factors affecting the performance of sodium dodecyl sulfate gel-filled capillary electrophoresis

Kiyoshi Tsuji

Control Biotechnology, Pharmaceutical Product Control Division, The Upjohn Company, Kalamazoo, MI 49001 (USA)

ABSTRACT

Effects of factors, such as column temperature, internal column diameter, and column length, on the performance of sodium dodecyl sulfate gel-filled capillary electrophoresis were evaluated for the analysis of protein. Increase of column temperature resulted in exponential decrease of peak efficiency. The maximum performance for a 40 cm × 75 μm I.D. column was obtained at the column temperature of *ca.* 21–24°C. Effect of column temperature on peak migration time was minimal. Increase of the internal column diameter resulted in peak migration time to decrease linearly while theoretical plate decreased exponentially. Linear relationship existed between the length of the capillary column and peak migration time and/or theoretical plates.

INTRODUCTION

Sodium dodecyl sulfate–polyacrylamide slab gel electrophoresis (SDS-PAGE) is an indispensable technique for separation of proteins based on their apparent molecular mass [1]. However, SDS-PAGE represents a collection of labor-intensive and time consuming techniques and quantification by means of an optical scanner is often sub-optimum. High-performance size-exclusion chromatography (HPSEC) is routinely employed to determine the composition of proteins. However, peak resolution capability of HPSEC is not always ideal [2].

Advances in high-performance capillary electrophoresis (HPCE) instrumentation [3–6] have made it possible to exploit potential of SDS gel-filled capillary systems for separation of proteins with promises of rapid and automated analysis with improved reproducibility and quantification. Hjertén [7] was the first to utilize a polyacrylamide gel-filled capillary column to demonstrate separation of a membrane protein. Cohen and Karger [8] applied SDS polyacrylamide gel-filled capillaries for electrophoresis of peptides and proteins. Neither publications presented quantitative data. Tsuji prepared SDS polyacrylamide gel-filled capillary columns and provided data for molecular mass separation and quantification of recombinant proteins [9].

Zhu *et al.* [10] expanded molecular sieving action of non-acrylamide polymers, *e.g.* dextran, methylcellulose, and polyethylene glycol, and used them as additives in the HPCE buffer to facilitate separation of DNA and proteins [11]. Karger *et al.* [12] also examined a branched dextran and a linear polyethylene glycol polymer networks and successfully achieved separation of proteins. Bode demonstrated sieving effect of a linear polyacrylamide for separation of RNA and proteins based on their molecular masses [13,14]. Widhalm *et al.* [15] used a non-derivatized fused-silica capillary column and applied the linear polyacrylamide for electrophoresis of proteins. Since no attempt was made to eliminate the electroosmotic flow, data presented were preliminary. Just recently such non-cross-linked and/or non-polyacrylamide based gel-filled capillary systems became commercially available

SSDI 0021-9673(93)E0879-Y

[16,17]. This paper examines factors affecting performance of such SDS gel-filled capillary electrophoresis systems.

EXPERIMENTAL

Instrumentation

Beckman P/ACE system 2100 high-performance capillary electrophoresis (HPCE) instrument (Beckman, Fullerton, CA, USA) was used.

Non-acrylamide gel-filled capillary system from Beckman [16]. Each analytical run consists of rinsing a coated capillary column (part No. 241521, Beckman; 100 μm I.D. × 375 μm O.D.; effective length, 40 cm) with 1.0 *M* HCl for 2 min and the column was filled with an SDS non-acrylamide gel solution (part No. 241522, Beckman) for 4 min. Use of a coated capillary column is required to eliminate electroendosmosis.

The column temperature was maintained at 20°C by a circulating coolant to minimize band diffusion for effective size separation. An electrophoretic run was conducted at −300 V/cm (24 μA) using the SDS non-acrylamide gel solution (Beckman) as reservoirs at both anode and cathode terminals. About 1 mg protein per ml solution was injected for 60 s under nitrogen pressure (total injection volume, *ca.* 60 nl) onto the SDS non-acrylamide gel-filled capillary column.

SDS gel-filled capillary system from ABI [17]. A bare fused-silica capillary column (75 μm I.D. × 375 μm O.D.; effective length, 40 cm, Polymicro Technologies, Phoenix, AZ, USA) was activated by a 0.1 *M* NaOH solution for 5 min. Analytical run starts by coating the capillary with the SDS gel solution (parts No. 401482, Applied Biosystems, (ABI), Foster City, CA, USA) for 20 min. Since the gel formulation contains a linear polymer of acrylamide [17] to minimize an electroendosmotic flow, use of a specially coated capillary column is not required. After a couple of electrophoretic runs, the capillary was rinsed and regenerated for 5 min with 1 *M* HCl followed by 0.1 *M* NaOH for another 5 min.

The column temperature was maintained at 20°C by a circulating coolant. Each electrophoretic run was conducted at −300 V/cm (37 μA) using the SDS gel solution (ABI) as reservoirs at both anode and cathode terminals. A sample solution containing about 100 μg protein per ml was injected for 40 s under nitrogen pressure (total injection volume, *ca.* 6 nl) onto the SDS gel-filled capillary column.

Peaks migrating in the capillary columns were monitored on-column by UV at 214 nm. The area under the peak was integrated by means of an in-house GC/LC program residing on a VAX mainframe computer and with an electronic integrator (Model 3392A, Hewlett-Packard, Palo Alto, CA, USA).

Reagents

The molecular mass protein standard solution containing hen egg white lysozyme (molecular mass 14 400), soybean trypsin inhibitor (21 500), bovine carbonic anhydrase (31 000), hen egg white ovalbumin (45 000), bovine serum albumin (BSA) (66 200), rabbit muscle phosphorylase *b* (97 400) was obtained from Bio-Rad (No. 161-0304, SDS-PAGE low range molecular mass standard).

Sample buffer solution, containing 1% SDS (Sigma, St. Louis, MO, USA) in 0.12 M Tris–HCl, pH 6.6 (part No. 241525, Beckman), was used to dilute the protein sample. The 2-mercaptoethanol (Sigma) was used to reduce the protein sample.

Preparation of protein samples

Molecular mass protein standard. A 5-μl quantity of the molecular mass protein standard solution (Bio-Rad) was diluted in 40 μl of the sample buffer solution. After through mixing, 2 μl of 2-mercaptoethanol was added and the mixture was heated at 80°C for 5 min.

Protein samples were diluted in the sample buffer solution to approximately 1 mg/ml concentration. To reduce and denature the protein, 2 μl of 2-mercaptoethanol was pipetted into a protein solution. After through mixing, the sample was heated at 80°C for 5 min.

RESULTS AND DISCUSSION

In the presence of SDS, protein forms a SDS–protein complex with a constant SDS–protein ration of 1.4 g/g [1]. Since the SDS gel-filled

capillary system utilizes means to eliminate electroosmotic flow, separation of SDS–protein complexes is strictly based on their size.

Factors affecting performance of SDS gel-filled capillary column

Column temperature. Effects of column temperature on the performance of the SDS gel-filled capillary columns were evaluated using the gel solutions obtained from ABI and Beckman. Effect of column temperature on peak migration time was minimal Fig. 1(I,II). Increase of the column temperature resulted in decrease of the peak migration time of phosphorylase *b*, for example, by approximately $1\%°C^{-1}$ [Fig. 1(I,II)].

Effects of column temperature on the performance/theoretical plate of the gel-filled capillary columns were then evaluated. For the Beckman's system, increase of the column temperature resulted in exponential decrease of theoretical plate (Fig. 2). Theoretical plate of the lysozyme and the carbonic anhydrase peaks, for example, decreased from about 80 000 to 25 000 and about 45 000 to 16 000 by increase of the column temperature from 18 to 30°C, respectively.

According to Jorgenson and Lukacs [19], once thermal equilibrium is established in the capillary, parabolic temperature gradient forms across the radius of the column resulting band broadening. Thus, as the column temperature rises loss of theoretical plates would result. Guttman *et al.* [20] presented a mathematical relationship between the column temperature and efficiency of the Beckman's gel-filled capillary column.

Effects of column temperature on theoretical plate of the ABI's system were complex (Figs. 3 and 4). For a 20 cm × 50 μm I.D. column, increase of the column temperature resulted in slow, yet exponential decrease of theoretical plates (Fig. 3). For example, theoretical plates of the lysozyme peak decreased gradually from about 150 000 to 110 000 by 12°C increase of the column temperature (from 19–33°C.). However, a 40 cm × 75 μm I.D. column behaved differently (Fig. 4). Theoretical plate of the carbonic anhydrase, lysozyme and phosphorylase *b* peaks first increased by increase of the column temperature form 19–20°C, then reached a plateau at the column temperature of *ca.* 21–23°C. This phenomenon, observed with a 40 cm × 75 μm I.D. column, of the theoretical plate to decrease by the decease of the column temperature from 20 to 18°C was confirmed by use of two other columns with the identical dimensions. Explana-

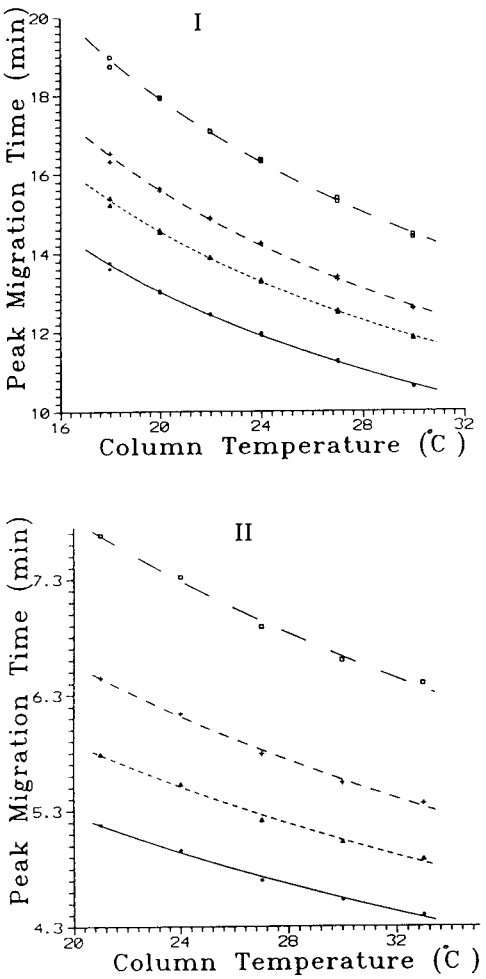

Fig. 1. Effect of column temperature on peak migration of proteins by the SDS gel-filled capillary systems of (I) Beckman and (II) ABI, indicating decrease of peak migration time by increase of column temperature. Conditions: (I) −300 V/cm (24 μA); column temperature: 20°C; effective peak migration distance: 40 cm; coated capillary: 100 μm I.D.; running buffer: SDS non-acrylamide gel solution (Beckman). (II) −300 V/cm (20 μA); column temperature: 30°C; effective peak migration distance: 20 cm; bare fused-silica capillary: 50 μm I.D.; running buffer: SDS gel solution (ABI). □ = Phosphorylase *b*; + = ovalbumin; △ = carbonic anhydrase; ● = lysozyme.

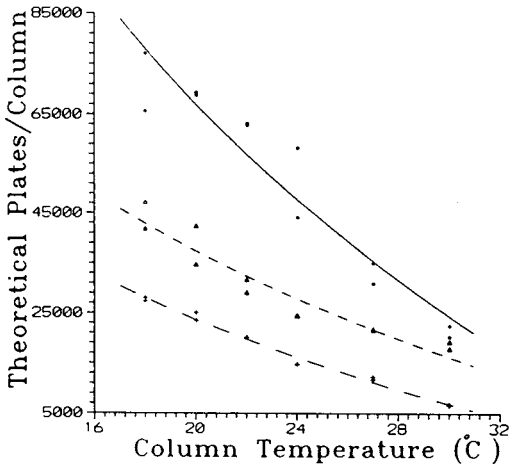

Fig. 2. Effect of column temperature on theoretical plate of the SDS non-acrylamide gel-filled capillary column (coated by Beckman, 40 cm × 100 μm I.D.) indicating exponential decrease of the theoretical plate by the increase of column temperature. Conditions: −300 V/cm (24 μA); column temperature: 20°C; running buffer: SDS non-acrylamide gel solution (Beckman). O = Lysozyme; △ = carbonic anhydrase; + = phosphorylase *b*.

tion on the phenomenon is not possible without knowing the exact composition of the proprietary gel formulation of the ABI.

Increase of the column temperature beyond

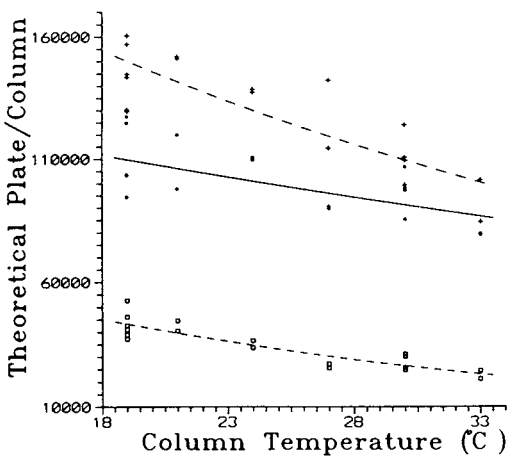

Fig. 3. Effect of column temperature on theoretical plate using a 20 cm × 50 μm bare fused-silica capillary column filled with the SDS gel from ABI indicating gradual decrease of theoretical plate by increase of column temperature. Conditions: −300 V/cm (20 μA); column temperature: 19 to 33°C; running buffer: SDS gel solution (ABI). + = Carbonic anhydrase; O = lysozyme; □ = BSA.

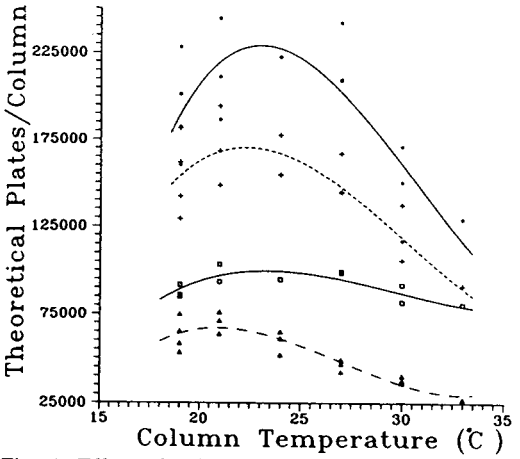

Fig. 4. Effect of column temperature on theoretical plate using a 40 cm × 75 μm bare fused-silica capillary column filled with the SDS gel from ABI indicating the optimum column temperature of 21–23°C for performance of the column. Conditions: −300 V/cm (32 μA); column temperature: 19 to 33°C; running buffer: SDS gel solute (ABI). O = Carbonic anhydrase; + = lysozyme; □ = trypin inhibitor; △ = phosphorylase *b*.

25°C resulted in theoretical plate of these three peaks to decrease from about 225 000 to 125 000, 170 000 to 90 000, and 65 000 to 25 000, respectively (Fig. 4). The BSA peak behaved similarly.

Effect of column temperature on theoretical plate of the trypsin inhibitor peak was minimal (Fig. 3). The trypsin inhibitor used contained two unresolved peaks of nearly equal proportions. Incomplete resolution of peaks resulted in unreliable theoretical plate numbers. Under such circumstances, minor trend of theoretical plates *vs.* column temperature relationship may not be detected.

Guttman *et al.* [20] evaluated influence of column temperature on the dextran and polyethylene oxide based gel-filled capillary systems. They observed that increase of column temperature resulted in decrease of peak efficiency in the polyethylene oxide based gel system while increase of peak efficiency was noted in the dextran based gel.

Evaluation of column diameter and length. Since the gel formulation of ABI contains a linear polymer of acrylamide [17] to minimize an electroendosmotic flow, use of a specially coated capillary column is not required

to separate proteins based on their molecular masses. Thus, the ABI's gel solution was utilized to evaluate effects of column diameter and column length on the performance of the gel-filled capillary columns.

I. Internal column diameter. 20 cm long columns with an internal diameter (I.D.) ranging from 50 to 150 μm (350 μm O.D.) were used to evaluate effect of internal column diameter on performance of the capillary columns. Experiments were conducted at the column temperature of 20°C with the constant electric potential gradient of −300 V/cm.

As shown in Fig. 5(I), increase of the internal column diameter resulted in exponential decrease of theoretical plate. Theoretical plate of the carbonic anhydrase peak, for example, decreased from about 115 000 to 7 000 by increase of the internal column diameter from 50 to 150 μm, respectively.

Loss of peak efficiency by the increase of the internal column diameter may be attributable to the Joule heating. Column radius significantly affects temperature differential within the capillary column, hence on the column performance. Indeed, effect of column radius on temperature differential, ΔT, was expressed by Cohen *et al.* [18] as

$$\Delta T = (0.24\ Wr^2)/(4k)$$

where: W is the generated power ($W = I^2R$), r is radius of the capillary column, and k is thermal conductivity of the medium. Thus, ΔT is a function of r^2. Effect of column diameter on theoretical plate height (H) was given by

$$H = [7 \cdot 10^{-9}\varepsilon_r\varepsilon_0\zeta\lambda^2\varepsilon^2 d_c^6 E^5 c^2]/(D_m\eta K^2)$$

(refer to the ref. 21) where; d_c is a diameter of the capillary, E is an electric potential gradient, and c is the electrolyte concentration. Under the current experimental condition, ε_r, ε_0, ζ, λ, ε, d_c, E, c, D_m, η, and K but not d_c are all constant. Thus, the H is a function of d_c^6. Since $N = 1/H$, N is proportional to $1/d_c^6$. Thus, two equations clearly indicate significant contribution of the column diameter on ΔT and N. For example, when the internal column diameter increases from 50 μm to 100μm, ΔT is expected to increase by 4 times and N decreases by 64 fold.

Although the effects of column diameter on peak migration time was not pronounced, migration time of the carbonic anhydrase peak showed a trend to decrease linearly from 4.8 to 4.2 minutes by increase of the internal diameter from 50 to 150 μm [Fig. 5(II)]. Peak migration time on five other proteins tested, lysozyme, trypsin inhibitor, ovalbumin, BSA, and phosphorylase *b*, behaved similarly.

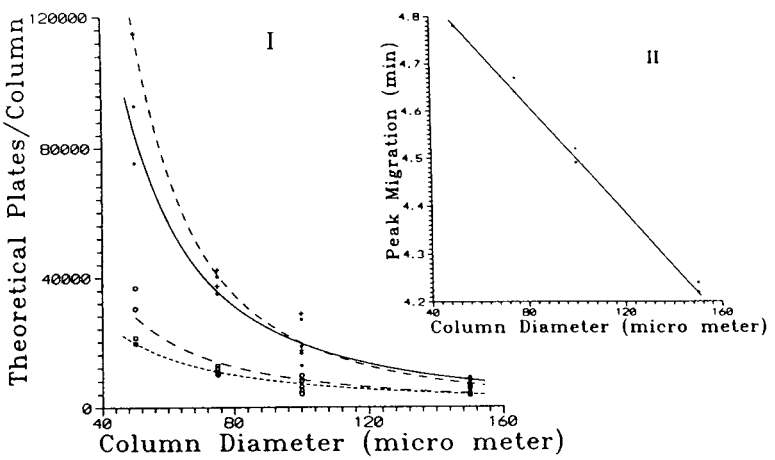

Fig. 5. Effects of column diameter on (I) theoretical plate of the carbonic anhydrase, lysozyme, BSA, and ovalbumin peaks and (II) peak migration time of carbonic anhydrase, using 20 cm long bare fused-silica capillary columns (50 to 150 μm I.D.) filled with the SDS gel from ABI. Conditions: −300 V/cm (*ca.* 20–37 μA); column temperature: 20°C; running buffer: SDS gel solution (ABI). ● = Lysozyme; + = carbonic anhydrase; □ = ovalbumin; ○ = BSA.

Use of a capillary column with an internal diameter smaller than 50 μm would be impractical since it requires longer than 90 min to effectively coat the bare fused-silica capillary column with the gel solution for a successful electrophoretic run.

II. Column length. Experiment was conducted using 75 and 100 μm I.D. columns at the column temperature of 20°C. Electrophoretic run was made at the constant electric potential gradient (E) of −300 V/cm.

For a 100 μm I.D. column, a linear relationship existed between the peak migration time and the column length. Migration time of the phosphorylase *b* peak, for example, increased from about 7 to 28 min by increase of the column length from 20 to 80 cm (Fig. 6). Similar linear relationship between the peak migration time and the column length was observed by the 75 μm I.D. column.

Since the experiment was conducted under the constant electric potential gradient (E) of −300 V/cm ($E = V/L$), the equation of Jorgenson and Lukacs [22] for the expression of peak migration time t_m of

$$t_m = L^2/(V\mu)$$

becomes

$$t_m = L/(E\mu)$$

where: t_m is the solute migration time, L is the column length, V is the voltage, and μ is the solute mobility. Thus, under the current experimental conditions, the relationship between the peak migration time and the column length is linear.

Relationship between the theoretical plate and the length of the column has been expressed as

$$N = (L\mu)/2D_m$$

(refer to ref. 21) where: L is the column length, μ is the solute mobility, and D_m is the diffusion coefficient. Under the current experimental conditions, both μ and D_m are constant. Thus, existence of a linear relationship between the theoretical plate and the column length is indicated. Indeed, for a 75 μm I.D. column, theoretical plates of protein peaks increased linearly by increase of the column length (Fig. 7); theoret-

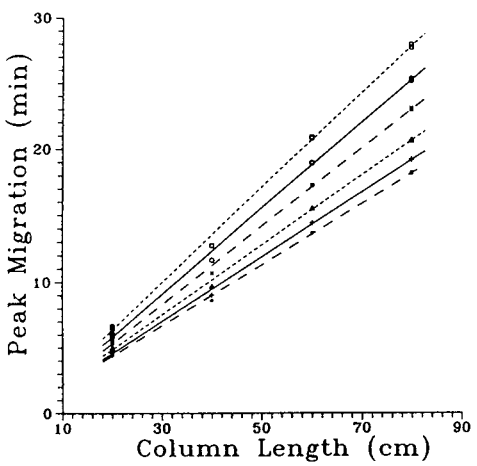

Fig. 6. Effect of column length on peak migration time of proteins using 100 μm I.D. bare fused-silica capillary columns filled with the SDS gel from ABI indicating existence of a linear relationship between the column length and the peak migration time. Conditions: −300 V/cm (20 μA); column temperature: 20°C; effective peak migration distance: 20 to 80 cm; running buffer: SDS gel solution (ABI). □ = Phosphorylase *b*; ○ = BSA; × = ovalbumin; △ = carbonic anhydrase; + = trypsin inhibitor; ● = lysozyme.

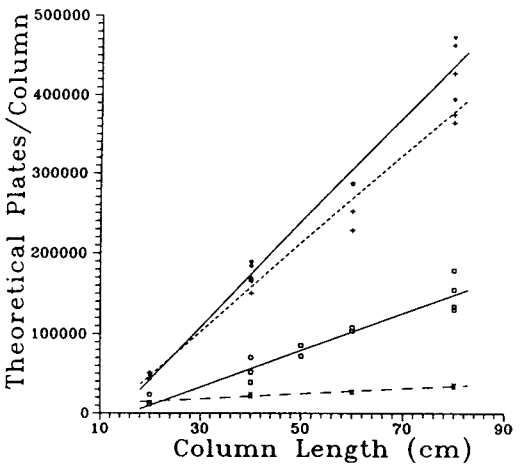

Fig. 7. Effect of column length on theoretical plate numbers of carbonic anhydrase, lysozyme, phosphorylase *b*, and ovalbumin peaks using 75 μm I.D. bare fused-silica capillary columns filled with the SDS gel from ABI indicating existence of a linear relationship between the column length and theoretical plates. Conditions: −300 V/cm (37 μA); column temperature: 20°C; effective peak migration distance: 20 to 80 cm; running buffer: SDS gel solution (ABI). * = Carbonic anhydrase; + = lysozyme; □ = phosphorylase *b*; × = ovalbumin.

ical plates of the carbonic anhydrase peak, for example, increased from about 50 000 to 440 000 by increase of the column length from 20 to 80 cm. However, increase of the theoretical plate was non-linear by use of various lengths of the 100 μm I.D. column (Fig. 8). Increase of theoretical plates of the lysozyme, trypsin inhibitor, and ovalbumin peaks reached a plateau at the column length of *ca.* 60–70 cm (Fig. 8). Non-linear relationship between the theoretical plates and the column length observed for the 100 μm I.D. column may be due to increased Joule heating.

Rs is a factor that is also expected to increase by increase of the column length. *Rs* is given by

$$Rs = 0.177(\mu_1 - \mu_2)[V/(D\mu_{av})]^{1/2}$$

(refer to the ref. 19). Since $E = V/L$, *Rs* can be expressed as

$$Rs = 0.177(\mu_1 - \mu_2)[EL)/(D\mu_{av})]^{1/2}$$

where: μ_1 and μ_2 are mobility and μ_{av} an average mobility of the 2 solutes 1 and 2, V is voltage, and D is the diffusion coefficient. The μ can be expressed as

$$\mu = (\varepsilon\zeta)/\eta$$

(refer to ref. 20) where: ε, ζ, and η are dielectric constant of the medium, zeta potential, and viscosity of the medium, respectively. Under the current experimental conditions, μ, E, and D are constant. Thus, *Rs* is a function of the square root of L. The *Rs* between the carbonic anhydrase and the ovalbumin peaks, obtained by use of a 20, 40, 60 and 80 cm long, 75 μm I.D., columns at the column temperature of 20°C, were 3.65, 5.73, 6.44, and 7.30, respectively. Indeed, these *Rs* values are in close agreement (correlation coefficient: 0.98) with those of 3.65, 5.16, 6.32 and 7.43, predicted form the equation.

Use of a 40 cm × 50 μm I.D. column was also attempted. However, in spite of over 90 min of the column coating operation, no migration of protein peak was detected. As the inner column surface increases, operation to effectively coat the bare fused-silica capillary column by use of the gel-solution from ABI became progressively difficult.

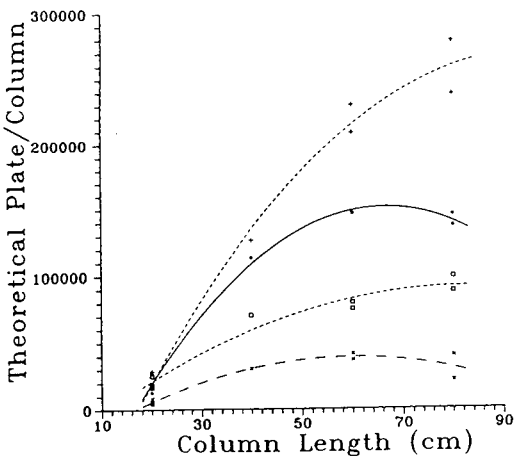

Fig. 8. Effect of column length on theoretical plates of the carbonic anhydrase, lysozyme, trypsin inhibitor, and ovalbumin peaks using 100 μm I.D. bare fused-silica capillary columns filled with the SDS gel from ABI indicating that theoretical plate number reaches a plateau at the column length of *ca.* 60–70 cm due to the Joule heating. Conditions: −300 V/cm (20 μA); column temperature: 20°C; effective peak migration distance: 20 to 80 cm; running buffer: SDS gel solution (ABI). + = Carbonic anhydrase; ● = lysozyme; □ = trypsin inhibitor; × = ovalbumin.

Practical consideration

In order for any assay method to be adopted by the pharmaceutical quality control laboratories, the method must improve quality of the assay results (*e.g.* precision and accuracy of the molecular mass determination) and/or productivity of the laboratory operation (*e.g.* speed and ease of the assay).

At the column temperature of 20°C, peak migration time of phosphorylase *b* (the largest molecular mass among the proteins examined) was approximately 8, 16, and 16 min for 20 cm × 50 μm I.D., 40 cm × 75 μm I.D., and 40 cm × 100 μm I.D. columns, respectively. It took about 40, 20, and 20 min to effectively coat these bare fused-silica capillary columns with the gel solution. After a couple of assay operations, the capillary column must be stripped and regenerated with HCl and NaOH solutions. Thus, cumulatively, each one assay operation took approximately 60, 45, and 45 min by these three columns, respectively.

Theoretical plate numbers of approximately

90 000, 1650 000, and 80 000 for the lysozyme peak were obtained by use of 20 cm × 50 μm I.D., 40 cm × 75 μm I.D., and 40 cm × 100 μm I.D. columns, respectively. Theoretical plates of the carbonic anhydrase peak were about 115 000, 450 000, and 250 000 for these three columns, respectively. Thus, the 40 cm × 75 μm I.D. column consistently outperformed the other two columns examined. The 75 μm I.D. column also gave a reasonable assay operation time and thus would be the SDS gel-filled column of choice for the assay of proteins. If critical analysis of a protein sample is required and one can afford a longer analysis time, then use of a longer capillary column to obtain an additional resolution may be justified. Development of a mathematical model to optimize column parameters, such as temperature, diameter, and length for the performance of the gel-filled capillary column is being contemplated.

ACKNOWLEDGEMENTS

Assistance of Devon K. Andres, a student intern from Western Michigan University, Kalamazoo, MI, is greatly acknowledged.

REFERENCES

1 F.M. Ausubel, R. Brent, R.E. Kingston, D.D. Moore, J.G. Seidman, J.A. Smith and K. Struhl (Editors), *Current Protocols in Molecular Biology*, Wiley, New York, 1990, p. 10.0.5.
2 Y. Kato, *LC · GC*, 9 (1983) 540.
3 R.A. Wallingford and A.G. Ewing, *Adv. Chromatogr.*, 29 (1989) 1.
4 F.E.P. Mikkers, F.M. Everaerts and Th. P.E.M. Verheggen, *J. Chromatogr.*, 169 (1979) 11.
5 J.W. Jorgenson and K.D. Lukacs, *Science*, 222 (1983) 266.
6 B.L. Karger, A.S. Cohen and A. Guttman, *J. Chromatogr.*, 492 (1989) 585.
7 S. Hjertén, in Hirai (Editor), *Electrophoresis '83*, Walter de Gruyter, New York, 1984, p. 71.
8 A.S. Cohen and B.L. Karger, *J. Chromatogr.*, 397 (1987) 409.
9 K. Tsuji, *J. Chromatogr.*, 550 (1991) 823.
10 M. Zhu, D.L. Hansen, S. Burd and F. Gannon, *J. Chromatogr.*, 480 (1989) 311.
11 H.-J. Bode, *FEBS Lett.*, 65 (1976) 56.
12 K. Ganzler, K.S. Greve, A.S. Cohen and B.L. Karger, *Anal. Chem.*, 64 (1992) 2665.
13 H.-J. Bode, *Anal. Chem.*, 83 (1977) 204.
14 H.-J. Bode, *Anal. Chem.*, 83 (1977) 364.
15 A. Widhalm, C. Schwer, D. Blaas and E. Kenndler, *J. Chromatogr.*, 549 (1991) 446.
16 A. Guttman, J.A. Nolan and N. Cooke, *J. Chromatogr.*, 632 (1993) 171.
17 W.E. Werner, D.M. Demorest, J. Stevens and J.E. Wiktorowicz, *Anal. Biochem.*, 212 (1993) 253.
18 A.S. Cohen, A. Paulus and B.L. Karger, *Chromatographia*, 24 (1987) 15.
19 J.W. Jorgenson and K.D. Lukacs, *Anal. Chem.*, 53 (1981) 1298.
20 A. Guttman, J. Horvath and N. Cooke, *Fifth International Symposium on High Performance Capillary Electrophoresis (HPCE '93), Orlando, FL, January 26, 1993*, p. 55.
21 J.H. Knox and I.H. Grant, *Chromatographia*, 24 (1987) 135.
22 J.W. Jorgenson and K.D. Lukacs, *J. Chromatogr.*, 218 (1981) 209.

Journal of Chromatography A, 661 (1994) 265–278
Elsevier Science B.V., Amsterdam

CHROMSYMP. 2894

Numerical algorithms for capillary electrophoresis

Sergey V. Ermakov[☆] Michael S. Bello[☆☆] and Pier Giorgio Righetti*

Faculty of Pharmacy and Department of Biomedical Sciences and Technologies University of Milano, Via Celoria 2, Milan 20133 (Italy)

ABSTRACT

Three groups of algorithms applied to mass transport equations in electrokinetic processes are described and compared. They are used for solving a set of partial differential equations expressing the conservation of mass and charge laws, the dissociation equilibria and electroneutrality. These equations should be able to predict the shape and structure of the boundaries and peak diffusion and anomalies as the analytes are driven in the electric field past the detector port. Three different numerical algorithms have been proposed: by Mosher *et al.* (*The Dynamics of Electrophoresis*, VCH, Weinheim, 1992), by Dose and Guiochon [*Anal. Chem.*, 63 (1991) 1063–1072] and by Ermakov *et al.* [*Electrophoresis*, 13 (1992) 838–848]. The first two algorithms offer numerical solutions which can only be implemented at unrealistically low current densities, two to three orders of magnitude lower than normally adopted in practical electrophoresis. When applied to real experimental conditions, both previous algorithms break down: the separated analyte zones, as obtained by simulation, decay into several solitary waves (solitons), resulting from the action of numerical dispersion. In contrast, the numerical algorithms proposed by Ermakov *et al.* still allow the prediction of peaks of with the correct shape, with only minor non-physical spikes.

INTRODUCTION

Progress in theoretical studies of electrophoresis processes nowadays depend more and more on computer simulations, because only with the help of a computer can one move forward in solving the set of numerical non-linear electrophoresis equations. Only a few simplified limiting cases of these equations could be solved analytically. The alternative to an analytical solution for complex equations is a numerical solution with the help of a computer which allows one to model a practical process governed by non-linear partial differential equations (PDEs). Computer simulations are able to help an experimenter to investigate the effects of the ion mobilities, pH and other parameters on the results of the separation run and/or to optimize the analysis conditions.

In the field of electrophoresis, numerical modelling was commenced by Bier's group about 10 years ago. An extensive review of what has been done since then with relevant references can be found in a recently published book by Mosher *et al.* [1]. Previous work demonstrated that all types of electrophoresis are governed by the same set of PDEs expressing the conservation laws of mass and charge, dissociation equilibria and electroneutrality. Examples of modelling give good qualitative agreement with experiments for different modes of electrophoresis.

Nevertheless, there is still a gap between numerical modelling and experiments. In order to bridge the gap and make numerical modelling a useful tool for a practitioner (as it is in fluid dynamics, heat transfer and some other fields), one has to be convinced that the results of

* Corresponding author.
☆ Permanent address: Keldysh Institute of Applied Mathematics, Russian Academy of Sciences, Miusskaya Sq. 4, Moscow 125047, Russian Federation.
☆☆ Permanent address: Institute of Macromolecular Compounds, Russian Academy of Sciences, Bolshoi 31, St. Petersburg 199004, Russian Federation.

0021-9673/94/$07.00
SSDI 0021-9673(93)E0827-H

modelling are in agreement with those given by real experiments. Today, most of the papers dealing with numerical solutions of electrophoresis equations present solely calculated concentration, pH and conductivity profiles *along the column axis* or, in the best case, compare them with *time dependences* of a UV sensor signal. Hence quantitative comparison of the experimental and calculated results is impossible and, usually, is not the goal of such simulations. However, as has been pointed out in a review [2] of the book by Mosher *et al.* [1], "Quantitative evidence, *e.g.*, simulated and experimental results side by side with a graphical output format that uses the same coordinate system..." is desirable. We believe that the aforesaid describes not only what the particular book lacks but what the whole field of numerical modelling in electrophoresis is missing.

Numerical algorithms help only if they are very carefully elaborated and adjusted to the equations they are supposed to solve. This is well known in fluid mechanics where the development of new algorithms and numerical modelling has become a separate scientific field called "computational fluid dynamics". Electrophoresis equations are very similar to those of fluid dynamics and, therefore, most of the problems encountered there might be expected to appear in numerical simulations of electrophoresis processes. The main difficulty in a numerical solution of electrophoresis equations arises from a solution for the unsteady (*i.e.*, time-dependent) mass transport equations when they describe moving zones with sharp non-uniformities of concentrations, velocities, temperature, etc., similar to shock waves in gas dynamics.

There are several approaches for a numerical solution of electrophoresis equations based on finite-difference techniques [1,3–13]. All algorithms applied to the mass transport equations in electrophoresis simulations may be divided into three groups: that used in refs. 1 and 4–6, that used in refs. 3 and 7–10 and that used in refs. 13 and 14. The first two groups [1,3–10] use similar methods for representing space derivatives in the transport equation and differ mostly in the method of temporal discretization. The algorithms used there under certain circumstances give solutions with spurious oscillations (see ref. 1, p. 58, and ref. 3). In order to avoid these oscillations and numerical instabilities, one is forced either to use high-speed computers [3] or to simulate separations at current densities more than two orders of magnitude less than experimental current densities [4]. In the first case these algorithms cannot be used on the personal computers usually provided with a capillary electrophoresis unit. In the second case, a prediction made for current densities two orders of magnitude less than those routinely adopted experimentally can hardly be interpreted as being quantitative.

In an attempt to improve numerical methods for unsteady electrophoresis equations, a high-resolution finite-difference algorithm based on a finite-difference scheme with artificial dispersion [11] has recently been developed by Ermakov *et al.* [12,13]. This algorithm was successfully applied to the simulation of capillary zone electrophoresis (CZE) and capillary isotachophoresis (ITP) [14], where it showed its ability to resolve sharp isotachophoretic boundaries and demonstrated excellent agreement with exact analytical results [15]. The algorithm [13] has been extended to multi-dimensional simulations, particularly to column electrophoresis, where two-dimensional sample evolution was studied [16].

This paper aims at testing and comparing the different numerical algorithms, particularly the properties of finite-difference schemes used for the solution of mass transport equations. All three numerical schemes, used for electrophoretic simulations, are implemented and applied to electrophoretic problems having explicit analytical solutions. This approach shows drawbacks inherent in specific numerical methods. Examples of simulations for CZE and ITP runs allow one to compare three numerical algorithms. The results of these numerical experiments exhibit limits of validities for these schemes and thus shed light on their applicability to real electrophoresis problems. The results of simulations are presented in the same form as seen by an experimenter, namely as dependences of concentration *versus* time for parameters of simulations corresponding to normal experimental conditions.

This is not the only approach we have adopted in bringing computer science into the realm of electrophoresis. In a recent development, Bello *et al.* [17] proposed a computer program able to predict buffer temperature and electric current in CZE as a function of capillary diameter, type of cooling device, buffer conductivity and applied voltage gradient. This program calculates with high precision the temperature inside the capillary, and can thus predict mobility shifts of analytes run with different voltage gradients. Given that today a number of CZE units are laboratory made and lack forced liquid cooling, this program should enable the experimenter to program precisely the temperature at which to perform a separation. This parameter is of utmost importance in, *e.g.*, micellar electrokinetic chromatography (since the partition coefficient of the analyte is strongly temperature dependent) [18] and in DNA separations, for runs below or above the melting point of double-stranded DNAs [19]. In yet another approach, we have applied computer science to the optimization of pH gradients to be adopted in isoelectric focusing separations with insolubilized buffers and titrants [20]. This program, developed over a 10-year period [21], allows the modelling of linear and non-linear (convex and concave exponentials, sigmoidal) gradients utilizing mixtures of up to 50 buffers and titrants. Its use in single- and two-dimensional separations of protein mixtures is now routine and its use has been instrumental in novel findings in, *e.g.*, molecular biology, biochemistry and human pathology [22]. This program is now being introduced into chromatographic science for separations performed under non-isocratic conditions.

THEORY

All modes of electrophoresis are governed by the general set of PDEs including mass transport equations for all components of the solution, the equation of charge conservation, the equation of electroneutrality and algebraic equations of ionic equilibria [1]. These equations form the basis for a general theoretical treatment of electrophoresis and the starting point for numerical simulations in particular. For the solution containing monovalent weak acids and bases the equations are reported in Appendix A. Further, we restrict ourself to capillary electrophoresis and particularly to CZE and ITP. This section presents known analytical solutions for mass transport PDE, which are further used as reference patterns for comparing different numerical methods. Numerical methods for mass transport equations used for electrophoresis simulations are also described.

Analytical solutions to unsteady mass transport equations in electrophoresis

Only in a few limiting cases are analytical solutions for these equations known. Here we mention two of them for zone electrophoresis:

(1) Sample zones migrate with constant velocities determined by their electrophoretic mobilities and do not interact either with each other or with the buffer. The mass transport equation is linear and the well known solution in this instance for the sample introduced as an infinitely narrow band is the Gaussian peak migrating with constant velocity in the direction parallel to the direction of applied electric field, *i.e.*, along the capillary axis.

(2) A sample zone changes the electric conductivity of the background electrolyte σ_0, but not its pH, and migrates without diffusion. The conductivity σ in the sample zone is linearly dependent on the concentration of the sample C according to $\sigma = \sigma_0(1 - \alpha C)$, where α is a proportionality coefficient. Both sample and buffer are uni–univalent electrolytes (see Refs. 23 and 24 and references cited therein). The analytical solution is a discontinuous function.

In both instances the concentration of the sample constituent is governed by the mass transport equation [23];

$$\frac{\partial C}{\partial t} + \frac{\partial (uC)}{\partial x} = D \cdot \frac{\partial^2 C}{\partial x^2} \tag{1}$$

$$u = u_0/(1 - \alpha C) \tag{2}$$

where u_0 is the migration velocity at the sample infinite dilution, x is the axis coordinate along the capillary, t is time and D is the diffusion coefficient.

The first case of a linear equation can be obtained from eqns. 1 and 2 by setting $\alpha = 0$ in eqn. 2, whereas the equation for the second case corresponds to $\alpha \neq 0$, $D = 0$.

It is convenient to take analytical solutions for eqn. 1 corresponding to particular forms of initial conditions: to the form of a Gaussian peak of unit height in the first case and to the form of a rectangular pulse of a height C_0 in the second case. The initial conditions are shown graphically in Fig. 1 and are represented by the following equations:

$$C(x, 0) = \exp\left[-\frac{(x - x_0)^2}{2\sigma_0^2}\right] \tag{3}$$

and

$$C(x, 0) = C_0,\ 0 \leq x \leq \Delta l \text{ and } C(x, 0) = 0,\quad x > \Delta l,\ x < 0 \tag{4}$$

where x_0 is the initial peak position, σ_0 is its initial dispersion, Δl is the initial width of the rectangular pulse and C_0 is the initial concentration in the pulse.

Assuming that the capillary is infinite, then the boundary conditions for eqn. 1 are the conditions at infinity and are given by

$$C(\pm\infty, t) = 0 \tag{5}$$

The analytical solution to eqn. 1 with the initial condition of eqn. 3 and the boundary condition of eqn. 5 is given by

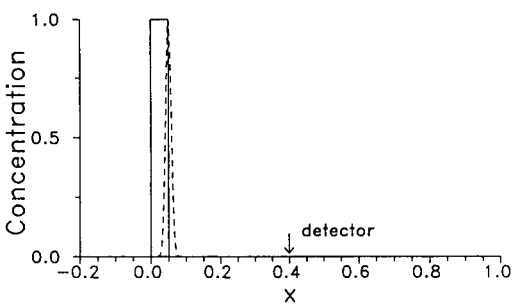

Fig. 1. Initial concentration profiles for model electrophoresis problems. The dashed line gives the profile for the linear equation ($\alpha = 0$) and the solid line gives that for the non-linear equation ($\alpha \neq 0$); detection point $x_d = 0.4$.

$$C(x_d, t) = \frac{A}{\sqrt{4\pi D(t^* + t)}} \exp\left[\frac{-(x_d - x_0 - ut)^2}{4D(t^* + t)}\right] \tag{6}$$

$$t^* = \frac{A^2}{4\pi D},\ A = \int_{-\infty}^{+\infty} C(x, t)\,dx = \sqrt{2\pi}\sigma_0$$

where x_d is the coordinate of the detection point. Eqn. 6 gives the concentration at the detection point as a function of time.

The second type of solution for eqns. 1 and 2 in a non-diffusional, non-linear case ($\alpha \neq 0$ and $D = 0$) with the initial condition of eqn. 4 is given by

(1) $\alpha < 0$:

$$C(x_d, t) = \left\{\begin{array}{ll} \frac{1}{\alpha}\left(1 - \sqrt{\frac{u_0 t}{x_d - \Delta l}}\right), & t_{min} < t < t_{max} \\ 0, & t < t_{min} \text{ or } t > t_{max} \end{array}\right\} \tag{7}$$

$$t_{min} = \frac{x_d - \Delta l}{u_0}$$

$$t_{max} = \frac{1}{u_0}\left(\sqrt{|\alpha|\Delta l\, C_0} + \sqrt{x_d - \Delta l}\right)^2$$

(2) $\alpha > 0$:

$$C(x_d, t) = \left\{\begin{array}{ll} \frac{1}{\alpha}\left(1 - \sqrt{\frac{u_0 t}{x_d}}\right), & t_{min} < t < t_{max} \\ 0, & t < t_{min} \text{ or } t > t_{max} \end{array}\right\} \tag{8}$$

$$t_{min} = \frac{1}{u_0}\left(\sqrt{\alpha\, \Delta l\, C_0} - \sqrt{x_d}\right)^2$$

$$t_{max} = x_d / u_0$$

where t_{min} and t_{max} are the moments when the zone appears and disappears at the detection point. Eqns. 7 and 8 are obtained from eqns. 10 and 14 in ref. 23, and their validity has the same limits as those of ref. 23.

The analytical solutions presented above are important for understanding diffusion (case 1) and electrochemical broadening (case 2) in zone electrophoresis. However, they describe only the

simplest possible cases and fail when applied, *e.g.*, to the case when both electrochemical and diffusion broadening are significant. The way to simulate complex behavior is to apply numerical methods to the electrophoresis equations.

Numerical solutions

The process of numerical solution usually includes two major stages. During the first, it is necessary to reduce the set of PDEs, derived in terms of infinitely small increments for continuous variables, to their discrete analogues as a set of finite-difference equations. The second stage assumes the choice of a numerical method for solving the large number of linear or non-linear algebraic equations, resulting from the previous stage of discretization. The final result and the quality of numerical solution depend on both stages. However, most of the work on computer simulation of electrophoresis [3,5,9,10] in the sections devoted to numerical algorithms pay attention mainly to the second stage of a solution process. In their considerations they are restricted to the problem of numerical stability of the algorithm [3,5], its computational efficiency [5,9] or the organization of calculations [7]. However, as has been shown [13], it is also very important to analyse theoretically the stage of discretization, accounting for the specifics of the governing equations. In this paper we demonstrate how the appropriate choice of a finite-difference scheme for the mass transport equation may significantly improve the quality of a solution and, hence, fulfil simulations more efficiently and for a much wider range of experimental parameters.

The characteristic feature of electrophoresis simulations is the necessity to solve numerically the set of non-stationary mass transfer equations similar to eqn. 1, which are PDEs with a small parameter D multiplying the second derivative (indeed, it is more correct to consider as a small parameter the combination $\tilde{D} = D/UL$, where U and L are the velocity and the linear dimension scales, respectively). This is a difficult task even for problems with one space dimension because, as has been pointed out [13], one should use a finite-difference grid with very small space increments to avoid some negative effects of a purely computational nature. These effects originate from discretization of PDEs when one replaces eqn. 1 with its discrete analogue, *i.e.*, finite-difference scheme. Discretization includes the introduction of a finite-difference grid with space step h and time step τ instead of continuous space and time variables and projection of all functions on the nodes of the grid (for details and notation, see Appendix B). One of the crucial points here is how to approximate the convective term $\partial(uC)/\partial x$. The two simplest and most commonly used approaches are the "upwind" difference and central difference approximations. The approximation with "upwind" difference gives the finite-difference scheme with an approximation error proportional to the first power of space step h [25]. The effects of numerical diffusion, which often is much greater than the physical diffusion (especially for small $\tilde{D}$), is inherent in such schemes. This numerical diffusion could entirely obscure the physical results, which has been demonstrated for ITP separations [13]. The finite-difference schemes used by most workers [3,5,9,10] approximate the convective term by a central difference, having an error of approximation proportional to the second order of h. These schemes are free from numerical diffusion, but they give spurious oscillations in the regions with sharp gradients if the space step h in a finite-difference grid is not small enough. It has been shown [13] that the oscillations are associated with the dispersion, introduced by the discretization.

The origin of these two non-physical effects (numerical diffusion and numerical dispersion) lies in the discretization stage, so they cannot be eliminated in the stage of solution of finite-difference equations. Theoretically, to reduce their negative influence, it is necessary to use a finite-difference grid with space steps h much less than $\tilde{D}$, but in practice it is often sufficient to use $h \sim \tilde{D}$. However, for very small $\tilde{D}$ values this restriction on h becomes too severe. In order to overcome it, a special finite-difference scheme with artificial dispersion was developed for electrophoresis problems [13]. It allows one to solve eqn. 1 accurately using the finite-difference grid with $h \sim \sqrt{\tilde{D}}$, which considerably reduces the calculation effort.

In our simulations we compare three basic finite-difference algorithms. In the first, similar to those used by others [3,9,10], the convective term is approximated in eqn. 1 by a central difference equation and the diffusive term with the usual three-point equation. In the second algorithm [1,5], the convective term is approximated as in the previous case, but the diffusive term is replaced with a five-point equation. The third algorithm implements the finite-difference scheme with artificial dispersion as reported in ref. 13. All these algorithms are described in Appendix B and denoted as B1, B2 and B3, respectively. As mentioned above, the numerical algorithm is determined by (i) the stage of discretization and, particularly, the space discretization, and (ii) the solution method for ordinary differential equations resulting from space discretization or, if the temporal discretization leads to a set of algebraic equations, the solutions method for algebraic equations. As it was difficult to establish exactly what method was used in previous work [3,5,7,9,10], we chose the Euler method for integration of the set of ordinary differential equations with temporal derivative (finite-difference scheme B1) and the Runge–Kutta method for integration of the set of ordinary differential equations with temporal derivative (algorithm B2). The set of linear equations resulting from discretization by the finite-difference scheme B3 was solved by the Gauss exclusion algorithm. In this paper we do not compare these calculation methods, as our aim was to study the advantages of finite-difference schemes. Therefore, the results presented here reflect the quality of a finite-difference scheme, or more exactly its space discretization. It should be pointed out that the algorithms considered differ only in this respect. All other parts, including the solution of the non-linear algebraic equation of electroneutrality, were the same in all three.

The properties of the three algorithms were compared by solving model electrophoresis problems described above, which admit exact analytical solutions. They were also applied to simulation of two-component sample separations by means of CZE and ITP.

EQUIPMENT

All calculations were performed on an IBM PS/2 Model 70 386 computer. Computer programs were written in Microsoft FORTRAN Version 5.1. Figures were drawn by using GRAPHER (Golden Software).

RESULTS AND DISCUSSION

During the first series of simulations, three finite-difference schemes, B1, B2 and B3, were applied to eqn. 1 governing translation and diffusion of an initial pulse (eqn. 3) along the x-axis with a constant dimensionless velocity $u_0 = 1$. Three dimensionless diffusion coefficients were used for simulations: $\tilde{D} = 2 \cdot 10^{-5}$, $\tilde{D} = 1 \cdot 10^{-4}$ and $\tilde{D} = 1 \cdot 10^{-3}$. The first case might correspond to the electrophoretic run of a sample with a diffusion coefficient of $2 \cdot 10^{-5}$ cm^2 s^{-1} in a capillary of length 50 cm and a migration time from end to end of 42 min. The second case corresponds to a five times longer migration time of the same sample, *i.e.*, *ca.* 3.5 h. The detection point was at $x_d = 0.4$. The initial distribution of concentration was given by a Gaussian peak (eqn. 3), positioned at $x_0 = 0.05$ and having unit height and mass $A = 0.02$. All simulations were performed with the spatial increments being equal to $h = 2 \cdot 10^{-3}$. Temporal increments were found from the condition of stability and were equal to $\tau = 1 \cdot 10^{-3}$ for schemes B2 and B3 and $\tau = 1 \cdot 10^{-4}$ for scheme B1. The data on space and time increments on this and all subsequent simulations are summarized in Table I.

Figs. 2 and 3 compare the three numerical results with the exact analytical solution (eqn. 6) for the two diffusion coefficients $\tilde{D} = 2 \cdot 10^{-5}$ and $\tilde{D} = 1 \cdot 10^{-4}$, respectively. The numerical electropherograms are shown by solid lines and the analytical solutions by dashed lines. For the first case, Fig. 2A and B show large-amplitude oscillations of numerical electropherograms, obtained by algorithms B1 and B2, whereas scheme B3 gives a non-oscillating solution (Fig. 2C) that agrees well with the exact analytical solution. In both instances $\tilde{D} \ll h$, but $h \geq \sqrt{\tilde{D}}$. In addition to the absence of oscillations, another advantage

TABLE I

FINITE-DIFFERENCE GRID PARAMETERS USED FOR CALCULATIONS

The space increment in all simulations was $h = 2 \cdot 10^{-3}$.

Algorithm	Time step, τ	Parameter $\tilde{D}$	Parameter α or separation technique	Fig.
B1	10^{-4}			2A
B2	10^{-3}	$2 \cdot 10^{-5}$	0	2B
B3	10^{-3}			2C
B1	10^{-4}			3A
B2	10^{-3}	$1 \cdot 10^{-4}$	0	3B
B3	10^{-3}			3C
B1	$5 \cdot 10^{-5}$			4A
B2	10^{-3}	$2 \cdot 10^{-5}$	−0.5	4B
B3	10^{-3}			4C
B1	10^{-5}			5A
B2	10^{-4}	$1 \cdot 10^{-4}$	0.3	5B
B3	$5 \cdot 10^{-4}$			5C
B1	$5 \cdot 10^{-5}$			6A
B2	$2.5 \cdot 10^{-4}$	$(1.46–2.52) \cdot 10^{-3}$	ITP	6B
B3	$2.5 \cdot 10^{-4}$			6C
B1	Unstable			–
B2	$2.5 \cdot 10^{-4}$	$(3.65–6.3) \cdot 10^{-4}$	ITP	7A
B3	$2.5 \cdot 10^{-4}$			7B
B1	Unstable			–
B2	Unstable			–
B3	$2.5 \cdot 10^{-4}$	$(1.46–2.52) \cdot 10^{-5}$	ITP	–
B1	$5 \cdot 10^{-5}$			8A
B2	$2 \cdot 10^{-3}$	$(2.93–5.16) \cdot 10^{-5}$	CZE	8B
B3	$2 \cdot 10^{-3}$			8C
B1	Unstable			–
B2	$2 \cdot 10^{-3}$	$(2.93–5.16) \cdot 10^{-6}$	CZE	9A
B3	$2 \cdot 10^{-3}$			9B

of the numerical solution given by scheme B3 is that it gives the least error in the peak position and the peak width. Fig. 3 shows that for higher diffusion coefficients the numerical oscillations become smaller. Nevertheless, algorithms B1 and B2 still produce numerical oscillations and asymmetric peaks, although the discrepancy between the analytical and numerical solutions is much less than in Fig. 2. For larger diffusion coefficients, the deviations of numerical solutions from the analytical solution become less and for $D = 1 \cdot 10^{-3}$, when $\tilde{D} \approx h$, all three algorithms give excellent agreement with the analytical solution. However, this value of the dimensionless diffusion coefficient corresponds to a migration time of *ca.* 35 h and can hardly be considered as realistic.

Figs. 4 and 5 give examples of the calculation of an electrophoresis run by using the three finite-difference algorithms, when a sample interacts with the background electrolyte, $\alpha \neq 0$ and the velocity is not constant. The initial condition

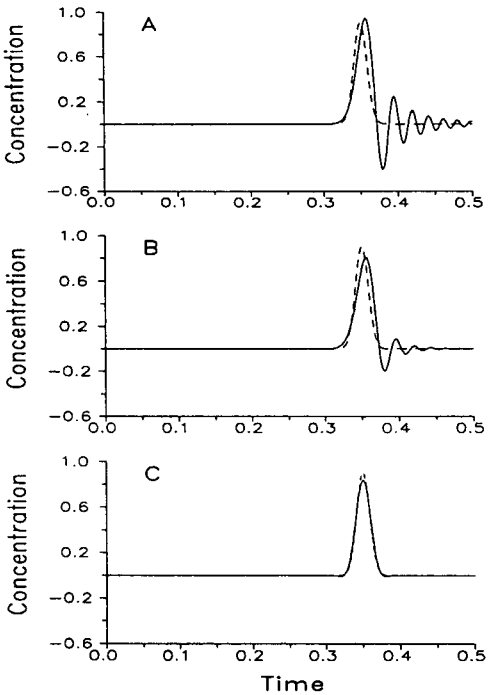

Fig. 2. Electropherograms for linear equation ($\alpha = 0$) calculated by three different finite-difference algorithms. Dimensionless diffusion coefficient $\tilde{D} = 2 \cdot 10^{-5}$. Here and also in Figs. 3–5 simulated results are plotted as solid lines and analytical results as dashed lines. Panels A, B and C represent the results obtained using finite-difference algorithms B1, B2 and B3, respectively. Concentration and time are measured in units of the maximal initial concentration and total migration time (L/u_0), respectively, with L being the length of the capillary.

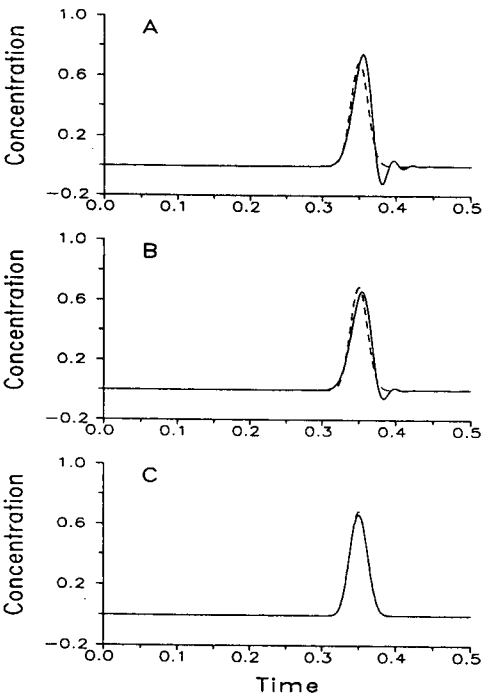

Fig. 3. Electropherograms for linear equation ($\alpha = 0$). Dimensionless diffusion coefficient $\tilde{D} = 1 \cdot 10^{-4}$. Other details as in Fig. 2.

was a rectangular pulse (see Fig. 1) of unit height and width equal to 0.05 starting at $x = 0$. Numerical results are compared in Fig. 4 for $\alpha = -0.5$ and in Fig. 5 for $\alpha = 0.3$ with analytical diffusionless solutions given by eqns. 7 and 8. As all three numerical schemes need a finite value of the diffusion coefficient, the relatively low values of $D = 2 \cdot 10^{-5}$ for $\alpha = -0.5$ and $D = 1 \cdot 10^{-4}$ for $\alpha = 0.3$ were chosen for all schemes. The detection point was at $x_d = 0.4$, $u_0 = 1$. The space increment was the same in all three instances, but temporal increments varied so as to provide stability of calculations. It is seen from Figs. 4 and 5 that for both $\alpha < 0$ and $\alpha > 0$ only the scheme with artificial dispersion (B3) is able to calculate electropherograms close to the exact analytical solution, whereas algorithms B1 and B2 give solutions with spurious large-amplitude oscillations behind the concentration jump in the profile. Calculations with a smaller time increment τ do not lead to improvements in numerical solutions because, as stated in Theory section, they result from an improper space discretization. The diffusion effects, as seen from Figs. 4C and 5C, are small, so that the comparison of the numerical solution with $\tilde{D} \neq 0$ and the analytical solution for $\tilde{D} = 0$ can be considered as correct. In these simulations the correlation between parameters $\tilde{D}$ and h, the finite-difference algorithms and the shapes of concentration profiles, obtained using these schemes, is similar to that in the previous simulations.

In the following example, two series of simulations were applied to CZE and ITP separations for a two-component sample composed of the weak bases aniline and pyridine. It was necessary to investigate the behaviour of different numerical algorithms for conditions close to those in real experimental runs. For this purpose, simula-

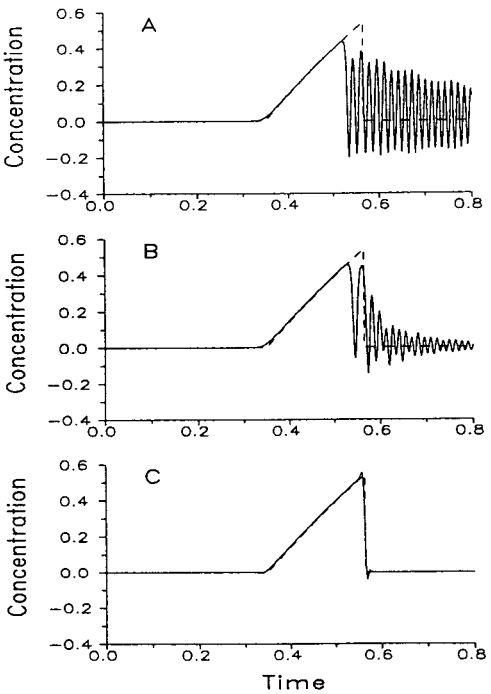

Fig. 4. Electropherograms for non-linear equation ($\alpha = -0.5$). Dimensionless diffusion coefficient $\tilde{D} = 2 \cdot 10^{-5}$. Other details as in Fig. 2.

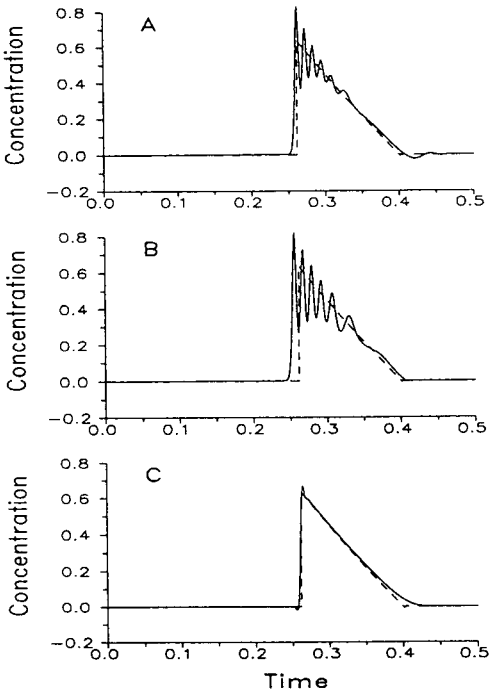

Fig. 5. Electropherograms for non-linear equation ($\alpha = 0.3$). Dimensionless diffusion coefficient $\tilde{D} = 1 \cdot 10^{-4}$. Other details as in Fig. 2.

tions were performed at several constant but different values of applied current, approaching separation times with reasonable values. The mathematical model used in the simulations was based on the same assumptions as stated in ref. 14. The set of equations is presented in Appendix A and it was solved by using the three calculation algorithms as described above. All simulations assumed a capillary of 50 μm I.D. thermostated at 25°C and with the detector located at a point with coordinate $x_d = 10$ cm. The volumes of injected samples were 20 nl for ITP runs and 10 nl for CZE runs. The lengths of the initial sample plugs corresponding to these volumes were *ca.* 1 and 0.5 cm, respectively. In the ITP simulation, the sample was placed in the capillary between $x_l = 1$ cm and $x_r = 2$ cm, whereas for CZE it was located within the interval $x_l = 0.5$ cm and $x_r = 1$ cm, so that the migration path to the detector in the former instance was 8 cm and in the latter 9 cm.

In the series of ITP simulations the leading electrolyte was composed of 18 m*M* sodium hydroxide and 20 m*M* acetic acid, which was the common counter ion in the system, the terminating electrolyte being 40 m*M* β-alanine plus 50 m*M* acetic acid. In the sample zone the initial concentrations were 10 m*M* aniline, 10 m*M* pyridine and 20 m*M* acetic acid. The data on ionic mobilities and p*K* values for specified substances used in the simulations are presented in Table II.

TABLE II

INPUT DATA FOR COMPUTER SIMULATIONS

Substance	pK_a	$\mu(10^{-8}$ m^2/V·s)
Tris	8.3	2.41
β-Alanine	3.3	3.6
Pyridine	5.18	3.0
Aniline	4.8	3.25
Acetate	4.75	4.24
Na^+	–	5.19
H^+	–	36.3
OH^-	–	20.5

Simulations were performed for four values of applied current, 0.05, 0.2, 0.5 and 5 μA.

As in previous simulations, the results are presented in the form of detector signals measured separately for each substance. For a current value of $J = 0.05$ μA, the concentration profiles are depicted in Fig. 6, where A, B and C show the simulation data obtained with finite-difference algorithms B1, B2 and B3, respectively. In order to provide computational stability, the temporal increment τ for algorithm B1 was chosen to be five times smaller than the increments used in the other two algorithms (see Table I). The dimensionless parameter $\tilde{D}$ here

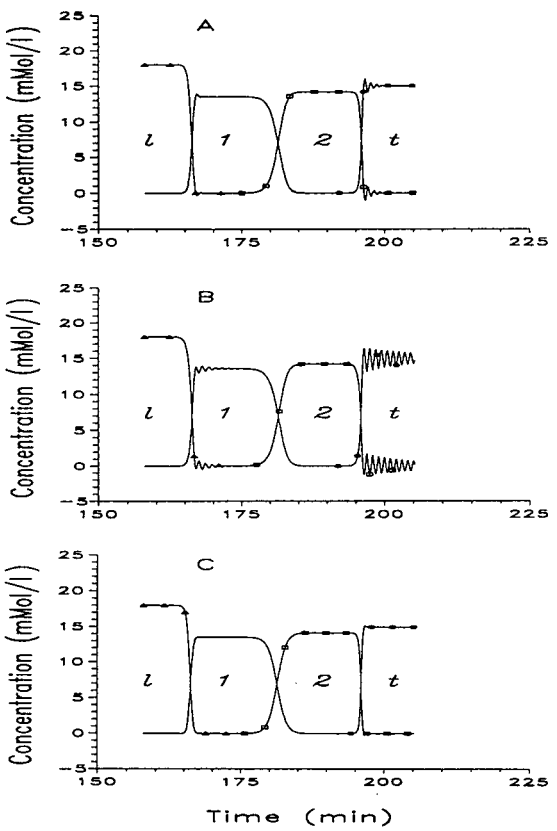

Fig. 6. Simulation for ITP separation of aniline and pyridine. Current, 0.05 μA. Panels A, B and C represent the results obtained using finite-difference algorithms B1, B2 and B3, respectively. Here and also in Fig. 7 pure zones of leader, substance components pyridine and aniline and terminator are designated by l, 1, 2 and t, respectively. ▲ = Sodium hydroxide (leader); line without symbols = pyridine (component 1); □ = aniline (component 2); ○ = β-alanine (terminator).

lies within the range $1.46 \cdot 10^{-3} \leq \tilde{D} \leq 2.52 \cdot 10^{-3}$ and have the order of magnitude of the space increment $h(\tilde{D} \approx h$, see Table I). Fig. 6 shows that only the solution given by finite-different scheme B3 is free from spurious oscillations. Conversely, the concentration profiles obtained by schemes B1 and B2 contain substantial oscillations in the regions close to the zone boundaries. The amplitude and the number of oscillations depend on the magnitude of the concentration gradients. For example, at the interface between sample species 1 and 2 the gradients are smaller than at the other interfaces and no oscillations are observed here. In contrast, the oscillations have the greatest amplitude at the 2–T interface (Fig. 6A and B), where the self-sharpening effect is the strongest and concentrations are changing most sharply. Nevertheless, these two solutions may be considered to be feasible, as they allow one to obtain valuable information on separation times and concentration distributions.

However, this simulation was performed for small current values, so that the migration path of barely 8–9 cm took between 2 and 3 h, which would be unsatisfactory in real experiment. The next example was simulated for a current four times greater, *i.e.*, $J = 0.2$ μA, and the results are shown in Fig. 7, obtained with algorithms (A) B2 and (B) B3 only; attempts to perform simulations with algorithm B1 demanded too much computational effort because, in order to provide the necessary computational stability one would have to use very small time increments. The concentration profiles calculated with algorithm B2 are severely distorted by false oscillations, which obscure the separation pattern. The solution given by B3 demonstrates only small spikes just near the zone interfaces. The other feature observed in Fig. 7 is the different lengths of zone 2 in A and B. According to Fig. 7A, the terminating electrolyte reaches the detector by $t = 48$ min, whereas in Fig. 7B this time is 49 min. The last value is correct as it corresponds to the value obtained in the previous simulation (Fig. 6) divided by four (the electric current is four times greater and, therefore, the migration time must be exactly four times less).

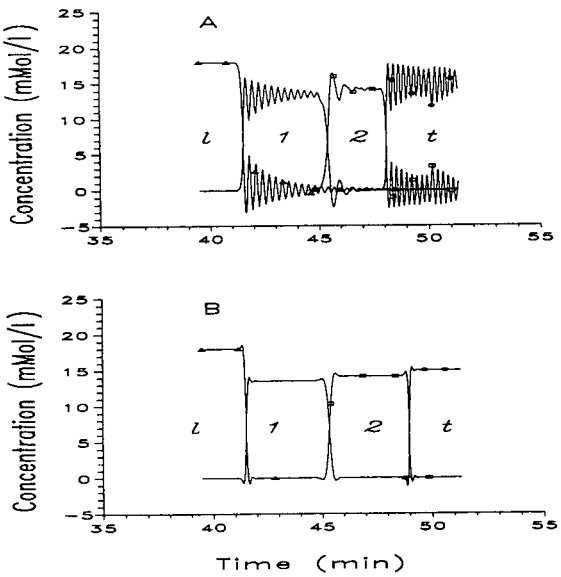

Fig. 7. Simulation for ITP separation of aniline and pyridine. Current, 0.2 μA. Panels A and B represent the results obtained using finite-difference algorithms B2 and B3, respectively. Other details as in Fig. 6.

The simulations at greater current values, $J =$ 0.5 and 5 μA, could be performed only by using algorithm B3, as the other two exhibit computational instability. For these currents the solution given by B3 was slightly distorted by spikes analogous to those in Fig. 7B. However, their amplitude was smaller than that of the oscillations in Fig. 7A, and the zone length was resolved correctly.

In the next series of simulations, modelling of a CZE separation of aniline and pyridine, Tris–acetate buffer was used with concentrations of Tris = 12 mM and acetic acid = 20 mM. This mixture gives a buffer with pH $\approx$ 5, which is approximately half way between the pK values of aniline and pyridine and thus provides the most suitable separation conditions. The concentration of both sample species was 1 mM. The simulations were performed for current values $J = 1$ and 10 μA.

Concentration profiles for $J = 1$ μA calculated using the three algorithms B1, B2 and B3 are plotted in Fig. 8A, B and C, respectively. As in the previous cases, satisfactory results are obtained only with the algorithm using the finite-difference scheme B3. The other two give con-

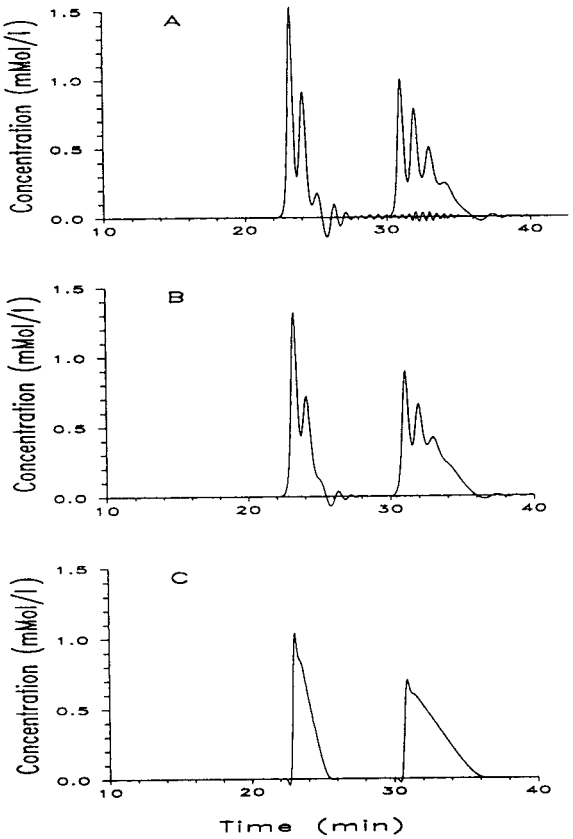

Fig. 8. Simulation for CZE separation of aniline and pyridine. Current, 1 μA. The first substance detected is pyridine (left zone, between 20 and 30 min) and the second is aniline (right zone, between 30 and 40 min). Panels A, B and C represent the results obtained using finite-difference algorithms B1, B2 and B3, respectively.

centration profiles distorted by large-amplitude oscillations and contain several peaks that could cause confusion. The positions of the first peak in Fig. 8A and B are close to the position of that in Fig. 8C, but the corresponding concentration values are different. In Fig. 8A and B they are unrealistic, as they exceed 1 mM. The profiles in Fig. 8C contain only small spikes just before and after the concentration jump. For larger currents ($J = 10$ μA, Fig. 9), the calculations by algorithm B1 were unstable up to time increments $\tau \geqslant 10^{-5}$, so the simulation run required too much time to be performed. Scheme B2 gave a solution totally distorted by oscillations (Fig. 9A). Indeed, the separated zones decay into several

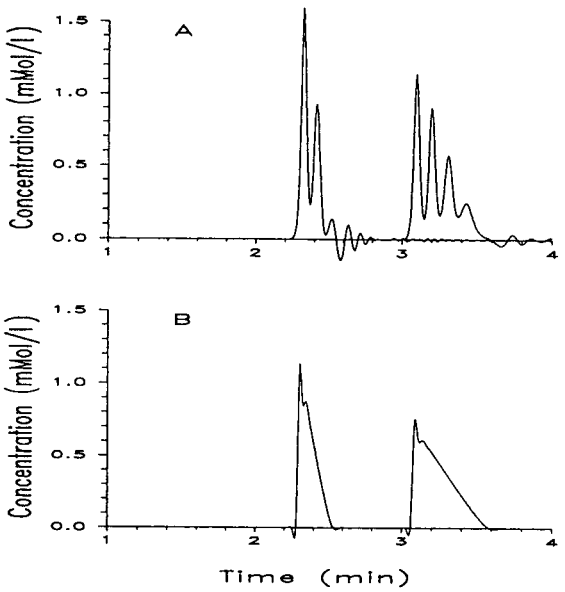

Fig. 9. Simulation for CZE separation of aniline and pyridine. Current, 10 μA. The first substance detected is pyridine (left zone, between 2 and 3 min) and the second is aniline (right zone, between 3 and 4 min). Panels A and B represent the results obtained using finite-difference algorithms B2 and B3, respectively.

solitary waves (solitons), resulting from the action of numerical dispersion [11]. The concentration profiles obtained by algorithm B3 (Fig. 9B) still retain the correct shape, but the non-physical spikes become greater.

CONCLUSIONS

Computer science is today applied with increasing frequency to the solution of problems in separation science. This is welcome in the field of electrokinetic processes, owing to the great complexity and non-linearity of electrophoresis equations. Thus, the efforts undertaken years ago by Bier's group at the Center for Separation Science in Tucson, AZ [5,6], by Dose and Guiochon [3], by Gaš and co-workers [9,10] and by Fidler *et al.* [7,8] represent an important step in the right direction, because in principle they should allow the experimenter to predict and optimize the separation by a "dry chemistry" approach (*i.e.*, by computer simulations) prior to the "wet chemistry" run. Unfortunately, so far none of these approaches has found its way into laboratory practice (except perhaps in the few laboratories which have developed such programs), so they have been of no utility to most of the potential users. As it turns out from this study, this is not because such programs have not been offered on the market, but rather because they were unable to predict real experimental conditions. Previously reported algorithms could only be adopted for solving separations at unrealistically low current densities, in general two to three orders of magnitude lower than those generally utilized in routine practice. Under these conditions, the transit times of analytes would be of the order of one to two days of electrophoresis, which does not compare favourably with modern electrophoretic science, where analyte peaks (especially in CZE) could be swept past the detector in a few minutes. When these algorithms were tried by us at real current densities, all of them broke down in a nightmare of numerical oscillations, which bore no resemblance to reality. We therefore feel that the solutions proposed and adopted here, which can still predict the correct peak shape and structure under real experimental conditions, could be an important step forward in computer science as applied to electrophoresis and facilitate the approach of newcomers to this important field of separation science. In conclusion, we believe that computer science applied to separation processes will grow more and more in importance and will soon become the basis on which to build any type of separation.

ACKNOWLEDGEMENTS

This work was supported in part by grants from Agenzia Spaziale Italiana (ASI, Rome), the European Space Agency (ESA, Paris) and the Consiglio Nazionale delle Ricerche (CNR, Rome), Progetti Finalizzati Chimica Fine II and Biotecnologie e Biosensori.

APPENDIX A

Governing equations

Our mathematical model is based on assumptions formulated in refs. 1 and 14.

An aqueous solution contains weak monoval-

ent acids HA_n and bases B_m, for which the association–dissociation reactions can be represented by

$$HA_n \rightleftharpoons A_n^- + H^+,\ n = 1, 2, \ldots, N \quad \text{(A1)}$$

$$H^+B_m \rightleftharpoons B_m + H^+,\ m = 1, 2, \ldots, M \quad \text{(A2)}$$

$$H_2O \rightleftharpoons H^+ + OH^- \quad \text{(A3)}$$

Dissociation equilibrium constants K_n^a and K_m^b and degrees of dissociation α_n and β_m are given by

$$K_n^a = \frac{[A_n^-][H^+]}{[HA_n]}, \quad \alpha_n = \frac{K_n^a}{K_n^a + [H^+]}, \quad n = 1, 2, \ldots, N \quad \text{(A4)}$$

$$K_m^b = \frac{[B_m][H^+]}{[H^+B_m]}, \quad \beta_m = \frac{[H^+]}{K_m^b + [H^+]}, \quad m = 1, 2, \ldots, M \quad \text{(A5)}$$

$$[H^+][OH^-] = K_w \quad \text{(A6)}$$

where $K_w = 10^{-14}$ is the ionic product of water.

The analytical concentrations of acids, $a_n = [HA_n] + [A_n^-]$, and bases, $b_m = [B_m] + [H^+B_m]$, obey the mass conservation laws:

$$\frac{\partial a_n}{\partial t} + \nabla(z_n^a \alpha_n \mu_n^a a_n \vec{E} - D_n^a \nabla a_n) = 0,\ z_n^a = -1,\ n = 1, 2, \ldots, N \quad \text{(A7)}$$

$$\frac{\partial b_m}{\partial t} + \nabla(z_m^b \beta_m \mu_m^b b_m \vec{E} - D_m^b \nabla b_m) = 0,\ z_m^b = +1,\ m = 1, 2, \ldots, M \quad \text{(A8)}$$

where μ_n^a and μ_m^b are the ionic mobilites and D_n^a and D_m^b are the diffusion coefficients for acids (a) and bases (b), which are expressed by the Einstein equation:

$$D = RT\mu/F$$

where $F = 96\,484$ C/mol is the Faraday constant, T is the absolute temperature and $R = 8.314$ J/mol · K is the universal gas constant.

The continuity equation for an electric current has the form

$$\nabla \cdot \vec{j} = 0 \quad \text{(A9)}$$

The generalized Ohm's law is given by

$$\vec{j} = F\Big\{\Big(\sum_n (z_n^a)^2 \alpha_n \mu_n^a a_n + \sum_m (z_m^b)^2 \beta_m \mu_m^b b_m + \mu_H[H^+] + \mu_{OH}[OH^-]\Big) \cdot \vec{E} - \sum_n z_n^a D_n^a \nabla(\alpha_n a_n) - \sum_m z_m^b D_m^b \nabla(\beta_m b_m) - D_H \nabla[H^+] + D_{OH} \nabla[OH^-]\Big\} \quad \text{(A10)}$$

The electroneutrality equation is valid:

$$q = F\Big(\sum_m z_m^b \beta_m b_m + [H^+] + \sum_n z_n^a \alpha_n a_n - [OH^-]\Big) = 0 \quad \text{(A11)}$$

APPENDIX B

We introduce the finite-difference grid Ω by dividing the calculation interval $[0, L]$ into I equal subintervals (space steps) $h = L/I$, and by dividing the time interval $[0, T]$ into K equal time subintervals (time steps) $\tau = T/K$, *i.e.*, $\Omega = \{x_i = (i-1) \cdot h, i = 1, 2, \ldots, I+1,\} \times \{t^k = k \cdot \tau, k = 1, 2, \ldots, K+1\}$.

The following notation is introduced:

$$f_i^k = f(x_i, t^k) = f_i,\ f_i^{k+1} = f(x_i, t^{k+1}) = \hat{f}_i,$$

$$f_i^{(0.5)} = \frac{1}{2}(\hat{f}_i + f_i),\ f_{i+1/2}^k = \frac{1}{2}(f_{i+1}^k + f_i^k)$$

where $f = f(x, t)$ is an arbitrary function.

For the finite-difference approximation of derivatives we use the notation

$$f_t = \frac{\hat{f}_i - f_i}{\tau}, \quad f_x = \frac{f_{i+1} - f_i}{h}, \quad f_{\bar{x}} = \frac{f_i - f_{i-1}}{h},$$

$$f_{\bar{x}} = \frac{f_{i+1/2} - f_{i-1/2}}{h}, \quad f_{\mathring{x}} = \frac{f_{i+1} - f_{i-1}}{2h},$$

$$f_{x\bar{x}} = \frac{f_{i+1} - 2f_i + f_{i-1}}{h^2},$$

$$f_{\bar{x}x\bar{x}} = \frac{f_{i+1} - 3f_i + 3f_{i-1} - f_{i-2}}{h^3},$$

$$f_{x\bar{x}x} = \frac{f_{i+2} - 3f_{i+1} + 3f_i - f_{i-1}}{h^3}$$

In the text we refer to $f_{\bar{x}}$ and $f_{\dot{x}}$ as the "upwind" and "central" differences, respectively.

The first algorithm we consider uses the Euler integration method for the set of ordinary differential equations resulting from the space discretization. It is written at every space grid node as

$$C_t + (uC)_{\dot{x}} - D \cdot C_{x\bar{x}} = 0 \quad \text{(B1)}$$

In the second algorithm we have the set of ordinary differential equations, written at every x_i node:

$$\frac{dC}{dt} + (uC)_{\dot{x}} - D \cdot (C_{\dot{x}})_{\dot{x}} = 0 \quad \text{(B2)}$$

which are integrated using the Runge–Kutta method [26].

The finite-difference scheme underlying the third algorithm in the above notation has the form

$$C_t + (uC^{(0.5)})_{\dot{x}} - D \cdot C^{(0.5)}_{x\bar{x}} + \mathscr{A} + \mathscr{B} + \mathscr{C} = 0 \quad \text{(B3)}$$

where

$$\mathscr{A} = -\frac{h^2}{6}[\text{sign}(u) \cdot (uC^{(0.5)})_{\bar{x}x\bar{x}} + (1 - \text{sign}(u)) \cdot (uC^{(0.5)})_{x\bar{x}x}]$$

$$\mathscr{B} = \frac{h^2}{4}(u_x C^{(0.5)}_x)_{\bar{x}}$$

$$\mathscr{C} = \frac{\tau^2}{12h}[u_{i+1/2}(u \cdot C_t)_x - u_{i-1/2}(u \cdot C_t)_{\bar{x}}]$$

$$\text{sign}(u) = 1 \text{ if } u > 0$$

$$\text{sign}(u) = 0 \text{ if } u \leq 0$$

The finite-difference scheme B3, in addition to three common terms contained in all the schemes, also has three additional terms, $\mathscr{A}$, $\mathscr{B}$ and $\mathscr{C}$, responsible for artificial dispersion [13]. The terms $\mathscr{A}$ and the $\mathscr{C}$ were used for all simulations, whereas $\mathscr{B}$ was set to zero in simulations of CZE and ITP.

REFERENCES

1 R.A. Mosher, D.A. Saville and W. Thormann, *The Dynamics of Electrophoresis*, VCH, Weinheim, 1992.
2 D. Tietz, *Electrophoresis*, 13 (1992) 339.
3 E.V. Dose and G.A. Guiochon, *Anal. Chem.*, 63 (1991) 1063–1072.
4 R.A. Mosher, P. Gebauer, J. Caslavska and W. Thormann, *Anal. Chem.*, 64 (1992) 2991–2997.
5 O.A. Palusinski, A. Graham, R.A. Mosher, M. Bier and D.A. Saville, *AIChE J.*, 32 (1986) 215–223.
6 R.A. Mosher, D. Dewey, W. Thormann, D.A. Saville and M. Bier, *Anal. Chem.*, 61 (1989) 362–366.
7 V. Fidler, J. Vacík and Z. Fidler, *J. Chromatogr.*, 320 (1985) 167–174.
8 Z. Fidler, V. Fidler and J. Vacík, *J. Chromatogr.*, 320 (1985) 175–183.
9 B. Gaš, J. Vacík and I. Zelenský, *J. Chromatogr.*, 545 (1991) 225–237.
10 E. Durovčáková, B. Gaš, J. Vacík and E. Smolková-Keulemansová, *J. Chromatogr.*, 623 (1992) 337–344.
11 S.I. Muhin, S.B. Popov and Yu.P. Popov, *Zh. Vychisl. Mat. Mat. Fiz.*, 23 (1983) 1355–1369.
12 S.V. Ermakov, O.S. Mazhorova and Yu.P. Popov, Preprint of Keldysh Institute of Applied Mathematics, 1990, No. 89, p. 28 (in Russian).
13 S.V. Ermakov, O.S. Mazhorova and Yu.P. Popov, *Informatica*, 3, No. 2 (1992) 173–197.
14 S.V. Ermakov, O.S. Mazhorova and M.Yu. Zhukov, *Electrophoresis*, 13 (1992) 838–848.
15 M.Yu. Zhukov, *Zh. Vychisl. Mat. Mat. Fiz.*, 24 (1984) 549–565.
16 S.V. Ermakov, O.S. Mazhorova and Yu.P. Popov, in V.S. Advuevsky (Editor), *Proceedings of the International Symposium on Hydromechanics and Heat/Mass Transfer in Microgravity, Perm–Moscow, July 1991*, Gordon and Breach, Philadelphia, PA, 1992, pp. 409–413.
17 M. Bello, S. Levine and P.G. Righetti, *J. Chromatogr. A*, 652 (1993) 329.
18 H. Nishi and S. Terabe, *Electrophoresis*, 11 (1990) 691–701.
19 M. Chiari, M. Nesi and P.G. Righetti, *J. Chromatogr. A*, 652 (1993) 31.
20 E. Giaffreda, C. Tonani and P.G. Righetti, *J. Chromatogr.*, 630 (1993) 313–327.
21 P.G. Righetti, *Immobilized pH Gradients: Theory and Methodology*, Elsevier, Amsterdam, 1990.
22 G. Hughes, S. Frutiger, N. Paquet, F. Ravier, C. Pasquali, J.C. Sanchez, R. James, J.D. Tissot, B. Bjellqvist and D.F. Hochstrasser, *Electrophoresis*, 13 (1992) 707–714.
23 F.E.P. Mikkers, F.M. Everaerts and Th.P.E.M. Verheggen, *J. Chromatogr.*, 169 (1979) 1–10.
24 V. Šustáček, F. Foret and P. Boček, *J. Chromatogr.*, 545 (1991) 239–248.
25 C.A.J. Fletcher, *Computational Techniques for Fluid Dynamics 1, Fundamental and General Techniques*, Springer, Berlin, Heidelberg, 1988.
26 L. Lapidus and J. Seinfeld, *Numerical Solutions of Ordinary Differential Equations*, Academic Press, New York, 1971.

Journal of Chromatography A, 661 (1994) 279–285
Elsevier Science B.V., Amsterdam

CHROMSYMP. 2881

Analysis of derivatized peptides by capillary electrophoresis

Kathryn M. De Antonis and Phyllis R. Brown
University of Rhode Island, Kingstown, RI 02881 (USA)

Yung-Fong Cheng and Steven A. Cohen*
Millipore Corp., Milford, MA 01757 (USA)

ABSTRACT

Thirteen synthetic prothrombin leader peptides differing only in C terminus were analyzed by capillary electrophoresis. These peptides were derivatized using the novel, fluorescent derivatizing agent, 6-aminoquinolyl-N-hydroxysuccinimidyl carbamate. Derivatized peptides were detected using fluorescence and ultraviolet absorption signals, and underivatized peptides were detected using ultraviolet absorbance at 185 nm. Data are presented which compare the analysis of the derivatized and underivatized peptides.

INTRODUCTION

The analysis of peptides is important for a wide variety of samples such as physiological fluids, foods, protein digests and synthetic mixtures. Peptide analysis is frequently performed using either high-performance liquid chromatography (HPLC) or capillary electrophoresis (CE). Historically, high sensitivity peptide detection has been difficult because peptides lack a strong UV absorbing chromophore. Detection in the low UV range (215 nm and below) is often used, but interference from the solvents and other modifiers present can be prohibitive. In order to avoid the complications involved with low UV measurements, peptide derivatization techniques are often employed which allow mid UV and fluorescence detection [1]. In addition, fluorescence detection greatly enhances analytical selectivity and sensitivity.

There are a number of essential requirements for successful peptide derivatization. Ideally, the derivatizing agent should produce a single, stable derivative for each target analyte. The derivatization reaction should be rapid and simple, and quantitative yields should be obtained easily. The derivatizing agent should generate a strong signal especially for high-sensitivity analyses, and the reaction byproducts should not complicate the separation and analysis.

A number of peptide derivatizing agents have been recently reported including *ortho*-phthalaldehyde (OPA), ninhydrin, fluorescamine, naphthalene-2,3-dicarboxaldehyde (NDA/CN), 9-fluorenylmethyl chloroformate (FMOC), 1-dimethyl aminonaphthalenesulfonyl chloride (Dansyl), and phenylisothiocyanate (PITC) [2–5]. All of these tags are sensitive for the analysis of primary amines, but each has unique disadvantages. OPA, which is the most popular derivatizing agent, ninhydrin and fluorescamine produce relatively unstable derivatives. In addition, ninhydrin is not useful for CE since post capillary derivatization is not available. NDA/CN, the naphthalene analogue of OPA, produces

* Corresponding author.

0021-9673/94/$07.00
SSDI 0021-9673(93)E0813-A

stable derivatives, but the reaction byproducts produced when in the presence of an excess of reagent complicate the analysis [5]. Also, the pH conditions for derivatization are very specific and vary from peptide to peptide, rendering quantitative derivatization of peptide mixtures very difficult. Both FMOC and Dansyl react with water to produce large hydrolysis product peaks which interfere with the analysis. In the case of PITC, the derivatization is complicated by the fact that excess reagent must be removed prior to analysis.

The derivatization of amino acids using the highly fluorescent derivatizing agent, 6-aminoquinolyl - N - hydroxysuccinimidyl carbamate (AQC) has been demonstrated and has a number of advantages [6,7]. This derivatizing agent reacts quickly and easily with both primary and secondary amines, and the derivatives are highly stable (see Fig. 1). Due to the unique fluorescence characteristics of the derivatizing agent, the fluorescence signal produced by the hydrolysis byproducts is significantly reduced, eliminating the problem of interference with the analysis [6]. In addition, the reaction is not hindered by buffer salts such as sodium phosphate, sodium acetate, sodium citrate, sodium chloride and sodium dodecyl sulfate which may

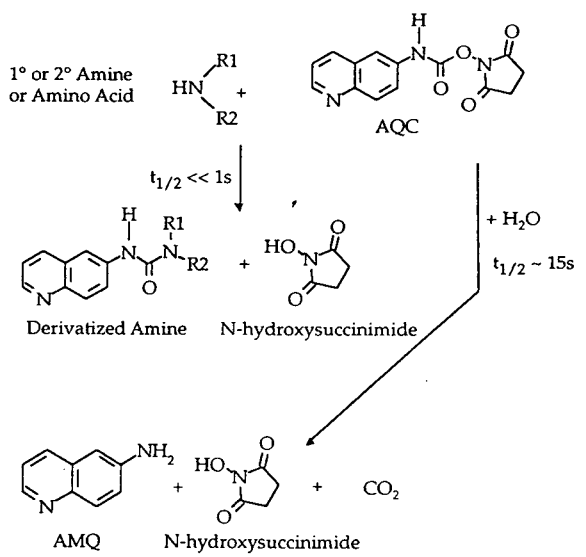

Fig. 1. AQC derivatization reaction [6,7].

be present in peptide containing samples. In this research, the feasibility of peptide derivatization with AQC was evaluated.

Thirteen synthetic prothrombin leader sequences, ANKGFLEEX (where X is valine in the unmodified sequence), differing only in C terminus were chosen as the model. The different C termini were aspartic acid (PT-Asp), serine (PT-Ser), glutamic acid (PT-Glu), glycine (PT-Gly), threonine (PT-Thr), alanine (PT-Ala), valine (PT-Val), methionine (PT-Met), lysine (PT-Lys), isoleucine (PT-Ile), leucine (PT-Leu), phenylalanine (PT-Phe), and tryptophan (PT-Trp). AQC reacts with the N terminal amine group as well as the amine groups of all lysine residues. As a result, all of the peptides except PT-Lys have two possible derivatization sites, and PT-Lys three potential sites. The effect of differing numbers of tags will be discussed.

EXPERIMENTAL

Materials, chemicals and reagents

Acetonitrile (ACN) and boric acid were purchased from J.T. Baker (Phillipsburg, NJ, USA), and ethylenediaminetetraacetic acid (calcium disodium salt, EDTA) was purchased from EM Science (Gibbstown, NJ, USA). AQC (Waters AccQ · Fluor reagent, Millipore, Milford, MA, USA) was synthesized according to ref. 6. Deionized water, which was used in all eluents, was purified on site using a Milli-Q water purification system (Millipore, Bedford, MA, USA). Glass tubes (50 × 6 mm) were purchased from Corning Glassworks (Corning, NY, USA), and were pyrolyzed at 500°C for 6 h prior to use.

Peptide synthesis

Solid-phase peptide synthesis was performed using FMOC methodology on a 9050 Plus flow peptide synthesizer (Millipore) [8]. Preactivated pentafluorophenyl esters were used for peptide assembly on a solid polyethylene glycol polystyrene support (Millipore). After synthesis, the peptide was cleaved from the solid support and deprotected using a solution of trifluoroacetic acid–triethylsilane (95:5).

Sample preparation

A 10-μl aliquot of a peptide containing solution was delivered to a pyrolyzed 50 × 6 mm glass tube. A 70-μl volume of borate buffer (200 m*M* boric acid and 5.0 m*M* EDTA, pH 8.8) was added and the mixture was vortexed. A 20-μl volume of a solution containing the AQC reagent (3 mg/ml dissolved in acetonitrile) was added and the solution was vortexed quickly to insure complete derivatization of all amines. The samples were then heated for 10 min at 50°C and injected. The underivatized peptide samples were prepared in the same fashion using ACN instead of AQC reagent.

Apparatus

The derivatized and underivatized peptides samples were analyzed under identical conditions using two separate CE systems (described below as systems 1 and 2). The eluent was an aqueous borate buffer (50 m*M*, pH 8.5). Fused-silica capillaries (Polymicro Technologies, Phoenix, AZ, USA) were 69 cm to the window × 75 mm I.D. The applied voltage was 14 kV and the resulting current was 11–12 μA. The samples were injected hydrostatically for 6 s unless otherwise noted.

CE System 1 was a Waters Quanta 4000 (Millipore). The UV absorbance signal was measured at 254, 214 and 185 nm. Electrophoretic data were collected using Expert Ease software (Millipore).

CE System 2 was a homemade system consisting of a DA-30 high-voltage power supply (Spectrovision, Chelmsford, MA, USA) and a Waters M470 scanning fluorescence detector (Millipore) with a modified flow cell for CE. The excitation wavelength was 250 nm and the emission wavelength was 395 nm. Hydrostatic injections were made using a pneumatic piston (Bimba, Monee, IL, USA) which drove a timed lift. Electrophoretic data were collected using Maxima software (Millipore).

RESULTS

Peptide detection by UV and fluorescence

Both the derivatized and underivatized PT-Ser peptide were analyzed on both systems using four different detection conditions. The peptide was analyzed on system 1 using 254, 214 and 185 nm detection, and on system 2 using fluorescence detection. The optimal fluorescence excitation and emission wavelengths for the aminoquinolyl tag are 250 and 395 nm, respectively. The absorbance signal generated by the underivatized peptide was strongest at 185 nm, and it was not detected at all at 254 nm. Apparently, the presence of phenylalanine in the peptide was insufficient to produce a peak. The derivatized peptide was detected strongly at all UV and fluorescence wavelengths. See Fig. 2 for the electropherograms of derivatized and underivatized PT-Ser.

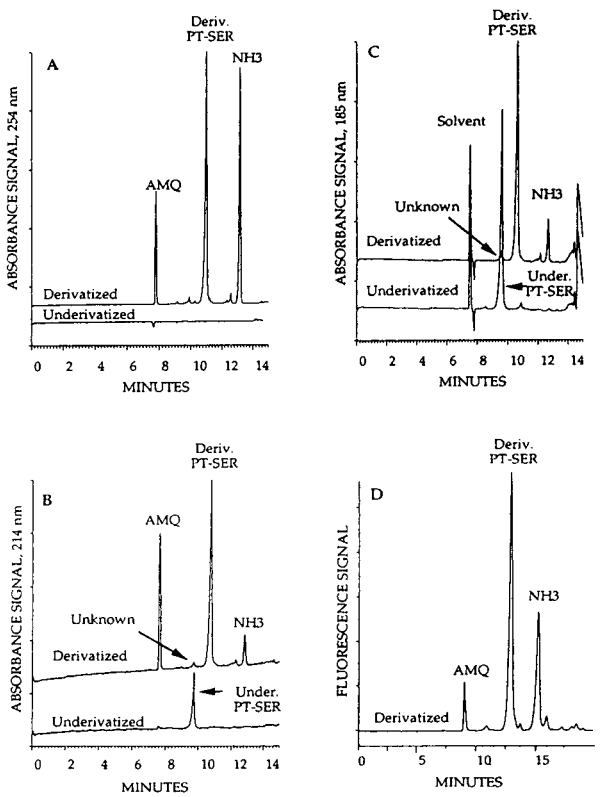

Fig. 2. (A) Derivatized and underivatized PT-Ser detected on system 1 at 254 nm. (B) Derivatized and underivatized PT-Ser detected on system 1 at 214 nm. (C) Derivatized and underivatized PT-Ser detected on system 1 at 185 nm. (D) Derivatized PT-Ser detected on system 2 using fluorescence detection. The excitation wavelength is 250 nm, and the emission wavelength is 395 nm.

Derivatization

We have recently demonstrated the rapid, quantitative formation of stable urea derivatives via reaction of AQC with amine compounds such as amino acids. Thus, the derivatization is expected to label the peptide at the free amino terminus, and on the amino-containing side chain of any lysine residues in the peptide. Excess reagent is hydrolyzed to AMQ, N-hydroxysuccinimide and carbon dioxide.

Derivatization yields of better than 95%, as determined by a loss of starting material, were observed for all peptides studied. Fig. 2 shows overlayed electropherograms of underivatized and derivatized PT-Ser peptides. At 214 nm, where both the underivatized and derivatized peptides generate a strong signal, a small unknown peak in the electropherogram of the derivatized peptide appears to be coeluted with the underivatized peptide. This peak, which correlates to 3% of underivatized peptide, is not the underivatized peptide because it is also visible at 254 nm where the underivatized peptide is not detected.

The addition of insufficient reagent will result in incomplete derivatization [6]. Fig. 3 contains overlays of two derivatized PT-Lys samples. In the upper electropherogram, there are two peaks corresponding to derivatized PT-Lys. The later peak is the completely derivatized peptide, and the earlier peak is mono- and/or di-derivatized PT-Lys. As has been shown for amino acids, addition of a second aliquot of reagent to the sample eliminated the first peak indicating that the derivatization was completed.

Linearity and reproducibility

Reproducibility of migration time (MT) and peak height was determined for six consecutive injections of derivatized PT-Ser using system 1 at 254 nm and system 2. Reproducibility of migration time increases significantly when the relative migration time (RMT) is calculated with respect to the AMQ peak. The relative standard deviation of the RMT is 0.3% for system 1 and 0.2% for system 2. These numbers are significantly improved from the R.S.D. of the MT which were 3 and 2% for systems 1 and 2, respectively (Table I).

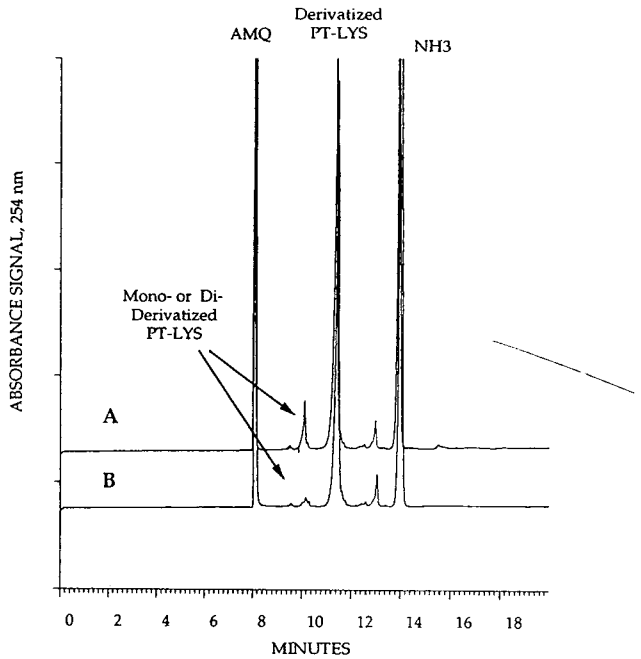

Fig. 3. (A) Incomplete derivatization of PT-Lys. (B) PT-Lys sample after the addition of another aliquot of reagent.

Linearity and the lower detection limits (LDL) were determined for derivatized and underivatized PT-Ser (Table II). Derivatized and underivatized peptide samples were prepared at the concentration levels of 660, 2700, 11 000, 42 000 and 170 000 n*M*. The derivatized samples were analyzed on system 1 at 254 nm and system 2, and the underivatized samples were analyzed on system 1 at 185 nm. Good linearity was achieved for all three systems with correlation coefficients better than 0.997 in the cases. The LDL ($S/N = 3$) was determined for each of the three condi-

TABLE I

REPRODUCIBILITY OF SYSTEM 1 AND SYSTEM 2

$n = 6$.

System	R.S.D. (%)		
	MT	RMT	Height
1 (254 nm)	3	0.3	2
2 (Fluorescence)	2	0.6	8

TABLE II

LINEARITY AND LOWER DETECTION LIMITS

System	Peptide	Correlation coefficient	LDL (nm)	LDL (fmol)
1 (185 nm)	Underivatized PT-Ser	0.997	300	11
1 (254 nm)	Derivatized PT-Ser	0.999	400	15
2 (Fluorescence)	Derivatized PT-Ser	0.999	300	11

tions. The LDL for both the underivatized peptide at 185 nm and the derivatized peptide on system 2 with fluorescence detection was 300 n*M* which corresponds to a mass detection limit of approximately 11 fmol of peptide on capillary. The LDL for the derivatized peptide on system 1 at 254 nm was slightly higher than these at 400 n*M* which corresponds to a mass detection limit of approximately 15 fmol of peptide on capillary.

Peptide resolution

Each of the thirteen peptides was analyzed in the underivatized state on system 1 at 185 nm and derivatized state on system 1 with UV detection at 254 nm. The underivatized peptides had positively charged lysine residues and, most likely, neutral N termini under the analysis conditions used (pH 8.5). In addition, the free carboxyl terminus and both of the glutamic acid residues were in the carboxylate form. Thus, the overall net charge of the underivatized peptides was −1 for PT-Lys, −3 for PT-Asp and PT-Glu, and −2 for the others except for PT-Ala. The net charge on PT-Ala was −1 because a glutamic acid was accidentally deleted from the sequence (as determined by amino acid analysis). Table III lists the RMT values for the underivatized peptides. As expected, PT-Asp and PT-Glu have the largest RMT values (1.44) because they have the largest negative charge. PT-Ala and PT-Lys have the smallest RMT values (1.14 and 1.12, respectively) because they had the smallest negative charge.

The aminoquinolyl tag is uncharged pH 8.5. As a result, derivatization at the positive lysine residues reduces the overall positive charge on the peptide causing it to be eluted later on the CE system (positive power supply). Since PT-

TABLE III

PEPTIDE MIGRATION

Peptide	MT		RMT		ΔRMT
	Underivatized	Derivatized	Underivatized	Derivatized	
PT-Asp	12.136	12.675	1443	1.586	0.143
PT-Ser	10.642	11.369	1.283	1.429	0.146
PT-Glu	11.917	12.617	1.442	1.584	0.142
PT-Gly	10.675	11.421	1.291	1.437	0.146
PT-Thr	10.500	11.242	1.287	1.418	0.140
PT-Ala	9.367	10.146	1.139	1.284	0.145
PT-Val	10.225	11.242	1.278	1.421	0.143
PT-Met	10.188	11.533	1.279	1.427	0.148
PT-Lys	8.291	11.454	1.124	1.415	0.291
PT-Ile	10.129	11.575	1.278	1.425	0.147
PT-Leu	10.158	11.613	1.278	1.425	0.146
PT-Phe	10.161	11.767	1.279	1.430	0.151
PT-Trp	10.138	11.800	1.275	1.427	0.152

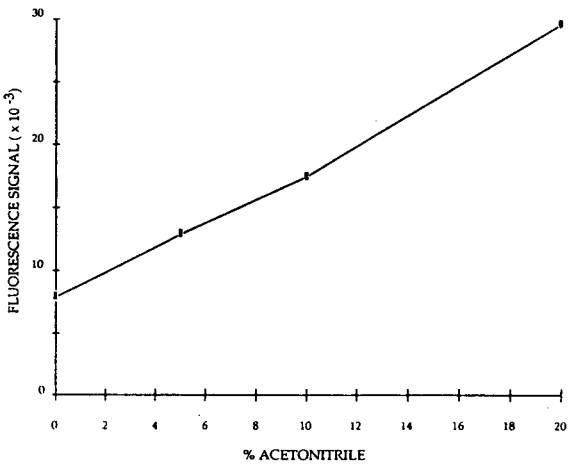

Fig. 4. Fluorescence signal enhancement in the presence of ACN. Signal intensity was measured for derivatized PT-Ile in the presence of 0, 5, 10 and 20% ACN.

Lys is doubly positive in the underivatized state, derivatization has a larger relative effect on its migration time. Table III lists the differences in RMT between the derivatized and underivatized peptides (ΔRMT). The values for all of the peptides except PT-Lys are approximately the same (0.14 to 0.15). PT-Lys has an RMT difference value that is twice the other values (0.29). This is to be expected because two positive charges are eliminated from the PT-Lys upon derivatization, but only one positive charge is eliminated from the others.

Fluorescence signal enhancement

Derivatized PT-Ile was analyzed using four different eluents containing varying percentages of ACN. The eluents were the borate buffer (50 m*M*, pH 8.5) with 0, 5, 10 and 20% ACN. The eluent containing 20% ACN was found to enhance the fluorescence signal by a factor of 3 to 4 over the buffer without ACN. These results agree with data previously generated for derivatized alanine [6] (Fig. 4).

DISCUSSION

AQC was shown to be an effective reagent for the derivatization of peptides. Complete derivatization took less than one minute, and the derivatives were stable for at least several days. It has been demonstrated for amino acids that the derivatives are stable for a minimum of one week at room temperature [6]. Unreacted AQC was hydrolyzed, and the byproducts of derivatization and hydrolysis did not interfere with the CE analysis. Derivatization yields of close to 100% were routinely achieved. It has been previously reported for amino acids that a 4–5-fold excess of AQC to amine is sufficient to generate quantitative yields of derivatized product [6]. However, when insufficient reagent was added to the PT-Lys peptide sample, quantitative conversion was achieved simply by adding a second aliquot of reagent.

RMT is a useful indicator for peptide charge characteristics. The underivatized peptides with the smallest RMT values were the peptides with the smallest negative charge (PT-Lys and PT-Ala which had a glutamic acid deletion), and the peptides with the largest RMT were those with the largest negative charge (PT-Asp and PT-Glu). The remaining underivatized peptides have a median RMT of approximately 1.28. In the case of the derivatized peptides, PT-Ala (net charge −2) is the only peptide with a low RMT value (1.28), and PT-Glu and PT-Asp still have the highest RMT values (1.58). The RMT value for derivatized PT-Lys is in line with the median peptides (1.43) since both of its positive charges have been eliminated. Note that derivatized PT-Ala has an RMT which is approximately equal to those underivatized peptides with net −2 charge, and that underivatized PT-Asp and PT-Glu have similar RMT values to the majority of the derivatized peptides, all of which have a net charge of −3.

The RMT value for derivatized PT-Lys is 1.42, and the RMT value for the incompletely derivatized peptide peak was 1.25. The ΔRMT value for these peaks were 0.29 and 0.13, respectively. Since 0.13 is close to the ΔRMT value generated for the peptides which have a net charge change of one, it is likely that the small peak is the result of incomplete derivatization at one of the lysine residues, rather than the N terminus. This is consistent with the RMT data and with data reported previously which indicated that the ε amine on lysine is less reactive than the α amino

group, and when reagent is limited, lysine is incompletely derivatized [6].

Selectivity of derivatized peptides is influenced by the number of derivatizable lysine residues. The ΔRMT was greater for PT-Lys because it had one more derivatization site than the other peptides, and thus the change in net charge was larger. Electrolyte pH will influence the effect that the number of derivatizable lysine groups will have on migration time. For instance, if the pH of the buffer is below the pK_a of the lysine residues, the N terminus, and the AMQ tag, or above the pK_a of all three, the effect will not be as dramatic. In both situations, the net peptide charge will not be changed upon derivatization. In the pH range used in this study, the addition of the derivatizing agent changed the overall charge of the peptide. In addition, though it was not demonstrated here, the sulfhydryl group of the amino acid cysteine is also derivatizable and could potentially be used to influence resolution.

A potential problem with fluorescence detection in aqueous environments is fluorescence quenching. The use of cyclodextrins in the eluent has been reported to be useful for fluorescence signal enhancement of derivatized peptides [9,10]. In this paper, a non-polar solvent was used to enhance the fluorescence signal by a factor of 3 to 4. As a result, the LDL was reduced to below 100 n*M* (mass detection limit less than 4 fmol) which is significantly better than the LDL for the underivatized peptides under their optimal detection conditions at 185 nm.

REFERENCES

1 M.C. Polo, D. Gonzalez de Llano and M. Ramos, in L.M.L. Nollet (Editor), *Food Analysis by HPLC*, Marcel Dekker, New York, 1992, pp. 117–140.
2 H. Konig, H. Wolf, K. Venema and J. Korf, *J. Chromatogr.*, 533 (1990) 171.
3 S. Lunte and O.S. Wong, *Curr. Sep.*, 10 (1990) 19.
4 R.G. Carlson, K. Srinivasachar, R.S. Givens and B.K. Matuszewski, *J. Org. Chem.*, 51 (1986) 3978.
5 S.M. Lunte and O.S. Wong, *LC·GC*, 7, 11 (1989) 908.
6 S.A. Cohen and D.P. Michaud, *Anal. Biochem.*, 211 (1993) 279.
7 S.A. Cohen, K.M. De Antonis and D.P. Michaud, in R.H. Angelletti (Editor), *Techniques in Protein Chemistry IV*, Academic Press, New York, 1993, pp. 289–298.
8 A. Rustici, M. Velucchi, R. Faggioni, M. Sironi, P. Ghezzi, S. Quataert, B. Green and M. Porro, *Science*, 259 (1993) 361.
9 J. Liu, K.A. Cobb and M. Novotny, *J. Chromatogr.*, 519 (1990) 189.
10 J. Liu, Y.-Z. Hsieh, D. Wiesler and M. Novotny, *Anal. Chem.*, 63 (1991) 408.

Journal of Chromatography A, 661 (1994) 287–295
Elsevier Science B.V., Amsterdam

CHROMSYMP. 2930

Indirect fluorescence determination of lactate and pyruvate in single erythrocytes by capillary electrophoresis

Qifeng Xue and Edward S. Yeung*

Department of Chemistry and Ames Laboratory–US Department of Energy, Iowa State University, Ames, IA 50011 (USA)

ABSTRACT

A scheme of using fluorescein as the fluorophore for indirect detection of anions was demonstrated. This system is quite stable at a fluorescein concentration of 100 μM even without any other buffer components. Different injection modes affect the limit of detection (LOD). A LOD of about 20 amol was obtained for lactate under optimal conditions. Lactate and pyruvate in the intracellular fluid of erythrocytes were measured in this manner. The average amounts in a single erythrocyte for lactate and pyruvate are 1.3 and 2.1 fmol, respectively, or a ratio of 1.6 for pyruvate to lactate. Variations of the absolute amounts and the ratios are fairly large among a group of 27 cells examined. This is consistent with the difference of cells in size and composition. Although the migration times changed by up to 20% during a series of runs from the influence of concomitants in the cells, the migration time ratio was maintained around 1.072 with 3% relative standard deviation.

INTRODUCTION

Indirect detection, as a universal detection approach for ions in capillary electrophoresis (CE), is widely used for the determination of both organic and inorganic compounds that do not possess a suitable detection property [1,2]. To a first approximation, this detection scheme is based on charge displacement between the analyte and a background ion. As many interesting compounds do not always possess a physical property suitable for direct detection, indirect detection became a popular scheme in both absorption [3,4] and fluorescence [5,6]. The limit of detection (LOD) for indirect detection is directly proportional to the concentration of the fluorophore used in the running buffer. By lowering the concentration of the background ions without sacrificing the dynamic reserve, the LOD can be further improved. Despite the impressive LOD obtained in ref. 1, further improvement is necessary for the application of this detection mode to the determination of certain components at the single-cell level. Fluorescein is well-known for its high fluorescence efficiency [7], and is conveniently excited by visible light. So far, little work has been done to optimize the conditions necessary for using fluorescein for the indirect detection of anions.

Determining the chemical and biochemical composition of a single cell can help to elucidate the detailed functions of some organisms. Potentially, it can provide useful information for diagnosis of diseases at an early stage. Much work has been done recently regarding the chemical analysis of individual cells because of the promising biomedical applications. Various schemes [8–11] were developed for determination of different components in different kinds of cells. The analysis of single neurons conducted by Olefirowicz and Ewing [12] and Kennedy *et*

* Corresponding author.

0021-9673/94/$07.00
SSDI 0021-9673(93)E0920-P

al. [13] showed the applicability of microscale separation to the analysis of individual cells. Other investigations [13–17] demonstrated the quantitative determination of multiple constituents in individual cells coupled with electrochemical detection modes.

Recent work in this group centered around the determination of several components within single erythrocytes [18–20] with both direct and indirect fluorescence detection. The red blood cell is the smallest cell so far subjected to chemical analysis. The successful analysis of such a small entity demonstrated that laser-induced fluorescence (LIF) is by far the most sensitive approach for direct and indirect detection of intracellular components. The indirect detection method described earlier [18,21,22] provided a general approach for the quantitation of intracellular ions normally with undetectable properties. This is accomplished without the tedious steps associated with derivatization. It also avoids the problems of incomplete reaction and of slow kinetics at low analyte concentrations.

Lactate and pyruvate that exist in the red blood cell play an important role in the glycolysis process [23]. The determination of the amounts of each in a single erythrocyte should provide some information about the carbohydrate metabolism, as these are products during the carbohydrate substrate conversion process. Lactate and pyruvate convert to each other via the following reaction cycle:

$$\text{Pyruvate} \xleftrightarrow[\text{LDH}]{\text{NADH}\rightarrow\text{NAD}} \text{Lactate}$$

This cycle also brings about the conversion of nicotinamide adenine dinucleotide (reduced form) (NADH) to nicotinamide adenine dinucleotide (NAD), and is catalyzed by lactate dehydrogenase (LDH). The determination of pyruvate and lactate can further be correlated to the concentrations of NADH and NAD indirectly. Also it is possible to relate these to the activity of LDH. Both lactate and pyruvate do not contain any physical properties amenable for sensitive detection. They are also not easily derivatized.

In the present work, the use of fluorescein as the fluorophore for the indirect detection of anions was evaluated. It was then used as the background ion for the determination of pyruvate and lactate in single human red blood cells. The variations in the amounts of pyruvate and lactate from cell to cell were depicted.

EXPERIMENTAL

Instrumentation

The CE system used in this work is similar to that described before [21,22]. For single cell analysis, a 70 cm long, 55 cm to detector, 14 μm I.D. and 350 μm O.D. fused-silica capillary (Polymicro Technologies, Phoenix, AZ, USA) and a high-voltage power supply (Spellman Electronics, Plainview, NY, USA) were used throughout the study. The running voltage was kept at 25 kV. An on-capillary detection window was created by burning off a short section of the polyimide coating. The cell injection end was conditioned by removing a 2-mm section of the polyimide coating for visual monitoring. About 3.2 mW of 330 nm laser light (after separation from the 350 and 360 nm lines) from an argon ion laser (Model Innova 90; Coherent, Palo Alto, CA, USA) was used for excitation. The laser beam was focused onto the detection region by a 1-cm focal length lens and the emitted fluorescence was collected using a 20× microscope objective lens at an angle of 90° to the laser beam. A spatial filter and a 400 nm longpass filter plus an interference filter at 516 nm were used to eliminate the scattered light before imaging onto the photomultiplier tube (PMT). The current produced was converted to voltage by an electrometer. Then, via a 24-bit A/D conversion interface (ChromPerfect Direct, Justice Innovations, Palo Alto, CA, USA), data was collected and stored on an IBM-compatible PC/AT computer.

For evaluation of the fluorescein system, a modified setup was also used. The major change is that a visible argon ion laser (Model 2211-10SL; Cyonics, Uniphase, San Jose, CA, USA) was used. The laser beam was not focused in order to simplify optical alignment. Basically, the original laser beam with a diameter of about 1.5 mm directly irradiates the capillary at the detection window. Since indirect detection involves a fair background concentration of a

fluorophore, the signal level is adequate even though only a few percent of the unfocused laser intensity is used.

Cell preparation and injection

Human erythrocytes were isolated from the fresh plasma of a healthy adult male. Usually 5 ml of plasma were obtained, with heparin and EDTA added to protect the red blood cells from coagulating during storage at 4°C in a refrigerator for as long as 4 days. Before detection of the anions, the red blood cells were separated from the serum by centrifuging, and also were washed by a process similar to that described in ref. 18. A different wash solution (8% glucose, 100 μM fluorescein disodium salt, 2-hydrate with no further adjustments in pH) was used. Multiple washings were performed so that the cells were free from the extracellular ions.

The cells were suspended in the wash solution at a concentration of about 0.1% (v/v). A 50-μl droplet of cell suspension was mixed with an identical volume of running buffer already deposited on the glass microscope slide. An individual red blood cell was selected for injection by manually guiding the capillary orifice close to the cell of interest with the help of the microscope and a 3-dimensional micromanipulator. A vacuum pulse produced by pulling on a syringe connected to the ground end of the airtight buffer vial was applied to draw the cell into the capillary. The whole process was clearly monitored and easily controlled under 100× magnification. It is easy to push out any air bubbles from the capillary that are inadvertently introduced during the injection process by squeezing on the piston of the syringe.

Red blood cells are easily distinguished from other constituents in blood by their number, size and uniform shape. In order to move the capillary orifice to the cell as close as possible, the injection end was etched to form a tip of about 50 μm O.D. with HF using the similar procedure as reported in ref. 17. By using the etched capillary, we can decrease the injected amount of the suspension solution, which was the main interfering component in this detection scheme. Injection of large amounts of suspension solution resulted in instability of the baseline. After a red blood cell was drawn into the capillary, the capillary was immediately moved back into the vial containing the running buffer. After 30 s to allow lysing, the separation begins. In the running buffer, erythrocytes typically lysed in a time shorter than 1 s. The fast lysis is desirable for the determination of intracellular components without extra manipulation. The 30 s waiting period allows the running buffer to mix with the suspension solution and to reach the cell.

Injection of standard samples

The standard samples were injected hydrodynamically at a height of 20 cm relative to the ground end. The hydrodynamic injection mode is comparable to and consistent with the cell injection process. Also, it is not biased for ions with different mobilities and the injected amount is easier to control based on the Poiseuille equation.

Reagents

Sodium pyruvate was obtained from Fluka (Buchs, Switzerland). Sodium lactate was purchased from Sigma (St. Louis, MO, USA). Fluorescein disodium salt, 2-hydrate ($C_{20}H_{10}Na_2O_5 \cdot 2H_2O$, M_r 412.3) was purchased from Eastman Kodak (Rochester, NY, USA). Other chemicals were obtained from Fisher Chemical (Fair Lawn, NJ, USA).

Solutions

Running buffer was made with 1% glucose (W), 100 μM fluorescein disodium salt, 2-hydrate, and 500 μM Tris with pH 8.5 without further adjustment. The standards were dissolved in the running buffer. For the evaluation of fluorescein, different running buffer solutions were used as described below. All solutions were prepared in deionized water and were filtered with a 0.22-μm filter before using.

RESULTS AND DISCUSSION

Evaluation of fluorescein performance

Since fluorescein is a highly efficient fluorophore, we expect that even at low concentration a stable baseline can still be obtained for small capillaries. For a new bare capillary and buffer solutions without cetyltrimethylammonium bro-

mide (CTAB), a positive system peak comes out very early at the running conditions tested. After that the baseline becomes quite stable and clean. When using a DB-1 capillary (J&W Scientific, Folsom, CA, USA) the system peak shows up much later, as the capillary coating and the low concentration of CTAB (20 μM) lead to a slow electroosmotic flow (EOF) rate. The system is also quite stable and clean. The relationship between anion migration and EOF is different for these two conditions. In first case, the anions migrate upstream. The EOF rate is greater than the electrophoretic rate so that the anions are carried to the grounded buffer vial. The more mobile anions will come out later. However, for the second case, the capillary walls are positively charged, leading to EOF and anion migration in the same direction. The more mobile anions will come out earlier. Both systems are suitable for the detection of common anions.

Fig. 1 shows that 8 anions were nicely separated in a DB-1 column, except that nitrate and iodide coeluted. Corresponding concentrations and migration times are listed in Table I. A dynamic reserve of >400 is easily obtained when using fluorescein as the fluorophore at this low concentration. This is a promising feature for the detection of anions. However, the LOD in indirect detection is not simply determined by the concentration of the background fluorophore

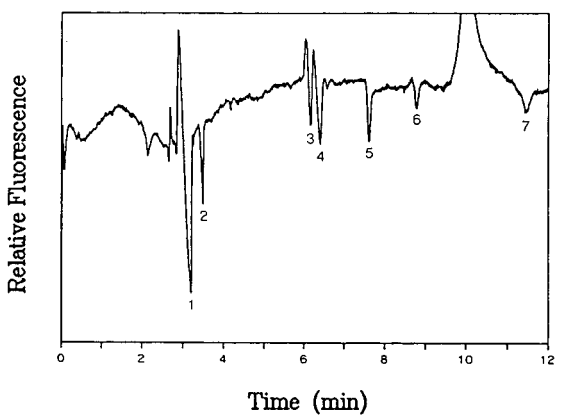

Fig. 1. Electropherogram of anion separation. Concentrations and migration times are listed in Table I. 50-μm DB-1 capillary, 76 cm long and 44 cm to detector. Running voltage: 30 kV. Injection: 30 kV, 0.5 s. Buffer: 100 μM fluorescein and 20 μM CTAB.

TABLE I

CONCENTRATIONS AND MIGRATION TIMES FOR THE SEPARATION SHOWN IN FIG. 1

No.	Anion	Concentration (μM)	Migration time (s)
1	Nitrate	47.2	191.6
	Iodide	15.1	191.6
2	Chlorate	17.8	210.1
3	Pyruvate	34.5	371.6
4	Acetate	23.3	385.4
5	Benzoate	20.1	460.4
6	Lactate	18.8	533.1
7	Glutamate	16.3	698.1

and the dynamic reserve. The displacement ratio is also an important factor that affects the LOD. The problems with fluorescein are the relatively large M_r and the double charge at pH 8.5, which may degrade the LOD. From the pyruvate peak area and peak height, the estimated displacement ratio is 0.2 to 0.08, which is dependent on the buffer components and the capillary size. The buffer components can introduce additional interaction between the analytes and the fluorescein ions. The effect of capillary size is not clear. Generally, simpler systems (using only 100 μM fluorescein as the running buffer) and smaller capillaries give larger displacement ratios.

Table II lists the LOD for different experimental conditions. Certain conditions provide improvements in LOD compared to that reported previously [1,22]. Even though different anions were tested, the LODs are comparable because the M_r values are similar and the charge is the same. The lowest LOD was obtained for electromigration injection in bare fused-silica column. A possible reason is that the total injection period is much shorter than hydrodynamic injection when injecting the same volume of sample. Therefore the baseline disturbance is smaller in magnitude. However, for electromigration injection in bare columns, the separation is not as good as that obtained for hydrodynamic injection. The LODs listed in Table II confirm the applicability to the detection of pyruvate and lactate in single red blood cells.

TABLE II

ABSOLUTE LOD (10^{-16} mol) UNDER DIFFERENT OPERATING CONDITIONS

Conditions: 1 = buffer: 100 μM fluorescein and 20 μM CTAB, pH 6.3; capillary; DB-1, 350 μm O.D., 50 μm I.D.; length 76 cm and 44 cm to the detector; voltage: 30 kV; injection: 30 kV, 0.5 s; laser: unfocused 488 nm beam; sample was dissolved in running buffer. 2 = Buffer: 100 μM fluorescein, 1% glucose and 500 μM Tris, pH 8.5; capillary: bare fused-silica, 362 μm O.D., 14 μm I.D., length 70 cm and 55 cm to the detector; voltage: 25 kV; injection: gravity 20 cm, 30 s; laser: focused 330 nm beam; sample was dissolved in 8% glucose and 100 μM fluorescein. 3 = As 2 except that the sample was dissolved in the running buffer. 4 = As 3 except that the running buffer did not contain glucose. 5 = As 4 except that injection was conducted by electromigration at 25 kV, 0.5 s. 6 = Buffer: 250 μM sodium salicylate, pH 6.0. Other conditions as in 4.

	Conditions					
	1	2	3	4	5	6
Pyruvate	4.49	1.58	1.49	0.68	0.32	1.79
Lactate	[a]	1.35	1.23	0.88	0.20	1.05
Glutamate	7.51	[a]	[a]	1.36	0.34	1.40

[a] Not measured.

Determination of intracellular pyruvate and lactate in a single erythrocyte

Bare fused-silica capillaries (14 μm I.D.) were used because this size is suitable for injection of cells with a diameter of 8–9 μm and a volume of 53–87 fl [24]. There is only a small dilution effect after the lysis of the cell and optical alignment is not very tricky. Also, it allows a reasonable vacuum injection time (<15 s) for introducing one cell into the capillary without drawing in too much extracellular fluid. The separation efficiency and detection sensitivity are still well maintained for both fluorescence detection [21] and electrochemical detection [25]. The results shown in Table II provide support for selecting small bore capillaries for single-cell studies.

LIF [19,26] provides the high sensitivity needed for small amounts of sample when the analyte possesses natural fluorescence. Unfortunately, most ionic components existing within a single erythrocyte do not have appreciable natural fluorescence except proteins, DNA and some amino acids. *In vivo* derivatization [18,27] is one of the possibilities for detecting certain compounds. Nevertheless, the tedious process and possible contamination during treatment are formidable challenges for applying that to such a tiny organism as the red blood cell. Some kind of a specific biosensor is an alternative. The high selectivity however limits its applicability for multiple component analysis. The indirect detection approach [1,18] proves to be practical for determining the ionic analytes inside a cell. Even though it is far from being a perfect method, especially near the LOD due to instability of the baseline and system peak interference, the advantages of easy operation and suitability for monitoring compounds without specific functionality make this a unique technique for the analysis of single cells.

We might expect that many peaks would be present in the electropherograms if the amounts of typical anions within the red blood cell were higher than the LOD obtained in this work (Table II). In actual fact most of them are at concentrations well below the LOD. The potentially troublesome components were proteins if they could displace enough fluorescein to produce peaks. At the pH and the low concentration of buffer used in this system, proteins interact strongly with the capillary wall and adsorb there. Also, generally the large biomolecules have poor displacement ratios leading to poor LOD [28]. This is in contrast to operation at pH 10 with native fluorescence detection [29]. Actually, for the low absolute amounts of proteins in a cell, they could not produce significant interferences except for changing the EO flowrate due to adsorption. According to Table II, only pyruvate (*ca.* 1.29 fmol) and lactate (*ca.* 0.78 fmol) [30] are at detectable levels in a single erythrocyte.

Preliminary results showed that the high concentration of glucose used in the cell suspension solution caused an unstable baseline. The disturbance was so strong that no recognizable peak was obtained. To reduce the disturbance, 1% glucose was added into the running buffer. Also, the capillary was equilibrated for 24 h at the same voltage before the analysis of single cells. The system became quite stable and could toler-

ate the injection of a high concentration of glucose. Furthermore, the mixing of an equivolume of running buffer with the cell suspension on the microscope slide before injection of a cell decreased the actual concentration of glucose to about 4% and reduced the disturbance. Examination under a microscope shows that red blood cells in 4% glucose can last up to 6 h with no obvious hemolysis. Naturally, leaving cells in the glucose solution for a long time can promote the leakage of intracellular components. Our experiments are performed immediately after washing of the cells to protect pyruvate and lactate from leaking out.

Fig. 2 shows the electropherograms for injection of the running buffer (A), cell suspension solution (B), standards (C), a single cell (D) and a lysed-cell suspension (E). The clean background in (A) and (B) demonstrates a desirable condition for the detection of anions. Considering the detectable components in the cell as well as the consistency of migration times for the standard samples and the cell, one can attribute the two peaks in (D) and (E) to lactate and pyruvate. The stability of the baseline for single cell analysis is dependent on the amount (volume) of suspension solution drawn into the capillary. Sometimes a system peak appeared at the position of the lactate peak, which affects the precise quantitation of intracellular lactate. Therefore, minimizing the volume of the suspension solution injected is crucial for the determination of lactate. With the HF-etched fine tip, the injection orifice can be more easily moved to approach the cell of interest without pushing it away. The other approaches used for controlling the excess injection volume are to use a slightly more concentrated cell suspension and to apply the vacuum pulse gradually after the orifice is near the selected cell.

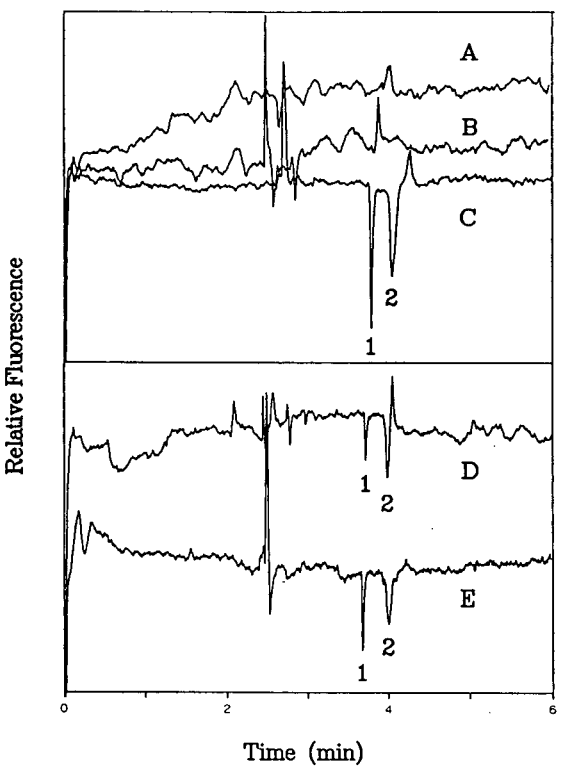

Fig. 2. Electropherograms for the analysis of the running buffer (A), cell suspension solution (B), standards (C), a single red blood cell (D) and a lysed-cell suspension (E). Peaks 1 and 2 refer to lactate and pyruvate, respectively.

Nevertheless, the carefully manipulated injection process is still not good enough to make every run informative. Some other factors can make the system unstable, *e.g.* shaking when moving the capillary in and out of the buffer vial, etc. Several electropherograms for cell separation are shown in Fig. 3. Variations among these trials are presumably due to the individual cell volumes and actual compositional differences. Runs 11 and 23 show other detectable components, which denote unusual cells. According to the analysis of whole blood extracts [31], the chemical composition of normal cells are dramatically different from those of abnormal cells. The common feature for these runs are the peaks for pyruvate and lactate.

In total, 32 cells were analyzed consecutively. Due to unpredictable disturbances, five runs were affected by serious baseline jumps and shifts. Therefore, those five data files were eliminated from further processing to quantify the individual components. A significant feature is that the individual cells are very different from each other with regard to the contents of pyruvate and lactate, as shown in Fig. 4. This is consistent with earlier observations [18,19]. One of the reasons for the large variability among these results may be that the red blood cells have significant differences in content, since volume

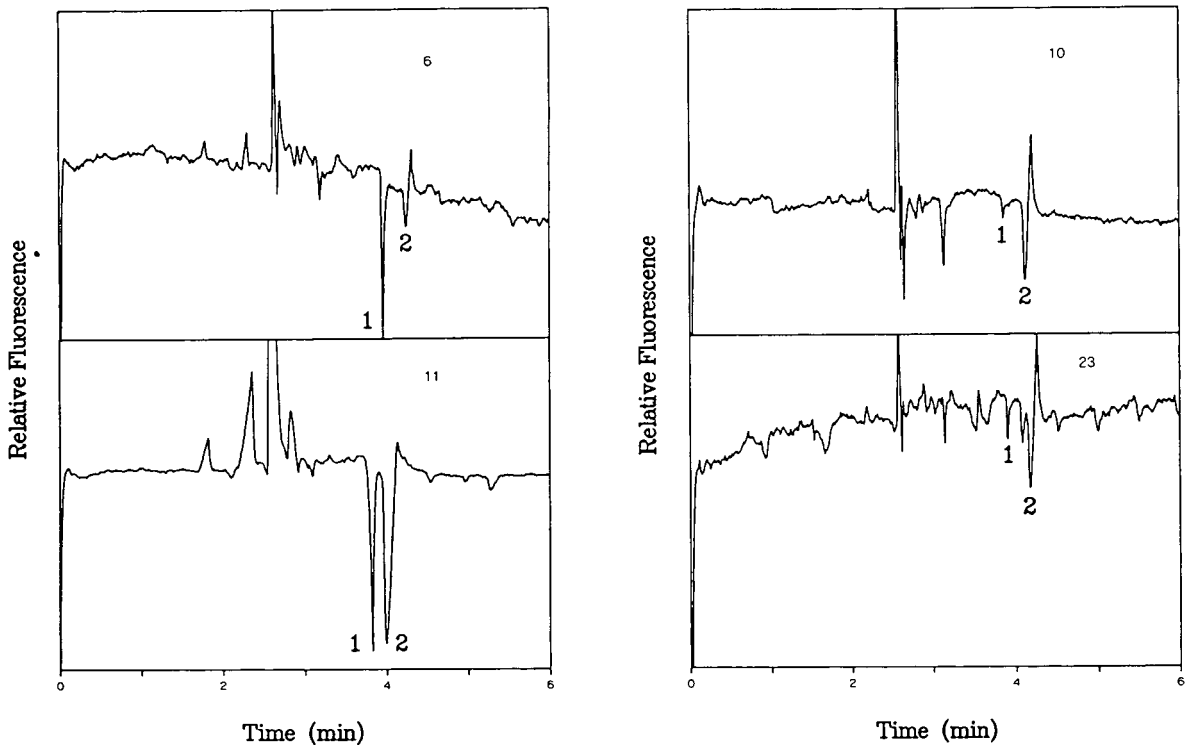

Fig. 3. Electropherograms for the analysis of individual red blood cells. Numbers (6, 11, 10, 23) refer to chronological order of the experiments. Peaks 1 and 2 refer to lactate and pyruvate, respectively.

and age variations can lead to compositional differences. In fact, lactate and pyruvate reflect enzyme activity that can be very different among cells. Another possibility is associated with the stability and accuracy of the indirect detection [3]. Owing to the low concentration of fluorescein used here, the reproducibility is not very good. Up to 40% deviation is observed sometimes, while typical deviations are below 20%. Another possible cause is the stability of the column after several hours of running. From the result of standard samples examined after 32 cell analyses, the peak area and height of four injections yielded a 20% deviation compared to the same standard samples injected before the analysis of cells. The deviation was still within the individual precisions for standard injections. This indicates that the low concentration buffer and the adsorbed material do not damage the capillary. Also, no obvious decreasing or increasing trend was observed in Fig. 4. The average intracellular contents of pyruvate and lactate are found to be 2.1 fmol and 1.3 fmol, respectively (a ratio of 1.6 for pyruvate to lactate). These values are different from the literature values of 1.29 and 0.78 fmol (a ratio of 1.6) for pyruvate and lactate, respectively. The ratio of pyruvate to lactate for each cell is shown in Fig. 5. A considerable variation was observed even though this is a cell-size independent quantity. This is further evidence that metabolism and enzyme activity can be very different in individual cells.

The migration time is always a useful marker for identifying the analyte in capillary electrophoresis. The migration times for pyruvate and lactate are shown in Fig. 6 for each cell injection. We note there is no significant change with run number except for the first several runs, where there is a change of up to 20%. A longer equilibration time between runs leads to a small-

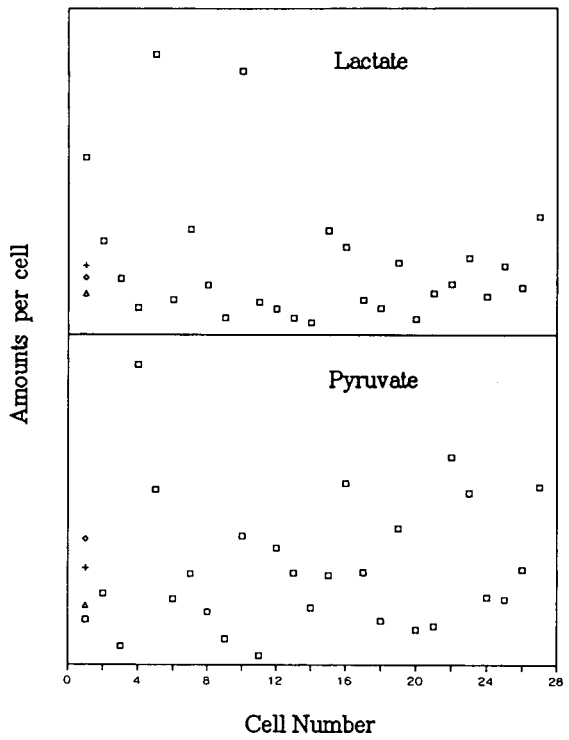

Fig. 4. Distributions of signals from lactate and pyruvate in individual human red blood cells over a series of 27 trials. Zero is indicated by the x-axis in each plot. □ = Amount in individual cells; △ = literature value; + = average for all 27 cells; ◇ = amount measured from a lysed-cell suspension.

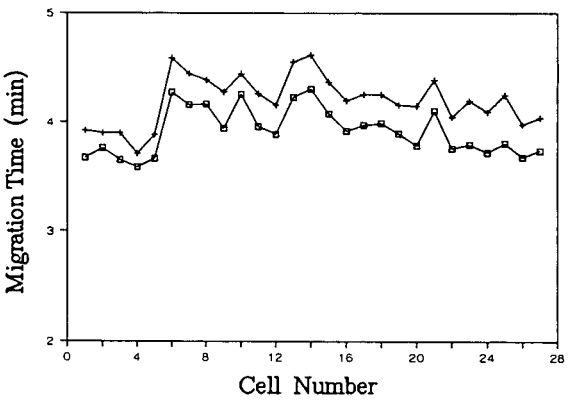

Fig. 6. Changes in migration times over the entire experiment. □ = Lactate; + = pyruvate.

er change in the migration times. We conclude that the change in migration is mainly caused by changing ζ potential due to the injection of cells, because the running voltage and the buffer ionic strength are kept constant for the entire set of runs. Fortunately, the system peak can be used as an internal standard for migration time calibration and for identifying the sample peaks. The ratios of the migration times for pyruvate and lactate are almost constant, as shown in Fig. 7, with an average of 1.072 and a relative standard deviation of only 3%. For standard samples, the ratio is 1.078. This provides positive evidence for identification of the two peaks as pyruvate and lactate.

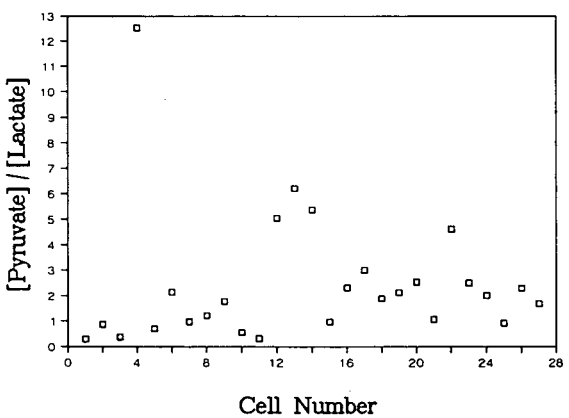

Fig. 5. Ratio of pyruvate to lactate in individual red blood cells for 27 trials.

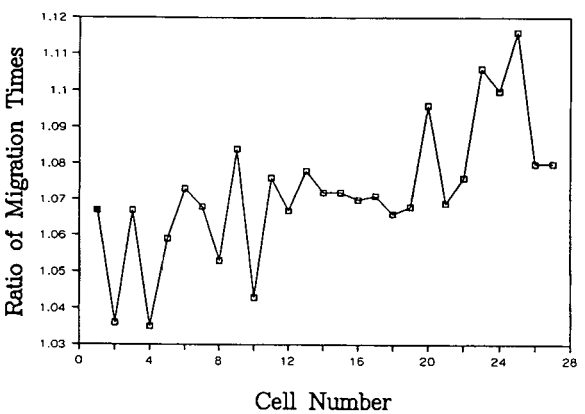

Fig. 7. Ratios of migration times for pyruvate to lactate for 27 runs.

CONCLUSIONS

We have demonstrated the advantages of using fluorescein as the background ion for the indirect detection of anions. The system shows good stability at 100 μM fluorescein. LOD of 20 amol for lactate was achieved. For the best performance in indirect detection, good equilibration is necessary before running the samples. Fluorescein can also be excited by visible laser sources, paving the way for a more compact and a less costly instrument.

The separation and determination of intracellular anions show an important application of this detection approach in the study of mammalian cells. Variations observed from cell to cell should be useful in understanding the biological functions of different components in cells, and perhaps can help to determine whether cells are normal. This scheme might allow the determination of NADH, NAD or LDH by measuring the amounts of pyruvate and lactate, because these are the products of catalysis by those enzymes. This kind of correlation requires very accurate determinations of pyruvate and lactate. Further improvements in stability and reproducibility for this system would thus be necessary to reach this goal.

ACKNOWLEDGEMENTS

The Ames Laboratory is operated for the US Department of Energy by Iowa State University under Contract No. W-7405-Eng-82. This work was supported by the Director of Energy Research, Office of Basic Energy Sciences, Division of Chemical Sciences.

REFERENCES

1 E.S. Yeung and W.G. Kuhr, *Anal. Chem.*, 63 (1991) 275A.
2 E.S. Yeung, *Acc. Chem. Res.*, 22 (1989) 125.
3 M.W.F. Nielen, *J. Chromatogr.*, 588 (1991) 321.
4 G.A. Pianetti, M. Taverna, A. Baillet, G. Mahuzier and D. Baylocq-Ferrier, *J. Chromatogr.*, 630 (1993) 371.
5 L. Gross and E.S. Yeung, *Anal. Chem.*, 62 (1990) 427.
6 H. Kawazumi, H. Nishimura and T. Ogawa, *J. Liq. Chromatogr.*, 15 (1992) 2233.
7 J.D. Ingle, Jr. and S.R. Crouch, *Spectrochemical Analysis*, Prentice-Hall, Englewood Cliffs, NJ, 1988, p. 346.
8 G.F. Bahr and E. Zeitler, *Lab. Invest.*, 11 (1962) 912.
9 R.T. Kennedy, R.L. St. Claire, J.G. White and J.W. Jorgenson, *Mikrochim. Acta*, II (1987) 37.
10 C.M. Lent, R.L. Mueller and D.A. Haycock, *J. Neurochem.*, 41 (1983) 481.
11 R.M. McCaman, D. Weinrich and H. Borys, *J. Neurochem.*, 21 (1973) 473.
12 T.M. Olefirowicz and A.G. Ewing, *Chimica*, 45 (1991) 106.
13 R.T. Kennedy, M.D. Oates, B.R. Cooper, B. Nickerson and J.W. Jorgenson, *Science*, 246 (1989) 57.
14 R.T. Kennedy and J.W. Jorgenson, *Anal. Chem.*, 61 (1989) 436.
15 M.D. Oates, B.R. Cooper and J.W. Jorgenson, *Anal. Chem.*, 62 (1990) 1573.
16 B.R. Cooper, J.A. Jankowski, D.J. Leszcyzyszyn, R.M. Wightman and J.W. Jorgenson, *Anal. Chem.*, 64 (1992) 691.
17 T.M. Olefirowicz and A.G. Ewing, *Anal. Chem.*, 62 (1990) 1872.
18 B.L. Hogan and E.S. Yeung, *Anal. Chem.*, 64 (1992) 2841.
19 T.T. Lee and E.S. Yeung, *Anal. Chem.*, 64 (1992) 3045.
20 B.L. Hogan and E.S. Yeung, *Trends Anal. Chem.*, 12 (1993) 4.
21 L. Gross and E.S. Yeung, *J. Chromatogr.*, 480 (1989) 169.
22 W.G. Kuhr and E.S. Yeung, *Anal. Chem.*, 60 (1988) 1832.
23 G.J. Brewer, in D.M. Surgenor (Editor), *The Red Blood Cell*, Academic Press, New York, 1974, Ch. 9.
24 R.S. Weinstein, in D.M. Surgenor (Editor), *The Red Blood Cell*, Academic Press, New York, 1974, p. 232.
25 R.A. Wallingford and A.G. Ewing, *Anal. Chem.*, 60 (1988) 1972.
26 J.V. Sweedler, J.B. Shear, H.H. Fishman, R.N. Zare and R.H. Scheller, *Anal. Chem.*, 63 (1991) 496.
27 J.W. Parce, J.C. Owicki, K.M. Kercso, G.B. Sigal, H.G. Wada, V.C. Muir, L.J. Bousse, K.L. Ross, B.I. Sikic and H.M. McConnell, *Science*, 246 (1989) 243.
28 K.C. Chan, C. Whang and E.S. Yeung, *J. Liq. Chromatogr.*, 16 (1993) 1941.
29 T.T. Lee and E.S. Yeung, *J. Chromatogr.*, 595 (1992) 319.
30 R.B. Pennell, in D.M. Surgenor (Editor), *The Red Blood Cell*, Academic Press, New York, 1974, p. 133.
31 R.H. Haas, J. Breuer and M. Hammen, *J. Chromatogr.*, 425 (1988) 47.

Journal of Chromatography A, 661 (1994) 297–303
Elsevier Science B.V., Amsterdam

CHROMSYMP. 2942

Comparative study of non-porous anion-exchange chromatography, capillary gel electrophoresis and capillary electrophoresis in polymer solutions in the separation of DNA restriction fragments

Chinuyo Sumita, Yoshinobu Baba*, Kayoko Hide, Naomi Ishimaru, Kazuko Samata, Atsuko Tanaka and Mitsutomo Tsuhako

Kobe Women's College of Pharmacy, Kitamachi, Motoyama, Higashinada-ku, Kobe 658 (Japan)

ABSTRACT

HPLC using a 100-mm column packed with a non-porous anion exchanger gave high-resolution separations of DNA restriction fragments up to 8000 base pairs (bp). High-resolution separation of DNA restriction fragments up to 12 000 bp was achieved using capillary gel electrophoresis (CGE) and capillary electrophoresis (CE) in entangled polymer solutions. These methods were compared with respect to their performance and efficiencies in the resolution of DNA restriction fragments. The resolving power of CGE is higher than those of the other techniques. The 50–100 bp resolution of DNA fragments up to 500 bp was realized using HPLC, 50 bp resolution using CE in entangled polymer solutions and 10 bp resolution using CGE. The plate number that was achieved with CGE of $3 \cdot 10^6$ plates/m was higher than those of HPLC of $1 \cdot 10^6$ and CE in polymer solutions of $7 \cdot 10^5$ plates/m. The advantages and limitations of HPLC and capillary electrophoretic techniques are discussed.

INTRODUCTION

During the past decade, high-performance liquid chromatography (HPLC) has been developing rapidly as a technique for separating mixtures of DNA fragments [1], because the availability of numerous separation columns makes HPLC an attractive alternative to conventional methods. Among the several novel packing materials developed for the separation of DNA fragments, a non-porous microparticulate (<5 μm) anion exchanger [2] has shown a high resolving power for DNA restriction fragments [3–7] and oligonucleotides in single-base resolution [8–11]. Potentially, non-porous anion-exchange chromatography offers rapid separation and determination when combined with reliable area integration. More recently, capillary electrophoresis (CE) has become an important technique for high-resolution and high-speed separations of DNA fragments. DNA restriction fragments of up to 12 000 base pairs (bp) and polynucleotides of up to 500 bases can be separated with high efficiency by capillary gel electrophoresis (CGE) [7,11–14]. Additionally, CE in entangled polymer solutions is effective for the high-resolution separation of DNA restriction fragments up to 12 000 bp [7,15,16].

As HPLC, CGE and CE in polymer solutions have their own advantages and limitations, they should each have suitable specific applications. Previously, we compared HPLC with CGE with respect to their performance in the single-base resolution of oligonucleotides [11]. In this study, we examined the performance and efficiencies of non-porous anion-exchange chromatography in comparison with CGE and CE in polymer solu-

* Corresponding author.

0021-9673/94/$07.00
SSDI 0021-9673(93)E0969-2

tions with respect to the resolving power and the speed of separation of DNA restriction fragments up to 12 000 bp. For this purpose, we investigated the suitability of a laboratory-made cross-linked polyacrylamide gel-filled capillary [12–14] for CGE, a laboratory-made linear polyacrylamide coated-capillary [7,15,16] for CE in entangled polymer solutions and a commercially available column for HPLC, namely a TSKgel DEAE-NPR non-porous anion-exchange column [2,5,8] in the separation of DNA restriction fragments.

EXPERIMENTAL

Chemicals

The DNA samples used were obtained as follows: a 1-kbp DNA ladder (1.0 μg/μl) from Gibco (Tokyo, Japan); a pBR322 DNA-*Hae III* digest (1 unit) from Sigma (St. Louis, MO, USA); and a ΦX174 DNA-*Hae III* digest (0.24 μg/μl) from Toyobo (Osaka, Japan). The DNA samples were diluted to *ca.* 0.1 μg/μl with water purified in a Milli-Q system (Millipore) and stored at −18°C until used. The 1-kbp DNA ladder contains 23 fragments of 75, 134, 154, 201, 220, 298, 344, 396, 506, 517, 1018, 1636, 2036, 3054, 4072, 5090, 6108, 7126, 8144, 9162, 10 180, 11 198 and 12 216 bp. The pBR322 DNA-*Hae III* digest contains 22 fragments of 8, 11, 18, 21, 51, 57, 64, 80, 89, 104, 123, 124, 184, 192, 213, 234, 267, 434, 458, 504, 540 and 587 bp. The ΦX174 DNA-*Hae III* digest contains eleven fragments of 72, 118, 194, 234, 271, 281, 310, 603, 872, 1078 and 1353 bp. Methylcellulose (4000 cP) was purchased from Sigma. All other chemicals were of analytical-reagent or electrophoretic grade from Wako (Osaka, Japan).

HPLC equipment, column and eluents

An LC-800 HPLC system (Jasco, Tokyo, Japan) was used for the separation of DNA fragments. A TSKgel DEAE-NPR column (35 mm × 4.6 mm I.D.) purchased from Tosoh (Tokyo, Japan) contains an anion exchanger based on a non-porous polymer support, having a particle diameter of 2.5 μm. A 100-mm long TSKgel DEAE-NPR column was donated from Tosoh. The eluents were (A) 0.25 *M* sodium chloride in 20 m*M* tris(hydroxymethyl)-aminomethane (Tris)–HCl buffer (pH 9.0) and (B) 1 *M* sodium chloride in 20 m*M* Tris–HCl buffer (pH 9.0). Sample solution (10–20 μl) was injected into the column and chromatographed at a flow-rate of 1.0 ml/min (35-mm column) or 0.5 ml/min (100-mm column). The column temperature was kept constant (30, 40, 50 and 60°C) to within 0.2°C. DNA fragments were detected at 260 nm.

Capillary electrophoresis

CGE separations were carried out by using an Applied Biosystems Model 270A capillary electrophoresis system. Polyimide-coated fused-silica capillaries (375 μm O.D., 100 μm I.D.; GL Sciences, Tokyo, Japan) of 30 cm effective length and 50 cm total length were used. Gel-filled capillaries, in which polyacrylamide gel is chemically bonded to the capillary wall, were prepared according to the literature [14] with slight modifications as follows. The polyimide coating was removed at a distance of *ca.* 20 cm from the outlet end. The capillary was rinsed with 1 *M* NaOH solution for 15 min and with Milli-Q-purified water for 30 min by using a vacuum injection system [13]. A solution of 0.4% 3-methacryloxypropyltrimethoxysilane in 6 m*M* acetic acid was continuously passed through the capillary for 10 min. The capillary was left for 1 h at 40°C and then rinsed with Milli-Q-purified water for 10 min. The acrylamide solution (3%T, 0.5%C) was prepared in a buffer solution (100 m*M* Tris–borate–2 m*M* EDTA, pH 8.3) and carefully degassed in an ultrasonic bath for 5 min. Polymerization is initiated with the addition of both 80 μl of 10% N,N,N′,N′-tetramethylethylendiamine (TEMED) solution and 20 μl of 10% ammonium peroxodisulphate solution into 5 ml of acrylamide solution. The polymerizing solution was quickly introduced into the capillary for 5 min. Polymerization in the capillary was completed within 5 h at 40°C. Sample solution was introduced into the capillary electrophoretically at a negative polarity of 5 kV for 5 s. Gel-filled capillaries were run with the buffer solution described above at negative polarity of 13 kV (260 V/cm, 15–25 μA) at 25°C. DNA fragments were detected at 260 nm.

CE separations in entangled polymer solutions were carried out by using a Waters Quanta 4000 capillary electrophoresis system. Polyimide-coated fused-silica capillaries (375 μm O.D., 100 μm I.D.; GL Sciences) of 42 cm effective length and 50 cm total length were used. Linear polyacrylamide-coated capillaries were prepared according to the literature [16]. The buffer was 50 m*M* Tris–borate–2.5 m*M* EDTA–0.5% or 0.7% methylcellulose (pH 8.0). Sample solution was introduced into the capillary electrophoretically at negative polarity of 5 or 10 kV for 10 s. CE in entangled polymer solutions was performed using linear polyacrylamide-coated capillaries with the buffer solution at a negative polarity of 10 kV (200 V/cm, 18–20 μA) at room temperature (23–25°C). DNA fragments were detected at 254 nm.

RESULTS AND DISCUSSION

Non-porous anion-exchange chromatography of DNA restriction fragments

Fig. 1 shows a chromatogram of pBR 322 DNA-*Hae III* restriction fragments obtained by HPLC using a 35-mm TSKgel DEAE-NPR column. The separation was performed by gradient elution at 40°C. The gradient and column temperature were optimized by preliminary experiments with the aid of an HPLC computer simulation system [17–19]. Multi-linear gradient elution as shown in Fig. 1 gave a better solution of large DNA fragments than linear gradient elution, whereas both elution techniques separated completely shorter DNA fragments. When the column temperature was changed for optimization, some DNA fragments could not be separated at low temperature (30°C). Separation at high temperatures (50 and 60°C) required longer analysis time, whereas the resolution of DNA fragments was similar to that in Fig. 1. The DNA fragments were separated approximately in proportion to the chain length under the optimum conditions in Fig. 1 and identified according to the literature [4,5]. The fragments of 8 and 11 bp could not be identified owing to their very low detectability. The peaks of the 123, 192, 458 and 504 bp fragments are eluted slightly later than expected from their chain lengths, because they are A-T-rich fragments [5].

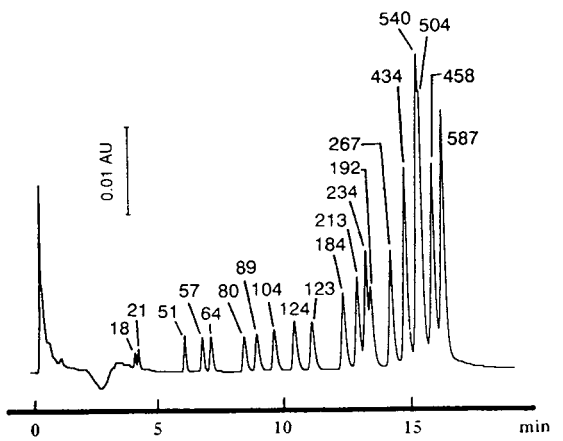

Fig. 1. HPLC separation of pBR322 DNA-*Hae III* digest. Column: TSKgel DEAE-NPR (35 mm × 4.6 mm I.D.). Eluents: (A) 0.25 *M* sodium chloride in 20 m*M* Tris–HCl buffer (pH 9.0) and (B) 1 *M* sodium chloride in 20 m*M* Tris–HCl buffer (pH 9.0). Gradient programme: 0–3 min from 27 to 34% B, 3–60 min from 34 to 100% B at 40°C. Flow-rate: 1.0 ml/min (70 kg/cm^2). Detection: 260 nm.

Fig. 1 illustrates that under optimum conditions eleven fragments ranging from 18 to 184 bp are baseline resolved and all the other components except for the fragments of 192 and 504 bp are almost completely separated. The separation of twenty kinds of the DNA fragments was completed within 17 min. The plate number of each peak was estimated to be $(4–6)\cdot 10^4$ [$(1.1–1.7)\cdot 10^6$ per metre]. The resolution, R_s, was calculated to be in the range 0.2–1.5. The reproducibility of the retention time was in the range 1–2% relative standard deviation (R.S.D.) ($n = 5$).

Fig. 2a shows chromatograms of the 1-kbp DNA ladder with the 35-mm column under the same conditions as in Fig. 1. The DNA fragments were identified according to the literature [5] and the peaks of 201 and 1018 bp fragments were eluted later than expected, for the same reason as described above. The mixture of DNA fragments ranging from 75 to 517 bp was separated almost completely. Some peaks of DNA fragments ranging from 2036 to 8144 bp appeared, but were poorly resolved. Large fragments around 10 kbp in length could not be resolved. The separation was completed within 20 min. We tried to improve the resolution of

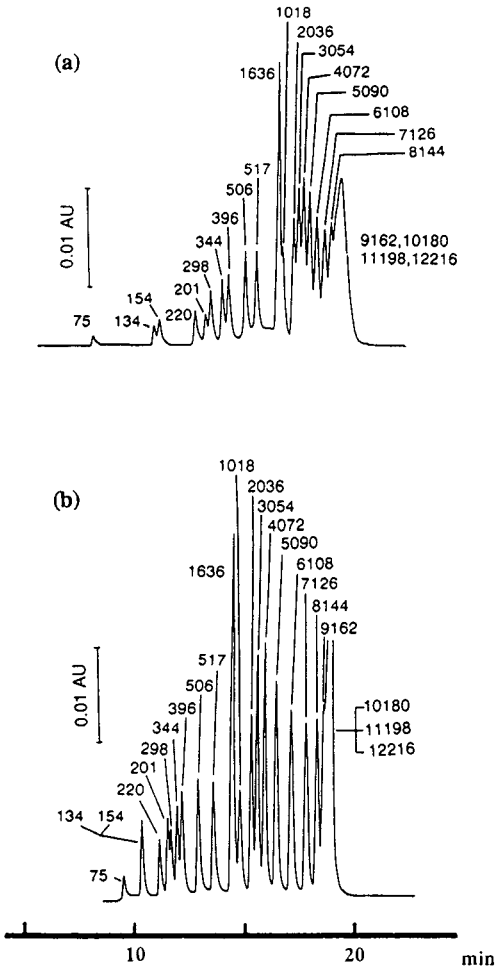

Fig. 2. (a) HPLC separation of a 1-kbp DNA ladder using the 35-mm column. Separation conditions as in Fig. 1. (b) HPLC separation of a 1-kbp DNA ladder, using the 100-mm column. Column: TSKgel DEAE-NPR (100 mm × 4.6 mm I.D.). Eluents A and B as in Fig. 1. Gradient programme: 0–47 min from 50 to 100% B at 50°C. Flow-rate: 0.5 ml/min (100 kg/cm^2). Detection: 260 nm.

large fragments of more than 2000 bp by varying the column temperature and the gradient elutions, but could not achieve a better resolution. The plate number, resolution and reproducibility were almost the same as those in Fig. 1.

We then used a longer column in order to obtain a better resolution of large fragments. The resolution of DNA fragments ranging from 1018 to 8144 bp was greatly improved by using a 100-mm TSKgel DEAE column under the same separation conditions as in Fig. 2a, but a very long time was required for the analysis of all fragments. The gradients were optimized to obtain the rapid and complete resolution of large fragments, instead of the loss of the resolution of short fragments up to 396 bp. A linear gradient with an increasing ratio of eluent B to A at the initial gradient stage was found to be effective in minimizing the analysis time and maximizing the resolution of large fragments, as shown in Fig. 2b. The large fragments ranging from 2036 to 8144 bp were almost completely resolved within less than 20 min, whereas the resolution of short fragments ranging from 134 to 396 bp was inferior to that in Fig. 2a. The plate number, which was $(0.4–1)\cdot 10^5$ [$(0.4–1)]\cdot 10^6$ per metre] using the 100-mm column, was slightly higher than that achieved with the 35-mm column, because the values of the plate number per metre were very similar to each other.

Capillary electrophoresis of DNA restriction fragments

Fig. 3 shows an electropherogram for the 1-kbp DNA ladder obtained with the linear polyacrylamide-coated capillary using 0.5% methylcellulose at 200 V/cm. The electrophoretic conditions were optimized according to the literature [16]. The resolving power of 0.5% methylcellulose solution was adequate for the rapid and

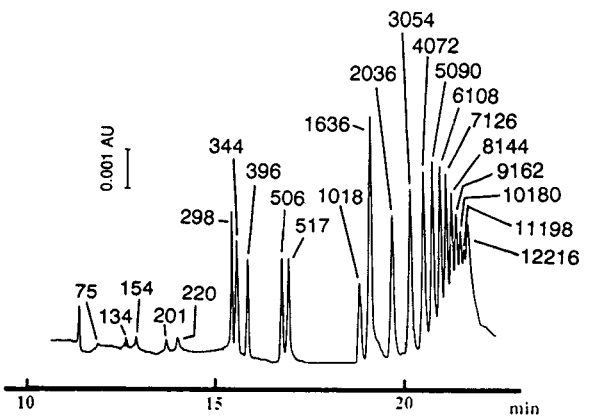

Fig. 3. Separation of a 1-kbp DNA ladder by CE in polymer solutions. Linear polyacrylamide-coated capillary, 100 μm I.D., 375 μm O.D., total length 50 cm, effective length 42 cm. Running buffer: 50 m*M* Tris–borate–2.5 m*M* EDTA–0.5% methylcellulose (pH 8.0). Field: 200 V/cm. Current: 20 μA. Injection: 5 kV for 10 s. Detection: 254 nm.

complete separation of these DNA fragments. The fragments were identified by their sizes in base pairs, and the assignments agreed with the reported separation of the 1-kbp DNA ladder [14,15]. Fig. 3 demonstrates that the separation of individual ladder fragments is excellent. DNA fragments ranging from 75 to 4072 bp are baseline resolved and larger fragments ranging from 5090 to 12 216 bp are almost resolved under the conditions given, yet the separation was completed in less than 24 min. The plate number of each peak was estimated to be $3 \cdot 10^5$ ($7 \cdot 10^5$ per metre). R_s was in the range 0.8–2.0. The reproducibility of the migration time was in the range 1–2% R.S.D. ($n = 5$).

Fig. 4 illustrates the separation of the 1-kbp DNA ladder sample by CGE with a cross-linked polyacrylamide gel (3%T and 0.5%C)-filled capillary at 260 V/cm. The separation conditions were optimized in several preliminary experiments with differing gel composition, electric field and capillary size. The fragments were identified by their sizes in base pairs, and the assignments agreed with the reported separation of a 1-kbp DNA ladder [14]. Fig. 4 clearly demonstrates that DNA fragments ranging from 75 to 4072 bp are baseline resolved and larger fragments ranging from 5090 to 12 216 bp are almost resolved, yet the separation was completed within 15 min. The plate number was $(4–6) \cdot 10^5$ [$(1.3–2.0) \cdot 10^6$ per metre]. R_s for each band was in the range 0.5–2.0. The reproducibility of the migration time was in the range 2–4% R.S.D. ($n = 5$).

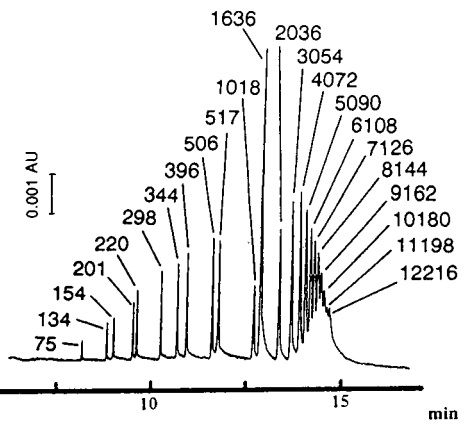

Fig. 4. CGE separation of a 1-kbp DNA ladder. Capillary: 100 μm I.D., 375 μm O.D., total length 50 cm, effective length 30 cm. Running buffer: 100 m*M* Tris–borate–2 m*M* EDTA (pH 8.3). The gel contained 3% T and 0.5% C. Field: 260 V/cm. Current: 20 μA. Injection: 5 kV for 5 s. Detection: 260 nm.

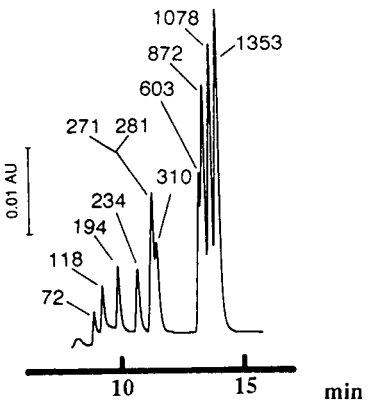

Fig. 5. HPLC separation of a ΦX174 DNA-*Hae III* digest. Separation conditions as in Fig. 2b.

Comparison of the resolving powers of the techniques

Figs. 5–7 illustrate comparisons of these techniques in the separation of a mixture of DNA restriction fragments (ΦX174 DNA-*Hae III* digest) including a critical pair of 271 and 281 bp fragments, which differ in length by only 10 bp.

HPLC separation (Fig. 5) with the 100-mm column gave a baseline resolution of short frag-

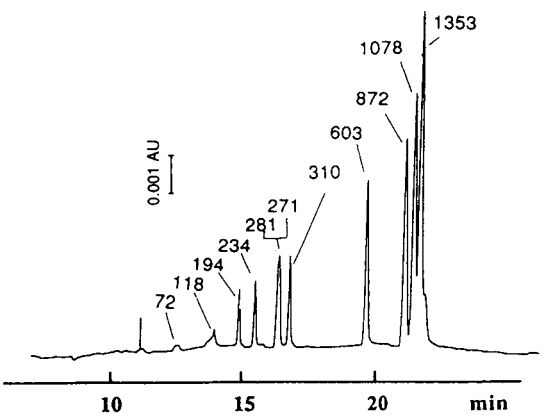

Fig. 6. Separation of a ΦX174 DNA-*Hae III* digest by CE in polymer solutions. Running buffer: 50 m*M* Tris–borate–2.5 m*M* EDTA–0.7% methylcellulose (pH 8.0). Injection: 10 kV for 10 s. Other conditions as in Fig. 3.

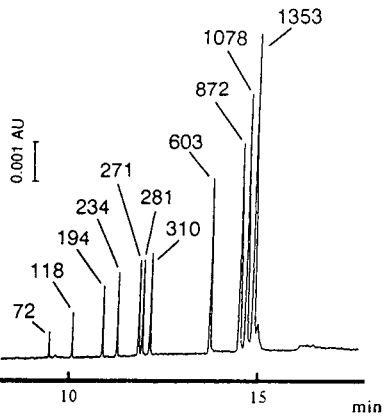

Fig. 7. CGE separation of a ΦX174 DNA-*Hae III* digest. Separation conditions as in Fig. 4.

ments ranging from 72 to 234 bp, but no separation between the 271 and 281 bp fragments was obtained. Some peaks of large fragments ranging from 603 to 1353 bp were separated. A further increase in the resolution was not achieved even by changing the separation conditions. CE separation (Fig. 6) in the entangled polymer solution achieved almost complete resolution of all fragments. No separation between the 271 and 281 bp fragments was obtained, however, in spite of the high resolution. A further improvement in resolution was reported to be achieved by the addition of ethidium bromide to the running buffer [10]. The CGE separation (Fig. 7) gave an excellent resolution of all fragments and two fragments of 271 and 281 bp, which differ by only 10 bp and were not separated by the other two techniques (Figs. 5 and 6), were baseline resolved. Overall, Figs. 5–7 demonstrate that the CGE technique gives a superior performance to the other techniques in the separation of the critical pair of 271 and 281 bp fragments.

HPLC offers a rapid separation of DNA fragments, as shown in Figs. 1, 2 and 5. Especially the 100-mm column appears very suitable for high-resolution separations of DNA fragments. For example, DNA fragments up to 500 bp are baseline resolved when two fragments differ by 50–100 bp. Larger fragments ranging from 2000 to 8000 bp can be separated completely when there is sufficient difference in their size in base pairs (1000 bp). However, HPLC cannot achieve a 10 bp resolution of the fragments of 271 and 281 bp and it is difficult to obtain complete 200–300 bp resolution of large fragments ranging from 600 to 1300 bp, as shown in Fig. 5. The resolving power of CE in polymer solution is slightly higher than that of HPLC. The 20–50 bp resolution of DNA fragments up to 500 bp was achieved, as shown in Figs. 3 and 6. Additionally, large fragments ranging from 1000 to 4000 bp are resolved almost completely, when two fragments differing by 150–1000 bp and larger fragments up to 12 000 bp are separated. CE in polymer solution and HPLC failed to resolve the critical pair of fragments of 271 and 281 bp, as shown in Fig. 6. Of these techniques, CGE offers the highest resolving power of DNA restriction fragments, as shown in Figs. 4 and 7. All fragments up to 5000 bp are baseline resolved when two fragments differ by 10–500 bp, and even two fragments of 271 and 281 bp were completely resolved from each other, as shown in Fig. 7. Larger fragments ranging 6000 to 12 000 bp were separated.

The resolving power of these techniques can be evaluated from their plate numbers. The plate number in HPLC with the 100-mm column is comparable to that of CE in polymer solutions, and that of CGE is higher than those of the other techniques. The plate number per metre of HPLC $[(0.4–1)\cdot 10^6]$ is higher than that of CE in polymer solution $[(5–7)\cdot 10^5]$. The use of a 1000-mm column, therefore, is expected to realize high-resolution separations of DNA fragments by HPLC, but leads to severe damage of the packing material, because a very high pressure drop (*ca.* 1000 kg/cm^2) may be applied in elution even at 50°C and a flow-rate of 0.5 ml/min. In contrast, longer capillary is easily available in CE techniques and will accomplish higher resolution of DNA fragments. These results clearly illustrate that the resolving power of CGE is the highest of these techniques.

We have found that CGE and CE in entangled polymer solutions were suitable for the rapid separation of a wide base pair range of DNA fragments and the resolving power of CGE is higher than that of CE in entangled polymer solutions. However, the use of linear polyacrylamide-coated capillaries and polymer solu-

tions as the molecular sieving medium avoids the difficulties associated with the preparation and use of gel-filled capillaries, such as bubble formation during polymerization and electrophoresis [12]. Additionally, the resolving power of CE in entangled polymer solutions can be improved by the combined use of polymer and ethidium bromide.

Although the resolving power of CGE cannot be matched by non-porous anion-exchange chromatography at present, HPLC has some advantages with respect to quantification and fractionation. HPLC offers accurate quantification when combined with reliable integration, whereas accurate quantification by CE techniques remains a problem. Additionally, HPLC is the only choice for preparative work on DNA fragments, because HPLC is suitable for large-scale preparative separations.

In conclusion, the results suggest that HPLC, CGE and CE in polymer solutions are equally sufficient for the high-resolution separation of DNA restriction fragments. These techniques may be a preferred alternative to slab gel electrophoresis and are applicable to the high-speed analysis of polymerase chain reaction (PCR) products and the rapid and high-precision restriction mapping of DNA fragments.

ACKNOWLEDGEMENTS

We are indebted to Mr. Hiroyuki Moriyama at Tosoh for the gift of an HPLC column. We gratefully acknowledge support for this research by a travel grant from the Kato Memorial Foundation for Bioscience Research and Tsukuba Research Laboratory, Nippon Oil and Fats. This work was partially supported by a Grant-in-Aid for Creative Basic Research (Human Genome Program), a Grant-in-Aid for Cancer Research and a Grant-in-Aid for Scientific Research from the Japan Ministry of Education, Science and Culture.

REFERENCES

1 R. Hecker and D. Riesner, *J. Chromatogr.*, 418 (1987) 97.
2 T. Hashimoto, *J. Chromatogr.*, 544 (1991) 257.
3 D.J. Stowers, J.M.B. Keim, P.S. Paul, Y.S. Lyoo, M. Merion and R.M. Benbow, *J. Chromatogr.*, 444 (1988) 47.
4 M. Merion, W.J. Warren, C. Stacey and M.E. Dwyer, *BioTechniques*, 6 (1988) 246.
5 Y. Kato, Y. Yamasaki, A. Onaka, T. Kitamura, T. Hashimoto, T. Murotsu, S. Fukushige and K. Matsubara, *J. Chromatogr.*, 478 (1989) 264.
6 M.A. Strege and A.L. Lagu, *J. Chromatogr.*, 555 (1991) 109.
7 Y. Baba, C. Sumita, K. Hide, N. Ishimaru, K. Samata, A. Tanaka and M. Tsuhako, *J. Liq. Chromatogr.*, 16 (1993) 955.
8 Y. Kato, T. Kitamura, A. Mitsui, Y. Yamasaki, T. Hashimoto, T. Murotu, S. Fukushige and K. Matsubara, *J. Chromatogr.*, 447 (1988) 212.
9 W.J. Warren and G. Vella, *BioTechniques*, 14 (1993) 598.
10 P.J. Oefner, G.K. Bonn, C.G. Huber and S. Nathakarnkitkool, *J. Chromatogr.*, 625 (1992) 331.
11 Y. Baba, T. Matsuura, K. Wakamoto and M. Tsuhako, *J. Chromatogr.*, 558 (1991) 273.
12 Y. Baba and M. Tsuhako, *Trends Anal. Chem.*, 11 (1992) 280; and references cited therein.
13 Y. Baba, T. Matuura, K. Wakamoto, Y. Morita, Y. Nishitu and M. Tsuhako, *Anal. Chem.*, 64 (1992) 1221.
14 D.N. Heiger, A.S. Cohen and B.L. Karger, *J. Chromatogr.*, 516 (1990) 33.
15 M. Strege and A. Lagu, *Anal. Chem.*, 63 (1991) 1233.
16 Y. Baba, N. Ishimaru, K. Samata and M. Tsuhako, *J. Chromatogr. A*, 653 (1993) 329.
17 Y. Baba, M. Fukuda and N. Yoza, *J. Chromatogr.*, 458 (1988) 385.
18 Y. Baba and M.K. Ito, *J. Chromatogr.*, 485 (1989) 647.
19 Y. Baba, *J. Chromatogr.*, 618 (1993) 41.
20 H.E. Schwartz, K. Ulfelder, F.J. Sunzeri, M.P. Busch and R.G. Brownlee, *J. Chromatogr.*, 559 (1991) 267.

Journal of Chromatography A, 661 (1994) 305–313
Elsevier Science B.V., Amsterdam

CHROMSYMP. 2984

Electrophoresis of proteins in uncoated capillaries with amines and amino sugars as electrolyte additives

Danilo Corradini*, Andrew Rhomberg and Claudio Corradini

Istituto di Cromatografia del CNR, Area della Ricerca di Roma, P.O. Box 10, I-00016 Monterotondo Stazione (Rome) (Italy)

ABSTRACT

The effect of triethylamine and triethanolamine in the running electrolyte on the electroosmotic flow and the migration of four standard basic proteins in bare fused-silica capillaries was examined. At pH 2.5 the direction of the electroosmotic flow was anodal with both additives and at constant ionic strength its magnitude increased with increasing additive concentration. The observations are in qualitative agreement with a theoretical model which is based on the Gouy–Chapman–Stern theory and incorporates a Langmuir-type relationship and also the Von Smoluchowski expression for the electroosmotic mobility, with the approximation to identify the zeta potential with the potential at the Stern plane. From the independence of the electrophoretic mobilities of the additive concentration and type the absence of interactions between the four basic proteins and the two alkylamines is inferred. The utility of glucosamine and galactosamine as additives for the capillary electrophoresis of basic proteins is also demonstrated and their effectiveness is compared with that of the alkylamines.

INTRODUCTION

Protein separations by capillary electrophoresis in untreated fused-silica capillaries are strongly affected by interactions of the proteins with the capillary wall. As a consequence, the efficiency, resolution, reproducibility of migration times and recovery are compromised. Several strategies have been addressed to overcome these problems: chemical or physical coating of the internal surface of the capillary to deactivate the free silanols [1–5]; extremes of electrolyte pH, whether acidic (below pH 2.0), to remove the negative charges to the capillary wall [6], or basic (higher than the isoelectric point), to have both the protein and the capillary wall negatively charged [7]; and the use of electrolytes at high ionic strength, to repress electrostatic interactions between the proteins and the capillary wall [8]. The drawbacks of the above strategies are that coated capillaries often suffer from a gradual loss of surface coverage, particularly at high pH. Extremes of electrolyte pH tend to denature proteins and to compromise recovery by reducing solubility, whereas the current derived from high ionic strength limits the voltage that can be applied.

A further strategy is to use an additive in the running electrolyte. Several compounds have been proposed as electrolyte additives and have been reported to aid in suppressing protein–capillary interactions or to improve separations [9–12]. Few of these additives have been reported to reverse the direction of the electroosmotic flow from cathodic to anodic [13–18]. Reversal of the direction of the electroosmotic flow in fused-silica capillaries occurs when specific adsorption of counter ions at the interfacial region between the capillary wall and the electrolyte takes place. These specifically adsorbed ions are located in the compact part of the double layer, the so-called Stern layer.

The potential changes from ψ_0 (the surface or wall potential) to ψ_δ (the Stern potential), in the Stern layer, and decays from ψ_δ to zero in the diffuse part of the double layer. The potential at

* Corresponding author.

0021-9673/94/$07.00
SSDI 0021-9673(93)E1185-3

the surface of shear between the Stern layer (plus that part of the double layer occupied by the solvent associated with the adsorbed ions in the Stern layer) and the diffuse part of the double layer is the zeta potential, ζ, which affects the direction and magnitude of the electroosmotic flow.

Although several papers [19–30] have reported the effect of the electrolyte composition on the electroosmotic flow, an exact relationship between the electroosmotic mobility and the concentration of ions in the running electrolyte which adsorb in the Stern layer has not been reported. The purpose of this study was to gain further insight into the effect of cationic additives on electroosmotic mobility and protein separation performance. We therefore examined the effect of the concentration of two alkylamines, triethylamine and triethanolamine, on the electroosmotic mobility and on the migration behaviour of four model basic proteins. We developed an equation that correlates the charge density at the capillary wall, due to silanol dissociation, and the charge density in the Stern layer, due to counter-ion adsorption, with the electroosmotic mobility. The model is based on the Gouy–Chapman–Stern theory [31] and incorporates a Langmuir-type adsorption equation and also the Von Smoluchowski expression for the electroosmotic mobility, with the approximation to identify the zeta potential with the potential at the Stern plane.

Further, we examined the use of two amino sugars, glucosamine and galactosamine, as additivies for the capillary electrophoresis of basic proteins and their effectiveness was compared with that of triethylamine and triethanolamine.

THEORY

According to the Gouy–Chapman–Stern (GCS) model of the double layer, as outlined by Shaw [31], a Langmuir-type adsorption model, modified by the incorporation of a Boltzmann factor, may be used to describe the specific adsorption of ions in the Stern layer from the electrolyte solution.

Considering only the adsorption of counter ions, the surface charge density σ_S of the Stern layer is related to the ion concentration C (mol/l) in the bulk solution by the following equation [32]:

$$\sigma_S = \frac{zen_0 \cdot \dfrac{C}{1000/M} \cdot \exp\left(\dfrac{ze\psi_\delta + \Phi}{kT}\right)}{1 + \dfrac{C}{1000/M} \cdot \exp\left(\dfrac{ze\psi_\delta + \Phi}{kT}\right)} \quad (1)$$

where e is the elementary charge, z is the valence of the ion, k is the Boltzmann constant, T is the absolute temperature, n_0 is the number of accessible sites, M is the molecular mass of the solvent (water in this instance), ψ_δ is the potential at the Stern plane and Φ allows for any specific adsorption potential. The surface charge density of the diffuse part of the double layer is given by the Gouy–Chapman equation [32]:

$$\sigma_G = -\left(\frac{2\kappa\varepsilon kT}{ze}\right) \sinh\left(\frac{ze\psi_\delta}{2kT}\right) \quad (2)$$

which at low potentials reduces to

$$\sigma_G = -\frac{\varepsilon\kappa}{4\pi}\psi_\delta \quad (3)$$

where κ is the reciprocal Debye length, defined as

$$\kappa = \left(\frac{4e^2 I}{\varepsilon kT}\right)^{1/2} \quad (4)$$

in which I is the ionic strength and ε is the permittivity of the aqueous solution.

The ionized surface silanol groups of the fused-silica capillary generate a surface charge density, σ_0, which is related to electrolyte pH by the following relationship [33]:

$$\sigma_0 = \frac{\gamma}{1 + \dfrac{[H^+]}{K_a}} \quad (5)$$

where γ is the sum of the ionized and protonated surface silanol group concentration, $[H^+]$ is the bulk electrolyte hydrogen ion concentration and K_a is the dissociation constant.

Hence the surface charge density, σ_0, of the capillary wall should be considered constant at a given pH and of opposite sign to σ_S if reversal of charge takes place within the Stern layer due to specific adsorption of counter ions.

For overall electric neutrality throughout the whole of the double layer,

$$\sigma_G = \sigma_s - \sigma_0 \quad (6)$$

The electroosmotic mobility, μ_{eo}, can be obtained by using the Von Smoluchowski equation [32]:

$$\mu_{eo} = -\frac{\varepsilon}{\eta} \cdot \zeta \quad (7)$$

where ε and η are the permittivity and the viscosity, respectively, of the running electrolyte and ζ is the zeta potential. For a number of simple systems [32,34,35], the zeta potential can be identified with ψ_δ. If this approximation is made, substituting the value of ψ_δ from eqn. 3, then eqn. 7 can be rewritten as

$$\mu_{eo} = \frac{4\pi}{\kappa\eta} \cdot \sigma_G \quad (8)$$

Thus, the combination of eqns. 1, 5 and 8 yields the following expression for the electroosmotic mobility:

$$\mu_{eo} = \frac{4\pi}{\kappa\eta}\left\{\frac{zen_0 \cdot \frac{C}{55.6} \cdot \exp\left(\frac{ze\psi_\delta + \Phi}{kT}\right)}{1 + \frac{C}{55.6} \cdot \exp\left(\frac{ze\psi_\delta + \Phi}{kT}\right)} - \left(\frac{\gamma}{1 + \frac{[H^+]}{K_a}}\right)\right\} \quad (9)$$

EXPERIMENTAL

Instrumentation

Capillary electorphoresis was performed on a P/ACE 2100 instrument, operated under System Gold control, data acquisition and analysis software (Beckman, Fullerton, CA, USA). A fused-silica capillary (Quadrex, New Haven, CT, USA), 0.075 mm I.D., 0.375 mm O.D., with a total length of 37 cm (30 cm to the detector), was mounted in the cartridge. The capillary tube temperature was maintained at 25 ± 1°C by means of a fluorocarbon liquid continuously circulating through the cartridge. A deuterium light source with either a 214- or 280-nm bandpass filter was used. The samples were injected by applying 0.5 p.s.i. (1 p.s.i. = 6894.76 Pa) pressure for 1 s, and the approximate sample volume of 9 nl was calculated according to ref. 36.

Chemicals

Triethylamine was obtained from Pierce (Rockford, IL, USA), triethanolamine from Fluka (Buchs, Switzerland) and D-glucosamine hydrochloride, D-galactosamine hydrochloride and 5-(hydroxymethyl)-2-furaldehyde from Aldrich (Milwaukee, WI, USA). Cytochrome *c* (from horse heart), lysozyme (from chicken egg white), ribonuclease A (from bovine pancreas) and α-chymotrypsinogen A (from bovine pancreas) were supplied by Sigma (St. Louis, MO, USA). Analytical-reagent-grade phosphoric acid, hydrochloric acid, sodium hydroxide, sodium chloride and HPLC-grade water were obtained from Carlo Erba (Milan, Italy) and were used as received.

Procedures

All experiments were carried out with uncoated fused-silica capillaries. Prior to use, the untreated capillary was flushed successively with 0.5 *M* sodium hydroxide solution (30 min), water (10 min) and 0.1 *M* hydrochloric acid (30 min), followed by a second treatment with 0.5 *M* sodium hydroxide solution (30 min) and water (10 min), and then rinsed with the running electrolyte.

The running electrolyte was renewed after five or six runs, and before each run the capillary was rinsed with the running electrolyte for 3 min. For storage the capillary was rinsed with water for 10 min and then dried by flushing nitrogen for 10 min.

The capillary was flushed with 0.5 *M* sodium hydroxide solution (3 min) and water (3 min) each time a running electrolyte of new composition was used. All experiments were carried out applying a constant voltage of 10 kV.

The electroosmotic mobility was determined by measuring the migration time of 5-(hydroxymethyl)-2-furaldehyde, used as an inert tracer, detected at 280 nm at the anodic end of the capillary, upon reversing the polarity. Protein solutions of 1.0–3.0 mg/ml were prepared in water. Running electrolytes at various additive

concentrations and constant ionic strength were prepared by adding the appropriate amount of sodium chloride to the electrolyte solution, containing 50 m*M* phosphate buffer (pH 2.5), for compensation of the changes in the additive concentration. All solutions were filtered through a 0.22-μm Type HA membrane filter (Millipore, Bedford, MA, USA) and degassed by sonication before use.

RESULTS AND DISCUSSION

All experiments were performed with running electrolytes containing 50 m*M* phosphate buffer (pH 2.5). Under such conditions basic proteins are fully protonated and the internal wall of the fused-silica capillaries still exhibits negative charges, as a consequence of incomplete silanol protonation [37]. However, in the presence of positively charged additives that adsorb at the interfacial region between the capillary wall and the electrolyte, the zeta potential becomes positive and the concomitant electroosmotic flow is directed towards the anode.

We first investigated the effect of the concentration of triethylamine (TEA) and triethanolamine (TEOHA) on the electroosmotic mobility and the migration behavior of proteins. Examination of eqn. 9 suggests that at a given pH and constant ionic strength, the electroosmotic mobility would depend mainly on the surface density of adsorbed counter ions in the Stern layer, which should follow a Langmuirian-type adsorption model. Hence, in order to verify this prediction, the effect of varying the additive concentration in the running electrolyte was examined for both additives at the same constant ionic strength and pH. The above requirements were obtained by adding the appropriate amounts of sodium chloride to the running electrolyte for compensation of the changes in the amine concentration.

The dependence of the electroosmotic mobility on the concentration of the two additives in the running electrolyte, as measured with 5-(hydroxymethyl)-2-furaldehyde as a neutral marker, is reported in Fig. 1. Experimental trends in the data are in good agreement with the theoretical prediction of eqn. 9. The curves, the slopes of which decrease, are Langmuirian or quasi-Langmuirian in shape with an initial linear region which is typical of adsorption behaviour at low concentration [38,39].

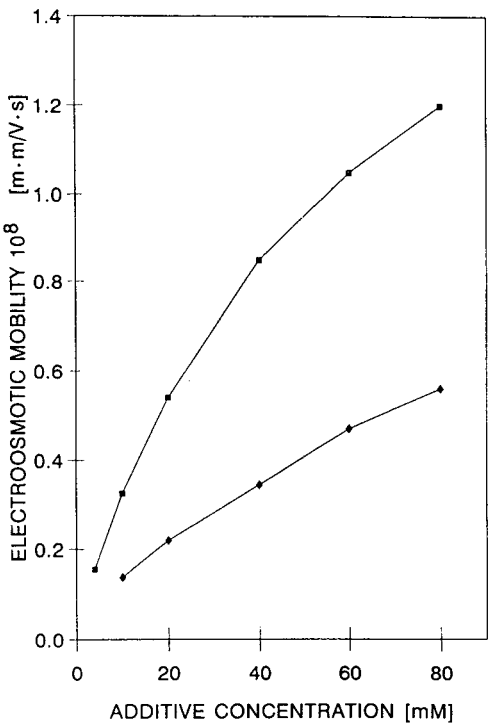

Fig. 1. Dependence of electroosmotic mobility on the concentration of additive in the running electrolyte at constant ionic strength (83 m*M*) and pH (2.5). Capillary, fused-silica, 0.075 mm I.D. × 370 mm total length (300 mm to the detector); applied voltage, 10 kV; temperature, 25°C; neutral marker, 5-(hydroxymethyl)-2-furaldehyde; detection wavelength, 280 nm at the anodic end. ◻ = Triethylamine; ◆ = triethanolamine.

The differences in the slopes of the two curves in Fig. 1 can be accounted for by differences in the specific adsorption energy of triethylamine and triethanolamine. Specific adsorption of TEA is likely to involve hydrogen bonding between the silanols and the amino group and may be stabilized by hydrophobic interactions between the alkyl chains and the siloxane groups, which are known to exhibit hydrophobic character [37,38]. Triethanolamine is also likely to have specific interactions via the amine group, but it is expected to establish much lower hydrophobic

interactions than TEA, which does not have polar groups besides the amino function.

The effect of varying the concentration of TEA or TEOHA in the running electrolyte on the electrophoretic mobility, μ_e, of four standard basic proteins was investigated at pH 2.5 over the same concentration range, constant ionic strength and experimental conditions employed to study the influence of these additives on the electroosmotic mobility. The values of the electrophoretic mobility of proteins vary within 4.4% (R.S.D. of the mean value) when measured with either additive over the whole investigated concentration range, and within 2.4% and 2.6% when measured over the same concentration range with TEOHA or TEA, respectively. This is an indication that the electrophoretic mobilities are virtually independent of the nature and concentration of the two additives, revealing the absence of interactions between proteins and additives. On the other hand, the apparent mobility, μ_{app}, which is the resultant of the oppositely directed vectors of the electrophoretic and electroosmotic mobility, vary from TEOHA to TEA and decreases with increasing additive concentration. For each additive a plot of the apparent mobility versus the additive concentration in the running electrolyte yields a set of curves that parallel each other and differ in shape and slope from those obtained with the other additive (see Fig. 2). Thus, for either TEA or TEOHA, an increase in the additive concentration leads to an increase in the protein migration times without any practical improvement in separation.

The effectiveness of TEA and TEOHA with decreasing protein–capillary wall interactions at pH 2.5 was compared with that of the amino sugars glucosamine (GluA) and galactosamine (GalA). In all experiments the running electrolyte consisted of 40 m*M* additive in 50 m*M* phosphoric acid, adjusted to pH 2.5 with 0.1 *M* NaOH, and containing 40 m*M* chloride ions added either as hydrochloric acid with the additive (GalA and GluA) or as NaCl. Hence all running electrolytes had the same additive concentration, the same ionic strength ($I = 83$ m*M*) and concentrations of phosphate and chloride ions in the same ratio.

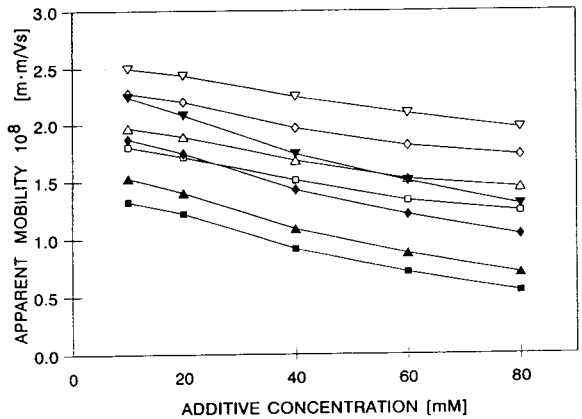

Fig. 2. Apparent mobility of standard basic proteins as a function of additive concentration in the running electrolyte. Open symbols, triethylamine; closed symbols, triethanolamine. ▽, ▼ = cytochrome *c*; ◇, ◆ = lysozyme; △, ▲ = ribonuclease A; □, ■ = α-chymotrypsinogen A. Detection at 214 nm at the cathodic end. Other conditions as in Fig. 1.

Typical electropherograms of the four model basic proteins performed with TEA, TEOHA, GluA and GalA at an applied voltage of 10 kV are depicted in Fig. 3. The values of the measured current were 104, 96, 82 and 89 μA with TEA, TEOHA, GluA and GalA, as the additive, respectively.

The electropherograms show significant dissimilarity in the migration times, which reflects the differences in the electroosmotic mobility produced by the four additives. The model basic proteins are positively charged at pH 2.5 and therefore move towards the cathode against the electroosmotic flow, which takes place in the opposite direction in the presence of the additives.

The average theoretical plate number per metre, N_{AV}, is reported on each electropherogram. These efficiency values may indicate differences in the effectiveness of the additives in preventing protein–capillary wall interactions, which contribute to peak broadening [40,41]. Another factor that has been reported to play a significant role in peak broadening is the longitudinal diffusion that takes place during the migration time between injection and detection [40,41]. Further, it should be considered that the

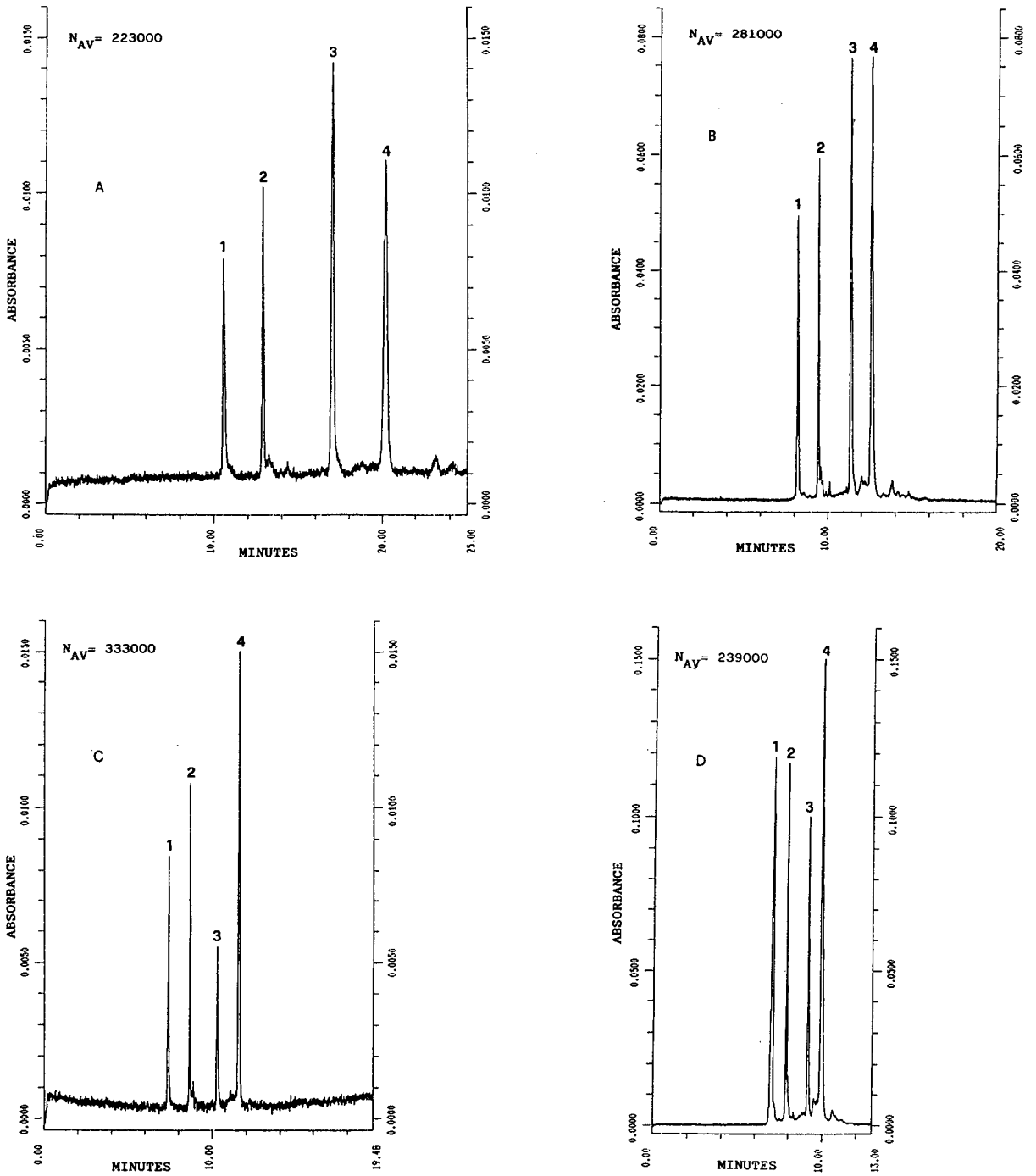

Fig. 3. Electropherograms of standard basic proteins obtained with different additives at the same concentration (40 mM), ionic strength (83 mM) and pH (2.5). (A) Triethylamine; (B) triethanolamine; (C) galactosamine; (D) glucosamine. Proteins: 1 = cytochrome c; 2 = lysozyme; 3 = ribonuclease A; 4 = α-chymotrypsinogen A. Conditions as in Fig. 2, except detection at 280 nm with galactosamine.

TABLE I

REPRODUCIBILITY OF MIGRATION TIMES WITH VARIOUS ADDITIVES

Electrophoretic conditions as in Fig. 3.

Additive	Protein							
	Cyt		Lys		RNase		Chy	
	Mean (min)	R.S.D. (%)	Mean (min)	R.S.D. (%)	Mean (min)	R.S.D. (%)	Mean (min)	R.S.D. (%)
TEA	11.04	0.52	13.16	0.48	17.62	0.61	20.08	0.85
TEOH	8.17	0.33	9.41	0.37	11.31	0.62	12.54	0.43
GluA	7.08	0.52	7.95	1.06	9.24	1.62	10.02	1.91
GalA	7.43	0.54	8.69	0.66	10.32	0.79	11.56	0.86

separated zones do not pass the detector at the same velocity. This causes unequal peak widths arising solely from differences in zone velocity [42], which induce differences in N_{AV} not related to protein–capillary wall interactions.

The run-to-run reproducibility of the protein migration times was determined by replicate injections ($n = 6$) on the same capillary. No washing of the capillary was performed between runs in order to detect irreversible protein adsorption that would affect the electroosmotic mobility and consequently the migration times. The high reproducibility of the migration times reported in Table I indicate that irreversible protein adsorption does not take place, as also evidenced in the electropherograms by the absence of peak tailing.

Peak capacity, which is another measure of the separation efficiency, was calculated using the equation $n = 1 + 0.25\sqrt{N}\ln(t_\omega/t_\alpha)$ [43]. where t_ω and t_α are the migration times of the last and the first peak in the electorpherogram, respectively. The calculation values of peak capacity were 41, 32, 35 and 24 with triethylamine, triethanolamine, galactosamine and glucosamine as the additive, respectively. The high value of the peak capacity obtained with triethylamine may be primarily related to the large separation space, which is taken in this case as the interval between cytochrome *c* and α-chymotrypsinogen A, obtained with this additive, owing to the high counter-electroosmotic flow. On the other hand, a high value of the peak capacity is also obtained with galactosamine, which displays a shorter separation space and a higher separation efficiency. The effect of the different additives on the selectivity is apparent from examination of the four electropherograms. The migration order of the four basic proteins is not affected by changing the additive and with all running electrolytes secondary peaks, due to impurities present in the authentic protein standards, are detected.

From the results reported in Table II, it is observed that the high resolution obtained with TEA and TEOHA, which generate a counter-electroosmotic flow, is in agreement with the expression for resolution proposed by Giddings [44] and Jorgenson and Lukacs [45], which predicts that the best resolution in capillary electrophoresis is obtained when electroosmotic

TABLE II

RESOLUTION OF PROTEINS WITH DIFFERENT ADDITIVES

Electrophoretic conditions as in Fig. 3.

Additive	Cyt–Lys	Lys–RNase	RNase–Chy
TEA	13.02	19.07	10.02
TEOHA	9.07	12.08	5.02
GluA	7.09	12.01	5.04
GalA	11.09	14.05	8.05

and electrophoretic mobilities are of the same order of magnitude and opposite in direction. However, it should be noted that galactosamine, which almost suppresses the electroosmotic flow, displays similar resolution, owing to the higher separation efficiency.

CONCLUSIONS

We have shown that at a given pH and constant ionic strength, increasing the concentration of a cationic species that adsorbs at the silica–electrolyte interface leads to an increase in the electroosmotic mobility. The effect depends on the nature and concentration of the cationic additive and has been qualitatively described by a model based on the Gouy–Chapman–Stern theory. Eqn. 9 correlates a complete expression for the Stern model of the double layer with the electroosmotic mobility. Although it inevitably entails oversimplifications, this model provides a framework for the study of the effect on the electroosmotic mobility of additives that are useful to control electroosmotic flow and solute–capillary wall interactions. Extrapolation of our theoretical model to the analysis of the double-layer parameters from capillary electrophoretic data obtained under a variety of conditions is under investigation.

Triethylamine and triethanolamine were selected as model cationic additives owing to their known effectiveness at masking silanophilic activity in RP-HPLC [46]. It is seen that the two alkylamines are also effective at preventing protein–capillary wall interactions, although the conditions selected may not be the most appropriate for protein analysis. Similar results are also displayed by the two amino sugars galactosamine and glucosamine.

ACKNOWLEDGEMENTS

A.R. was the recipient of a predoctoral fellowship from the Italian Government. The valuable contribution of Dr. Emanuela Fabbri to some of the experiments is gratefully acknowledged.

REFERENCES

1 S. Hjertén, *J. Chromatogr.*, 347 (1985) 191.
2 J.W. Jorgenson and K. DeArman Lukacs, *Science*, 222 (1983) 266.
3 S.A. Swedberg, *Anal. Biochem.*, 185 (1990) 51.
4 W. Nashabeh and Z. El Rassi, *J. Chromatogr.*, 559 (1991) 367.
5 J.T. Smith and Z. El Rassi, *Electrophoresis*, 14 (1993) 396.
6 R. McCormick, *Anal. Chem.*, 60 (1990) 2322.
7 J.S. Green and J.W. Jorgenson, *J. Chromatogr.*, 478 (1989) 63.
8 M.M. Bushey and J.W. Jorgenson, *J. Chromatogr.*, 480 (1989) 301.
9 M. Zhu, R. Rodriguez, D. Hansen and T. Wehr, *J. Chromatogr.*, 516 (1990) 123.
10 H.H. Lauer and D. McManigill, *Anal. Chem.*, 58 (1986) 166.
11 F.S. Stover, B.L. Haymore and R.J. McBeath, *J. Chromatogr.*, 470 (1989) 241.
12 J.A. Bullock and L.C. Yuan, *J. Microcol. Sep.*, 3 (1991) 241.
13 D. Corradini, C. Böhler and C. Corradini, presented at the *8th International Symposium on Capillary Electrophoresis and Isotachophoresis, Rome, October 6–9, 1992*, Lecture O-19.
14 T. Tsuda, Y. Kobayashi, A. Hori, T. Matsumoto and O. Suzuki, *J. Microcol. Sep.*, 2 (1990) 21.
15 J.E. Wiktorowicz and J.C. Colburn, *Electrophoresis*, 11 (1990) 769.
16 A. Emmer, M. Jansson and J. Roeraade, *J. High Resolut. Chromatogr.*, 14 (1991) 738.
17. A. Emmer, M. Jansson and J. Roeraade, *J. Chromatogr.*, 547 (1991) 544.
18 W. Nashabeh and Z. El Rassi, *J. Chromatogr.*, 596 (1992) 251.
19 T. Tsuda, K. Nomura and G. Nakagawa, *J. Chromatogr.*, 248 (1982) 241.
20 T. Tsuda, *J. High Resolut. Chromatogr. Chromatogr. Commun.*, 10 (1987) 622.
21 H.J. Issaq, I.Z. Atamna, G.M. Muschik and G.M. Janini, *Chromatographia*, 32 (1991) 155.
22 I.Z. Atamna, H.J. Issaq, G.M. Muschik and G.M. Janini, *J. Chromatogr.*, 588 (1991) 315.
23 I.Z. Atamna, C.J. Metral, G.M. Muschik and H.J. Issaq, *J. Liq. Chromatogr.*, 13 (1990) 2517.
24 K. Salomon, D.S. Burgi and J.C. Helmer, *J. Chromatogr.*, 549 (1991) 375.
25 K. Salomon, D.S. Burgi and J.C. Helmer, *J. Chromatogr.*, 559 (1991) 69.
26 B.B. VanOrman, G.G. Liversidge, G.L. McIntire, T.M. Olefirowicz and A.G. Ewing, *J. Microcol. Sep.*, 2 (1990) 176.
27 S. Fujiwara and S. Honda, *Anal. Chem.*, 58 (1986) 1811.
28 S. Nathakarnkitkool, P.J. Oefner, G. Bartsch, M.A. Chin and G.K. Bonn, *Electrophoresis*, 13 (1992) 18.

29 K.D. Altria and C.F. Simpson, *Chromatographia*, 24 (1987) 527.
30 C. Schewer and E. Kenndler, *Anal. Chem.*, 63 (1991) 1801.
31 D.J. Shaw, *Introduction to Colloidal and Surface Chemistry*, Butterworths, London, 3rd ed., 1980, pp. 148–159.
32 R.J. Hunter, *Zeta Potential in Colloid Science*, Academic Press, Sydney, 1981, pp. 33–61 and 219–235.
33 M.A. Hayes, I. Kheterpal and A.G. Ewing, *Anal. Chem.*, 65 (1993) 27.
34 D.C. Grahame, *Chem. Rev.*, 41 (1947) 441.
35 J.T. Davies and E.K. Rideal, *Interfacial Phenomena*, Academic Press, London, 1961, pp. 84–93.
36 R.S. Rush and B.L. Karger, *Sample Injection with P/PACE System 2000: Importance of Temperature Control with Respect to Quantitation* (*Technical Bulletin* TIBC-104), Beckman Instruments, Spinco Division, Palo Alto, CA, 1990.
37 K.K. Unger, *Porous Silica*, Elsevier, Amsterdam, 1979.
38 J. Vacík, in Z. Deyl (Editor), *Electrophoresis*, Elsevier, Amsterdam, 1979, pp. 6–8.
39 J. Jacobson, J. Frenz and Cs. Horváth, *J. Chromatogr.*, 316 (1984) 53.
40 X. Huang, W.F. Coleman and R.N. Zare, *J. Chromatogr.*, 480 (1989) 95.
41 W.G.H.M. Muijselaar, C.H.M.M. de Bruijn and F.M. Everaerts, *J. Chromatogr.*, 605 (1992) 115.
42 S. Hjertén, K. Elenbring, F. Kilar, J.L. Liao, A.J.C. Chen, C.J. Siebert and M.D. Zhu, *J. Chromatogr.*, 403 (1987) 43.
43 Cs. Horváth and W. Melander, in E. Heftmann (Editor), *Chromatography*, Elsevier, Amsterdam, 1983, p. A45.
44 J.C. Giddings, *Sep. Sci.*, 4 (1969) 181.
45 J.W. Jorgenson and K. DeArman Lukacs, *Anal. Chem.*, 53 (1981) 1298.
46 K.E. Bij, Cs. Horváth, W.R. Melander and A. Nahum, *J. Chromatogr.*, 203 (1981) 65.

Journal of Chromatography A, 661 (1994) 315–321
Elsevier Science B.V., Amsterdam

CHROMSYMP. 2892

Preparation and characterization of a stable polyacrylamide sieving matrix-filled capillary for high-performance capillary electrophoresis

Manabu Nakatani*

Pharmaceutical Research Department, Nippon Boehringer Ingelheim Co., Ltd., 3-10-1 Yato, Kawanishi, Hyogo 666-01 (Japan)

Akimasa Skibukawa and Terumichi Nakagawa

Faculty of Pharmaceutical Science, Kyoto University, Sakyo-ku, Kyoto 606 (Japan)

ABSTRACT

A stable sieving matrix of polyacrylamide filled in a capillary was developed. The inner wall of a fused-silica capillary was covalently bonded with a linear polyacrylamide through Si–C linkages, in which cross-linked polyacrylamide gel or linear polyacrylamide solution was filled. The stability of the coating was examined by exposure of the capillaries to alkaline buffer (pH 8) for up to 30 days. Compared with the coatings with linear polyacrylamide bonded through siloxane linkages, the present capillary markedly reduced the electroosmotic flow. Thus, the sieving matrix in the capillary was stabilized, resulting in a prolonged lifetime of the capillary and good reproducibility of separations. The migration behaviours of oligonucleotides were compared for the cross-linked gel and linear polyacrylamide solution at the same concentration.

INTRODUCTION

High-performance capillary electrophoresis is a rapidly growing technique for the separation of a wide range of analytes, especially biopolymers such as proteins and polynucleotides. However, good reproducibility of the separation of proteins is difficult because of the instability of the gel and the considerable adsorption on the capillary wall. Many reports [1–6] have described the techniques to overcome this difficulty by coating the inner wall of the capillary with hydrophilic polymers through siloxane (Si–O–Si–C) bonds. However, these bonds are prone to nucleophilic cleavage under basic conditions [7,8]. Coating with stable Si–C bonds is a more successful approach to this problem [9].

When polyacrylamide gel was directly bonded to the capillary through siloxane bonds [10–14], it was often found that the bubbles are generated inside the capillary during polymerization and electrophoretic separation. In order to prepare bubble-free gels, the procedure was modified by applying high pressures of up to 400 bar during polymerization [15]. Another modification is that the capillary wall is first covalently bonded with linear polyacrylamide through siloxane linkages to eliminate electroosmotic flow [16], then filled with polyacrylamide gel under moderate pressure.

A gel-filled capillary without a coating is not stable. The separation efficiency decreases rapidly because a small part of the gel is slowly extruded out of the capillary by the electroosmotic pressure generated by the zeta potential on the untreated capillary surface. We solved this problem by employing the Si–C bond coating

* Corresponding author.

0021-9673/94/$07.00
SSDI 0021-9673(93)E0819-G

technique mentioned above [9], but this needed to be improved because it was time consuming. Cross-linked or linear polyacrylamide was formed in a fused-silica capillary which was covalently bonded with linear polyacrylamide through Si–C linkages. This type of capillary suppressed the electroosmotic flow so that the sieving matrix in the capillary became sufficiently stable.

EXPERIMENTAL

Reagents

3-Methacryloxypropyltrimethoxysilane (MAP-S) was purchased from Shin-etsu Chemicals (Tokyo, Japan), vinylmagnesium bromide (1 *M* solution in tetrahydrofuran) from Aldrich (Milwaukee, WI, USA) and thionyl chloride, acrylamide (AA), N,N′-methylenebis(acrylamide) (bisAA), N,N,N′,N′-tetramethylethylenediamine (TEMED), ammonium peroxodisulphate (APS), tris(hydroxymethyl)aminomethane (Tris), tetrahydrofuran (THF), boric acid, urea and Orange G from Wako (Osaka, Japan). Polydeoxyadenylic acids $[p(dA)_{12-18}]$, polydeoxycytidylic acids $[p(dC)_{12-18}]$, polydeoxyguanylic acids $[p(dG)_{12-18}]$ and polydeoxythymidylic acids $[p(dT)_{12-18}]$ were purchased from Pharmacia (Piscataway, NJ, USA). Crude oligonucleotide products (S-1, 5′-TTCAGCAGCCACGCCCAG-3′; S-2, 5′-TGATCTTCCCCTACTACG-3′; A-1, 5′-TAGGCGTATGGACGGCTG-3′; and A-2, 5′-TGGAGCAGGTGAAGAAGC-3′) were prepared by an oligonucleotide synthesizer.

Apparatus

Fused-silica capillaries (50 μm × 75 μm I.D. × 375 μm O.D.) were purchased from GL Sciences (Tokyo, Japan). Separations were performed on a CE-800 capillary electrophoresis system (Jasco, Tokyo, Japan). The operating conditions are given in the figure captions.

Preparation of linear polyacrylamide-coated capillary through siloxane linkages

A detection window was prepared by removing the polyimide coating from a small section of a fused-silica capillary before coating. The inner surface of the capillary was first treated with 1 *M* NaOH for 3 h at room temperature, then reacted with MAPS by the method described by Hjerten [2].

Preparation of linear polyacrylamide-coated capillary through Si–C linkages

A non-cross-linked monolayer of polyacrylamide was bonded to the inner surface of the capillary through Si–C linkages by the reaction shown schematically in Fig. 1, where the procedure employed was the improved version of the reported method [9].

The capillary with a detection window was treated with 1 *M* NaOH, washed with distilled water for 1 h and dried at 110°C under nitrogen overnight. Thionyl chloride was introduced into the capillary using a suction pump for several minutes. After both ends of the capillary had been sealed with a small torch, it was kept at 70°C for 6 h. After reaction, both ends of the capillary were opened and excess thionyl chloride was blown out with nitrogen. A solution of 0.25 *M* vinylmagnesium bromide–THF was introduced into the chlorinated capillary by suction for several minutes, then both ends were sealed and the capillary was kept at 70°C for 6 h for the Grignard reaction to proceed. The capillary was opened and rinsed with THF and distilled water. An aqueous solution containing 3% AA, 0.1% APS and 0.1% TEMED was filled into the capillary, which was kept for 1 h at 28 ± 2°C for polymerization to take place. The capillary was then washed with distilled water by suction until small drops of water appeared rapidly at the end of the suction side.

Preparation of cross-linked polyacrylamide gel-filled capillary

A 5-ml volume of aqueous solution containing 0.1 *M* Tris, 0.25 *M* boric acid, 7 *M* urea and AA–bisAA (7%T, 5%C) was degassed in an ultrasonic bath. A 30-μl volume of 10% TEMED and 10 μl of 10% APS were added to the solution and mixed thoroughly. The mixed solution was immediately filled into the above-mentioned coated capillary. The polymerization proceeded under a pressure of 200 bar to prevent bubbling. After polymerization, the gel-filled

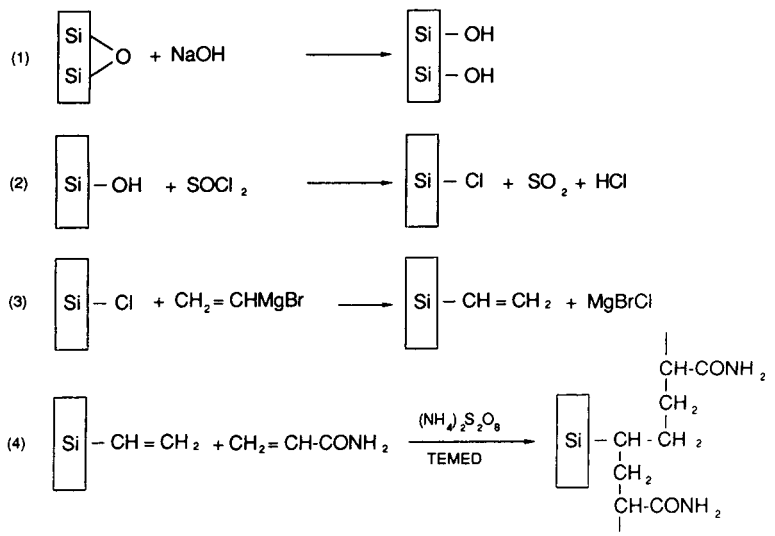

Fig. 1. Reaction scheme for coating a capillary with linear polyacrylamide through Si–C bonds.

capillary was conditioned at −100 V/cm for 30 min before electrophoretic runs.

Preparation of linear polyacrylamide solution-filled capillary

A 5-ml volume of aqueous solution containing 0.1 *M* Tris, 0.25 *M* boric acid, 7 *M* urea and AA (7%T, 0%C) was degassed in an ultrasonic bath, then 30 μl of 10% TEMED and 10 μl of 10% APS were added and mixed thoroughly. The mixed solution was immediately filled into the coated capillary. After polymerization under atmospheric pressure, the gel-filled capillary was conditioned at −100 V/cm for 30 min before electrophoretic runs.

Assessment of durability of coatings under alkaline conditions

The uncoated capillary and the polyacrylamide-coated capillaries (50 μm I.D., total length 50 cm, effective length 30 cm) involving Si–O–Si–C and Si–C linkages prepared by the above methods were filled with 50 m*M* Tris–HCl buffer (pH 8) and kept at room temperature for up to 30 days. The electroosmotic flow was measured using mesityl oxide as a neutral marker and 50 m*M* Tris–HCl buffer (pH 8) as a running buffer, with an applied potential of 400 V/cm.

RESULTS AND DISCUSSION

Fig. 2 illustrates the electroosmotic mobilities observed in the uncoated and coated capillaries after exposure to alkaline conditions (pH 8) for up to 30 days. The coated capillaries involving Si–O–Si–C linkages showed a gradual increase in mobility, whereas those involving Si–C linkages showed a low and constant mobility unchanged from the initial value. The initial values of electroosmotic mobility in both types of coated capillary were very low, such that the

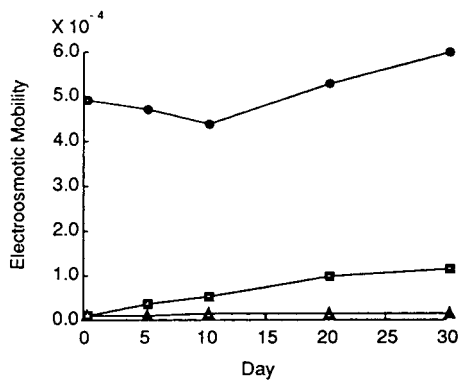

Fig. 2. Time course of electroosmotic mobility ($cm^2/V \cdot s$) as a function of number of days of exposure under alkaline conditions (50 m*M* Tris–HCl, pH 8.0). ○ = Uncoated capillary; □ = coated capillary through siloxane linkages; ▲ = coated capillary through Si–C linkages.

migration times of the marker substance exceeded 6 h. This indicates that the capillary wall has virtually no electric charge because of the almost complete conversion of silanol groups into AA derivatives. After exposure for 30 days, the electroosmotic mobilities in the coated capillaries were $5.21 \cdot 10^{-6}$ cm^2/V·s (Si–C) and $1.04 \cdot 10^{-4}$ cm^2/V·s (Si–O – Si–C), whereas the mobilities in the uncoated capillaries were as high as $4.61 \cdot 10^{-4}$–$5.89 \cdot 10^{-4}$ cm^2/V·s. This indicates that the Si–C bond is more stable than the siloxane bond which links silanol groups to AA. It is also suggested that the polyacrylamide network bonded through Si–C linkages can protect the siloxane bondings of the capillary wall itself from attack by hydroxyl anions. This effect may be stronger than that due to the polyacrylamide coatings through siloxane linkages.

The separations of p(dA) ranging from 12 to 18 bases [p(dA)$_{12-18}$] in the cross-linked polyacrylamide (7%T, 5%C) gel and the linear polyacrylamide (7%T, 0%C) solution-filled capillaries are shown in Figs. 3 and 4, respectively. The inner wall of both capillaries was coated

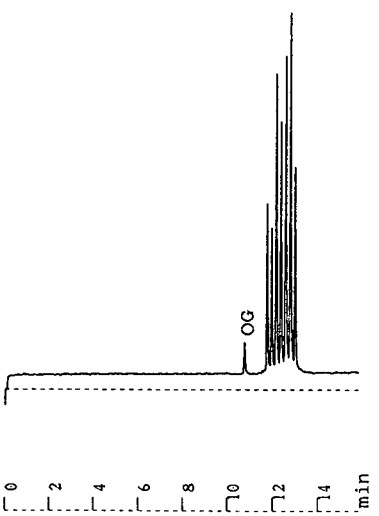

Fig. 3. Electropherogram of p(dA)$_{12-18}$ on cross-linked polyacrylamide gel-filled capillary. Capillary, 75 μm I.D. × 50 cm (30 cm to detector), inner surface coated with linear polyacrylamide through Si–C linkages; gel, polyacrylamide, 7%T, 5%C; buffer, 0.1 *M* Tris–0.25 *M* boric acid–7 *M* urea; electric field, −300 V/cm, 7 μA; injection, −5 kV, 2 s; detection, UV at 260 nm.

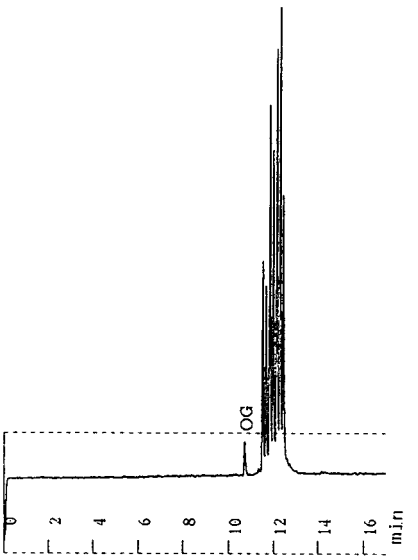

Fig. 4. Electropherogram of p(dA)$_{12-18}$ on linear polyacrylamide solution-filled capillary. Capillary, 75 μm I.D. × 50 cm (30 cm to detector), inner surface coated with linear polyacrylamide through Si–C linkages; gel, polyacrylamide, 7%T, 0%C; buffer, 0.1 *M* Tris–0.25 *M* boric acid–7 *M* urea; electric field, −300 V/cm, 7 μA; injection, −5 kV, 2 s; detection, UV at 260 nm.

with linear polyacrylamide through Si–C linkages in order to suppress electroosmotic flow and to stabilize the matrices. The peaks are clearly separated with baseline resolution. The peak marked OG corresponds to the internal standard (Orange G). The separation efficiency is almost the same as that found with conventional gel-filled capillaries [13,14,17].

The run-to-run reproducibilities of the migration times and relative migration times were determined by repeated injections of p(dA)$_{12-18}$ using the cross-linked polyacrylamide (7%T, 5%C) gel and the linear polyacrylamide (7%T, 0%C) solution-filled capillaries and are given in Table I. The relative migration time is given as the ratio of the migration time of the tested oligomer to that of Orange G. Although the reproducibility of the migration times obtained in the linear polyacrylamide solution-filled capillary is better than that in the cross-linked gel-filled capillary, there were no significant differences between relative migration times in the two capillaries.

TABLE I

REPRODUCIBILITY OF MIGRATION TIMES ($n = 10$)

Gel concentration	Sample	Migration time (min) (mean ± S.D.)	Relative migration time (mean ± S.D.)
7%T, 5%C	$P(dA)_{12}$	11.553 ± 0.21	1.087 ± 0.004
	$P(dA)_{15}$	12.135 ± 0.22	1.143 ± 0.004
	$P(dA)_{18}$	12.746 ± 0.23	1.201 ± 0.005
7%T, 0%C	$P(dA)_{12}$	11.453 ± 0.05	1.077 ± 0.003
	$P(dA)_{15}$	11.913 ± 0.05	1.122 ± 0.003
	$P(dA)_{18}$	12.359 ± 0.06	1.165 ± 0.003

The day-to-day reproducibilities (R.S.D.s) of the migration times ($n = 30$) using the cross-linked gel and the linear polyacrylamide solution-filled capillaries were *ca.* 3.5% and *ca.* 4.5%, respectively.

The four different homooligonucleotide mixtures, $p(dA)_{12-18}$, $p(dT)_{12-18}$, $p(dC)_{12-18}$ and $p(dG)_{12-18}$, were also applied to the cross-linked and the linear polyacrylamide solution-filled capillaries. The migration times relative to that of the internal standard (Orange G) showed linear relationships (correlation coefficient $r > 0.999$) with the base number of each homologous series, as shown in Figs. 5 and 6. The four lines in each figure are parallel to each other, but a comparison of the slopes in Figs. 5 and 6 suggests that the cross-linked polyacrylamide gel (Fig. 5) gives a slightly better resolution than linear polyacrylamide (Fig. 6). These oligonucleotides can be completely deformed by 7 *M* urea in the running buffer solution. If this is the case, p(dA) and p(dG) with purine bases are expected to have a larger molecular size than p(dT) and p(dC) with pyrimidine bases, and hence their migration times should be in the order p(dT), p(dC) < p(dA), p(dG). Further, if the total charge of each molecule can be regarded as the sum of independent dissociations of these bases and phosphate groups, the net charge in the running buffer solution, depending on the dissociation constant of the base, differs

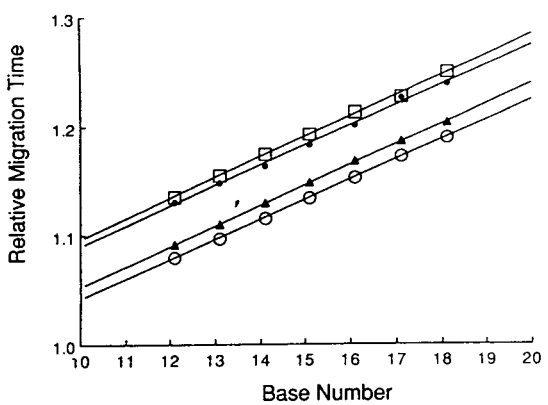

Fig. 5. Relationship between the base number and the relative migration time of the homooligonucleotide mixtures on a cross-linked polyacrylamide gel-filled capillary. Separation conditions as in Fig. 3. The calculation of relative migration times was based on the migration time of Orange G. ○ = $p(dA)_{12-18}$; □ = $p(dT)_{12-18}$; ▲ = $p(dC)_{12-18}$; ● = $p(dG)_{12-18}$.

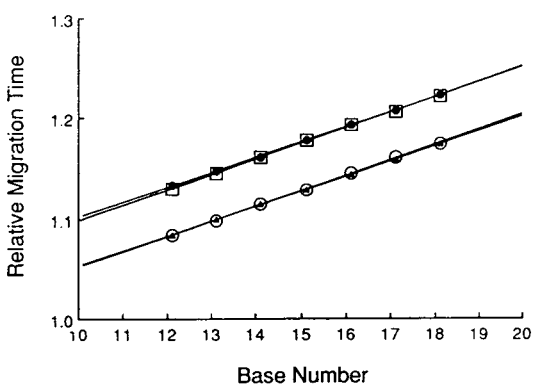

Fig. 6. Relationship between the base number and the relative migration time of the homooligonucleotide mixtures on a linear polyacrylamide solution-filled capillary. Separation conditions as in Fig. 4. The calculation of relative migration times was based on the migration time of Orange G. Symbols as in Fig. 5.

among homooligonucleotides having same number of base groups. The reported pK_a values [18–20] are *ca.* 4 for adenine and cytosine and 9.5 for guanine and thymine. These values suggest that only guanine and thymine nucleotides may have weak negative charges in the running buffer (pH 8.3), resulting in the migration time order p(dT), p(dG) < p(dC), p(dA). The experimental results in Figs. 5 and 6 indicate the order p(dA) < p(dC) < p(dG) < p(dT) in the linear polyacrylamide-filled capillaries. Further studies are required in order to resolve this discrepancy.

The electropherograms of a mixture of the four synthesized heterooligonucleotides using the cross-linked and the linear polyacrylamide-filled capillaries are shown in Figs. 7 and 8, respectively. These oligonucleotides have same chain length (18mer), but the sequence of base units differs. Both capillaries gave the same migration order, but the separation efficiency was slightly better with the cross-linked polymer than with the linear polymer. The relative migration times of these synthesized oligonucleotides were calculated by the following equation, which was

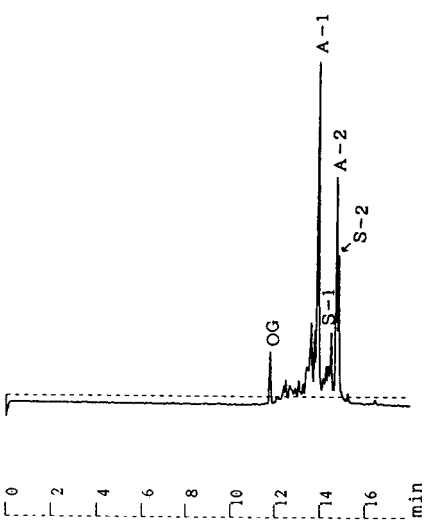

Fig. 7. Electropherogram of crude oligonucleotide products on a cross-linked polyacrylamide (7%T, 5%C) gel-filled capillary. Separation conditions as in Fig. 3. Sample: S-1 = 5′-TTCAGCAGCCACGCCCAG-3′; S-2 = 5′-TGATCTTCCC-CTACTACG-3′; A-1 = 5′-TAGGCGTATGGACGGCTG-3′; A-2 = 5′-TGGAGCAGGTGAAGAAGC-3′.

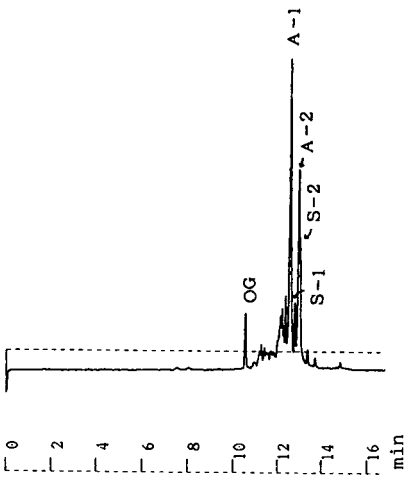

Fig. 8. Electropherogram of crude oligonucleotide products on a linear polyacrylamide (7%T, 0%C) solution-filled capillary. Separation conditions as in Fig. 4. Sample: S-1 = 5′-TTCAGCAGCCACGCCCAG-3′; S-2 = 5′-TGATCTTC-CCCTACTACG-3′; A-1 = 5′-TAGGCGTATGGACGGC-TG-3′; A-2 = 5′-TGGAGCAGGTGAAGAAGC-3′.

obtained from the linear relationship given in Figs. 5 and 6 according to Guttman *et al.*'s method [20]:

$$t'(A_aT_tC_cG_g) = a/nt'(A_n) + t/nt'(T_n) + c/nt'(C_n) + g/nt'(G_a)$$

where n is the oligonucleotide chain length ($n = a + t + c + g$) and a, t, c and g are numbers of the individual bases in the oligonucleotide, and $t'(A_n)$, $t'(T_n)$, $t'(C_n)$ and $t'(G_n)$ are the relative migration times of the n-mers of adenylic, thymidylic, cytidylic and guanylic acid homooligonucleotides, respectively. The results obtained were different from the observed values of relative migration time and migration order. This indicates that Guttman et al. equation, which was applied to three kinds of heterooligonucleotides having a different base only at the tenth residue from the 5′-terminus, cannot be applied to those having entirely different base arrangements. Therefore, not only the kind and number of bases but also their location and sequence in the chain need to taken into consideration in order to predict migration times.

CONCLUSION

As the capillary was coated with linear polyacrylamide which was covalently bonded to the silica wall through Si–C linkages, the cross-linked polyacrylamide gel or linear polyacrylamide solution in the capillary became stable even under alkaline conditions and could be used repeatedly owing to the easy refilling of sieving matrices. This type of the stable capillary will allow a wide range of soft gel or polymer solutions of low viscosity to be used for high-performance capillary electrophoresis.

ACKNOWLEDGEMENT

We thank Dr. Ito for supplying the crude oligonucleotide products.

REFERENCES

1 J.W. Jorgenson and K.D. Lukacs, *Science*, 222 (1983) 266.
2 S. Hjerten, *J. Chromatogr.*, 347 (1985) 191.
3 R.M. McCormick, *Anal. Chem.*, 60 (1988) 2322.
4 G.J.M. Bruin, J.P. Chang, R.H. Kuhlman, K. Zegers, J.C. Kraak and H. Poppe *J. Chromatogr.*, 471 (1989) 429.
5 J.K. Towns and F.E. Regnier, *J. Chromatogr.*, 516 (1990) 69.
6 S.A. Swedberg, *Anal. Biochem.*, 185 (1990) 51.
7 R.K. Iler, *The Chemistry of Silica*, Wiley, New York, 1979, Ch. 6.
8 K.K. Unger, *Porous Silica*, Elsevier, Amsterdam, 1979, Ch. 8.
9 K.A. Cobb, V. Dolnik and M. Novotny, *Anal. Chem.*, 62 (1990) 2478.
10 A.S. Cohen and B.L. Karger, *J. Chromatogr.*, 397 (1987) 409.
11 A.S. Cohen, A. Paulus and B.L. Karger, *Chromatographia*, 24 (1987) 15.
12 A. Guttman, A. Paulus, A.S. Cohen, N. Grinberg and B.L. Karger, *J. Chromatogr.*, 448 (1988) 41.
13 A.S. Cohen, D.R. Najarian, A. Paulus, A. Guttman, J.A. Smith and B.L. Karger, *Proc. Natl. Acad. Sci. U.S.A.*, 85 (1988) 9660.
14 A. Guttman, A.S. Cohen, D.N. Heiger and B.L. Karger, *Anal. Chem.*, 62 (1990) 137.
15 H. Drossman, J.A. Luckey, A. Kostichka, J.D'Cunha and L.M. Smith, *Anal. Chem.*, 62 (1990) 900.
16 J.A. Lux, H. Yin and S. Schomburg, *J. High Resolut. Chromatogr.*, 13 (1990) 436.
17 A. Guttman, R.J. Nelson and N. Cooke, *J. Chromatogr.*, 593 (1992) 297.
18 B.L. Horecker, *J. Biol. Chem.*, 183 (1950) 593.
19 P. Strittmatter and S.F. Velic, *J. Biol. Chem.*, 221 (1956) 227.
20 P. Strittmatter and S.F. Velic, *Biochim. Biophys. Acta*, 25 (1957) 228.

Author Index

Abbas, N.M., see Iob, A. 661(1994)245
Achilli, G., Cellerino, G.P. and Melzi d'Eril, G.
Determination of amines in wines by high-performance liquid chromatography with electrochemical coulometric detection after precolumn derivatization 661(1994)201
Aguilar, M.I., see Round, A.J. 661(1994)61
Aguilar, M.-I., see Yarovsky, I. 660(1994)75
Al-Yousef, F., see Iob, A. 661(1994)245
Au, T., see Woolf, E.J. 660(1994)307
Baba, Y., see Sumita, C. 661(1994)297
Bagchi, D., see Cordis, G.A. 661(1994)181
Balke, S.T., see Schunk, T.C. 661(1994)227
Balmér, K., Persson, B.-A. and Lagerström, P.-O.
Stereoselective effects in the separation of enantiomers of omeprazole and other substituted benzimidazoles on different chiral stationary phases 660(1994)269
Barnaby, R.J. and Iavarone, L.
Automated assay for GV104326, a novel tribactam antibiotic, in human plasma by high-performance liquid chromatography and solid-phase extraction 660(1994)319
Basileo, G., see Fontana, E. 660(1994)293
Beinert, W.-D., see Kirschbaum, J. 661(1994)193
Bello, M.S., see Ermakov, S.V. 661(1994)265
Below, E., see Thede, R. 660(1994)25
Berger, H., see Brudel, M. 661(1994)55
Bienert, M., see Rothemund, S. 661(1994)77
Bonora, C., see Vitali, P. 660(1994)219
Brown, P.R., see De Antonis, K.M. 661(1994)279
Brudel, M., Kertscher, U., Berger, H. and Mehlis, B.
Liquid chromatographic–mass spectrometric studies on the enzymatic degradation of gonado-tropin-releasing hormone 661(1994)55
Brunt, K., see Houben, R.J. 661(1994)169
Burgess, A.W., see Nice, E. 660(1994)169
Calori, R., see Vitali, P. 660(1994)219
Carini, M., see Pietta, P. 661(1994)121
Caruso, U., Fowler, B., Minniti, G. and Romano, C.
Determination of tryptophan and ten of its metabolites in a single analysis by high-performance liquid chromatography with multiple detection 661(1994)101
Cellerino, G.P., see Achilli, G. 661(1994)201
Chen, B.H. and Chen, Y.C.
Evaluation of the analysis of cholesterol oxides by liquid chromatography 661(1994)127
Chen, Y.C., see Chen, B.H. 661(1994)127
Cheng, Y.-F., see De Antonis, K.M. 661(1994)279
Cheung, P., see Schunk, T.C. 661(1994)227
Chmelík, J., see Pazourek, J. 660(1994)113
Chu, A.H.T., see Ludolph, B.S. 660(1994)3
Cohen, S.A. and De Antonis, K.M.
Applications of amino acid derivatization with 6-aminoquinolyl-N-hydroxysuccinimidyl carbamate. Analysis of feed grains, intravenous solutions and glycoproteins 661(1994)25
Cohen, S.A., see De Antonis, K.M. 661(1994)279
Constanzer, M., see Woolf, E.J. 660(1994)307
Cordis, G.A., Bagchi, D., Maulik, N. and Das, D.K.
High-performance liquid chromatographic method for the simultaneous detection of malonaldehyde, acetaldehyde, formaldehyde, acetone and propionaldehyde to monitor the oxidative stress in heart 661(1994)181
Corradini, C., see Corradini, D. 661(1994)305
Corradini, D., Rhomberg, A. and Corradini, C.
Electrophoresis of proteins in uncoated capillaries with amines and amino sugars as electrolyte additives 661(1994)305
Cserháti, T. and Forgács, E.
Retention of some monoamine oxidase inhibitory drugs on a β-cyclodextrin polymer-coated silica column 660(1994)313
Cserháti, T., see Forgács, E. 661(1994)239
Cserpán, E., see Péter, A. 660(1994)283
Csizmadia, F., see Fekete, J. 660(1994)33
Darvas, F., see Fekete, J. 660(1994)33
Das, D.K., see Cordis, G.A. 661(1994)181
Davankov, V., see Kurganov, A. 660(1994)97
De Antonis, K.M., Brown, P.R., Cheng, Y.-F. and Cohen, S.A.
Analysis of derivatized peptides by capillary electrophoresis 661(1994)279
De Antonis, K.M., see Cohen, S.A. 661(1994)25
Desbène, P.L. and Desmazieres, B.
Analytical study of polyoxyethylene surfactants of high degree of condensation by normal-phase liquid chromatography on p-nitrophenyl-bonded silica 661(1994)207
Desmazieres, B., see Desbène, P.L. 661(1994)207
Dyas, A.M., Robinson, M.L. and Fell, A.F.
Influence of the structure of the alcoholic modifier on the enantioselective separation of nadolol 660(1994)249
Ehrlich, A., see Rothemund, S. 661(1994)77
Eisenbeiss, F., see Kurganov, A. 660(1994)97
Emmrich, F., see Guse, A.H. 661(1994)13
Eriksson, B.-M., see Hedenmo, M. 661(1994)153
Ermakov, S.V., Bello, M.S. and Righetti, P.G.
Numerical algorithms for capillary electrophoresis 661(1994)265
Fabri, L., see Nice, E. 660(1994)169
Facino, R.M., see Pietta, P. 661(1994)121
Fekete, J., Morovján, G., Csizmadia, F. and Darvas, F.
Method development by an expert system. Advantages and limitations 660(1994)33
Fell, A.F., see Dyas, A.M. 660(1994)249
Fontana, E., Pianezzola, E., Basileo, G. and Strolin Benedetti, M.
High-performance liquid chromatographic determination of FCE 24928, a new aromatase inhibitor, in human plasma 660(1994)293
Forgács, E. and Cserháti, T.
Retention behaviour of tributylphenol ethylene oxide oligomers on an alumina high-performance liquid chromatographic column 661(1994)239

Forgács, E., see Cserháti, T. 660(1994)313
Fowler, B., see Caruso, U. 661(1994)101
Friebe, S., Hartrodt, B., Neubert, K. and Krauss, G.-J.
High-performance liquid chromatographic separation of *cis–trans* isomers of proline-containing peptides. II. Fractionation in different cyclodextrin systems 661(1994)7
Friedl, Z., see Šlais, K. 661(1994)249
Frigerio, E., Pianezzola, E. and Strolin Benedetti, M.
Sensitive procedure for the determination of reboxetine enantiomers in human plasma by reversed-phase high-performance liquid chromatography with fluorimetric detection after chiral derivatization with (+)-1-(9-fluorenyl)ethyl chloroformate 660(1994)351
Fujima, H., see Haginaka, J. 660(1994)275
Gaberc-Porekar, V., see Luksa, J. 661(1994)161
Galushko, S.V., Kamenchuk, A.A. and Pit, G.L.
Calculation of retention in reversed-phase liquid chromatography. IV. ChromDream software for the selection of initial conditions and for simulating chromatographic behaviour 660(1994)47
Galushko, S.V., Shishkina, I.P. and Soloshonok, V.A.
Ligand-exchange high-performance liquid chromatography of fluorine-containing phenylglycine and phenylalanine 661(1994)51
Ganajová, M., see Oriňák, A. 660(1994)67
Garrigues, P., see Pyell, U. 660(1994)223
Geschwill, K., see Niedwetzki, G. 661(1994)175
Glusa, E., see Rothemund, S. 661(1994)77
Gorton, L., see Marko-Varga, G. 660(1994)153
Gottschlich, N., see Kasche, V. 660(1994)137
Grahn, A., see Hermansson, J. 660(1994)119
Grishina, G.A., see Klyushnichenko, V.E. 661(1994)83
Guse, A.H., Milton, A.D., Schulze-Koops, H., Müller, B., Roth, E., Simmer, B., Wächter, H., Weiss, E. and Emmrich, F.
Purification and analytical characterization of an anti-CD4 monoclonal antibody for human therapy 661(1994)13
Gyoryová, K., see Oriňák, A. 660(1994)67
Haberland, D., see Thede, R. 660(1994)25
Haginaka, J., Seyama, C., Murashima, T., Fujima, H. and Wada, H.
Retention and enantioselective properties of ovomucoid-bonded silica columns. Influence of physical properties of base materials and spacer length 660(1994)275
Haldna, U., see Kaljurand, M. 660(1994)147
Hartrodt, B., see Friebe, S. 661(1994)7
Hearn, M.T.W., see Round, A.J. 661(1994)61
Hearn, M.T.W., see Yarovsky, I. 660(1994)75
Hedenmo, M. and Eriksson, B.-M.
On-line solid-phase extraction with automated cartridge exchange for liquid chromatographic determination of lipophilic antioxidants in plasma 661(1994)153
Hees, T., see Wenclawiak, B.W. 660(1994)61
Hermansson, J. and Grahn, A.
Determination of drugs by direct injection of plasma into a biocompatible extraction column based on a protein-entrapped hydrophobic phase 660(1994)119
Hide, K., see Sumita, C. 661(1994)297
Horká, M., Kahle, V. and Šlais, K.
Parallel-current open-tubular liquid chromatography with fluorimetric detection 660(1994)187
Houben, R.J. and Brunt, K.
Determination of glycoalkaloids in potato tubers by reversed-phase high-performance liquid chromatography 661(1994)169
Huang, C.-Y., see Lee, Y.-C. 660(1994)299
Iavarone, L., see Barnaby, R.J. 660(1994)319
Iob, A., Al-Yousef, F., Tawabini, B.S., Mohammed, A.I. and Abbas, N.M.
Simultaneous determination of benzotriazole copper inhibitor and microbiocidal isothiazolinenones by high-performance liquid chromatography 661(1994)245
Isajeva, T., see Kurganov, A. 660(1994)97
Ishibashi, M., see Toyo'oka, T. 661(1994)105
Ishimaru, N., see Sumita, C. 661(1994)297
Ito, M., Miura, J., Ito, M., Umesato, F., Yasuda, K., Takata, Y. and Stanislawski, B.
Correlative retention time peak identification method for glycated haemoglobin in high-performance liquid chromatography 661(1994)143
Ito, M., see Ito, M. 661(1994)143
Jekel, M., see Reemtsma, T. 660(1994)199
Jeng, C.-Y., see Ludolph, B.S. 660(1994)3
Johansson, K., see Marko-Varga, G. 660(1994)153
Jones, D., Scarborough, A. and Tier, C.M.
Quantitative determination of a dipeptide in personal wash liquid by capillary electrophoresis 661(1994)1
Josic, D., see Luksa, J. 661(1994)161
Juan, H., see Wintersteiger, R. 660(1994)205
Kahle, V., see Horká, M. 660(1994)187
Kaljurand, M., Urbas, E. and Haldna, U.
Improvement of the performance of single-column ion chromatography by computerized detector signal processing and correlation chromatography 660(1994)147
Kamenchuk, A.A., see Galushko, S.V. 660(1994)47
Kapustin, D.V., see Kataev, A.D. 660(1994)131
Kasche, V., Gottschlich, N., Lindberg, A., Niebuhr-Redder, C. and Schmieding, J.
Perfusible and non-perfusible supports with monoclonal antibodies for bioaffinity chromatography of *Escherichia coli* penicillin amidase within its pH stability range 660(1994)137
Kasper, M., see Woolf, E.J. 660(1994)307
Kataev, A.D., Saburov, V.V., Reznikova, O.A., Kapustin, D.V. and Zubov, V.P.
Polytrifluorostyrene-coated silica as a packing for column liquid chromatography 660(1994)131
Kehr, J.
Determination of catecholamines by automated pre-column derivatization and reversed-phase column liquid chromatography with fluorescence detection 661(1994)137
Kertscher, U., see Brudel, M. 661(1994)55
Khoshab, A. and Teasdale, R.
Application of high-performance gel-permeation chromatography clean-up in the determination of hexaflumuron residues in soil 660(1994)195
Kirkland, J.J., see Kirkland, K.M. 660(1994)327

Kirkland, K.M., McCombs, D.A. and Kirkland, J.J.
Rapid, high-resolution high-performance liquid chromatographic analysis of antibiotics 660(1994)327
Kirschbaum, J., Luckas, B. and Beinert, W.-D.
Pre-column derivatization of biogenic amines and amino acids with 9-fluorenylmethyl chloroformate and heptylamine 661(1994)193
Klyushnichenko, V.E., Koulich, D.M., Yakimov, S.A., Maltsev, K.V., Grishina, G.A., Nazimov, I.V. and Wulfson, A.N.
Recombinant human insulin. III. High-performance liquid chromatography and high-performance capillary electrophoresis control in the analysis of step-by-step production of recombinant human insulin 661(1994)83
Koulich, D.M., see Klyushnichenko, V.E. 661(1994)83
Krause, E., see Rothemund, S. 661(1994)77
Krauss, G.-J., see Friebe, S. 661(1994)7
Kurganov, A., Davankov, V., Isajeva, T., Unger, K. and Eisenbeiss, F.
Characterization of covalently bonded and adsorbed polymer coatings on silica, alumina and zirconia by means of physico-chemical and chromatographic methods 660(1994)97
Kus, B., see Luksa, J. 661(1994)161
Lach, G., see Niedwetzki, G. 661(1994)175
Lackmann, M., see Nice, E. 660(1994)169
Lagerström, P.-O., see Balmér, K. 660(1994)269
Langer, S.H., see Ludolph, B.S. 660(1994)3
Lee, Y.-C., Huang, C.-Y., Wen, K.-C. and Suen, T.-T.
Determination of paeoniflorin, ferulic acid and baicalin in the traditional Chinese medicinal preparation Dang-Guei-San by high-performance liquid chromatography 660(1994)299
Levsen, K., see Volmer, D. 660(1994)231
Liapis, A.I. and McCoy, M.A.
Perfusion chromatography. Effect of micropore diffusion on column performance in systems utilizing perfusive adsorbent particles with a bidisperse porous structure 660(1994)85
Lindberg, A., see Kasche, V. 660(1994)137
Lindner, W., see Veigl, E. 660(1994)255
Luckas, B., see Kirschbaum, J. 661(1994)193
Ludolph, B.S., Jeng, C.-Y., Chu, A.H.T. and Langer, S.H.
Quantitative study of retention processes in reversed-phase liquid chromatography by means of reaction kinetics 660(1994)3
Luksa, J., Menart, V., Milicic, S., Kus, B., Gaberc-Porekar, V. and Josic, D.
Purification of human tumour necrosis factor by membrane chromatography 661(1994)161
Maltsev, K.V., see Klyushnichenko, V.E. 661(1994)83
Marko-Varga, G., Johansson, K. and Gorton, L.
Enzyme-based biosensor as a selective detection unit in column liquid chromatography 660(1994)153
Matisová, E., see Oriňák, A. 660(1994)67
Matuszewski, B., see Woolf, E.J. 660(1994)307
Maulik, N., see Cordis, G.A. 661(1994)181
Mauri, P., see Pietta, P. 661(1994)121
McCombs, D.A., see Kirkland, K.M. 660(1994)327
McCoy, M.A., see Liapis, A.I. 660(1994)85
Mehlis, B., see Brudel, M. 661(1994)55
Melzi d'Eril, G., see Achilli, G. 661(1994)201
Menart, V., see Luksa, J. 661(1994)161
Meyer, K., see Simat, T. 661(1994)93
Milicic, S., see Luksa, J. 661(1994)161
Milton, A.D., see Guse, A.H. 661(1994)13
Minniti, G., see Caruso, U. 661(1994)101
Miura, J., see Ito, M. 661(1994)143
Mohammed, A.I., see Iob, A. 661(1994)245
Molnár-Perl, I.
Advances in the high-performance liquid chromatographic determination of phenylthiocarbamyl amino acids (Review) 661(1994)43
Morovján, G., see Fekete, J. 660(1994)33
Motellier, S. and Pitsch, H.
Determination of aluminium and its fluoro complexes in natural waters by ion chromatography 660(1994)211
Müller, B., see Guse, A.H. 661(1994)13
Murashima, T., see Haginaka, J. 660(1994)275
Nakagawa, T., see Nakatani, M. 661(1994)315
Nakatani, M., Skibukawa, A. and Nakagawa, T.
Preparation and characterization of a stable polyacrylamide sieving matrix-filled capillary for high-performance capillary electrophoresis 661(1994)315
Nazimov, I.V., see Klyushnichenko, V.E. 661(1994)83
Neubert, K., see Friebe, S. 661(1994)7
Nice, E., Lackmann, M., Smyth, F., Fabri, L. and Burgess, A.W.
Synergies between micropreparative high-performance liquid chromatography and an instrumental optical biosensor 660(1994)169
Niebuhr-Redder, C., see Kasche, V. 660(1994)137
Niedwetzki, G., Lach, G. and Geschwill, K.
Determination of aflatoxins in food by use of an automatic work station 661(1994)175
Noguchi, K., see Seki, T. 661(1994)113
Ofner, B., see Wintersteiger, R. 660(1994)205
Oriňák, A., Gyoryová, K., Matisová, E., Šlesárová, L., Skoršepa, J., Rosival, I. and Ganajová, M.
Mobile phase selection for high-performance liquid chromatographic analysis of novel zinc(II) carboxylates with N-donor ligands 660(1994)67
Orita, Y., see Seki, T. 661(1994)113
Parissi-Poulou, M., see Piperaki, S. 660(1994)339
Patthy, M.
Explanation of the selectivity differences between reversed-phase ion-pair chromatographic systems containing trifluoroacetate or heptafluorobutyrate as pairing ion 660(1994)17
Pazourek, J., Urbánková, E. and Chmelík, J.
Experimental study on the separation of silica gel supports by gravitational field-flow fractionation 660(1994)113
Perakis, A., see Piperaki, S. 660(1994)339
Persson, B.-A., see Balmér, K. 660(1994)269
Péter, A., Tóth, G., Cserpán, E. and Tourwé, D.
Monitoring of optical isomers of β-methylphenylalanine in opioid peptides 660(1994)283
Pianezzola, E., see Fontana, E. 660(1994)293
Pianezzola, E., see Frigerio, E. 660(1994)351

Pietta, P., Facino, R.M., Carini, M. and Mauri, P.
Thermospray liquid chromatography–mass spectrometry of flavonol glycosides from medicinal plants 661(1994)121
Piperaki, S., Perakis, A. and Parissi-Poulou, M.
Liquid chromatographic retention behaviour and separation of promethazine and isopromethazine on a β-cyclodextrin bonded-phase column 660(1994)339
Pit, G.L., see Galushko, S.V. 660(1994)47
Pitsch, H., see Motellier, S. 660(1994)211
Pyell, U. and Garrigues, P.
Clean-up by high-performance liquid chromatography of polychlorodibenzo-*p*-dioxins and polychlorodibenzofurans on a pyrenylethylsilica gel column 660(1994)223
Raffaelli, R., see Vitali, P. 660(1994)219
Reemtsma, T. and Jekel, M.
Analysis of sulphonated polyphenols, synthetic tanning agents in heavily polluted tannery wastewaters 660(1994)199
Renard, J. and Vidal-Madjar, C.
Kinetic study of the adsorption of human serum albumin on immobilized antibody using the split-peak effect in immunochromatography 661(1994)35
Reznikova, O.A., see Kataev, A.D. 660(1994)131
Rhomberg, A., see Corradini, D. 661(1994)305
Righetti, P.G., see Ermakov, S.V. 661(1994)265
Robinson, M.L., see Dyas, A.M. 660(1994)249
Romano, C., see Caruso, U. 661(1994)101
Rosival, I., see Oriňák, A. 660(1994)67
Roth, E., see Guse, A.H. 661(1994)13
Rothemund, S., Krause, E., Ehrlich, A., Bienert, M., Glusa, E. and Verhallen, P.
Determination of peptide hydrophobicity parameters by reversed-phase high-performance liquid chromatography 661(1994)77
Round, A.J., Aguilar, M.I. and Hearn, M.T.W.
High-performance liquid chromatography of amino acids, peptides and proteins. CXXXIII. Peak tracking of peptides in reversed-phase high-performance liquid chromatography 661(1994)61
Saburov, V.V., see Kataev, A.D. 660(1994)131
Samata, K., see Sumita, C. 661(1994)297
Scarborough, A., see Jones, D. 661(1994)1
Schmieding, J., see Kasche, V. 660(1994)137
Schulze-Koops, H., see Guse, A.H. 661(1994)13
Schunk, T.C.
Composition distribution separation of methyl methacrylate–methacrylic acid copolymers by normal-phase gradient elution high-performance liquid chromatography 661(1994)215
Schunk, T.C., Balke, S.T. and Cheung, P.
Quantitative polymer composition characterization with a liquid chromatography–Fourier transform infrared spectrometry–solvent-evaporation interface 661(1994)227
Seki, T., Orita, Y., Yamamoto, S., Ueda, N., Yanagihara, Y. and Noguchi, K.
Column-switching liquid chromatographic method for the simultaneous determination of iothalamic acid and creatinine in biological fluids 661(1994)113
Seyama, C., see Haginaka, J. 660(1994)275
Shishkina, I.P., see Galushko, S.V. 661(1994)51
Simat, T., Meyer, K. and Steinhart, H.
Synthesis and analysis of oxidation and carbonyl condensation compounds of tryptophan 661(1994)93
Simmer, B., see Guse, A.H. 661(1994)13
Skibukawa, A., see Nakatani, M. 661(1994)315
Skoršepa, J., see Oriňák, A. 660(1994)67
Šlais, K. and Friedl, Z.
Low-molecular-mass p*I* markers for isoelectric focusing 661(1994)249
Šlais, K., see Horká, M. 660(1994)187
Šlesárová, L., see Oriňák, A. 660(1994)67
Smyth, F., see Nice, E. 660(1994)169
Soloshonok, V.A., see Galushko, S.V. 661(1994)51
Stanislawski, B., see Ito, M. 661(1994)143
Steinhart, H., see Simat, T. 661(1994)93
Strolin Benedetti, M., see Fontana, E. 660(1994)293
Strolin Benedetti, M., see Frigerio, E. 660(1994)351
Suen, T.-T., see Lee, Y.-C. 660(1994)299
Sumita, C., Baba, Y., Hide, K., Ishimaru, N., Samata, K., Tanaka, A. and Tsuhako, M.
Comparative study of non-porous anion-exchange chromatography, capillary gel electrophoresis and capillary electrophoresis in polymer solutions in the separation of DNA restriction fragments 661(1994)297
Takata, Y., see Ito, M. 661(1994)143
Tanaka, A., see Sumita, C. 661(1994)297
Tawabini, B.S., see Iob, A. 661(1994)245
Teasdale, R., see Khoshab, A. 660(1994)195
Terao, T., see Toyo'oka, T. 661(1994)105
Thede, R., Haberland, D. and Below, E.
Determination of rate constants in a liquid chromatographic reactor by means of a fitting algorithm 660(1994)25
Tier, C.M., see Jones, D. 661(1994)1
Tóth, G., see Péter, A. 660(1994)283
Tourwé, D., see Péter, A. 660(1994)283
Toyo'oka, T., Ishibashi, M. and Terao, T.
Sensitive determination of N-terminal prolyl peptides by high-performance liquid chromatography with laser-induced fluorescence detection 661(1994)105
Tsuhako, M., see Sumita, C. 661(1994)297
Tsuji, K.
Factors affecting the performance of sodium dodecyl sulfate gel-filled capillary electrophoresis 661(1994)257
Ueda, N., see Seki, T. 661(1994)113
Umesato, F., see Ito, M. 661(1994)143
Unger, K., see Kurganov, A. 660(1994)97
Unger, K.K.
Foreword 660(1994)1
Urbánková, E., see Pazourek, J. 660(1994)113
Urbas, E., see Kaljurand, M. 660(1994)147
Veigl, E. and Lindner, W.
Epimeric N-substituted L-proline derivatives as chiral selectors for ligand-exchange chromatography 660(1994)255
Venturini, E., see Vitali, P. 660(1994)219
Verhallen, P., see Rothemund, S. 661(1994)77
Vidal-Madjar, C., see Renard, J. 661(1994)35

Vitali, P., Venturini, E., Bonora, C., Calori, R. and Raffaelli, R.
Determination of triazines and dinitroanilines in waters by high-performance liquid chromatography after solid-phase extraction 660(1994)219
Volmer, D., Levsen, K. and Wünsch, G.
Thermospray liquid chromatographic–mass spectrometric multi-residue determination of 128 polar pesticides in aqueous environmental samples 660(1994)231
Wächter, H., see Guse, A.H. 661(1994)13
Wada, H., see Haginaka, J. 660(1994)275
Weiss, E., see Guse, A.H. 661(1994)13
Wen, K.-C., see Lee, Y.-C. 660(1994)299
Wenclawiak, B.W. and Hees, T.
Optimization of high-performance liquid chromatography and solvent parameters for the separation of polycyclic aromatic hydrocarbons compared with supercritical fluid chromatography with UV detection 660(1994)61
Windisch, M., see Wintersteiger, R. 660(1994)205
Wintersteiger, R., Ofner, B., Juan, H. and Windisch, M.
Determination of traces of pyrethrins and piperonyl butoxide in biological material by high-performance liquid chromatography 660(1994)205
Woolf, E.J., Au, T., Kasper, M., Constanzer, M. and Matuszewski, B.
Simultaneous determination of L-693,612, a topical carbonic anhydrase inhibitor, and two potential metabolites in human whole blood by ion-pair high-performance liquid chromatography 660(1994)307
Wulfson, A.N., see Klyushnichenko, V.E. 661(1994)83
Wünsch, G., see Volmer, D. 660(1994)231
Xue, Q. and Yeung, E.S.
Indirect fluorescence determination of lactate and pyruvate in single erythrocytes by capillary electrophoresis 661(1994)287
Yakimov, S.A., see Klyushnichenko, V.E. 661(1994)83
Yamamoto, S., see Seki, T. 661(1994)113
Yanagihara, Y., see Seki, T. 661(1994)113
Yarovsky, I., Aguilar, M.-I. and Hearn, M.T.W.
High-performance liquid chromatography of amino acids, peptides and proteins. CXXV. Molecular dynamics simulation of *n*-butyl chains chemically bonded to silica-based reversed-phase high-performance liquid chromatography sorbents 660(1994)75
Yasuda, K., see Ito, M. 661(1994)143
Yeung, E.S., see Xue, Q. 661(1994)287
Zubov, V.P., see Kataev, A.D. 660(1994)131

PUBLICATION SCHEDULE FOR THE 1994 SUBSCRIPTION

Journal of Chromatography A and *Journal of Chromatography B: Biomedical Applications*

MONTH	O 1993	N 1993	D 1993	J	F	
Journal of Chromatography A	652/1 652/2 653/1	653/2 654/1 654/2 655/1	655/2 656/1 + 2 657/1 657/2	658/1 658/2 659/1 659/2	660/1 + 2 661/1 + 2 662/1 662/2	The publication schedule for further issues will be published later
Bibliography Section						
Journal of Chromatography B: Biomedical Applications				652/1	652/2 653/1	

INFORMATION FOR AUTHORS

(Detailed *Instructions to Authors* were published in *J. Chromatogr. A*, Vol. 657, pp. 463–469. A free reprint can be obtained by application to the publisher, Elsevier Science B.V., P.O. Box 330, 1000 AH Amsterdam, Netherlands.)

Types of Contributions. The following types of papers are published: Regular research papers (full-length papers), Review articles, Short Communications and Discussions. Short Communications are usually descriptions of short investigations, or they can report minor technical improvements of previously published procedures; they reflect the same quality of research as full-length papers, but should preferably not exceed five printed pages. Discussions (one or two pages) should explain, amplify, correct or otherwise comment substantively upon an article recently published in the journal. For Review articles, see inside front cover under Submission of Papers.

Submission. Every paper must be accompanied by a letter from the senior author, stating that he/she is submitting the paper for publication in the *Journal of Chromatography A* or *B*.

Manuscripts. Manuscripts should be typed in **double spacing** on consecutively numbered pages of uniform size. The manuscript should be preceded by a sheet of manuscript paper carrying the title of the paper and the name and full postal address of the person to whom the proofs are to be sent. As a rule, papers should be divided into sections, headed by a caption (*e.g.*, Abstract, Introduction, Experimental, Results, Discussion, etc.) All illustrations, photographs, tables, etc., should be on separate sheets.

Abstract. All articles should have an abstract of 50–100 words which clearly and briefly indicates what is new, different and significant. No references should be given.

Introduction. Every paper must have a concise introduction mentioning what has been done before on the topic described, and stating clearly what is new in the paper now submitted.

Experimental conditions should preferably be given on a *separate* sheet, headed "Conditions". These conditions will, if appropriate, be printed in a block, directly following the heading "Experimental".

Illustrations. The figures should be submitted in a form suitable for reproduction, drawn in Indian ink on drawing or tracing paper. Each illustration should have a caption, all the *captions* being typed (with double spacing) together on a *separate sheet.* If structures are given in the text, the original drawings should be provided. Coloured illustrations are reproduced at the author's expense, the cost being determined by the number of pages and by the number of colours needed. The written permission of the author and publisher must be obtained for the use of any figure already published. Its source must be indicated in the legend.

References. References should be numbered in the order in which they are cited in the text, and listed in numerical sequence on a separate sheet at the end of the article. Please check a recent issue for the layout of the reference list. Abbreviations for the titles of journals should follow the system used by *Chemical Abstracts*. Articles not yet published should be given as "in press" (journal should be specified), "submitted for publication" (journal should be specified), "in preparation" or "personal communication".

Vols. 1–651 of the *Journal of Chromatography*; *Journal of Chromatography, Biomedical Applications* and *Journal of Chromatography, Symposium Volumes* should be cited as *J. Chromatogr.* From Vol. 652 on, *Journal of Chromatography A* (incl. Symposium Volumes) should be cited as *J. Chromatogr. A* and *Journal of Chromatography B: Biomedical Applications* as *J. Chromatogr. B.*

Dispatch. Before sending the manuscript to the Editor please check that the envelope contains four copies of the paper complete with references, captions and figures. One of the sets of figures must be the originals suitable for direct reproduction. Please also ensure that permission to publish has been obtained from your institute.

Proofs. One set of proofs will be sent to the author to be carefully checked for printer's errors. Corrections must be restricted to instances in which the proof is at variance with the manuscript.

Reprints. Fifty reprints will be supplied free of charge. Additional reprints can be ordered by the authors. An order form containing price quotations will be sent to the authors together with the proofs of their article.

Intelligent Software for Chemical Analysis

Edited by **L.M.C. Buydens** and **P.J. Schoenmakers**

Data Handling in Science and Technology Volume 13

Various emerging techniques for automating intelligent functions in the laboratory are described in this book. Explanations on how systems work are given and possible application areas are suggested. The main part of the book is devoted to providing data which will enable the reader to develop and test his own systems. The emphasis is on expert systems; however, promising developments such as self-adaptive systems, neural networks and genetic algorithms are also described.

Contents:

1. Introduction. Automation and intelligent software. Expert systems. Neural networks and genetic algorithms. Reader's guide. Concepts. Conclusions.

2. Knowledge-based Systems in Chemical Analysis (P. Schoenmakers). Computers in analytical chemistry. Sample preparation. Method selection. Method development. Instrument control and error diagnosis. Data handling and calibration. Data interpretation. Validation. Laboratory management. Concluding remarks. Concepts. Conclusions. Bibliography.

3. Developing Expert Systems (H. van Leeuwen). Introduction. Prerequisites. Knowledge acquisition. Knowledge engineering. Inferencing. Explanation facilities. The integration of separate systems. Expert-system testing validation and evaluation. Concepts. Conclusions. Bibliography.

4. Expert-System-Development Tools (L. Buydens, H. van Leeuwen, R. Wehrens). Tools for implementing expert systems. Tool selection. Knowledge-acquisition tools. Concepts. Conclusions. Bibliography. **5. Validation and Evaluation of Expert Systems for HPLC Method Development - Case Studies** (F. Maris, R. Hindriks). Introduction. Case study I: Expert systems for method selection and selectivity optimization. Case study II: System-optimization expert system. Case study III: Expert system for repeatability testing, applied for trouble-shooting in HPLC. Case study IV: Ruggedness-testing expert system. General comments on the evaluations. Concepts. Conclusions. Bibliography.

6. Self-adaptive Expert Systems (R. Wehrens). Introduction - maintaining expert systems. Self-adaptive expert systems: Methods and approaches. The refinement approach of SEEK. Examples from analytical chemistry. Concluding remarks. Concepts. Conclusions. Bibliography.

7. Inductive Expert Systems (R. Wehrens, L. Buydens). Introduction. Inductive classification by ID3. Applications of ID3 in analytical chemistry. Concluding remarks. Concepts. Conclusions. Bibliography. **8. Genetic Algorithms and Neural Networks** (G. Kateman). Introduction. Genetic algorithms. Artificial neural networks. Concepts. Conclusions. Bibliography. **9. Perspectives.** Limitations of Intelligent Software. Dealing with intelligent software. Potential of intelligent software. **Index.**

© 1993 366 pages Hardbound
Price: Dfl. 350.00 (US $ 200.00)
ISBN 0-444-89207-9

ORDER INFORMATION

For USA and Canada
ELSEVIER SCIENCE INC.
P.O. Box 945
Madison Square Station
New York, NY 10160-0757
Fax: (212) 633 3880

In all other countries
ELSEVIER SCIENCE B.V.
P.O. Box 330
1000 AH Amsterdam
The Netherlands
Fax: (+31-20) 5862 845

US$ prices are valid only for the USA & Canada and are subject to exchange rate fluctuations; in all other countries the Dutch guilder price (Dfl.) is definitive. Customers in the European Community should add the appropriate VAT rate applicable in their country to the price(s). Books are sent postfree if prepaid.